UNIVERSITY OF STRATHCLYDE

DEPARTMENT OF MECHANICAL AND PROCESS ENGINEERING

DIVISION OF MECHANICS OF MATERIALS

THE MECHANICS AND MATHEMATICAL MODELLING OF WIRE ROPE

Thesis presented for the

Degree of Doctor of Philosophy

by

Wai Kong Lee

1989

To my dear wife Connie who saw

to everything else while I wrote...

and to my parents, my wife's parents,

other members of both families, for

encouraging and supporting me

during this period.

UNIVERSITY OF STRATHCLYDE

FULL NAME : Wai Kong Lee

DEGREE FOR WHICH SUBMITTED: PhD

DEPARTMENT: Mechanical and Process Engineering

TITLE OF THESIS: The Mechanics And Mathematical Modelling Of Wire Rope.

ABSTRACT

Wire rope is a structure formed by a large number of helical wires which combine in a complex manner to form a composite whole. The work presented in this thesis is concerned with unravelling the geometrical and mechanical complexities of stranded rope in a manner which promotes understanding of the mechanical behaviour and eventual failure of typical ropes.

The thesis presents methods and computed results which provide detailed descriptions of single, double and triple helical shapes of individual wires in strands and ropes. Equations governing the possible spatial configurations of wires in multi-layered and stranded rope are also given and the dependence of the configuration on the number of wires per layer, wire diameter and helix angle is highlighted.

This understanding of rope geometry is used to interpret extensive post-test examinations of full-scale ropes which have failed during systematic laboratory fatigue testing.

Finally, closed-form mathematical models for the study of the mechanical behaviour of various rope and strand types are developed and presented. In all cases, these are built on the earlier geometric foundation described. In some cases, a modification of Costello's and Velinsky's approach is used. In single layer strand modelling, comparisons have been make between the author's analytical models and the experimental results from Martin and Packard as well as Machida and Durelli. Good agreement is shown.

DATE OF DEPOSIT	STRATHCLYDE REF.	BLLD REF.	MORATORIUM EXPIRES

ACKNOWLEDGEMENTS

To Members At The Department Of Mechanical And Process Engineering, University Of Strathclyde, Glasgow

I acknowledge with gratitude my academic supervisor Professor T G F Gray, BSc., PhD., CEng., MIMechE., M.INST.W., of the Department of Mechanical & Process Engineering, for his guidance and valuable suggestions.

I would like to express my sincere gratitude to Professor John Spence, BSc., MEng., ARCST., PhD., DSc., FIMech.E., CEng., Head of Department of Mechanical & Process Engineering, for his kindness and the use of the Department's facilities.

I would like to thank to my undergraduate councillor, Dr. J Hossack, BSc., PhD., C.ENG., senior lecturer of the Department of Mechanical & Process Engineering, for his enthusiastic guidance and help.

My sincere thank to the Department Secretary, Miss Janet Harbidge for her valuable help in many ways.

To Members At The National Engineering Laboratory East Kilbride, Glasgow

I acknowledge with the gratitude my industrial supervisor Dr.

N F Casey, Principal Scientific Officer at the National Engineering Laboratory for his tireless guidance and suggestions during the period of this project.

I would like to acknowledge with gratitude the assistance and help provided by Dr. J Fairbairn, Manager of the Structural Testing and Analysis Division and D. Waters, Principal Scientific Officer of the Structural Testing and Analysis Division, at the National Engineering Laboratory.

I would also like to thank Dr. R Haq, senior scientific officer of Structural Testing and Analysis Division, at the National Engineering Laboratory, for his valuable suggestions.

My sincere thanks to all staffs of the library and photographic section at the National Engineering Laboratory for their delicate work in helping me to search through papers & journals and taking photographs of wire failures for this thesis.

All my project work was carried out both at the Department of Mechanical and Process Engineering, University of Strathclyde and at the National Engineering Laboratory, East Kilbride, Glasgow.

I would like to thank the many other people who have given enthusiastic assistance in my project in both establishments.

I would also like to thank both establishments for providing equipments for the use of this project. Finally, financial support given by the National Engineering Laboratory is gratefully acknowledged.

Note On Computer Programming And Illustrations

All the computer programs for this project were written by the author. They were run on the Amstrad PC1512, which has a colour monitor.

All the figures and illustrations were also drawn by the author.

CONTENTS	PAGE

CHAPTER ONE

LITERATURE REVIEW

1.1 INTRODUCTION

1.1-1 Wire Rope Application

In the early days, wire ropes were closely related with the mining industry, bridge building and rigging of ships. Wire rope applications nowadays are widespread and diverse. Many applications go unnoticed, such as submarine cable for communication, power transmission, mooring of oil production platforms, aircraft components, suspension of bridges & cable cars, hoisting for various industries, antenna supports or roof suspension for large span buildings. There are also many other commercial and domestic applications, such as shop windows and suspension of display shelves, lift and elevator operation in sky-scrapers, false ceilings & suspension of air conditioning ducts and so on.

1.1-2 The Design Potential of Wire Rope

A large variety of wire ropes are available, formed according to different geometrical patterns. However, not more than twenty basic configurations are commonly used. The main reason for using wire rope as tensile member is related to its high strength-to-weight ratio, flexibility and comparative ease of installation in structures and machines. Nevertheless, wire rope has disadvantages which are discussed in Chapter Three.

Under normal applications, wire ropes are generally designed to carry tensile load;eg as tensile members of a structure in which people and equipment are housed. As a result, the aim of good wire rope practice is to establish the most economical, efficient and reliable rope service, commensurate with the appropriate degree of safety to both personnel and equipment. Research, design, evaluation, production and selection of the proper rope for a given application is important, as well as efficient storage, installation, inspection and maintenance practice.

1.1-3 Development of Wire Rope Technology

Although wire rope have been used for several hundred years[1.9], early advancement of wire technology was essentially in manufacturing techniques and material improvements. Rope design, evaluation and selection rely heavily on tests and experiments. Extensive tests and experiments date back to at least one hundred and fifty years ago. However, information on analytical aspects, such as knowledge of the stress level that causes wire failure at various local points, description of the mechanical response of wires (eg in double helical wire and triple helical wire) and understanding the influences of the mechanical interactions between wires and strand, have not yet become apparent in the history of wire rope research. Therefore, in the author's opinion, the present investigations into theoretical aspects are still elementary. More theoretical work is necessary to complement experimental work in the wire rope field.

1.1-4 Difficulties Encountered in Rope Research

The complex geometrical patterns of wire rope construction have limited attempts to investigate the behaviour of wire rope through tests and experiments. Wire rope tests, on one hand, are very costly and only gross parameters can be obtained. Experimental results and data, on the other hand, are difficult to interpret and to isolate from constructional and environmental factors which may occur during tests.

1.1-5 Reviews

The present chapter presents a brief and somewhat subjective view of existing literature on the behaviour of wires, strand ropes. Since a complete review of the past 50 years work would be a difficult task to achieve, only work which is regarded as interesting and significant in relation to the present investigation, will be dealt with. The objectives of this chapter are essentially to establish the scope of various interests in wire rope, to highlight the difficulties and to link the early major achievements in theoretical studies of wire rope with the present investigations. The literature review covers the following aspects.

a. Historical review of wire rope and strand technology
b. Mathematical modelling of wire rope and strand.
c. Termination of rope and end attachments.
e. Other studies on wire ropes.

The literature on wire rope history essentially revolves about wire rope origin and development, wire rope patents in the early days and wire rope research. The history of the wire rope industry in Great Britain from 1830 to 1952 was recorded by Forseter-Walker[1.3]. The birth and evolution of the wire rope industry in America was traced by Sayenga[1.6]. The historical review in the present chapter is confined to a brief introduction only.

Literature on experiments and non-destructive tests have been explored extensively. Only a brief review of these aspects will be given in the present chapter.

Literature on the theory and mathematical modelling of wire rope and strand dates back to 1948. There were three main streams of theory which were initiated by Hruska, Machida and Costello respectively. Detailed reviews will be introduced on these aspects in the present chapter.

1.1-6 Structure Of Chapter One

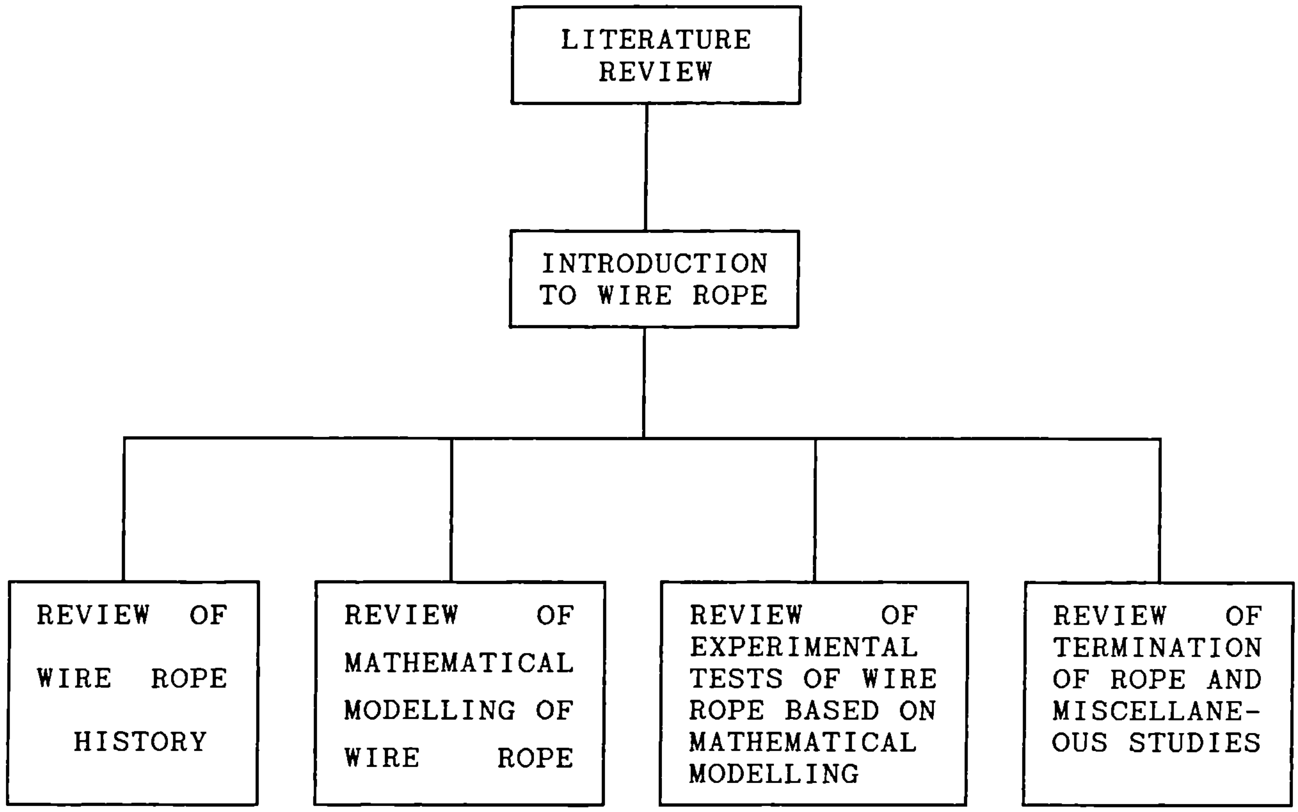

BLOCK DIAGRAM 1

STRUCTURE OF CHAPTER ONE

1.2 HISTORICAL REVIEW

The present section is a brief review of three main aspects of rope history. Namely,

a. Origin and development of the wire rope industry.
b. Development of wire rope and rope production machines.
c. Wire rope research.

A brief review of historical events in wire rope technology is given in table 1.1.

1.2-1 Origin and Development of Wire Rope Industry

Reference [1.1] noted that manufacture and use of wire dated back to 3000 B.C. It was also said that copper cable was found in the ruins of Ninevah as early as 700 B.C. [1.9]. Reference [1.4] claimed that a fifteen foot sample of 1" Lang's lay bronze rope used by Romans over 2400 years ago, was found in Muzio Barbonic at Naples, Italy. A book about Leonardo da Vinci [1.10] shows sketches of mechanised wire production accessories dated approximately 1500 A.D. and manuscripts and books on the history of technology constantly reveal reports of wire which have been in service in Roman times [1.10]. Reference [1.4] noted that the Vikings were using crude wire rope lashings in the 8th century and the Chinese used wire rope to construct rope-ways across rivers as long as 1500 years ago. A book in the library at Vienna dated 1400 shows a sketch of rope-way. During the 16th and 17th centuries, manuscripts were frequently coded "iron rope", however this does not refer to wire rope but to chains [1.4].

a. Wire Rope Industry in Britain

References to helically wound wire rope, as known nowadays, were first found between the years of 1832 to 1837 in the Proceedings of the Institution of Mechanical Engineers (Charles Shelley, London 1862, pages 170-209, plate 57). Figures 1.1 shows the configurations of these ropes. The French-Style Selvage suspension bridge cable, with Selvage ship rigging was patented by Andrew Smith in 1835 [1.6] and "formed" wire rope was actually made by Smith and Binkes during that period at Grimsby. According to record[1.6], forty year after G.W. Binkes established his factory in Grimsby, there were more than thirty manufacturers producing wire rope in Britain. In 1874 alone, 36,692 tons of wire were exported (worth more than three-quarters of a million pounds). At that time, the wire ropes were closely related with bridge building, the mining industry and the shipbuilding industry. The early nineteenth century was the most flourishing period for the wire rope industry in Britain. There were more than 46 companies in business in 1914. However, the rope industry declined suddenly due to takeovers and amalgamations. British Ropes was formed during 1924 by the conglomeration of eight wire rope manufacturing companies. This organisation has continued to absorb small rope businesses since and has become the sole company that still manufactures a variety of ropes at the present time in Britain.

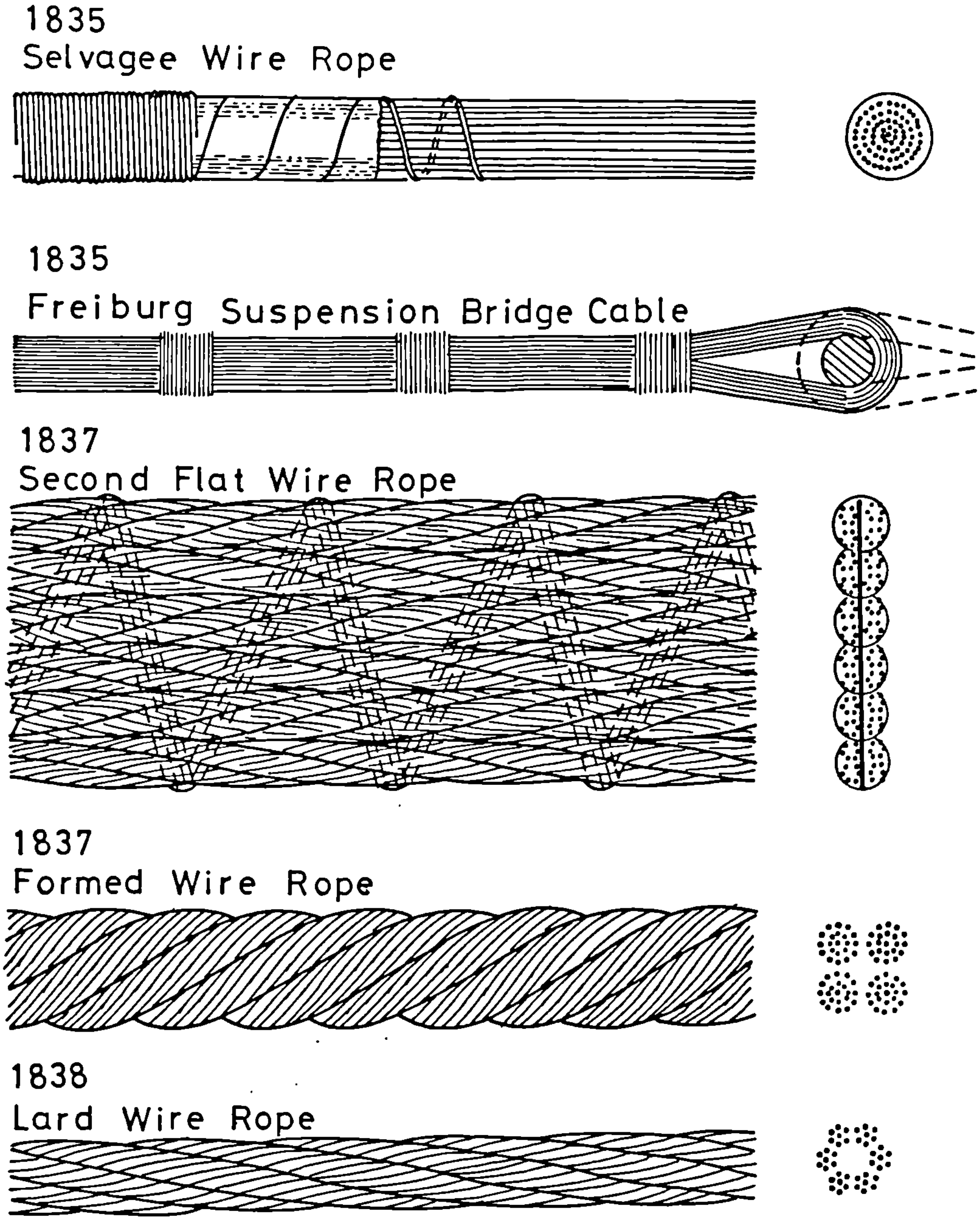

Figure 1·1
Construction Of Wire Rope By L.Gorden & R.S. Newall From Proceeding Of The Institution Mechanical Engineers Charles Shelley, London. 1862 Page 170 -209. Plate 57

Remark: Forstier-Walker [1.3] has detailed records on the history of wire rope industry in Great Britain from 1830 to 1952.

b. Wire Rope Industry In U.S.A.

The development of the wire rope industry in America [1.6] took place at more or less the same time as in Great Britain. The growth of this industry was essentially encouraged by coal (anthracite) mining and the construction of suspension bridges. The pioneers in this field were largely influenced by the European philosophy of wire rope and bridge building. Many of them actually went to Germany, France and Britain to study bridge design and the application of wire ropes in haulage and ropeways. The main reason was simply because there were no American colleges offering engineering degrees at that time.

In 1839, the first American wire rope patent was obtained by Isaac McCord. However, John Roebling was the most dominant figure in American wire rope history. He founded a wire rope company which bore his own name; and was a brilliant bridge engineer who built a most spectacular bridge across the gorge at Niagara Falls. Figure 1.2 is a schematic diagram which illustrate the appearance of his bridge. In fact, through the efforts of his three brilliant sons, his company was made highly successful after his death. Other impressive achievements through the use of wire rope were the invention of the cable car, steam shovels, draglines and passenger

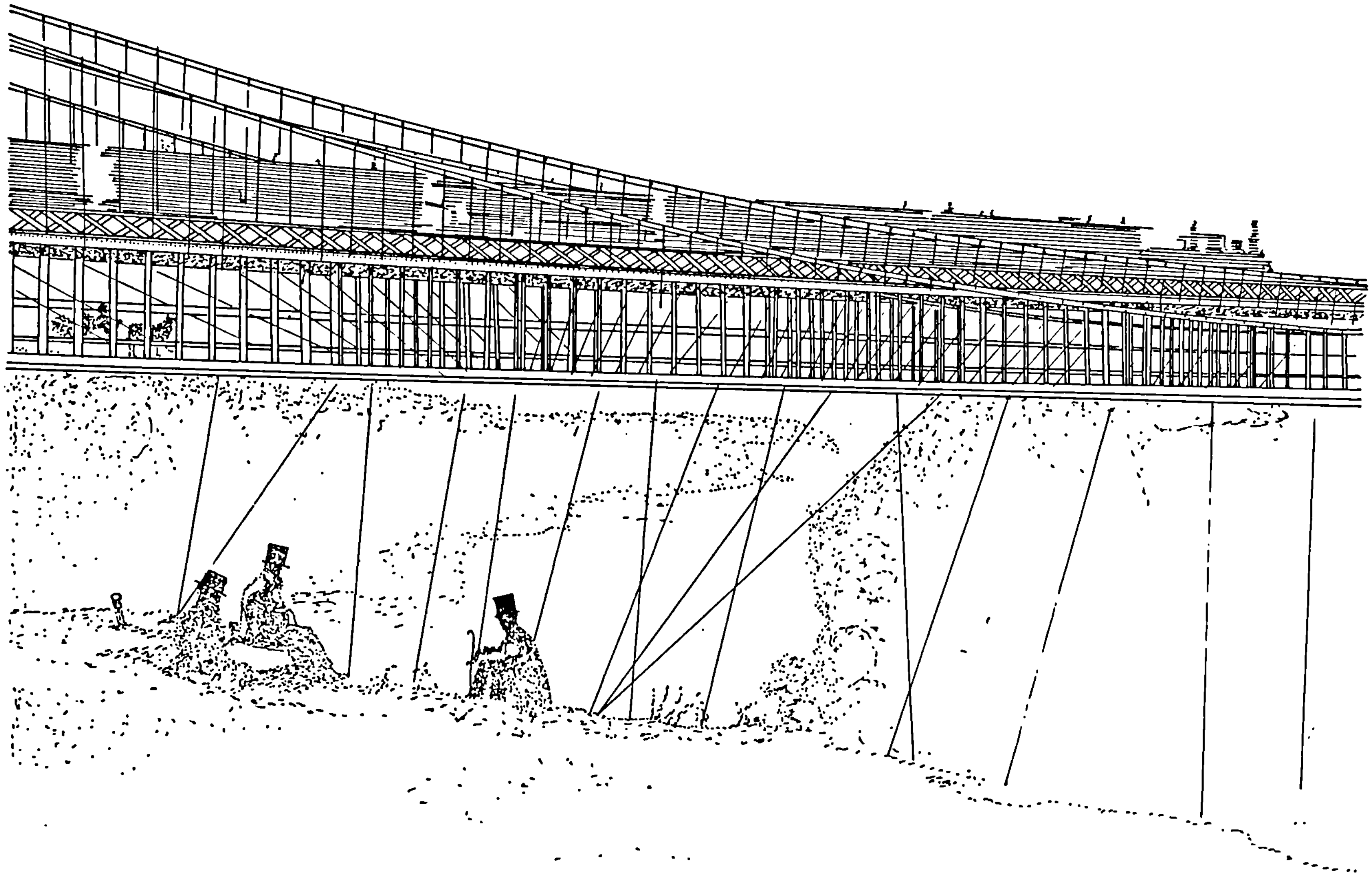

Suspension Bridge Across The Gorge At Niagara Falls

(Built By John Roebling In The Late 1850's Ref.1.6)

Figure 1·2

lifts in this period. Rope industry started to decline from the early 20th century. This was due to the enormous quantities of wire ropes imported from abroad at very low price which made it almost impossible for American producers to make an adequate profit. In the early 1970's the entire American consumption on 7-wire steel strands was 150,000 tons per year, yet, 100,000 tons were imported annually from Japan alone. During 1969-1979, Korean wire rope imports exceeded 45,000 tons to US and the Korean wire rope industry did not really exist in 1969. Within the same decade, American companies who manufactured 7-wire steel strands for use in prestressed concrete construction, in Hampton, Houston, Los Angeles, Muncy, Palmer, Roebling, San Francico, Trenton, Waukegan and Wilkes-Barre were all closed.

1.2-2 Development Of Wire rope And Rope Production Machines

Although the exact origin of helically wound wire rope is difficult to trace, this type of configuration was first found between the years 1832 to 1837.

a. Development Of Wire Ropes

In Britain, production of wire rope probably began in 1828. Many experimental iron wire ropes were produced by Andrew Smith and George Binks. They used conventional cordage machinery and fine iron wires to form such stranded iron rope. In 1839, Andrew Smith obtained his most significant patent (No. 8009 - September 20, 1839) which covered the use of malleable iron or other metal wire to make ropes. Three main types of ropes were produced by Binkes and Smith. Namely,

i. Parallel wire selvage cables.

ii. Helically laid "formed" ropes.

iii. Flat wire rope.

During that time, attempts were made to apply selvage rope and "formed" rope in mine hoists. But they soon found that Selvage ropes were found to be too stiff, and the iron wires broke up rapidly in "formed" rope due to fatigue.

Meanwhile, in 1834, a German mining official named Wilhem August Julius Albert discovered how to lay a wire rope together using relatively large iron wires. His first successful hand-made ropes were 3x4 construction. Figure 1.3 is a contemporary portrait of Wilhelm Albert. Figure 1.4 (a) is a schematic diagram of twisting wrenches for producing strands or ropes according to Albert's construction and Figure 1.4 (b) is a schematic representation of rope construction in Albert's time.

In 1835, Albert published all the details of his work which then stimulated widespread experimental studies and production. In 1837, Albert invented Lang's lay type of rope in Clausthal as shown in Figure 1.4 (b). The rope construction is known as Lang's lay because John Lang was successful in obtaining the patent in Britain forty years

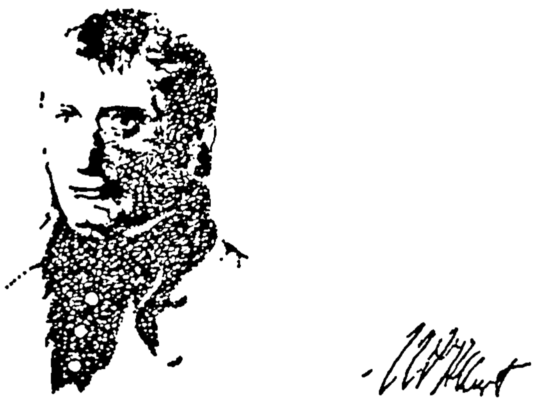

Contemporary Portrait Of Wilhelm August Julius Albert, Born 24 January 1787 In Hanover, Died 5 July 1846 At Clausthal (Ref. 1.11)

Figure 1·3

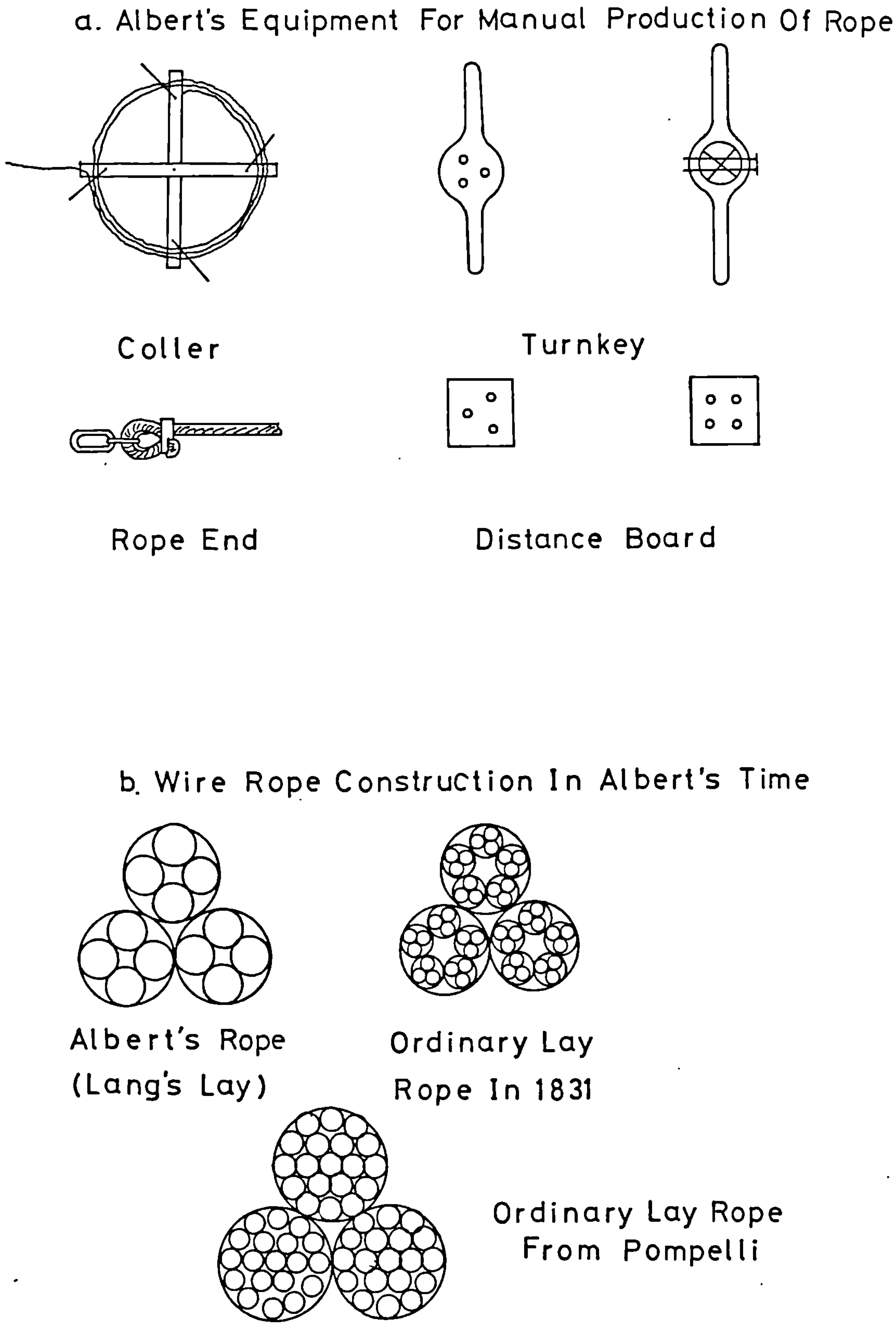

Figure 1.4

Albert's Equipment And Wire Rope In His Time later, even though this construction had been in use in Britain more than ten years before Lang's rope was patented. A few year later, a Scottish engineer, Lewis Gordon, visited Albert and obtained a comprehensive understanding of the techniques for producing these types of rope. Figure 1.1 is a schematic representation of the types of ropes that Gordon learnt to make from Albert. He then returned to Britain and founded a wire rope factory with his friend R.S. Newall. In the meantime, John Heimann also produced wire ropes similar to the German development. But they were sued by Andrew Smith who claimed the exclusive right to produce these types of ropes. Figure 1.5 is the schematic representation of Andrew Smith's rope patterns. However, Smith lost his suit later.

Thereafter, rope patterns were patented one by one, either in Britain or elsewhere. In 1884, the lock coil ropes, as shown in Figure 1.6 b, c, were patented by E.C. Batchelor. In 1886, the flat rope, as shown in Figure 1.6 d, was patented by H.R.I. Webeter. In 1888, the flattened stranded rope, as shown in Figure 1.6 e and f, was patented by Latch and Batchelor. In 1897, Lang's lay rope was successfully patented by John Lang. In 1909, the non-twist rope of elliptical strands, as shown in Figure 1.6 g and h, was patented by Newall and Skelton, and in 1910, a rope with inter-mixed elliptical and triangular strands, as shown in Figure 1.6 i, was patented by E.C. Batchelor.

In America, wire rope development was stimulated by totally different problems. In 1832, a law was passed by Congress

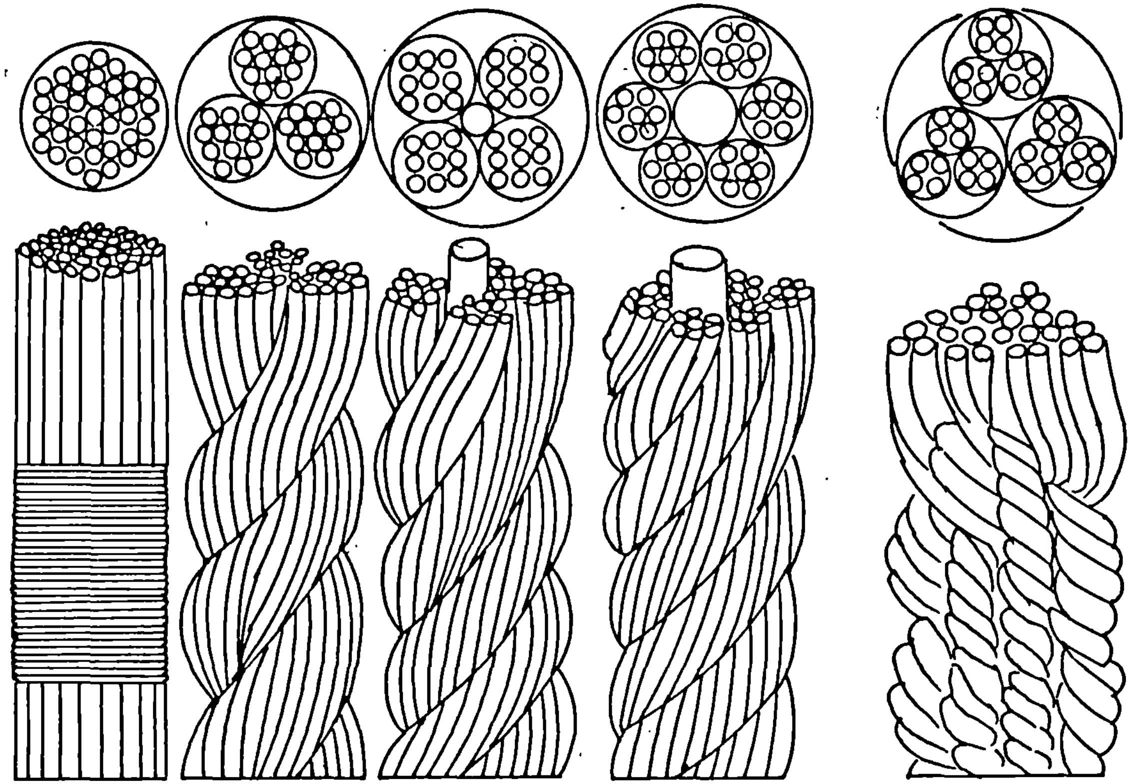

Figure 1·5

Construction Of Wire Rope Patented By Andrew Smith Mining Journal, London, Dec.,7, 1844 PP 422

a. b. c.

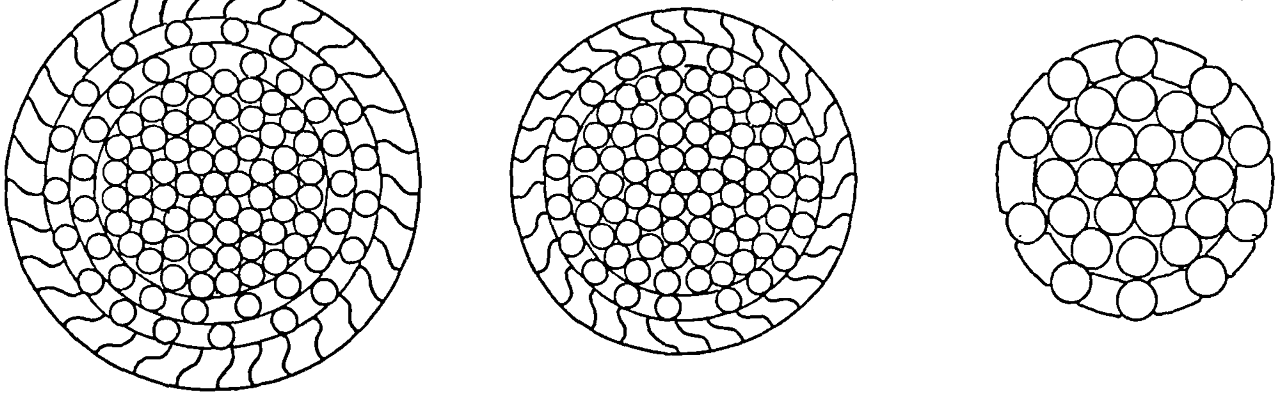

Variety Of Wire Ropes Which Had Been Patented By Rope Makers (Ref.1.1)

d.

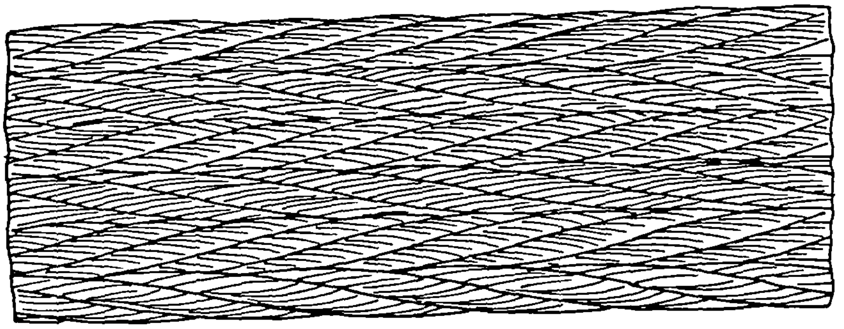

Figure 1·6

e. f. g.

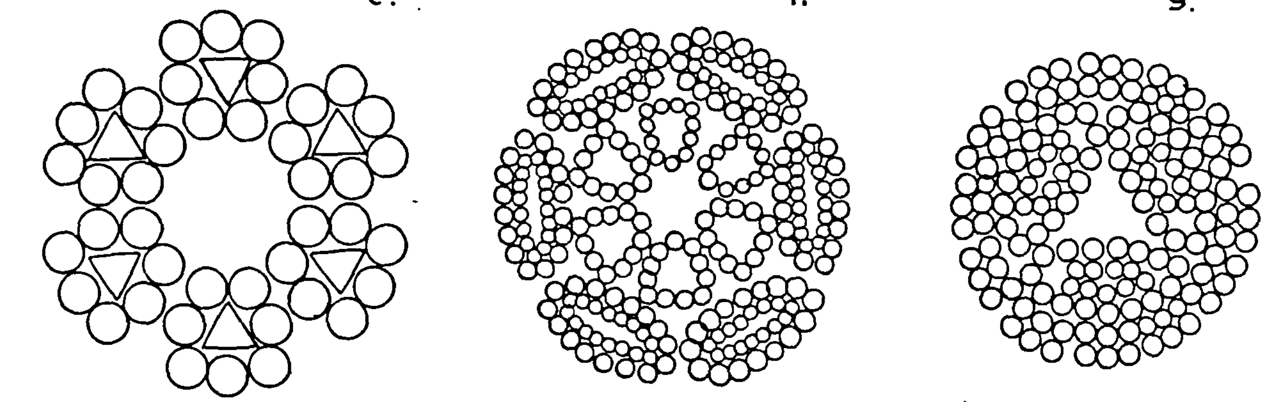

h. i j.

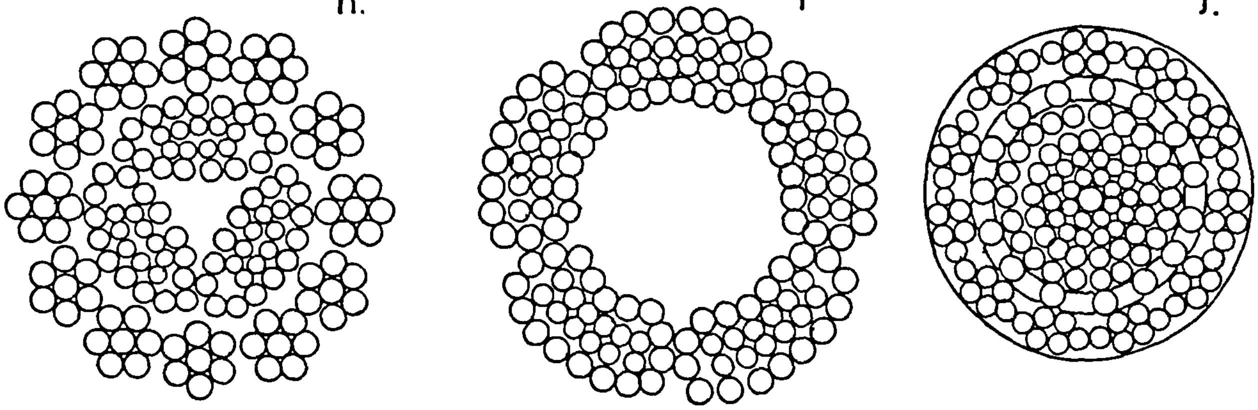

which stated that in existing paddle-wheel river boats with fibre cordage the tiller ropes had to be replaced by "metallic" ropes to achieve required safety standards. This law motivated American to the design of "metallic" cordage. In 1839, the first American wire rope was patented by Isaac McCord who proposed to make ropes from three small selvage cables twisted together like cordage. Since then, Americans developed a number of good rope types, such as the "three side" construction (which is now called "Warrington") patented by John Roebling in 1886, the "alternative lay" which was patented by Ferdinand Roebling in 1875, and the filler wire rope which was patented by Jame Stone in 1889. These types are still being used today. In 1921 Roebling covered a rope with metal band as shown in Figure 1.6 j.

b. Rope Production Machines

Wherever in Europe or in America, there were always three main objectives to be pursued in the wire rope industry. They were to:

i. improve the quality of wire used in rope manufacture.
ii. design better machines for production and
iii. further improve rope design.

After Albert's equipment for manual production of rope was successfully introduced in the Harz Mountains of Bavaria, as shown in Figure 1.4 (a). Various type of stranding machines were designed, such as a Wooden stranding machine designed by

Franz Wurm, as shown in Figure 1.7, a manually operated stranding machine designed by Westmeyer, a combined stranding and rope closing machine with rope transmission for relative movement of bobbins was developed by Westmeyer. Figure 1.8 is a schematic diagram of this machine which was patented by R.S. Newall in August 1840 in Dundee. The "tubular strander" which was designed by Andrew Smith and improved by his son in America, was the most important machine design for rope production. This design eventually became a universally applied tool in rope making all over the world. Figure 1.9 is a schematic drawing of the "tubular strander" which was patented by Andrew Smith in 1849 and improved by his son later.

1.2-3 Wire Rope Research

The present section is a brief review of wire rope research in both Germany and Britain.

a. Wire Rope Research in Germany

Although Albert was not the inventor of the wire rope, his efforts in promoting the application of wire rope on an extremely wide scale undoubtedly deserves credit. Albert published all the details of his work in 1835. His breakthrough in wire rope stimulated widespread experimental studies in Europe. However, intensive wire rope research was actually begun around 1860. This activity was initiated by Professor Reuleaux at the Technische Hochschule in Berlin.

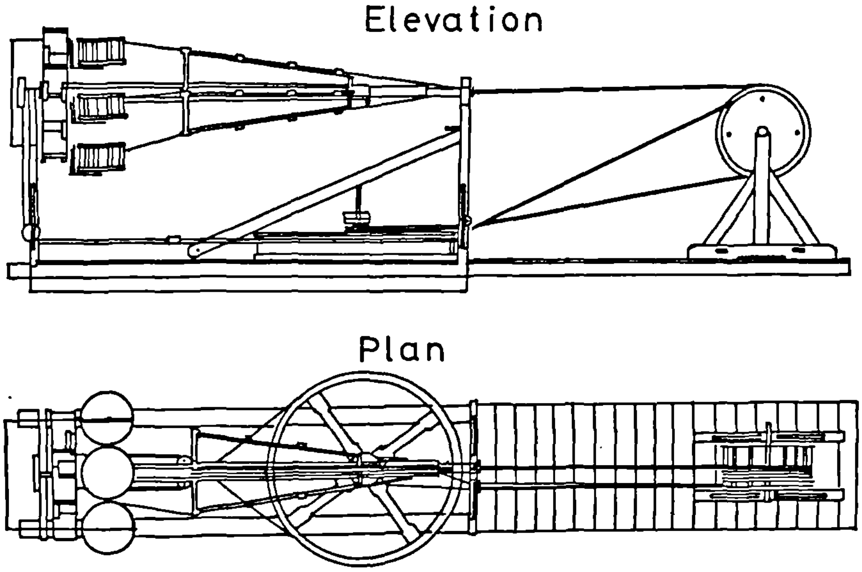

Figure 1·7

Wooden Stranding Machine For Rope Manufacture According To A Design By Wurm Of Vienna Ref.1.7

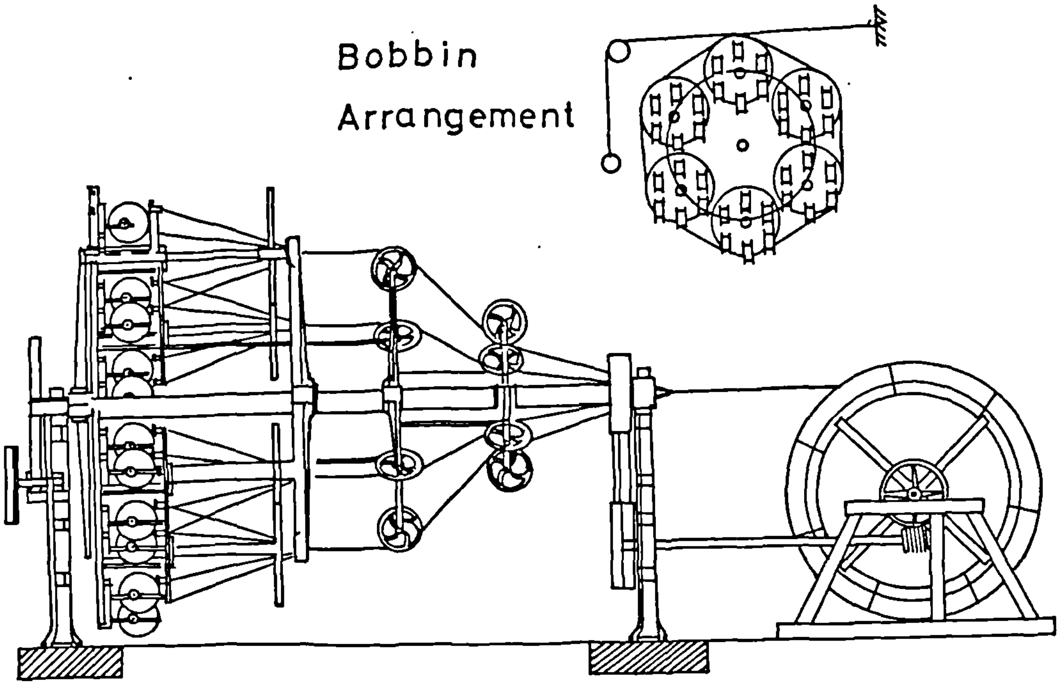

Figure 1·8

Combined Stranding & Closing Machine Ref. 1.7

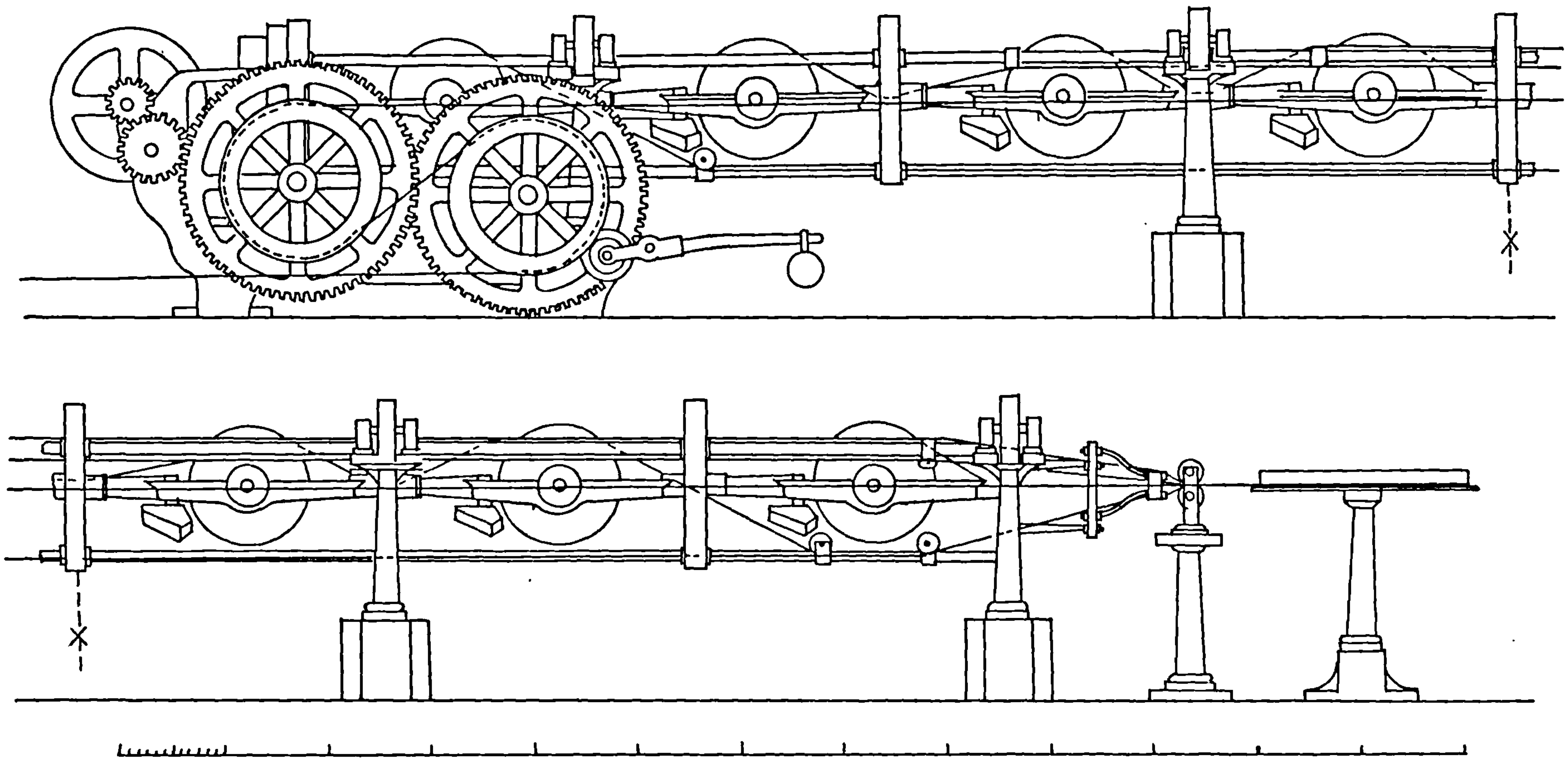

Figure 1·9

Tubular Strander Designed By Andrew Smith And Improved By His Son. From Rope Manufacture Proceedings Inst., ME 1862, Page 170, Plate 60

These works were carried on by several professors, but most of their research was done on small diameter rope for use in hoist and cranes. Tests on relatively large diameter wire rope such as those used for shaft haulage installations, were carried out at the Westphalian Mining Union-Rope testing Station in Bochum, founded in 1903, under the direction of Dr. Ing. Eh. Hermann Herbst (Seilprufstelle Bochum). From 1951 onwards, rope tests were still carried on at the Technische Hochschule of Karlsruhe. Wire rope tests are still carried on in Germany at present. These tests are essentially done on safety devices and driving sheaves in lift construction. Figure 1.10 illustrates some of the rope endurance test equipment from 1829-1927 in Germany.

b. Wire Rope Research In Britain

A considerable amount of experimental studies on wire ropes were undertaken in Britain, during the First World War, but extensive rope tests were actually started around 1920. Under the British Wire Rope Research Commission, these tests supervised by Scoble, were concentrated on wire ropes for use over pulleys. Five detailed reports between 1920 to 1930 were presented. In 1983 the Department of Energy commissioned the National Engineering Laboratory to undertake a survey to examine the published literature on the fatigue performance of large diameter wire ropes[9.14]. As a result of this survey the Department of Energy sponsored a short test programme which was carried out during the period 1984-85. The primary objective was to investigate the repeatability of the endurances of wire ropes of different diameter (40, 70 and 127 mm) but of the same general construction when subjected to fluctuating tensile loads of constant amplitude. It was observed during this study that the changes in rope stiffness and elongation which took place allowed one to distinguish between good fatigue test result from ones which failed resulting from the influence of the termination. A secondary objective was to evaluate available non-destructive testing techniques for assessing the condition of large diameter wire

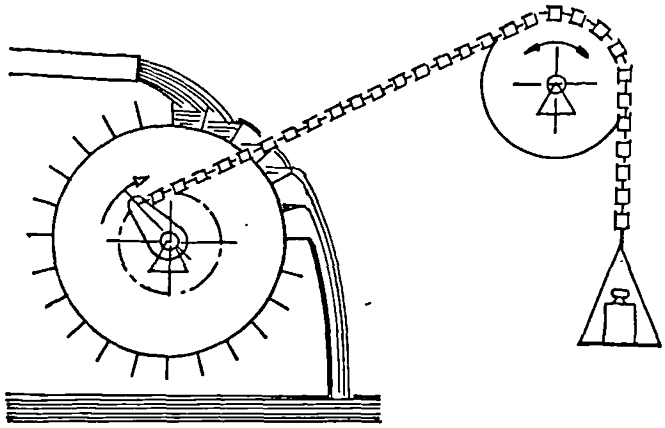

a. Chain Testing Machine Designed By Albert In 1829

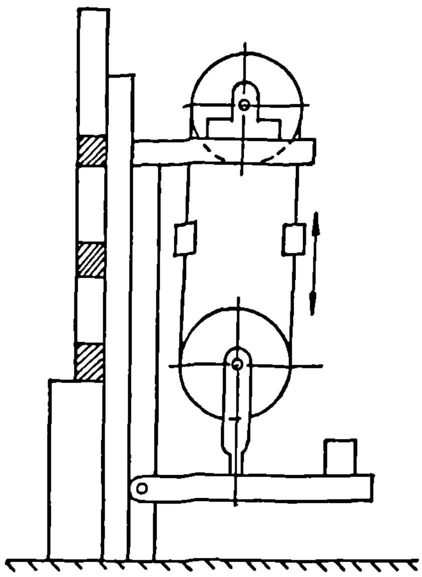

b. Bending Machine By Biggart 1890.

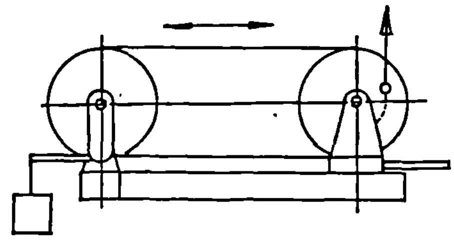

c. Bending Machine By Rudeloff 1893.

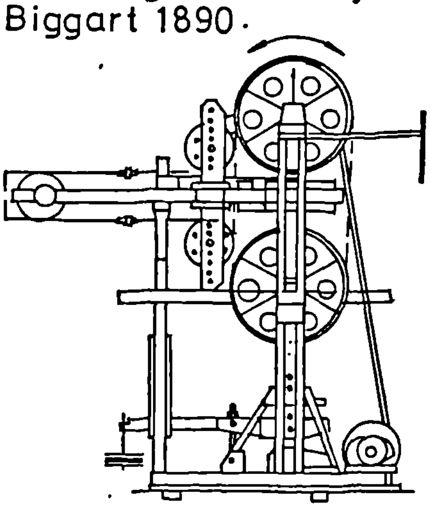

e. 60 KN Alternating Bending Machine By R. Woernle 1927

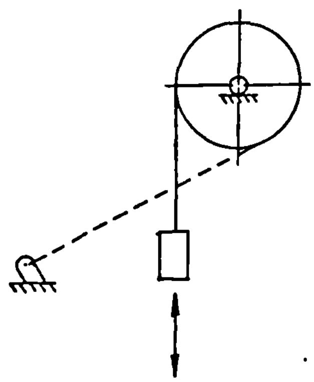

d. Testing Machine By Isaachaen 1909

Figure 1.10

Rope Endurance Testing (Ref. 1.11)

ropes. The results of this work has led to a number of publications (Ref. 4.7 and 4.8).

NEL is now the major participant in a collaborative Joint Industry Study which look into the fatigue behaviour of large diameter wire rope and strand used for mooring offshore structures. The objective and scope of the study which is covered in the original proposal by Potts and Chaplin[7.13], is to produce an experimental database on the fatigue performance of these products and develop a method for predicting the fatigue life of large diameter wire rope and strand based on reference S-N curves obtained for 40 mm diameter six strand rope.

In addition to this, NEL has actively pursued mathematical modelling of wire rope by sponsoring research students at Strathclyde University and allowing them to carry out their work at NEL. The author of this thesis is being one of the students.

This comprehensive approach to wire rope research, which has been developed over the last four years, has resulted in NEL being at the forefront of wire rope research.

Figure 1.11 and 1.12 illustrated the most advanced full scale endurance testing rigs equipped with modern data acquisition system for the large diameter wire ropes. The testing rig illustrated in Figure 1.12 is regarded as the world largest full scale multi-function large diameter wire rope bending-tension testing rig at the present time.

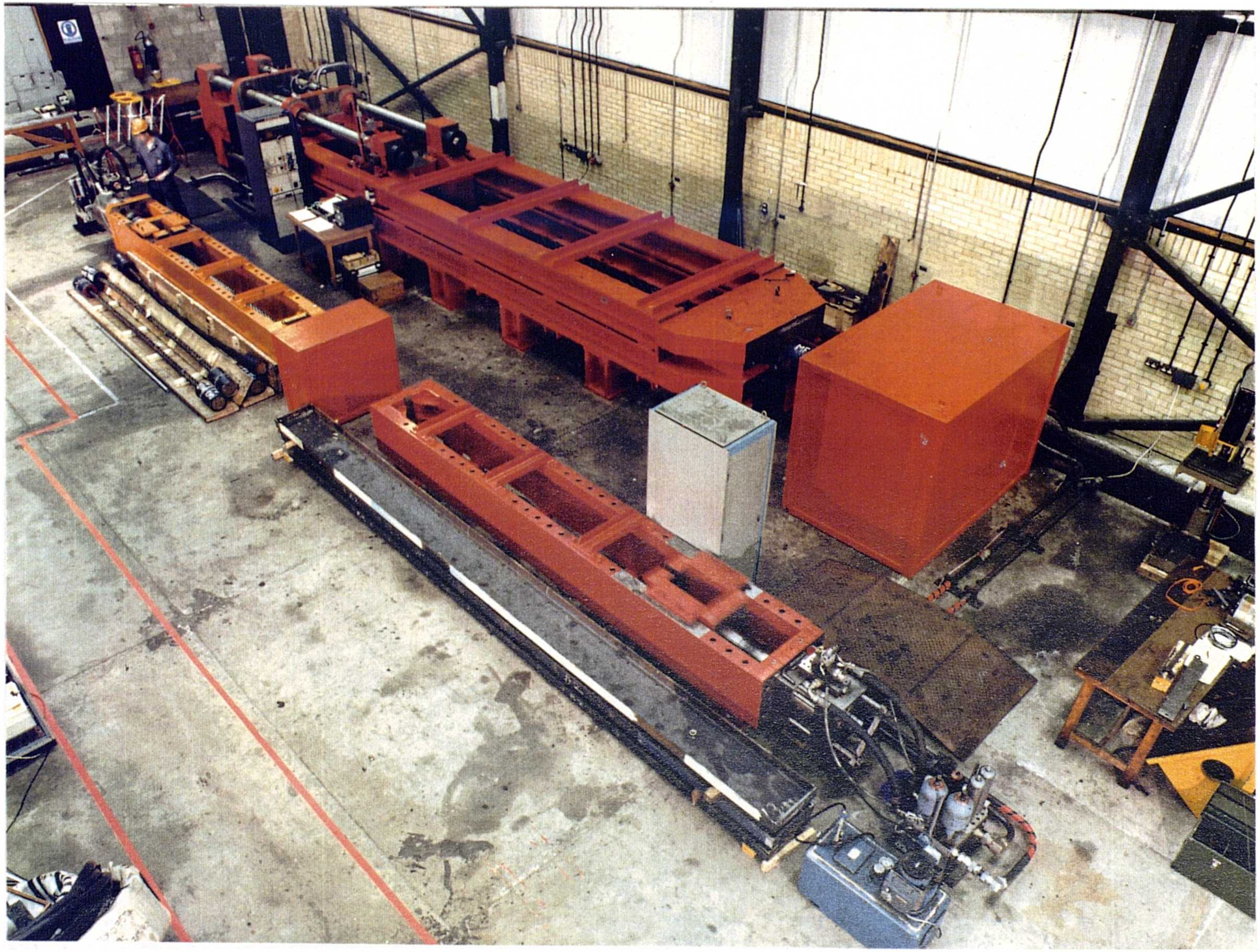

Figure 1·11

Tension–Tension Endurance Testing Machine Equipped In NEL

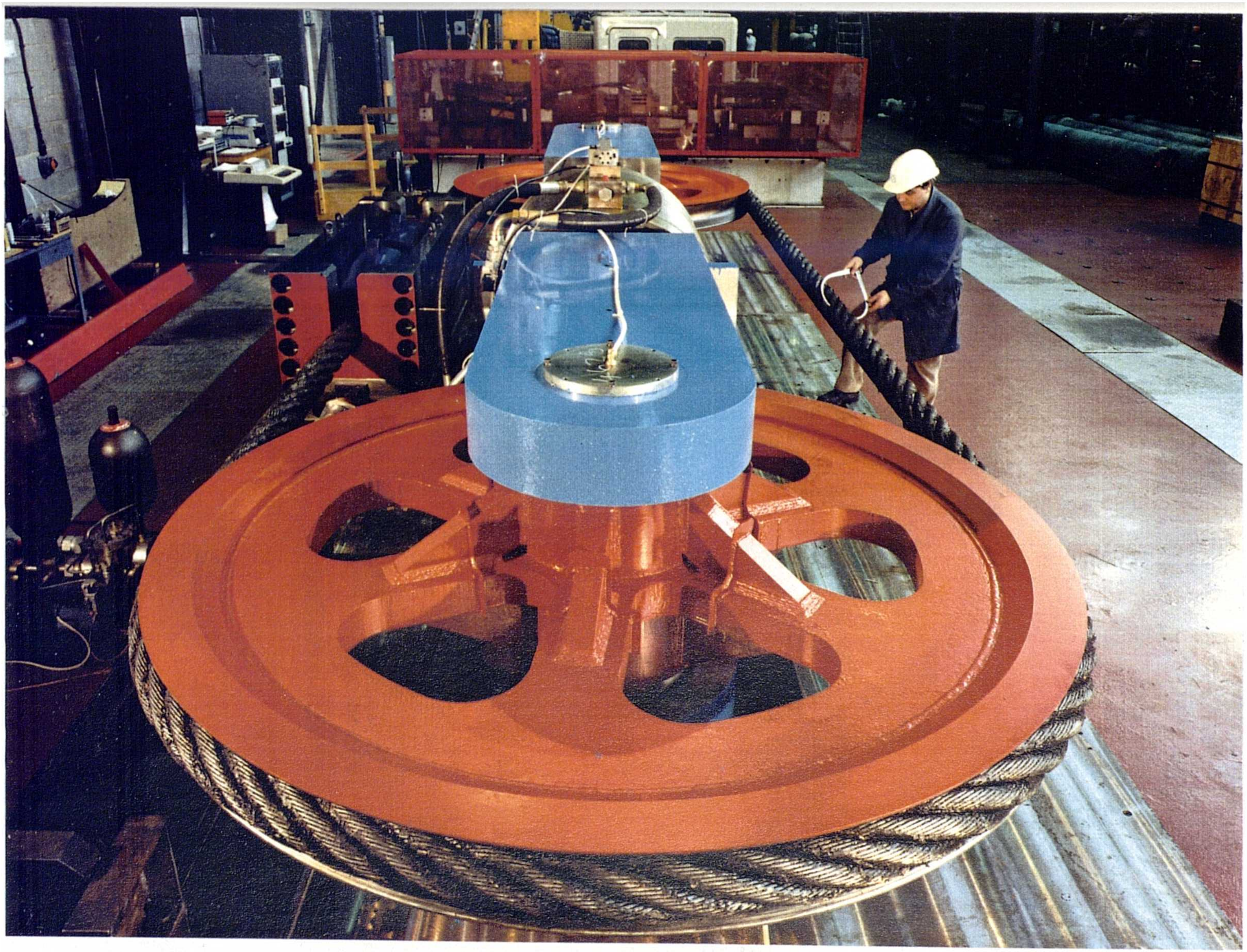

Bending-Tension Endurance Testing Machine Equipped In NEL

Figure 1·12

1.3 REVIEW OF THE MATHEMATICAL MODELLING OF STRANDS AND ROPES

In this section, a review is made of available information on the static response of wire strands and ropes published in various sources journals and theses. From this survey, it was found that theoretical works on wire rope have only emerged strongly in the last two decades. Most of the published works were essentially focused on the static mechanical responses of strands and ropes. Before the 1970's, Only a scattered number of papers were found. The prominent figure was Hruska. The literature review is divided into the following categories.

a. Work by Hruska and his followers.

b. Work by Costello, his fellow workers and his students.

c. Work by Machida, Huang, Knapp and miscellaneous works.

d. Geometry of strands and ropes.

1.3-1 Mathematical Modelling of Strand and Rope (Hruska, F.H. And Other Investigations)

H.M.Hall and F.H.Hruska can be regarded as pioneering rope modellers who attempted to find out the tensile stresses on a core wire and helical wires at different layers of a strand within a rope by using the "Strength of Material" approach.

Most of their published works are reviewed and summarized as follows:

In an analytical paper by Hall[2.1], attempt has been made to show that the tensile stress on the helical wires of outermost layer is greater than that of the helical wires of the inner layer within a strand subjected to tensile load. However, this analysis was proved to be wrong by Hruska.

Having been stimulated by Hall's work, Hruska[2.2 - 2.5] carried out a series of analytical studies on the mechanical behaviour of wires within strands and ropes. His contributions included work on:

a. Tensile stress ratio between core wire and helical wire,

b. Evaluation of radial force between wires at regions of contact,

c. Tangential force acting on helical wire and torque provoked at the rope termination and

d. Approximation of the cross section shape of a helical wire on a transverse section which is made through a strand or rope. A similar analytical approach is also found in Costello and Phillips' paper[2.2].

However, Hruska's work ignored friction and all helical wires within a rope were considered as single helical wires. In his analysis, attempt had been also made to model ropes with zero moment (ie unwinding moment) by using moment equilibrium and single helix geometry. This model ignores the fact that the majority of helical wires are double helical wires and that rope geometry will be changed as applied load changes. Besides, only the tensile component was considered to be acting on each of the wires.

Summary Remarks on Hruska's Stress Analysis of Wire Rope

Hruska's strength of materials approach used to study wire ropes have been relatively simple and almost entirely restricted to strands made up of single helical wires; since his model considered only the tensile component acting on the single helical wire. Furthermore, the double helix geometry, geometry of wire cross-section, many other internal components (such bending, twisting and shear components) have not been adequately considered. However, his concept, idea and approach were improved in the later studies by other investigators who considered force and moment equilibrium, extensional stress and strain on a core wire and single helical wire, displacement, helix geometry and friction. All these parameters, to some extent, have been explored by later investigators.

Hruska's approach applied by other investigators used in other areas, are briefly reviewed as follows:

Contact stresses in a 6 x 7 wire rope were investigated by Cress[2.6]. Based on Hruska's work and Hertzian contact theory from Seeley and Smith[9.12], three principal compressive stresses equations taken from Ref. 9.12 were written as functions of tensile load, single helix geometry and elastic properties of the material. However, the complicated contact geometry was idealised by parallel and cross cylinders with equal diameters.

Contact stresses analysis for a 6 x 7 wire rope, published in an article by Leissa[2.8], was similar to the work of Cress[2.6].

In response to Leissa's paper[2.8], an analysis of the critical stresses and mode of failure of a wire rope was made by Starkey and Cress[2.7]. It was a minor improvement to the earlier work of Cress and offered further analytical results based on Hertzian contact theory. The geometry of wires at the contact points was still idealised by the geometry of parallel and cross cylinders. In their study, they point out that the critical stresses occur between wires are at the crossover points between adjacent strands.

Bert and Stein[2.9] selected a more complex rope structure (6 x 37) for the contact force analysis. Additional improvement was made by introducing curvature geometry at the contact positions which were initially idealised by parallel and cross cylinder as shown in Cress and Leissa's works. They even showed that the calculated contact stress value was five times greater than the yield stress of the wire material.

Torque characteristics (ie unwinding moment) of wire ropes were studied by Gibson and others [2.10]. In their analysis, Hruska's approach for strands and ropes was still pursued. They pointed out that for six stranded ordinary lay rope, Lang's lay rope and fibre core ropes, the unwinding torque generated is linearly with respect to tensile load.

Hruska's analytical approach to the study of the mechanical behaviour of strands and ropes was summarized by Reensnyder[2.11].

Brief Summary Remarks On contact Stress Analysis

Hertzian contact stresses analysis and Hruska's strength of materials approach were applied throughout Cress, Leissa and others analysis. Two cross and parallel straight cylinders with equal diameter were used to simulate the contact feature between the core wire and helical wire of the 6/1 strand and the core strand & helical strand of the 6 x 7 wire rope. However, this analysis did not consider the relationships between the R/r ratio and the admissible helix angle of helical wires within a layer of a strand (see chapter 6). Besides, they did not consider the influence of double helix angle and the curvature of double helical wires at the contact point used in the contact stress analysis of the 6 x 7 wire rope.

Overall Remarks On Hruska's Approach And His Followers' On Wire Rope Analysis

Hruska's strength of material approach used to solve the wire rope problem (ie straight strand) is thought to be original and is an approximate method to evaluate forces and torque components acting on the helical wires and helical strands. However, this approach has a number of limitations and ignored the following mechanical and geometrical influences on the strand and rope under external loading:

a. The geometrical relationships between the core and the helical wire i.e. the spatial configuration of strand and R/r ratio. For details, see Chapter Six of this thesis.

b. The mechanical interactions between adjacent wires and strands. For example, friction, wear secondary bending and twisting.

c. The change in helical geometry resulting from the incremental change in external applied load. For instance, change in curvature, torsion and helix angle.

d. Mechanical components other than tension. For example, shear force, bending and twisting moment acting on the single helical wire.

e. Geometry of double helical wires in a rope.

Hruska's approach was soon applied to deal with the contact problem in the 6/1 strand and 6 x 7 wire rope by Cress, Leissa, Starkey, Bert and Stein in the same decade. Nevertheless, the parallel cylinder, cross cylinder and the improved curvature method did not consider the 3 dimensional interaction between wires at the contact location which may be important in the actual situation, depend upon the strand and rope geometry. For instance, they did not consider:

a. The three dimensional slippage, friction, wear and thermal effects.
b. The influence of galvanized coating.
c. The influence of mechanical interactions other than radial force.
d. The geometry at the contact locations. For example, the double helix angle and curvature.
e. The influence of lubricants.
f. The spatial relationship between the radius of core wire, radius of helical wire, helix angle and the number of helical wires per layer.

Remarks:

The approaches adopted by Cress, Leissa, Strakey, Bert and Stein to the contact problem were basically similar with the exception that Bert and Stein considered the curvature of wire at the contact point of wires.

The improved mathematical method of Gibson, Cress, Kaufman and Gallant to deal with the unwinding torque of wire rope under tension, was the minor modification of Hruska's approach.

1.3-2 Mathematical and Theoretical Study of Strand and Rope (By Costello, His Fellow Workers and His Students)

Analytical and mathematical studies on strands and ropes (American type of wire rope, eg Seale rope) was actually stimulated during the dramatic decline of the American wire rope industry in the early 1970's. Detailed strand (6/1 strand without core wire) modelling work was published by S. Machida and A.J. Durelli . Since then, a series of joint academic papers on mathematical modelling of strands and ropes emerged in State and were chiefly published by G.A. Costello, his fellow workers and students[3.1 - 3.25] at the University of Illinois; the static and dynamic response of 6/1 strand and 6 x 19 construction of Seale rope with IWRC were their main interests.

In their earlier analysis, a more fundamental approach was taken to model the responses of a helical wire within a strand, in which the individual wires of a 6/1 strand were modelled by initially thin curved rods subject to internal tension, bending moment, twisting moment, shear force and radial force per unit length of the helical wire. The nonlinear displacements and the axial strain of the helical wire were derived from the "developed triangle" of a deformed helix. The nonlinear displacement equations were then linearized by dropping the 2nd and higher order differential terms. Eventually, a linearized model was developed for the evaluation of the static response of the helical wire within a strand. Frictional effects were not introduced until the early 80's when Buston[3.11] one of the Costello's PhD students introduced frictional effects into a 6/1 strand model for the analysis of strand mechanical responses. Buston also studied the dynamic response of alike strand.

Later, the rod theory and single helix strand model were applied to study the mechanical responses of Seale rope. For instance, Velinsky[3.18 & 3.19] selected a more complex rope construction to study. It was a structural modelling of an 6x19 type of Seale rope either with a fibre core or with an IWRC, by introducing an effective fibre core radius and effective Poisson's ratio respectively. A survey of their literature from the early 1970's to the mid 1980's has been collected in the appendix of this thesis.

Comments on Costello and His Fellow Worker's Theory for Modelling of Strand and Rope.

Within the last decade, a series of joint papers by Costello and his fellow workers emerged in the United States. In their earlier works, fundamental approach was taken in modelling the radial force between wires in contact and the ratio of radius of helical wire to the wire helical radius of strand as functions of number of helical wires per layer and helix angle. However, similar work had been published by Hruska in "Geometrie im Drahtseil". The similarity found in their works are as shown below:

In Costello's paper, 1974

$$\frac{r_1}{R} = \{ 1 + \frac{\tan^2 (\pi/2 - \pi/n)}{\sin^2 \alpha'} \}^{1/2} \qquad (1.2.3)$$

In Hruska's paper, 1958

$$\frac{D'}{d} = \{ 1 + \frac{\cot^2 (180/n)}{\cos^2 \alpha} \}^{1/2} \qquad (1.2.4)$$

There is no difference between these two equations, since $\alpha' = 90 - \alpha$.

Kirchhoff's naturally curved rod theory was also introduced to solve the static mechanical response of single helical wires within strand or single helical strands within a rope. This concept was not new since similar concept had been proposed by Hansom[6.2]; in a PhD thesis called "*The Mechanics Of Locked Coil Ropes*", published in 1949, at the University of Birmingham. However, Hansom himself did not actually apply rod theory to analyze his rope problem, whereas, Costello and his fellow workers actually used the rod theory to analyze the static response of strands and ropes.

In a paper called "*Simplified Bending Theory For Wire Rope*", Costello and others showed that the core wire was separated from the helical wires within a strand. This implies that the importance of curvature effect influencing the spatial configuration of a strand and a rope has not been appreciated. As long as the helical wires are laid around a core wire, each layer of helical wires must always touching the layer immediate beneath. Because, there is an admissible value which prevents helical wires jamming each other in each layer within a strand, see Chapter six.

For static strand modelling, the rod theory with the frictionless assumption, proposed by Costello and others, is considered as a rational approach for the analysis of the mechanical responses of strand and helical wires subjected to static tensile load. For a strand with fixed ends subject to quasi-static tensile loading, the deformation of the strand is very small. Although their model is frictionless model. There are almost no significant differences between full-friction and full-slip (ie frictionless) strand model provided the helix angle of the wires is large enough (eg 80 degrees).

For ropes modelling, Costello's and others' approach use strand approach and rope theory to analyze some global mechanical behaviour of rope (eg effective stiffness). However, single helix strand approach can not used to analyze stresses and strains on double helical wires since geometry of single helix differ from that of the double helix. Besides, the mechanical interactions which are very significant in relation with the geometrical configuration of rope, were not be fully appreciated in their theory.

1.3-3 Mathematical Modelling Of Strands And Cables By Other Investigators

In addition to Hruska's and Costello's approach, several other strand and cable investigators also understood the importance of single helix geometry in governing the static response of strands and cables under tensile and twisting load. The following is a review of their work.

Machida and Durelli[4.1] proposed an explicit mathematical model to analyse the static response of a 6/1 strand. Strength of materials approach was used and change of helix geometry as the result of loading was considered. Component forces and moments acting on each wire were summed up to the direction of applied loads. Four termination conditions were considered, namely fixed ends, free ends, twisting and combined loads (tension and twisting). However, shear force, mechanical interaction (include friction) and spatial configuration* of helical wires within a strand were ignored. It is because they showed that the diameter of core wire equals the diameter of helical wires in a 6/1 strand.

Note:

Spatial configuration of strand* is relating to the circumferential space of strand core occupying by the helical wires that laid around it. This geometrical configuration is closely related with the helix angle, number of wires per layer, helical radius and radius of helical wire within a strand.

Nowak[4.2] dealt specifically with core wire strain, pressure acting on cable core, normal and shear stress provoked in any layer of helical wire in an electro-mechanical cable. Nowak also showed that if a transverse section was made through a strand, the section of a helical wire is a "kidney shaped" section.

Knapp[4.3 and 4.5] specialized in the mechanical behaviour of helically armored cable. In his earlier work, linearized and non-linear analytical models for cable subjected to tension were also proposed. Knapp's analytical approaches were quite similar to those of Machida. However, improvements were made to deal specially with the cable problems. In his latest work[4.6], the analytical models dealing with the bending of cable over sheaves were proposed. Frictionless and full-friction conditions were considered. Analytical results were then compared with experimental results and good agreement was claimed.

Like Costello and others, Huang[4.4] also made use of rod theory in the analytical study of static response of a 6/1 strand. Inter-wires friction was considered in his work. However, he did not seem to appreciate the significance of the spatial configuration of the strand; the author does not agree with Huang's conclusion that if the central core and the surrounding wires were made of the same material, the extension of the strand always caused a separation between core wire and helical wires.

1.3-4 Helix Geometry and Sectional Geometry of Helical Wires in Rounded Stranded Rope

The term '*helix geometry*' describes the three dimensional coordinates of the centroidal axis of a helical wire. The term '*sectional geometry*' describes a mathematical means to determine the cross sectional shape of a helical wire as a function of helix angle, number of helical wires per layer and the ratio of helical radius to the radius of the helical wire. Complete and comprehensive studies of these aspects are still scarce. This section provides a review of available literature.

Until recently mathematical models used to study wire ropes have been relatively simple and entirely restricted to strand made up of single helical wires. This is simply because the influence of the rope geometrical pattern are not known and the understanding of the geometrical properties of double helical wire are limited. Furthermore, the geometry of wire cross-sections and its significance has not been adequately considered.

A relatively small amount of work has been published on the geometry of single and double helices in ordinary lay rope. Despite the fact that wires in a rope may be triple helices, triple helix geometry has not previously been considered.

Stein and Bert [5.1] considered double helical wire in an ordinary lay rope. They presented the coordinate equations and the curvature equation for this helix. However, the derivations given were very brief.

Karamchetty [5.2] attempted a study on the geometry of double helical wires. However, his equations do not agree either with these of Stein and Bert [5.1] or these presented in Chapter 4 of this thesis. For example, it should be possible to obtain the equations for Lang's lay from the equations of ordinary lay simply by reversing the direction of the wire rotational coordinate. This is not so for equations presented by Karamchetty. Indeed, Karamchetty's equations do not distinguish between Lang's lay and ordinary lay at all. Karamchetty [5.3] went on further to calculate the number of contact points in a rope by using his previous geometrical model for double helical wire in a rope.

The papers by Wiek [5.5] dealt mainly with the calculation of the radius of curvature of a single helical wire bent over a sheave. His work on double helical wires is restricted to the degenerate case of a strand bent into a circular arc.

Lee and other [5.9] carried out a more comprehensive study into rope geometry. They considered, for example, radii of curvature and torsion for the constituent wires when strand or rope is bent around a sheave or wound around a drum.

Although work has been done on the approximation of the cross sectional shape of helical wires by an ellipse, for example by Costello and Huang, the influences of the spatial configuration of strands have not been fully appreciated. The "kidney shaped" helical wire section was first published in Nowak's paper[4.2]. Kunoh and Leech [5.4] went further: They explained that the "kidney shaped" wire section is the result of curvature effect of a single helical wire.

1.4 Experimental Study Of Wire Rope And Strand

The complicated construction of wire rope and strand imposes enormous difficulties with respect to the experimental study of the mechanical responses, mechanical interactions, stress and strain variations and the behaviour of wires within a rope. As a result, most experimental studies of wire ropes are confined to the macroscopic behaviour of strands and ropes. Comprehensive experimental study of mechanical responses, mechanical interactions, stresses and strains variation on individual wires have not yet been considered adequately. However, some available wire rope experimental literature (quantitative or qualitative) relevant to the present study is briefly reviewed. The work can be divided geographically into the following categories:

a. Experimental and mathematical study of wire rope and strand in Britain.

b. Experimental study on wire ropes and strand outside Britain.

1.4-1 Mathematical Modelling And Experimental Work On Wire Ropes And Strands In Britain

In this section, the review is particularly concerned with the literature on mathematical modelling and experimental study of strand and rope in Britain from 1948 to 1987.

Matheson[6.1] and Hansom[6.2] were the earliest investigators in connection with experimental and mathematical study of the static response of locked coil rope (ie strand). They were particularly interested in the tensile and rotation characteristics of lock coiled strands. The strength of material approach was employed by Matheson. However, the locked coil strand was considered as an indeterminate structure by Hansom. The naturally curved rod theory for the analysis of the static response of helical wire within a locked coil strand was first introduced by Hansom's in his thesis. Simultaneous equations were developed to deal with load sharing amongst wire layers in the strand. Experimental and mathematical results were then compared and the discrepancy was noted. He then concluded that the discrepancy was due to the initial looseness of the strand (also defined as constructional displacement as shown in Appendix) and the elasticity of the core wire as a foundation.

An experimental study on the torsional properties (ie static response on twisting) of three and seven strand rope (ie 3 helical wire strand and 6/1 strand) was carried out by Slight[6.3]. A simple mathematical model based on the open coil spring theory was introduced for the study of the 3 helical wires strand and 6/1 strand. The analytical calculations were then compared with the results obtained from the experiment.

Experimental study on the tensile stress on a core wire and helical wires within a 6/1 strand was conducted by Martin and Packard [6.4]. Electrical strain gauges and extensometer were used to measure both the strains on the surface of the wires and the overall extension of the strand. Results were then compared with Hruska's analytical approach for strands and agreement was claimed.

Inter-wire slippage, contact force, hysteresis and fatigue properties of large diameter multi-layer structural strand were examined by Hobbs and Raoof[6.6 and 6.7]. Both experimental and analytical methods were used in their study. In Raoof's strand modelling, each layer of wires was considered as a concentric orthotropic sheet. Full friction and full slip assumptions were made in this model. Experimental results on hysteresis, wire slippage and wire stress were claimed to be in substantial agreement with the model.

In the same time as Raoof, Utting and Jones[6.8 & 6.10] also developed their own model of the static response of a 6/1 strand. They also made use of rod theory. Friction and flattening effects due to contact force were considered. They developed their own testing rig to study the stresses and load-extension characteristics of a 6/1 strand. Experimental results were then compared with analytical calculations obtained from their model and other modellers; includes Machida, Velinsky and Matheson.

In other areas, Casey[6.9] successful employed acoustic emission technique to monitor the reliability of wire rope during the service life of the rope.

A plastic collapse model for 6/1 strand has been developed by Jones and Christodoulides[6.5] based on the classical upper and lower bound theorems of plasticity. They assumed that the core wire of the strand was inextensible and the wires of outer layer were made of perfectly plastic material. Hill and Siebel's yield criterion was applied throughout the analysis.

1.4-2 Experimental Work On Strand And Ropes Outside Britain

In this section, some interesting experimental work on wire rope are also briefly reviewed for the purpose of completeness. They are presented in the following.

Dong and Steidel[7.2] attempted to study the contact stresses distribution between each layers of wires within a strand. A photo-elastic cable model was clamped laterally. The normal contact stress distributed between inter-wires within the strand model were obtained by means of stress freezing photo-elastic technique. Experimental results were then compared with the analytical calculations obtained from the Hertz contact stress analysis for two crossover cylinders. Agreement was claimed.

Vanderceldt and others[7.4] studied the mechanical properties of cables (ie strands) under monotonic tensile test, properties such as equivalent elastic modulus of cable, effective Poisson's ratio and total input energy required to cause failure of a strand. The acoustic emission provoked from the breakage of a wire within a strand was also studied.

Durelli and others[7.5 & 7.6] conducted a series of tests on a epoxy oversized strand model and steel wire strand; ie 6/1 strand construction. Strains and responses of wires in the strand resulting from axial and torsion displacements applied to the models were studied by means of brittle lacquer coating, electrical resistance strain gauge and extensometer techniques. The extension and rotation between terminations were recorded under fixed end and free end condition. Results were then compared with Machida's strand theory and agreement was also claimed.

Wiek[7.7, 7.10 & 7.11] reported experimental studies on the surface strain of cover wires of different ropes. Strain gauges were mounted on the surface of the wires in both Lang's lay and ordinary lay ropes. He pointed out that for nominally identical wires on both ropes stresses found to be more uneven in the case of Lang's lay. As a consequence, he doubted that Lang's lay rope has greater endurance than ordinary lay rope.

Nesterov[7.1] examined the load shared by each layer of strands in a rope. The rope was loaded to a predetermined extension. Both tensile load and resisting torque were recorded and followed by cutting away the outer layer strands. The final tensile load and resisting torque were then recorded again. The difference between the initial and final load carried by the rope is the load shared by the strands layer.

Hankus[7.8 - 7.10] reported tests on 35 mining ropes or various diameters and constructions. Various rope properties were published, eg torque generated by the rope under tension.

Gibson and others[7.3] made use of an electrical strain gauge load cell to monitor tensile tests on a Lang's lay rope. The rope was loaded to 60 % of its breakage strength. Agreement between experiment results and analytical method (Hruska's method) was claimed to be within 2 %.

Summary Remarks on Experimental Studies of Wire Rope

The preceding experimental studies resulted in some qualitative understanding on the mechanical behaviour of wire ropes. Conventional methods were normally used throughout experimental tests, (for example, electrical strain gauge, load cell methods, Photo-elastic technique and extensometry). However, these methods have confined applications because of the complicated structure of a rope, (cf to chapter three).

In order to understanding the interactive mechanical behaviour within a rope. Future experimental studies should aim to separate parameters from the influences of mechanical responses and mechanical interactions within a rope. Hence, improvement of experimental techniques are essential.

1.5 Attachments and Termination of Wire Rope and Strand

End terminations for wire rope installations are of the greatest importance to safety and transmission of the load to the rope. It is commonly realised that even properly made and well installed terminations will develop less strength than the full strength of the rope and strand themselves. This sub-section gives a brief review on the study of rope terminations.

Christen and Hilgers[8.1-8.2] described detailed procedures for securing a rope termination to the end attachment. The former investigator suggested that hooking over the round wires at the rope termination will increase the effectiveness of wires gripping in the attachments. However, the latter investigator did not agree this; he suggested that the strength of a wire will be reduced by 4 to 6 % if the wire is bent more than 90 degrees.

Myers[8.3] discussed a wide range of end attachments for wire ropes, He recommended that swaged fittings are more effective with respect to resistance to fatigue.

Gathman[8.4] even went further, he reported 800 laboratory tests on resin attachments for wire ropes. He suggested that resin-poured sockets are more durable than zinc poured sockets on 7/8" diameter wire rope under fatigue test at moderate loads. Besides, the penetration of resin was found to be better than zinc.

A test programme was conducted by Matanzo and Metcalf[8.6]. In order to determine the efficiency of rope terminations, nine different types of wire rope terminations were tested under static tensile condition.

Dodd[8.5] discussed the development of work on resin socket. He pointed out that the major restraining force on a rope termination is the wedging action within a socket, not the bounding force of the filling material. He then listed number of advantages of resin over zinc in many applications.

Chaplin and Sharman[8.7] discussed the gripping characteristics of resin sockets. They argued that the gripping mechanism depends initially on the adhesion between the surface of wires and solidified resin.

Utting[6.8 and 8.6] in his PhD thesis, presented the results of strand resin termination pull out from end attachments for 6/1 strand. He then published work on the mathematical study of stresses in wires near termination.

Summary Remarks On The Rope Termination

Investigations on rope terminations suggested that the gripping efficiency between rope termination and end attachment depends on both the wedging action and the adhesion between wires and the filling media (eg resin or zinc).

1.6 OTHER STUDY ON ROPES

There is a wide range of literature on other aspects of wire rope studies eg fatigue performance tests, non-destructive tests, inspections, discard criteria and general applications. However, these subjects are outside the scope of this study and will not be covered in this review.

TABLE 1.1

SOME HISTORICAL EVENTS IN WIRE ROPE DEVELOPMENT

YEAR	DESCRIPTION OF EVENTS	NAMES & VENUES
700B.C.S	METALLIC COPPER WIRE DISCOVERED	RUINS OF NINEVAH
1452 - 1519 A.D.	WIRE ROPE WAS FIRMLY FOUND IN THE TECHNICAL BOOK	LEONARD DA VINCI
1500 A.D.	MECHANISED WIRE PRODUCTION ACCESSORIES	LEONARD DA VINCI
1816	1ST WIRE ROPE USED IN U.S.A. AS EMERGENCY FOOT BRIDGE	BUILT BY JOSIAH WHITE
1824	LARGE SCALE TESTS ON WIRE ROPE SUSPENSION BRIDGE	CARRIED OUT IN AUSTRIA
1830	1ST AMERICAN SUSPENSION BRIDGE DESIGNED	BUILT BY CHARLES ELLET
1832	1ST HELICOID WIRE ROPE APPEARED	UNKNOWN
1834	BEGINNING OF WIRE ROPE TESTS	BY ALBERT,W.A.T. GERMAN REMARK: THE FIRST ONE WHO PRODUCED ROPE IN LANG LAY (ALBERT LAY)
1835	FIRST VESSEL (MARSHALL OF GRIMSBY) RIGGED WITH WIRE ROPE	WOOLWICH DOCKYARD
1840	1ST WIRE ROPE MAKING MACHINE PATENTED	BY NEWALL (ENGLISH)
1860	INTENSIVE WIRE ROPE RESEARCHES BEGAN IN GERMANY	BY PROFESSOR REULEAUX AT THE TECHNICAL SCHOOL OF BERLIN
1864	TRANS-ATLANTIC CABLE LAID	GREAT EASTERN
1875-1879	WIRE ROPE WAS DEVELOPED INTO ALTERNATIVE LAY & LANG LAY	FERDINARD ROEBLING AND JOHN LANG RESP.

CONT...TABLE 1.1

1884	LOCK COIL ROPE WAS PATENTED	BATCHELOR,E.C.
1886	FLAT ROPE INTRODUCED	WEBSTER,H.R.I.
1888	FLATTENED ROPE WAS PATENTED	LATCH AND BATCHELOR
1890	IDEA IF FILLING THE INTER-STITIAL SPACES WITH FINE FINE WIRE WAS CONCEIVED	STONE,J.B.
1909	NON-TWIST ROPE OF ELLIPT-ICAL STRAND WAS PATENTED	NEWAL AND SKELTON (ENGLISH)
1910	A ROPE WITH INTERMIXED ELLIPTICAL STRAND APPEARED	LESCHEN E.C. BATCHELOR
1913	PATENTED LOCK-COIL ROPE SURROUNDED FLATTENED STRAND	UNKNOWN
1921	ROPE IN WHICH CORE WAS ENCLOSED IN A METAL BAND	ROEBLING
1940-1950	MATHEMATICAL MODEL FOR STRESS ANALYSIS OF WIRE ROPE	HRUSKA,F.H. (ORIGIN) AND HIS FOLLOWERS
1970-1980	MORE PRECISE MATHEMATICAL MODEL FOR STRESSES ANALYSIS	COSTALLO'S AND HIS FOLLOWERS

REMARK:

A. WEBER,W.[1.7] RECORDED HOW ALBERT'S ROPES WERE PROMOTED IN MINING INDUSTRY AND TRACED THE DEVELOPMENT OF WIRE ROPE MACHINERY.

B. FORESTIER-WALKER,E.R[1.2] RECORDED THE HISTORY OF WIRE ROPE INDUSTRY IN GREAT BRITAIN FROM 1830 TO 1952

C. SAYENGA,D[1.6] RECORDED THE HISTORY OF WIRE ROPE INDUSTRY IN U.S.A.

TABLE 1.2

HRUSKA,F.H. AND HIS FOLLOWERS
MATHEMATICAL MODELLING OF WIRE ROPE

YEAR	INVESTIGATOR	FIELD OF STUDY	ORIGIN
1951	HRUSKA,F.H.	TENSILE STRESS FOR WIRE ROPE	UNKNOWN
1952	HRUSKA,F.H.	RADIAL FORCE FOR WIRE ROPE	UNKNOWN
1953	HRUSKA,F.H.	TANGENTIAL FORCE FOR WIRE ROPE	UNKNOWN
1953	HRUSKA,F.H.	CONTACT FORCE & STRAND GEOMETRY	UNKNOWN
1954	LEISSA,A.W.	STRESS ANALYSIS FOR 6/1 STRAND SUBJECTED PURE TENSILE LOAD	HRUSKA,F.H.
1955	CRESS,H.A.	CONTACT STRESS FOR 6/1 STRAND	HRUSKA,F.H. HERTZIAN CONTACT STRESS
1959	LEISSA,A.W.	CONTACT STRESS	HRUSKA,F.H. HERTZIAN CONTACT STRESS
1959	STARKEY,W.L. CRESS,H.A.	CRITICAL STRESS ANALYSIS AND MODE OF FAILURE	LEISSA & HERTZIAN CONTACT STRESS
1966	MARTIN,B.C. PACKARD,T.J.	STRESS IN WIRE STRAND	VERIFY HRUSKA'S MODEL
1970	GIBSON,P.T. CRESS,H.A.	TORSIONAL PROPERTIES OF WIRE ROPE	HRUSKA
1972	REEMSNYDER, H.S.	THE MECHANICAL BEHAVIOR AND FATIGUE RESISTANCE OF STEEL WIRE, STRAND AND ROPE	HRUSKA

TABLE 1.3

COSTELLO AND HIS FELLOWS
ON MECHANICAL RESPONSE OF WIRE ROPE

YEAR	INVESTIGATOR	*FIELD OF STUDY*	*ORIGIN*
1973	PHILLIPS,J.W. COSTELLO,G.A.	CONTACT STRESS OF 6/1 CABLE	CURVED ROD THEORY LOVE.A.E.H. HRUSKA,F.H.
1974	COSTELLO,G.A. PHILLIPS,J.W.	MORE EXACT OF CONTACT STRESS	HRUSKA,F.H.
1976	COSTELLO,G.A. PHILLIPS,J.W.	EFFECTIVE MODULUS OF CABLES	COSTELLO, G.A
1977	COSTELLO,G.A. SINHA,S.A.	TORSIONAL STIFF- NESS OF CABLE	COSTELLO, G.A.
1979	COSTELLO,G.A. MILLER,R.E.	LAY EFFECT OF WIRE ROPE	COSTELLO, G.A.
1980	COSTELLO,G.A. MILLER,R.E.	STATIC RESPONSE OF REDUCED ROT- ATION ROPE	COSTELLO, G.A.
1980	COSTELLO,G.A. PHILLIPS,W.J. MILLER,R.E.	CONTACT STRESSES IN STRAIGHT CROSS LAY WIRE ROPE	COSTELLO, G.A.
1980	VELINSKY,S COSTELLO,G.A.	AXIAL RESPONSE OF OVAL WIRE ROPE	COSTELLO, G.A.
1981	BUTON,G.J. COSTELLO,G.A.	STATIC & DYNAMIC OF AXIALLY LOADED WIRE ROPES	COSTELLO, G.A.
1982	COSTELLO,G.A. BUTSON,G.J.	SIMPLIFIED BENDING THEORY FOR WIRE ROPE	COSTELLO, G.A.

CONTINUE TABLE 1.3

1983	PHILLIPS,J.W. FOTSCH,P.D.	PRELIMINARY. ANALYSIS OF FILLER-WIRE HOISTING ROPE	COSTELLO, G.A.
1983	COSTELLO,G.A.	STRESS IN MULTI LAYERED CABLES	COSTELLO, G.A.
1984	VELINSKY,S.A. ANDERSON,G.L. COSTELLO,G.A.	WIRE ROPE WITH COMPLEX CROSS SECTIONS	COSTELLO, G.A.
1985	VELINSKY,S.A.	ANALYSIS OF FIBRE CORE WIRE ROPE	COSTELLO, & HIS OWN
1985	CHIEN,C.H. COSTELLO,G.A.	EFFECTIVE LENGTH OF A FRACTURED WIRE ROPE	COSTELLO, & HIS OWN
1985	PHILLIPS,J.W. COSTELLO,G.A.	ANALYSIS OF WIRE ROPE WITH IWRC	COSTELLO, G.A.
1985	VELINSKY,S.A.	GENERAL NONLINEAR THEORY FOR COMPL- EX WIRE ROPE	COSTELLO, G.A.
1988	R.A.LECLAIR & COSTELLO,G.A.	AXIAL, BENDING & TORSIONAL LOADING OF A STRAND WITH FRICTION	COSTELLO, G.A.
1988	S.A.VELINSKY J.D.SCHMIDT	A SIMPLIFIED TREA- TISE ON THE EFFECT OF WEAR IN CABLES	UNKNOWN

TABLE 1.4

MATHEMATICAL MODELLING OF ROPES IN BRITAIN

YEAR	INVESTIGATOR	FIELD OF STUDY	ORIGIN
1948	MATHESON,J.A.L.	MECHANICS OF LOCKED COIL WIRE ROPES (PHD PROJECT) 1ST PERSON WHO MENTIONED KIR-CHHOFF'S SLENDER ROD THEORY	HIS OWN
1949	HANSOM.O.P.	MECHANICS OF LOCKED COIL ROPE	HIS OWN
1980	JONES, N AND CRISTODOULIDES	STATIC PLASTIC BE-HAVIOUR OF A 6 / 1 STRAND	HIS OWN
1982	HOBBS, R.E.	INTERWIRE SLIPPAGE AND FATIGUE PRE-DICTION IN STRAND CABLES FOR TLP TETHERS	HRUSKA, COSTELLO
1985	KUNOH, T & LEECH, C.M.	CURVATURE EFFECTS ON CONTACT POSITION	COSTELLO & HIS OWN
1987	UTTING,W.S, & JONES, N	RESPONSE OF WIRE ON 6/7 STRAND DUE TO AXIAL TENSILE LOADS	COSTELLO & HIS OWN

CHAPTER TWO

OBJECTIVE OF THIS PROJECT

2.1 INTRODUCTION

Wire ropes are often considered to be consumable items, in contrast to more expensive capital equipment; however, the use of wire rope in the mooring of North Sea oil exploration platforms has gained attention in recent years. In such a hostile environment, rope failure resulting in catastrophic failure of a structure, may lead to loss of life and money. Safety considerations have led to a gradual increase in the size and quantity of ropes used in mooring. Using bigger sizes of structural members to carry the dead load of a structure does not necessarily ensure greater safety, and it is important to understand how wire rope will behave at each stage of its life so that necessary precautions can be taken.

Conventional approaches and concepts of design for tensile members using '*safety factors*' emphasis the quantity or cross-sectional area of material used in the structure. Ideally, the load distribution in the structure and the associated stresses and strains along and across each member should be analysed in order to assess the actual safety factor against initial yield or plastic failure of a structure. Unfortunately, this approach is often found to be impracticable and difficult to use[9.9] when applied directly to wire rope design. Basically, the complicated geometrical construction of wire rope make it difficult to obtain reliable theory and data to describe the behaviour in service. The research reported in this thesis arose as part of a department of Energy Joint Industry Studies (J.I.S) programme to investigate the behaviour of wire rope. The main objectives were

a. To examine the relationship between the number of individual wire failure and fatigue endurance.

b. To investigate the scale effect and repeatability of endurance between ropes of different diameters.

c. To provide an opportunity to evaluate the use of non-destructive testing devices applied to large diameter wire ropes.

The programme included literature surveys, experimental studies on the fatigue performance of large diameter (40, 70 and 127 mm) steel wire ropes and visits to experienced investigators at the University of Liverpool, University of reading and Imperial College London. A number of papers and confidential reports have been published.

In 1984, a non-destructive testing device based on acoustic emission principles was successfully applied by Dr. N F Casey for monitoring wire failures in ropes during tension-tension fatigue tests. This device is currently being used for monitoring the number of wire failure in a large diameter wire rope during full scale fatigue tests. Wire counts in each failed rope were performed after tests in order to verify the acoustic emission results.

The rope testing work of NEL has been focused on obtaining evidence for structural property changes cyclic loading and using it to predict rope endurance. However, it is also important to understand how the mechanical behaviour of individual wires is related to the structural behaviour of the rope; this has been the motivation for the mathematical modelling of strand and rope behaviour in this thesis.

The main objectives of this thesis and the approach taken to achieve these objectives are now outlined below:

2.2 OBJECTIVE

The principal objective of the present project was originally to provide a better understanding of the mechanical behaviour of wires in a general type of rope subjected to axial loadings at the terminations. However, the complicated geometrical patterns of wire, the complications in contact conditions, the large variety of rope constructions and insufficient previous theoretical research led to the decision to confine studies to circular-wire, round-stranded rope. The structure of the approach to the objective is illustrated in Figure 2.2.1. The following headings summarize the project: (p67

a. Post-Test Examination of Large Diameter Wire Ropes

This activity was mainly concentrated on visual examination of wire failure and contact patches in ropes which had experienced constant-amplitude, tension-tension fatigue tests. A summary of the findings is presented in Chapter Three. Some 40 mm diameter and 70 diameter ropes of 6x41 (IWRC) construction and 127 mm diameter of 6x49 (IWRC) construction have been examined.

b. Mathematical Study of Helix Geometry in Strands and Ropes

The helix geometry of circular wires in round stranded ropes must be understood before the mechanical behaviour of wires can be understood. The study includes methods of finding coordinates of the wires, path lengths, and the torsion and curvature of wires in stranded rope subject to general engineering applications; for example, a straight rope subject to tension, or a rope subject to bending over a sheave or wound around a drum.

c. Sectional Geometry of Helical Wires in Round Strands

A mathematical study of the relationships between the helix angle of wires, the number of helical wires per layer and the admissible ratio of helical radius to wire cross-sectional radius has been carried out. These relations determine the spatial configuration of circular wires laid around a core and their geometrical relationships.

d. Structural Modelling of Single Layer Strands

Closed form mathematical models have been developed to predict the stiffness of ropes by considering the Poisson's effect in wires which constitute a single layer strand. This model includes the evaluation of the mechanical response of each wire, the stresses and strains due to the responses and the structural properties such as the stiffness and load-extension relationship of the strand under static conditions within the limit of proportionality (ie the limit of Hookes' law). The accuracy of this approach has been compared with Machida and Durelli's model [4.1] of 6/1 strand and B.C. Martin and T.J. Packard's experimental studies of 6/1 strands.[6.4]

e. Structural Modelling of Multilayer Strand

Closed form mathematical models have been developed, based on the stiffness approach with Poisson's effect, in two layer-strands. The purpose was again to study the static mechanical behaviour of these strands.

f. Structural Modelling On Round Stranded Ropes

Closed from mathematical model based on Velinsky's stiffness approach and the author's own approach for a simple Lang's lay and ordinary lay rope (ie IWRC) have been developed. The main different between Velinsky's stiffness approach and the author's approach is that Velinsky's approach only uses single helix geometry to approximate the double helix geometry of the double helical wires whereas the author make use of the double helix geometry to model the double helical wires. This is important because more than 73 % wires in the IWRC are in double helical form.

2.2.1 STRUCTURED APPROACH TO THE OBJECTIVE

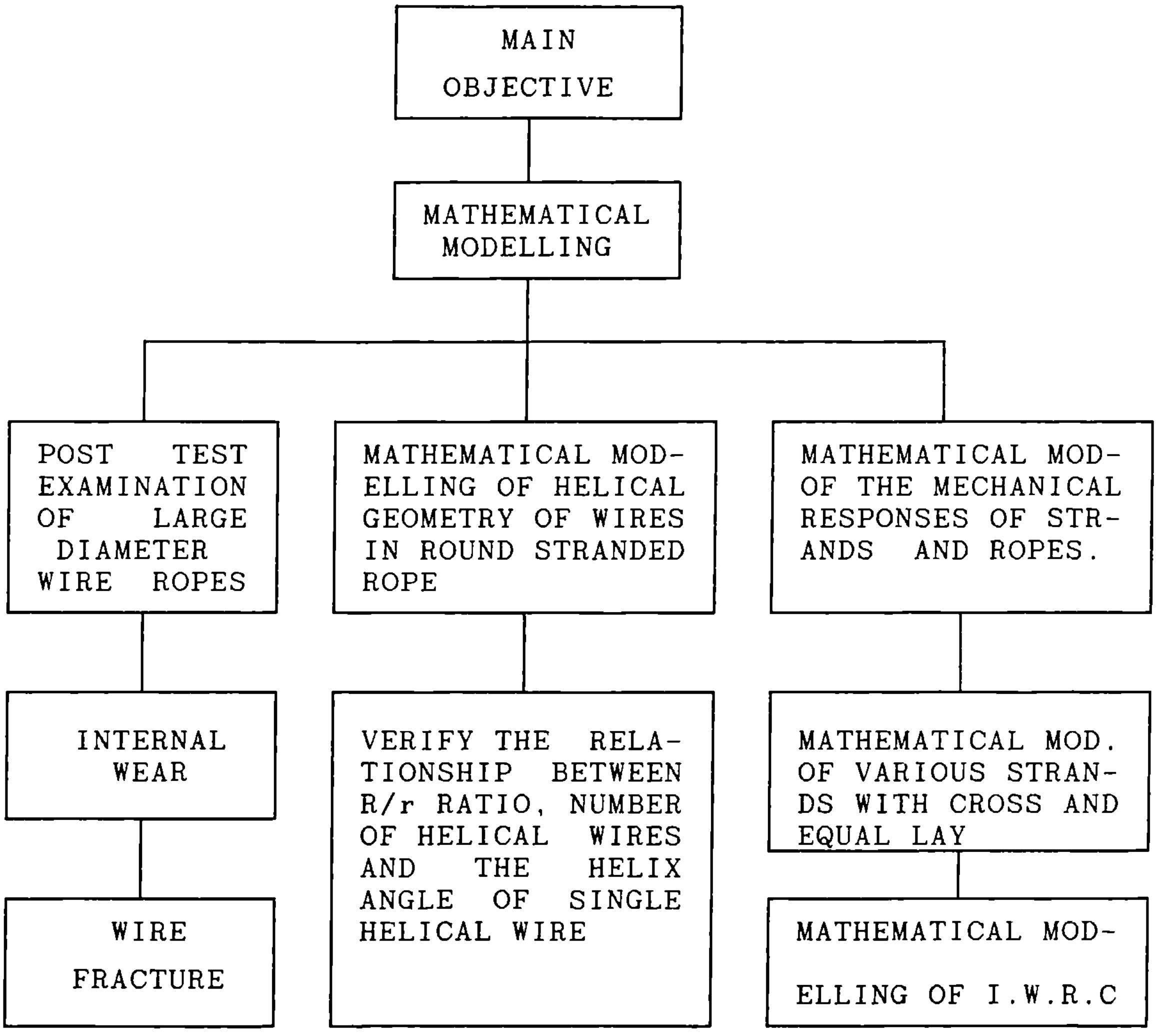

WHERE:

D.HELIX = DOUBLE HELIX
MOD. = MODELLING
I.W.R.C = INDEPENDENT WIRE ROPE CORE

BLOCK DIAGRAM 2.2.1

STRUCTURE OF THIS PROJECT

2.3 THE LAYOUT AND CONCEPT USED FOR THIS THESIS

The present research work was divided essentially into two principal studies, one is of a observational nature and the other theoretical. The observational studies included the post-test examination of wire failures in large diameter wire ropes after fatigue testing. The theoretical study included

(a) mathematical study of rope geometry (ie the helix geometry and sectional wire geometry) in order to interpret the significance and implications of mechanical responses.

(b) a mathematical model for the mechanical response of a single layer and multi-layer strand (including cross and equal lay multi-layer strand) and

(c) a mathematical model of the mechanical response of an IWRC (including Lang's lay and ordinary lay type of IWRC) in order to understand the mechanical and structural behaviour of rope.

The layout and basic concepts used in this thesis are presented Chapter by Chapter as follows:

2.3.1 Chapters One, Two and Three

Chapter one presents a brief description of the origin of wire rope, the historical background, the rise and fall of the rope industry and a literature survey for the present study. Chapter two is the present chapter. Chapter three introduces brief descriptions of wires and round stranded rope configuration, the micro structure of wire for rope production, the mechanical responses and mechanical properties of rope, common problems encountered in rope applications and the preliminary practical study of wire degradation during tensile fatigue by testing. This study is a prerequisite for the understanding of ropes and wires behaviour under static loading and fatigue.

2.3.2 Chapter Four, Five and Six

It is of great interest to relate the helix geometry of the wire to its mechanical responses in various strand and rope configurations. Through this analysis one can gain insight into the sharing of loads. In addition, a full understanding of the helix geometry enables one to understand the contact pattern along a particular wire in a strand or in a rope and to provide important information for the analysis of mechanical interactions in round stranded rope. Most importantly an understanding of the geometry facilitates the analysis of stresses and strains resulting from the global displacements applied at the rope terminations.

Helix geometry descriptions also enable one to visualise the mechanical interactions at a point and to understand the significance of the helix geometry in relation to these interactions. Chapter four therefore, presents the application of a vector method to analyse the helix geometry found in the circular-wire round-stranded rope. Three dimensional paper models have been made in order to visualise the Cartesian coordinates of points on the centroidal axis of the helical wire. Eventually, the Cartesian coordinates, the helix angle, the radius of curvature, radius of torsion and the path length of any helical wire found in a straight rope, drum-wound rope or sheave-bent rope can be analysed. Chapter Five presents the implications of these geometrical features for the mechanical response of wire in ropes as applied in general engineering. Chapter Six explains the significance of helical parameters related to the selection of helix angle, admissible helical radius, diameter of wires, the number of wires per layer and the spatial configuration of strands.

2.3.3 Chapter Seven and Eight

Chapter Seven presents a closed form method to evaluate the mechanical response of a single layer strand. In this study, naturally curved rod theory and Costello's approach are modified in order to generated a stiffness matrix method to model the mechanical responses of a single layer strand. Chapter Eight presents a further modification of the approach to evaluate the mechanical responses of two layer multi-layer strand, for both cross lay and equal lay configuration.

Computer software has been developed for each of these models. Sample results, discussion and conclusion are also given at the end of each chapter.

2.3.4 Chapter Nine

This chapter presents two closed form methods to evaluate the mechanical responses of an IWRC with Lang's and ordinary lay construction. The first method is based on Velinsky's approach and the second method is based on the author's approach. The double helical wire geometry is considered in the second method. Again, computer software has been developed for these models. Sample results, discussion and conclusion are also presented at the end of this chapter.

2.3.5 Appendix And Glossary Of Terms

This final section presents summary on the previous works, a collection of expressions and parametric equations used in the preceding analysis together with common terms used in the rope industry.

CHAPTER THREE

CONSTRUCTION OF ROUND STRANDED ROPE

AND RESULTS OF POST TEST EXAMINATION

3 INTRODUCTION

The National Engineering Laboratory (NEL) is currently participating in a comprehensive collaborative research programme to assess the behaviour of large diameter wire ropes (40, 70 and 127 mm) and strands, especially for offshore mooring applications. The programme at NEL includes mathematical modelling as well as various rope testing procedures. A thorough understanding of practical aspects of strands and ropes is necessary to establish realistic mathematical models.

This chapter introduces the terminology used in the rope industry and discusses the construction of wire ropes, rope degradation, mechanical properties of round stranded rope, rope selection, and basic design considerations. The results of the author's detailed examination of wire failures in various tension-tension fatigue loaded ropes together with some of the new findings are also presented in this chapter.

3.1 ORGANIZATION OF CHAPTER THREE

The organization of this chapter is illustrated in the following block diagram :

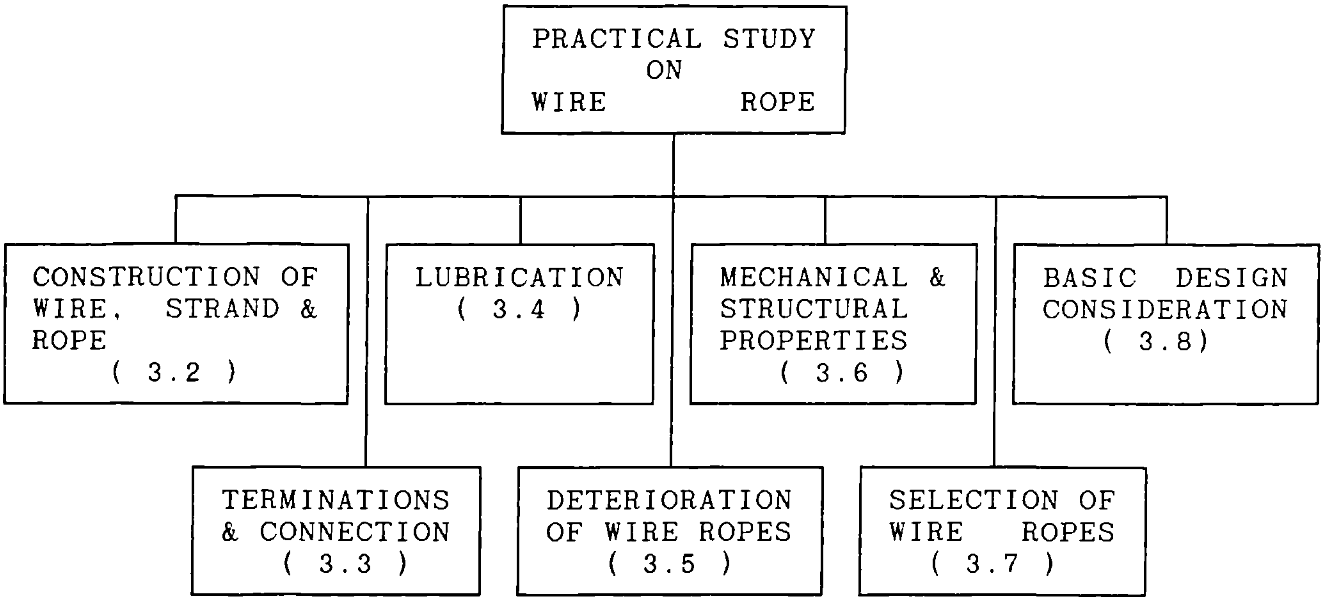

BLOCK DIAGRAM 3.1-1

STRUCTURE DAIGRAM OF CHAPTER THREE

3.2 WIRE, STRAND AND ROPE CONSTRUCTIONS

Rope steel may have a tensile strength (1765.8 N/mm^2 or even more) which is more than four times greater than that of mild steel[9.1]. For a given size of a rope, the strength of the wire rope is, in general, determined by the size and grade of wire used, the number of wires in the strand, the geometrical pattern of and the type of main core strand and outer layer strands. In this section the properties of wire and strand shapes and the features of common rope constructions are discussed.

3.2.1 Wire

Wire is the basic element employed for manufacturing strands. The following sub-sections present essential terms.

3.2.1-1 Wire Strength[9.5]

Wires of the same shape are generally categorised into grades in accordance with tensile strength. These vary from 160 grade (160 kgf) to 180 grade (180 kgf). The fatigue resistance of wire up to 110 kgf/sq mm tensile strength is proportional to breaking strength, but for higher tensile grades, the ratio of fatigue resistance to the breaking strength decreases with increase of breaking strength. In other words, the higher the tensile grade of wire, the more likely it is to subject to such fatigue problems.

3.2.1-2 Shape Of Wires

A particular wire shape may be suitable for some applications and rope construction geometries, but unsuitable for others. The most common wire shapes illustrated in Figure 3.2.1-1, are:

i. Round — ie transverse section of wire is in circular shape.

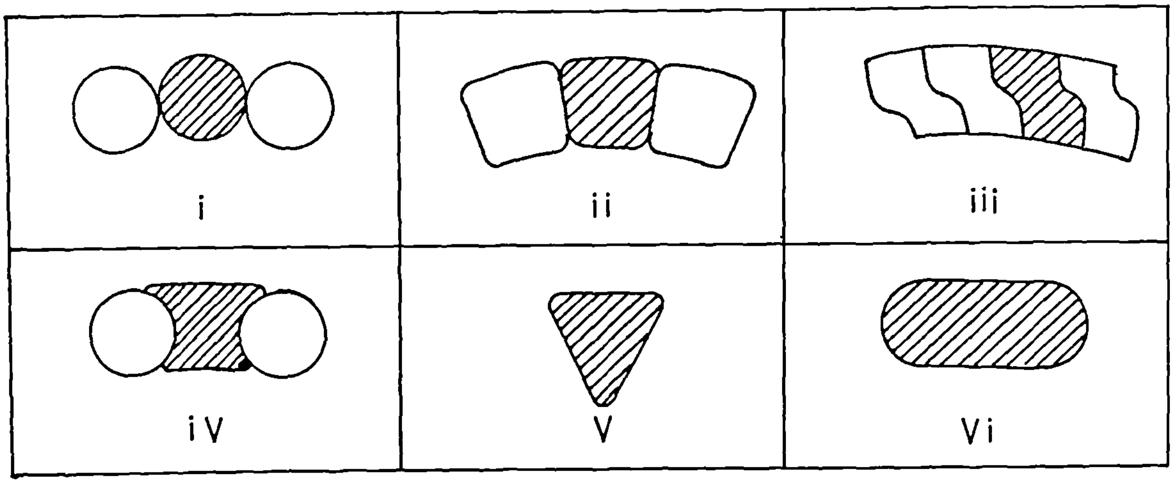

Where:

i Circular Wire

ii Trapezoidal

iii Full Lock

iV Half Lock

V Triangular

Vi Ribbon Wire

Figure 3·2·1-1
Wire Shape

ii. Trapezoidal ie transverse section of wire is in trapezoidal shape.

iii. Full Lock ie Z-Shaped wire as shown in the Figure.

iv. Half-Lock ie rail-shaped wire as shown in the Figure.

v. Triangular ie wire transverse section is a triangular shape and this is usually used for the core wires of particular strand.

vi. Ribbon Wire ie Oval-shape wire as shown in the Figure.

3.2.1-3 Surface Finish Of Wire

The surface texture of wires used for manufacturing wire rope is regarded as important in determining rope endurance and corrosion protection. Several commonly used surface finish are available. The most common one is called "galvanised coating". A wire can be supplied in one of the following surface finished ready for rope manufacturing. They are:

i. Ungalvanised (or black).

ii. Galvanised, Type A (heavy coating with Zinc)

iii. Galvanised, Type Z (lighter coating with Zinc)

Wire coating has a dual purpose

i. Corrosion protection.

ii. Provides a soft bed to distribute the contact force.

3.2.1-4 Wire Forms Found in a Round Stranded Rope

Circular wire in round stranded rope can be formed in the following shapes:

i.	A straight Wire	ie King wire.
ii.	A single helical wire,	ie as core wire of single helical strand
iii.	A double helical wire,	ie as layered wire of single helical strand.

3.2.1-5 Heat Treatments and Defects in Wire [9.6]

(1) Introduction

Wire manufacture is a complicated process. The drawn-wire tends to become brittle after a sequence of passes through the die. To reverse this work hardening tendency across the section of the drawn wire and to restore the ductility and drawability for subsequent drawing, carefully controlled heat treatments are needed from time to time during the drawing process. As a result, the material properties of the finished wire will be governed by the micro-structure after these complicated manufacturing processes. Defects, which are found in the wire at the final stage, are normally regarded as "*intrinsic*" defects.

(2) Patenting

Heat treatment applied during the wire manufacturing process is known as "PATENTING". The purpose of patenting is to reverse the highly deformed micro-structure of drawn wire to the original state and to restore the normal drawability of the wire for subsequent drawing processes. The micro-structure of steel wire after heat treatment is known as "SORBITE". Apart from its comparatively high strength, sorbite has excellent cold deformation capacities because of its globular structure which can easily be deformed in all directions. It is generally accepted that the mechanical properties of patented steel wire for rope manufacturing depend on the patenting conditions, such as the method of cooling (eg type of salt or lead bath), the quenching temperature and the speed of wire travelling through the quenching bath. Details of the procedure of how heat treatments are performed will not be discussed in this thesis. However, this section focuses on faults appearing during patenting and the type of micro-structures which will affect the mechanical properties and the fatigue performance of wires in a strand and rope.

NB. the difference between a pearlite and sorbite structures found in heat treated steel wire relates to the thickness of the cementite lamellae. The main characteristics of the structure of patented wires relate to the grain size and distance between lamellae of cementite crystals.

(3) Faults of Heat Treatment on Wire

Basically, two faults, which can occur in patented steel, are influenced by the carbon content and the furnace temperature for heat treatment.

For steel wire with .8% carbon content which are specially used for high strength wire ropes, the wire is heat treated to a high temperature (about 1000 deg. C.) and then quenched into a lead bath (about 450 to 470 deg. C). Thermal stress will be set up in the wire and this will often show in immediate cracking, or this may appear later during pickling. These cracks will occur normal to wire length and will typically occur at a hundred or more places along the wire. In some cases, the thermal stress will release during rope manufacturing or may not be revealed until the rope is in use. As the result, the rope is found to have a shortened service life. In more severe cases these cracks cause sudden breakage of the rope.

NB. In high carbon steel wire, poor control of quenching temperature will result in the formation of martensite along the wire. This is a highly brittle constituent and is very poor in resisting bending.

For a steel wire with low carbon content, too low a patenting temperature will result in the separation of ferrite from pearlite. A steel wire with such micro-structure will stand less deformation than those wires with a sorbite structure.

If patented wire with such a structure is drawn then this wire will again shown brittleness, and have low bend warping number. Rope with such micro-structure will show a relatively short service life. Of course, the micro-structure of such wire also shows less wear and corrosion resistance so that the wire will be poor in fretting fatigue performance in general.

The material properties of even heat treated steel wire are generally accepted to be homogeneous-isotropic or orthotropic.

3.2.2 Strand

Strand is formed by winding one or more layers of wires helically around either a core wire or a strand core. A strand could either remain as a strand core (employed either as a core of a strand or as a main core of a rope) or be further deformed helically as an outer layer helical strand of a rope. The following sub-sections present the terminology used in connection with strands which form part of the elements of wire rope.

3.2.2-1 Strand Cores

From the mechanical point of view, strand cores are mainly used to provide a bed to support outer the layer strands, to share loads carried by the rope, to provide flexibility and to give shape to the rope. The strand cores are commonly categorised into three types namely fibre core, wire core and built-up-core "BUC" (which is a die-formed core). Various strand cores are shown in Figure 3.2.2-1.

Strand cores are also classified according to their shape. The common types of strand cores are:

a. Round ie used for making round strand
b. Triangular ie used for making triangular strand
c. Oval ie used for making filled flat strand.

3.2.2-2 Helical Strands and Their Shapes

The common types of strand shape found in wire ropes presented in Figure 3.2.2-2, are:

a. Round as shown in Figure 3.2.2-2 except i, ii & iii
b. Triangular as shown in Figure 3.2.2-2 iii
c. Oval as shown in Figure 3.2.2-2 ii
d. Flat not shown
e. Hexagonal as shown in Figure 3.2.2-2 i

3.2.2-3 Construction Nomenclature of a Strand

Construction nomenclature normally quotes "shape" and number of wires in each layer, starting from the outer layer. eg,

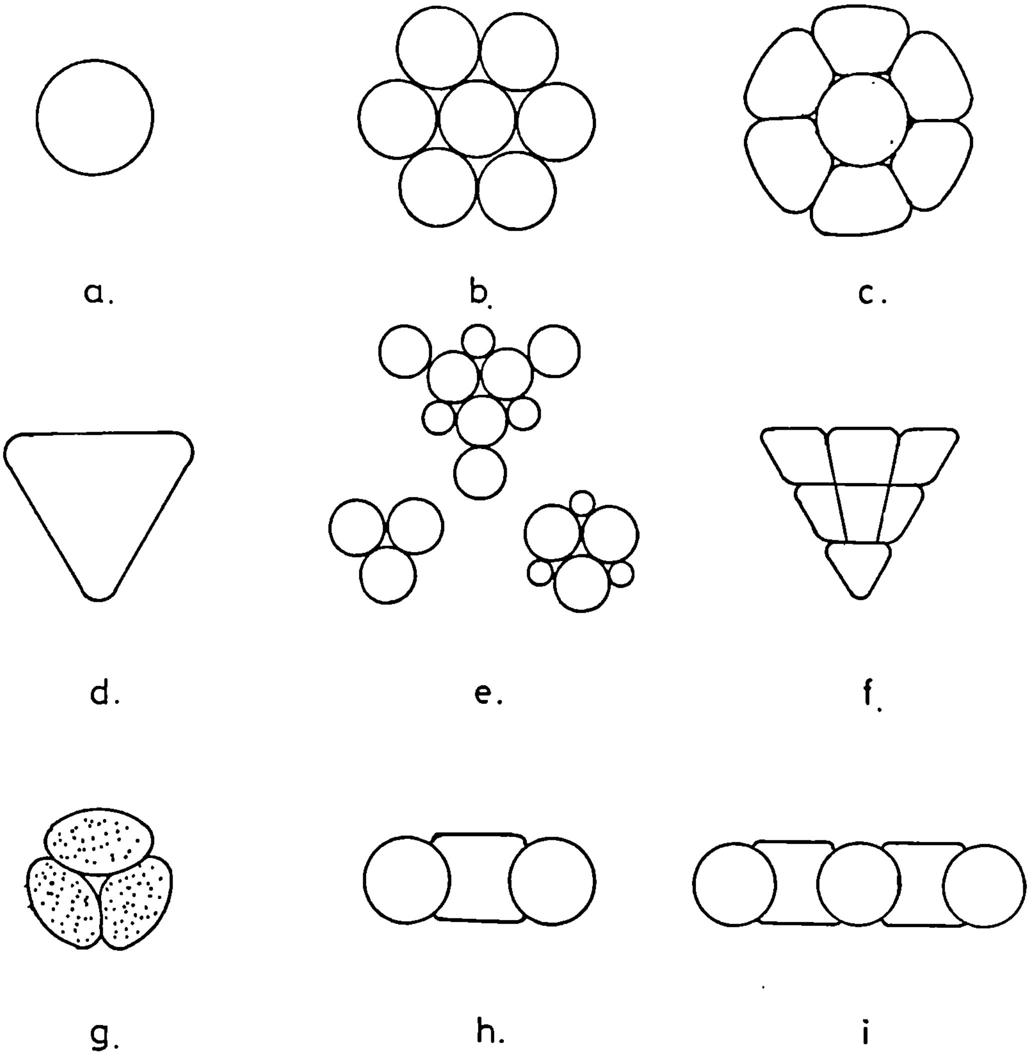

Where:

a b c	Round Core
d e f	Triangular
g	Fibre
h i	Oval

Figure 3·2·2–1
Strand Core

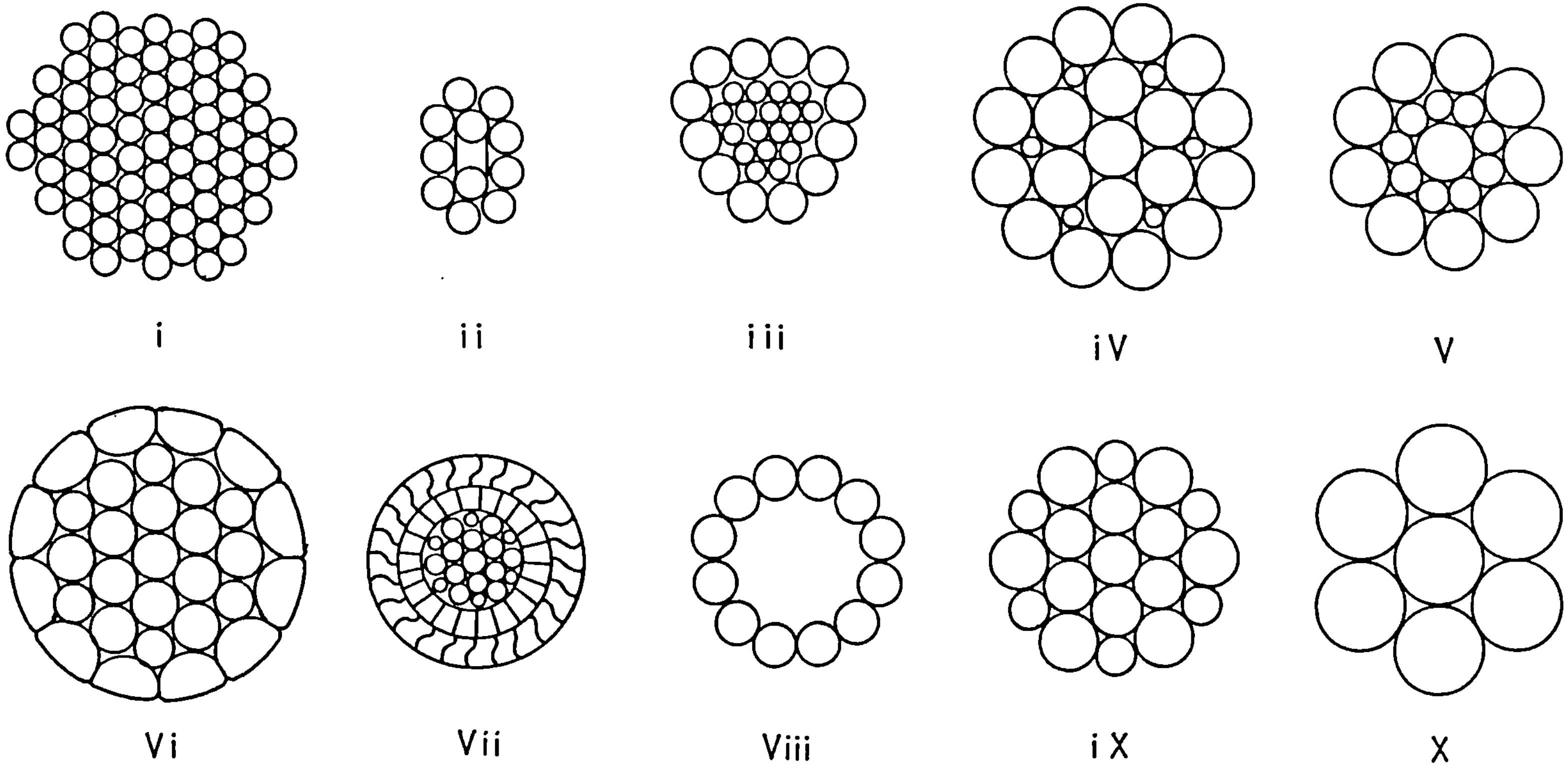

Where

i 1x73 Glass Strand
ii Oval Strand
iii Triangular
iV 12/6F/6/1 Strand
V 9/9/1 Strand
Vi Die Formed Strand
Vii Lock Coil Strand
Viii 12/Fibre Strand
iX 12/6/1 Strand
X 6/1 Strand

Figure 3·2·2-2
Strand Shapes

Figure 3.2.2-2 V. illustrates a strand section named as "round 9/9/1".

3.2.2-4 Form Of Strands And Wires.

In this thesis, interest is focused on round strand with circular wires. A round strand should always be made with a circular core wire or a round strand core. This type of strand should either be in straight form or deformed into helical form along its length. For a straight strand, all the wires are deformed permanently into single helical form except the core wire. For a helical strand, however, all the wires are deformed permanently into double helical form, with exception of the core wire which is deformed into single helical form. Details of wire forms will be discussed in Chapter 4.

3.2.2-5 Strand Flexibility

For a given grade of wire irrespective of the material stiffness of the wire, the flexibility of a strand can be adjusted by two methods namely,

a. Wire size and.

b. Wire lay angle.

(1) Wire Size

Apart from the influence of lay angle, the smaller the wire diameter used to construct a strand, the more flexible will be the strand. However, when the outer layer wires of a strand become less than 2 mm in diameter, they will be more likely to be subject to severe wear and corrosion damage. Therefore, in practice, no strand will be constructed with wire diameter less than 2 mm without considering appropriate protection against wear and corrosion.

(2) Wire Lay Angle

The flexibility of a strand can be adjusted by varying the lay angle of wires. Reducing the lay angle produces greater flexibility. However, this adjustment leads to complications related to geometry, mechanical responses and interactions. Lay angle can be varied between layers in two possible configurations: namely, "equal lay" and "cross lay" geometry.

a. Influence Of Geometrical Pattern

There is an admissible wire lay angle which can be used for constructing strand with given number of helical wires per layer, given size of core wire and helical wires. This problem will be discussed in Chapter 6.

Four well known geometrical patterns applied to strands are listed:

1. Seale Rope

For a Seale rope, the outer strand is constructed in such a way that the number of outer layer wires equals to the number of inner layer wires within the strand. This construction allows strand to have the biggest wires located at the outer-most layer. As the result, the construction may provide greater external abrasion resistance for the rope.

2. 6/1 Strand

For a 6/1 strand, the diameter of the core wire is always bigger than the diameter of the helical wires. This design is normally used for construction of multi-strand rope.

3. Filler Wire Strand

A filler wire strand can be regarded as the equal lay strand. The filler wires are used to prevent the outer layer wires from falling into the valley provided by the layer of wires immediate beneath. This construction provides better support between adjacent layers within a strand. Hence, greater interior abrasion and fatigue resistance can be expected.

4. Strand Of Warrington Rope

For a Warrington rope, the outer strand of is constructed in such a way that two different sizes of wires are laid alternately at the outer-most layer of the strand. Thus the crowns and valleys of the inner layer wires form support points. This construction provides good external abrasion resistance and can used to adjust strand flexibility.

b. Influence of Lay Angle for High Strength Steel Wires

The approach of using lay angle to adjust the flexibility of a strand is limited by the fatigue performance of high strength steel wire with brittle properties. Wires with high strength brittle properties are more likely to fail resulting from reversed bending and torsion, which increase significantly as the helix angle of wire is decreased.

c. Influence of Wire Helix Angle on the Mechanical Response of a Strand

A straight strand is formed by laying wires helically around either the core wire or a strand core. Wires which are laid around the core, can be wound either in right hand or left hand direction (as in right hand or left hand screw thread). The longitudinal length of one complete cycle of a single helical wire at the outer layer of a strand is defined as the lay length of the strand. The helix angle of the wire constitutes a significant influence on the mechanical responses of the strand. Strands can be constructed to give rise rotation or to minimize rotation when subjected to axial tension at terminations.

1. Rotational Strand

A strand with all wires laid helically around a core wire in the same direction is known as rotational strand; since the strand will rotate when subjected to axial tension at the terminations. This strand can be constructed either in cross lay or equal lay.

2. Minimized Rotation Strand

A strand with wires which are laid around a core wire with one layer in one direction and the other layer in opposite direction alternately, is *known as minimized* rotation strand (since the rotation of the strand will be minimized by the opposite twisting moment at each layer). This type of strand can only be constructed in cross lay.

d. Influences of Equal Lay and Cross Lay

A strand with wires which are laid helically around a core wire each with same lay angle, is said to be equal lay. Otherwise, is said to be cross lay.

1. Equal Lay

The advantage of equal lay strand is that this lay configuration provides greater wear surface at the expenses of rotation when the strand is subjected to tension at its terminations.

2. Cross Lay

The advantage of cross lay is obviously in minimizing unwinding rotation when the strand is subjected to tension at its terminations. However, wires will subject to cross cutting at the contact points between adjacent layers.

3.2.3 Ropes

A stranded rope is formed (except for flat rope) by laying up one or more layers of strands around a main core strand. Figure 3.2.3-1 presents the common constructions of "*round stranded ropes*". Ropes are normally constructed in the following forms (see ropeman hand book [9.1] for details of the following ropes):

a. Round stranded rope
b. Flattened stranded rope
c. Non-rotation rope
d. Flat rope
e. Locked-coil rope
f. Round guide rope
g. Half-lock guide rope

3.2.3-1 Construction Nomenclature of Wire Rope

The construction of a wire rope is conventional expressed terms:

a. Number of strands (from outer layer to inner layer)
b. Number of wires in the strand
c. Lay up of wires in the strand
d. Type of core
e. Direction of rope lay

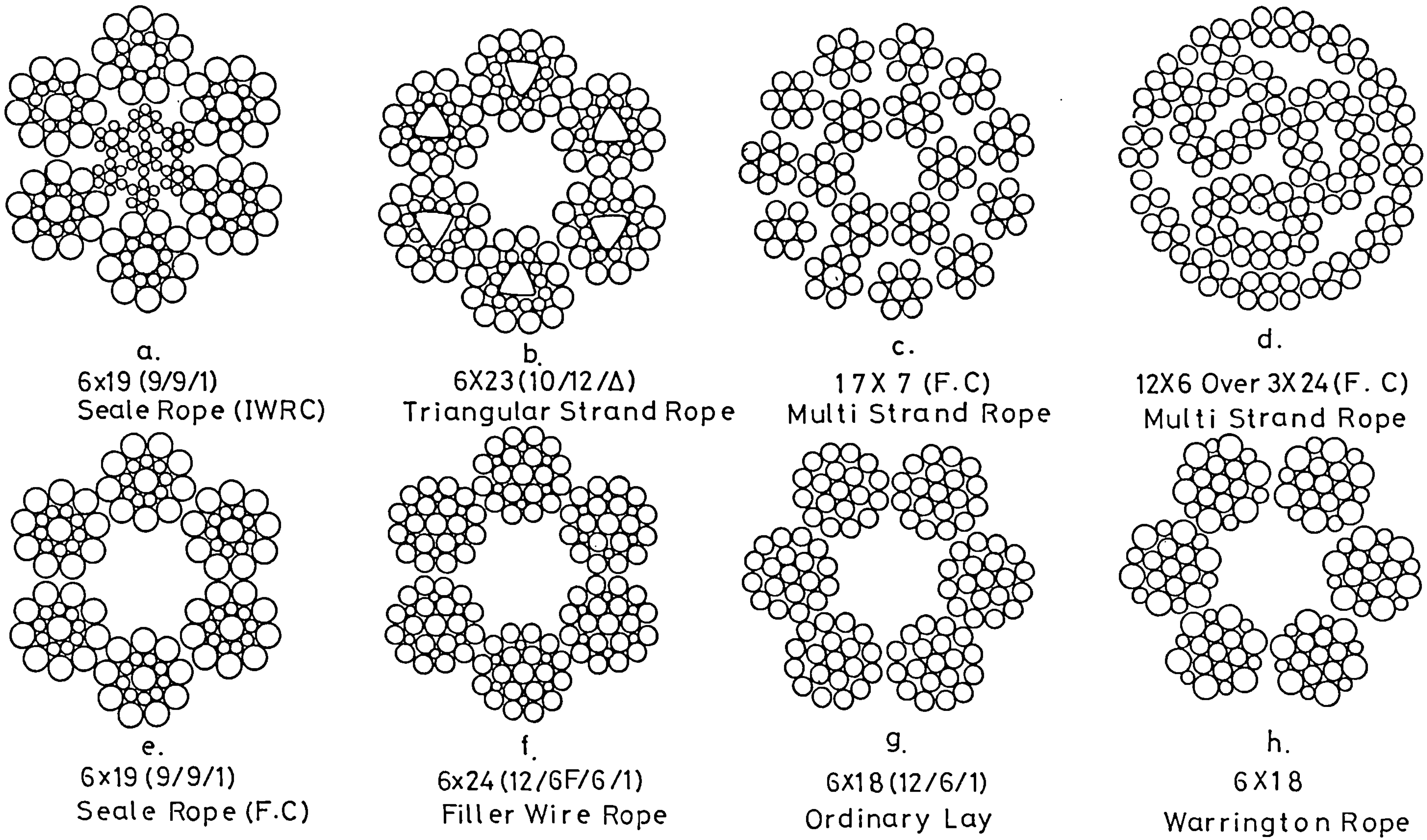

Figure 3·2·3-1
ROUND STRANDED ROPE

Presented in Figure 3.2.3-1.a is a typical schematic wire rope section which is known as 6 x 19 (9/9/1) IWRC right hand ordinary lay Seale rope, ie 6x19 is outer layer, the rest is IWRC.

3.2.3-2 Composition Of Round Stranded Rope

A round stranded rope consists of a main core and one or more layers of helical strands laid around the main core. A typical schematic wire rope construction is presented in Figure 3.2.3-2. A brief description of the components of a round stranded rope is presented in the following:

(1) Main Core of Rope

In this thesis, the focus is on round stranded rope with a circular core. These types of rope are essentially formed by winding strands helically around a main core. The main core of a stranded rope can be classified into the following types:

a. Fibre Main Core (ie fibre core and fibre-film core) (FMC)
b. Wire Main Core (ie steel core) (WMC)
c. Wire Strand Core (ie steel core) (WCS)
d. Dyform Core (ie steel core)
e. Independfent Wire Rope Core (ie IWRC)

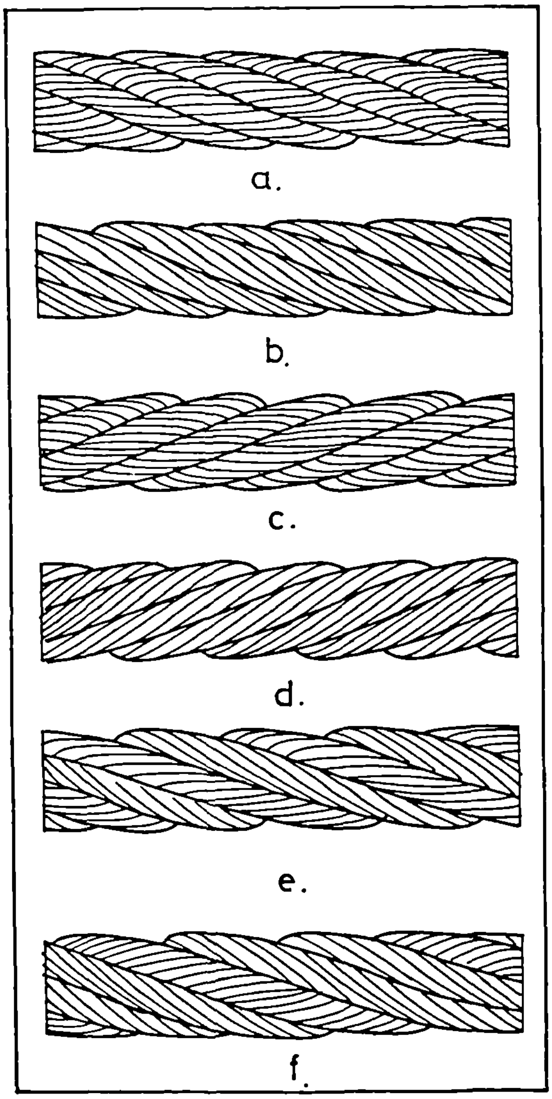

Lay Patterns

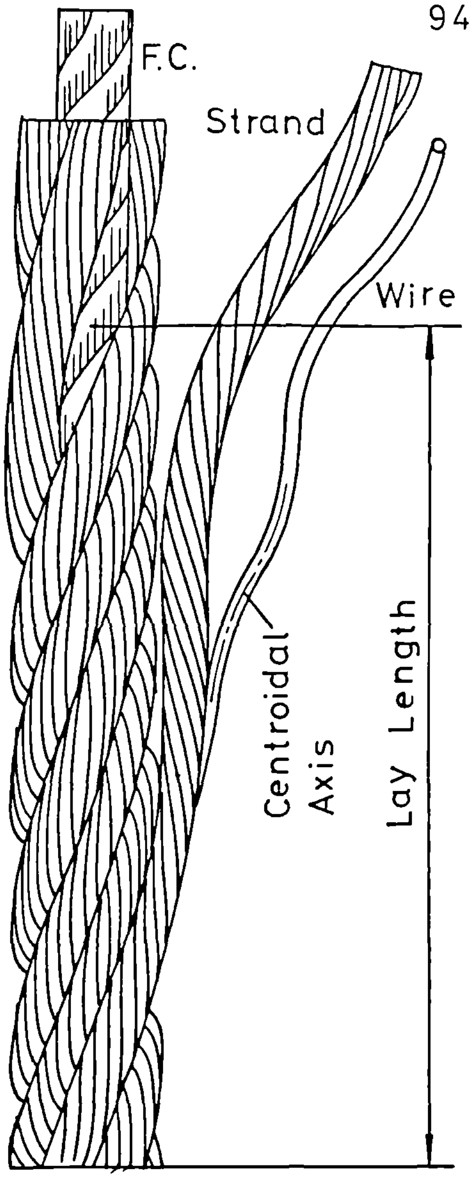

Rope.

Where:

a. Right Hand Ordinary Lay

b. Right Hand Lang's Lay

c. Left Hand Ordinary Lay

d. Left Hand Lang's Lay

e. Right Hand Alternate Lay

f. Right Hand Herringbore

Figure 3·2·3-2
Schematic Representation
Of Rope Configuration

The fibre main core is very flexible. Ropes constructed with fibre core are not suitable for operating in an environment with high temperature and cannot be used where there is severe core crushing. Ropes with a steel core, such as Wire Main Core and Independent Wire Rope Core, are less flexible than those with fibre main core. Those with a steel core can withstand higher core crushing and can be used in high temperature environment.

(2) Helical Strand of a Rope

Apart from the Main Core, ropes consists of one or more layers of helical strand. The following presents terms used for describing the helical strand of a rope

a Rope Lay

Helical strand can be laid in various combinations around the main core. Each of these lay configurations are designed to achieve its best mechanical properties and fatigue performances by the manufacturer. Figure 3.2.3-2 presents the most common lay configurations:

1. Ordinary Lay (or Regular Lay)

   If the orientation of wires laid in the outer layer strand is opposite to the orientation of that strand laid round the main core, then rope is known as ordinary lay rope.

2. Lang's Lay

If the orientation of wires laid in the outer layer strand is the same as the orientation of that strand laid around the main core, then rope is known as Lang's lay.

3. Alternate Lay

In this case, Lang's lay strand and ordinary lay strand are laid alternately around the main core of a rope.

4. Herringbone or Twinned Strand rope

If two pairs of right hand Lang's lay strands and one pair of left hand ordinary lay strands are laid alternately around the main core, then the rope is known as Herringbone rope.

b. Direction of Lay and Lay Length of Rope

Helical strand which is laid around the main core of a rope, can be either laid in the right hand direction or in the left hand direction. The lay directions are known as right hand lay and left hand lay respectively. The longitudinal length for one cycle (ie 360 degrees rotation of strand about the rope axis) of an outer strand is known as one rope lay; lay length of a rope. Figure 3.2.3-2 presents an illustration of one lay length of a 6 stranded rope.

c. Influence of Rope Lay

The helical structure of a rope geometry complicates mechanical responses when this structure is subject to tensile loading. Apart from many other responses of wire, the unwinding moment of strands at the terminations is one of the most obvious mechanical responses to be note. Two designs concerned with this problem are noted:

1. Rotational Rope

Figure 3.2.3-3(b) is a schematic representation of a rotational rope in which both wires and strands are laid in the same direction around the wire core and main core respectively. Ropes of such construction will subject to rotational movement at the terminations when they are subjecting to axial tensile load.

2. Non-Rotational Rope

Figure 3.2.3-3(a) is a schematic representation of a reduced-rotational rope in which wires and strands laid in the opposition direction around the strand core and main core respectively. Ropes of such construction will have rotational movement minimized at the terminations when they are subjecting to axial tensile load. If ropes are constructed with more than two layers of strands, strands at each layer will have to be laid in opposite directions. Thus, the tendency of one layer of strands

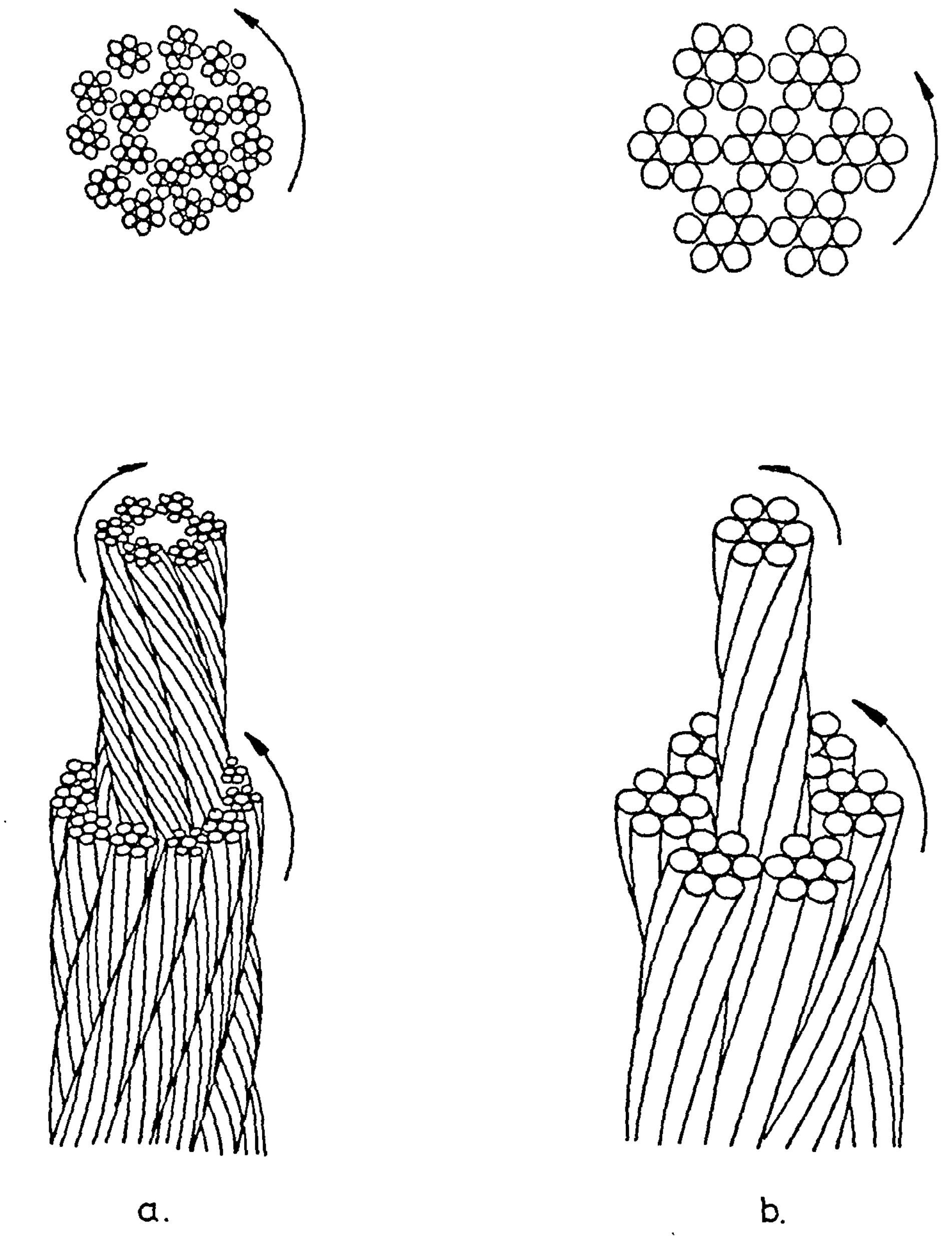

Where :

a. Reduced Rotation Rope

b. Rotation Rope

Figure 3·2·3-3

to rotate in one direction is counteracted by the tendency of the other layer of strands to rotate in opposite directions.

Care has to be taken when handling this type of rope because any twisting movement applied to the outer layer strand could cause the slippage of core strand (somewhat like untightening a screw) and it will protrude from the rope.

3.2.3-3 Methods of Rope Manufacture

Ropes are manufactured either by preforming or postforming. In other words, both wires and strands are set to their permanent shape in the rope without any tendency to unlay themselves while the rope is in the unloaded condition. Figure 3.2.3-4 illustrates the difference between preformed rope and postformed rope and the following present a summary for each method is presented below.

(1) Preforming

Wires are deformed permanently into their predetermined shaped before they are laid into the rope.

(2) Postforming

Wires are first laid into the form of a straight strand and then the strand is bent helically around a main core.

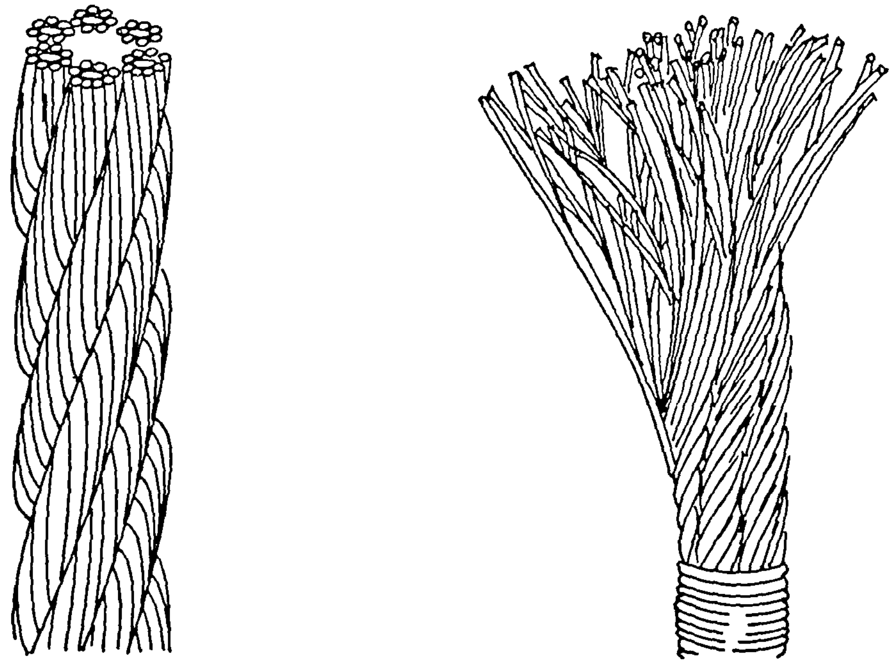

a.   b.

Where :

a. Preformed Rope

b Non Preformed Rope

Figure 3·2·3-4

Advantages of preforming rope:

a. Exposed ends will not be untwisted
b. Easy to handle during storing and installation
c. Less likely to kink and free from twisting tendencies.

3.2.3-4 The Overall Characteristics Of Round Stranded Rope

Round stranded ropes are comparatively easy to examine visually and generally provide a fairly wide range of flexibility. However, they have a tendency to twist as the load changes and are rather vulnerable to both external and internal wear. It should be borne in mind that the rotation movement of a non-rotating rope is only minimized at the rope terminations. The unwinding movements still appear between outer and inner layer strands. Figure 3.5.2-14 illustrates the typical damage on wires between two layers of strands resulted from unwinding movement of reduced-rotation rope. For a rotation rope, unwinding rotations are significant. In order to prevent this movement, some form of constraint has to be applied to the terminations of this rope. Otherwise, internal wear and bending of wires on the outer layer of strand are expected to be more prominent and will eventually shorten the rope service life.

3.2.3-5 Summary on the Characteristics of Lang's Lay and Ordinary Lay

Lang's lay rope behaves as rotational rope whereas ordinary lay rope behaves as reduced-rotational rope. Lang's lay ropes are constructed so as to offer better external wearing surface and therefore can be expected, in some cases, to have a longer fatigue life than ordinary lay. Since the Lang's lay rope is a rotational rope, it must not be allowed to used when the termination is free to rotate. Ordinary lay ropes, on the other hand, are thought to be easier to be handle than Lang's lay, since they are less liable to untwisting and kinking in general applications. (See chapter 5 for further discussion)

3.3 TERMINATIONS AND CONNECTION OF ROPE

Wire rope termination installations are of enormous importance with regard to the safety requirements. It is generally recognised that even properly made and carefully installed terminations will develop less strength than the full strength of the rope. It is not only necessary to know what type of termination is to be used and how to install it correctly, but the safe working load is also needed. The commonly used rope terminations are:

a. Socketing

"Socketing" is the most effective and efficient method of terminating wire rope. Correctly installed sockets will be more likely to allow a rope to develop its full breaking load (see British Rope Blue Standard [9.2]). Figure 3.3-1 illustrates two types of recommended sockets for rope terminations.

b. Capping Material

The common types of material for securing sockets to the rope terminations are:

1. White Metal
b. Zinc
c. Resin (polyester)

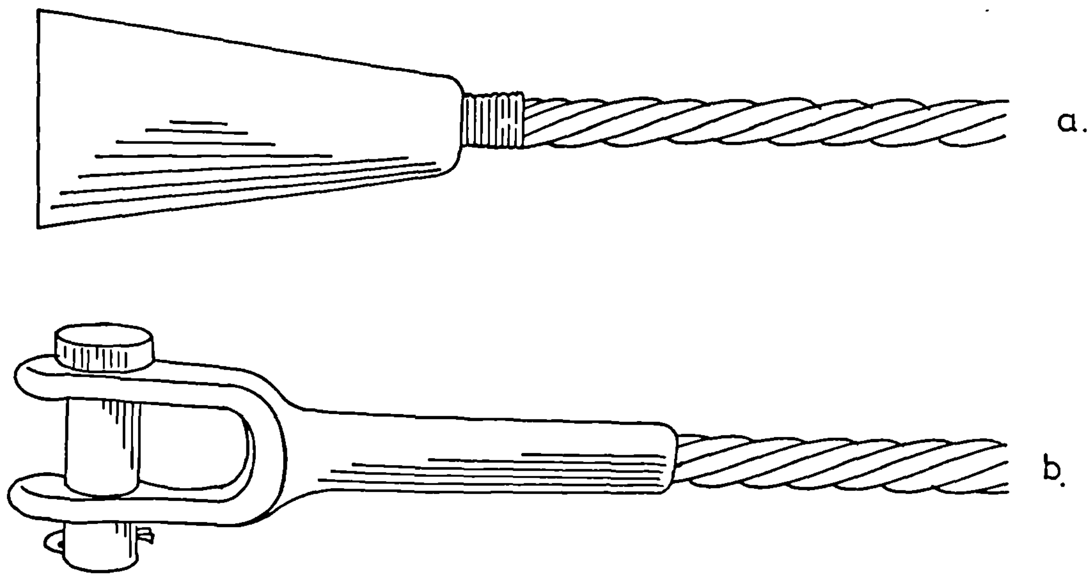

Where:

a. Cone Socket

b. Swaged Socket

Figure 3·3-1
Rope Termination

Procedures for rope capping can be found in the following standards.

ISO/DIS 7595	Molten Metal Socketing of Wire Rope.
ISO/TR 7596	Socketing procedures for Wire Rope. (Resin Socketing)

N.B.
Resin socketing [9.2] is not recommended for use in stainless steel ropes in a marine environment because of the potential for crevice corrosion. However, this combination can be used in an industrial environment.

Remarks:
Swaged socket attachment with zinc capping is commonly used for more permanent types of installation for rope terminations where the standing rope is subjected to little or no movement. When a rope is subjected to movement and vibrations, wires are gradually cracked and broken at the entrance of the socket resulted from fatigue. There is no way to prevent this type of fatigue and the majority of rope failures occur near the entrance of socket.

3.4 Lubrication

Lubrication serves several purposes. It provides corrosion resistance and minimizes internal wear between wires at local contact locations inside a rope. Good lubricants for ropes should basically have the following characteristics. [9.2].

a. Corrosion resistance.

b. Water repellence.

c. High viscosity.

d. Chemically neutral.

e. Penetrating ability.

f. Adhesiveness and affinity for steel.

g. Plastic coating.

h. Temperature stability.

3.5 ROPE DETERIORATION AND CONTACT PATCHES OCCURRENCE

Wire failures, which may be found in hundreds of places (internally and externally) along a rope under normal operating conditions, have long been recorded by rope workers probably as early as the eighteenth century. However, systematic examination of wire failures and correlation with positions related to wire geometry features has not yet been published. The following sub-sections present a brief summary of common rope deterioration patterns and the results of author's systematic post test examination on large diameter wire ropes (ie, Φ40, Φ70 and Φ127 mm) failed by tension-tension fatigue tests carried out in the N.E.L current rope research programme.

Organization Of Current Section

a. Summary of common rope deteriorations [9.1]

b. Author's post test examinations [9.8] on large diameter wire rope.

3.5.1 Rope Deteriorations

Ropes, like all other man-made tools, have their own mechanism of deterioration, even under careful and normal usage. Figure 3.5.1-1 presents the common deterioration patterns found in round stranded ropes. These are on:

a. Wire failures on outer strand.
b. IWRC failure.
c. Kinking.
d. High wires.
e. Rope fracture due to poor socketing.
f. High strands.
g. Bird cage.
h. Failure of outer strands.
i. Protruding core.
j. Wire crushing.
k. Loose strands due to fatigue.

According to reference [9.1], the factors which influence the deterioration of ropes can be summarized as

a. Wear (external and internal)
b. Fatigue (mechanical fatigue)
c. Corrosion (chemical attack or oxidation)
d. Surface embrittlement
e. Accidental damage and distortion. (lock deterioration)

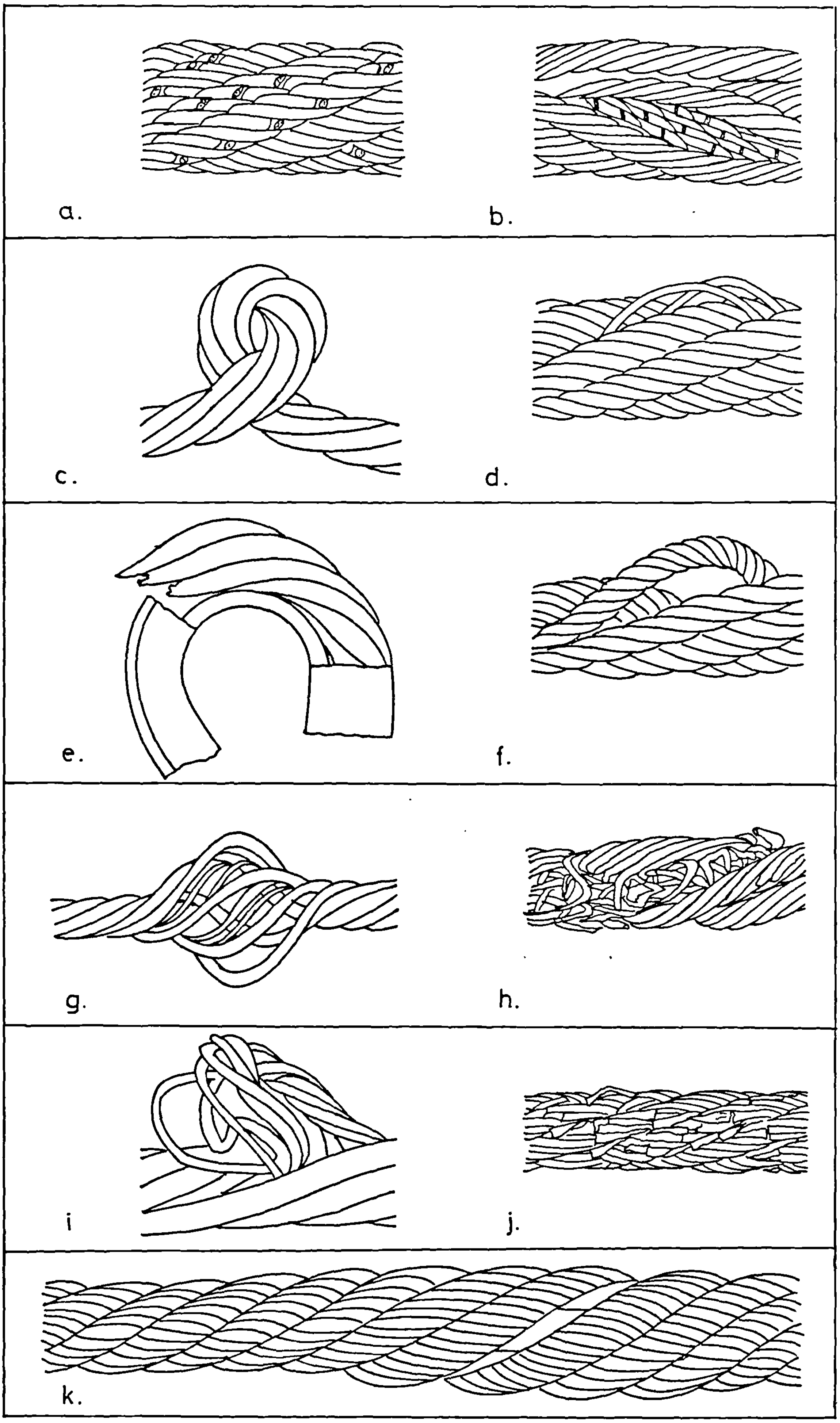

Figure 3·5·1-1

Common Types Of Rope Failures.

3.5.2 Post Test Examination of Large Diameter Wire Rope

If ropes are used in a normal condition and controlled environment (for instance, under fatigue tests in an experimental environment). Rope deterioration will normally be confined to two sources, namely, wear and fatigue. In general, wear is relatively easily identified as compared with fatigue, since wear appears as nicks and grocves on the surface of wires. The author's post test examination of large diameter wire ropes subject to tension-tension fatigue are presented below:

Detail of Rope Constructions are Listed Below:

a. 40 mm dia 6 x 41 (IWRC) ordinary lay rope

b. 70 mm dia 6 x 41 (IWRC) ordinary lay rope

c. 127 mm dia 6 x 49 (IWRC) ordinary lay rope

3.5.2-1 Wear

Although, rope steel has a tensile strength almost four times greater than that of mild steel, the cross sections of wires are much smaller than that of common structural members such as girders. Wires on the outer layer of strands are more vulnerable to damage. In general, wear is categorized into "External Wear" and "Internal Wear" respectively.

(1) External Wear

Wires in the outer-most layer of a rope are bound to be subject to abrasive wear, plastic wear or a combination of the two. Figure 3.5.2-1 (a) and (b) show two common types of external wear, namely, abrasive wear and plastic wear respectively. They result from different degrees of bearing pressure on the surface of the wire as it presses against the hard surface of the groove of a running sheave.

a. Plastic Wear

It is suggested that plastic wear is resulted from the wire surface bearing too heavily on the hard surface of a sheave groove.

b. Abrasive Wear

Abrasive wear, on the other hand, is resulted from the wire surface rubbing too much against the hard surface of a sheave groove.

Since rope steel is coated with galvanized material, in some cases, combined wear situation occurs.

Influence of Rope Lay on External Wear

The degree of damage due to external wear can be altered by using rope lays. Figure 3.5.2-2 (a) and (b) are schematic diagrams representing the damage due to external wear on the wire of Lang's lay rope and ordinary lay rope. Obviously, for wires in the outer-most layer of a Lang's lay rope, the lay configuration provides better and much longer worn crown than

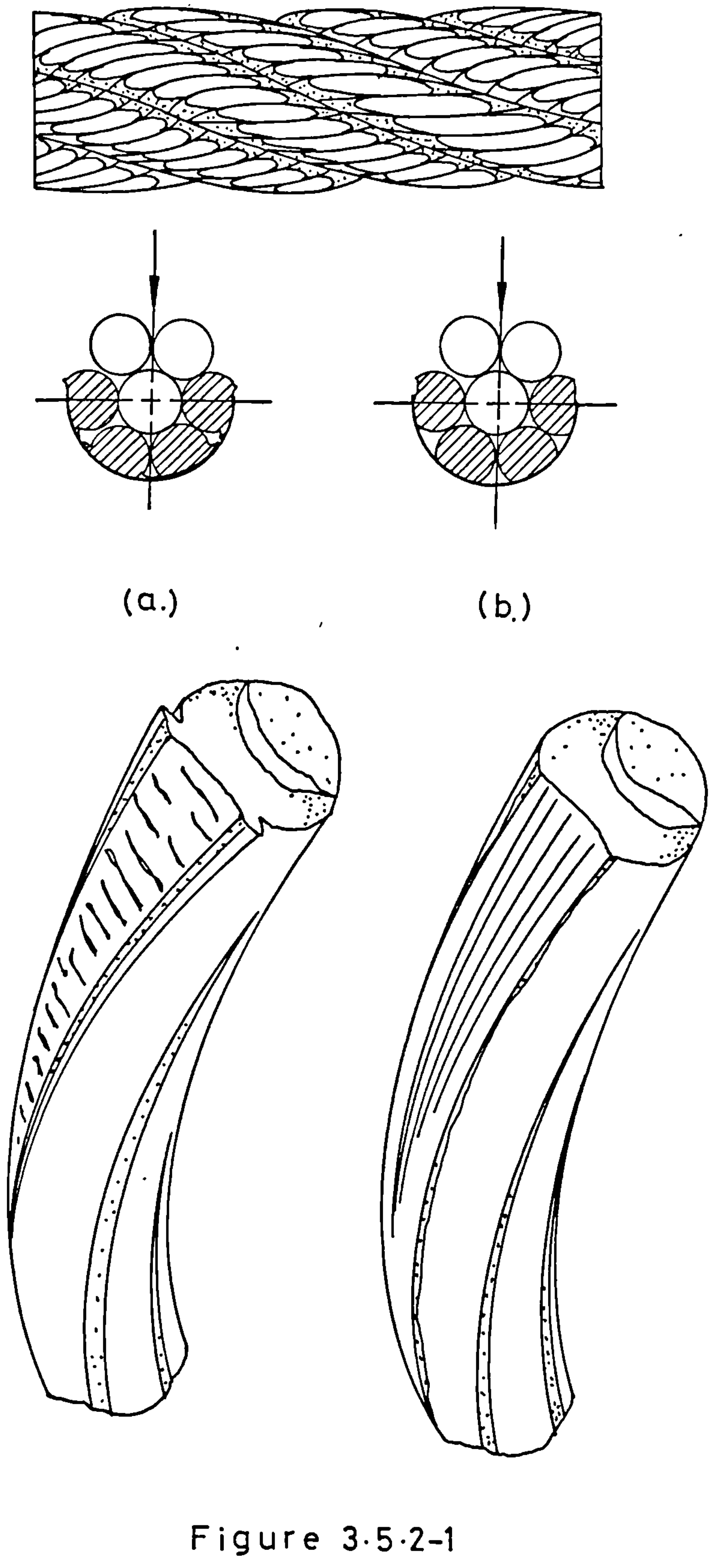

Figure 3.5.2-1

External Wears

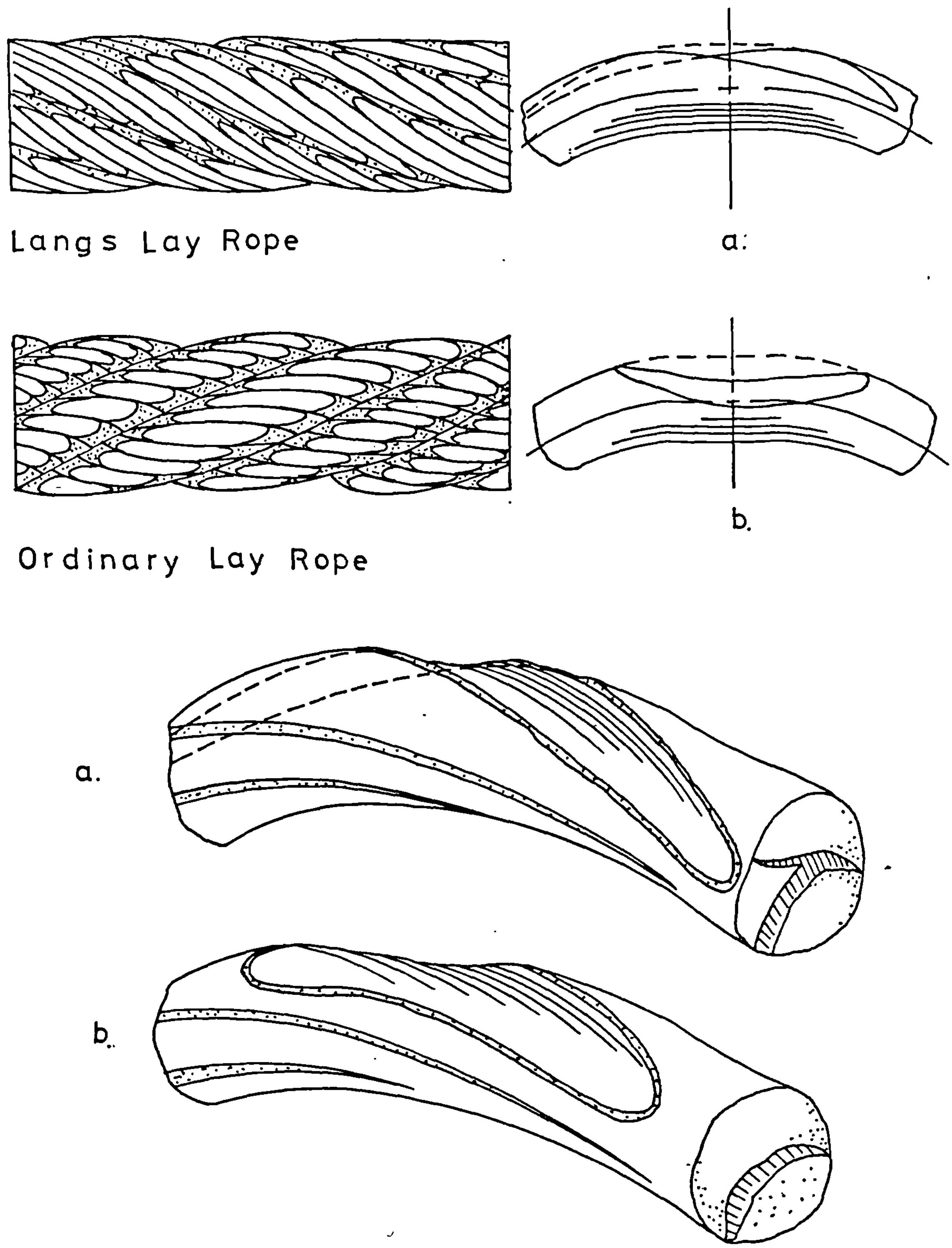

Figure 3·5·2-2

External Wear Features On

Langs Lay & Ordinary Lay Rope

that of the wires in an ordinary lay rope.

(2) Internal Wear

For a rope subjected to axial load, interior wires are bound to cut into one another at their contact points resulted from tightening the geometrical patterns. Figure 3.5.2-3 shows typical internal wear patterns on the wire surface inside the rope, namely, grooves and nicks. The differences between grooves and nicks depend on whether the contacts are continuous or of a discrete nature. The following presents the author's post test examinations on the internal wear of large diameter wire ropes carried out in N.E.L especially 6 x 41 (40 mm and 70 mm diameter rope) and 6 x 29 (127 mm diameter rope) ordinary lay construction, each with a Lang's lay 6/7 I.W.R.C. The work is based on the detailed examination of rope specimens which were subjected to constant amplitude tension-tension fatigue until one of the outer strands failed. Multi-layer outer strands and the IWRC have been considered separately. Figure 3.5.2-4 illustrates the physical appearance of the 6 x 49 construction, 127 mm diameter rope.

a. Multi-Layer Outer Strands

The multi-layer outer strand is a single helical strand located at the outer layer of the rope. All the wires in this strand are in double helical form with the exception of the core wire which is in single helical form. For wires in the

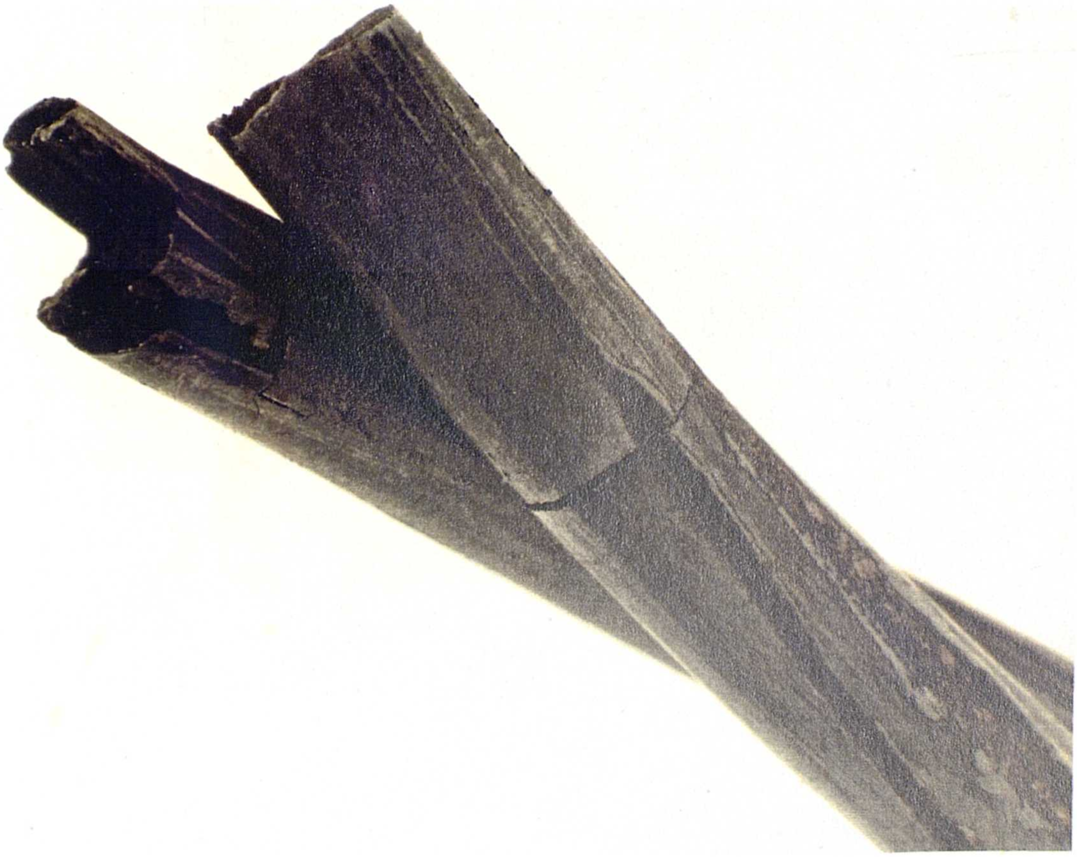

a. Grooving

b. Nicking

Figure 3·5·2-3 Grooving & Nicking

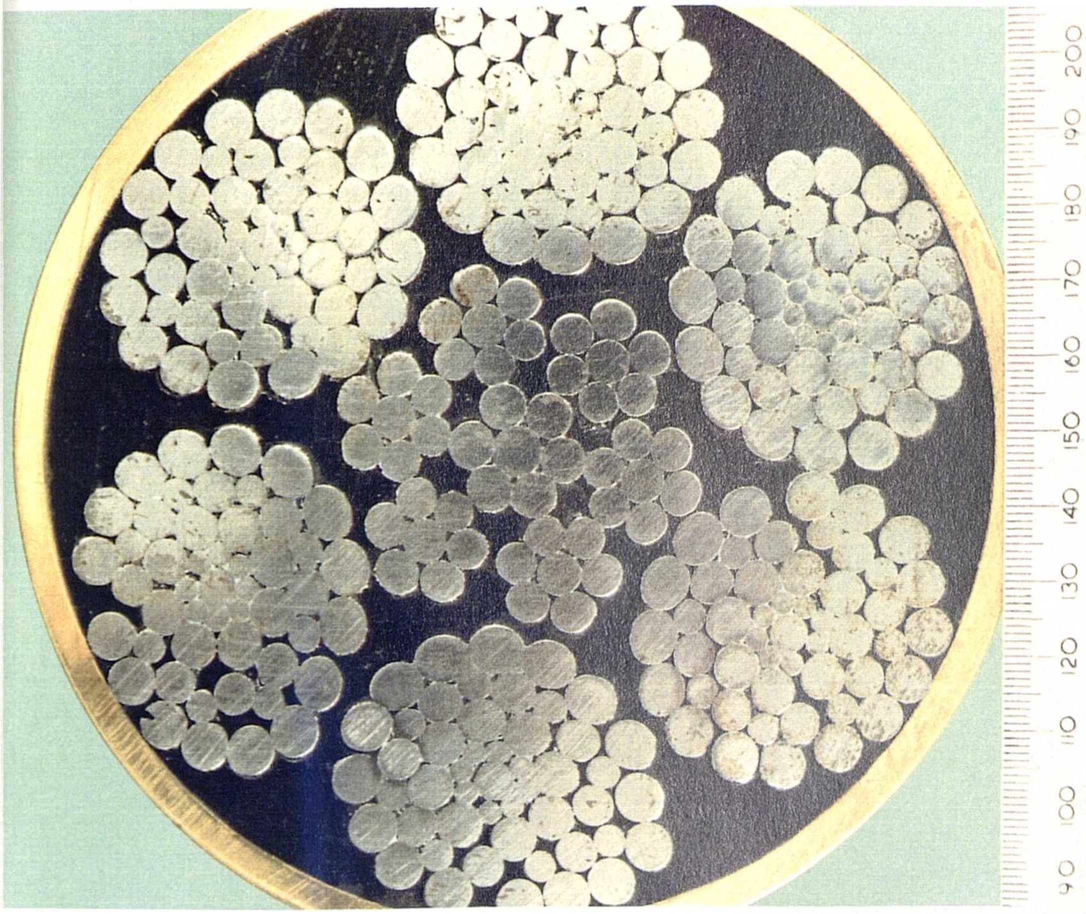

Cross Section Of Six Strand Rope Of 6×49 Construction

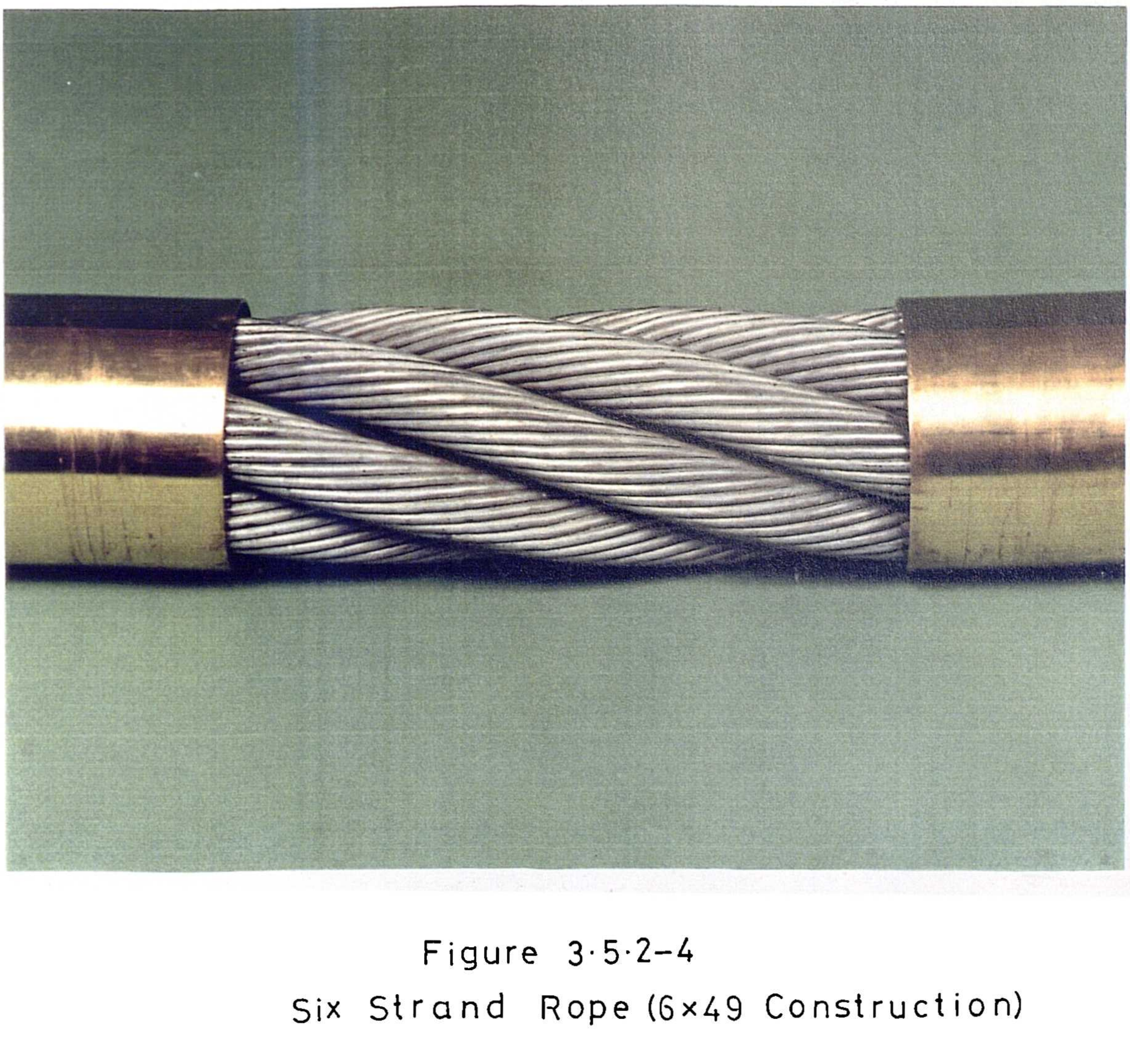

Figure 3·5·2–4
Six Strand Rope (6×49 Construction)

outer-most layer of a multi-layer outer strand, both grooves and nicks are present.

1. Grooves

Figure 3.5.2-5 shows the physical appearance of grooves on each wire of a multi-layer outer strand. For an equal lay multi-layer helical strand, grooves found on each of the wires within the strand are resulted from inter-wire contact amongst neighbouring wires in between adjacent layers. The number of grooves present around the circumference of a wire can be vary between four and eight, depending upon the location of the wire within the strand section. The grooves travel helically along the wires making a double helical pattern on both single and double helical wires. It is also found that the groove is heavier in some places than others along each of the helical wires. It is believed that the heavier grooves result from higher radial force and mechanical interactions of the strands. Grooves are less obvious, if the zinc coating is completely removed from the fatigue failure wire. The significance of the grooves upon fatigue life is not understood at the moment.

2. Nicking

By examining the wires in the outer layer of the strand after testing, the presence of a regular contact patches are revealed. Figure 3.5.2-6 shows the physical

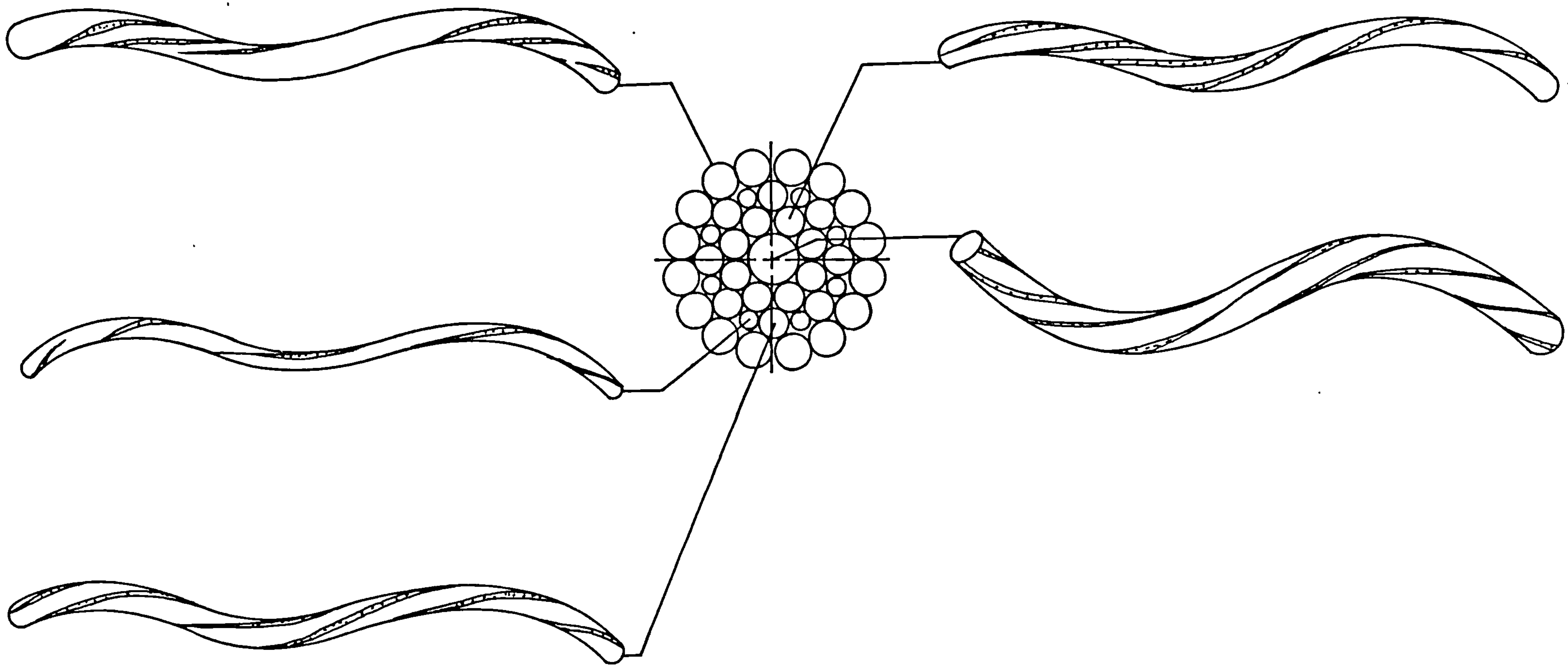

Grooving On The Wires Of The Multi-Layer Outer Strand

Figure 3·5·2-5

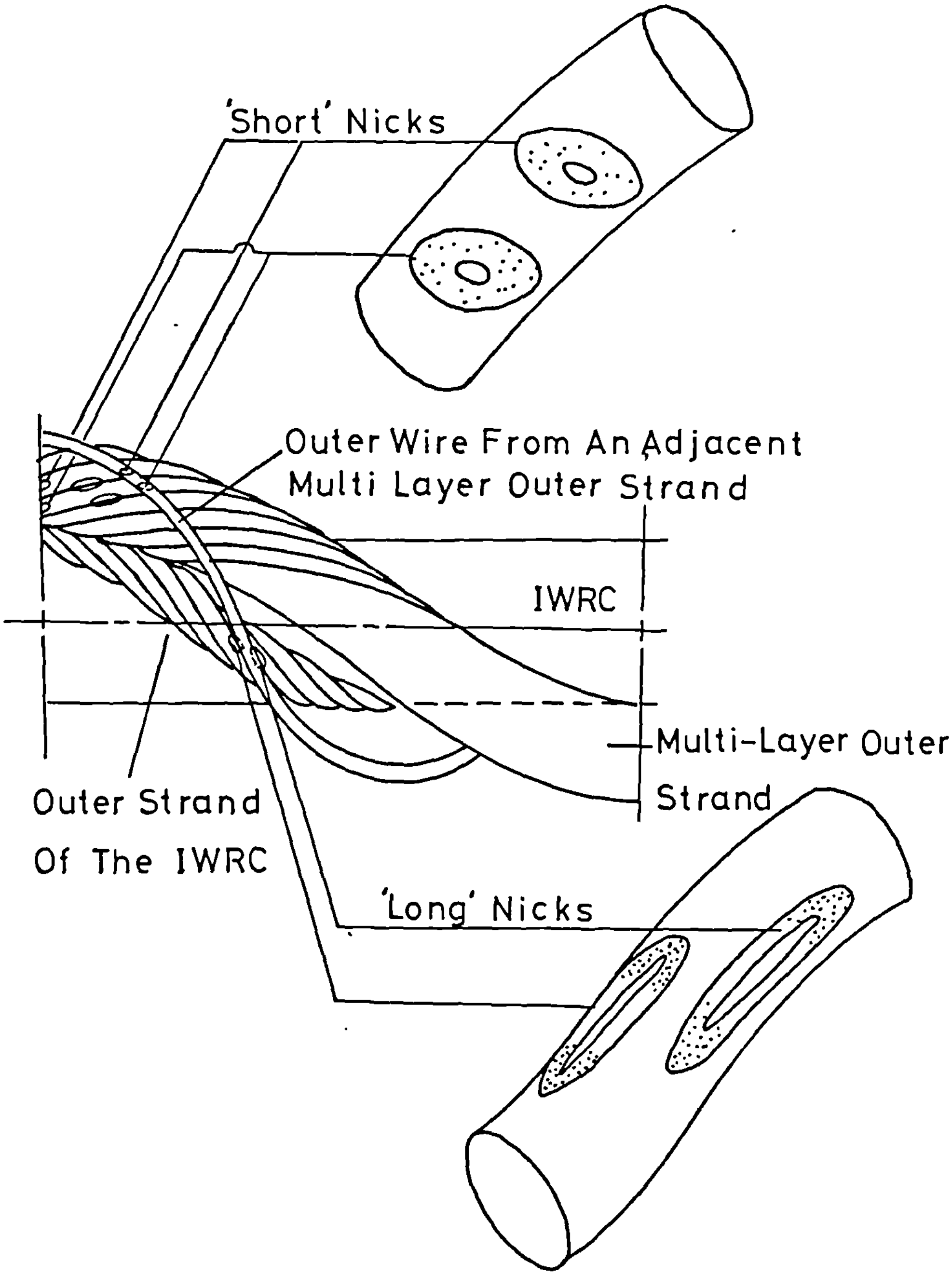

Figure 3·5·2-6
Formation Of Short And Long Contact Patches On The Outer Wires Of The Multi Layer Outer Strands

appearance of nicks on the wires in the outer-most layer of a multi-layer outer strands. Figure 3.5.2-7 helps to explain the pattern. The two pairs of '*short*' contact patches result from inter-wire contact between adjacent multi-layer strands. the central '*long* ' contact patches result from inter-wire contact with the IWRC. These nicks can be found on each of the outer layer wires of the multi-layer strand. It is found (by statistical means) that, under constant amplitude tension-tension fatigue, the vast majority of outer wire breaks occur within this system of contact patches.

b. I.W.R.C

The independent wire rope core is 6/7 Lang's lay type of main core strand which is constructed by laying six (6/1) single helical strands (ie 36 double helical wires and 6 single helical core wires) around a (6/1) straight strand (ie six single helical wires and one straight king wire). By examining the fatigue failed rope, all the physical appearance of wear pattern can be revealed.

1. Grooves

Figures 3.5.2-8 and 3.5.2-9, show the physical appearance of grooves which can be found on each wire of an I.W.R.C. The grooves result from the continuous contact with neighbouring wires. The outer wires (ie all double helical wires) of all the strands each have three

Figure 3·5·2–7

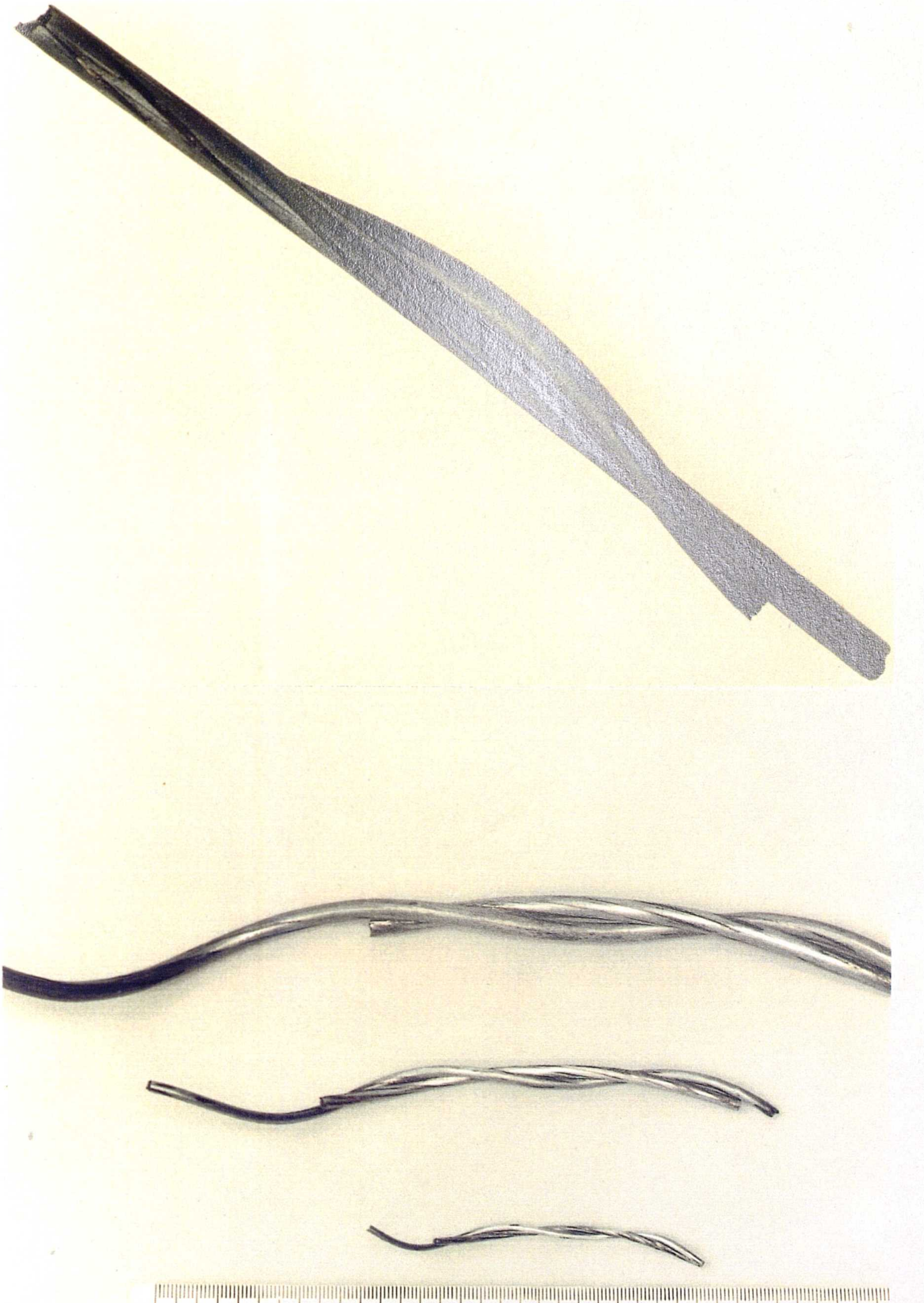

Figure 3·5·2-8

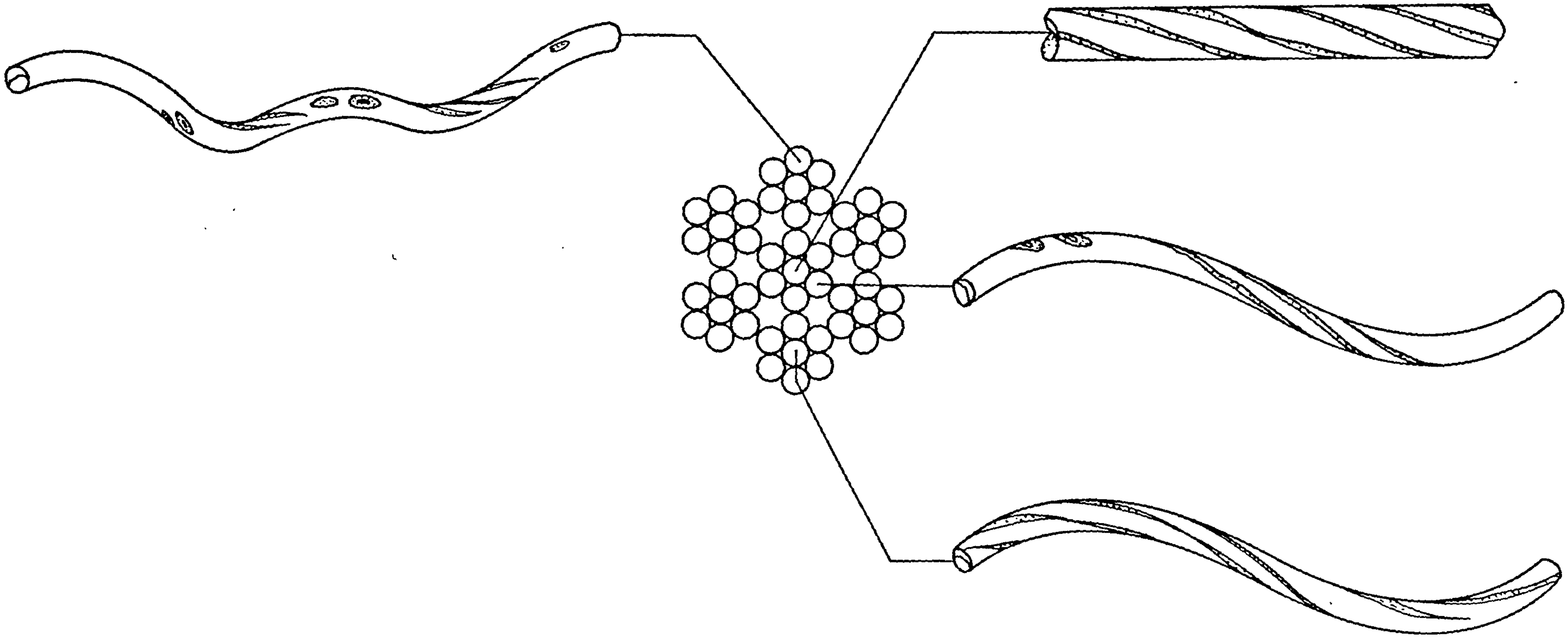

Figure 3·5·2–9
Grooving On The Wires Of The Independent Wire Rope Core

grooves present around their circumference, whereas the six single helical core wires and the king wire each have six. In contrast to the multi-layer outer strands, the grooving appears to be more severe; however, in some places along the double helical wires, the grooves effectively disappear. The variation of the groove severity appears to be result from complex mechanical responses and interactions along the double helical wires.

Again, grooves travelling along both double helical wire and single helical core wire have a double helical form. However, grooves along the straight king wire and the single helical wire of core strand have a single helical form.

2. Nickings

Figures 3.5.2-10, 3.5.2-11 and 3.5.2-12, show the four types of nicks identified. Formation of each of these nicks is described as follows:

i. Type 1 Contact Pairs

Result from contact between two double helical wires of an ordinary lay multi-layer strand with one double helical wires of a Lang's lay IWRC outer strand. These correspond to the 'long' contact patches on the wires of the multi-layer outer strands.

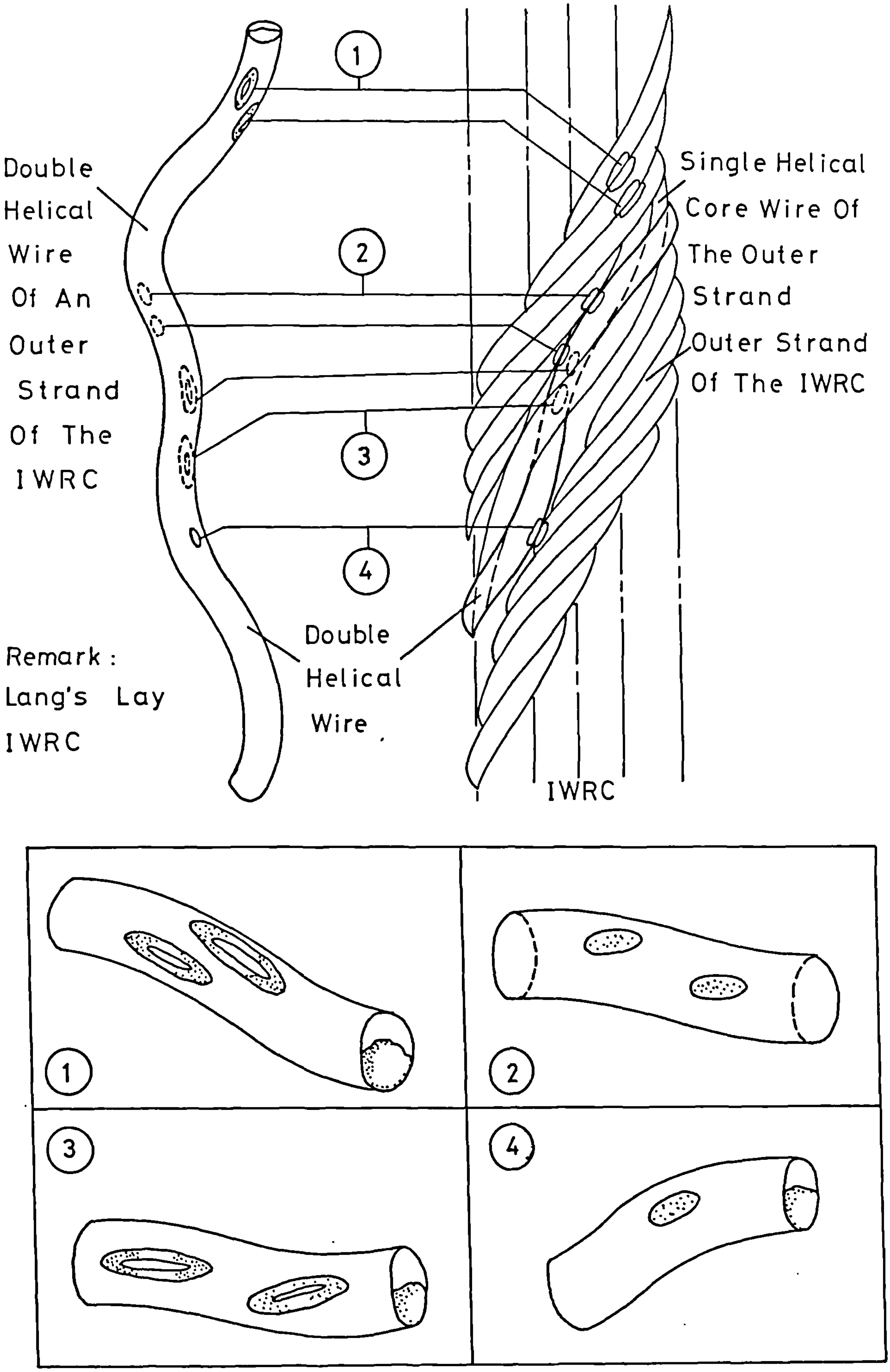

Figure 3·5·2-10

Types Of Discrete Contact Within The IWRC

Type 1.

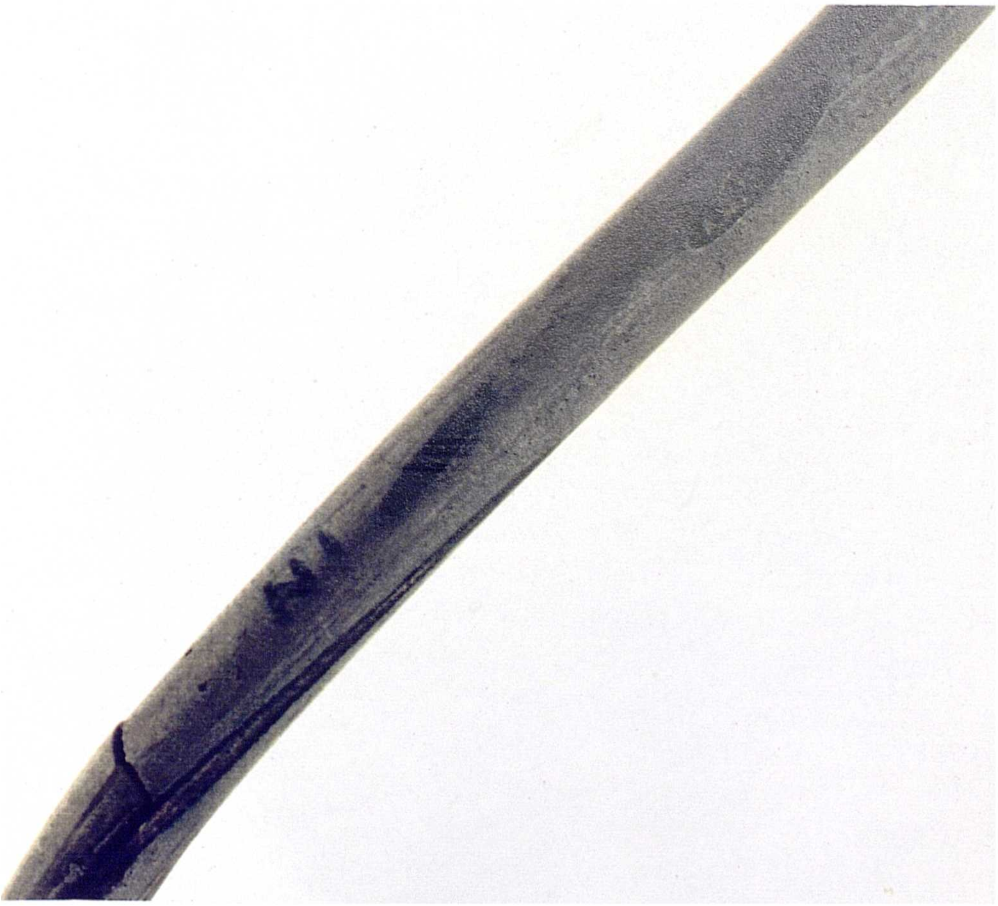

Type 2.

Figure 3·5·2–11

Type 3

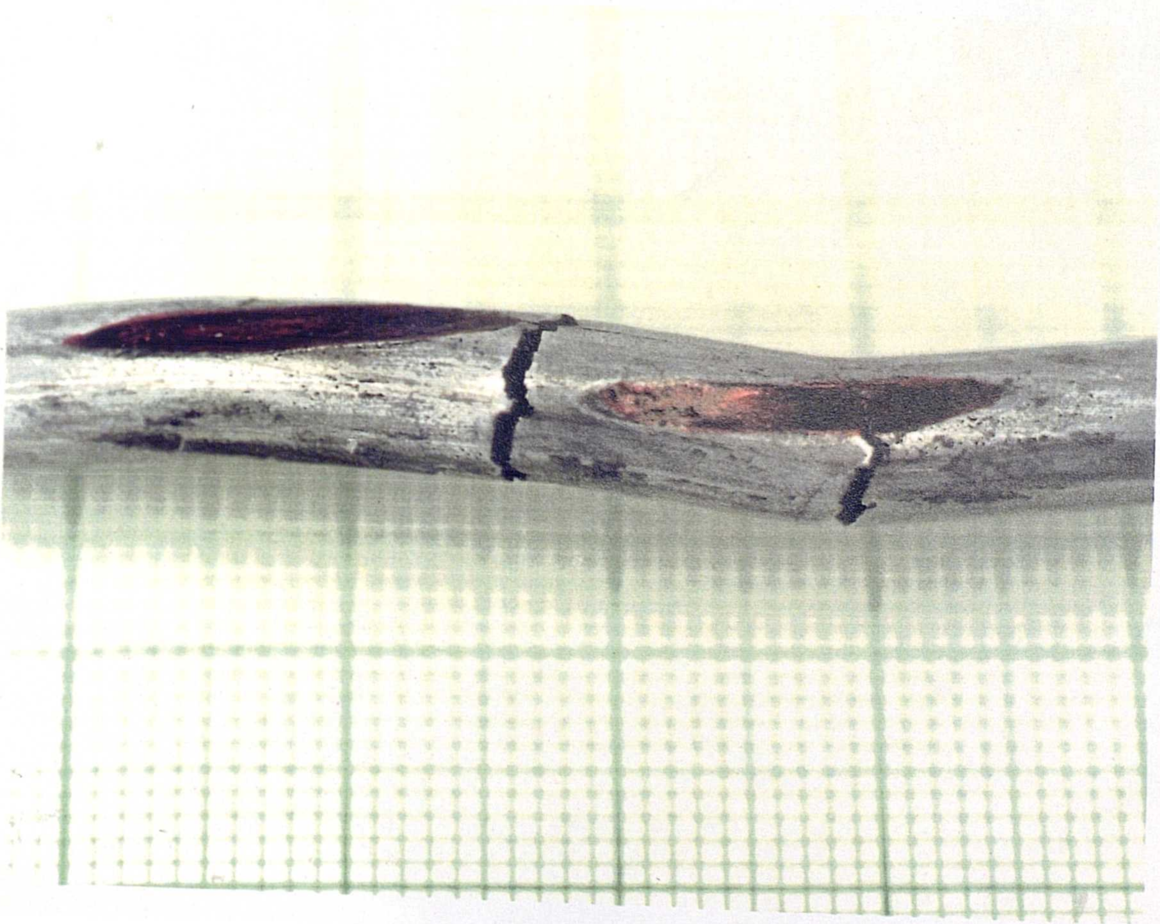

Type 4

Figure 3-5-2-12

ii. Type 2 Contact Pairs

Result from contact between adjacent double helical wires of two neighbouring Lang's lay outer strands of the IWRC. See Figure 3.5.2-10 and Figure 5.4-4 (2) for cross reference.

iii. Type 3 Contact Pairs

Result from contact with a double helical wire of the Lang's lay IWRC outer strand and two single helical wires of the straight core strand.

iv. Type 4 Contact

Result from contact between adjacent double helical wires of two adjacent Lang's lay outer strands of the IWRC. See Figure 3.5.2-10 and Figure 5.4-4(2) in Chapter 5. for cross reference. The contact feature of type 4 contact is similar to type 2 contact. However, both contact types locate at different places.

Figure 3.5.2-13 presents the nicking patterns found on the multi-layer outer strand and on the outer strand of the IWRC. For interest, Figure 3.5.2-14 shows the nicking patterns found on the ordinary lay type of IWRC of a multi-layer stranded rope. Although there is no quantitative evidence to illustrate the significant influence of contact patterns in respect of rope degradation, wear, clamping & pivoting at various contact locations provide favourable conditions for the fatigue crack to initiate and to grow.

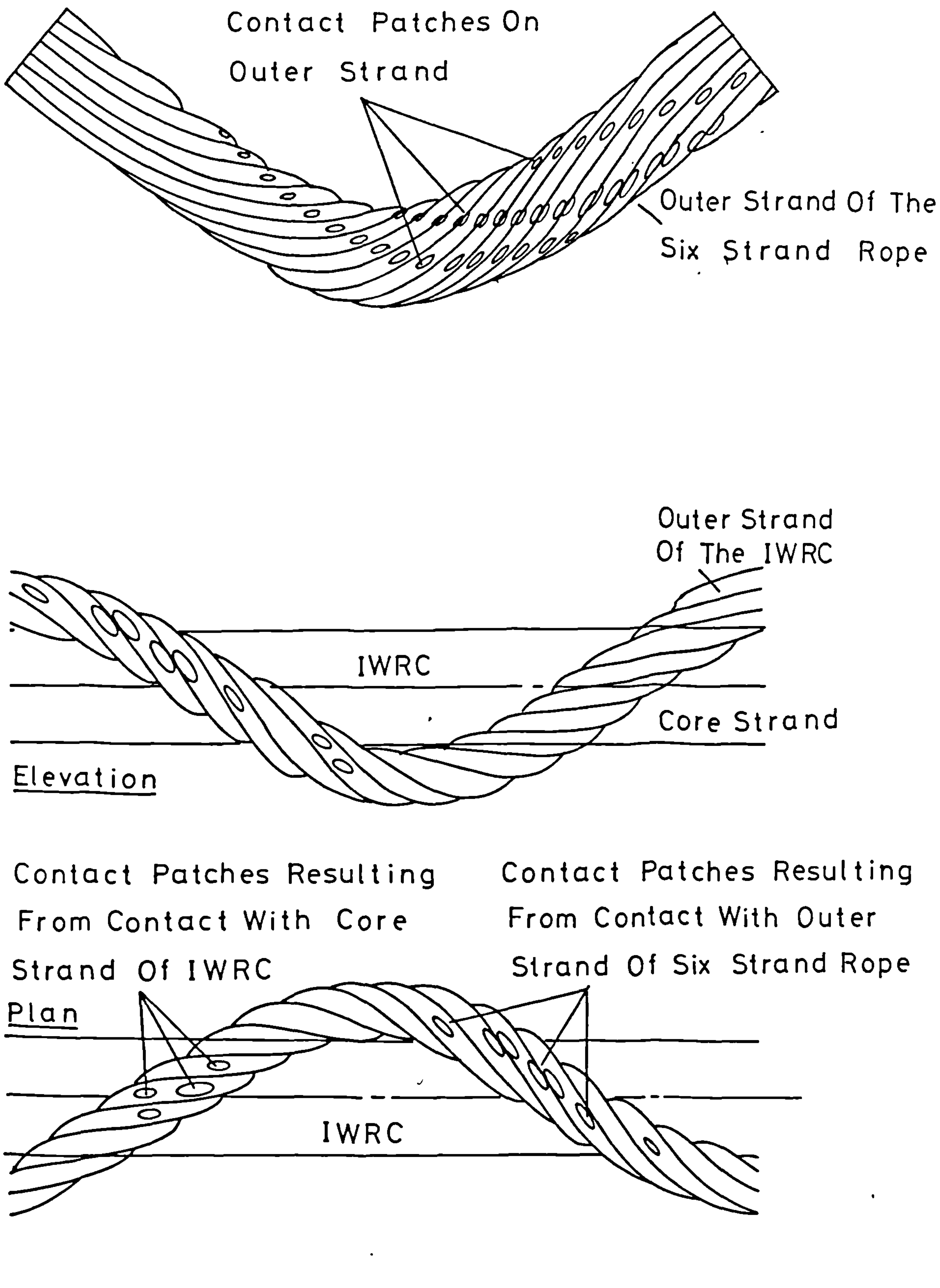

Figure 3·5·2–13

Contact Patches On Outer Wires Of The Helical Strand Of The Six Strand Rope

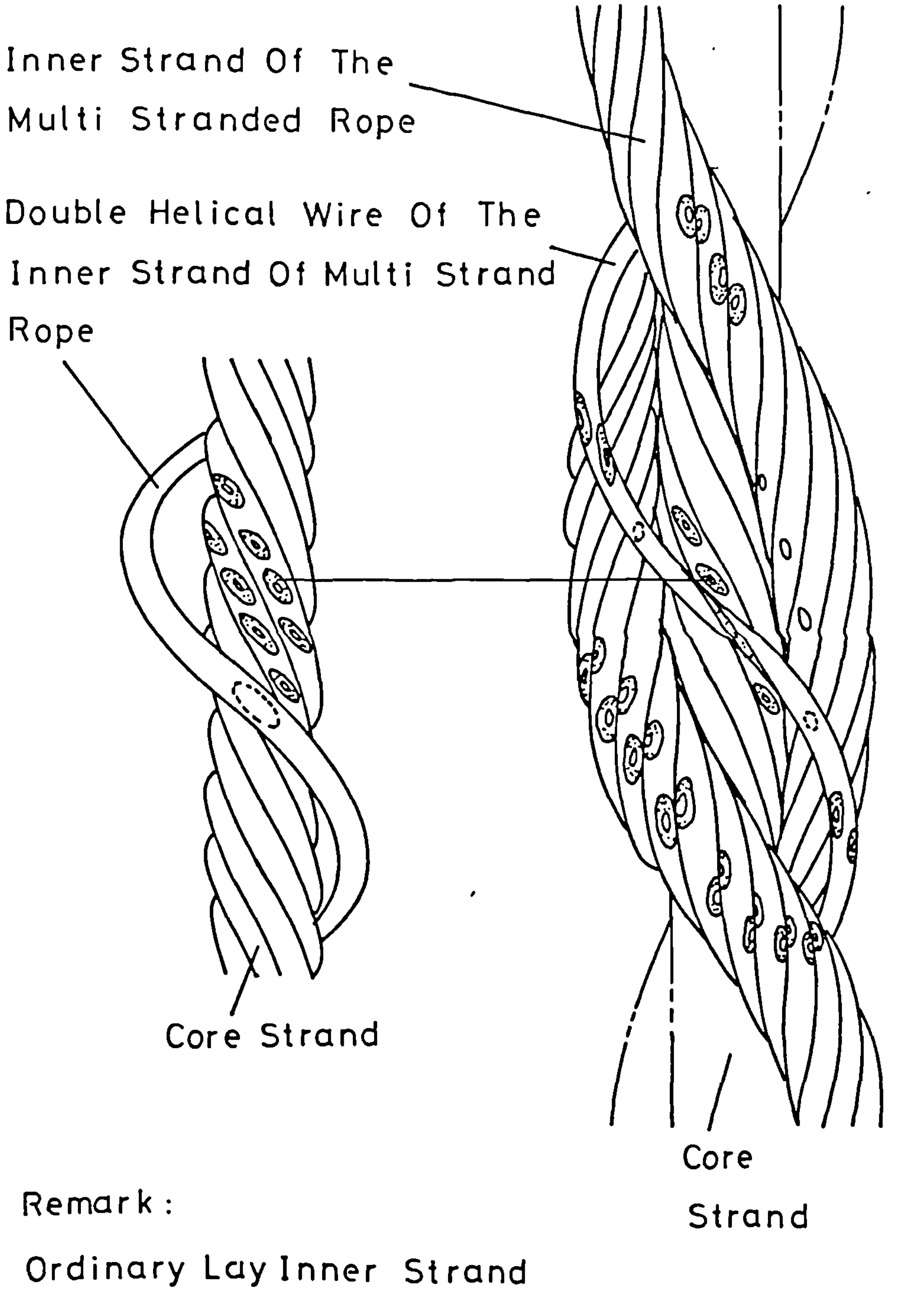

Figure 3.5.2-14

Types Of Discrete Contact Within The Inner Strand Of The Multi Layer Stranded Rope

3.5.2-2 Wire Breakage due to Fatigue

The following section is concerned with categorising the wire breakages which take place under constant amplitude tension-tension fatigue testing on large diameter wire ropes. Effectively, six types of wire breakage have been identified as a result of the very careful post test examinations of fatigued rope sections. In addition, each failure type has been related to the local loading condition present within the rope. These local loading conditions are heavily dependent upon the geometrical configuration of the rope section. Breakage types are:

Type 1 and 2

These failures mostly occur along double helical wires within the IWRC at the regions where mechanical interactions are significant. Cracks initiate at the surface of the wire and initially propagate transversely.

a. For Type 1 Failure (Figure 3.5.2-15 (1) a and Figure 3.5.2-16.a)

Localised torsional stresses alter the direction of crack propagation to that of a combined transverse/longitudinal crack. Failure takes place some distance away from where the crack first initiated.

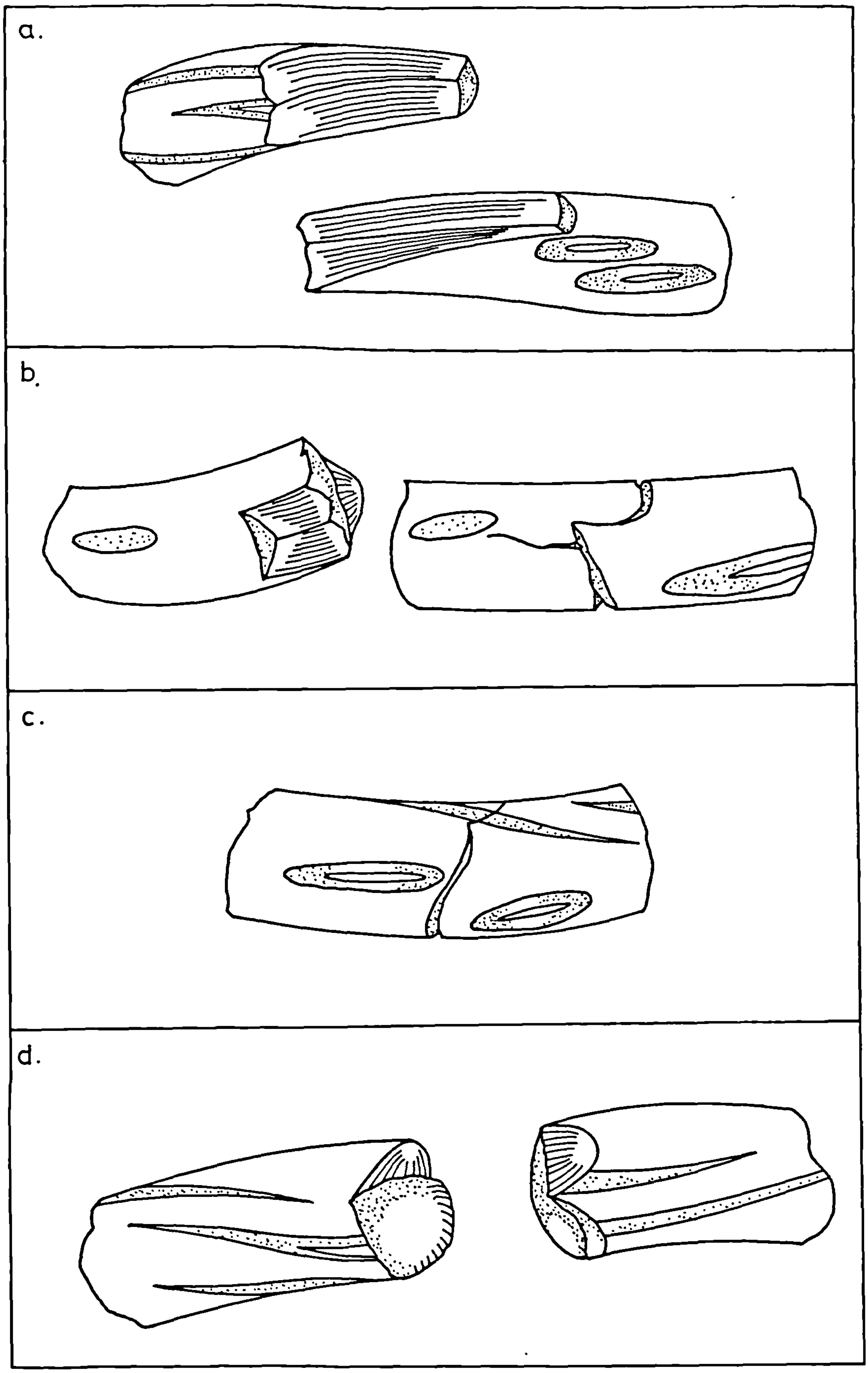

Figure 3.5.2-15 (1)

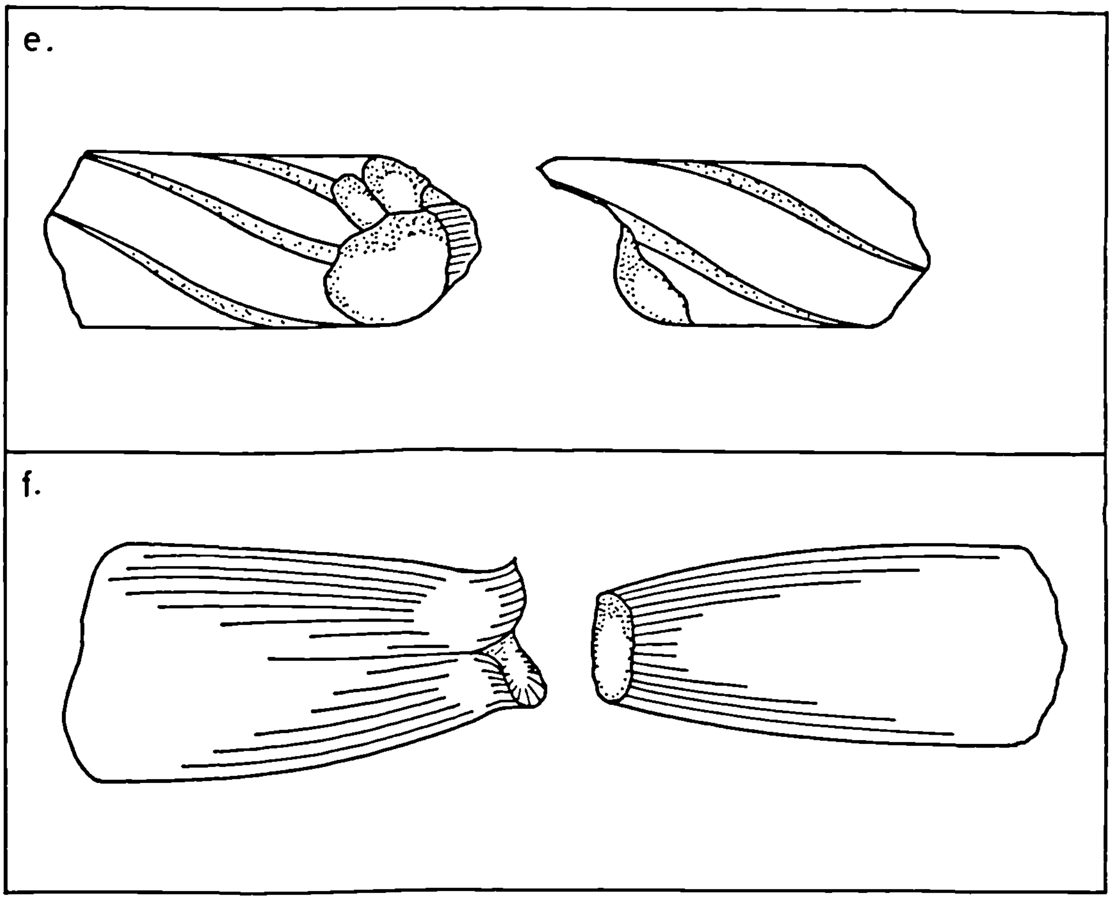

Typtical Wire Failure Found In
Tension Tension Fatigue Rope

Figure 3·5·2-15 (2)

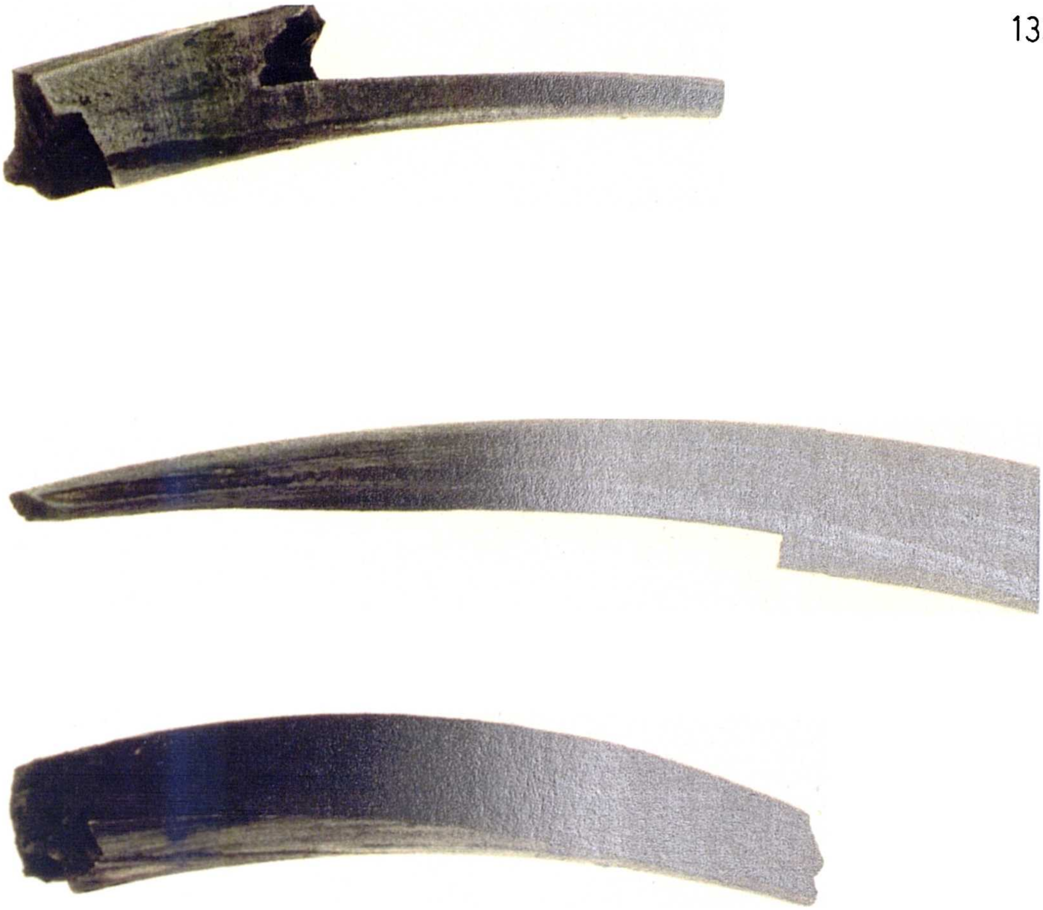

Type a.

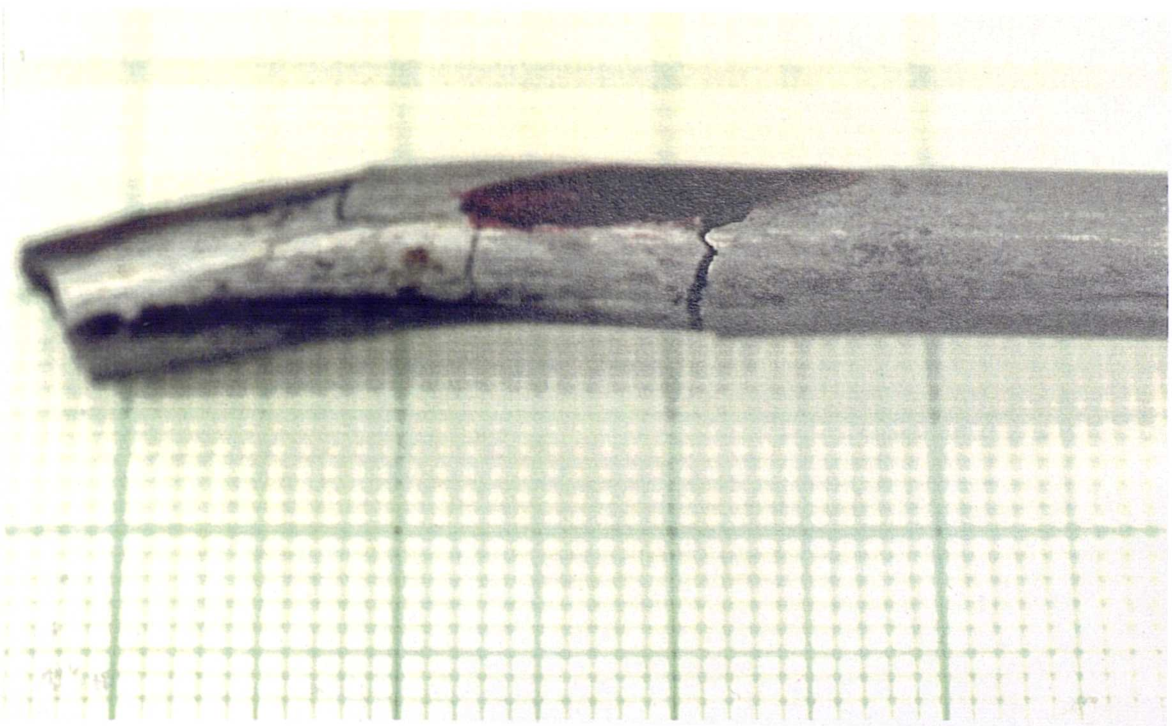

Type b.

Figure 3.5.2-16

b. For Type 2 Failure (Figure 3.5.2-15 (1) b and Figure 3.5.2-16 b)

Transverse crack growth is interrupted by complementary shear stress (resulting from bending component of the double helical wire) and crack propagation continues longitudinally. Transverse crack growth reinitiates at some distance along the wire finally resulting in a stepped fracture surface.

Type 3 (Figure 3.5.2-15 (1) c and Figure 3.5.2-17 a)

This failure type results from secondary 'point' bending due to large mechanical interactions. Failure usually occurs at the gap between any pair of type 3 contact patches.

Type 4 (Figure 3.5.2-15(1).d and Figure 3.5.2-17.b)

This is the most common type of fatigue failure and can occur in both single or double helical wires. Transverse crack propagation takes place and upon final failure a pronounced shear lip is present. This type of failure takes place in regions of low mechanical interactions; thus tensile forces predominate.

Type 5 (Figure 3.5.2-15 (2) e and Figure 3.5.2-18 a)

Failure of this type occurs in the King wire of the IWRC, as a result of combined tensile and torsional stresses. It can

Type c.

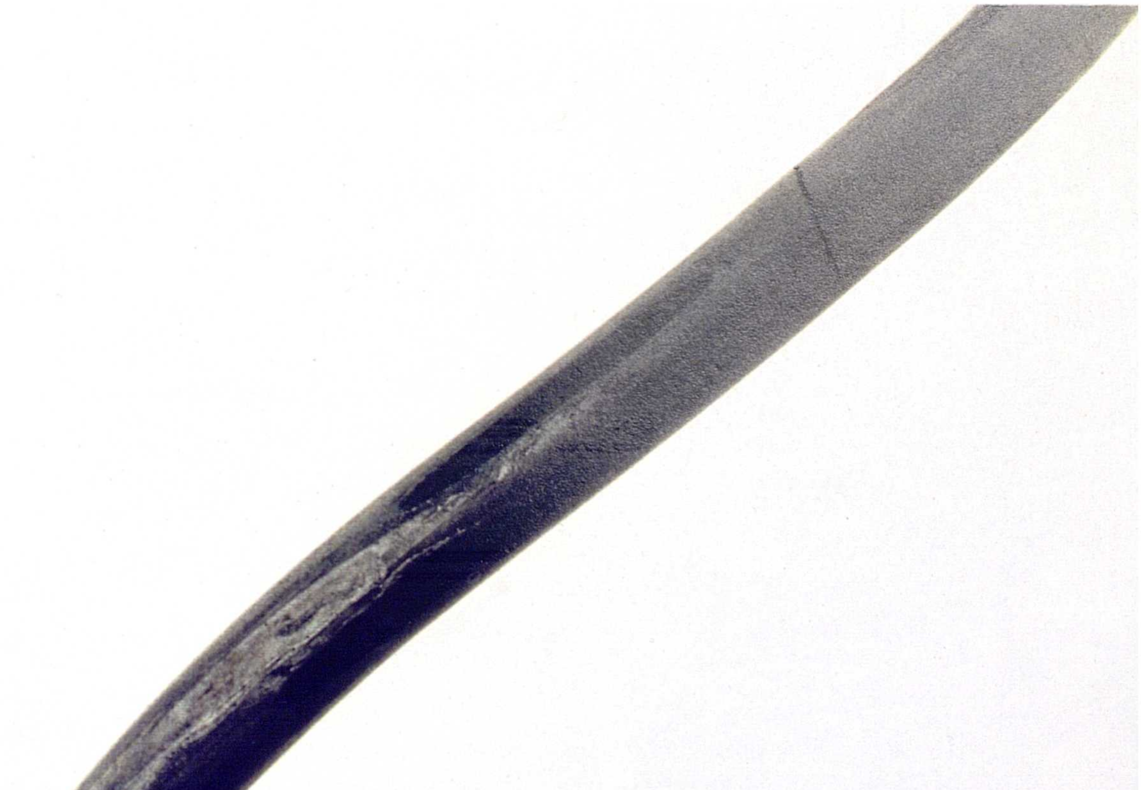

Type d.

Figure 3·5·2 –17

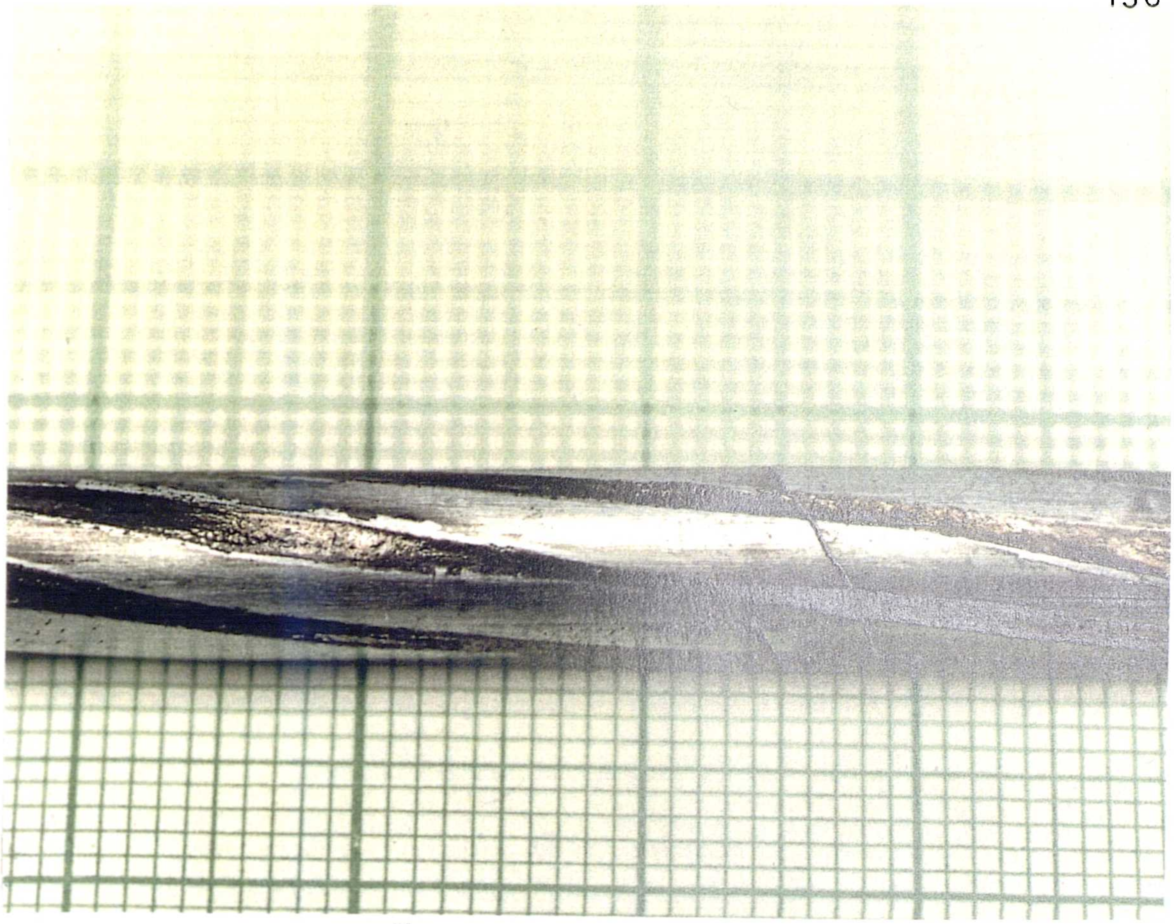

Type e.

Type f.

Figure 3·5·2-18

also be found in the helical core wires of the multi-layer outer strands under high loads.

Type 6 (Figure 3.5.2-15 (2) f and Figure 3.5.2-18 b)

Failures of this type are a direct result of tensile overload producing the cup and cone ductile failure appearances. This type of failure occurs where there are many localised fatigue failures in one or more of the multi-layer outer strands. The remaining unbroken wires within this region can no longer sustain the fatigue load and tensile overloading take place.

Wire failures can also result from other mechanisms, such as from combinations of crushing and abrasion as shown in Figure 3.5.2-19.

3.5.2-3 Broken Wire Counts

Figure 3.5.2-20, presents typical length distributions of broken wires found in the IWRC of large diameter wire ropes. This analysis confirmed that the vast majority of wires were broken within the length between contact patches. This finding was not indicated in reference [3.17].

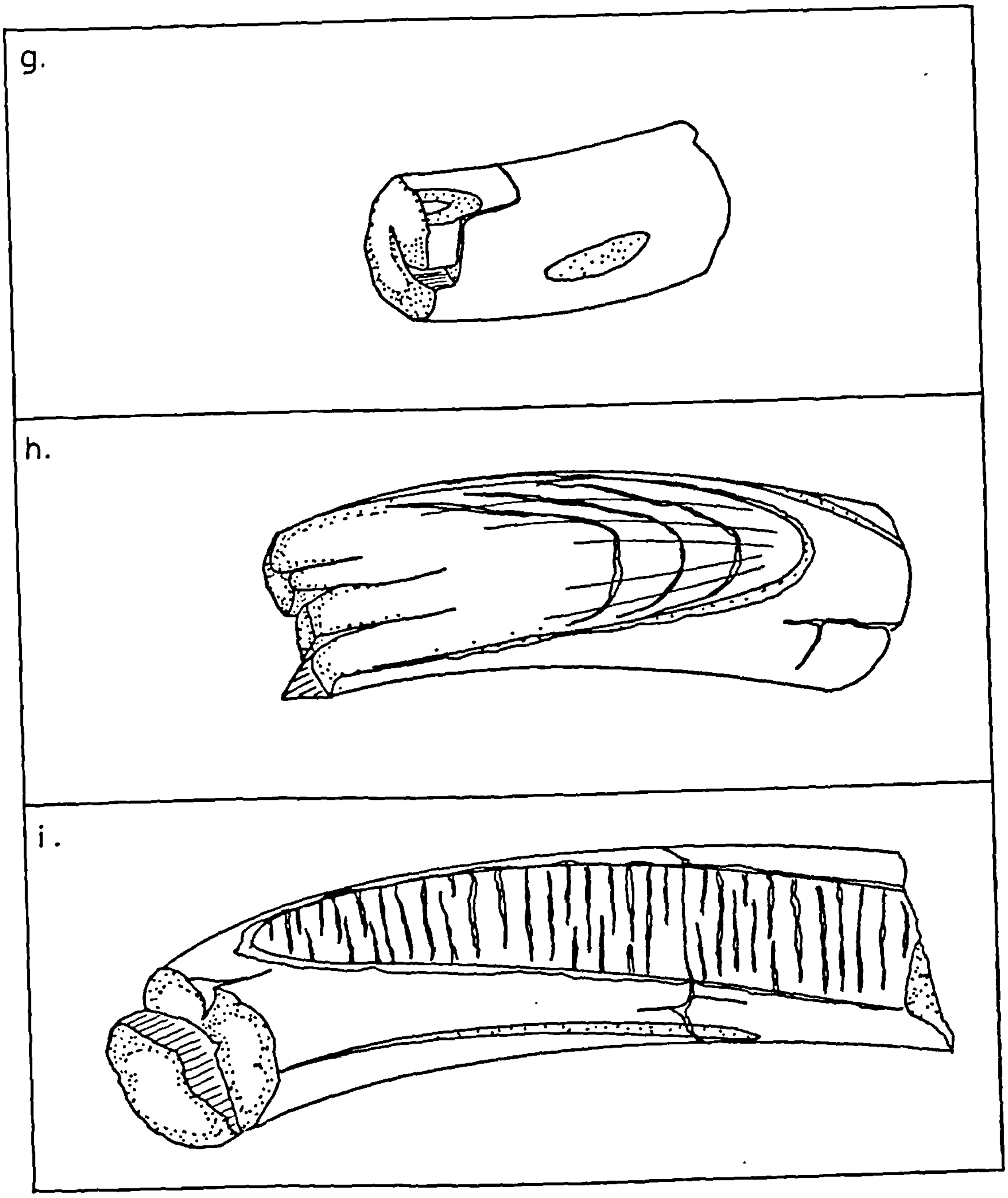

Figure 3·5·2-19

Wire Failure In Rope Due To Wear
And Crushing

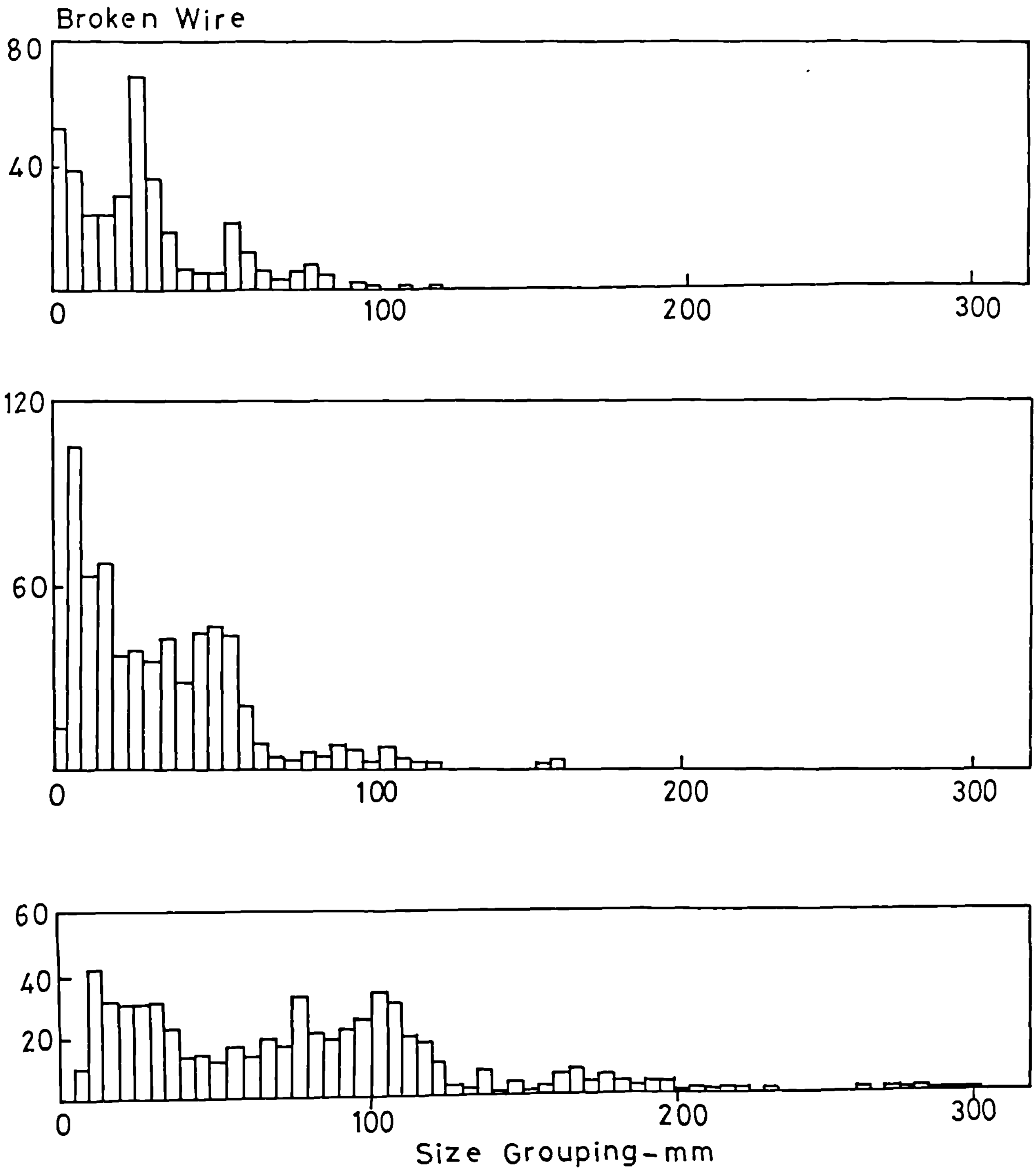

Figure 3.5.2-20

3.6 MECHANICAL AND STRUCTURAL PROPERTIES OF ROUND STRANDED ROPE

This section discusses the application of conventional methods used to evaluate the mechanical properties of round stranded ropes with 6- or 8-outer helical strands, having either a fibre core or a steel core. The author includes evidence of the structural properties of large diameter wire ropes (Φ40, Φ70 and Φ127 mm) obtained by Dr. N F Casey in an N.E.L research program on offshore mooring applications. The physical implications of these structural properties are then explained by the author on the basis of post test rope examinations. Although these conclusions are based an qualitative study, the experimental data reveal the significance of the structural change of large diameter wire rope undergoing tension-tension fatigue test.

The organization of this section is as follow:

Wire Rope Physical Properties

a. Mechanical properties under axial loading[9.9].
b. Structural properties under fatigue test[9.9].
c. Physical implications of structural properties.

3.6.1 Mechanical Properties of Rope Under Axial Loading

This sub-section deals with the mechanical properties of round stranded rope under axial loading within the proportional limit. These properties are summarized as follows:

(1) Extensional Properties

Round stranded ropes are generally used as tensile members which will be stretched under loading. The stretch of a rope aggregates three sources of axial displacements namely:

1. "*Constructional*" elongation
2. Elastic elongation
3. Rotational elongation

a. Constructional Elongation

When the rope is subject to axial tensile loading, the helically laid wires and strands act in a constricting manner thereby compressing the main core and bringing all the elements of the rope into closer contact by filling up all the possible inter-wire spacing. This property results in a slight reduction of rope diameter and lengthening. Constructional elongation is thought to be influenced by the following factors.

1. Type of strand core and main core.
2. Type of outer layer helical strand

3. Types of wire lay and types of rope lay
4. Material properties.

Rope which is constructed with wire main core, wire strand core and independent wire rope core has less constructional elongation than fibre core. Usually, constructional elongation is insignificant for the early stage of fatigue life, if the rope is constructed with steel core. However, some fibre core ropes, if lightly loaded, may exhibit a degree of construction elongation over the majority of their fatigue lives. There are number of complicated and inter-linked factors which will affect constructional elongation. No definite equations or values are assigned to this type of elongation at present in the rope industry.

b. Elastic Elongation

Elastic elongation results from the intrinsic recoverable deformation of the material, provided that it is still within the material elastic limit. Conventionally, elastic elongation cannot be calculated precisely due to the complicated geometry of the wires, the three dimensional changes and the clamping and pivoting which occur. However, a simplified equation in terms of a notional modulus commonly used in the rope industry to approximate this change for some situations. This equation is given by:

Change in length =

$$\frac{\text{Change in Load (N)} \quad \times \quad \text{Rope Length in mm}}{\begin{array}{ll}\text{Cross Sectional Area} & \times \text{ Elasticity Modulus} \\ \text{of a Rope (sq. mm)} & \text{(N/sq. mm)}\end{array}}$$

The cross sectional area of a rope is the sum of the approximate metallic area of strands, and the Modulus of Elasticity is obtained from a rope test. Both quantities are given by the rope manufacturer.

c. Rotational Elongation

Rotational elongation results from unwinding movement of helical strands if the rope terminations are not firmly secured. Again, no definite equations or quantities are assigned to this elongation.

(2) Structural Modulus Of Elasticity For Rope

Wire rope subjected to external tensile load exhibits a degree of nonlinearity on the load-extension curve. These nonlinear properties have long been recognised by rope workers. In order to evaluate the approximate rope elongation at any portion of the load-extension curve within the "proportional limit" of the rope, the slope of the load-extension curve is split into a low-load and high-load portion at 20 percent of the load range. In other words, the load-extension curve is approximated by two straight lines with different slopes. A schematic representation is given is Figure 3.6.1 in order to illustrate this method.

In the low-load portion, the sources of displacements are the sum of

a. Elastic elongation and
b. Constructional elongation. (the changes can be noted)

In the high-load portion (from 20% to 65%)of the rope nominal strength the sources of displacements are the sum of

a. Elastic elongation. (more changes as compared with b.)
b. Constructional elongation.

The method presented above is only applicable for a new formed rope provided that the loading is still within the proportional limit (similar to elastic limit).

(3) Proportional Limit of a Rope

Proportional limit has virtually the same meaning as elastic limit. This is a notional limit of a rope.

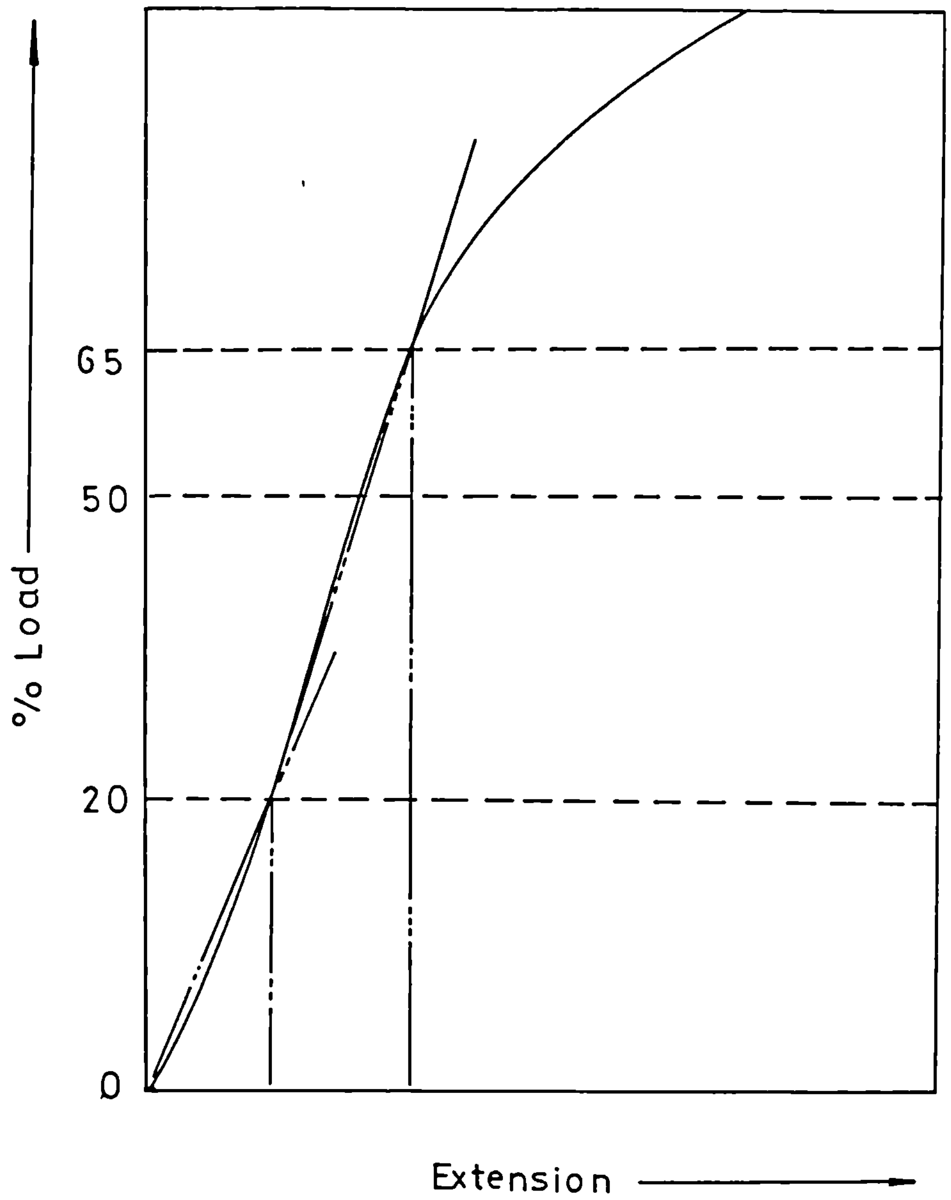

Typtical Load Extension
Curve For Wire Rope

Figure 3·6·1

3.6.1-1 Definitions of Breaking Loads

(1) Minimum breaking force (in kN)

The tensile force applied to a rope below which the rope shall not break when tested to destruction.

(2) Minimum breaking load. (in Tonnes)

The tensile load corresponding to the minimum breaking force.

(3) Calculated aggregate breaking load

This value is calculated from the product of the cross sectional metallic area of a rope and the tensile grades of the wires. The cross sectional metallic area of a rope is the sum of the cross sectional metallic areas of all the individual wires in a rope. In general, the metallic area of wires is directly proportional to the square of the nominal diameter of the rope.

3.6.2 Structural Properties of Rope Under Cyclic Loading (summarized from N.E.L internal report)

Rope with different geometrical pattern, different strand lay and rope lay configuration display different structural properties. However, by using the Load/Extension data obtained during a fatigue test, various structural properties of ropes can be measured. Figure 3.6.2 is a schematic representation of rope properties measured from the load

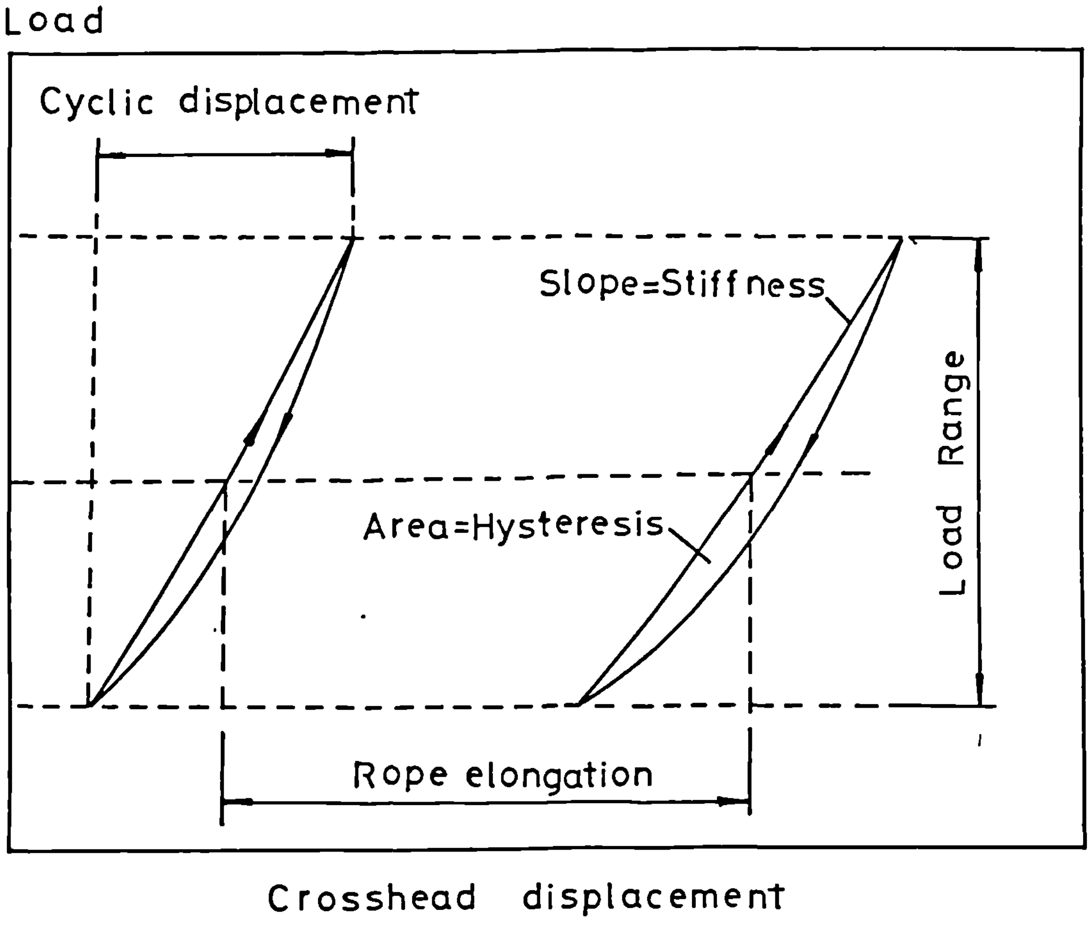

Schematic Representation Of Rope Properties
Measured From Load Extension Data

Figure 3·6·2

extension data. They are

a. Stiffness
b. Cyclic displacement
c. Hysteresis and
d. Elongation

(1) Rope Stiffness

Rope stiffness is defined as the gradient of the load-extension curve. Linear regression was used to produce a best fitting straight line to approximate this slope. The stiffness can be used to determine the proportional (elastic) modulus of the rope by using:

$$\text{Proportional modulus} = E = M \frac{L}{A}$$

where

M is the rope stiffness

L is the rope length at the date measurement point, and

A is the original metallic cross-sectional area of rope

N.B. The termination conditions (see Chapter 7) can alter the proportional modulus of a rope.

(2) Cyclic Displacement

Cyclic displacement is the movement of the rope between the minimum and maximum cyclic load. It can be expressed as percentage of strain by dividing the cyclic displacement by the original length of a rope.

(3) Rope Hysteresis

This is a measure of the energy dissipated in any given fatigue cycle, being the loss of energy of the entire rope and test system. Energy loss includes the elastic-plastic deformation, the frictional heat, the wire breakages and the collection of any other small losses from the rope and from the test system. The area within the hysteresis loop is termed as the loss of energy due to hysteresis. The area within the hysteresis loop is obtained by subtracting the area under the unloading curve from the area under the loading curve.

(4) Rope Elongation

Rope elongation is the increase in rope length which takes place during a fatigue test. It is measured using the mean cross-head displacement and is expressed in terms of percentage of strain by dividing by the original rope length.

3.6.3 Physical Implications Of Structural Change Rope During Tension-Tension Fatigue Test

Figures 3.6.3 (1), (2), (3) and (4) show the typical changes in rope structural properties which take place during tension-tension fatigue testing of wire rope. The tests were carried out at N.E.L on 40 mm, 70 mm and 127 mm diameter six stranded rope, with an independent wire rope core (IWRC). Figure 3.6.3 (5) is the change of rope stiffness against % of rope life for the same rope construction but at 19 mm diameter. This test was carried out at the Reading University [9.7].

Experimental results (see Figure 3.6.3) show that in the early stage of the rope life (approximately from 0 to 20 percentage of rope life), there are rapid increases in elongation, stiffness and temperature with a corresponding decrease in hysteresis and cyclic displacement. At approximately 20 to 30 percent of rope life, there is a transition period where the rope properties remain relatively constant. At approximately 30 percent of rope life, stiffness starts to decrease and hysteresis, cyclic displacement and temperature start to increase. Thereafter, the rate of change for each property is relatively constant until the last 15% of rope life where a significantly rapid changes take place.

From post-test examination of wire rope, the author has firm evidence to suggest that the first rapid changes in rope structural properties correspond to the significant "bedding in" of the outer strands; small number of wire breakage can

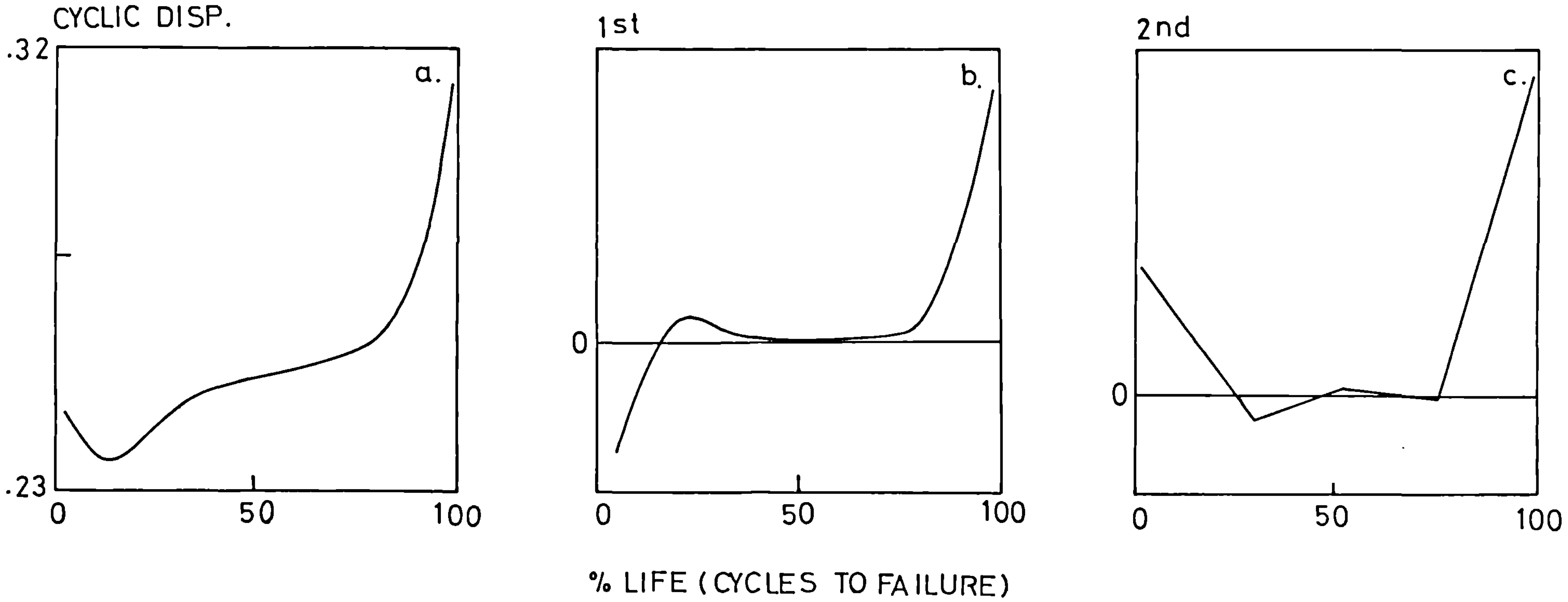

a. Cyclic Displacement vs % Life

b. 1st Derivative of Cyclic Disp. vs % Life

c 2nd Derivative of Cyclic Disp vs % Life

Figure 3·6·3 (1)

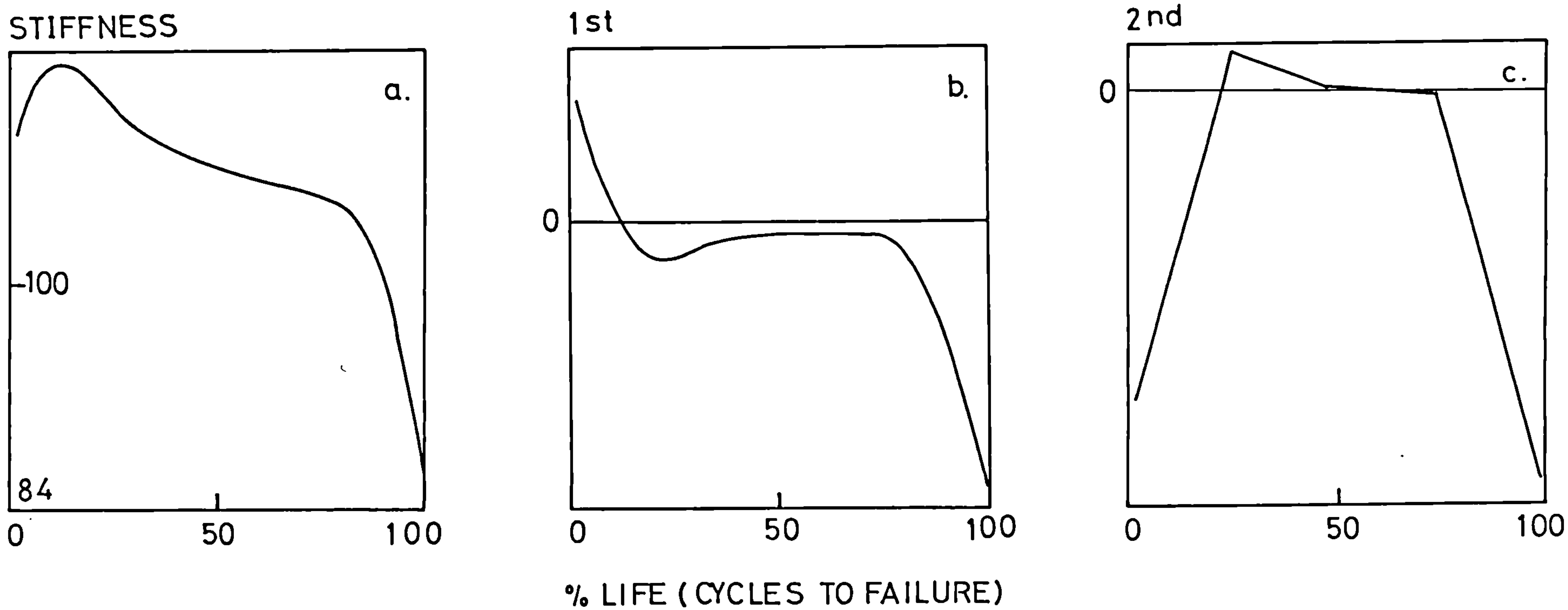

a. Stiffness vs % Life

b. 1st Derivative of Stiffness vs % Life

c. 2nd Derivative of Stiffness vs % Life

Figure 3·6·3 (2)

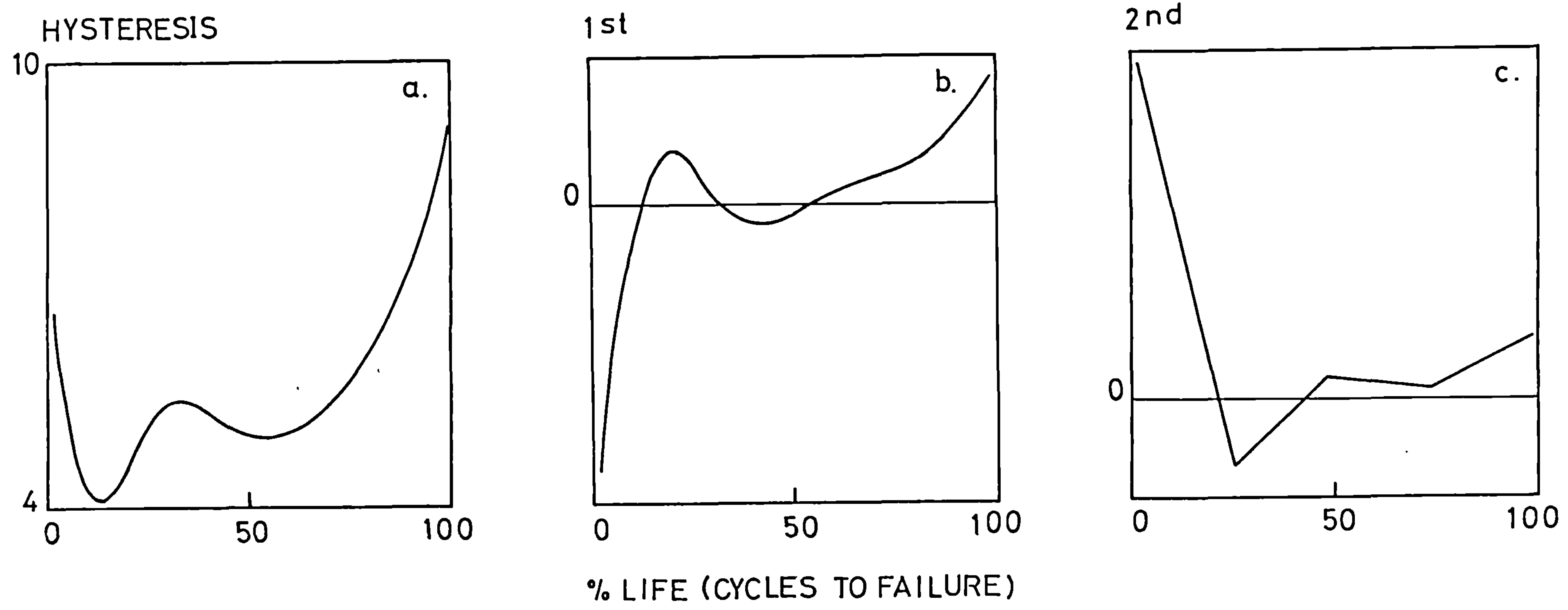

a. Hysteresis vs % LIfe

b. 1st Derivative of Hysteresis vs % Life

c. 2nd Derivative of Hysteresis vs % Life

Figure 3·6·3 (3)

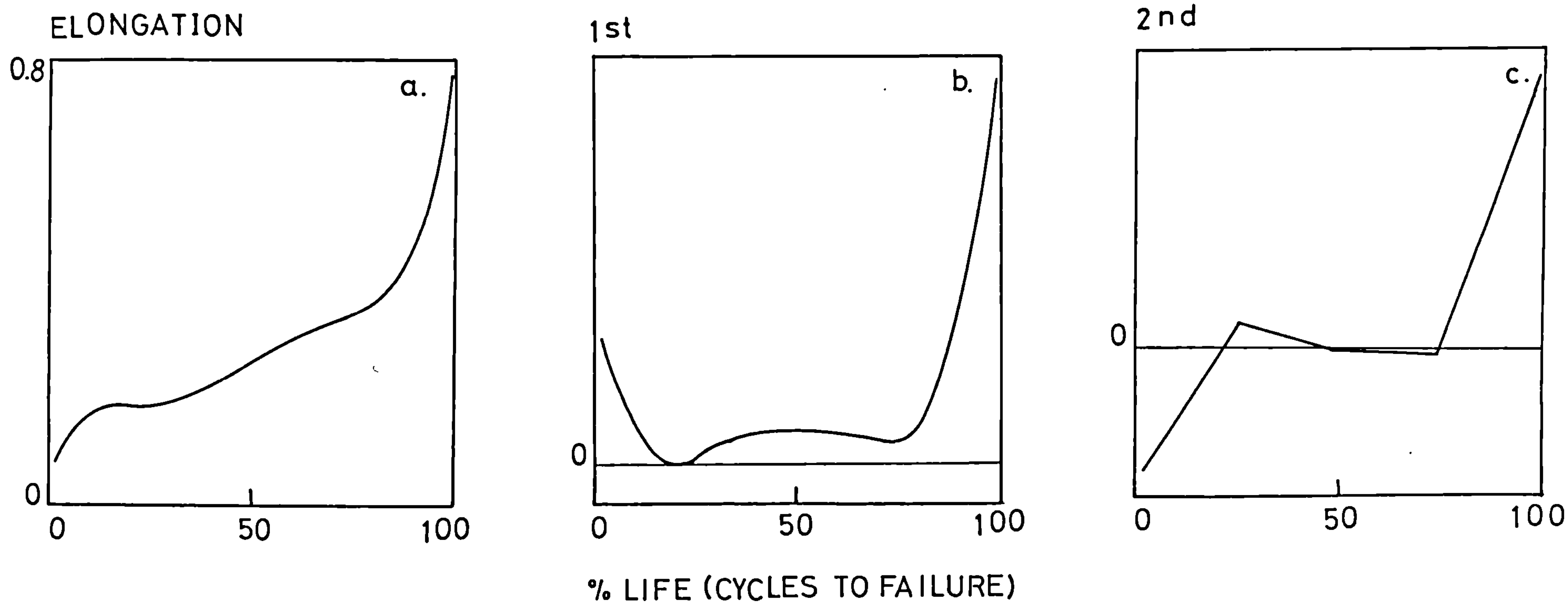

a. Elongation vs % Life

b. 1st Derivative of Elongation vs % Life

c. 2nd Derivative of Elongation vs % Life

Figure 3·6·3 (4)

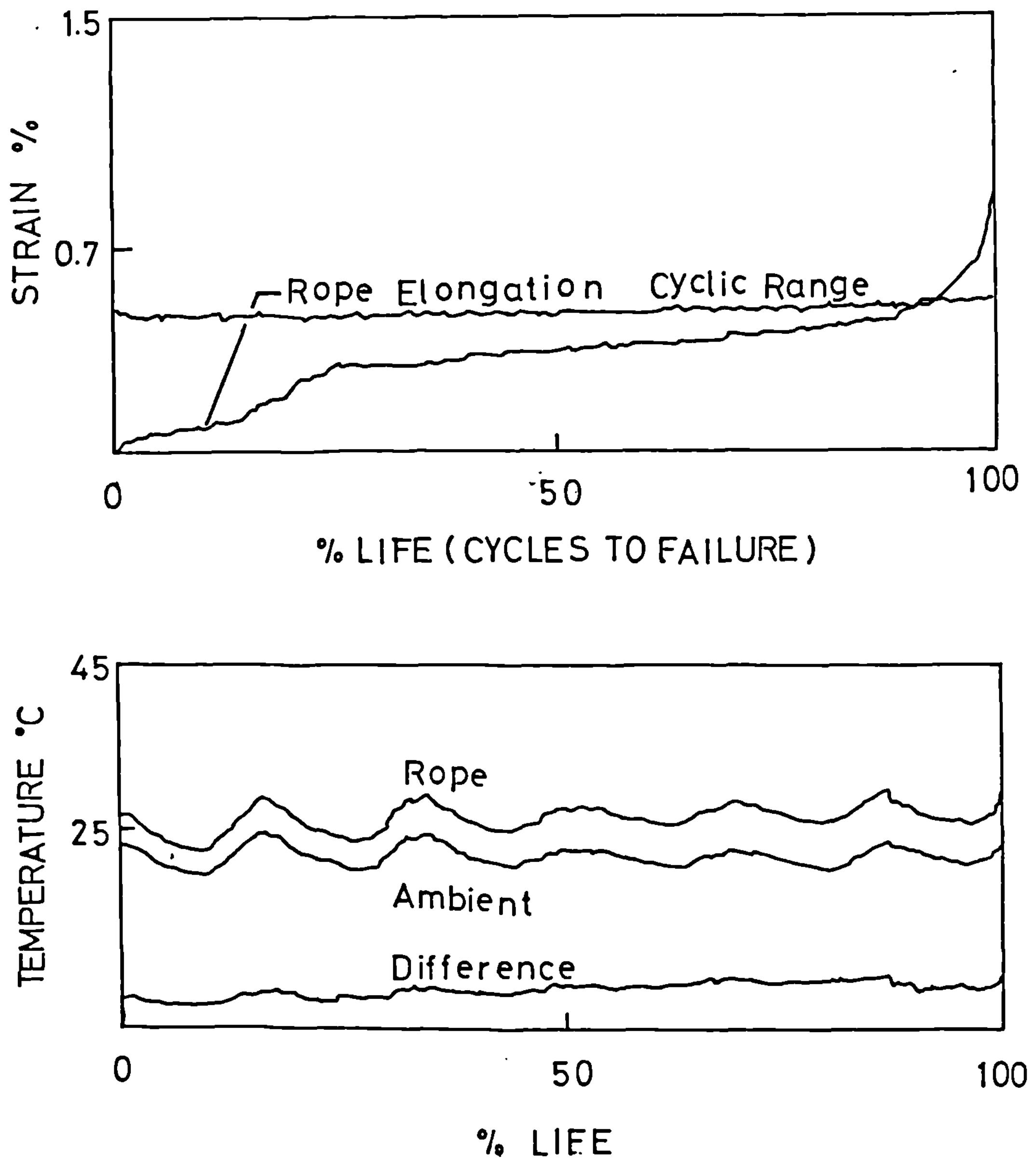

Property Monitoring Plots Over Life For Rope Subject To T-T Fatigue (From Chaplin & Tantrum)

Figure 3·6·3 (5)

be found in the IWRC. At the beginning transition region, the rope structure is brought to the tightest condition. The number of wire breakage is increased at a constant rate within this region. Until the last 15% of life where a problem has developed on one of the outer strands which causes the rapid change of structural properties. This study leads to important understanding of the fatigue performance of this particular type of rope based on the change of the structural properties at each stage.

3.7 Wire Rope Selection

The wide range of rope constructions are designed and have been developed to serve various engineering applications in a changing environment.

3.7-1 Grades Of Rope

To satisfy the requirements for varying strength, toughness, flexibility, abrasion resistance and corrosion resistance, wire rope is manufactured in the following grades for general crane and lifting safety operation.

a. Grade 200 (130 tonf/sq in or 2008 MN/sq m)

Used for installation where maximum rope tensile strength is required.

b. Grade 180 (115 tonf/sq in or 1776 MN/sq m)

Used for installation where tensile strength above grade 160 is needed and for rope needed which is to be run over sheaves or wound around drums.

c. Grade 160 (102 tonf/sq in or 1575 MN/sq m)

Used for installations where there are special needs for a combination of tensile strength and wearing qualities.

d. Grade 134 (92 tonf/sq in or 1420 MN/sq m)

Used for installation where lower tensile strength and resistance to wear are needed than Grade 160.

3.7-2 Rope Service Requirements

The six essential factors for selection of rope are

a. Tensile Strength Of Rope

Rope must possess sufficient strength to carry the required maximum load plus the necessary factor of safety. The strength of a wire rope depends on its size, grade of wire and type of strand core and main core. This table presents the most common safety factors:

Purpose	Safety Factor
Carry Personnel	12 : 1
Running Rope On Drum Or On Sheave Of Crane	4.5-5.5 : 1
Running Rope ON Drum Sheave For Erecting Jib	3.75 : 1
For Pendants Or Standing Rope	3.5 - 4 : 1
For Pendants Or Standing When Erecting Jib	3 : 1

For details, refer to BS. 302 for wire ropes for cranes, BS 1757 for power-driven mobile cranes and BS. 2799 for power-driven tower cranes.

b. Flexibility and Resistance to Bending Fatigue

Wires in a rope are subject to different degrees of bending while it is running over a sheave, a drum or simply under tensile load alone. Thus, a relative new wire rope must have the ability to be bent over small sheaves or to be wound around a relatively small drum without causing substantial number of wire breakages resulting from bending. To satisfy these requirements, strands should contain sufficient number of small wires and the strands should be laid with a relatively large helix angle so that there is no loss of flexibility.

c. Resistance to Abrasion

For wires laid at the outer-most layer of the outer strands, they are more likely subject to wear and abrasion while it is running over a sheave. For a rope bent over a small sheave and under high tensile load condition, wires pressed against the sheave surface will be subjected to high bearing pressure.

d. Resistance To Crushing

If a rope is forced to run over a narrow groove of a sheave or on drum where too many layers of rope wound over each other, it will be distorted or flattened resulted from crushing of the main core. In fact, there are other factors which will also cause crushing of the main core, namely:

1. wires used for the main core are too small.
2. too large helix angle for the wires of the main core.

To meet the requirements of resistance to crushing. IWRC is normally recommended, since IWRC is constructed with a tighter structural configuration without sacrifice of rope flexibility.

e. Resistance To Rotation

Wire ropes tend to rotate as tensile load is applied. This undesirable rotation or unwinding rotation will lead to rapid deterioration of main core due to mechanical interactions. Thus, in some applications, ropes are designed to counterbalance the unwinding rotation. For instance, ropes constructed with ordinary lay strand have greater stability than ropes constructed with Lang's lay strand.

f. Resistance to Corrosion

Uncoated wires are more likely to be corroded, especially, when the wire diameter smaller than 2 mm. The most common method to against corrosion is to coat the wire with a layer of Zinc. This type of wire is commonly known as "Galvanized wire". Other method such as use of stainless steel or special lubricants.

3.8 BASIC DESIGN CONSIDERATIONS OF ROPE

The following lists five basic design considerations for round stranded rope.

a. Grade and size of wire.
b. Number and pattern of wires configuration in the

strand.

c. Type of strand lay and rope lay.

d. Preforming or non-preforming.

e. Type of main core and strand core.

CHAPTER FOUR

HELIX GEOMETRY OF WIRE ROPE

NOMENCLATURE

a_h	Helical wire radius in mm
b	Binormal vector
$\bar{i}, \bar{j}, \bar{k}$	Unit vector associated with global Cartesian coordinates
k'	Curvature of centroidal axis of any wire in mm^{-1}
$\bar{r}$	Position vector of space curve
R_w	Helical radius of wire in mm
R_s	Helical radius of strand in mm
R_d	Drum radius in mm
R_r	Ring radius in mm
S_r	Path length of rope in mm
S_s	Path length of strand in mm
S_w	Path length of wire in mm
T	Tangent vector of any space curve
X, Y, Z	Global (ie Cartesian) coordinates of space curve
x, y, z	Local coordinates system of space curve
$\dot{X}, \dot{Y}, \dot{Z}$	
$\ddot{X}, \ddot{Y}, \ddot{Z}$	Derivatives of Cartesian coordinates with
$\dddot{X}, \dddot{Y}, \dddot{Z}$	respect to θ_w
$\overline{xy}$	Defined parameter
α	Helix angle of wire in a strand in degrees
β	Helix angle of strand in a rope in degrees
γ	Helix angle of rope wound around a drum in

	degrees
α^*	Double helix angle in degrees
θ	Angle of rotation in degrees
$d\theta$	Differential angle of rotation in degrees
θ_w	Angle of rotation of helical wire in degrees
θ_s	Angle of rotation of helical strand in degrees
θ_d	Angle of rotation of drum in degrees
τ	Torsion of helical wire in mm^{-1}
ρ_k	Radius Of curvature of the centroidal axis of a wire
ρ_τ	Radius of torsion of the centroidal axis of a wire

SUBSCRIPTS

SD	Double helix
DS	Drum single helix
RS	Ring single helix
DD	Drum double helix
RD	Ring double helix
w	Helical wire
s	Helical strand
r	Rope
D	Drum
R	Ring

4.1 INTRODUCTION

A wire rope is a complex geometrical structure made up of many individual wires. The nature of construction and operation of wire rope means that individual wires have helical form within the rope. Depending on the position of the wires in this structure, and on whether the rope is passed around a sheave or wound around a drum, the wire can be in the form of a single, double or even triple helix. These geometrical configurations play a significant role with respect to flexibility, mechanical response, inter-wire action, fatigue performance and service life.

A large variety of ropes are manufactured for various load carrying purposes. Amongst those varieties, round stranded ropes are the most widely used form in the majority of rope applications. As a result, there have been many experimental investigations dedicated to evaluating the structural properties of round stranded rope. However, the significance and influence of rope geometry relative to the rope performance, safety and reliability during engineering operation appears to have been largely neglected.

The aim of this chapter, therefore, is to obtain a mathematical model which can represent any wire in a rope subject to normal loading; eg tension, twisting and bending. In particular, this includes development of methods to determine curvature, torsion and path length of any wire within a rope. The results of this chapter are also necessary for further analysis of mechanical behaviour on individual helical wire (such as to determine component stresses and strains).

4.2 STRUCTURE OF CHAPTER FOUR

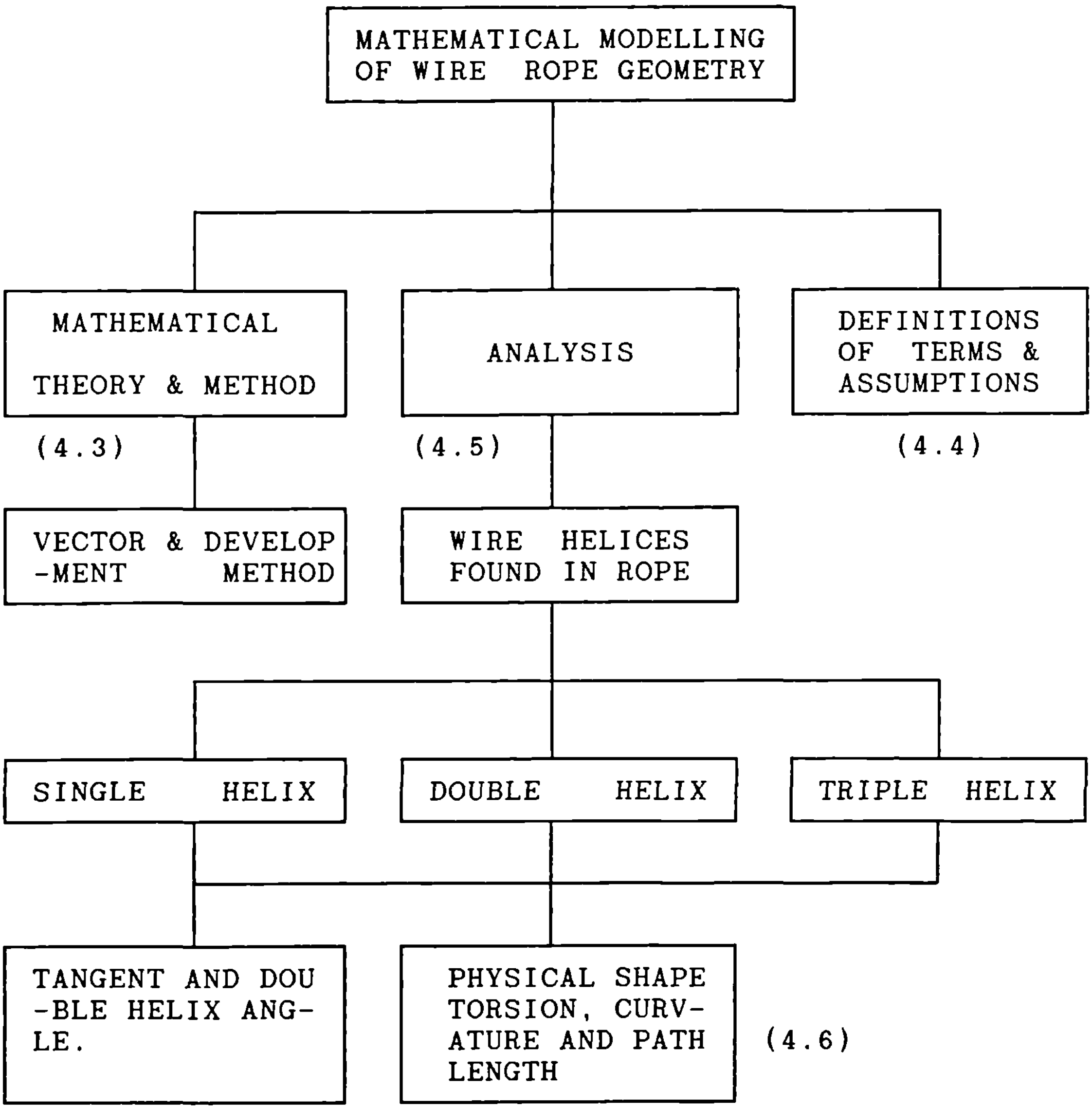

BLOCK DIAGRAM 4.1

STRUCTURE OF THE APPROACH TO THE

MATHEMATICAL MODELLING OF ROPE GEOMETRY

4.3 FUNDAMENTALS FOR WIRE HELIX MATHEMATICAL MODELLING

The following sub-sections are fundamental to the mathematical model representing circular helical wires in a round stranded rope. This section is organized under three main headings. Namely,

a. Formation of helices in a round stranded rope.

b. Vector method of geometrical analysis.

c. Development method of analysis.

4.3.1 Formation of Helices in a Round Stranded Rope

Details of how a rope is constructed, have been presented in Chapter Two. For convenience, the definitions used for a typical circular wire round stranded rope are represented in Figure 4.3.1 (hereinafter, 'rope' refers to round stranded rope).

Wires which are laid around a central straight wire (ie King wire) to produce a multi-wire strand, are in single helical form. If several strands are then laid around a central straight strand (ie the main core), the central wire (or core wire) in each of these strands also has a single helical form. However, the remaining wires in these outer strands each take on the form of a double helix. The rope now described is referred to as an independent wire rope core; ie

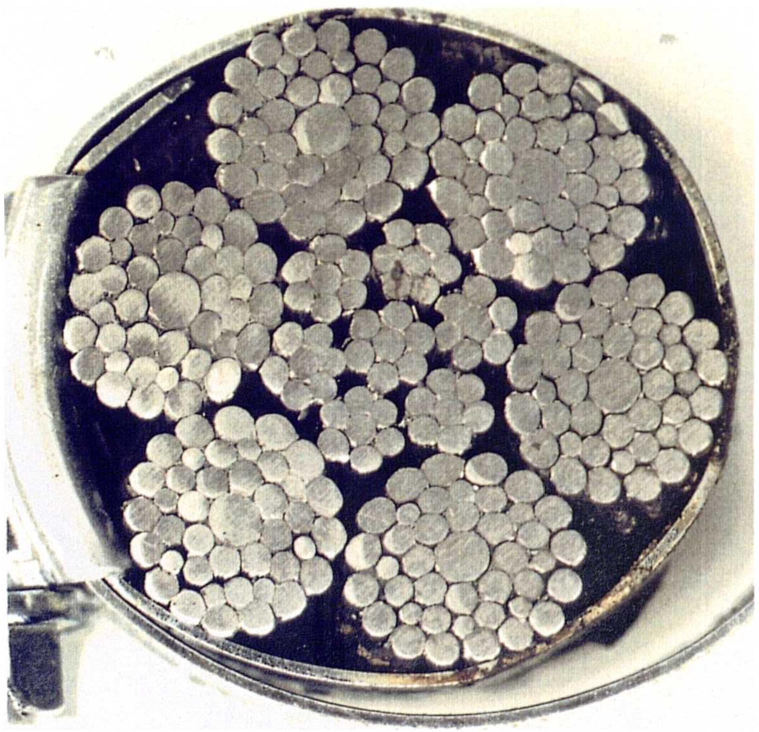

Transverse Section Of
40 mm Diameter Rope

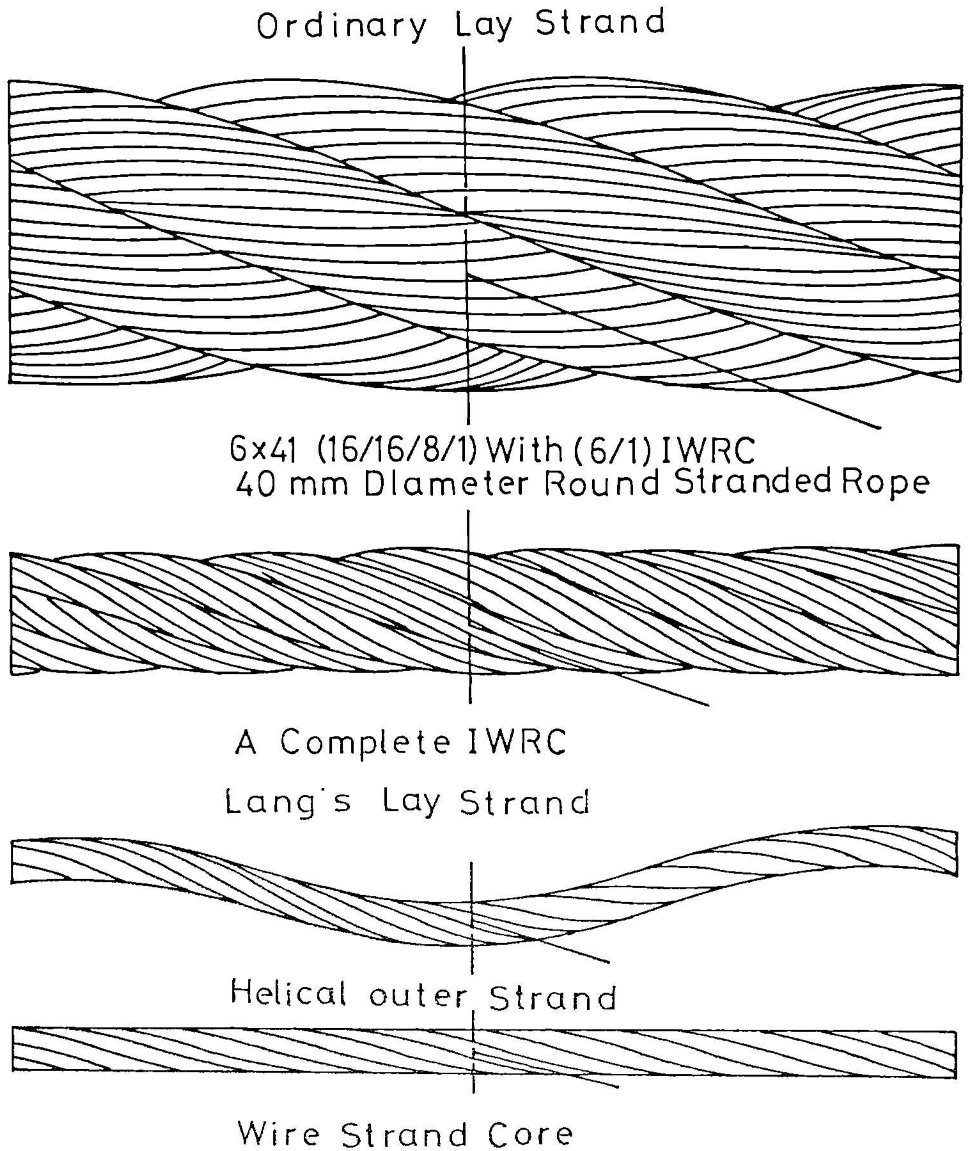

Figure 4·3·1
Typtical Large Diameter Wire Rope

IWRC. A schematic view of *straight* helices found in an IWRC is presented in Figure 4.3.2. If the rope is now wound around a drum, the King wire will take a single helical form whereas the straight single helical wire and double helical wires will take double and triple helical forms respectively. For clarity, these two helical forms are referred to as 'drum single' and 'drum double' helices respectively. On the other hand, if the rope is bent around a sheave, the King wire forms a circular ring whereas the straight single helical wires and double helical wires will take forms referred to as 'ring single' and 'ring double' helices respectively. In fact, ring single and ring double helices are degenerate cases of drum single and drum double helices where the strand and the rope helix angle on the drum are zero.

The *helix angle (or Lay angle) is defined* as the angle subtended by a helical wire or strand about the longitudinal axis of the rope. For a single helical wire of strand this angle is constant along its length. However, it is shown in a later chapter that the helix angle of a double helical wire varies along its length. This result has important implications for calculating component stresses and strains within rope subject to tensile load.

4.3.2 VECTOR METHOD OF GEOMETRIC ANALYSIS

An outline of the mathematical basis of the vector method used in reference (5.1-5.9) and in this thesis may be helpful at this point. The centroidal axis of any wire in a rope is a

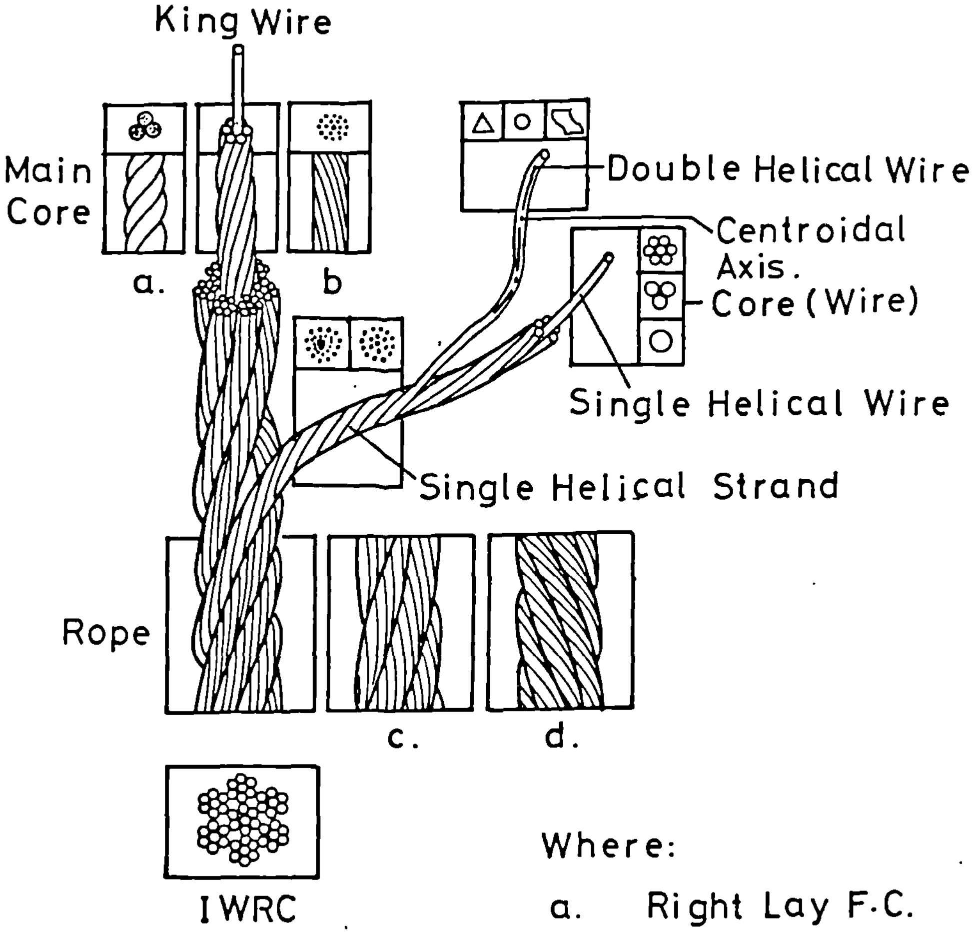

Where:

a. Right Lay F.C.

b. Left Lay Strand Core

c. Ordinary Lay Rope

d. Lang Lay Rope

Figure 4·3·2

Straight Helix Found In Rope

three dimensional space curve. It is convenient to use a local coordinate system at each point on the centroidal axis defined by the tangent, principal normal and binormal vectors at that point. This is referred to as the Frenet frame at that point, Figure 4.3.3. The position vector of a point on the centroidal axis is given in the global Cartesian coordinate by

$$\bar{r} = X\bar{i} + Y\bar{j} + Z\bar{k} \tag{4.3.2-1}$$

the derivative of this, with respect to the variable parametrising the curve, is

$$\dot{\bar{r}} = \dot{X}\bar{i} + \dot{Y}\bar{j} + \dot{Z}\bar{k} \tag{4.3.2-2}$$

If the curve is parametrised by the angle of rotation θ_w the distance dS between two nearby points on the curve is given by

$$dS = | \dot{\bar{r}} | \, d\theta_w \tag{4.3.2-3}$$

or

$$dS_w = \{ \dot{X}^2 + \dot{Y}^2 + \dot{Z}^2 \}^{1/2} \, d\,\theta_w \tag{4.3.2-4}$$

The arc length between two points $\theta_w = a$ and $\theta_w = b$, is given by

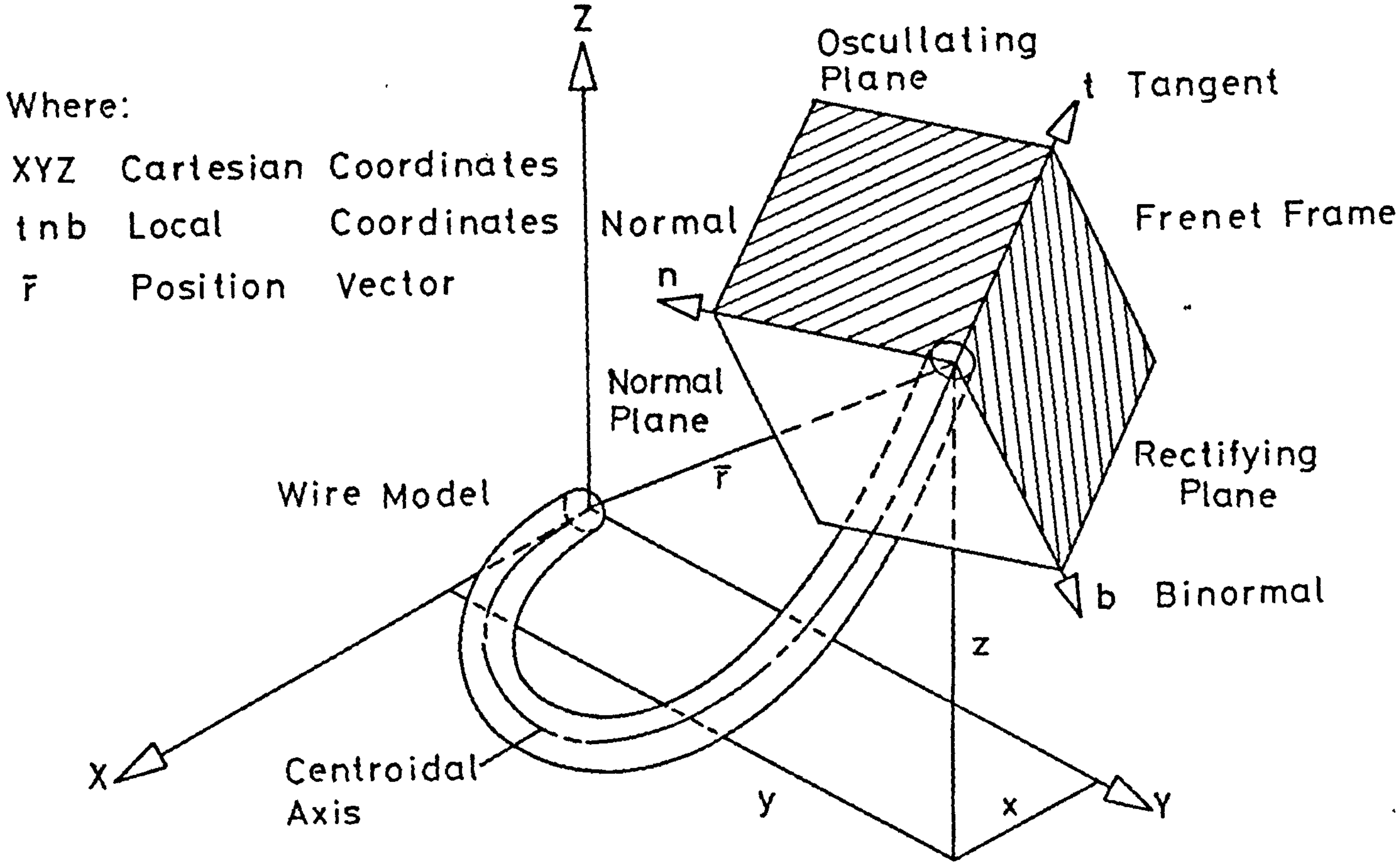

Figure 4·3·3
Coordinate System Of Space Curve

$$S = \int_a^b |\dot{\bar{r}}| \, d\theta_w \qquad (4.3.2\text{-}5)$$

provided that

$$\bar{r} = r(\theta_w), \quad X = x(\theta_w), \quad Y = y(\theta_w), \quad Z = z(\theta_w)$$

Several useful expressions which are useful in calculating the geometrical properties of space curves are given below:

Curvature of a space curve:

$$K = \frac{|\dot{\bar{r}} \times \ddot{\bar{r}}|}{|\dot{\bar{r}}|^3} \qquad (4.3.2\text{-}6)$$

$$K = \frac{\{ (\dot{Y}\ddot{Z}-\ddot{Y}\dot{Z})^2 + (\dot{Z}\ddot{X}-\ddot{Z}\dot{X})^2 + (\dot{X}\ddot{Y}-\ddot{X}\dot{Y})^2 \}^{1/2}}{(\dot{X}^2 + \dot{Y}^2 + \dot{Z}^2)^{3/2}} \qquad (4.3.2\text{-}7)$$

and the corresponding radius of curvature (ρ_k) of which is the reciprocal of equation 4.3.2-7.

Torsion of a space curve:

$$\tau = \frac{(\dot{\bar{r}} \times \ddot{\bar{r}}) \cdot \dddot{\bar{r}}}{|\dot{\bar{r}} \times \ddot{\bar{r}}|^2} \qquad (4.3.2\text{-}8)$$

$$\tau = \frac{\begin{vmatrix} \dot{X} & \dot{Y} & \dot{Z} \\ \ddot{X} & \ddot{Y} & \ddot{Z} \\ \dddot{X} & \dddot{Y} & \dddot{Z} \end{vmatrix}}{(\dot{Y}\ddot{Z}-\ddot{Y}\dot{Z})^2 + (\dot{Z}\ddot{X}-\ddot{Z}\dot{X})^2 + (\dot{X}\ddot{Y}-\ddot{X}\dot{Y})^2} \qquad (4.3.2\text{-}9)$$

the corresponding radius of torsion (ρ_τ) of which is the reciprocal of equation 4.3.2-9.

4.3.2-1 Tangent and Helix Angle of Space Curve

The vector method presented in the preceding sub-section can be extended to relate the unit tangent 'T' vector with the angle of rotation 'θ' of the space curve, Figure 4.5.5. This fundamental relationship will be applied to evaluate the helix angle (eg, double helix angle) in the later section.

The tangent vector of a space curve is given by:

$$T = \frac{dr}{dS} = \frac{dr}{d\theta} \cdot \frac{d\theta}{dS} \qquad (4.3.2\text{-}11)$$

Where dS is the infinitesimal length between two nearby points on the space curve.

$$\frac{dS}{d\theta} = \frac{|d\,\bar{r}|}{|d\,\theta|} \qquad (4.3.2\text{-}12)$$

and

$$\frac{|d\,\bar{r}|}{|d\,\theta|} = \{\dot{X} \cdot \dot{X} + \dot{Y} \cdot \dot{Y} + \dot{Z} \cdot \dot{Z}\}^{1/2} \qquad (4.3.2\text{-}13)$$

As shown in Figure 4.5.5, the helix angle of the helical curve is given by:

$$\alpha^* = \text{atn} \left(\frac{Z^*}{\overline{XY}} \right) \qquad (4.3.2\text{-}14)$$

Where $\overline{XY}$ and Z^* are the horizontal component and the vertical component of the tangent vector 'T'. By simplifying the equation 4.3.2-14. The helix angle of any helical curve can be given by:

$$\alpha^* = \tan^{-1} \left\{ \frac{\dot{Z}}{(\dot{X}^2 + \dot{Y}^2)^{1/2}} \right\} \qquad (4.3.2\text{-}15)$$

4.3.3 Development Approach to Geometric Analysis

The development technique applied to rope helical geometry is based on the idea of projecting the centroidal axes in this problem onto a plane, without stretching or shrinking. This uses the fact that a cylinder is a developable surface[9.13]. This technique provides:

(a) A method for evaluating the path length of the centroidal axis of a strand or of a helical wire in a strand, and

(b) Linear relationships between the wire, strand and rope rotational coordinates.

The developed path of a double helical wire in an undeformed rope is shown in Figure 4.5.4. The expression for the path length can be obtained from the same figure by using simple trigonometry.

$$S_w = \{ (\frac{r_s \theta_s}{\cos \beta})^2 + (r_w \theta_w)^2 \}^{1/2} \qquad (4.3.3\text{-}1)$$

Relationships for strands and ropes bent over sheaves or wound around drums can be obtained similarly, and are summarized in table 4.1.

Another application of the development technique is to relate the different rotational coordinates in a rope, (eg θ_w and θ_s in a straight rope, Figure 4.4.2 & 4.5.4). The rotational coordinates of helical wires and strands for a rope wound a drum or bent over a sheave can be obtained in terms of the rotational coordinate of the drum or the sheave. The equations for double and triple helices can then be written in terms of any one of the rotational coordinates.

The linear relationship between the helical wire coordinate θ_w and the strand coordinate θ_s in an undeformed rope is

$$\theta_s = \frac{R_w}{R_s} . \tan \alpha \ . \ \cos \beta \ . \theta_w \qquad (4.3.3\text{-}2)$$

The relationship between θ_s and θ_w for a strand wound around a drum is essentially the same, with γ, θ_d and R_d replacing β, θ_s and R_s respectively.

If the centroidal axis of a wire in an undeformed rope is a double helix then, when the rope is wound around a drum, the centroidal axis of double helical wire will become a triple helix. The relationship between θ_w and θ_d is then

$$\theta_d = \frac{R_w}{R_d} \cdot \tan\alpha \cdot \sin\beta \cdot \cos\gamma \cdot \theta_w \qquad (4.3.3-3)$$

4.4. ASSUMPTIONS AND DEFINITIONS

The vector method and the development technique are the basic mathematical tools for the analysis of helix geometry. To proceed further, assumption and terminologies used in this chapter must be defined in this section.

4.4.1 Assumptions

Assumptions which have been made for the analysis, are given as follows:

a. Any section normal to the centroidal axis of a wire (ie any transverse section) is circular both before and after being bent over a sheave or wound around a drum.

b. The shape of the centroidal axis is regarded as the most important geometrical characteristic of a wire within a rope.

c. The shape of the centroidal axis of a wire (straight or curved wire) within a rope is a helix. For example a straight king wire is a degenerated helix.

d. Sheaves, drums and all wires of a rope are perfect circular cylinder.

4.4.2 Definition of Geometrical Parameters:

a. Wire Helical Radius (R_w)

For a helical wire wound around any strand, the wire helical radius is defined as the perpendicular distance from the centroidal axis of the wire to the centroidal axis of the parent strand, Figure 4.4.1.

b. Strand Helical Radius (R_s)

For a strand wound around any type of cylindrical core, the strand helical radius R_s is defined as the perpendicular distance from the centroidal axis of this core to the centroidal axis of the central core wire of the helical strand, Figure 4.4.1.

c. Rotational Coordinate of Wire (θ_w)

For two nearby points on the centroidal axis of a wire the differential $d\theta_w$ of the rotational coordinate θ_w is given by the angle between the oscullating planes at the two points.

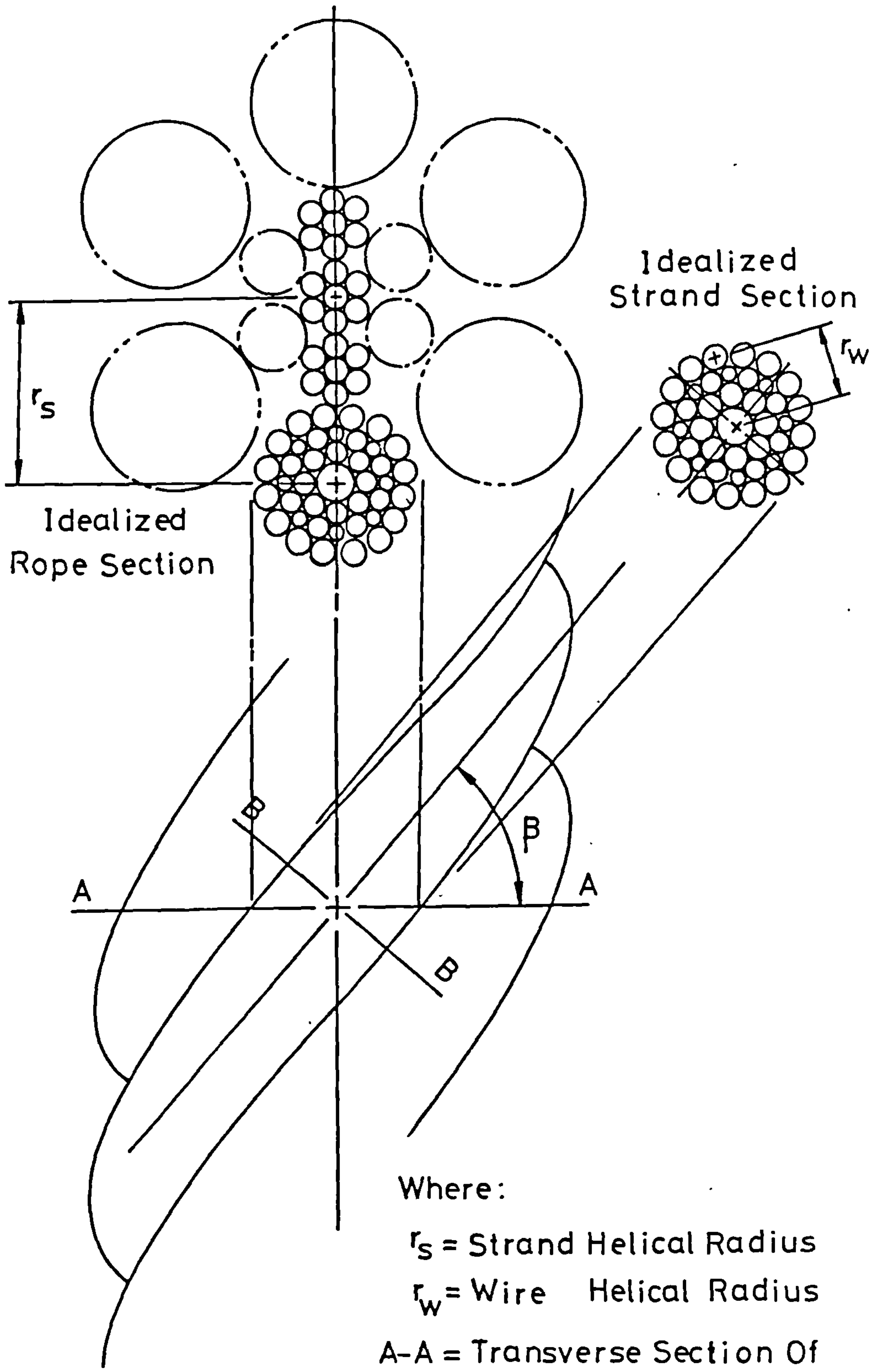

Where:

r_s = Strand Helical Radius

r_w = Wire Helical Radius

A-A = Transverse Section Of Rope.

B-B = Transverse Section Of Strand

Figure 4·4·1

Helical Radii

The oscullating plane at a point is defined as the plane formed by the tangential and normal vectors at that point, Figure 4.4.2. This is effectively a measure of the angular position of a point on the centroidal axis of a wire within a rope relative to an arbitrary fixed line.

d. Rotational Coordinate of Strand (θ_s)

For two nearby points on the centroidal axis of a strand wound around any type of cylindrical core the differential $d\theta_s$ of the rotational coordinate θ_s is defined as the angle between the osculating planes at the two points, Figure 4.4.2.

e. Ring/Drum Radius (R_r or R_d)

If a strand or rope is passed over a sheave then the ring radius R_r is defined as the perpendicular distance from the centre line of the sheave to the centroidal axis of the strand or rope. Similarly, the drum radius R_d is defined as the perpendicular distance from the centre line of a drum to the centroidal axis of the strand or rope wound around the drum, Figure 4.5.3-2 & 4.5.4-1.

f. Ring/Drum Rotation (θ_r & θ_d)

For two nearby points on the centroidal axis of a strand or rope passed over a sheave the differential $d\theta_r$ of the ring rotation coordinate θ_r is defined as the angle between the osculating planes at the two points. We can similarly define the drum rotation coordinate θ_d for a strand or rope wound

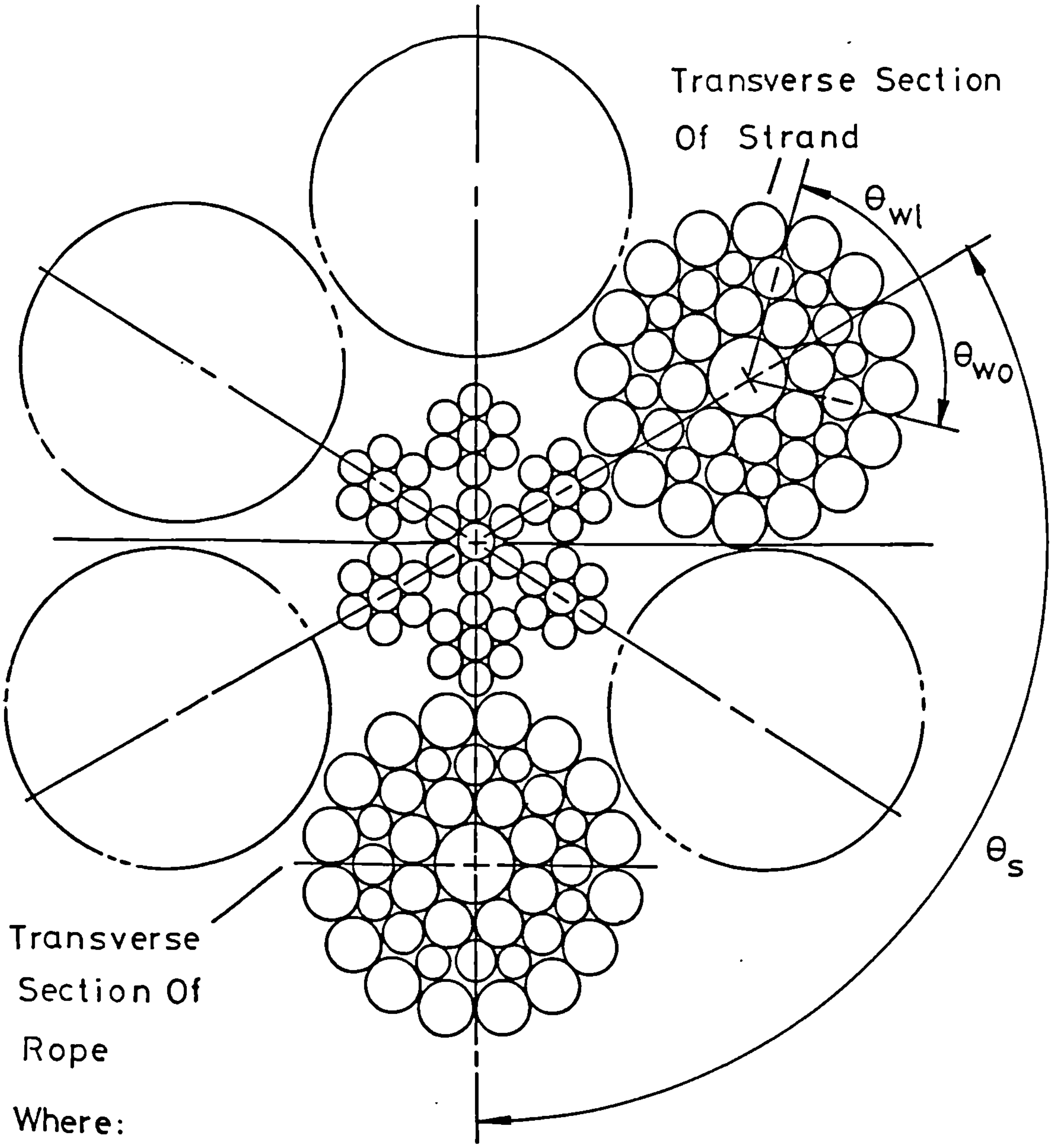

Where:

θ_s = Rotational Coordinate Of Strand

θ_{wl} = Rotational Coordinate Of Wire (Lang's Lay)

θ_{wo} = Rotational Coordinate Of Wire (Ordinary Lay)

Figure 4·4·2
Rotational Coordinate

around a drum, Figure 4.5.3-2 & 4.5.4-1.

g. Helix Angle (γ) of a Rope or Strand Wound Around a Drum

If a strand is wound around a drum then the helix angle γ is defined as the angle of inclination of the tangent vector to the centroidal axis of the strand to the plane normal to the axis of the drum, Figure 4.5.4-1 The helix angle of a rope is defined similarly.

Remark:

Any wire and strand within a rope has a helix angle; a straight wire and strand has a helix angle of 90 degrees. A strand and its central core wire share the same helix angle which is constant along the centroidal axis of the strand. However, the helix angle of a double helical wire is not constant. It is a periodical relationship between the helix angle and its position within a rope.

4.4.3 Definition of Helices

a. Single Helix

A curve with parametric equations

$$x = a \cos \theta$$

$$y = b \sin \theta$$

$$z = c \theta.$$

is a single helix whose axis is the Z axis. For a circular helix the constants a and b are equal. The constant c determines the pitch of the helix, Figure 4.3.4.

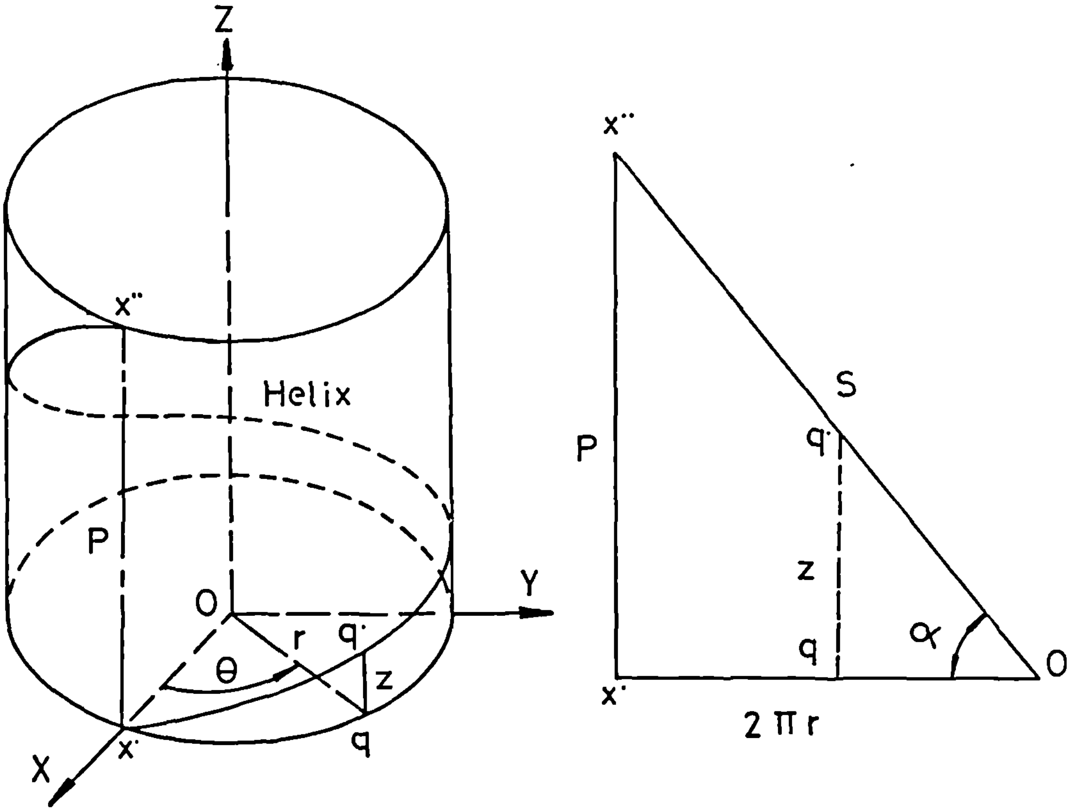

Where:

θ = Angle Of Rotation
S = Path Length
r = Helical Radius
α = Helix Angle

Figure 4.3.4

Development Method

b. Double Helix

A double helix is a helical curve whose axis is a single helix: for example wire wound around a single helical strand or a single helical strand wound around a drum.

c. Triple Helix

A triple helix is a helical curve whose axis is a double helix: for example, a wire wound around a helical strand which is itself wound around a drum.

Note:

Ring Single Helix And Drum Single Helix:

A ring single and a drum single can be regarded as special case of straight double helix. If a rope is bend over a sheave. The centroidal axis of the single helical wire in the bent rope is defined as ring single helix. Similarly, if a rope is wound around a drum. The centroidal axis of the single helical wire in the bent rope is defined as drum single helix

Ring Double Helix And Drum Double Helix:

The centroidal axis of the double helical wire in a rope wound around a drum is also defined as drum double helix. Besides, the centroidal axis of the double helical wire in a rope bent over a sheave is a degenerate case of triple helix. The curve which describes the centroidal axis is defined as ring double helix.

Remark:

A helix can be a single helix, double helix, triple helix or of even higher order. An n th order helix has a helical axis of (n-1)th order. A circle or a straight line can be considered as a degenerate limiting case of a single helix as the helix angle approaches 0 or 90 degrees respectively.

4.5 ANALYSIS

The geometrical mathematical modelling presented in the current sub-sections cover helices formed by the centroidal axis of wires within a round stranded rope. Although wire helices of the rope can be categorised into single, double and triple helices, the geometrical properties can vary, depending on the combination of lay direction of wire, strand and rope.

The general equations used to evaluate the geometrical properties (ie curvature, torsion and helix angle) and path length of any helical curve have been presented in section 4.3.2 and 4.3.3 respectively. The following describes the derivation of Cartesian coordinates equations of rope helices. In order to derive these coordinate equations, three dimensional paper models have been made and some of them are drawn in this section for the purpose of illustration.

4.5.1 Single Helix:

The standard model representing the parametric relationships between cylindrical coordinates and Cartesian coordinates of the straight single helix is given in Figure 4.3.4 & 4.5.1 (a). For completeness, the coordinate equations are given as follows:

$$X = r_w \cos \theta_w \qquad (4.5\text{-}1)$$

$$Y = r_w \sin \theta_w \qquad (4.5\text{-}2)$$

$$Z = r_w \theta_w \tan \alpha \qquad (4.5\text{-}3)$$

The helix described above is referred as a right hand circular helix. There are no differences in the geometrical properties of right hand and left hand circular helices in respect of their geometrical properties.

4.5.2 Straight Double Helix:

Straight double helical wires can be found in both Lang's lay and ordinary lay rope (also known as regular lay rope), depending on whether wires of the strand are laid in the same direction as the strand or in the opposite direction. A model which represents the centroidal axis of the double helical wire found in a right hand Lang's lay rope, is shown in Figure 4.5.1 (b).

In order to illustrate how Cartesian coordinate equations of double helix can be derived. Typical Lang's lay and ordinary

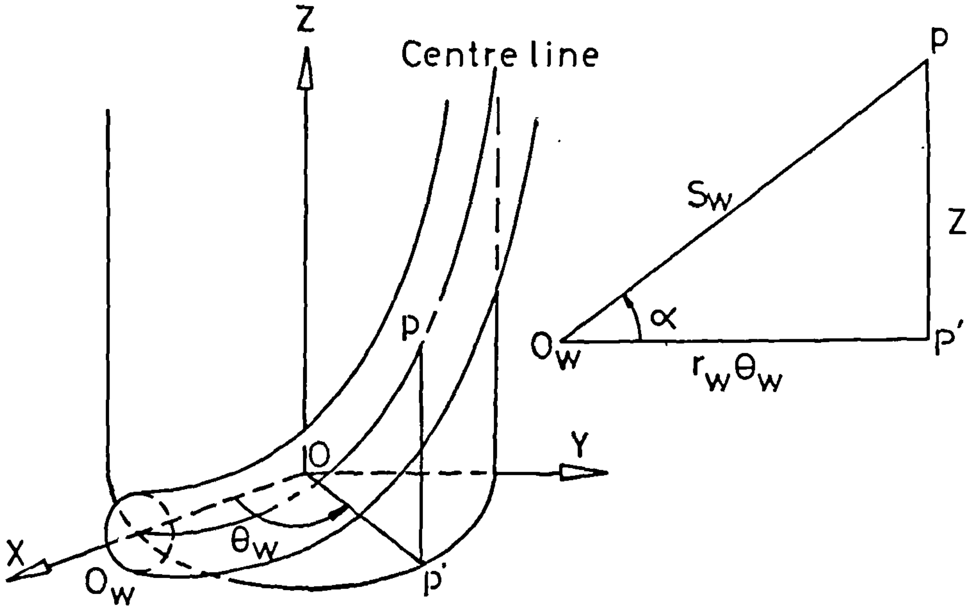

a. Single Helix Model

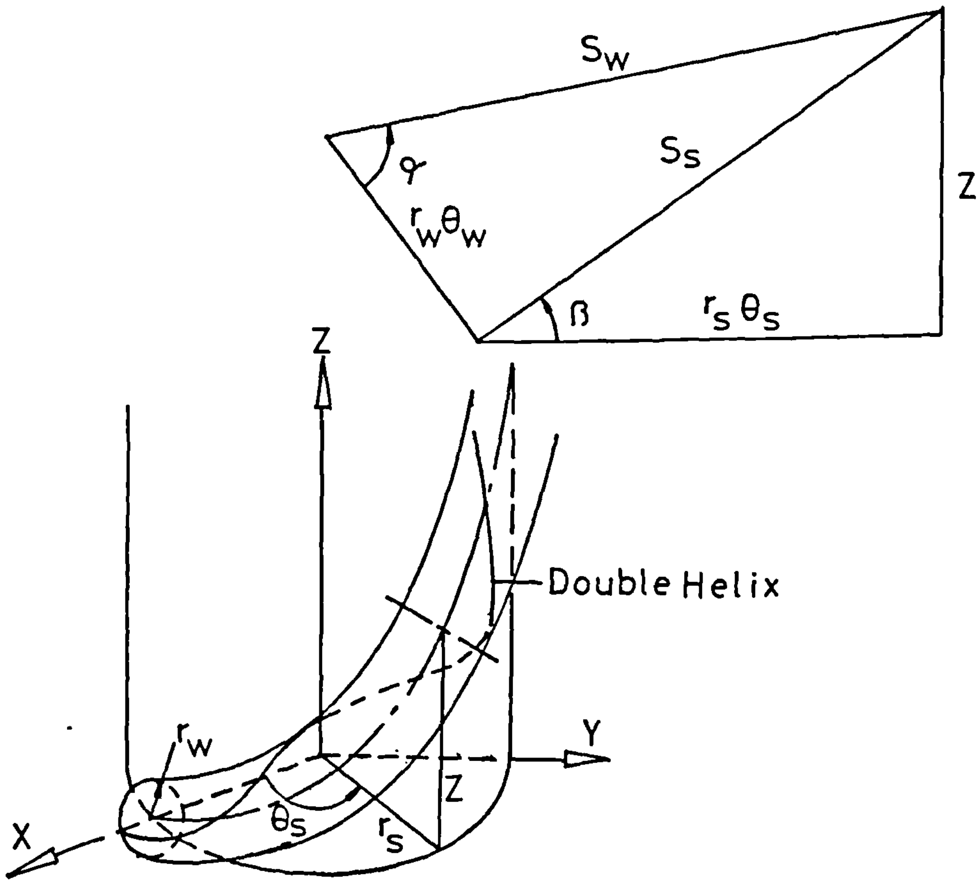

b. Double Helix Model

Figure 4·5·1

Straight Helix Model

lay models are considered, as shown in Figure 4.5.2 and Figure 4.5.3 respectively. The physical dimensions of wires within a helical strand which is cut by the transverse plane B-B, are resolved and projected onto plane A-A by means of trigonometry. A set of coordinate equations representing the Lang's lay and ordinary lay double helix in the Cartesian reference frame are given below

Cartesian Coordinate Equations of Lang's Lay Double Helix:

$$X = (R_s + R_w \cos\theta_w)\cos\theta_s + R_w \sin\theta_w \sin\theta_s \sin\beta$$
$$Y = (R_s + R_w \cos\theta_w)\sin\theta_s - R_w \sin\theta_w \cos\theta_s \sin\beta$$
$$Z = (R_s \tan\beta)\,\theta_s + R_w \sin\theta_w \cos\beta$$

(4.5.2-1)

Cartesian Coordinate Equations of Ordinary Lay Double Helix:

$$X = (R_s + R_w \cos\theta_w)\cos\theta_s - R_w \sin\theta_w \sin\theta_s \sin\beta$$
$$Y = (R_s + R_w \cos\theta_w)\sin\theta_s + R_w \sin\theta_w \cos\theta_s \sin\beta$$
$$Z = (R_s \tan\beta)\,\theta_s - R_w \sin\theta_w \cos\beta$$

(4.5.2-2)

4.5.2-1 Development Method for Double Helix:

The main purpose of using the development method in the analysis of double helix are of two-fold:

a. To relate the angle of rotation of the double helical wire θ_w with the corresponding angle of rotation of the single helical strand θ_s in the global Cartesian coordinates.

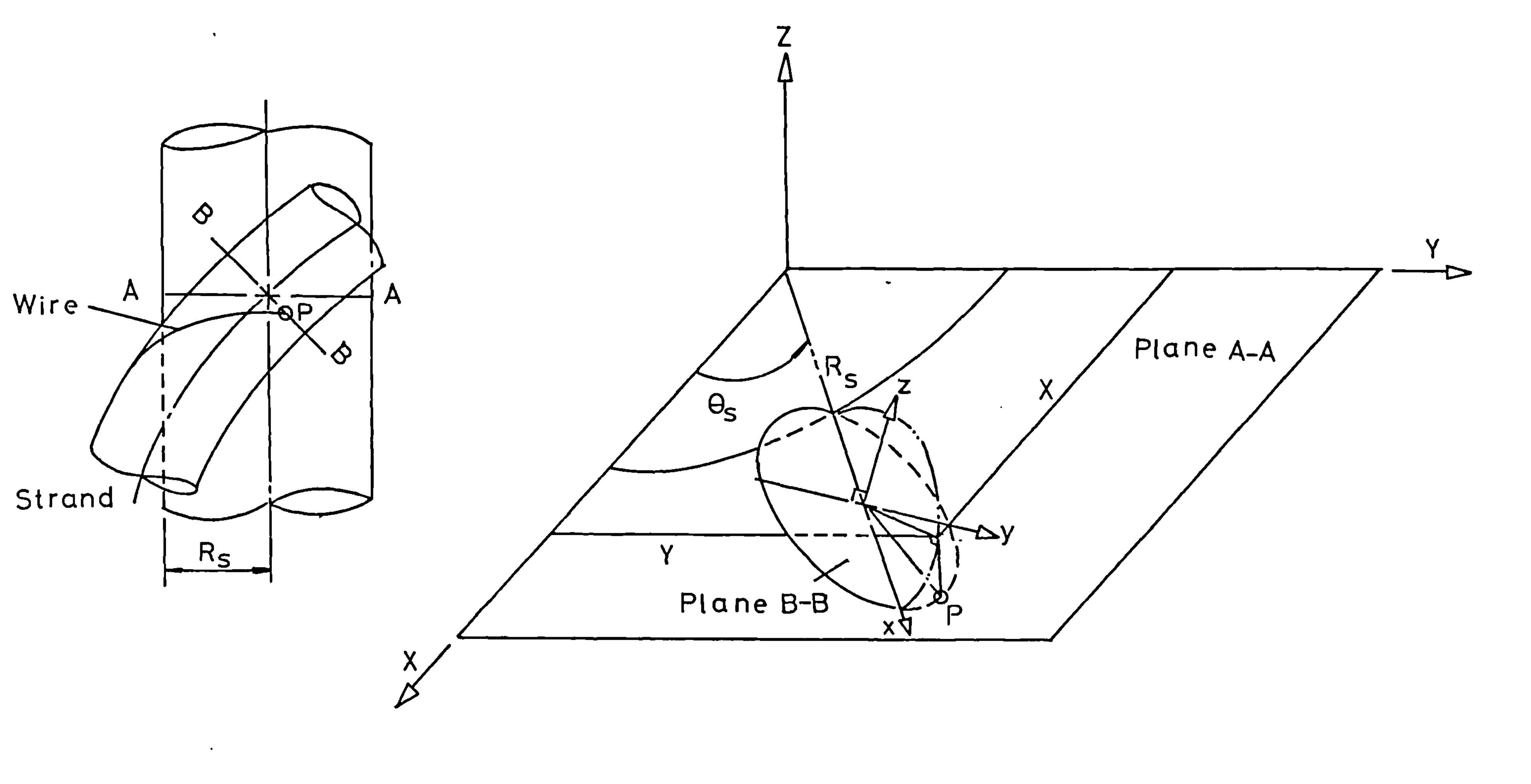

Figure 4·5·2

Double Helix Model (Lang's Lay)

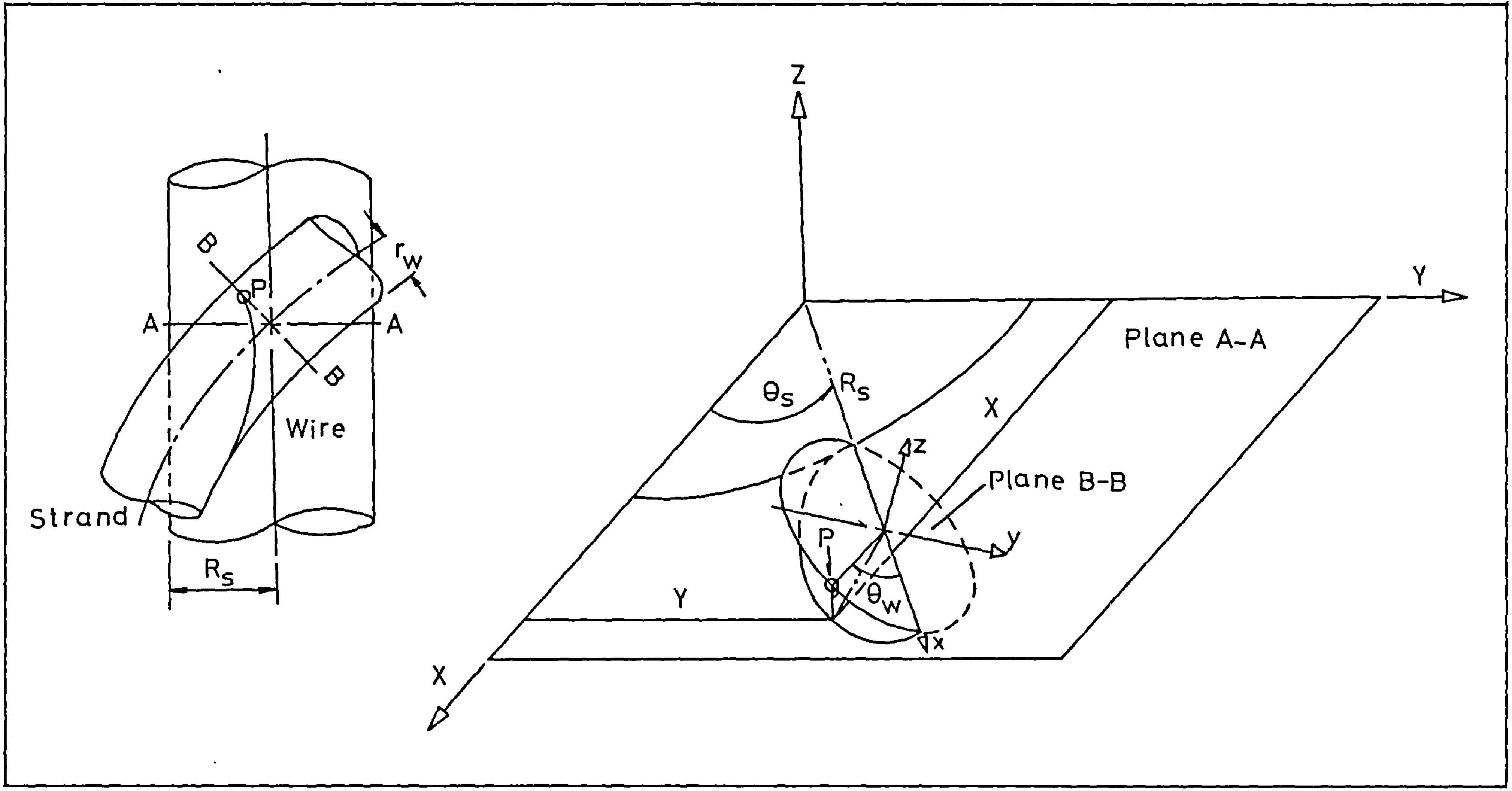

Figure 4·5·3
Double Helix Model (Ordinary Lay)

b. To evaluate the path length of the double helix which is given in table 4.1.

Figure 4.5.4 illustrates and explains how the development method works. The linear relationship between θ_s and θ_w has been given in equation 4.3.3-3.

4.5.2-2 Evaluation Of Double Helix Angle

Evaluation of the double helix angles of the double helical wire have two purposes namely:

a. to visualize the lay configuration from the transverse section of a rope.

b. to relate some mechanical responses along the double helical wire subjected to tensile load. Discussed in Chapter 9.

The following presents the procedure for evaluating the double helix angle by vector method, see Figure 4.5.5.

a. to evaluate the tangent vector to the centroidal axis of the double helical wire. This is given by

$$T = \frac{d\bar{r}}{dS} = \frac{d\bar{r}}{d\theta_w} \cdot \frac{d\theta_w}{dS} \qquad (4.5.2\text{-}4)$$

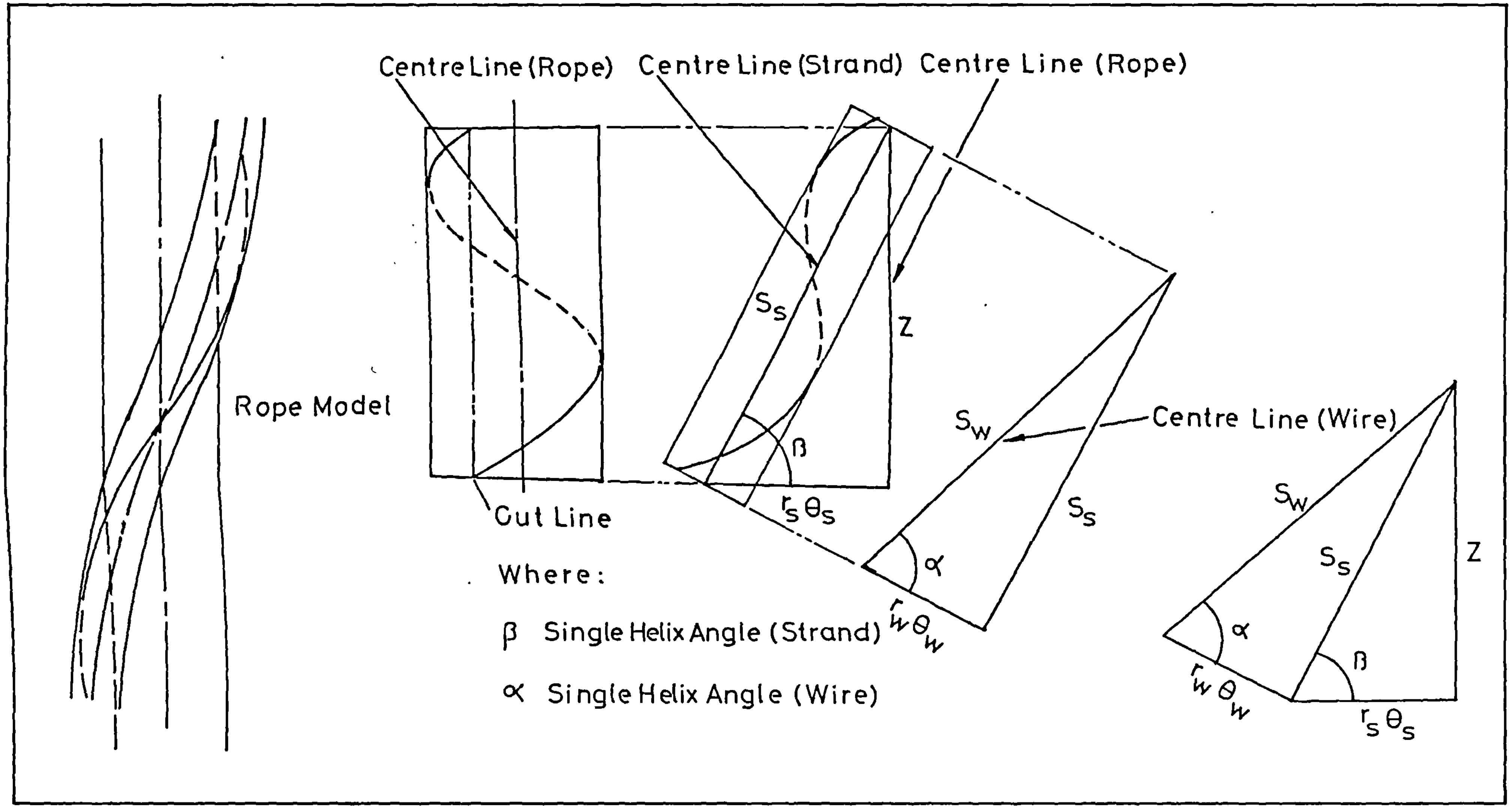

Figure 4.5.4
Development Method For Lang's Lay Rope

where

$$\frac{dS}{d\theta_w} = \frac{| d\bar{r} |}{| d\theta_w |} \qquad (4.5.2\text{-}5)$$

and

$$\frac{| d\bar{r} |}{| d\theta_w |} = (\dot{X} \cdot \dot{X} + \dot{Y} \cdot \dot{Y} + \dot{Z} \cdot \dot{Z})^{1/2} \qquad (4.55.2\text{-}6)$$

b. to resolve the tangent vector T into two components $\overline{XY}$ and Z^*, as shown in Figure 4.5.5. And the double helix angle is given by

$$\alpha^* = \text{atn} \left(\frac{Z^*}{\overline{XY}} \right) \qquad (4.5.2\text{-}7)$$

Where the vertical component of tangent vector is given by

$$Z^* = \frac{d\theta_w}{dS} \cdot | \dot{\bar{Z}} | \qquad (4.5.2\text{-}8)$$

$\overline{XY}$ is the horizontal component of tangent vector.

4.5.3 Drum Single Helix and Ring Single Helix

If a strand is laid helically around a cylinder, the single helical wire in the strand will take a double helical form. Similarly, if the strand is wound around a drum which is in fact a cylinder, the single helical wire in that strand will have exactly the same geometrical characteristic as those in a double helical wire. In other words, the single helical

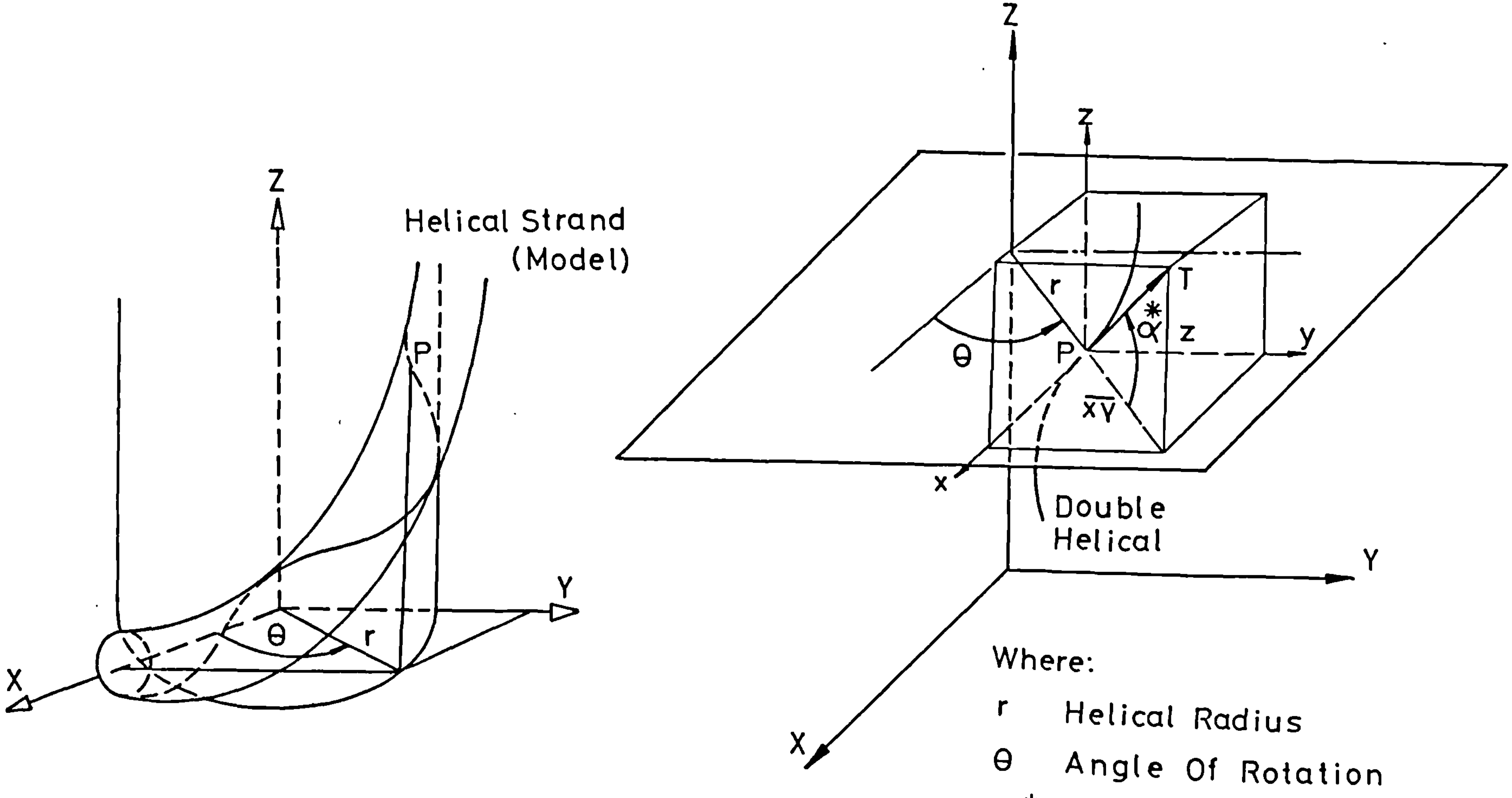

Where:

r Helical Radius

θ Angle Of Rotation

α* Double Helix Angle

T Unit Tangent Vector

Figure 4·5·5

Double Helix Angle (Model)

wire laid in a strand which itself wound around a drum, will eventually take a double helical form on that drum. On the other hand, if a strand is wound around a drum with a very small helix angle which is reduced to zero, the geometrical nature of the single helical wire in that strand is defined as ring single helix and a degenerate double helix. Figure 4.5.3-1 (a) is the schematic representation of a ring single helical model; Figure 4.5.3-2 shows a drum single helical model. For clarity, the following table lists the notation used to represent the strand helix angle which is common to double helix, ring single helix and drum single helix.

Table 4.5.3

	Double Helix	Drum single	Ring single
Helical Radius	R_s	R_d	R_s
Helix Angle	β	$0 < \gamma < \beta$	$\beta = 0$

4.5.3-1 Influence of Strand Lay on Drum:

If single helical wires in a strand are laid in the same direction as the strand wound around the drum, then the drum single helical wire will have exactly the same geometrical characteristics as the double helical wire in the Lang's lay rope. Otherwise, the drum single helical wire will have the geometrical characteristics of the double helical wire in a ordinary lay rope. Expressions which represent the Cartesian coordinates of ring and drum single helix are given in table 4.2.

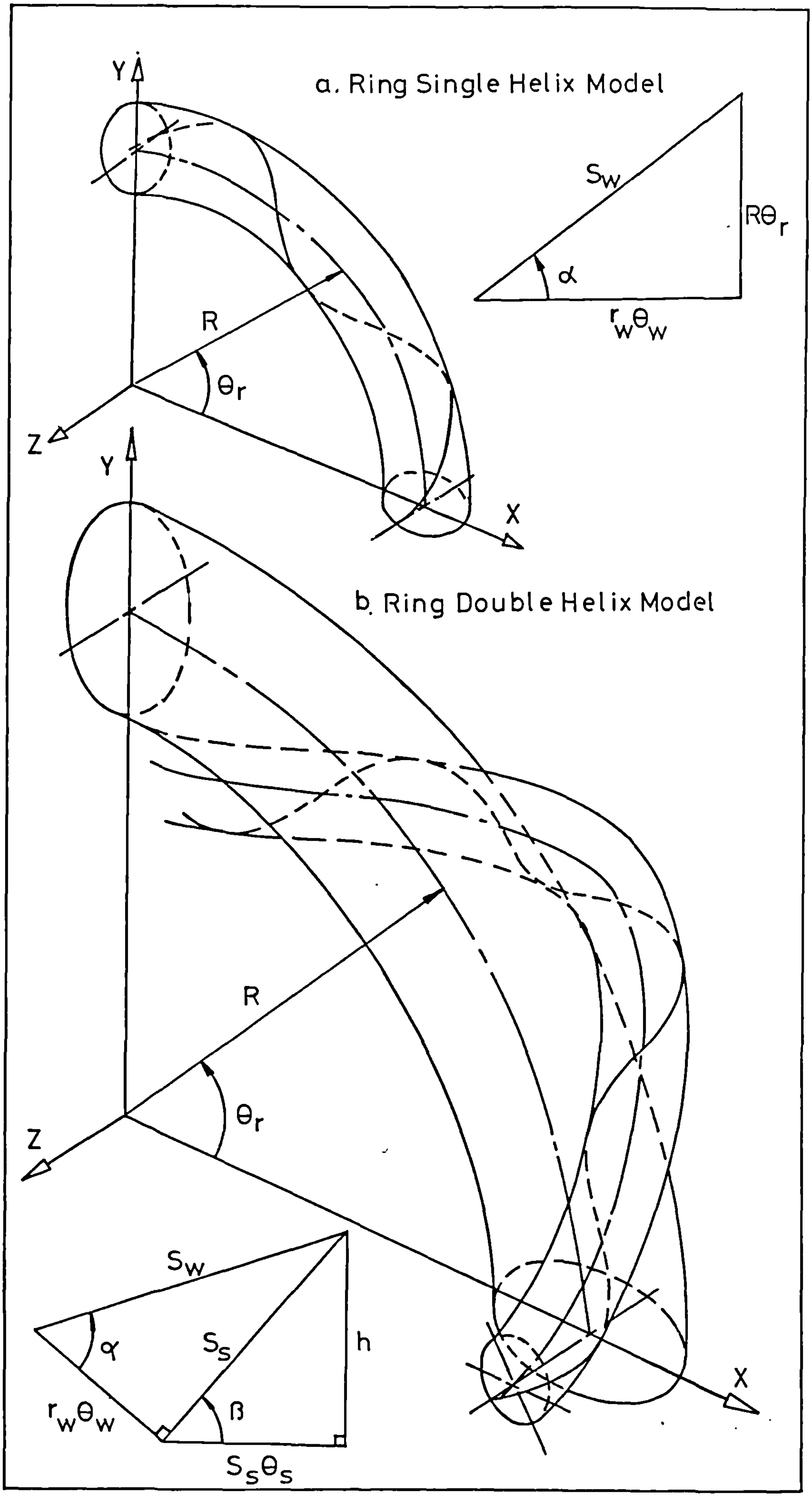

Figure 4·5·3-1 Ring Helix Model

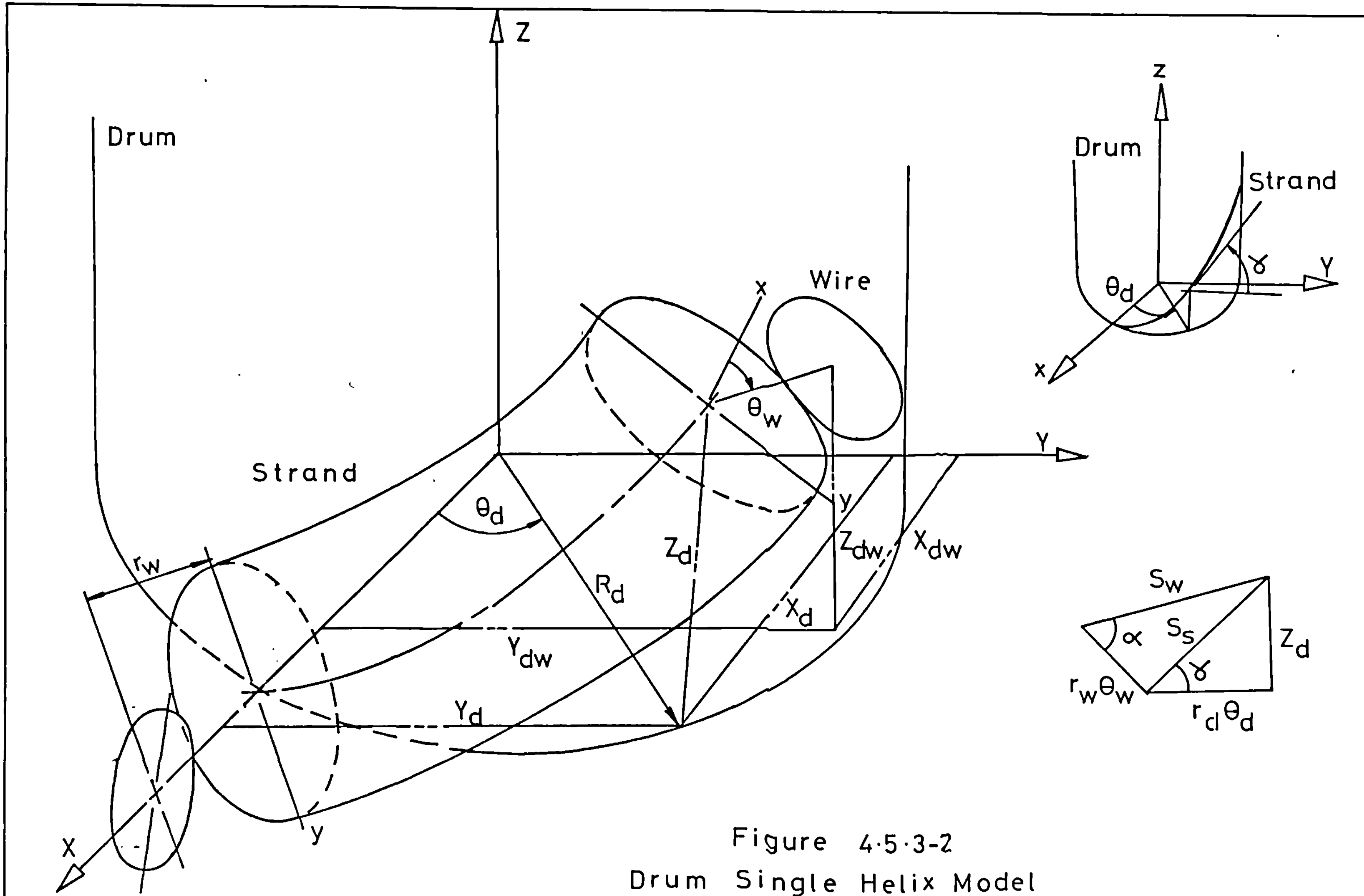

Figure 4·5·3-2
Drum Single Helix Model

4.5.4 Drum Double Helix and Ring Double Helix

If a rope is wound around a drum, all the single helical strands in the rope will take a double helical form and all the double helical wires in a single helical strand will take a triple helical form (also defined as drum double helix). However, if a rope is wound with zero helix angle, the double helical wire on the drum will take a slightly different geometrical shape which is defined as ring double helix. In fact, a ring double helix can be classified mathematically as a sub-set of a drum double helix. In other words, the coordinate expressions derived for the drum double helix will degenerate to ring double helix, if the rope helix angle approaching zero. Three dimensional models for a ring and a drum double helix found in a right hand Lang's lay rope, are illustrated in Figure 4.5.3-1 (b) and Figure 4.5.4-1 respectively.

In order to derive the Cartesian coordinate equations of the triple helix, three intersecting planes A-A, B-B and C-C which cut at the transverse plane of the drum, rope and strand, are considered. A typical triple helical model representing a drum double helical wire found in a right hand ordinary lay rope which wound around a drum in the right hand direction, is shown in Figure 4.5.4-2. The physical dimensions of the drum, and the related helical strand and wire cut by plane B-B and C-C are then resolved onto the plane A-A by means of the preceding method. A set of general

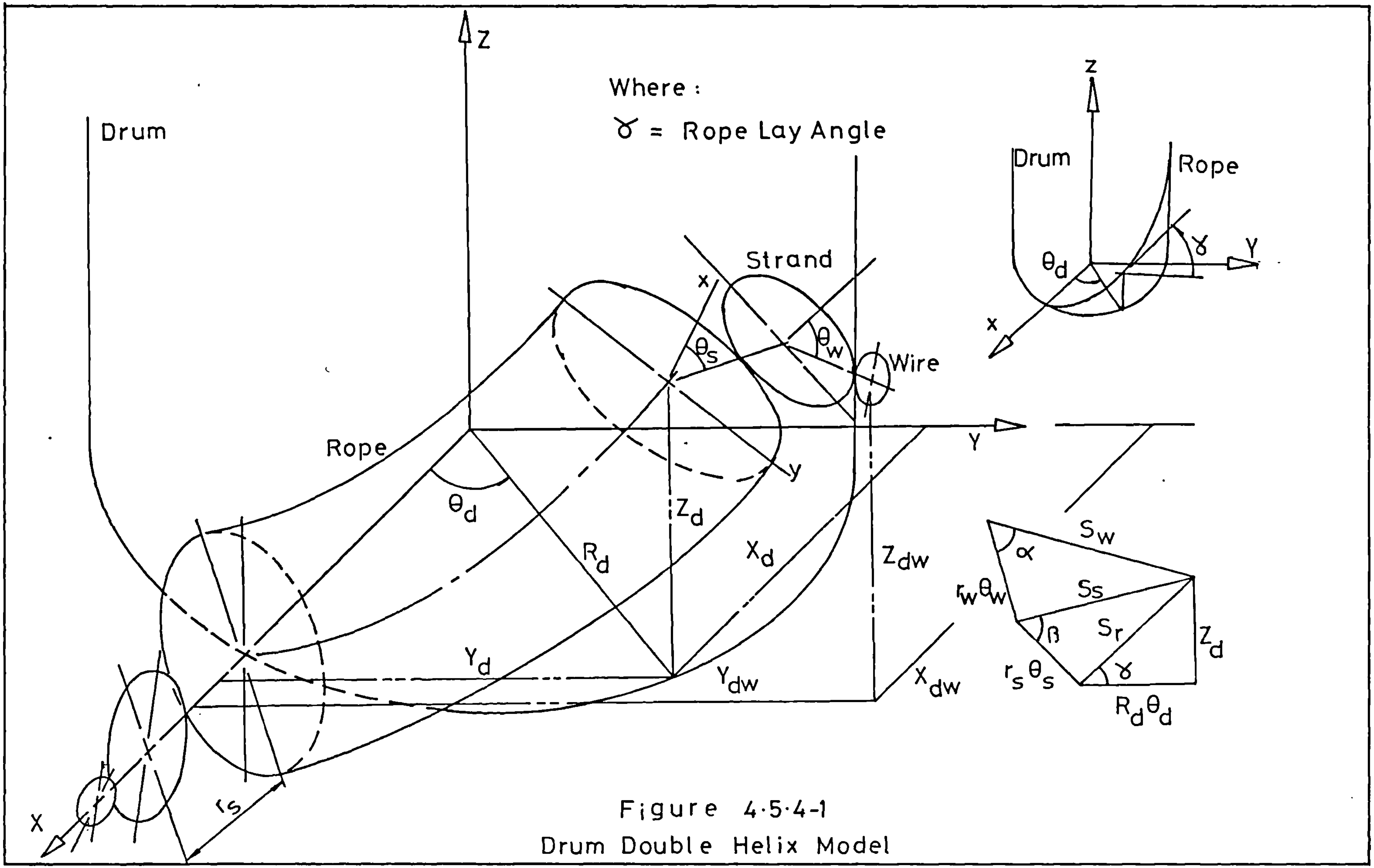

Figure 4·5·4-1
Drum Double Helix Model

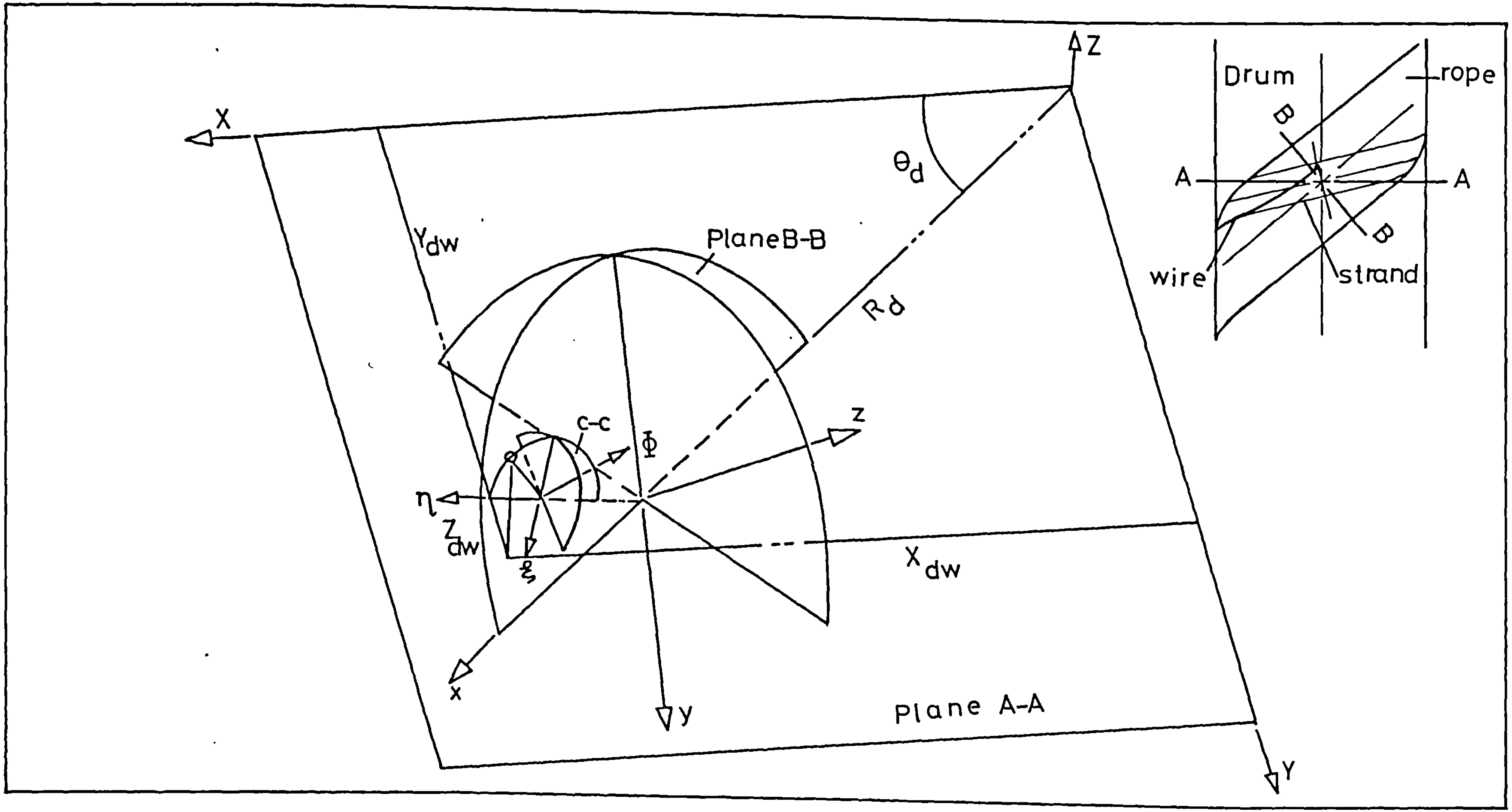

Figure 4·5·4-2
Drum Double Helix Model (Ordinary Lay)

coordinate equations representing a triple helix in a Cartesian reference frame is given by:

$$X_{DD} = X_D + X_{sd}$$
$$Y_{DD} = Y_D + Y_{sd}$$
$$Z_{DD} = Z_D + Z_{sd}$$

(14)

The coordinate equations given above are expressed in condensed form. Expansion for each terms can be found in Table 4.2. By setting the rope helix angle "γ" zero in the coordinate equations of triple helix, the coordinate equations of drum double helix will be degenerated into the coordinate equations of ring double helix.

Remark: All coordinate equations for rope helices are tabulated in Table 4.2.

4.6 GENERAL SUMMARY

The following is a brief summary of the procedure used to evaluate the geometrical properties of helices representing the wire in a rope.

4.6.1 Geometrical Shape of Rope Helices

The geometrical shape of any helical wire found in a rope can be readily visualised by plotting one of the Cartesian Coordinates of the helices derived in the preceding section.

4.6.2 Curvature of Rope Helices

The curvature of any helix formed by the centroidal axis of a rope can be obtained by substituting the first, second and third derivatives of any set of coordinate equations (as presented in Table 4.2) into equation 4.3.2-6. The corresponding radius of curvature of a helix is the reciprocal of the curvature of that helix.

4.6.3 Torsion of Rope Helices

Similarly, the torsion of any helix formed by the centroidal axis of a rope can be obtained by substituting the first, second and third derivatives of any set of coordinates equations (also presented in Table 4.2) into equation 4.3.2-8. The corresponding radius of torsion of that helix is the reciprocal of the torsion.

4.6.4 Path Length of Rope Helices

All expressions derived for evaluation of the path lengths of helices formed by the centroidal axis of helical wire within a rope, are based on the triangular relationship established by the "Development Technique". Note the arc lengths of the helices may be different from path lengths of helices. One must use equation 4.3.2-3 to evaluate the arc length of any helix.

In view of the complexity of the coordinate equations require to evaluate the geometrical shape and properties of helices representing the centroidal axes of wires in a rope, a PC type of computer package has been developed by the author and the results obtained from this package will be presented and discussed in next Chapter.

MICRO-COMPUTER SOFTWARE STRUCTURE FOR HELIX GEOMETRY

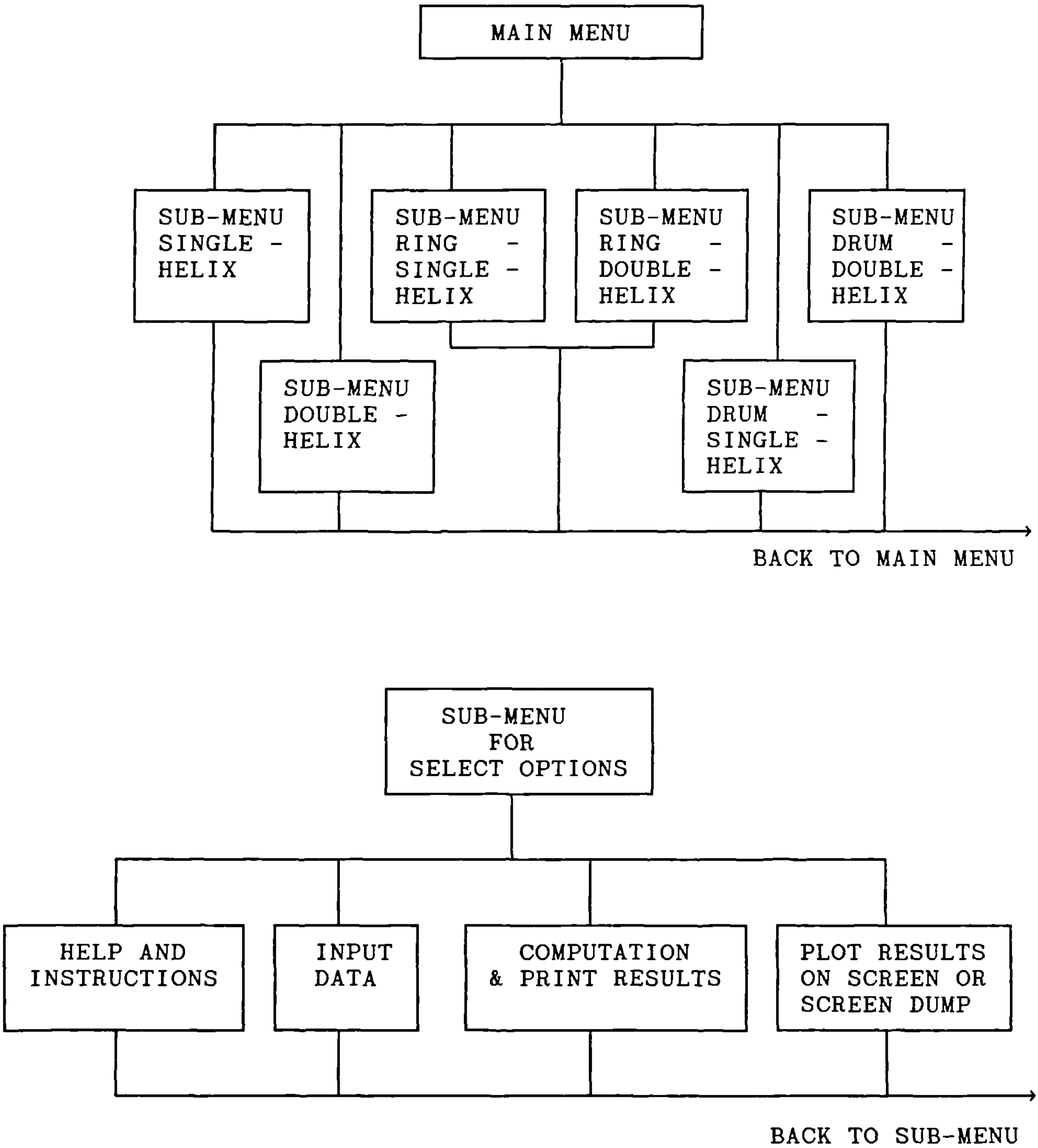

BLOCK DIAGRAM 4.2

STRUCTURE DIAGRAM OF THE APPROACH TO HELIX GEOMETRY MODELLING

Table 4.1

EQUATIONS REPRESENTING THE PATH LENGTH OF THE CENTRE LINE OF CONSTITUENT WIRES, STRAND OR ROPE USING THE DEVELOPMENT METHOD

PATH LENGTH (CENTRE LINE)	EXPRESSION
STRAIGHT SINGLE HELICAL WIRE	$S_w = \dfrac{\theta_w R_w}{\cos\alpha}$
STRAIGHT DOUBLE HELICAL WIRE	$S_w = \dfrac{h_s}{\sin\alpha \cos\beta}$; $h_s = R_s \theta_s$
(ALTERNATIVELY)	$S_w = \left\{ \left(\dfrac{R_s \theta_s}{\cos\beta} \right)^2 + R_w^2 \theta_w^2 \right\}^{1/2}$
RING SINGLE HELICAL WIRE	$S_W = \{ R_w^2 \theta_w^2 + R_R^2 \theta_R^2 \}^{1/2}$
STRAND AROUND A SHEAVE	$S_S = R_R \theta_R$
RING DOUBLE HELICAL WIRE	$S_w = \{ R_w^2 \theta_w^2 + R_R^2 \theta_R^2 + R_w^2 \theta_w^2 \}^{1/2}$
ROPE AROUND A SHEAVE	$S_R = R_R \theta_R$
DRUM SINGLE HELICAL WIRE	$S_w = \left\{ \theta_w^2 R_w^2 + \dfrac{R_D^2 \theta_D^2}{\cos^2\gamma} \right\}^{1/2}$
STRAND AROUND A DRUM	$S_s = \dfrac{R_D \theta_D}{\cos\gamma}$
DRUM DOUBLE HELICAL WIRE	$S_w = \left\{ R_w^2 \theta_w^2 + R_s^2 \theta_s^2 + \dfrac{\theta_D^2 R_D^2}{\cos^2\gamma} \right\}^{1/2}$
ROPE AROUND A DRUM	$S_R = \dfrac{R_D \theta_D}{\cos\gamma}$

Table 4.2 Cartesian Coordinate Equations Of Rope Helices

a. Single Helix

$$X = R_w \cos \theta_w$$

$$Y = R_w \sin \theta_w$$

$$Z = (R_w \tan \alpha)\ \theta_w$$

b. Double Helix

In Ordinary Lay Rope

$$X = (R_s + R_w \cos \theta_w) \cos \theta_s + R_w \sin \theta_w \sin \theta_s \sin \beta$$

$$Y = (R_s + R_w \cos \theta_w) \sin \theta_s - R_w \sin \theta_w \cos \theta_s \sin \beta$$

$$Z = (R_s \tan \beta)\ \theta_s + R_w \sin \theta_w \cos \beta$$

In Lang's Lay Rope

$$X = (R_s + R_w \cos \theta_w) \cos \theta_s - R_w \sin \theta_w \sin \theta_s \sin \beta$$

$$Y = (R_s + R_w \cos \theta_w) \sin \theta_s + R_w \sin \theta_w \cos \theta_s \sin \beta$$

$$Z = (R_s \tan \beta)\ \theta_s - R_w \sin \theta_w \cos \beta$$

c. Triple Helix

$$X_{DD} = X_D + X_{sd}$$

$$Y_{DD} = Y_D + Y_{sd}$$

$$Z_{DD} = Z_D + Z_{sd}$$

Expansion Of Terms Used In Coordinates Equation Of Triple Helix

$X_D = (R_D \tan \gamma)\ \theta_D$

$Y_D = R_D \cos \theta_D$

$Z_D = R_D \sin \theta_D$

$Z_{s1} = R_w \sin \theta_w \cos \beta \cos \gamma$

$Z_{s2} = R_w \sin \theta_w \cos \beta \sin \gamma$

Rope Wound Around Drum In The Left Hand Direction:

1. Right Hand Lang's Lay Rope

$X_{sd} = Y_{s2} - Z_{s2}$

$Y_{sd} = X_s \cos \theta_D + Y_{s1} \sin \theta_D + Z_{s1} \sin \theta_D$

$Z_{sd} = X_s \sin \theta_D - Y_{s1} \cos \theta_D - Z_{s1} \cos \theta_D$

$X_s = R_s \cos \theta_s + R_w \cos \theta_w \cos \theta_s - R_w \sin \theta_w \sin \theta_s \sin \beta$

$Y_{s1} = R_s \sin \theta_s \sin \gamma + R_w \cos \theta_w \sin \theta_s \sin \gamma + R_w \sin \theta_w \cos \theta_s \sin \beta \sin \gamma$

$Y_{s2} = R_s \sin \theta_s \cos \gamma + R_w \cos \theta_w \sin \theta_s \cos \gamma + R_w \sin \theta_w \cos \theta_s \sin \beta \cos \gamma$

2. Right Hand Ordinary Lay rope

$X_{sd} = Z_{s2} + Y_{s2}$

$Y_{sd} = X_s \cos \theta_D + Y_{s1} \sin \theta_D - Z_{s1} \sin \theta_D$

$$Z_{sd} = X_s \sin \theta_D - Y_{s1} \cos \theta_D + Z_{s1} \cos \theta_D$$

$$X_s = R_s \cos \theta_s + R_w \cos \theta_w \cos \theta_s + R_w \sin \theta_w \sin \theta_s \sin \beta$$

$$Y_{s1} = R_s \sin \theta_s \sin \gamma + R_w \cos \theta_w \sin \theta_s \sin \gamma - R_w \sin \theta_w \cos \theta_s \sin \beta \sin \gamma$$

$$Y_{s2} = R_s \sin \theta_s \cos \gamma + R_w \cos \theta_w \sin \theta_s \cos \gamma - R_w \sin \theta_w \cos \theta_s \sin \beta \cos \gamma$$

Rope Wound Round Drum In The Right Hand Direction

1. Right Hand Lang's Lay Rope

$$X_{sd} = - Y_{s2} - Z_{s2}$$

$$Y_{sd} = X_s \cos \theta_D - Y_{s1} \sin \theta_D + Z_{s1} \sin \theta_D$$

$$Z_{sd} = X_s \sin \theta_D + Y_{s1} \cos \theta_D - Z_{s1} \cos \theta_D$$

$$X_s = R_s \cos \theta_s + R_w \cos \theta_w \cos \theta_s - R_w \sin \theta_w \sin \theta_s \sin \beta$$

$$Y_{s1} = R_s \sin \theta_s \sin \gamma + R_w \cos \theta_w \sin \theta_s \sin \gamma + R_w \sin \theta_w \cos \theta_s \sin \beta \sin \gamma$$

$$Y_{s2} = R_s \sin \theta_s \cos \gamma + R_w \cos \theta_w \sin \theta_s \cos \gamma + R_w \sin \theta_w \cos \theta_s \sin \beta \cos \gamma$$

2. Right Hand Ordinary Lay Rope

$$X_{sd} = - Y_{s2} + Z_{s2}$$

$$Y_{sd} = X_s \cos \theta_D - Y_{s1} \sin \theta_D - Z_{s1} \sin \theta_D$$

$$Z_{sd} = X_s \sin \theta_D + Y_{s1} \cos \theta_D + Z_{s1} \cos \theta_D$$

$$X_s = R_s \cos\theta_s + R_w \cos\theta_w \cos\theta_s + R_w \sin\theta_w \sin\theta_s \sin\beta$$

$$Y_{s1} = R_s \sin\theta_s \sin\gamma + R_w \cos\theta_w \sin\theta_s \sin\gamma - R_w \sin\theta_w \cos\theta_s \sin\beta \sin\gamma$$

$$Y_{s2} = R_s \sin\theta_s \cos\gamma + R_w \cos\theta_w \sin\theta_s \cos\gamma - R_w \sin\theta_w \cos\theta_s \sin\beta \cos\gamma$$

d. Linear Relationship between Rotational Coordinates

1. Double Helix

$$\theta_s = \frac{R_w}{R_s} . \tan\alpha . \cos\beta . \theta_w$$

2. Triple Helix

$$\theta_d = \frac{R_w}{R_d} . \tan\alpha . \sin\beta . \cos\gamma . \theta_w$$

CHAPTER FIVE

IMPLICATION AND SIGNIFICANCE

OF HELIX GEOMETRY

5.1 INTRODUCTION

Tests carried out at NEL showed that the structural properties of ropes depend significantly on the geometry of the rope structure. The geometry of the structure also has a profound effect on the type of wire failure and the fatigue performance of the rope. This is because the geometry of the rope determined the clamping and pivoting environment for individual wires at periodic locations within a rope.

In this chapter, the author's main objective is to explain the implications and the influence of rope geometry on the mechanical behaviour of wires within a rope.

5.2 LAYOUT OF CHAPTER FIVE

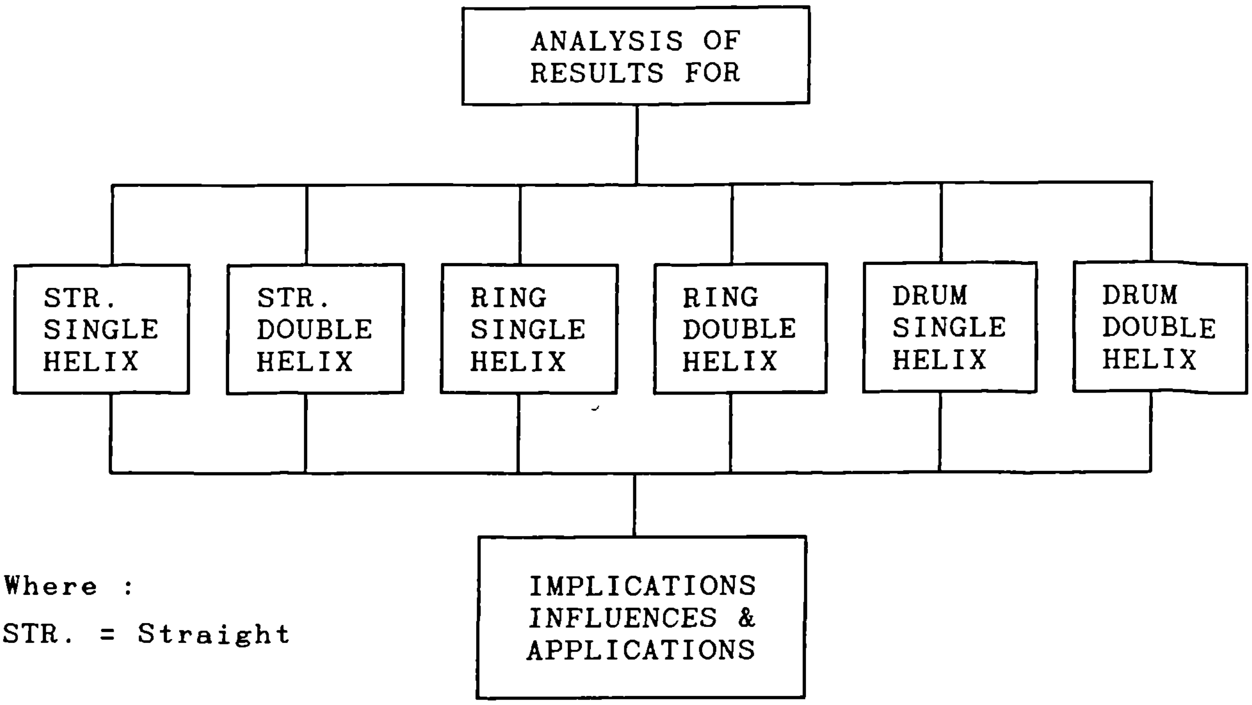

Where :

STR. = Straight

BLOCK DIAGRAM 5.1

5.3 SINGLE HELIX GEOMETRY AND ITS IMPLICATIONS

The following sub-sections are mainly concerned with the geometrical aspects of single helices and the implication of these to the mechanical responses.

5.3.1 Geometrical Properties of Single Helix

The centroidal axis of a single helical wire is a circular helix with constant pitch. For the single helix with any helix angle between 0 and 90 degrees and any helical radius, the projection of this curve on the ZY and ZX planes (referred to a right hand coordinate system) can be regarded as functions of θ_w, Figure 5.3-1. For a single helical wire, the radius of curvature, radius of torsion and helix angle are constant on the centroidal axis of a single helical wire, Figure 5.3 -2. The resulting effects of varying on strains, radius of curvature and torsion are shown in Figure 5.3-3 and 5.3-4. The effects of varying the helical radius on radius of curvature and torsion are shown in Figure 5.3-5 to 5.3-7.

5.3.2 Implications of Helix Geometry on Single Helical Wire

The component forces and moments on a single helical wire within a strand are depend upon the wire geometry as shown in many articles[3.1-3.20]. Based on the understanding of single helix geometry, in this sub-section, a qualitative summary of the implication of helix geometry on the static mechanical

SINGLE HELIX

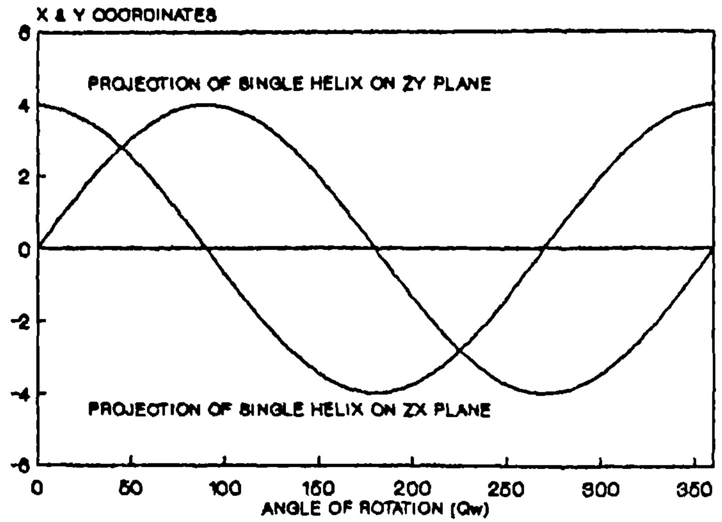

FIGURE 5.3-1
COORDINATES OF SINGLE HELIX

SINGLE HELIX

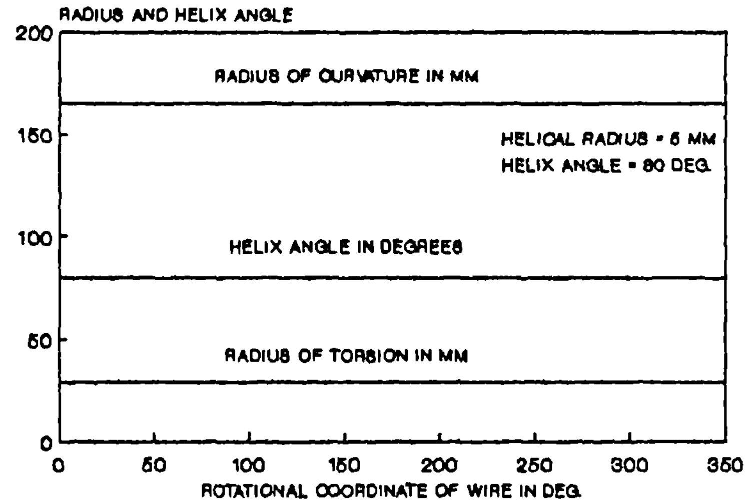

FIGURE 5.3-2
RADIUS OF CURVATURE, TORSION AND HELIX ANGLE Vs ANGLE OF ROTATION (Qw)

SINGLE HELIX

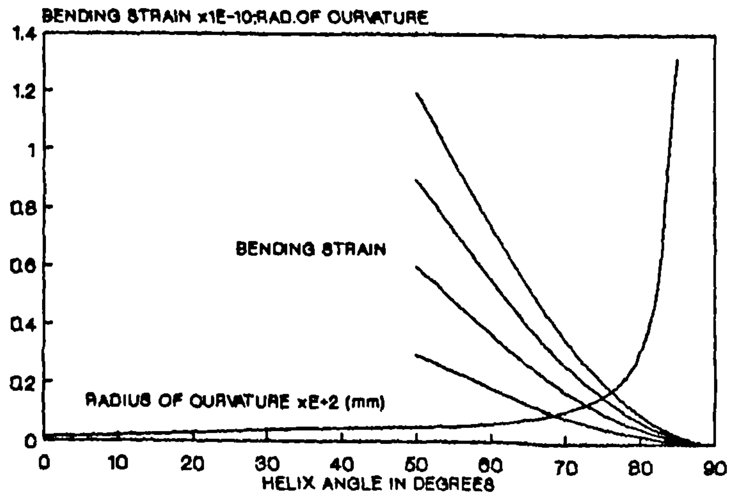

FIGURE 5.3-3
BENDING STRAIN, RADIUS OF CURVATURE VS HELIX ANGLE

SINGLE HELIX

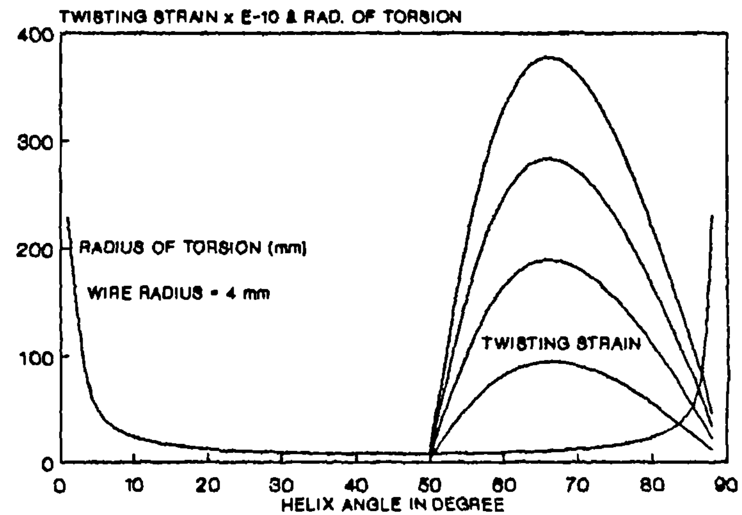

FIGURE 5.3-4
RADIUS OF TORSION VS HELIX ANGLE

SINGLE HELIX

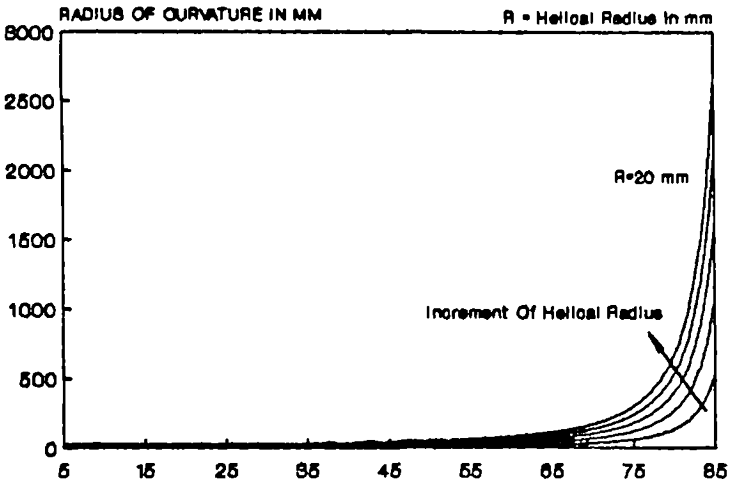

FIGURE 5.3-5
VARIATION OF RADIUS OF CURVATURE
Vs VARIATION OF HELIX ANGLE

SINGLE HELIX

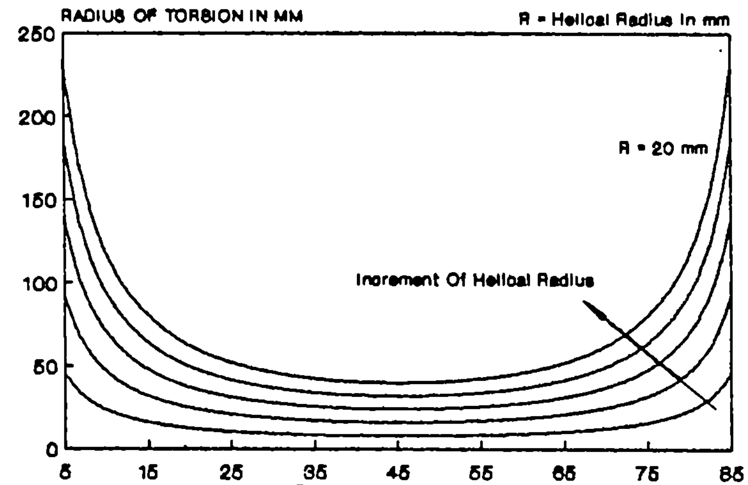

FIGURE 5.3-6
VARIATION OF RADIUS OF TORSION
Vs VARIATION OF HELIX ANGLE

SINGLE HELIX

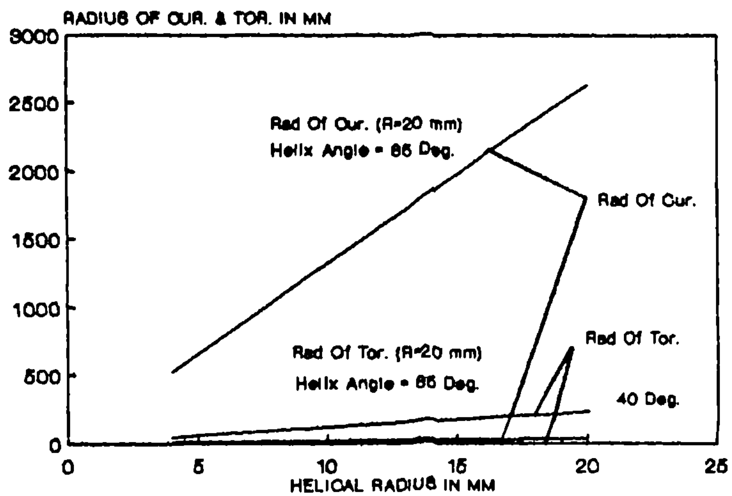

FIGURE 5.3-7
VARIATION OF RAD. OF CUR. & TOR.
Vs VARIATION OF HELICAL RADIUS

responses of single helical wire is given as follows:

a. The helix angle, curvature and torsion are related to the internal forces and moments by the equations of equilibrium presented by Love[3.21]. These equations imply that the internal forces and moments are constant on any single helical wire within a single layer straight strand and an equal lay multi-layer straight strand subjected to monotonic tensile loading. Under dynamic loading this may not be the case because of transient effects.

b. The helix angle of a single helical wire usually between 60 to 90 degrees; within this range the radius of curvature, and to a lesser extent the radius of torsion (see Figure 5.3-7) of the wire changes rapidly with helix angle, Figure 5.3-5 to 5.3-6. Thus the bending and torsional stress components along a large diameter single helical wire are very sensitive to small changes in helix angle. Quantities such as the radial force, contact force and complementary shear force which depend upon the bending and torsion, are also sensitive to changes in the helix angle. Bending and torsional stresses can be reduced by the use of smaller diameter wires; however, very small diameter wires (ie with diameter less than 2 mm) are more liable to corrosion[9.1].

c. For a straight strand subject to monotonic tensile load, if all the helical wires are being laid 90 degrees to the transverse plane of the strand, bending and twisting strains (see Figure 5.3-3 and 5.3-4) will not be induced on any helical wire. In other words, for helical wire with very large helix angle, bending moment, twisting moment, shearing force and radial force are reduced significantly. Tensile force, by contrast, becomes more dominant.

Note:

the mathematical model applied to evaluate the bending and twisting strain will be discussed in the latter chapters; Chapter Seven and Chapter Nine.

5.4 DOUBLE HELIX GEOMETRY AND ITS IMPLICATION

The geometrical properties of the double helical wire described in following sub-section are obtained from the author's computer results.

5.4.1 Geometrical Properties of Double Helix

If a main core is wound around by an outer strand which is in form of a cylindrical helix (also defined as a single helix). Each of the single helical wires in the same layer of the strand will take up the same geometrical shape which have been defined as a double helix in the preceding Chapter.

An outer strand can either be laid in the right hand or in the left hand direction. Likewise, a helical wire can either be laid in the same or in the opposite direction to the parent strand. The following table shows the four possible lay configurations which can be found in rope.

Table 5.4.1

ROPE TYPE	Lang's lay	Ordinary Lay
STRAND LAY	left or right	left or right

For the purpose of building picture on how a double helix will look like, the coordinates of a single helix, Lang's lay and ordinary lay double helix as functions of θ_w are shown in Figure 5.4-1. For further illustration, the X and Y coordinates of a Lang's lay double helix as functions of θ_w are also shown in Figure 5.4-1 (a).

For comparing purpose, the geometrical configurations of a single helix and double helices found in Lang's lay and ordinary lay rope are shown in Figures 5.4-1, 5.4-2 and 5.4-3. (Hereinafter, double helix found in Lang's lay rope is called "Lang's lay double helix", whereas double helix found in ordinary lay rope is called "ordinary lay double helix".)

For a double helical wire, the geometrical model shows that (for helix angles of wires and strands within a rope greater

X-COORDINATE OF DOUBLE HELIX

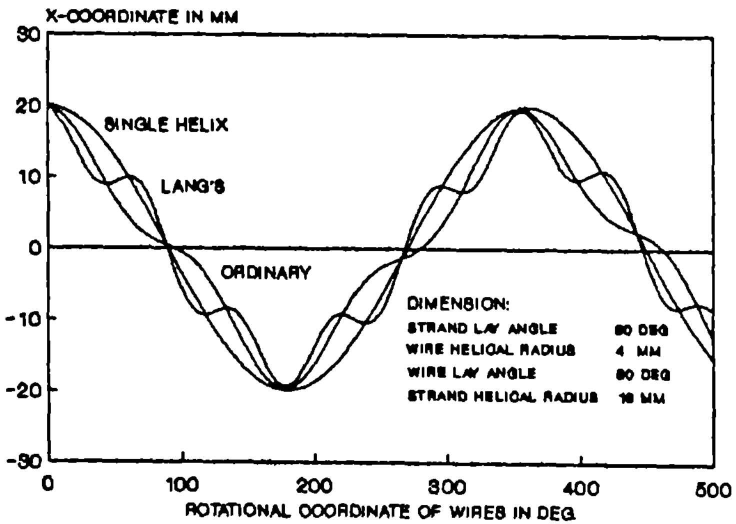

FIGURE 6.4-1
X-COORDINATE VS WIRE ROTATION

DOUBLE HELIX

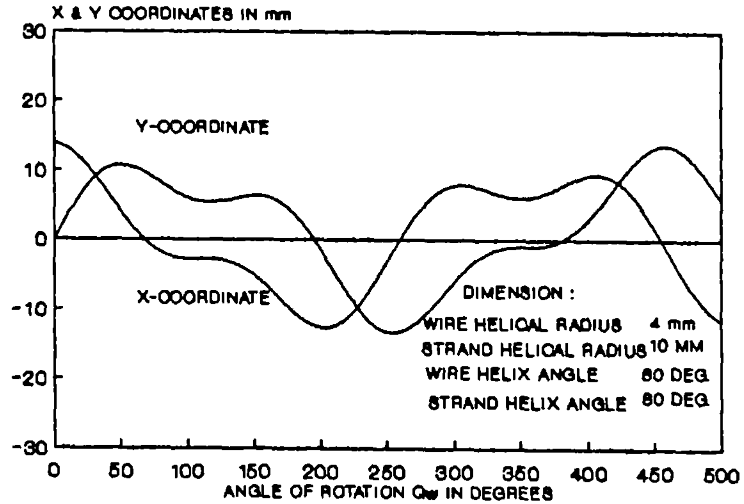

FIGURE 6.4-1 (a)
X & Y COORDINATES OF DOUBLE HELIX
(LANG'S LAY)

COMPARISON OF HELIX ANGLES
STRAIGHT DOUBLE HELIX

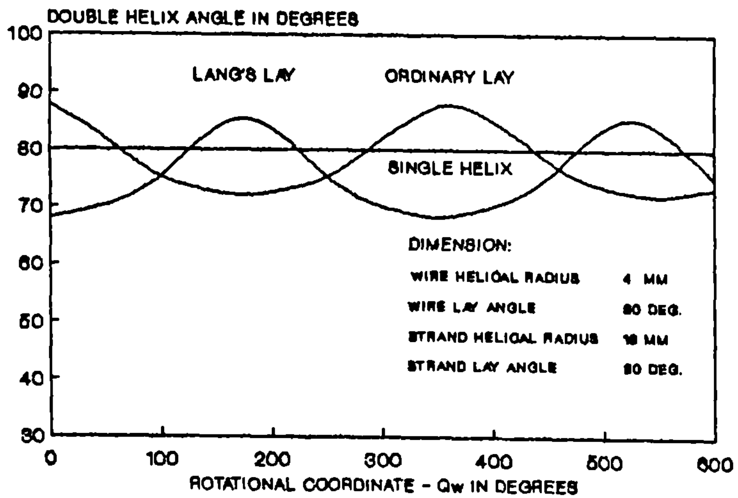

FIGURE 6.4-2
DOUBLE HELIX ANGLE VS WIRE ROT.

DOUBLE HELIX ANGLE V STRAND ROTATION
LANGS LAY AND ORDINARY LAY

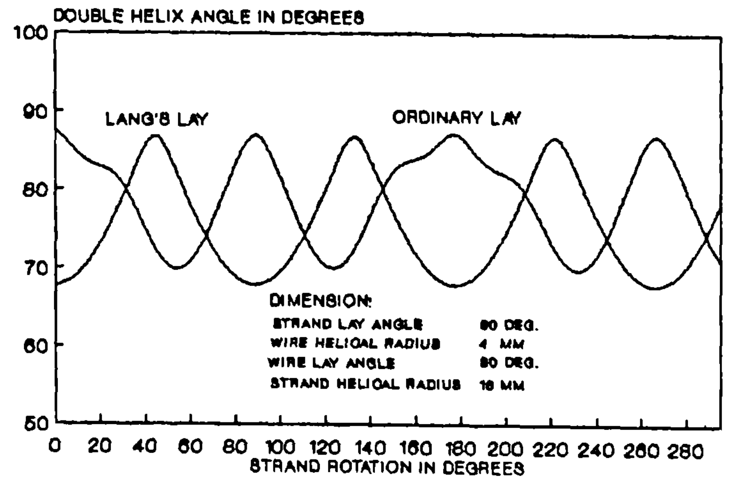

FIGURE 6.4-3
DOUBLE HELIX ANGLE VS ANGLE
OF ROTATION OF STRAND

than 60 degrees):

a. The coordinates, curvature, torsion and helix angle of a double helix can be regarded as functions of θ_w and θ_s, Figure 5.4-1 to 5.4-5.

b. For curvature and torsion of Lang's lay rope and ordinary lay rope expressed as functions of θ_w, the period of both functions is 360 degrees, with the two functions being 180 degrees out of phase, Figure 5.4-4 and 5.4-5. For curvature and torsion expressed as functions of θ_s , the period of both functions is less than 360 degrees. However, the out-of-phase characteristic remains change, Figure 5.4-4 (a) and 5.4-5 (a).

c. Lang's lay double helix is more tortuous than ordinary lay double helix, Figure 5.4-1.

d. For double helix angle expressed as functions of θ_w, the function of Lang's lay double helix angle is 180 degrees out-of-phase with the function of ordinary lay double helix angle, Figure 5.4-2.

e. When the wire helix angle is a minimum the curvature is a maximum and the torsion is a minimum. Similarly, when the wire helix angle is maximum the curvature is a minimum and the torsion is a maximum, Figure 5.4-2,

DOUBLE HELIX

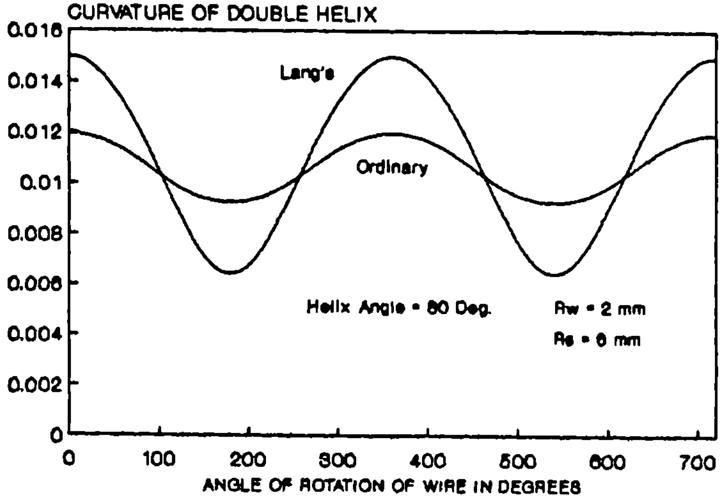

FIGURE 6.4-4
CURVATURE OF DOUBLE HELIX
Vs ANGLE OF ROTATION OF WIRE

DOUBLE HELIX

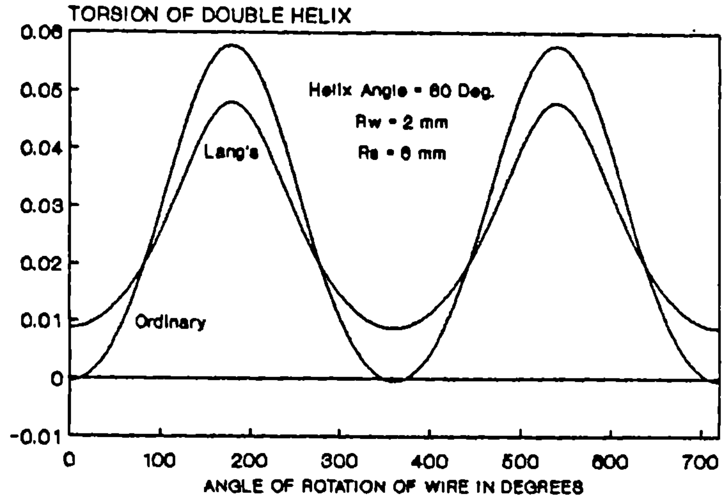

FIGURE 6.4-5
TORSION OF DOUBLE HELIX Vs
ANGLE OF ROTATION OF WIRE

DOUBLE HELIX

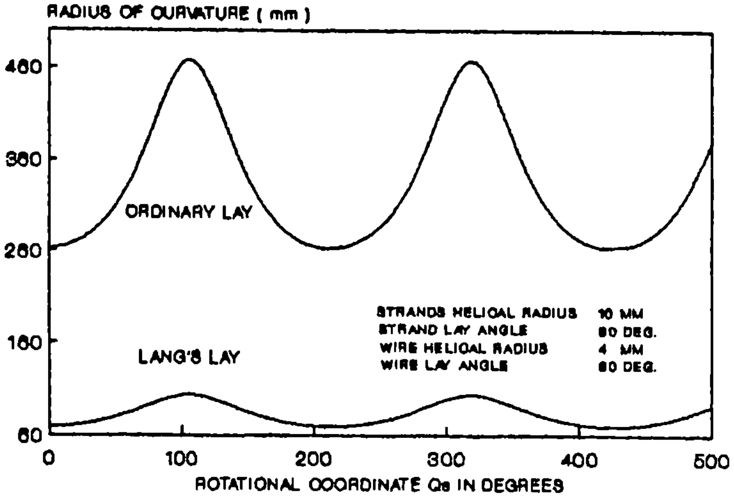

FIGURE 6.4-4 (a)
RADIUS OF CURVATURE VS
ANGLE OF ROTATION OF STRAND

DOUBLE HELIX

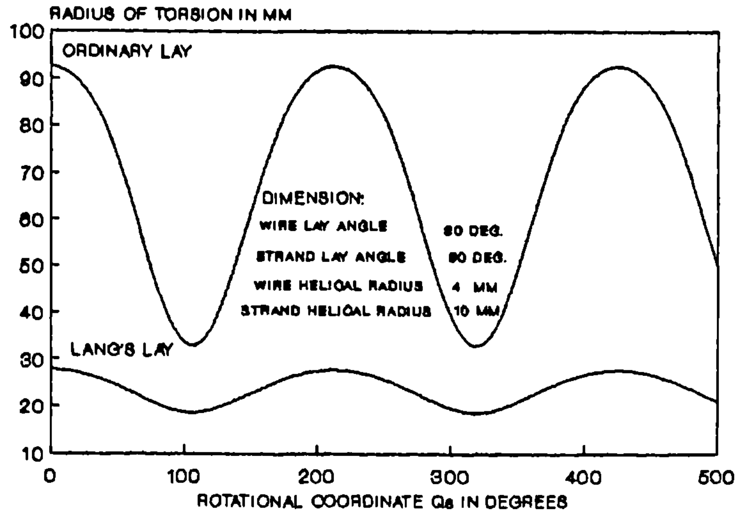

FIGURE 6.4-5 (a)
RADIUS OF TORSION VS STRAND ROT.

5.4-4 and 5.4-5.

Note:

a. Points for which θ_w is a multiple of 360 degrees are on the worn crown of the rope.

b. Points for which (θ_w - 180) degrees is a multiple of 360 degrees are point of contact with the strand layer immediately beneath the current strand layers.

c. Point for which (θ_w - 90) degrees is a multiple of 180 degrees are points of contact with neighbouring strands in the current strand layer.

5.4.2 Implications of Helix Geometry

Elastic rod theory shows that

Bending Moment = flexural bending stiffness x change in curvature

Twisting Moment = flexural twisting stiffness x change in torsion

Combining these equations with the results of the geometrical model, one can see that:

a. Internal components of forces and moments will vary periodically with θ_w along a double helical wires, irrespective of the frictional conditions imposed on the wire. For instance, the variation of groove width and depth on the surface of double helical wire, as shown on Figure 5.4-2 (1), is thought to be a result of variation of radial force along each cycle length. Bending and twisting moment also vary as the result of the wavy geometry of the double helical wire. In addition to the influence of the mechanical responses, mechanical interactions would also be responsible for causing the variation of the degree of damage (ie, width and depth of grooves and nicks) on the surface of the double helical wire. Groovings and nickings have been shown and defined in chapter two.

b. The periodic variation of double helix angle along a double helical wire implies that the pattern of contact patches along the double helical wire will also vary periodically with θ_w.

c. The periodic geometrical variations of a double helical wire implies that there are periodic stresses variation on the double helical wire. If a rope is subjected to tension-tension fatigue tests the failure modes along the double helical wire will also vary periodically with θ_w.

d. For a straight rope, a Lang's lay double helical wire is wavier than a ordinary lay double helical wire, as shown in Figure 5.4-1. This implies that the lang's lay double helical wire will likely subject to more fatigue

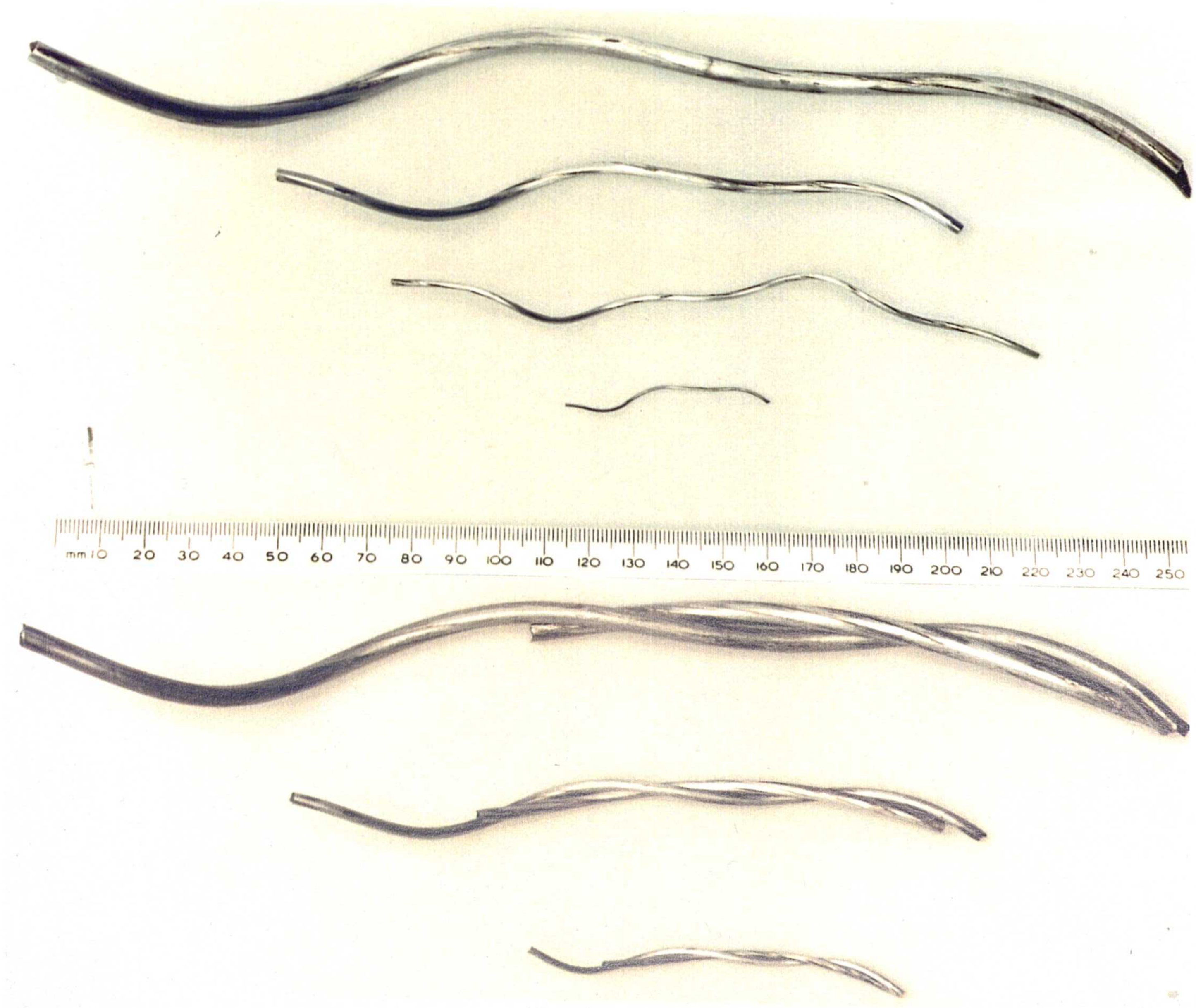

a. Grooves On Double Helical Wires

b. Single Helical Wire Incorporated With Double Helical Wire

Figure 5·4-2 (1)

problems than ordinary lay double helix.

e. For a rope which is not subject to bending wire helix angle will in practice always greater than 60 degrees. Thus curvature will, to a good approximation, be 180 degrees out of phase with torsion. This implies that, for a straight rope under tension, points of maximum bending will also be points of minimum twisting, and vice versa. Bending and twisting will be periodic in θ_w with a period of 360 degrees.

If a transverse section is made through the longitudinal axis of a rope the variation of the helix angle of a double helical wire is such that:

a. The wire cross-section is approximately elliptical when the wire helix angle is a minimum and is approximately circular when the wire helix angle is a maximum. The lay configuration of a rope can thus be identified from its transverse section, Figure 5.4-4 (3) and 5.4-2.

b. When the wire helix angle is a minimum the curvature is a maximum and the torsion is a minimum. Similarly, when the wire helix angle is maximum the curvature is a minimum and the torsion is a maximum. These characteristics allow high bending and twisting stresses along a wire to be located.

From (a) and (b) it can be shown that if an ordinary lay rope, with a Lang's lay IWRC is subjected to a tensile load, the maximum curvature and minimum torsion of a wire will occur in the regions of contact between the outer strands and the IWRC. The maximum torsion and minimum curvature occur at the worn crown of the outer strands.

5.4.3 Influences of Strand Helix Angle on Double Helix Geometry

The helix angle of wire and strand in a rope has a strong influence on the geometrical properties of the double helical wire and hence on the mechanical behaviour of this wire. Although the present analyses do not provide a picture of how mechanical behaviour is changed by the helix angle, they provide information on how the geometry of a double helix is changed by the helix angle.

a. Figure 5.4-7 shows the variation of maximum radii of curvature on the Lang's lay and ordinary lay double helices corresponding to the change of the strand helix angles. For strand helix angle larger than 50 degrees, Figure 5.4-7 shows that the radius of curvature of ordinary lay double helix increases more rapid than that on a Lang's lay double helix.

b. Figure 5.4-8 shows the variation of maximum radii of torsion on the Lang's lay and ordinary lay double

DOUBLE HELIX

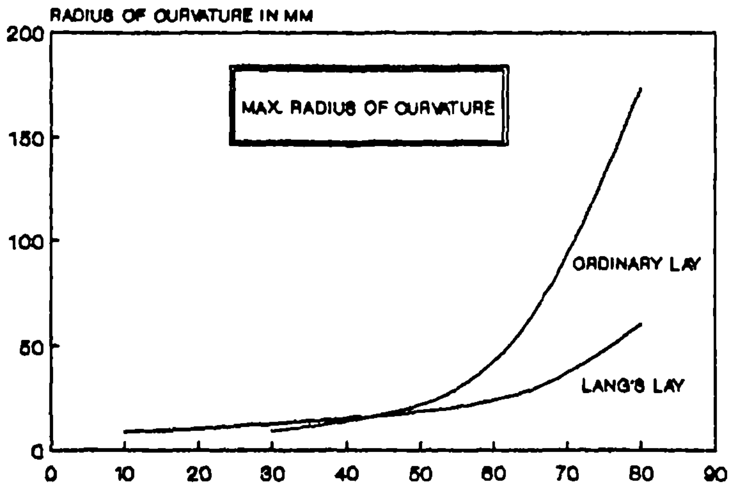

FIGURE 5.4-7
RADIUS OF CURVATURE VS STRAND LAY
(LANG'S LAY AND ORDINARY LAY)

DOUBLE HELIX

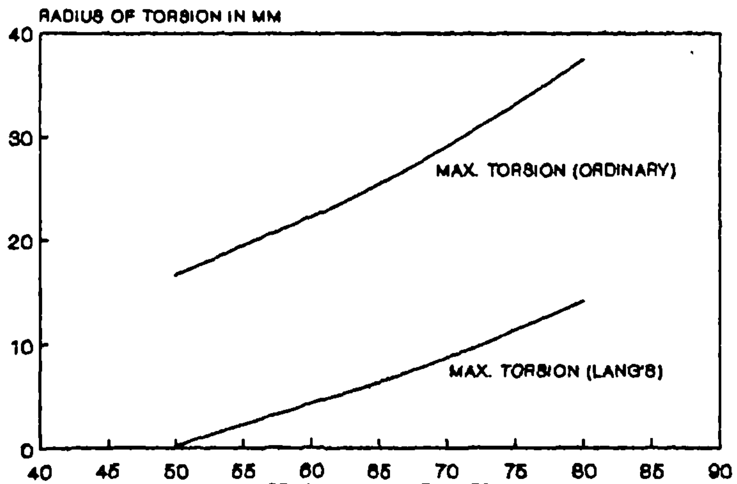

FIGURE 5.4-8
COMPARING RADII OF TORSION
BETWEEN LANG'S & ORDINARY LAY

DOUBLE HELIX ANGLE V STRAND LAY
LANG'S AND ORDINARY LAY

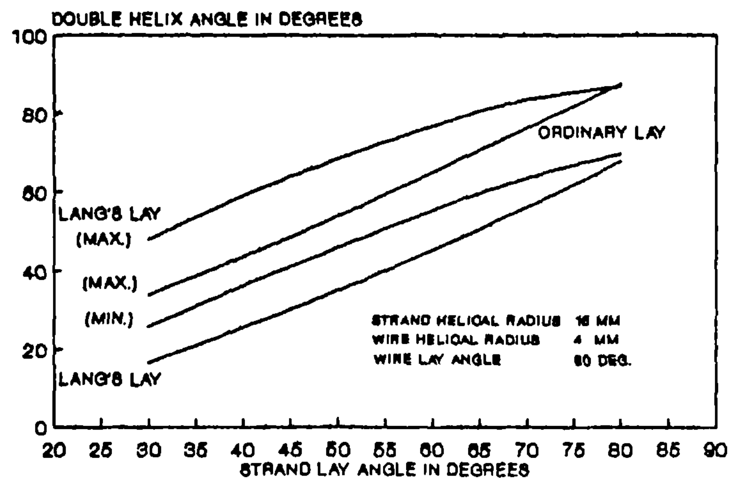

FIGURE 5.4-9
COMPARISON OF DOUBLE HELIX ANGLE BETWEEN
LANG'S LAY AND ORDINARY LAY (VS STR.ROT)

helices corresponding to the change of the strand helix angles. This diagram indicates that the maximum radius of torsion on an ordinary lay double helix is always larger than that of the Lang's lay double helix.

c. Figure 5.4-9 shows the variation of maximum and minimum double helix angle in Lang's lay and ordinary lay double helices corresponding to the change of the strand helix angle. This diagram indicates that the difference between maximum and minimum double helix angles on a Lang's lay double helical wire is larger than that on an ordinary lay double helical wire. In other words a Lang's lay double helix is more tortuous than an ordinary lay double helix.

These diagrams reveal the geometrical differences between Lang's lay and ordinary double helices. If relationships between helix geometry and mechanical behaviour were known, one could immediately tell from these diagrams that which type of lay would be better than the other.

5.4.4 Double Helix Angle And Its Applications

The double helix angle, defined in the previous chapter, is an important characteristic parameter for rope behaviour. The following sub-sections will focus on the practical and analytical aspects of this parameter, whose importance is identified in this thesis.

a. Practical Aspect

Many of the practical features of rope behaviour are related to the sectional shape of individual wires and it is of interest to know that for a rope with given transverse or oblique cross-section, individual and adjacent wires appear to have different sectional shape (circular, elliptical or kidney etc.) Figure 5.4-2 gives a clue to this aspect. It shows that double helix angle varies along the cyclic length of double helical wire. Photographs which illustrate this geometrical characteristic are now referred to.

1. Figure 5.4-4 (1) illustrates the elevation and plan view of a double helical wire in contact with the single helical wire in an IWRC. In the plan view, one will note that the double helical wire (the wire is marked by a red dash) is almost parallel to the axis of the core strand at the point of contact. Therefore, one can expect a circular cross section for that Lang's lay double helical wire at the contact point. Figure 5.4-4 (2) illustrates how this Lang's lay double helical wire (the wire is marked by two green dashes) is incorporated in the strand.

2. Figure 5.4-4 (3) illustrates a transverse section of a 6x41 ordinary rope with a Lang's lay IWRC. It can note that the Lang's lay double helical wire has a circular sectional shape when it comes in contact with the single

Elevation

Plan View

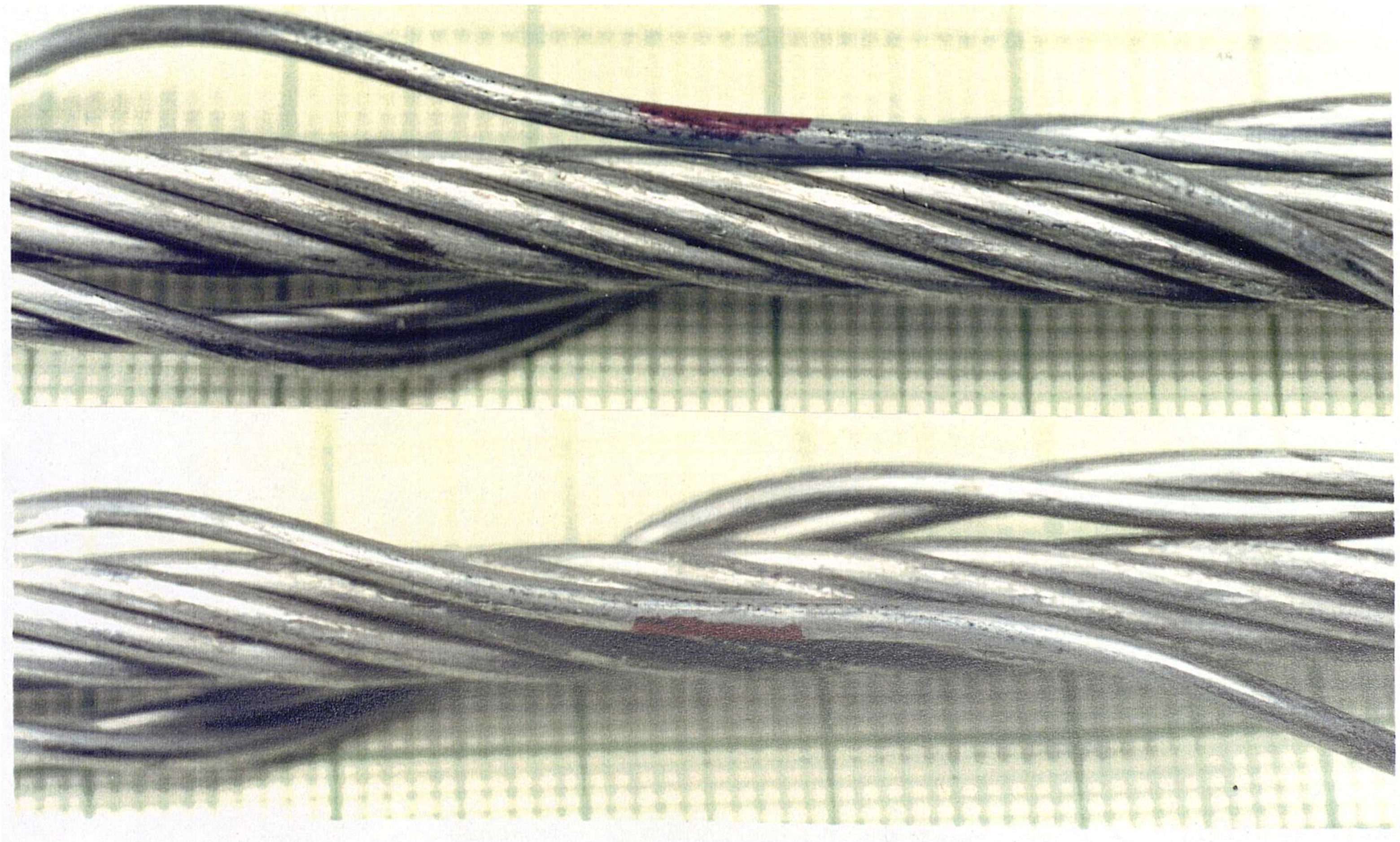

Contact Features Between Single

And Double Helical Wire In IWRC

Figure 5·4-4(1)

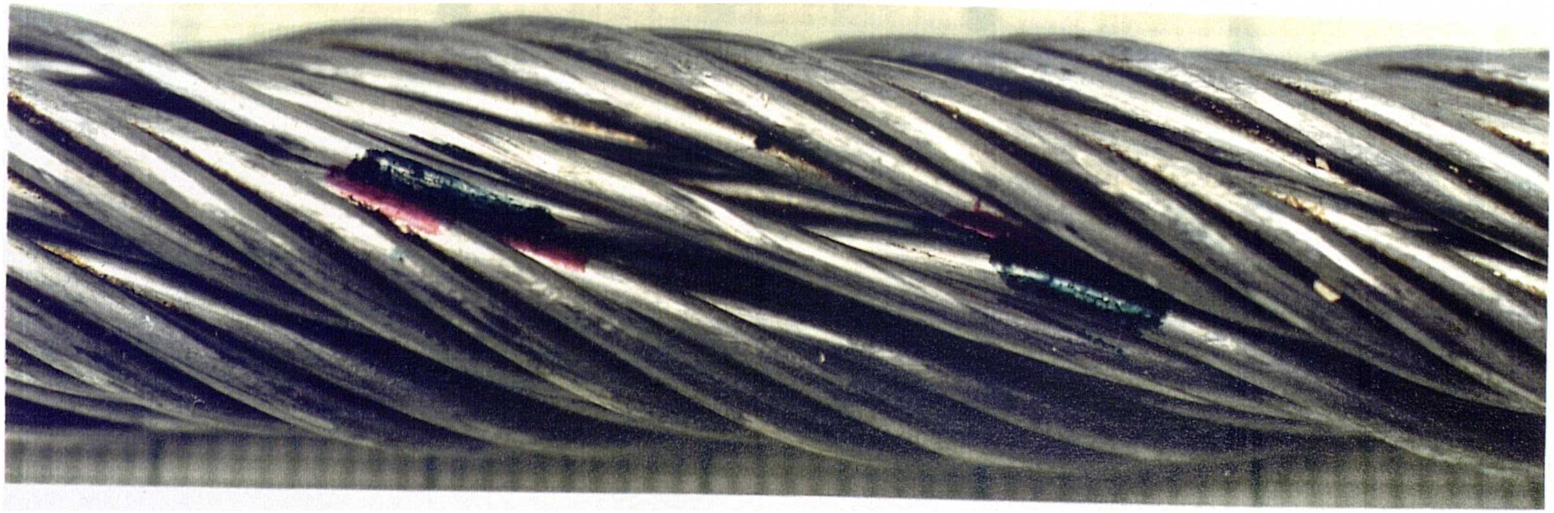

Plan View Of IWRC

Double Helical Wire Incorporated In

Strand And Contacting Core Wire In IWRC

Figure 5.4-4 (2)

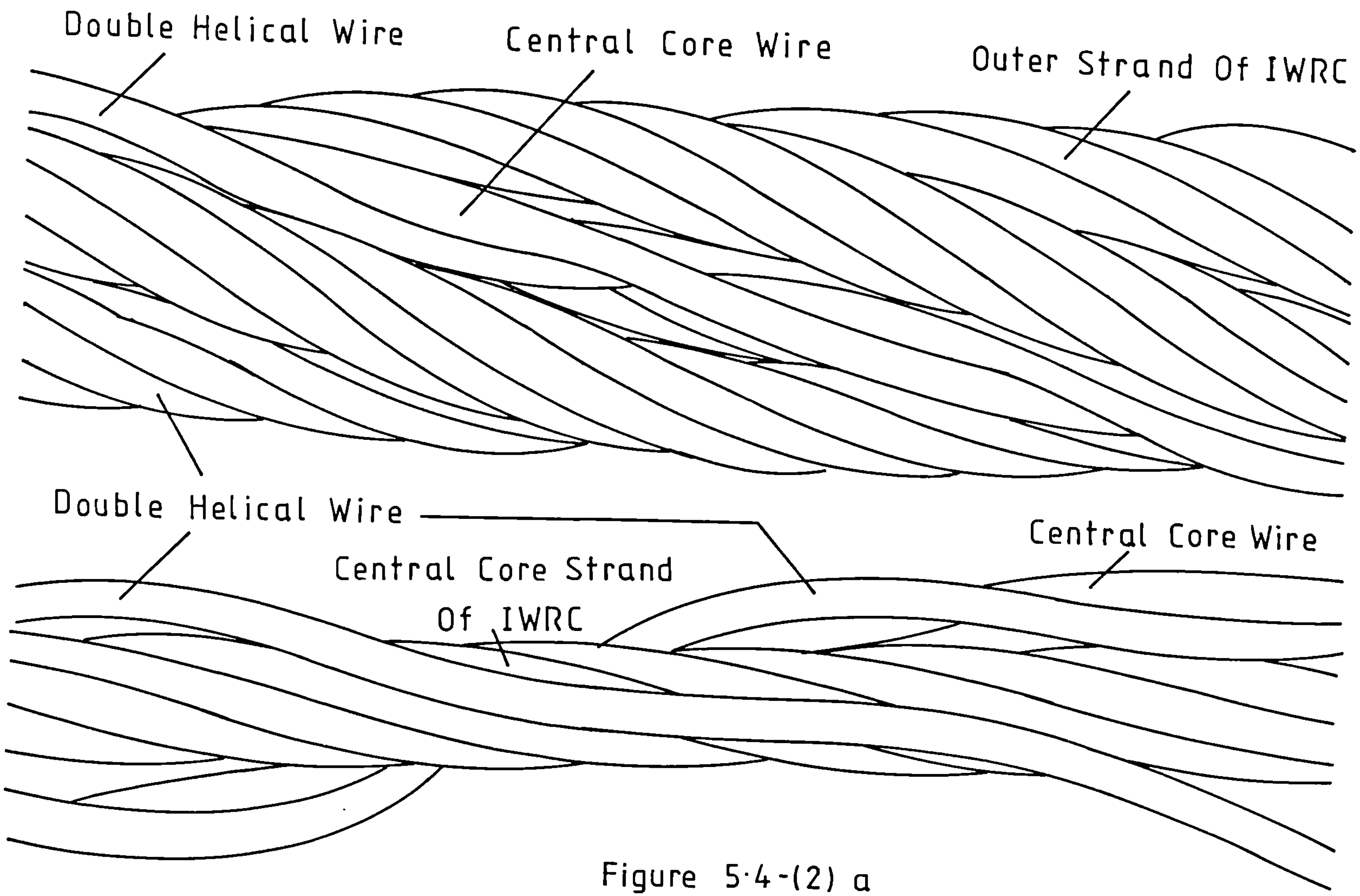

Figure 5·4-(2) a

Dissection Of IWRC

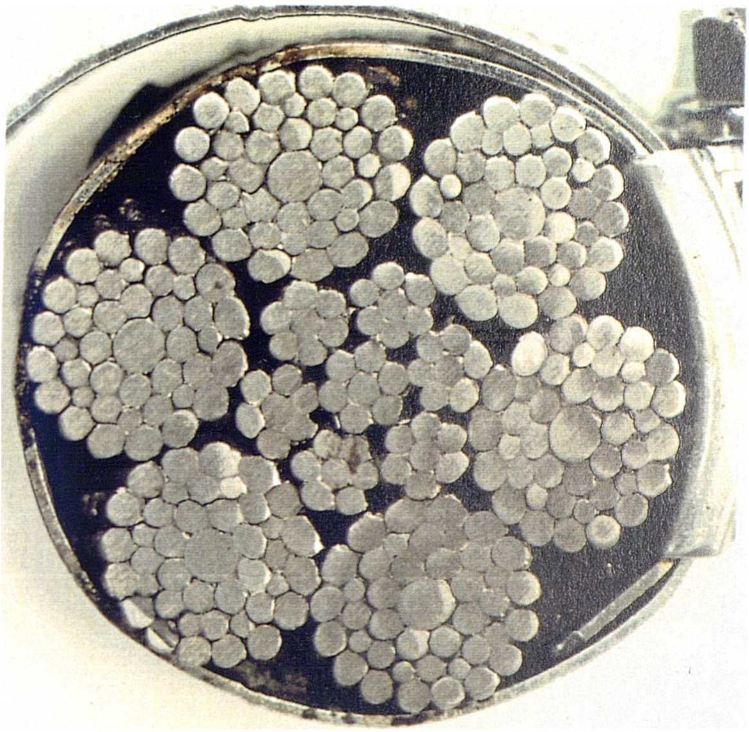

(a.)

Typtical Large Diameter Wire Rope
Transverse Section

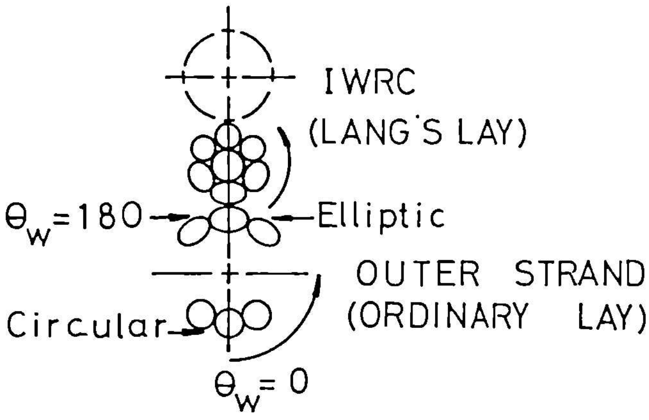

(b.)

Figure 5·4-4(3)

helical wire of the core strand. However, the double helical wire has a elliptical sectional shape where it contacts with the double helical wire of the outer strand. An ordinary double helical wire, on the other hand, has an elliptical sectional shape when it come in contact with double helical wire of the IWRC. This wire has a circular sectional shape when it located on the surface of the rope. In general, understanding of the double helix angle can be applied to distinguish between Lang's lay strands and ordinary lay in ropes.

b. Analytical Aspects

Grooves found on a double helical wires are the result of either contacting with equal lay wires or contacting with a single helical core wire. However, nicks found on the double helical wire are more complicated. It is because of the periodic variation of double helix angle along the double helical wire and the tolerance between adjacent wires at the outer layer of the strands. *Figure 5.4-4 (4) shows typical* nicks found on the double helical wire. The wires, shown in these photographs, have failed resulting from secondary bending (top) and secondary twisting (bottom). A study of double helix angle leads to understanding of two important features, namely.

a. the location of nicks constitute clamping and pivoting points.

a.

Plan View

Side View

Typtical Nicks On Double Helical Wire

b.

Wire Failed By

a. Secondary Bending

b. Secondary Twisting

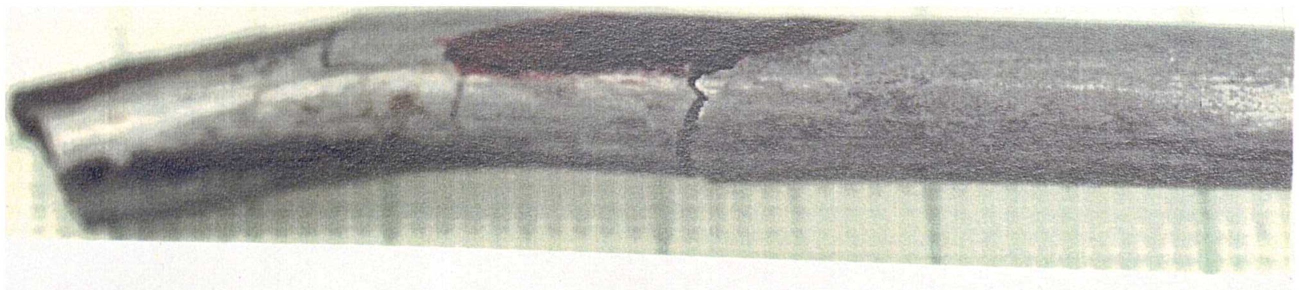

Figure 5·4-4 (4)

b. quantifying of the contact angle for contact analysis.

Figure 5.4-4 (5) is a schematic representation of the contact patterns between double helical wires. The following tables (tables 5.4.2.1, 5.4.2.2 and 5.4.3) give the contact angles obtained by applying mathematical manipulation of the double helix angles of wires at the contact points. The subscript notation for the double helix angles are defined as follows:

Subscript Notation:

chl	Single helical wire contact with Lang's Lay double helical wire within an IWRC
L	Lang's lay double helical wire in an IWRC
I	Single helical wire in an IWRC
cha	Single helical wire contacting ordinary Lay double helical wire within IWRC
A	Ordinary lay double helical wire in an IWRC
d	Contact of two double helical wires between two neighbouring strands in the same layer (Lang's layand ordinary lay)
wl	Single helix angle of outer layer wire in a helical strand
hhl	Contact of two double helical wires between two neighbouring strands at the adjacent layers of lang's lay strand.
lo	Double helical wire in an outer strand

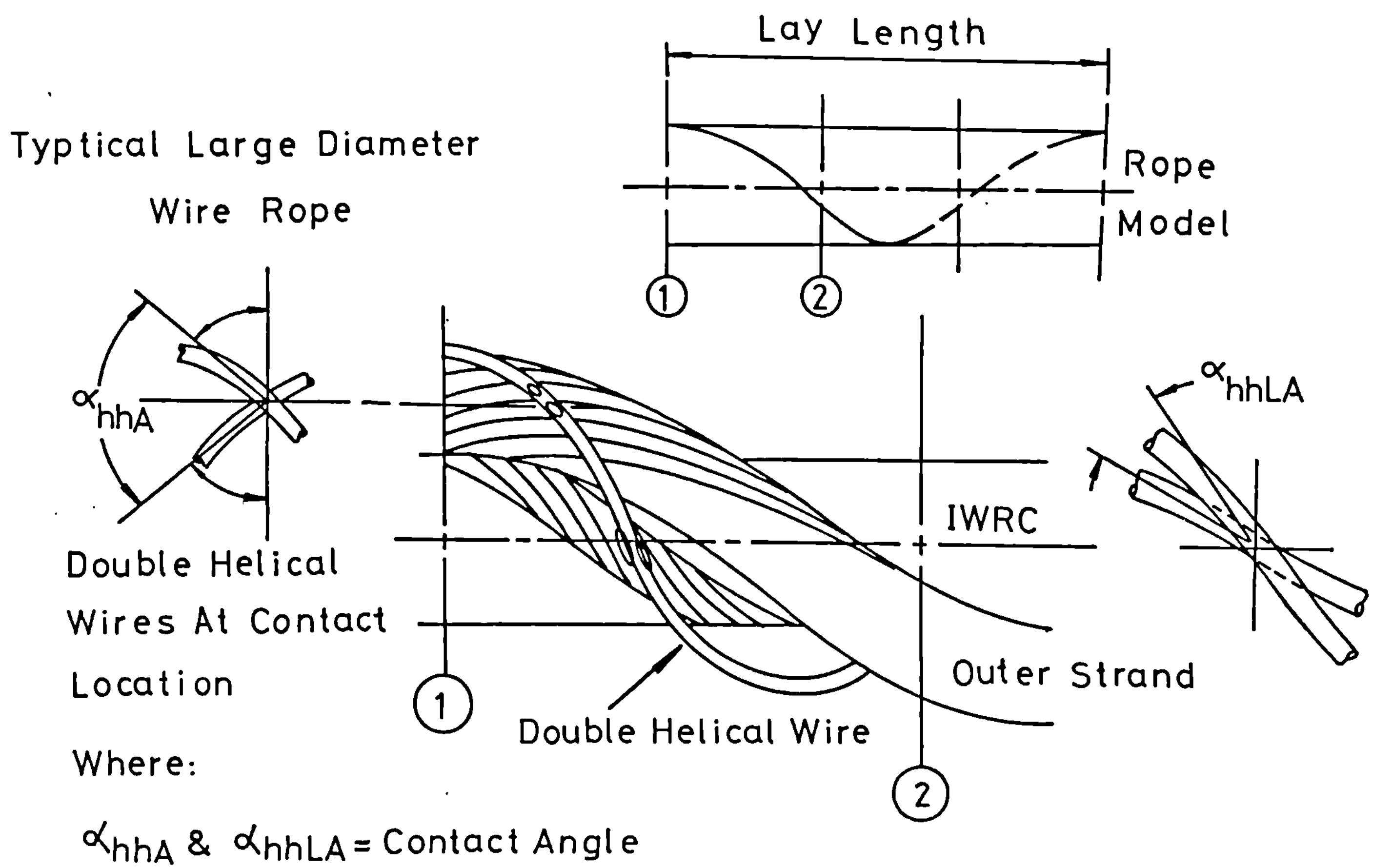

Figure 5·4-4 (5)
Contact Angle

Li Double helical wire in an inner strand

hhA Contact of two double helical wires between two neighbouring strands at adjacent layers of ordinary lay strand.

hhLA Contact of two double helical wires between two neighbouring strands which are inner layer Lang's lay strand and outer layer ordinary lay strand.

L Lang's lay wire

A Ordinary lay wire

Superscript Notation

* Double helix angle (Lang's lay or ordinary lay)

TABLE 5.4.2.1

WIRE CONTACT ANGLE BETWEEN CORE STRAND AND HELICAL STRAND OF A 6 STRANDED ROPE

DIRECTION OF TWO ADJACENT WIRE AT THE CONTACT POINT	CORE STRAND CONTACT WITH HELICAL STRAND (FOR LANG'S LAY ONLY)	LAY DIRECTION
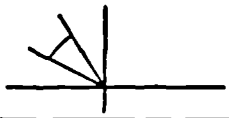	$\alpha_{chl} = \mid \alpha^*_l - \alpha_1 \mid$	LEFT-LEFT
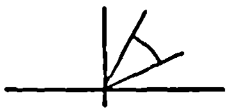	DITTO	RIGHT - RIGHT
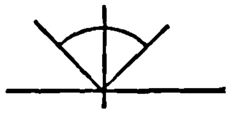	$\alpha_{chl} = \mid 180 - \alpha^*_l - \alpha_1 \mid$	LEFT - RIGHT
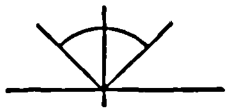	DITTO	RIGHT-LEFT

	(FOR ORDINARY LAY ONLY)	
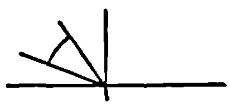	$\alpha_{chA} = \mid \alpha_1 - \alpha^*_A \mid$	LEFT-LEFT
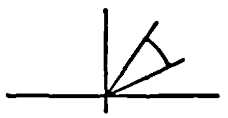	DITTO	RIGHT - RIGHT
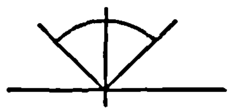	$\alpha_{chA} = \mid 180 - \alpha^*_A - \alpha_1 \mid$	LEFT - RIGHT
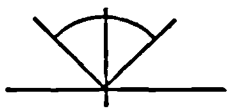	DITTO	RIGHT-LEFT

These two tables can be applied to reveal the contact angle between two wires of two adjacent strands at two adjacent layers.

TABLE 5.4.2.2

DIRECTION OF TWO WIRES	HELICAL STRAND + HELICAL STRAND (WIRE OUT) (WIRE IN)	REMARK
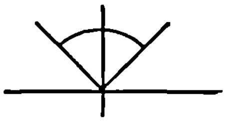	$\alpha_d = 180 - \alpha_{wi} - \alpha_{wo}$	TWO ADJACENT STRD

This table applys only to two adjacent contact strand in the same layer. It can be applied to reveal the contact angle of wires in both Lang's and ordinary lay strands.

TABLE 5.4.3

DIRECTION OF TWO ADJACENT WIRE AT THE CONTACT POINT	HEL. STRAND CONTACT HEL. STRAND (INNER LAYER) (OUTER LAYER) (THIS APPLY ONLY TO LANG'S LAY)	LAY DIRECTION
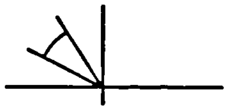	$\alpha_{chh} = \mid \alpha^*_{lo} - \alpha^*_{li} \mid$	LEFT-LEFT
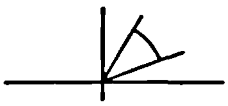	DITTO	RIGHT - RIGHT
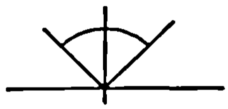	$\alpha_{chl} = \mid 180 - \alpha^*_{lo} - \alpha^*_{li} \mid$	LEFT - RIGHT
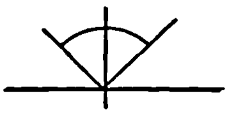	DITTO	RIGHT-LEFT

	(APPLY ONLY TO ORDINARY LAY)	
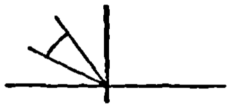	$\alpha_{chA} = \mid \alpha_1 - \alpha^*_A \mid$	LEFT-LEFT
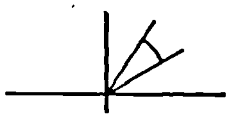	DITTO	RIGHT - RIGHT
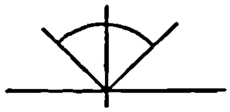	$\alpha_{chA} = \mid 180 - \alpha^*_A - \alpha_1 \mid$	LEFT - RIGHT
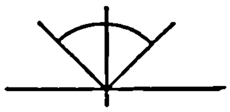	DITTO	RIGHT-LEFT

TABLE 5.4.4

DIRECTION OF TWO ADJACENT WIRE AT THE CONTACT POINT	HEL. STRAND CONTACT HEL. STRAND (LANG'S LAY) (ORDINARY LAY) (THIS APPLY ONLY TO LANG'S LAY)	LAY DIR- ECTION
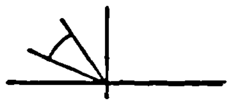	$\alpha_{chh} = \mid \alpha^*_L - \alpha^*_A \mid$	LEFT-LEFT
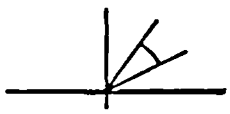	DITTO	RIGHT - RIGHT
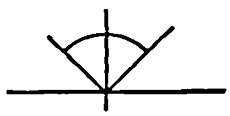	$\alpha_{chl} = \mid 180 - \alpha^*_L - \alpha^*_A \mid$	LEFT - RIGHT
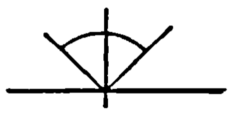	DITTO	RIGHT-LEFT

This table can be applied to reveal the contact angle between two contacting wires each in Lang's lay strand and ordinary lay strand located at two adjacent layers.

5.4.5 Summary of Findings and Postulations

Post-test examination of wire failures and geometrical modelling of double helical wire have enabled the author to make some postulates about the mechanical responses of double helical wire in a rope subjected to external tensile load.

1. Periodic variation of the radius of curvature, radius of torsion and double helix angle on a double helical wire implies that internal component forces and moments will also vary periodically with θ_w along double helical wire.

2. The out-of-phase characteristic between the radius of curvature and radius of torsion on a double helical wire implies that the maximum bending and minimum twisting stresses on the double helical wire will almost locate at the same position on the double helical wire and this characteristic will repeat each cycle.

3. For an ordinary lay rope with a Lang's lay IWRC, the maximum curvature and minimum torsion of a wire will occur in the regions of contact between the outer strands and the IWRC. the maximum torsion and minimum curvature occur at the worn crown of the outer strands. This characteristics is importance for design ' reduced rotation ' ropes.

4. For double helix angle expressed as functions of θ_w, the function of the double helix angle of a Lang's lay double helical wire is 180 degrees out of phase with the function of the double helix angle of a ordinary lay double helical wire.

This characteristic is importance for identifying contact patches and lay configuration of ropes.

Remark:
One important point that the author wishes to raise, is that the out-of-phase geometric characteristic must be carefully considered when designing 'reduced rotation' rope (eg multi-strand rope) in which the Lang's lay type of strand and ordinary type of strand are often laid alternately amongst adjacent layers. Wires at the contact locations between adjacent layers could fail much earlier as the results of

a. contact stresses
b. stresses resulting from interactions and
c. maximum stresses *which occur as the result of* mechanical response due to the out-of-phase geometrical characteristic between Lang' lay and ordinary lay double helical wire coinciding at the contact locations.

5.5 Ring and Drum Single Helix Geometry and Implications

Both ring and drum single helices are double helices. The former is a degenerate case with zero strand helix angle; it is because the strand is being bent over a sheave. The latter is a double helix with very small strand helix angle; it is because the strand is being wound around the drum. The following sub-sections present the author's computer results for ring/drum single helix and discuss the implications of these helix geometry for the mechanical responses of ring and drum single helical wire.

5.5.1 Physical Differences Between Ring / Drum Single Helix and Double Helix

There are some differences between a double helical wire within a straight rope and a ring/drum single helical wire within a bent strand.

a. Double helical wires are preformed permanently in a rope during rope manufacturing whereas ring or drum single helical wires within a strand are deformed, from single helical wires to double helical wires, by bending a strand over a sheave or by winding a strand around a drum.

b. For helical strands laid around a main core, a rope is formed with small strand helical radius and very large helix angle; for example strand helical radius = 10 mm and strand helix angle = 78 degrees. For a strand wound around a drum, the strand helix angle is very small and drum helical radius is very large; for example drum helical radius = 300 mm and strand helix angle < 10 degrees. For a strand bent over a sheave, the helix angle even equals zero. (N.B. the strand helical radius in a rope is equivalent to the ring or drum helical radius applied to a strand bent around a sheave or wound around a drum).

5.5.2 Geometrical Properties of Ring and Drum Single Helix

If a strand is wound around a drum in the same orientation as the helical wire laid in the strand, then the periodic variation of geometrical properties of a ring or a drum single helical wire should be similar to those of the double helical wires in a Lang's lay rope. On the other hand, if a strand is wound in the opposite orientation to the helical wire laid in the strand, then the periodic variation of geometrical properties of the ring and the drum single helical wire may be different from those of the double helical wires in an ordinary lay rope, Figure 5.4-5 and 5.5.2-2. The geometrical model shows:

a. For an ordinary lay rope, the torsion has a period of

DRUM SINGLE HELIX

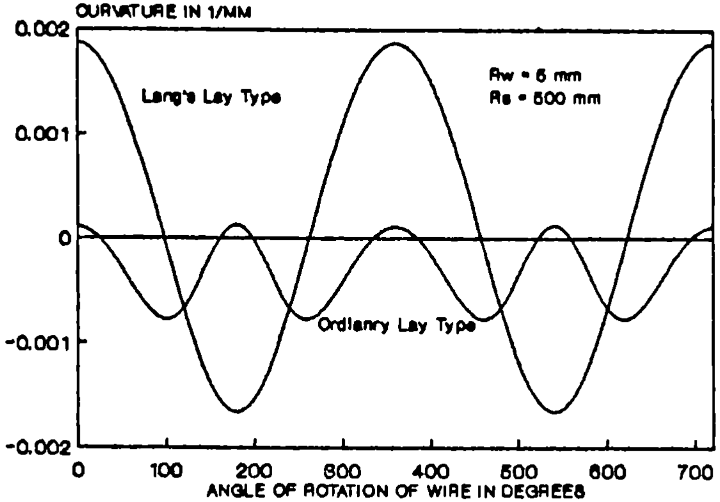

FIGURE 5.5.2-1
CURVATURE Vs ANGLE OF
ROTATION OF WIRE (Qw)

DRUM SINGLE HELIX

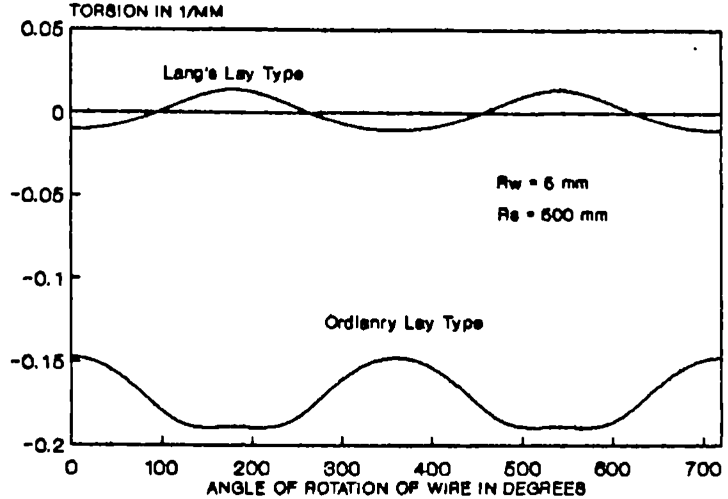

FIGURE 5.5.2-2
TORSION VS ANGLE OF
ROTATION OF WIRE (Qw)

DRUM SINGLE HELIX

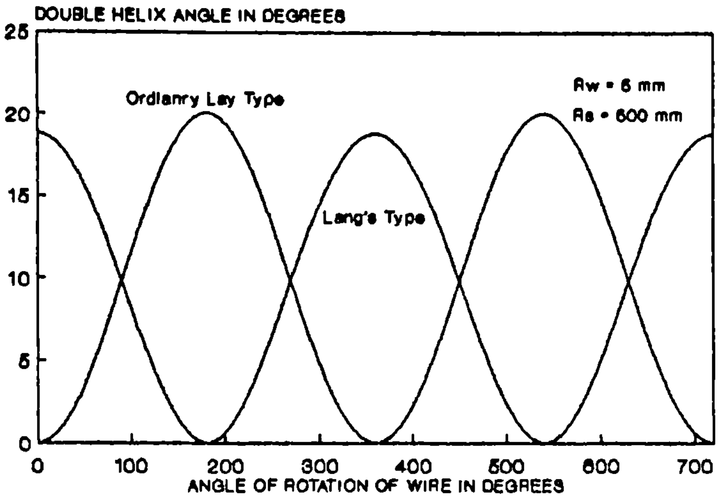

FIGURE 5.5.2-3
DOUBLE HELIX ANGLE Vs
ANGLE OF ROTATION OF WIRE

360 degrees but the period of the curvature may be less than this.

b. The curve of the helix angle function will shift downward as the strand helix angle reduces.

c. For a strand wound around a drum, the entire shape of the curves of change in curvature and torsion between a double and single helical wires remain the same as those of curvature and torsion of the double helical wire, with the exception that the change in curvature and torsion shift downward toward the zero axis or below the zero axis of the curvature and torsion graphs.

5.5.3 Implications Of Ring/Drum Single Helical Wire

The implications of geometrical properties of a ring single helical wire and a drum single helical wire are qualitatively discussed in the following.

a. For a given size of strand and drum, the maximum magnitude of curvature on the Lang's lay type of drum single helical wire is more significant than that of the curvature on the ordinary lay type of drum single helix, as shown in Figure 5.5.2-1. On the other hand, the magnitude of torsion on the ordinary lay type of drum single helical wire is more significant than that of the torsion on the Lang's lay type of drum single helical wire, Figure 5.5.2-2.

b. For a strand wound around a drum (the strand is being wound in the same orientation to its wires), the high bending stress appears to be at the points for which θ_w is a multiple of 360 degrees on the *double helical* wire. The reference datum for θ_w must be at either 0 or 180 degrees.

c. For a strand wound around a drum (the strand is being wound in the opposite orientation to its wires), the high bending stress appears to be at the points for which $(\theta_w - 90)$ is a multiple of 180 degrees.

Note:

By varying the strand helix angle and drum helical radius, the geometrical properties of ring and drum single will be changed.

5.6 RING/DRUM DOUBLE HELIX GEOMETRY AND THEIR IMPLICATIONS

Rope is not only designed to carry tensile load, but must also be designed withstand reversed bending as it runs over a sheave or a drum. For a rope running over a sheave or a drum, rope problems will silently develop and soon become apparent. Problems such as core crushing, external and internal wear resulting form using improper size of sheave or drum are the consequence of high bearing pressure. However, some physical parameters are not readily to be seen and, are hidden in the helix geometry of wires eg the change in radius of curvature and torsion along the triple helical wire. These parameters are rather sensitive to the diameter of a sheave or a drum. Examples chosen to illustrate these points are described as follows:

5.6.1 Geometrical Properties of Triple Helix

In addition to the geometrical influence of radii of wires, helical radii of wires and strands. The geometrical shape of a triple helix (included ring double helix and drum double helix) can be varied greatly by the combinations of orientations of wire lay, strand lay, rope lay (see table 5.6.1) as well as helix angle.

For a triple helical wire, the geometrical model shows that:

a. the coordinates, curvature, torsion and helix angle of a triple helix can be regarded as functions of θ_w and θ_d, Figure 5.6-1, 5.6-2 and 5.6-3.

Table 5.6.1. Lay Configurations Of Rope On Drum

TYPE OF ROPE LAY	ROPE DIRECTION ON DRUM	
	RIGHT HAND	LEFT HAND
RIGHT HAND LANG'S LAY	RIGHT-RIGHT LANG'S LAY	RIGHT-LEFT LANG'S LAY
LEFT HAND LANG'S LAY	LEFT-RIGHT LANG'S LAY	LEFT-LEFT LANG'S LAY
RIGHT HAND ORDINARY LAY	RIGHT-RIGHT ORDINARY LAY	RIGHT-LEFT ORDINARY LAY
LEFT HAND ORDINARY LAY	LEFT-RIGHT ORDINARY LAY	LEFT-LEFT ORDINARY LAY

(a) Possible lay configurations of rope wound around a drum.

TYPE OF ROPE LAY	ROPE DIRECTION ON DRUM	
	RIGHT HAND	LEFT HAND
RIGHT HAND LANG'S LAY	RIGHT-RIGHT LANG'S LAY	RIGHT-LEFT LANG'S LAY
RIGHT HAND ORDINARY LAY	RIGHT-RIGHT ORDINARY LAY	RIGHT-LEFT LANG'S LAY

(b) Four basic lay configurations of rope wound around a drum.

TRIPLE HELIX
(RIGHT LAID ON DRUM)

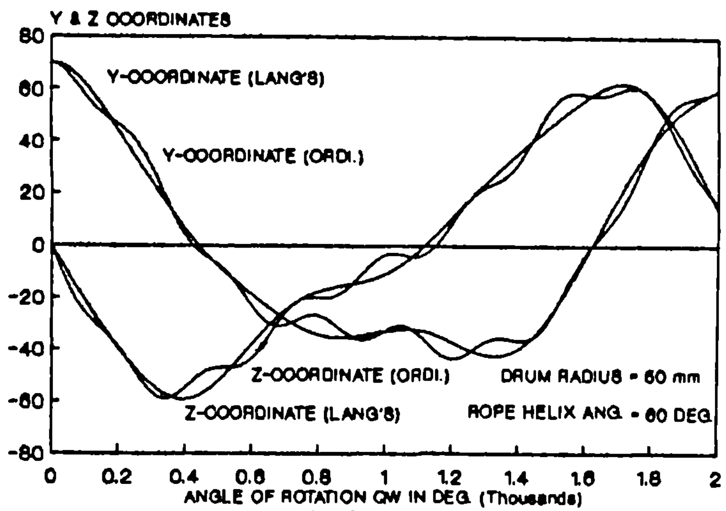

FIGURE 5.6-1 (a)
Y AND Z COORDINATES OF TRIPLE HELIX

RADIUS OF CURVATURE OF DRUM DOUBLE HELIX
(LANG'S LAY)

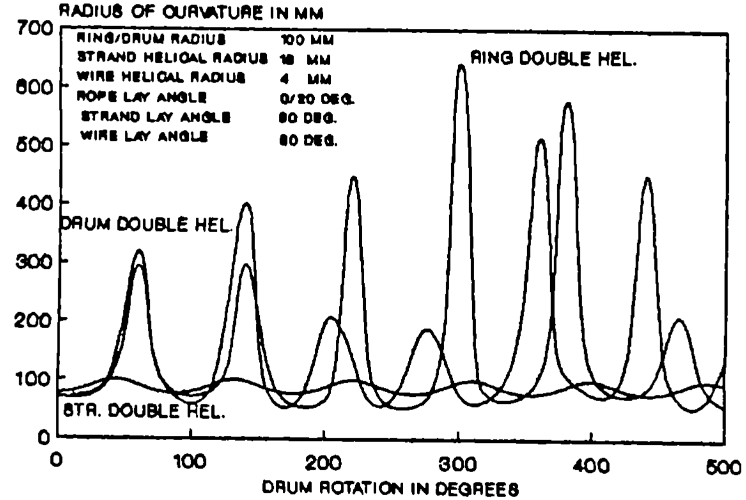

FIGURE 5.6-1(b)
RADIUS OF CURVATURE VS RING/DRUM ROT.

RADIUS OF CURVARURE OF DRUM DOUBLE HELIX
ORDINARY LAY

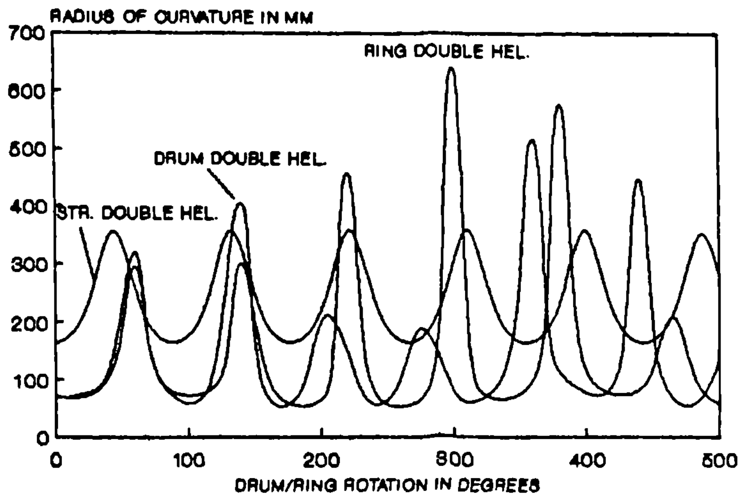

FIGURE 5.6-1(c)
RADIUS OF CURVATURE VS RING/DRUM ROT.

b. The magnitude of the curvature of a triple helical wire in an ordinary lay rope is smaller than that of a triple helical wire in a Lang's lay rope, Figure 5.6-2 (a) and 5.6-3 (a).

c. The variation in the torsion of triple helical wires in a Lang's lay rope is much less than that of the triple helical wire in an ordinary lay rope, Figure 5.6-2 (b) and 5.6-3 (b).

d. *the variation of the helix angle for a triple helical* wire in a Lang's lay rope is much greater than that for a triple helical wire in an ordinary lay rope, Figure 5.6-2 (c) and 5.6-3 (c).

N.B. All dimensions are in mm and in degrees.

5.6.2 Implication Of Ring And Drum Double Helix Geometry

For a rope wound around a drum, the geometrical model shows that the bending in double helical wires within a Lang's lay rope is , for all value of θ_w, greater than that on double helical wires within an ordinary lay rope. The torsion in a double helical wire in a Lang's lay rope is greater than that on a double helical wire in an ordinary lay rope for most values of θ_w.

TRIPLE HELIX
ROPE LAID IN THE LEFT HAND DIRECTION

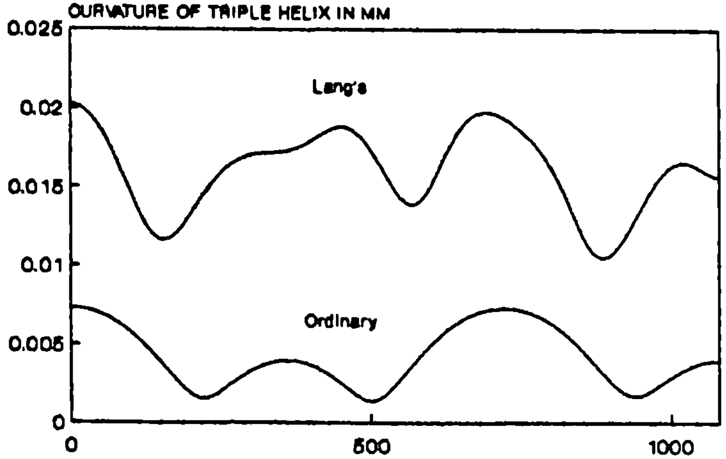

(a)
CRUVATURE OF TRIPLE HELIX Vs
ANGLE OF ROTATION OF WIRE

TRIPLE HELIX
ROPE LAID IN THE LEFT HAND DIRECTION

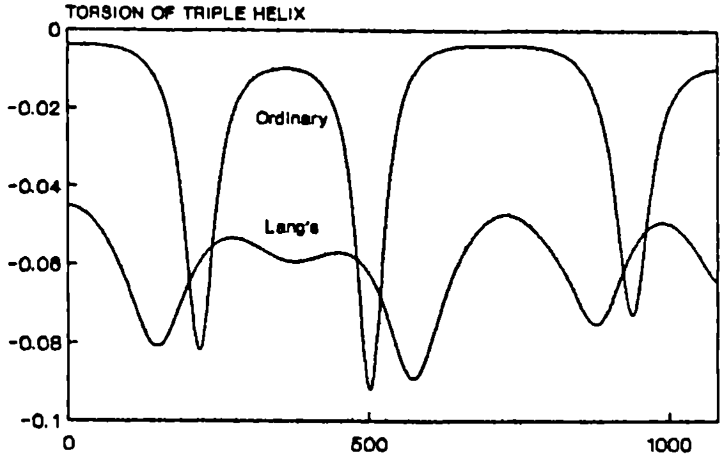

(b)
TORSION OF TRIPLE HELIX Vs
ANGLE OF ROTATION OF WIRE

TRIPLE HELIX ANGLE
ROPE LAID IN THE LEFT HAND DIRECTION

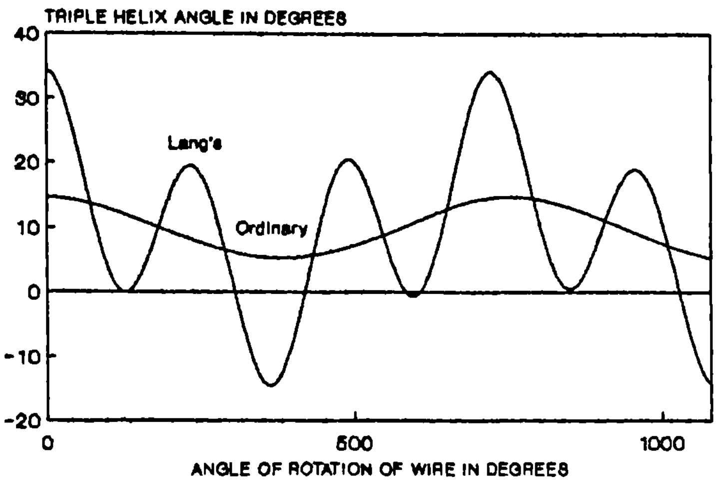

(c)
TRIPLE HELIX ANGLE Vs
ANGLE OF ROTATION OR WIRE

Key:

Helix Angle Of Wire = 80 Deg.

Helix Angle Of Strand = 80 Deg.

Helix Angle Of Rope = 10 Deg.

Helical Radius Of Wire = 4 mm

Helical Radius Of Strand = 8 mm

Drum Radius = 500 mm

FIGURE 5.6-2

GEOMETRICAL PROPERTIES OF DRUM DOUBLE HELIX

TRIPLE HELIX
ROPE LAID IN THE RIGHT HAND DIRECTION

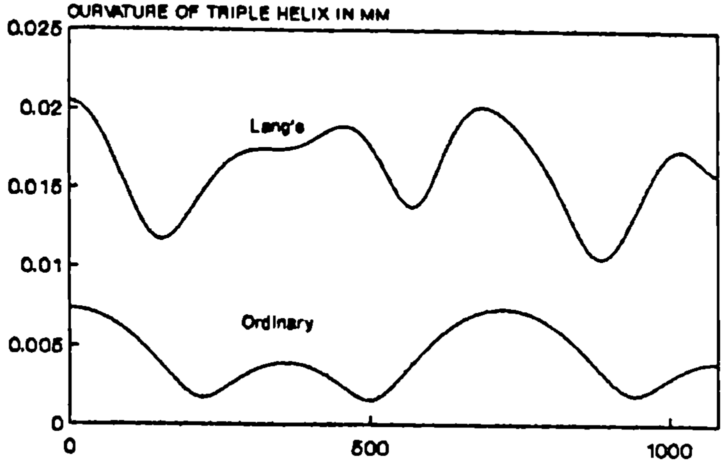

ANGLE OF ROTATION OF WIRE IN DEGREES
(a)
CURVATURE OF TRIPLE HELIX Vs
ANGLE OF ROTATION OF WIRE

TRIPLE HELIX
ROPE LAID IN THE RIGHT HAND DIRECTION

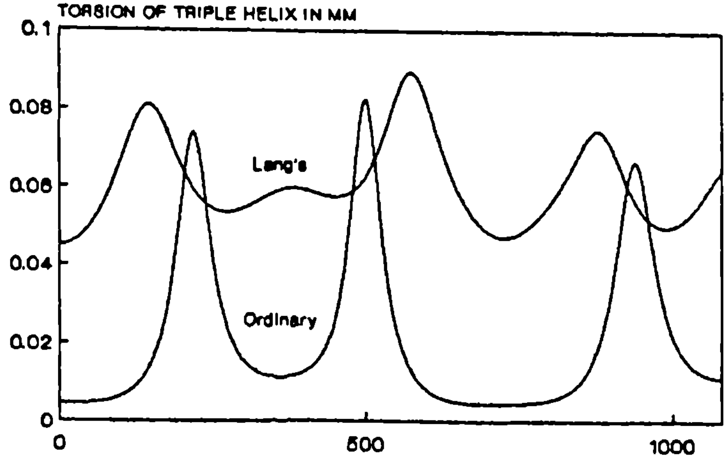

ANGLE OF ROTATION OF WIRE IN DEGREES
(b)
TORSION OF TRIPLE HELIX Vs
ANGLE OF ROTATION OF WIRE

TRIPLE HELIX
ROPE LAID IN THE RIGHT HAND DIRECTION

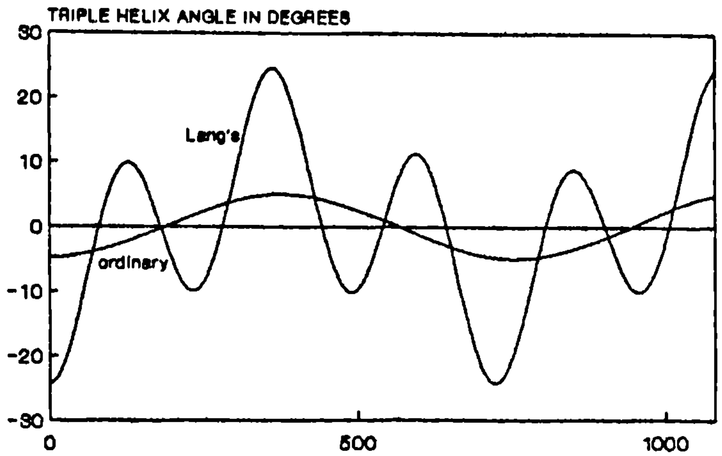

ANGLE OF ROTATION OF WIRE IN DEGREES
(c)
TRIPLE HELIX ANGLE Vs
ANGLE OF ROTATION OF WIRE

FIGURE 5.6-3

GEOMETRICAL PROPERTIES OF DRUM DOUBLE HELIX

5.7 CONCLUSION ON THE STUDY OF WIRE HELIX GEOMETRY

Rope manufacturers take full advantage of helix geometry to lay wires into an integral structure i.e. a strand or a rope. By carefully adjusting helical parameters within a strand or a rope, desired properties of the strand or the rope can be obtained. The following conclusion, based on the study of the rope geometry, are briefly drawn:

a. Single Helix

For a single helical wire in a straight strand, helix angle, curvature and torsion along the centroidal axis of a single helical wire are constant. These geometrical properties imply that the mechanical component forces and moments are also constant along the length of a single helical wire. However, as the helix angle is being changed within the practical range (ie 60 to 85 degrees), geometrical properties of single helix, such curvature and torsion, will significantly be changed. Thus, helix angle is one of the important parameters affecting the change of geometrical and mechanical properties of a strand.

b. Double Helix

For a double helical wire within a straight rope, the curvature, torsion and helix angle are periodic functions of wire rotational coordinate θ_w. The majority of helical wires in a rope are in double helical form; eg over 73% of wires are double helical wires in an IWRC. This implies that the macroscopic properties of a rope will significantly be influenced by the double helical wires. In addition to this, the periodic geometrical characteristics of double helical imply that the variation of contact patches, internal component forces and moments on the helical wire repeat every helix cycle

c. Ring And Drum Single Helix

Ring and drum single helices are degenerate and almost degenerate double helices respectively. The helix angle of a strand laid on a sheave and drum is very small between zero and 10 degrees. The curvature and torsion of helical wire will significantly be influenced by the diameter of the sheave or drum as the strand is being bent over the sheave or the drum.

d. Ring And Drum Double Helix

Ring and drum double helices are degenerate and almost degenerate triple helices respectively; a rope is being laid with a very small helix angle on a sheave or a drum. Again, curvature and torsion of triple helical wires will be significantly influenced by the diameter of the sheave or the drum. Since a rope can be either laid as a Lang's lay rope or as an ordinary lay rope. A rope can be laid on the drum either in the right hand orientation or in the left hand orientation. The orientation of rope laid on the drum will also contribute the mechanical behaviour of the rope depending upon the diameter of the drum and the rope lay (ie Lang's lay or ordinary lay). The model shows that the orientation of rope laid on the drum has more influence to the geometrical properties of triple helical wire within the Lang's lay rope than that of the triple helical wire within the ordinary lay rope.

CHAPTER SIX

SECTIONAL GEOMETRY OF HELICAL WIRE

Nomenclature

a	Semi-minor axis of an ellipse
A	Defined variable
b	Semi-major axis of an ellipse
c	Defined variable
K	Defined variable
m or M	Number of helical wires per layer
Q	Reaction force per unit length at the contact
r	Radius of a single helical wire
R	Helical radius of a single helical wire
X	Radial force acting on a helical wire per unit length
α	Helix angle of wire
β	Defined variable for contact angle
Q_c	Defined variable for contact angle
$\Delta\theta$	Defined variable
R_1, R_2, R_3	Reaction forces per unit length at the contact (For Figure 6.4.1 only)
R_i	Helical radius at ith layer of strand (i = 1, 2, 3, ... etc)

Subscritpt

s	strand

6.1 INTRODUCTION

For multi-layer strand design the number of helical wires (with given size and helix angle) which can be associated with a core wire of given size must be determined; the inverse procedure may also be required. In practice, the size of the helical wire is always smaller than the size of the core wire in a single layer strand, with the exception of "Selvagee" type of wire rope; that is all wires are parallel to each other. This will ensure that all helical wires in the inner-most layer will make contact with the core wire. Likewise, the size of helical wire in any particular layer must not be larger than the size of the inner strand immediate beneath; In this these, this geometrical problem is termed the "spatial configuration of wires within strand". The geometrical theory needed to deal with this problem is termed "sectional geometry of helical wire".

In this Chapter, the author intends to highlight the significance of the sectional geometry of helical wire in forming a reasonable mathematical model for single layer strand. This is in contract to some of the literature,[3.13, 4.1 & 4.4] where it is assumed either that the size of core wire is equal to that of the helical wire (provided that the helix angle of helical wire is 90 degrees) or that the core wire is separated from the inner layer helical wire. These assumptions ignore sectional geometry. There is, in fact, a geometric relationship which governs the "admissible helix angle"* for a given number of wires per layer and given size of core wire. This Chapter therefore aims:

a. to derive a mathematical method to evaluate the sectional shape of helical wire with a given helix angle.

b. to verify the approximate approach proposed by other strand modellers to handle the problem of "admissible helix angle" for a given number of helical wires.

c. to show some applications of sectional geometry .

* Definition:

For a given size and given number of helical wires per layer, the admissible helix angle is defined as the limiting helix angle that allows each of the helical wires to be in contact with their neighbouring wires without jamming or separation between adjacent wires.

6.2 LAYOUT OF CHAPTER SIX

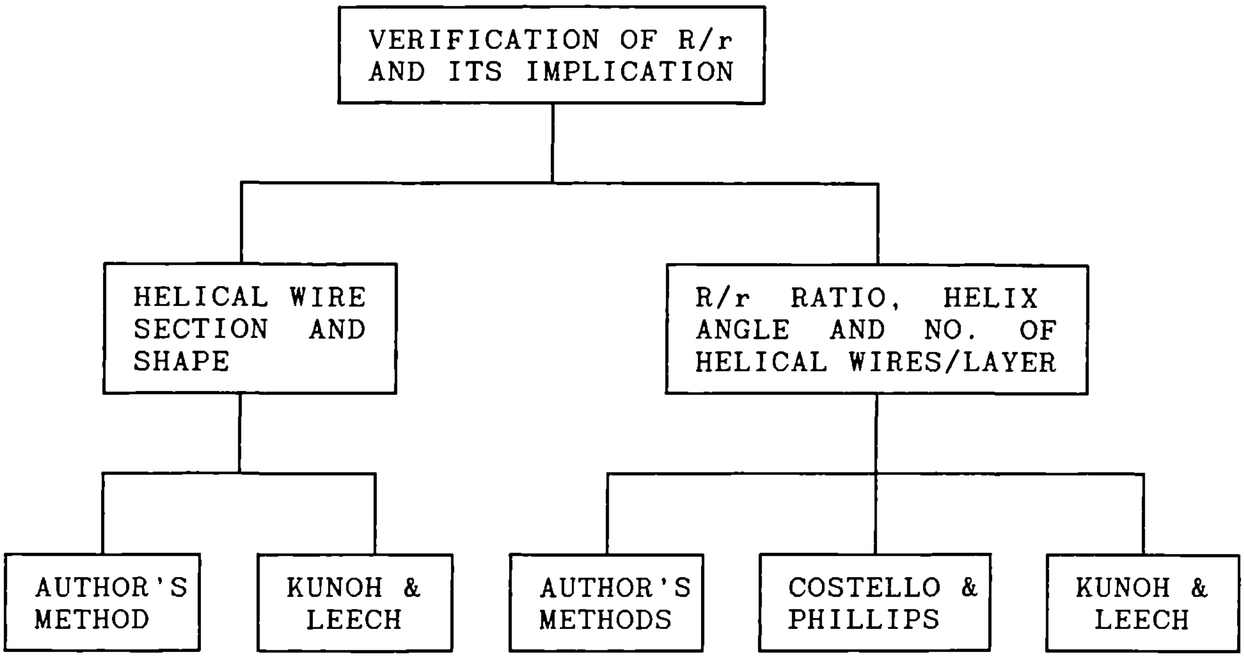

BLOCK DIAGRAM 6.1

STRUCTURE OF THE APPROACH TO THE

SPATIAL CONFIGURATION OF STRAND

6.3 BASIC ASSUMPTION

The main assumptions that have been made for the current analysis are:

a. Any wire within a strand is considered to be perfectly cylindrical.

b. The centroidal axis of any layer of wires, except the core wire, is in the form of a right cylindrical helix.

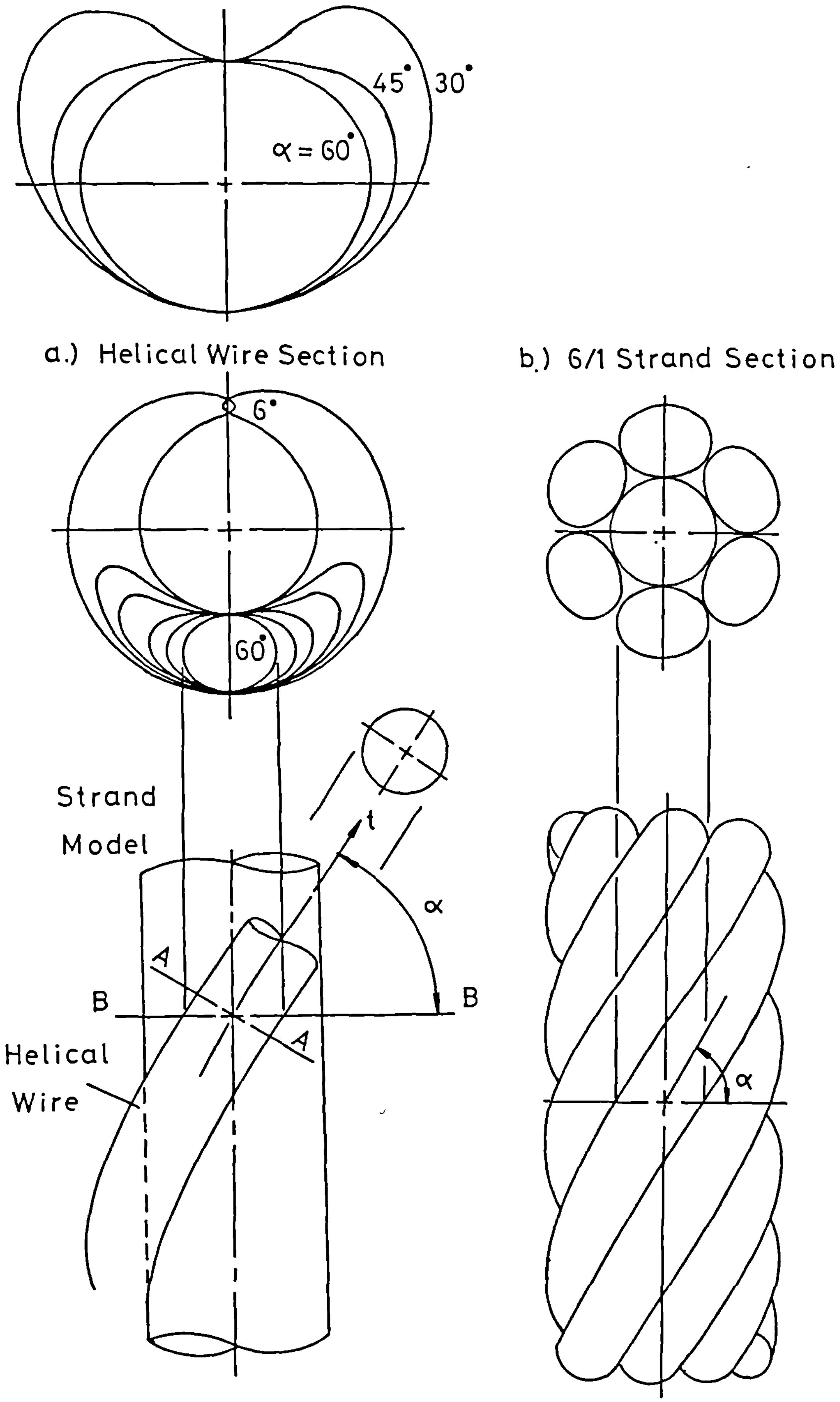

Figure 6·1
Helical Wire Section

c. Any transverse section of any wire is normal to the centroidal axis of that wire.

6.4 ANALYSIS OF HELICAL WIRE SECTION

If a transverse section is made through a helical wire, a circular shape can be expected. On the other hand, if a cut is made normal to axis of the straight strand; a "kidney shape" wire section can be expected. However, if the helix angle of the helical wire is gradually increased from 60 degrees, the wire section will gradually be changed from the "kidney shape" to an "approximately elliptical shape", Figure 6.1. Similar wire sectional shapes can also be found in Ref.5.4. The following method may be used to construct sectional shape:

Note: "Kidney shape" and "elliptical shape" are the names to describe the sectional shapes of a helical wire with the change of helix angle. They do not represent the exact mathematical meaning.

Method:

Let us consider a solid helical wire bundle which is formed by laying an infinite number of equal lay filaments. A point "P" is located on one of the filaments which form the surface of the helical wire, Figure 6.2. By joining the centre "0" of the strand with this point "P", the distance "0P" is designated by "R_p". An expression, which relates R_p with the helix angle,

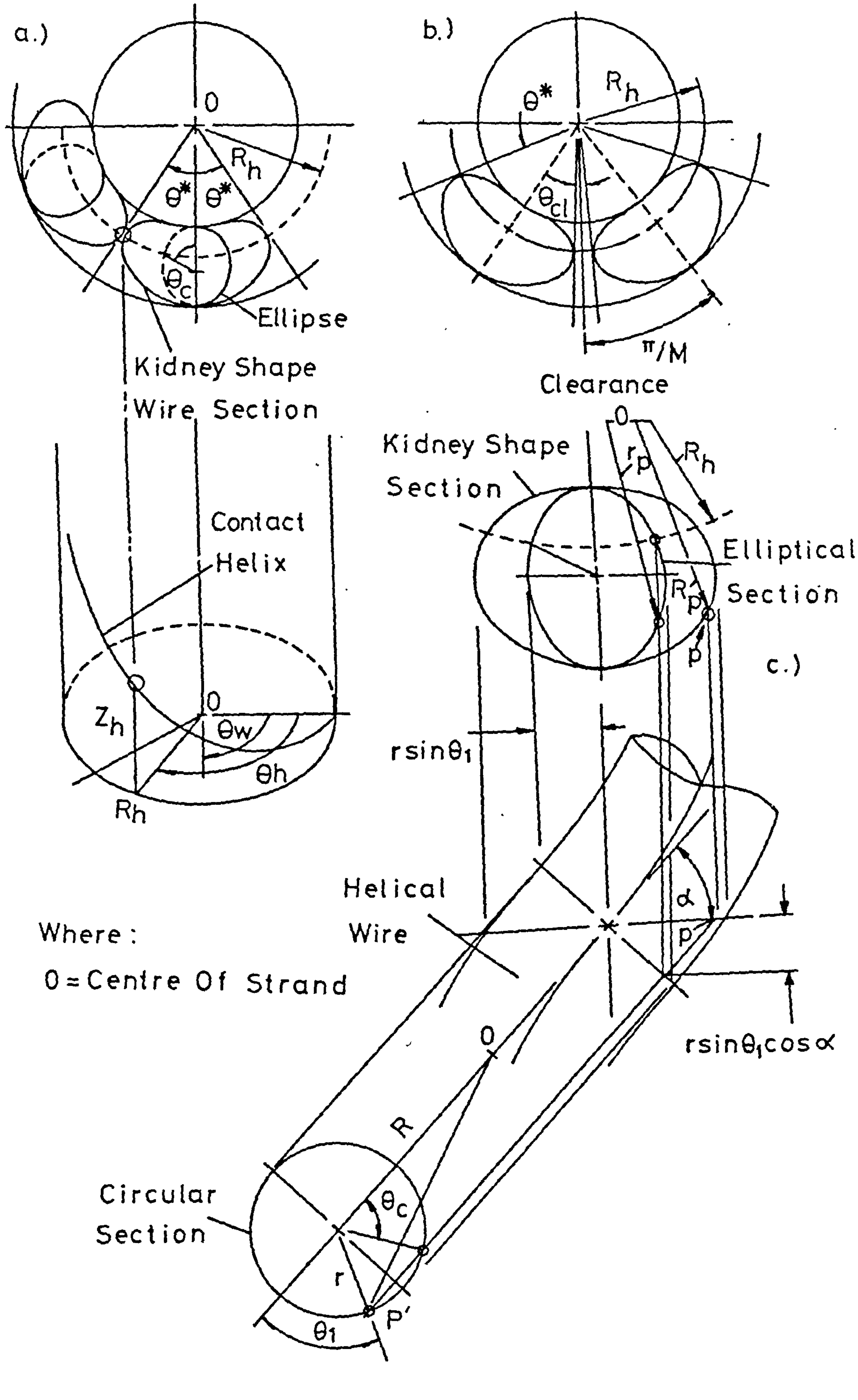
a.)
0
R_h
θ* θ*
$θ_c$
Ellipse
Kidney Shape
Wire Section
b.)
θ*
R_h
$θ_{cl}$
π/M
Clearance
Contact
Helix
Z_h
0
θw
θh
Rh
Kidney Shape
Section
0
r_p
R_h
Elliptical
Section
R_p
p
c.)
rsinθ1
Helical
Wire
α
p
Where:
0 = Centre Of Strand
rsinθ1cosα
0
R
Circular
Section
$θ_c$
r
P'
θ1

Figure 6·2

helical wire radius and the helical radius of the strand, can be derived based on the diagrams as illustrated in Figure 6.2. The parameter R_p is given by:

$$R_p = a_h \{ (\cos \theta_c + R_R)^2 + \sin^2 \theta_c \sin^2 \alpha \}^{1/2} \quad (6.1)$$

Where $R_R = R / a_h$

By varying R_p and θ_c (from 0 degree to 360 degrees) the sectional shape of a helical wire on the transverse plane of the given strand can be traced out for a given wire radius and helix angle, in equation 6.1. In order to illustrate this geometrical relationship, a computer program has been written and selected results are given in Figure 6.3.

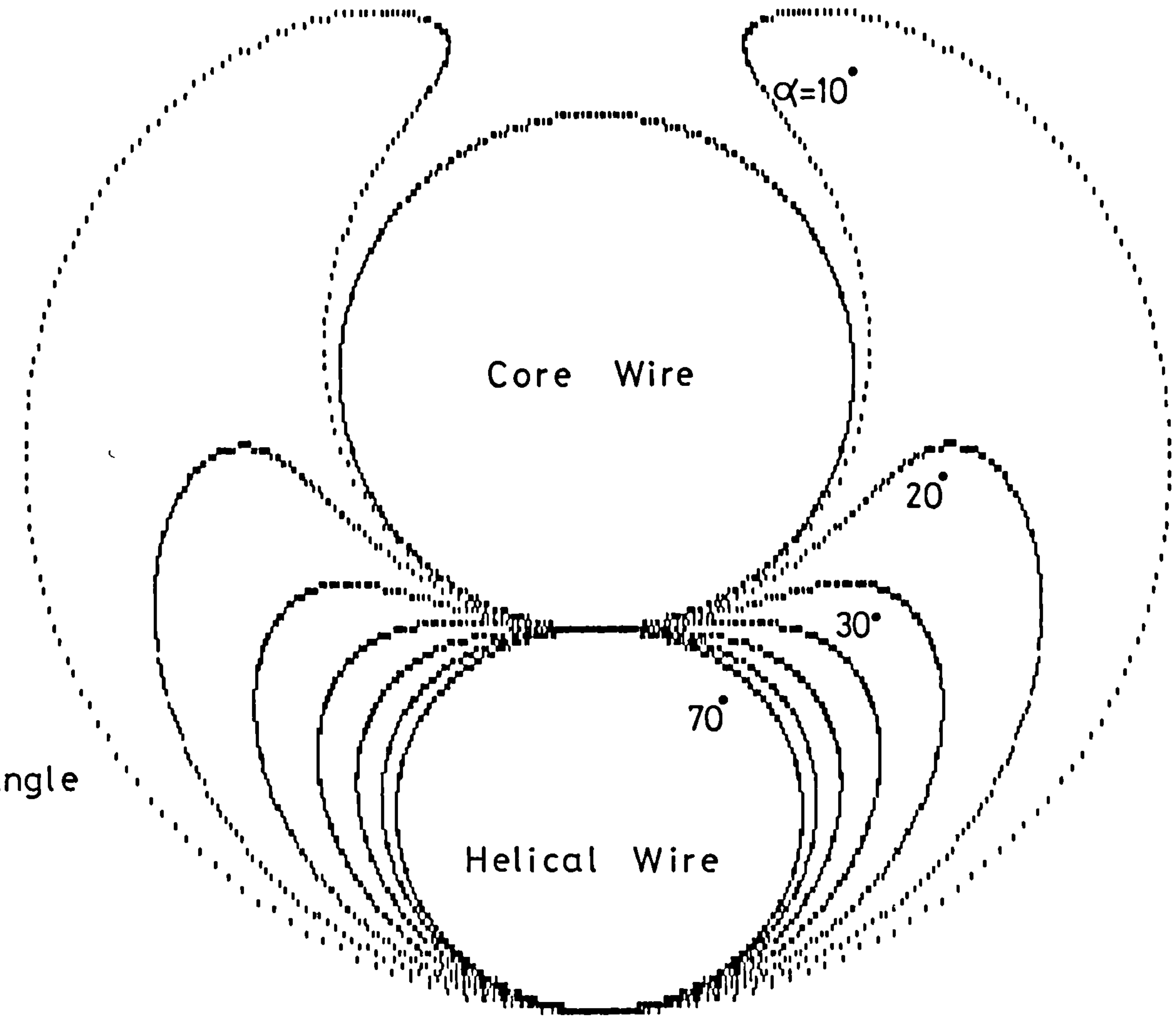

Where:

α = Helix Angle

Figure 6·3

Sectional Shape Of Helical Wire

6.5 ANALYSIS OF THE ADMISSIBLE R/r RATIO

This section presents both an approximate and an exact mathematical approach which can be applied to determine the R/r ratio* and the contact angle** in a single layer strand. These approaches include:

a. Huang, Costello and Phillips' method

b. T.Kunoh and C.M.Leech method

c. Author's methods

Definitions:

The *R/r ratio is defined as the ratio of helical radius to the helical wire radius. This ratio is closely related with the number of helical wires per layer and the "admissible helix angle" of the helical wire in any layer.

The **Contact angle θ_c is defined as the subtended angle of contact between helical wire in contact with the core wire and one of its neighbouring helical wires in the same layer, Figure 6.2

6.5-1 Huang, Costello and Phillips' Approach

Huang and Costello applied similar methods to determine the R/r ratio. Both modellers used an elliptical section, as illustrated in Figure 6.4, to approximate a "kidney section", Figure 6.3. The helical surface of the wire is also approximated by a straight line a_{hi} as shown in Figure 6.4 (a). The elliptic expressions used to evaluate the R/r ratio, are given by:

$$a = r \qquad (6.2)$$

$$b = r / \sin \alpha \qquad (6.3)$$

..(by Costello & phillips)

$$b = r \, (R^2 + k^2)^{1/2} / k \qquad (6.4)$$

................(by Huang)

Where $1 / \sin \alpha = (R^2 + k^2)^{1/2} / k$

$$k = R \tan \alpha \qquad (6.5)$$

By using Figure 6.4 and analytical geometry, it can be shown that:

$$\frac{R}{r} = \left(1 + \frac{\tan^2 (\pi / 2 - \pi / m)}{\sin^2 \alpha} \right)^{1/2} \qquad (6.6)$$

Based on the elliptic section approach, the contact angle "β" (illustrated in Ref.3.1). can be shown to be given by:

$$\cos \beta = \frac{1}{\cos^2 \alpha} \left\{ \left(1 + \frac{\tan^2 (\pi/2 - \pi/m)}{\sin^2 \alpha} \right)^{1/2} - \right.$$

a.

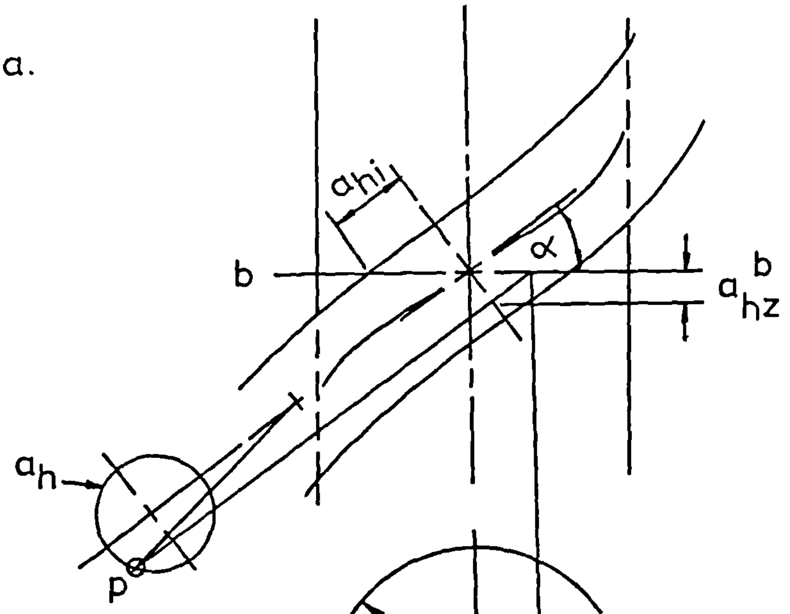

b.

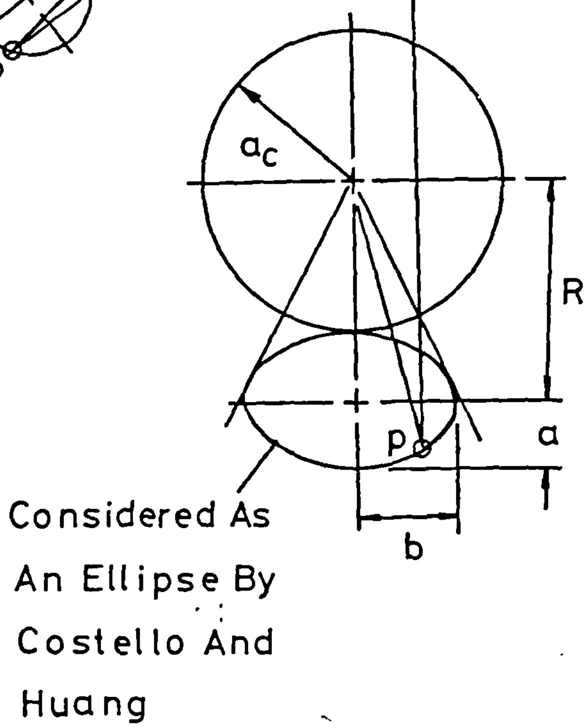

c.

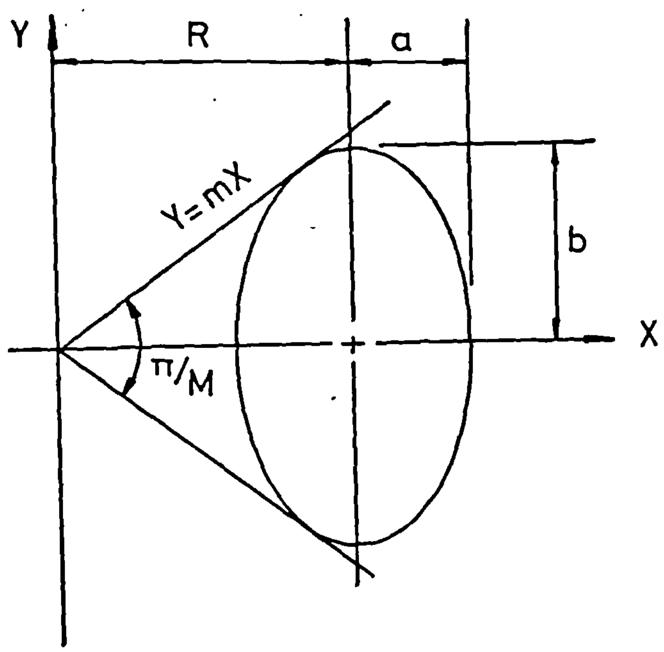

Figure 6·4

$$(\tan^2 (\pi/2 - \pi/m)) [1 + \frac{}{\tan^2 \alpha \cos^2 (\pi/2 - \pi/m)}$$

$$\frac{1}{(\sin^2 \alpha + \tan^2 (\pi/2 - \pi/m)}] + \sin^4 \alpha \} ^{1/2} \qquad (6.7)$$

According to Costello and Phillips[3.1], the contact force Q between neighbouring helical wires, (See Figure 6.5) is given by:

$$Q = - X / 2 \cos \beta \qquad (6.8)$$

Where $Q = R_2$ and R_3

$X = R_1$

Note: the notation Q and X has been used in Ref.3.1.

6.5-2 T. Kunoh and S.M. Leech Approach

T. Kunoh and S.M. Leech used a different method to evaluate the R/r ratio and compared their results with Costello and Phillips. However, the expressions for "R/r" and for the contact angle have not been given in their paper and no comments can therefore be made on their approaches.

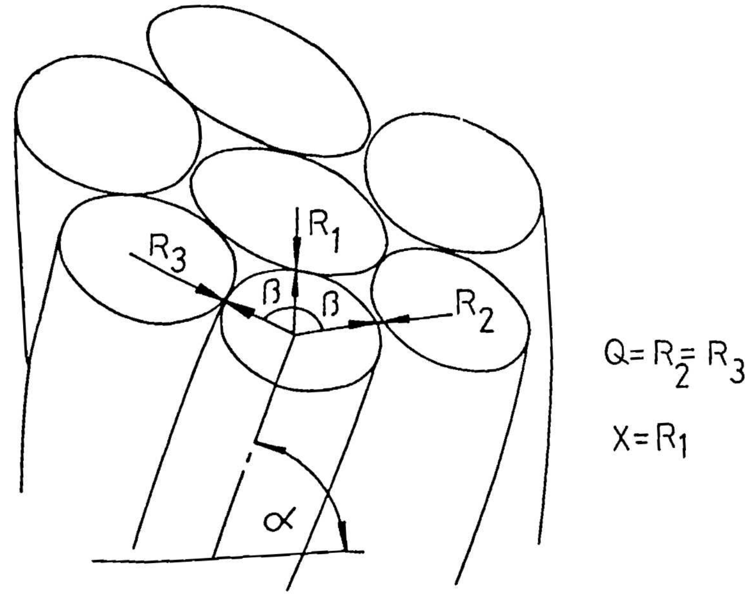

Oblique Section Of 6/1 Strand

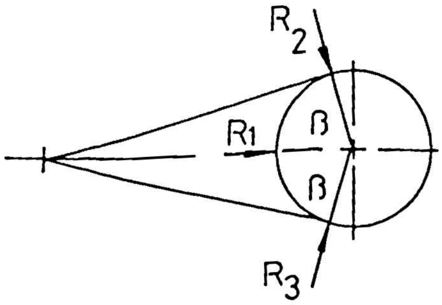

Contact Forces Between Wires

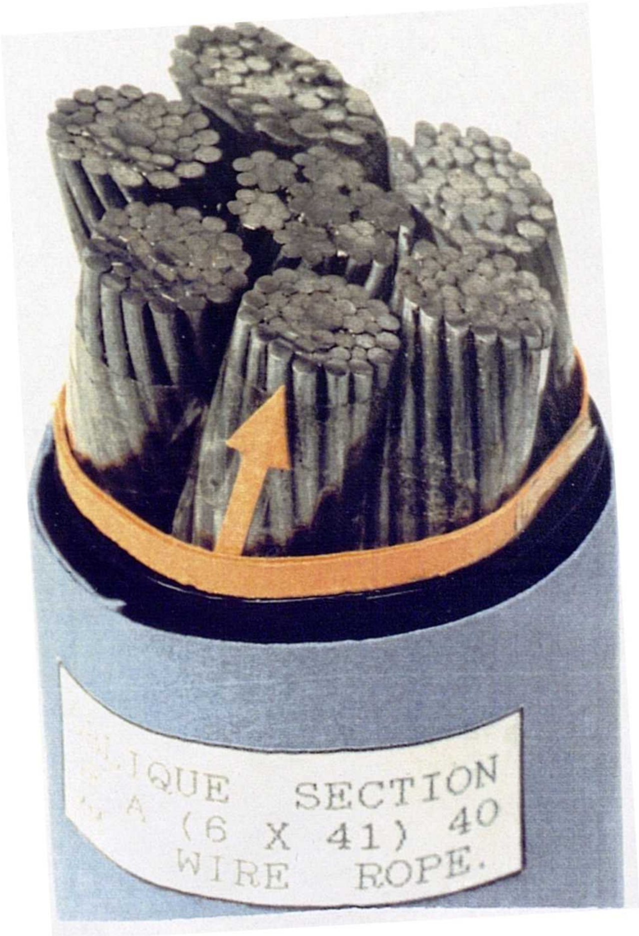

Figure 6·5

6.5-3 Approximate Methods and an Exact Method (of The Present Author)

Various approaches which can be applied to evaluate the R/r ratio, are presented.

a. Approximate By Elliptic Section

The elliptic section can be approximated:

$$a = r$$

$$b = k\, r \,/\, (R^2 + k^2)^{1/2} \qquad (6.9)$$

$$k = R \tan\alpha \qquad (6.10)$$

In this case, the author kept "a" as a constant radius and "b" as the dependent variable of the helix angle. Again, by using Costello's approach, the expression for R/r ratio is given by:

$$\frac{R}{r} = \frac{(1 + \tan^2\alpha)^{1/2}}{\{m^2 (1 + \tan^2\alpha)\}^{1/2}} \qquad (6.11)$$

N.B. This method is intended to show that the "kidney section" of helical wire which governs the permissible helix angle, has insignificant influence if this angle is greater than 85 degrees. Equation 6.11 has no practical use.

b. Projected Elliptic Method (with exact method)

In order to evaluate R/r ratio from the "kidney shape" section, one needs to consider the "contact helix" * and the "projection of the transverse section of the helical wire"** on the plane which cut the transverse section of a straight strand, Figure 6.2.

1. Contact Helix*

This is a helical contact line formed by the contact of two neighbouring helical wires in the same layer of the strand, as illustrated in Figure 6.2. The expressions which represent the Cartesian coordinates of the contact helix are:

$$X_c = a_c \cos \theta_w \qquad (6.12)$$

$$Y_c = a_c \sin \theta_w \qquad (6.13)$$

$$Z = a_c \theta_w \tan \alpha \qquad (6.14)$$

In cylindrical coordinates:

$$R_h = a_h \{ (\cos \theta_c + R_R)^2 + \sin^2 \theta_c \sin^2 \alpha \}^{1/2} \qquad (6.15)$$

$$\theta_h = \theta_w + \tan^{-1} \{ \frac{\sin \alpha \sin \theta_c}{R_R + \cos \theta_c} \} \qquad (6.16)$$

$$Z_h = R \theta_w \tan \alpha - a_h \sin \theta_c \cos \alpha \qquad (6.17)$$

Similar equations can also be found in Kunoh's[5.4] paper but they were used for other purposes.

2. Projection Of Transverse Section Of Helical Wire.**

If a section is made normal to the direction of a unit tangent vector on the centroidal axis of a helical wire, a circular transverse section of the helical wire can be expected. If this circular section is projected onto the plane of the transverse section of the straight strand. The projected shape becomes a true ellipse. By using this concept, to evaluate the "R/r" ratio, two results can be found. They are:

i. Approximate Method

In this approach, the helical radius of a contact helix and a projected ellipse are considered, see Figure 6.2 (a). Again, by using Costello's analytical geometry approach, the expression which gives the R/r ratio, is given by:

$$A\ R_R^2 - A - \sin^2 \alpha = 0 \qquad (6.18)$$

Where

$$A = \tan^2 \left\{\frac{\pi}{m} - \frac{a_h \sin \theta_c \cos \alpha}{R_p \tan \alpha}\right\} \qquad (6.19)$$

ii. Exact Method

In this analysis, the contact helix and the projected ellipse are considered, see Figure 6.2 (b). One can obtain the following mathematical relationships:

$$\theta_{cl} = 2\ (\pi/m - \theta^{*}) \qquad (6.20)$$

Where

$$\theta^{*} = \frac{a_h \sin\theta_c \cos\alpha}{R_p \tan\alpha} + \tan^{-1}\left\{\frac{\sin\theta_c \sin\alpha}{R_R + \cos\theta_c}\right\} \qquad (6.21)$$

In order to evaluate the admissible helix angle, One needs to set $\theta_{cl} = 0$. The corresponding R/r ratio can then be evaluated on this basis. (a computer program has been produced in order to evaluate the admissible ratio for various helix angles).

iii The Contact Angle "β"

The contact angle as published in Costello and Phillips paper[3.1] is similar to that considered in this sub-section. If a helical wire is considered as a perfect cylinder and its centroidal axis is considered as a right cylindrical helix. By using the contact helix and projected elliptic section method, one can show that this angle "β" is exactly equal to the angle 180 - θ_c at the contact point. To evaluate this angle, the expression is given by:

$$\cos \beta = 1/R_R \qquad (6.22)$$

6.6 DISCUSSION & CONCLUSION

This sub-section presents a brief discussion of the sample results obtained from various approaches; the R/r ratio and contact angle for the single layer strand is evaluated.

a. R/r Ratio

Figures 6.6 to 6.8 show the relationship between R/r ratio, the admissible helix angle and the number of helical wires per layer. Generally speaking, the results obtained from various approaches are quite close to each other provided the helix angle chosen for the helical wire is within the practical range, i.e. 60 to 90 degrees. However, there is an exception as shown in Figure 6.7. For a helix angle greater than 60 degrees, these graphs show that the elliptical method is also a close approximation.

Figure 6.6 illustrates sample results (R/r ratio vs helix angle) obtained from an approximated method of Costello and are due to the author. The methods agree with each other when the helix angle is greater than 40 degrees but then the results begin to diverge when the helix angle is smaller than 40 degrees.

Figure 6.7 illustrates sample results (R/r ratio vs helix angle) obtained from one of the elliptical approximate

R/r RATIO VS HELIX ANGLE OF WIRE
COSTELLO AND LEE'S METHOD

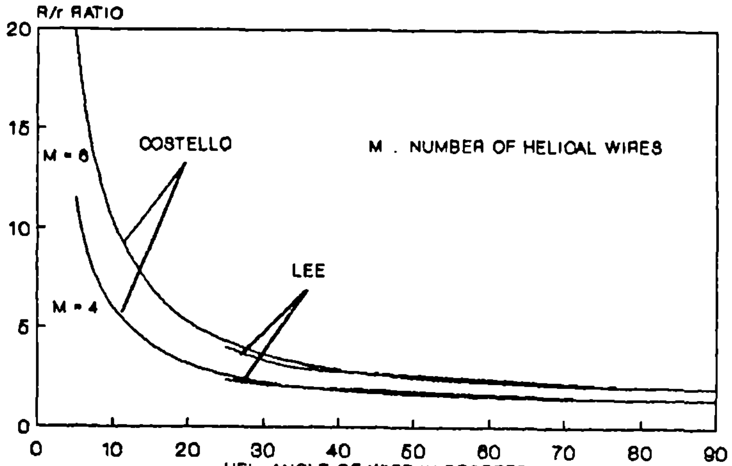

FIGURE 66
R/r RATIO VS HELIX ANGLE OF WIRE
(COMPARISON BETWEEN COSTELLO AND LEE)

R/r RATIO VS LAY ANGLE OF WIRE
COSTELLO AND DIFF. GEOM

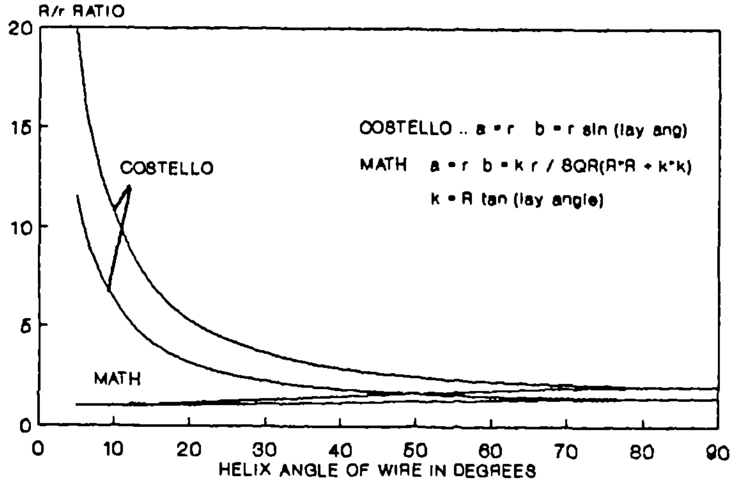

FIGURE 67
R/r RATIO VS HELIX ANGLE
WIRE SECTION APPROX BY AN ELLIPSE.

R/r RATIO VS LAY ANGLE OF WIRE
COSTELLO AND KUNOH

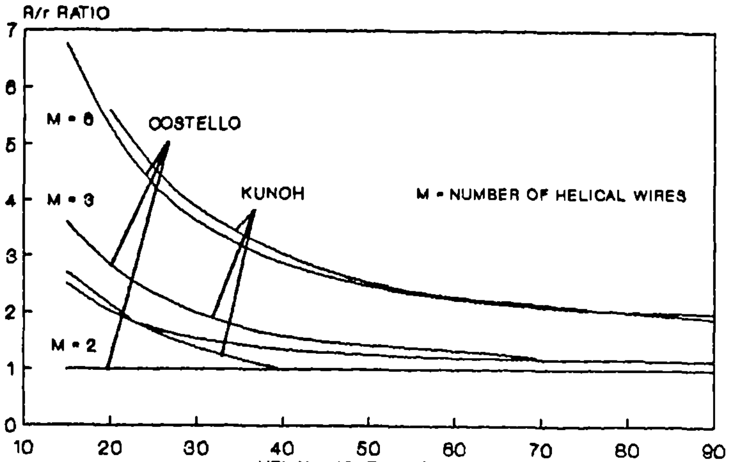

FIGURE 68
(COSTELLO AND KUNOH)
(COMPARISON BETWEEN COSTELLO AND KUNOH)

R/r RATIO VS LAY ANGLE OF WIRE
COSTELLO, HUANG, KUNOH AND LEE

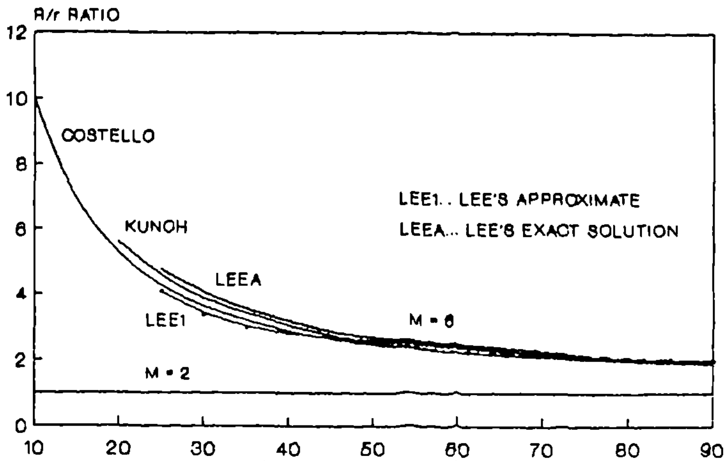

FIGURE 69
R/r RATIO VS HELIX ANGLE
(FOR 6/1 STRAND)

R/r RATIO VS HELIX ANGLE OF WIRE
COSTELLO AND LEE'S METHOD

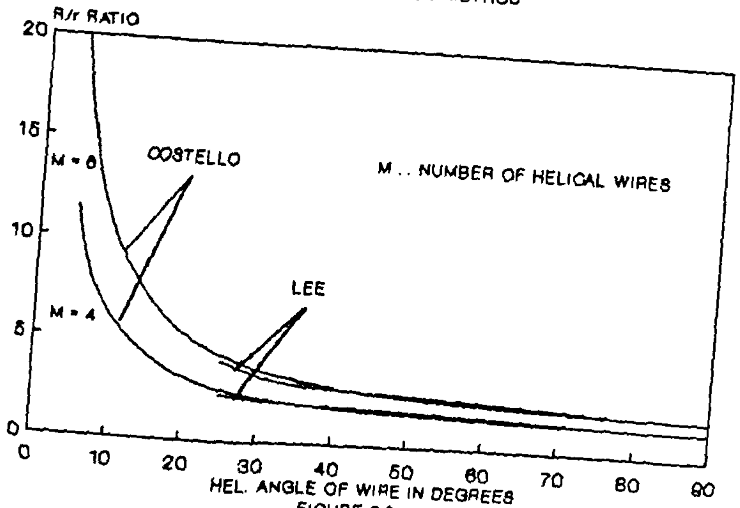

FIGURE 6 6
R/r RATIO VS HELIX ANGLE OF WIRE
(COMPARISON BETWEEN COSTELLO AND LEE)

R/r RATIO VS LAY ANGLE OF WIRE
COSTELLO AND DIFF. GEOM.

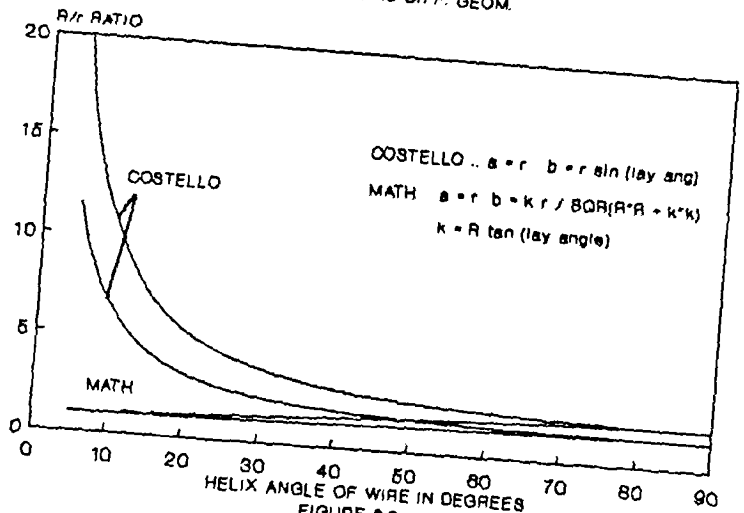

FIGURE 6 7
R/r RATIO VS HELIX ANGLE
WIRE SECTION APPROX. BY AN ELLIPSE.

R/r RATIO VS LAY ANGLE OF WIRE
COSTELLO AND KUNOH

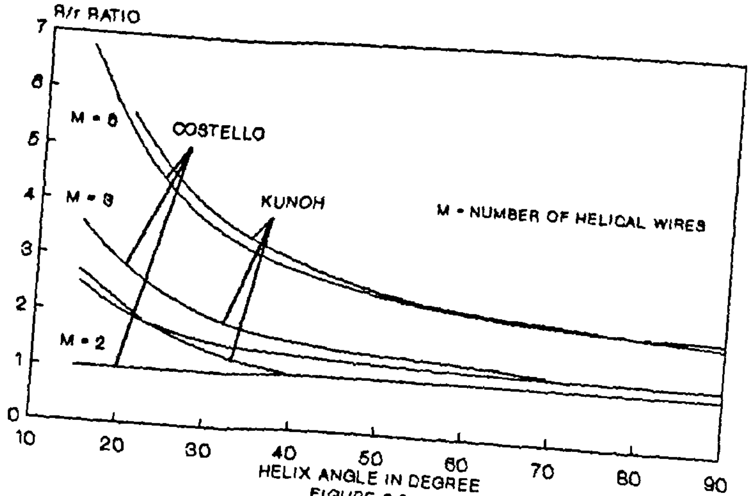

FIGURE 6 8
(COSTELLO AND KUNOH)
(COMPARISON BETWEEN COSTELLO AND KUNOH)

R/r RATIO VS LAY ANGLE OF WIRE
COSTELLO, HUANG, KUNOH AND LEE

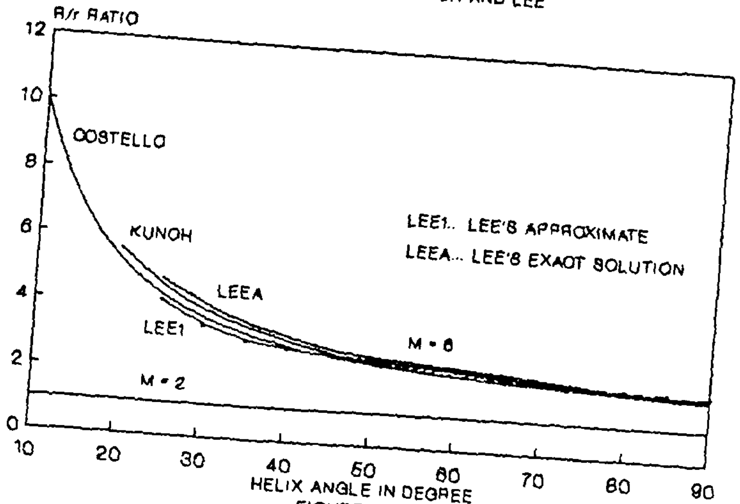

FIGURE 6 9
R/r RATIO VS HELIX ANGLE
(FOR 6/1 STRAND)

methods; for the evaluation of R/r ratio. The curve designated with "math" (note: "math" is just a legend given to the curves only) is definitely inappropriate. This is because when a helix angle is gradually decreased, the wire section changes from a "kidney shape" to "horse-shoe shape". In other words, the R/r ratio will increase as the result of "horse-shoe" effect, Figure 6.8 (a). However, Figure 6.7 show that the R/r ratio gradually decreases as the helix angle decrease.

Figure 6.8 illustrates the R/r ratio vs helix angle, extracted from Ref.5.4, Kunoh and Costello's approach. Again, both results agree with each other within the range 40 to 90 degrees and then gradually diverge as the helix angle become smaller than 40 degrees. For a strand with two helical wires (ie M=2), Kunoh clearly showed the "horse-shoe" effect in the prediction of the R/r ratio without pointing out the physical significance, i.e. when R/r > 1. Two wires will contact with each other at two contact points, Figure 6.8 (a).

Figure 6.9 presents the comparison of the results obtained from various approaches. Results obtained from various source agree reasonably within a practical range of helix angle for strand design.

b. Contact Angle

Figure 6.10 illustrates the variation of cos β as functions of

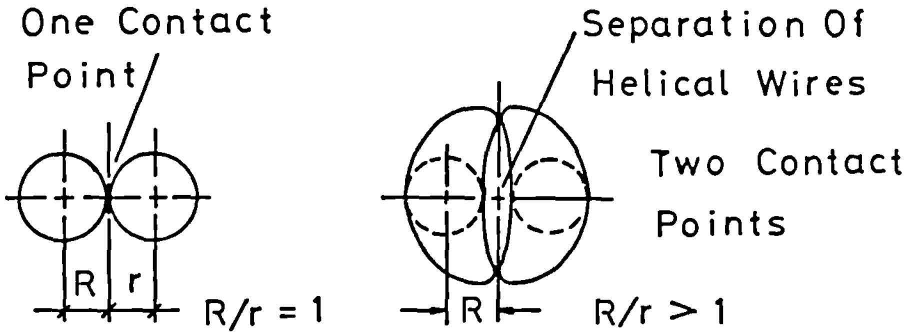

$40^\circ < \alpha < 90^\circ$ $\alpha < 40^\circ$ (Helix Angle)

(a) (b)

Figure 6·8 (a)

CONTACT ANGLE VS LAY ANGLE
LEE'S METHOD

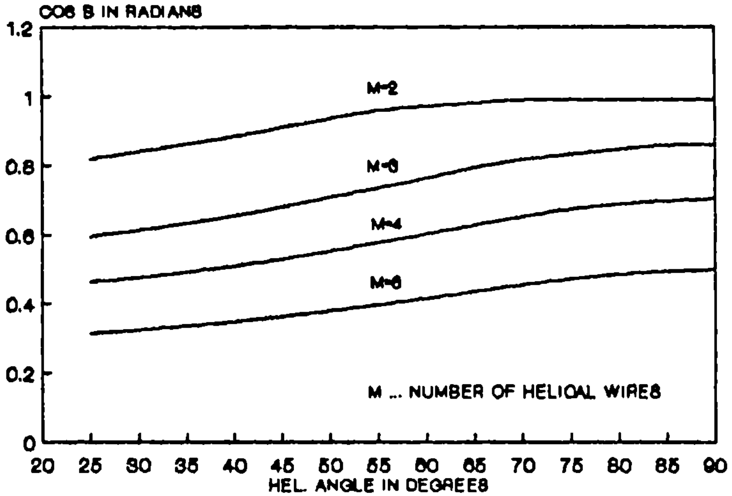

FIGURE 6.10
COS B VS HELIX ANGLE

CONTACT ANGLE VS HEL. ANGLE OF WIRE

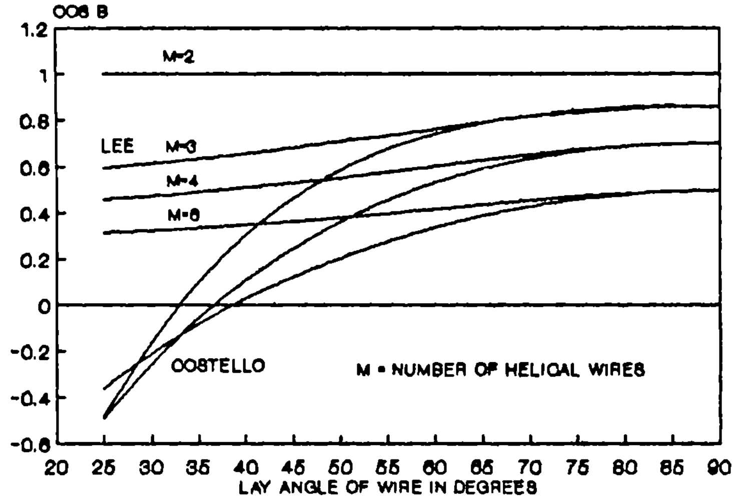

FIGURE 6.11 (a)
COS B VS HELIX ANGLE IN DEGREES
(COMPARISON BETWEEN COSTELLO AND LEE)

CONTACT ANGLE VS LAY ANGLE OF WIRE
COSTELLO AND KUNOH

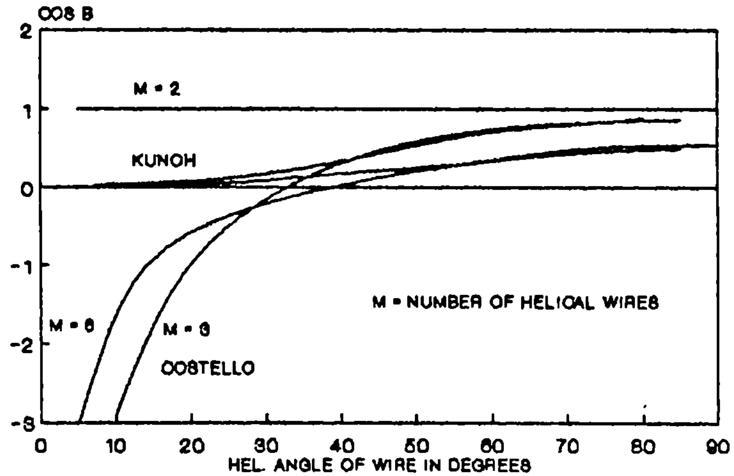

FIGURE 6.11 (b)
COS B VS HELIX ANGLE IN DEGREES
(COMPARISON BETWEEN COSTELLO AND KUNOH)

CONTACT ANGLE VS R/r RATIO

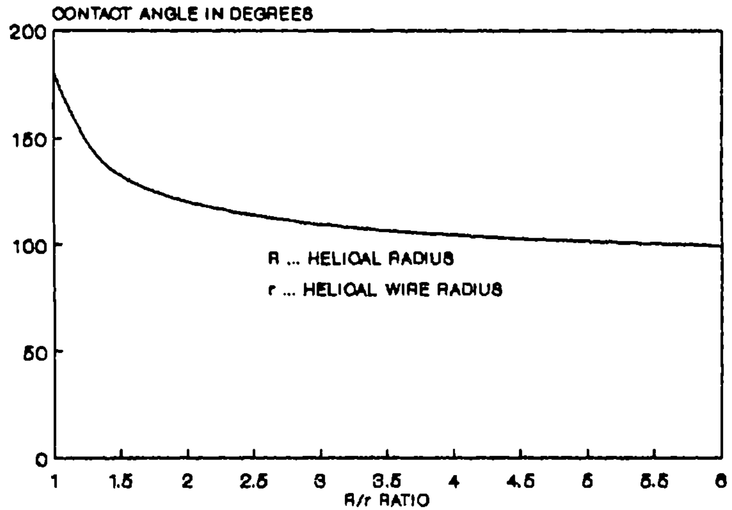

FIGURE 6.12
CONTACT ANGLE VS R/r RATIO

helix angle and number of helical wires predicted by the projected elliptic method.

Figure 6.11 (a) & (b) compare results for the contact angle obtained by using Costello, Kunoh and author's approaches. The author's results agree with Costello's results provided the helix angle is greater than 65 degrees. Kunoh's approach also agrees with Costello's approach provided the helix angle is greater than 50 degrees. However, when the helix angle approaches zero degrees, "cos β" neither approaches zero nor diverges to a very large quantity. This is due to the "horse shoe"effect of helical wire with small helix angle.

Figure 6.12 illustrates the variation of contact angle β with the corresponding R/r ratio.

CONCLUSION

Some simple but important conclusions can be drawn.

1. The ratio of helical radius to radius of helical wire must be related to the helix angle and the number of helical wires per layer.

2. The wire sectional shape varies from circular through approximately elliptical, kidney shape, horse-shoe to toroidal shape as the helix angle decreases from 90 to 0 degrees.

3. For any size of wires, helix angle and number of helical wires per layer within a strand, there is an "admissible

helix angle". For a given helix angle greater than the "admissible helix angle", the helical wires will be no longer touching their neighbouring wires in the same layer. On the other hand, if the helix angle is smaller than the "admissible helix angle", all the inner layer helical wires will be separated from their core wire. Therefore, one should not design strands with the latter case.

4. For a strand without a core wire, by decreasing the helix angle, a "separation" will occur when the "kidney shape" section is transformed to a "horse-shoe" section. For example, the strand with two helical wires, as shown in Figure 6.8 (a).

5. For designing single and multi-layer strands, the practical range of helix angle should be within 50 to 90 degrees. Costello's expression for "R/r" ratio is reasonable accurate and easy to use within this range.

6.7 APPLICATION

Figure 6.13 illustrates several simple strand constructions and the "lay" configurations encountered in various strand designs. Examples are given to illustrate application of sectional geometry principles.

6.7-1 R/r Ratio For Equal Lay Strand

a. R/r Ratio For 9/9/1 Strand

Figure 6.14 (a) represents the cross section of a 9/9/1 strand. By applying Costello's method for calculating the R/r ratio, the helical radii for each layer are given by:

$$\frac{R_1}{r_1} = \left\{ 1 + \frac{\tan^2 (7\pi / 18)}{\sin^2 \alpha_1} \right\}^{1/2} \tag{6.23}$$

$$\frac{R_2}{r_2} = \left\{ 1 + \frac{\tan^2 (7\pi / 18)}{\sin^2 \alpha_1} \right\}^{1/2} \tag{6.24}$$

b. R/r Ratio For 12/6F + 6/1 Strand

Figure 6.14 (b) represents a cross section of a 12/6F+6/1 Strand. By applying Costello's method for calculating the R/r ratio, the helical radii for each layer are given by:

$$\frac{R_1}{r_1} = \left\{ 1 + \frac{\tan^2 (\pi / 3)}{\sin^2 \alpha_1} \right\}^{1/2} \tag{6.25}$$

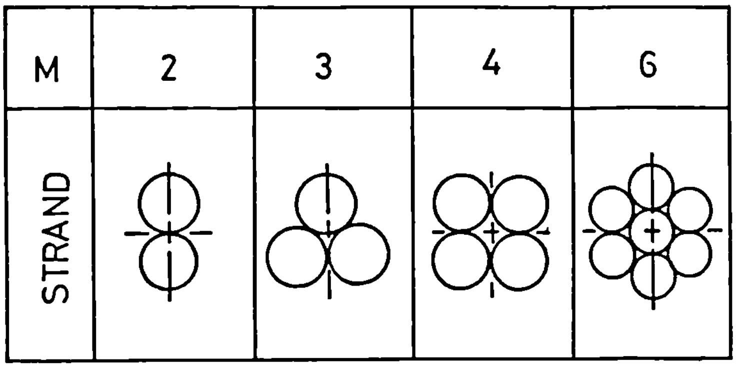

Schematic Representation
Of Simple Strand Section

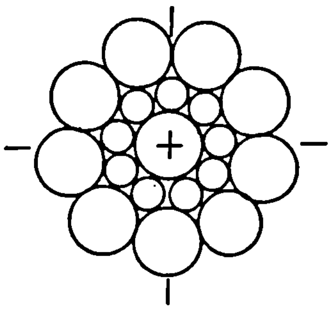

Equal Lay

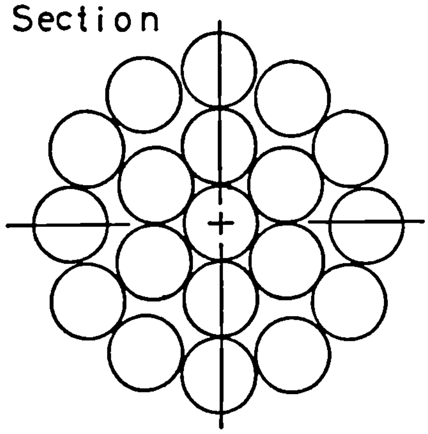

Cross Lay

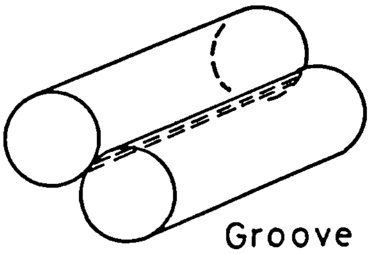

Groove

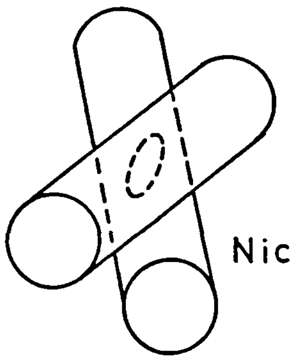

Nick

Figure 6·13

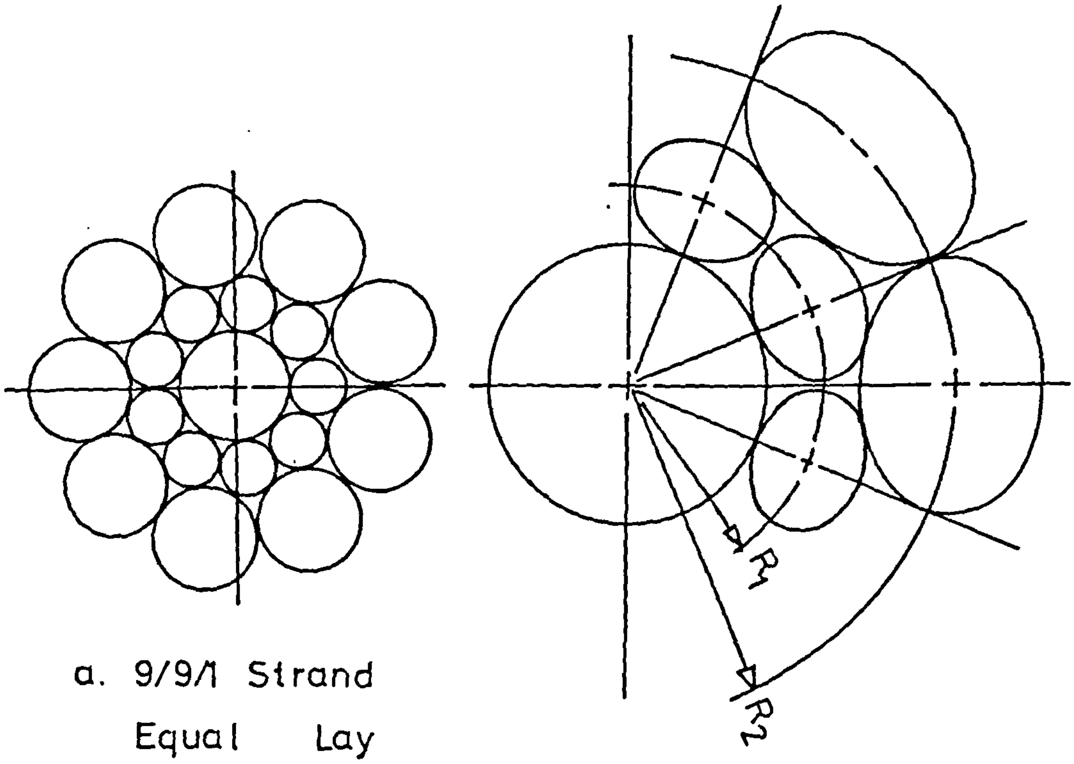

a. 9/9/1 Strand
Equal Lay

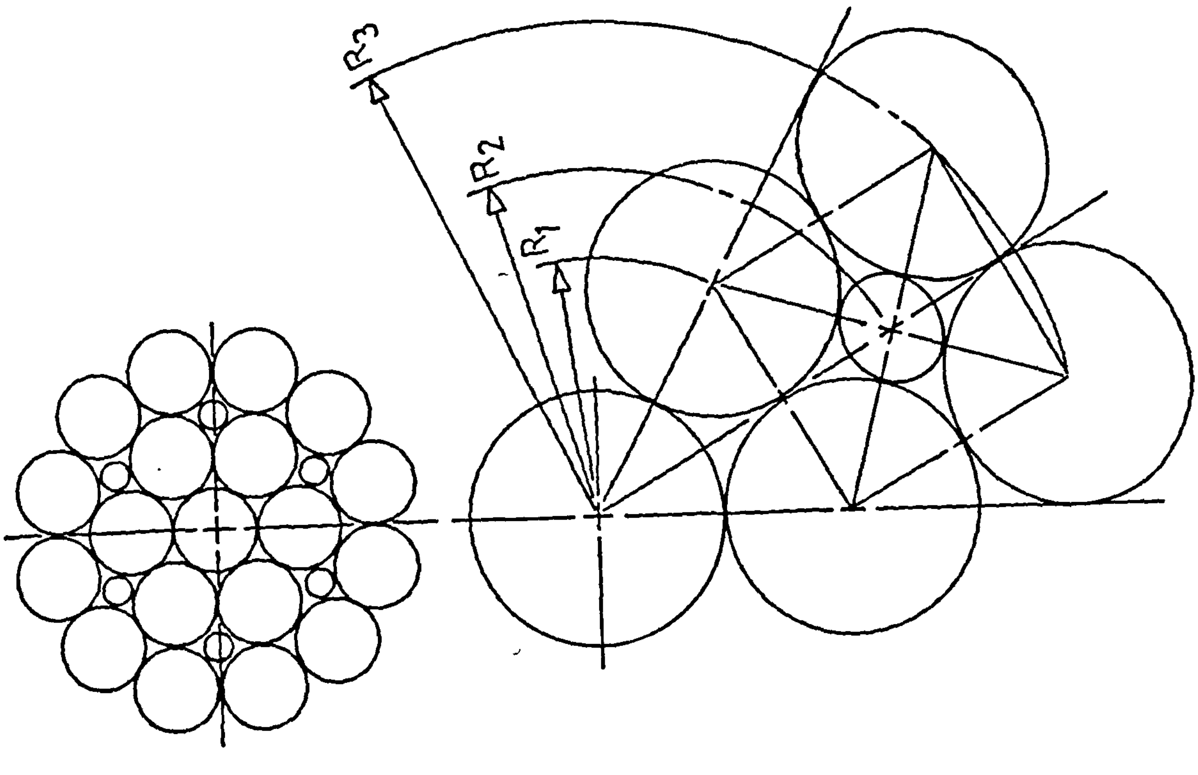

b. 12/6F + 6/1 Strand
Equal Lay

Where: R_i = Helical Radius
$i=1,2,3$

Figure 6·14

$$\frac{R_1}{r_1} = \{ 1 + \frac{\tan^2 (\pi / 3)}{\sin^2 \alpha_1} \}^{1/2} \tag{6.25}$$

$$\frac{R_2}{r_1} = \frac{R_1}{r_2} \cos (\frac{\pi}{6}) + (1 + \frac{r_1}{r_2}) \cos \theta_1$$

$$\theta_1 = \sin^{-1} (\frac{r_2}{r_2 + r_3}) \tag{6.26}$$

$$\frac{R_3}{r_3} = \{ 1 + \frac{\tan^2 (5\pi /12)}{\sin^2 \alpha_1} \}^{1/2} \tag{6.27}$$

c. R/r Ratio For Tri. 3 And Tri. 3/3

Figure 6.15 (a) represents a cross section of the core of the triangular strand. Again, by applying Costello's method for calculating the "R/r" ratio, the helical radii for the helical wires are given by:

For Tri. 3

$$\frac{R_1}{r_1} = \{ 1 + \frac{\tan^2 (\pi / 3)}{\sin^2 \alpha_1} \}^{1/2} \tag{6.28}$$

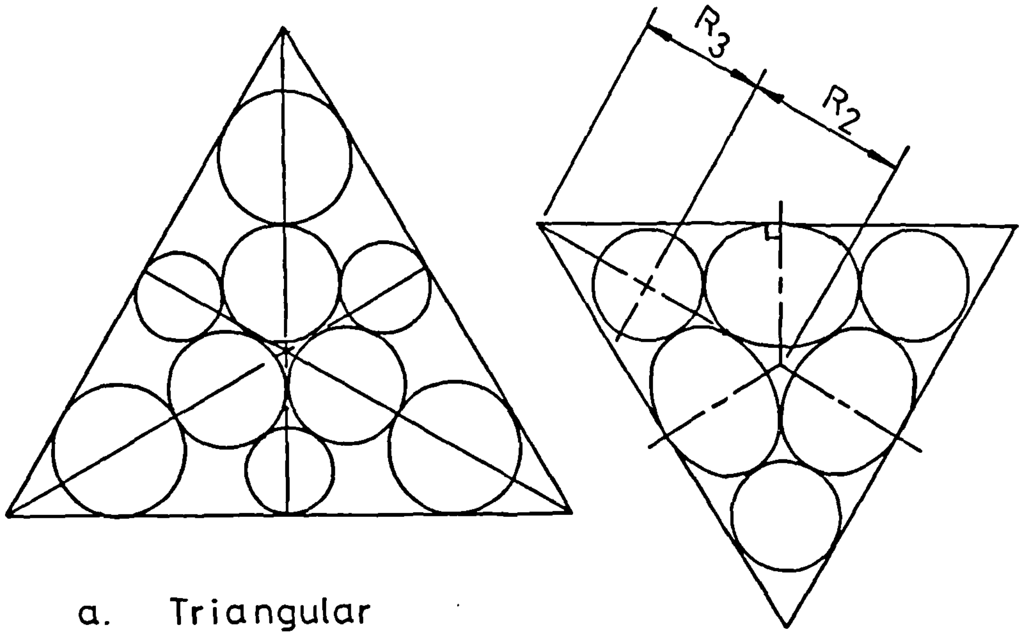

a. Triangular Strand

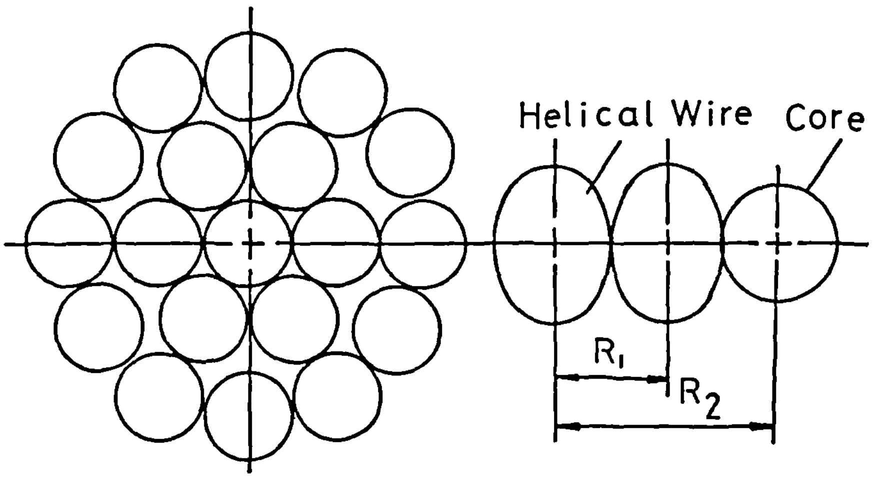

b. 12/6/1 Strand Cross Lay

Where R_i = Helical Radius
$i = 1,2,3$

Figure 6·15

For Tri. 3/3

$$\frac{R_2}{r_1} = \frac{R_1}{r_2} \cos\left(\frac{\pi}{3}\right) + \left(1 + \frac{r_1}{r_2}\right) \cos\theta_1$$

$$\theta_1 = \sin^{-1}\left(\frac{r_1}{r_1 + r_2}\right) \tag{6.29}$$

$$R_1 = r_1 \left(1 + \frac{\tan\ (\pi/3)}{\sin^2 \alpha}\right)^{1/2}$$

(6.30)

6.7-2 "R/r" Ratio For Cross Lay Strand

Figure 6.15 (b) represents a cross section of a cross lay 12/6/1 strand. In this case, the R/r ratios are given by:

$$\frac{R_1}{r_1} = \frac{r_0 + r_1}{r_1} = \left\{ 1 + \frac{\tan^2 (2\pi / 3)}{\sin^2 \alpha_1} \right\}^{1/2}$$

(6.31)

$$\frac{R_2}{r_2} = \frac{r_0 + 2r_1 + r_2}{r_2} = \left\{ 1 + \frac{\tan^2 (2\pi / 3)}{\sin^2 \alpha_2} \right\}^{1/2}$$

(6.32)

For interest, Table 6.1 shows the expressions which can be used to approximate the R/r ratio for cross and equal lay strands.

STRAND	R/r EXPRESSION	RANGE
	$\frac{R}{r} = 1$	≃ 50 TO 90
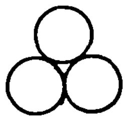	$\frac{R}{r} = \{ 1 + \frac{TAN^2 (\Pi/6)}{SIN^2 \alpha} \}^{1/2}$	≃ 50 TO 90
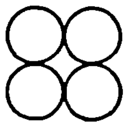	$\frac{R}{r} = \{ 1 + \frac{TAN^2 (\Pi/4)}{SIN^2 \alpha} \}^{1/2}$	≃ 50 TO 90
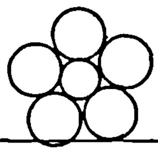	$\frac{R}{r} = \{ 1 + \frac{TAN^2 (\Pi/10)}{SIN^2 \alpha} \}^{1/2}$	≅ 50 TO 90
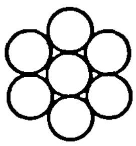	$\frac{R}{r} = \{ 1 + \frac{TAN^2 (\Pi/3)}{SIN^2 \alpha} \}^{1/2}$	≃ 50 TO 90
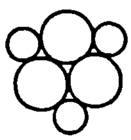	$\frac{R_1}{r_1} = \{ 1 + \frac{TAN^2 (\Pi/6)}{SIN^2 \alpha} \}^{1/2}$ $\frac{R_2}{r_1} = \frac{R_1}{r_2} \cos \frac{\pi}{3} + (1 + \frac{r_1}{r_2}) \cos \theta_1$	≃ 50 TO 90

TABLE 6.1

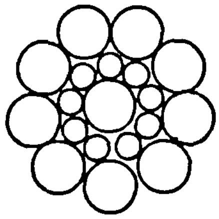	$\frac{R_1}{r_1} = \{ 1 + \frac{\tan^2(7\Pi/18)}{\sin^2 \alpha} \}^{1/2}$ $\frac{R_2}{r_2} = \{ 1 + \frac{\tan^2(5\Pi/12)}{\sin^2 \alpha} \}^{1/2}$	$\simeq$ 50 TO 90
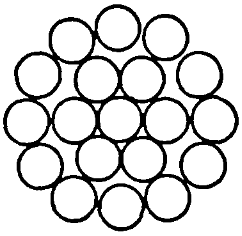	$\frac{R_1}{r_1} = \{ 1 + \frac{\tan^2(2\Pi/3)}{\sin^2 \alpha} \}^{1/2}$ $\frac{R_2}{r_2} = \{ 1 + \frac{\tan^2(5\Pi/12)}{\sin^2 \alpha} \}^{1/2}$	$\simeq$ 50 TO 90
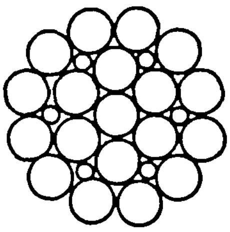	$\frac{R_1}{r_1} = \{ 1 + \frac{\tan^2(\Pi/3)}{\sin^2 \alpha} \}^{1/2}$ $\frac{R_2}{r_2} = \frac{R_1}{r_2} \cos \frac{\pi}{6} + (1 + \frac{r_1}{r_2}) \cos \theta_1$ $\frac{R_3}{r_3} = \{ 1 + \frac{\tan^2(5\Pi/12)}{\sin^2 \alpha} \}^{1/2}$	$\simeq$ 50 TO 90
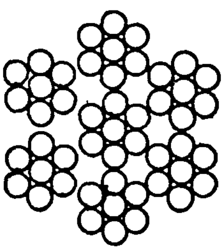	$\frac{R}{r_S} = \{ 1 + \frac{\tan^2(\Pi/6)}{\sin^2 \beta} \}^{1/2}$	$\simeq$ 50 TO 90

TABLE 6.1

CHAPTER SEVEN

STRUCTURAL MODELLING OF

SINGLE LAYER STRAND

NOMENCLATURE

A	Defined parameter
A_h	Sectional area of helical wire
a_c	Core wire radius
a_h	Helical wire radius
a_{cy}	Distance from the neutral axis to a point within a section of a core wire ore wire
a_{hy}	Distance from the neutral axis to a point within a section of a helical wire cal wire
B	Defined parameter
B_s B'_s	Flexual bending stiffness
C	Defined parameter
E	Young modulus
E_{eff}	Effective tensile stiffness
F	External tensile load applied to the strand
G	Shear modulus
G_{eff}	Effective modulus of rigidity
H_1 H_2	Defined parameters
I_h	Second moment of area of helical wire
J_c	Polar moment to area of core wire
J_h	Polar moment of area of helical wire
J_i	Geometrical constants; where i = 1, 2, 3,...22
K_1 K_2 K_3 K_4	Equivalent assemble stiffness for strand
k' & $\bar{k}'$	Initial and final curvature
M	External torsion applied to the strand
m	Number of helical wires per layer
N & N'	Internal shear force on a helical wire

N_h	Defined parameter
P_L	Lay length of strand
R & $\bar{R}$	Initial and final helical radius
R'	Defined parameter
T_c	Internal tensile load on core wire
T_h	Internal tensile load on helical wire
V & V'	Internal bending moment on helical wire
W & W'	Internal twisting moment on helical wire
W_c	Internal twisting moment on core wire
X, Y, Z	Radial forces along a naturally curve rod
$\Delta\theta$	Rotation of the strand per lay length
$\Delta k'$	Change in curvature
$\Delta\tau$	Change in torsion
$\Delta\alpha$	Change in lay angle
ε_s	Strand strain
ε_c	Helical wire strand
ε_{wb}	Bending strain on helical wire
γ_w	Shearing strain on helical wire
σ_b	Stress due to bending moment
τ_h	Shear stress due to twisting moment on helical wire
υ	Poisson's ratio of wire
υ_{eff}	Effect Poisson's ratio of strand
$\Delta\phi$	Rotation of helical wire
ΔS_w	Incremental length of helical wire
$\Delta\theta^*$	Defined parameter

7.1 INTRODUCTION TO STRUCTURAL MODELLING OF SINGLE LAYER STRAND

Stranded rope can be considered as an integrated structure which is cleverly constructed by twisting thin rods helically to form a tensile member. This structural design takes full advantage of the geometry of each individual element and does not use jointing or welding. As a result, structural flexibility is retained. The model presented in this chapter is developed by using this concept - ie that the mechanical responses of individual wires are orientated and summed with respect to global coordinates where external loads are exerted.

The approach applied here draws on several sources: the earlier studies of fatigue failed rope, the analysis of helix and sectional geometry, and the earlier treatments of 6/1 strand such as those given by S. Machida, Costello and Phillips. However, the author's models have been refined and modified. Some factors or assumptions which will affect the theoretical analysis and the structural properties of single layer strand are noted here;

a Type of Sockets for End Terminations

Cone sockets with white metal or epoxy are preferred for grasping the strand terminations.

b. Wire Material

Cold drawn rope steel is assumed to be used. Wires are assumed to be free from residual stresses and defects resulting from manufacturing, preforming and storing on the bobbin.

c. Termination Conditions

The termination conditions influence the structural properties of the strand. Four termination conditions are considered:

1. rotation of terminations is constrained (tensile load only).
2. terminations free to rotate (tensile load only).
3. torsional load applied to terminations.
4. combined tensile & torsional loads applied to termination.

7.2 STRUCTURE OF THE APPROACH TO THE MATHEMATICAL MODELLING OF SINGLE LAYER STRAND

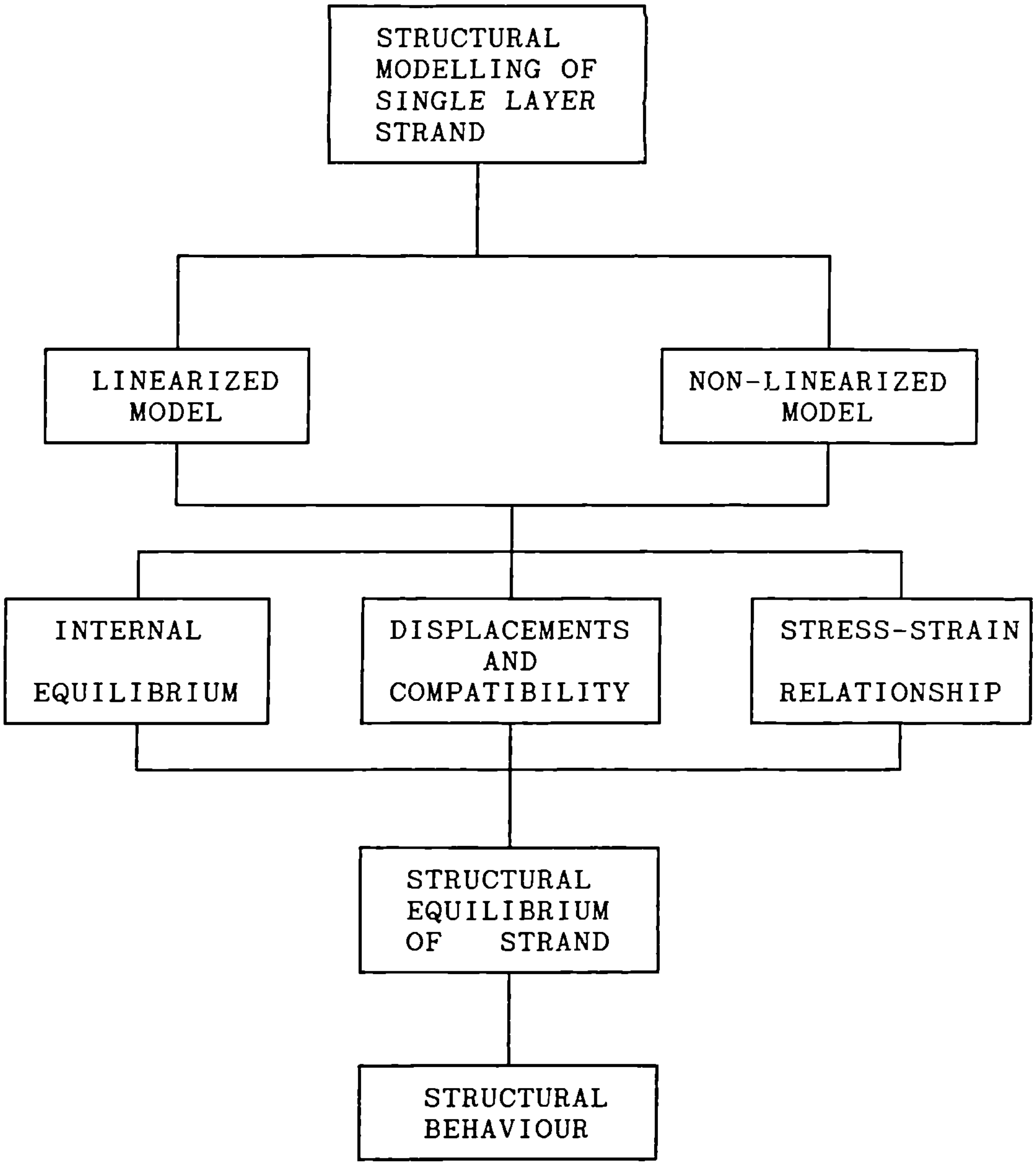

BLOCK DIAGRAM 7.2-1

STRUCTURAL MODELLING OF SINGLE LAYER STRAND

7.3 PRINCIPLES UNDERLYING METHOD OF SOLUTION AND ASSUMPTIONS

a. Principles

A strand structure is generally considered to be statically indeterminate[4.1], and hence the fundamental principles of solution must be based on:

1. Equation(s) of equilibrium of forces and moments, both internal (normally as a function of stress) and external (applied).
2. Equation(s) describing the geometry of deformation or compatibility of displacements and strains.
3. Constitutive relationships between load-deformation or stress-strain.

b. Assumptions

To apply the preceding statements logically and realistically, in accordance with the nature and characteristics of the problem (ie modelling of single layer strand), it is necessary to make the following assumptions.

1. Any section normal to the centroidal axis of a wire (ie any transverse section) is circular both before and after loading.
2. The centroidal axis of any wire within a

strand is regarded as the most important geometrical characteristic of that wire.

3. For a single helical wire, the helix angle should be between 50 to 90 degrees. this is the practical range for strands design.
4. The wire diameter should not be less than 2 mm (or .08 in). Although this may be mathematically possible, this is unrealistic in practice due to external wear and corrosion.
5. The mechanical response of a wire should be free from termination influences.
6. All helical wires in the same layer should touch the core wire and each of the helical wires may either touch neighbouring helical wires or separate from each other.
7. The wire material is assumed to be either orthotropic or isotropic and all wires remain elastic before and after loading.
8 The residual stresses set up in any wire during manufacturing, storing and strand production are ignored, as are frictional and flattening effects.
9. An oblique section of any helical wire can be approximated either by an ellipse or by a kidney shape.

7.4 INTRODUCTION TO LINEARIZED MODEL FOR SINGLE LAYER STRAND

The following sub-sections present the mathematical procedure and principal equations leading to the modelling of single layer strand in the monotonic, linear elastic regime. The model features are presented as follows:

a. Any helical wire is considered as a naturally curved rod so that naturally curved rod theory [3.21-3.22] can be applied to determine the internal components (forces and moments) exerted on the helical wire.

b. Costello-type equilibrium equations are applied to relate the internal components to the external applied loads.

c. For a strand subjected to a tensile load, the development method is applied to relate the displacement of a strand to that of the helical wires.

d. For model linearization, second and higher order derivatives of displacement equations are ignored.

e. Four termination conditions are considered in order to obtain the stiffness matrix representing the equilibrium of the strand structure.

f. Structural properties such as strand stiffness and effective Poisson's ratio can be obtained from the stiffness approach to the solution of the problem.

g. New-formed strand, free from any plastic deformations due to fatigue or wire failure, is assumed.

7.4.1 Internal and External Equilibrium

The current sections present applications of the theory to determine:

1. Internal equilibrium along the single helical wire and core wire.

2. External equilibrium on the strand.

7.4.1-1 Internal Equilibrium

a. Internal Equilibrium of a Naturally Curved Rod

This theory was first made known as Kirchhoff's linear theory of slender curved rods [3.22]. A similar theory applied to study the kinematic equilibrium of initially curved rod were also given in Love's treatise [3.21] " the mathematical theory of elasticity". In 1949, the possibility of applying the naturally curved rod theory to lock coil rope emerged in Hansom's [4.1] PhD thesis on "Mechanics of locked coil steel wire ropes". Since the mid 70's, naturally curved rod theory

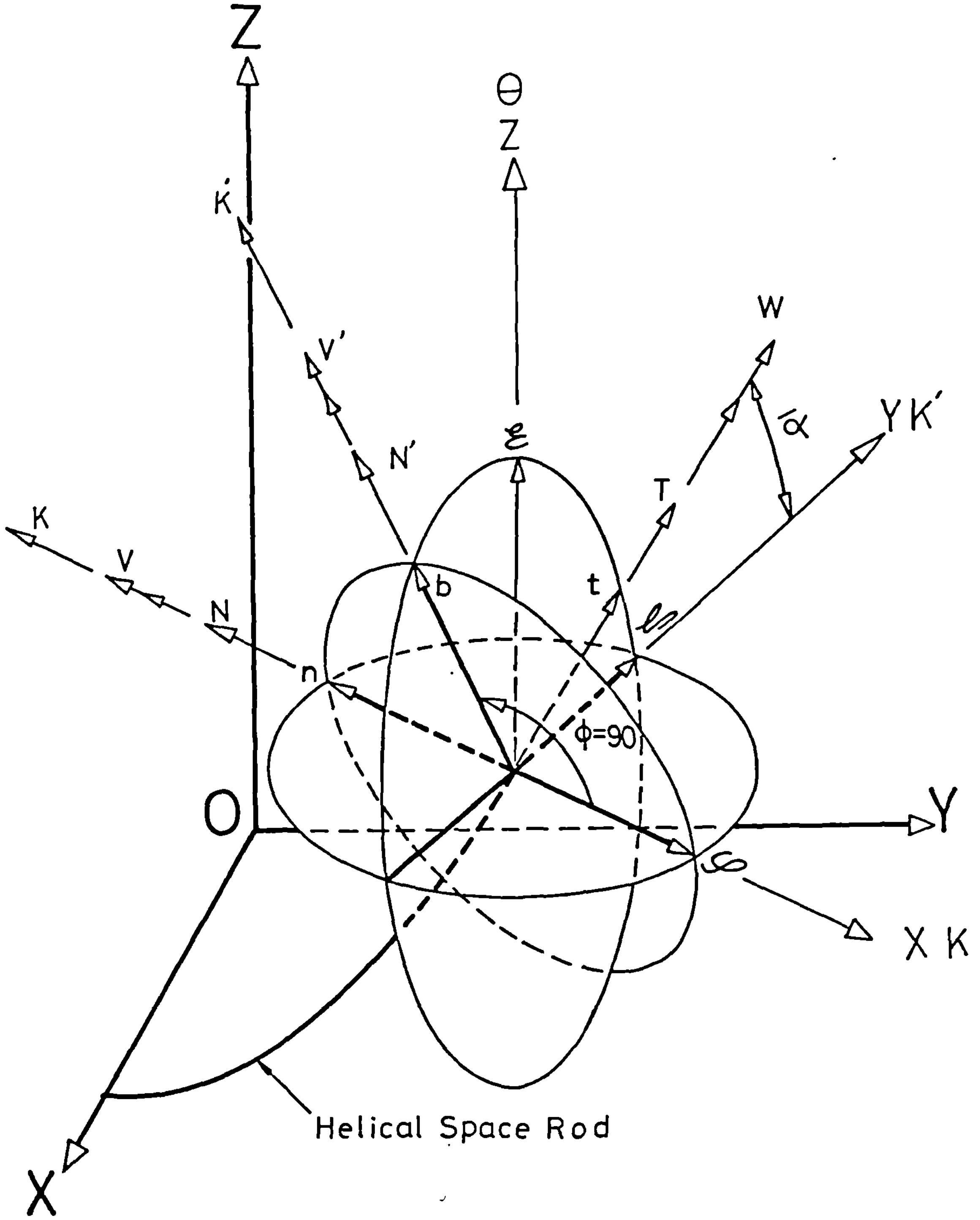

Internal Components Exerted On
A Naturally Curved Rod Subjected
To External Loads

Figure 7.4-1

was widely used to determine the internal component forces and moments on a single helical wire within a 6/1 strand by a number of strand modellers, such as Costello, Phillips and their fellow workers; For better understanding of rod theory, a schematic diagram which represents the orientation of component forces and moments on the naturally curved rod, is shown in Figure 7.4-1. A paper model which represents the orientation of similar component forces and moments on the helical rod, is also given in Figure 7.4-2. Principal differential equations of the rod model are presented in the following matrix.

Force Equilibrium:

$$\begin{vmatrix} 0 & \bar{k}' & -\bar{k} \\ \bar{\kappa} & -\bar{\tau} & 0 \\ -\bar{\kappa}' & 0 & \bar{\tau} \end{vmatrix} \begin{vmatrix} T \\ N \\ N' \end{vmatrix} = \begin{vmatrix} dT/ds \\ dN'/ds \\ dN/ds \end{vmatrix} + \begin{vmatrix} Z \\ Y \\ X \end{vmatrix} \qquad (7.4\text{-}1)$$

Moment Equilibrium:

$$\begin{vmatrix} 0 & \bar{k}' & -\bar{k} \\ \bar{\kappa} & -\bar{\tau} & 0 \\ -\bar{\kappa}' & 0 & \bar{\tau} \end{vmatrix} \begin{vmatrix} W \\ V \\ V' \end{vmatrix} = \begin{vmatrix} dW/ds \\ dV'/ds \\ dV/ds \end{vmatrix} + \begin{vmatrix} \underline{\theta} \\ \underline{K}' \\ \underline{K} \end{vmatrix} \qquad (7.4\text{-}2)$$

These sets of equations are derived from differential geometry. They are also known as "Frenet-Serret Formulae".

Top View

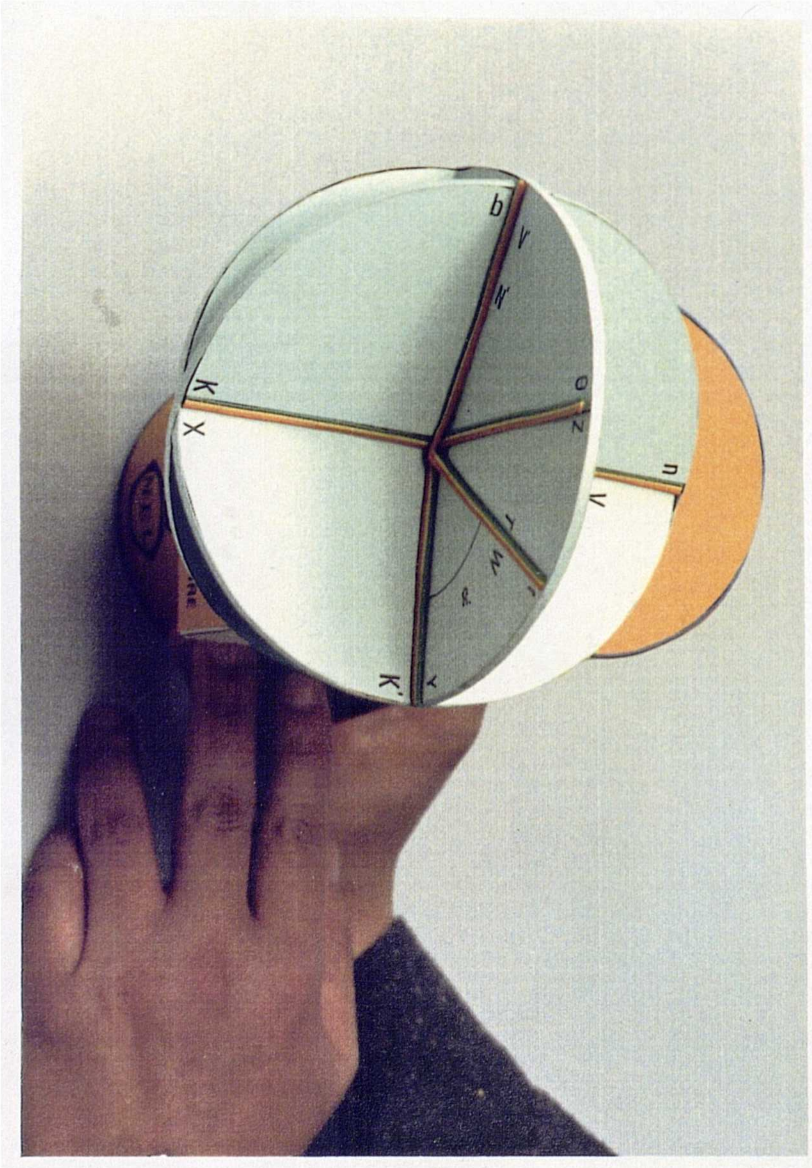

Elevation

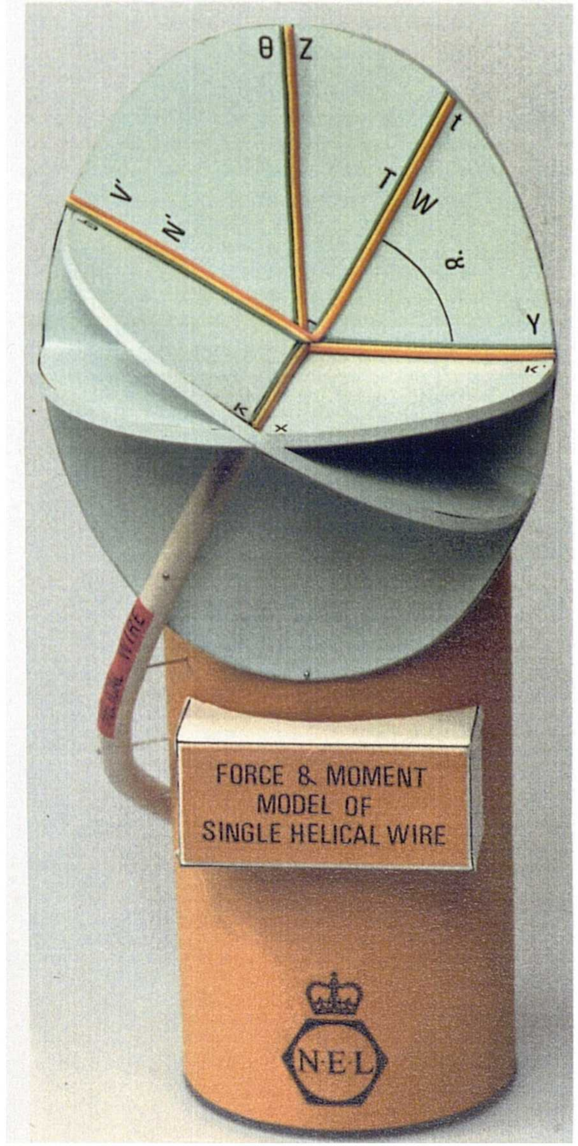

A Model Illustrates The Internal Components Along The Helical Wire

Figure 7·4-2

b. Internal Equilibrium of a Single Helical Helical Wire

When equations 7.4-1 and 7.4-2 are being applied to a single helical wire under static conditions, several component forces and moments will vanish in the preceding matrices. They are forces Y and Z per unit length and external moments $\underline{\theta}$, $\underline{K}'$ and $\underline{K}$ per unit length of the helical wire. Hence, the matrices representing the internal components of forces and moments along the single helical wire are given by:

Force Equilibrium:

$$\begin{vmatrix} 0 & \bar{k}' & -\bar{k} \\ \bar{k} & -\bar{\tau} & 0 \\ -\bar{k}' & 0 & \bar{\tau} \end{vmatrix} \begin{vmatrix} T \\ N \\ N' \end{vmatrix} = \begin{vmatrix} 0 \\ 0 \\ X \end{vmatrix} \qquad (7.4\text{-}3)$$

Moment Equilibrium:

$$\begin{vmatrix} 0 & \bar{k}' & -\bar{k} \\ \bar{k} & -\bar{\tau} & 0 \\ -\bar{k}' & 0 & \bar{\tau} \end{vmatrix} \begin{vmatrix} W \\ V \\ V' \end{vmatrix} = \begin{vmatrix} 0 \\ 0 \\ 0 \end{vmatrix} \qquad (7.4\text{-}4)$$

C Approximate Theory for Component Moments

Equations 7.4-3 and 7.4-4 represent a set of indeterminate equations. In order to solve them, some of the terms in the equations have to be approximated by the expressions[3.21] given below:

$$V = B_s \; (\bar{k} - k) \qquad (7.4\text{-}5)$$

$$V' = B_s' \; (\bar{k}' - k') \qquad (7.4\text{-}6)$$

$$W = T_s \; (\bar{\tau} - \tau) \qquad (7.4\text{-}7)$$

where B_s', B_s and T_s are the flexural bending stiffness and flexural twisting stiffness respectively.

$$B_s = B_s' = EI \qquad (7.4\text{-}8)$$

$B_s = B_s'$ due to axial symmetry of wire cross section

$$T_s = GJ \qquad (7.4\text{-}9)$$

For a single helical wire described by its centroidal axis, there is one curvature; ie binormal curvature " k' ". In other words, the normal curvature is zero. Therefore, the normal flexual bending moment "V" on the single helical wire vanishes.

The tensile component along the helical wire is given by

$$T_h = \pi \, a_h^2 \; E \, \varepsilon_w \qquad (7.4\text{-}10)$$

Having approximated these three important parameters (ie, W, V' and T_h), one should have sufficient parameters to evaluate shearing force "N'" and radial force "X" per unit length along the single helical wire, by substitution of equations 7.4-5, 7.4-6 and 7.4-10 into equation 7.4-1. Parameters *for* shearing force and radial force are then given by:

$$N' = W \bar{k}' - V' \bar{\tau} \qquad (7.4\text{-}11)$$

$$X = N'\bar{\tau} - T \bar{k}' \qquad (7.4\text{-}12)$$

The equations for internal force and moment equilibrium on the helical wire under static conditions can then be solved.

d. Internal Equilibrium Of Core Wire

For a straight strand subjected to combined axial loads (ie tension and twisting), internal force and moment can exist on the core wire of the strand. They are given by:

$$T_c = \pi a_c^2 E \varepsilon_s \qquad (7.4\text{-}13)$$

$$W_c = G J_c \Delta\theta \qquad (7.4\text{-}14)$$

7.4.1-2 External Equilibrium of Single Layer Strand

Soon after a rational mathematical model emphasizing the structural equilibrium of a 6/1 strand was developed by S. Machida and J.J Durelli[4.1], an improved approach to deal with the structural equilibrium of a 6 single helix strand was also proposed by Costello, Phillips and fellow workers [3.1-3.20]. This logical and reasonable approach is also applied by the present author. For a better understanding of how to derive the structural equilibrium of a single layer strand, a detailed schematic diagram indicating the orientation of the internal components exerted on a helical wire of a 6/1 strand (as an example) is presented in Figure 7.4.3. The equations which represent structural equilibrium of a single layer strand are given by:

$$F = m (T_h \sin \bar{\alpha} + N' \cos \bar{\alpha}) + T_c \quad (7.4\text{-}15)$$

$$M = m (W \sin \bar{\alpha} + V' \cos \bar{\alpha} + T_h \bar{R} \cos \bar{\alpha} - N' \bar{R} \sin \bar{\alpha}) + W_c \quad (7.4\text{-}16)$$

The strand termination conditions, as presented in the preceding section, have a significant influence on the structural properties of the single layer strand. The structural equilibrium equations have to be expressed in terms of structural translational and rotational displacements of the strand. They can be expressed in a matrix form:

$$\begin{vmatrix} K_1 & K_2 \\ K_3 & K_4 \end{vmatrix} \begin{vmatrix} \varepsilon_s \\ \Delta\theta \end{vmatrix} = \begin{vmatrix} F \\ M \end{vmatrix} \quad (7.4\text{-}17)$$

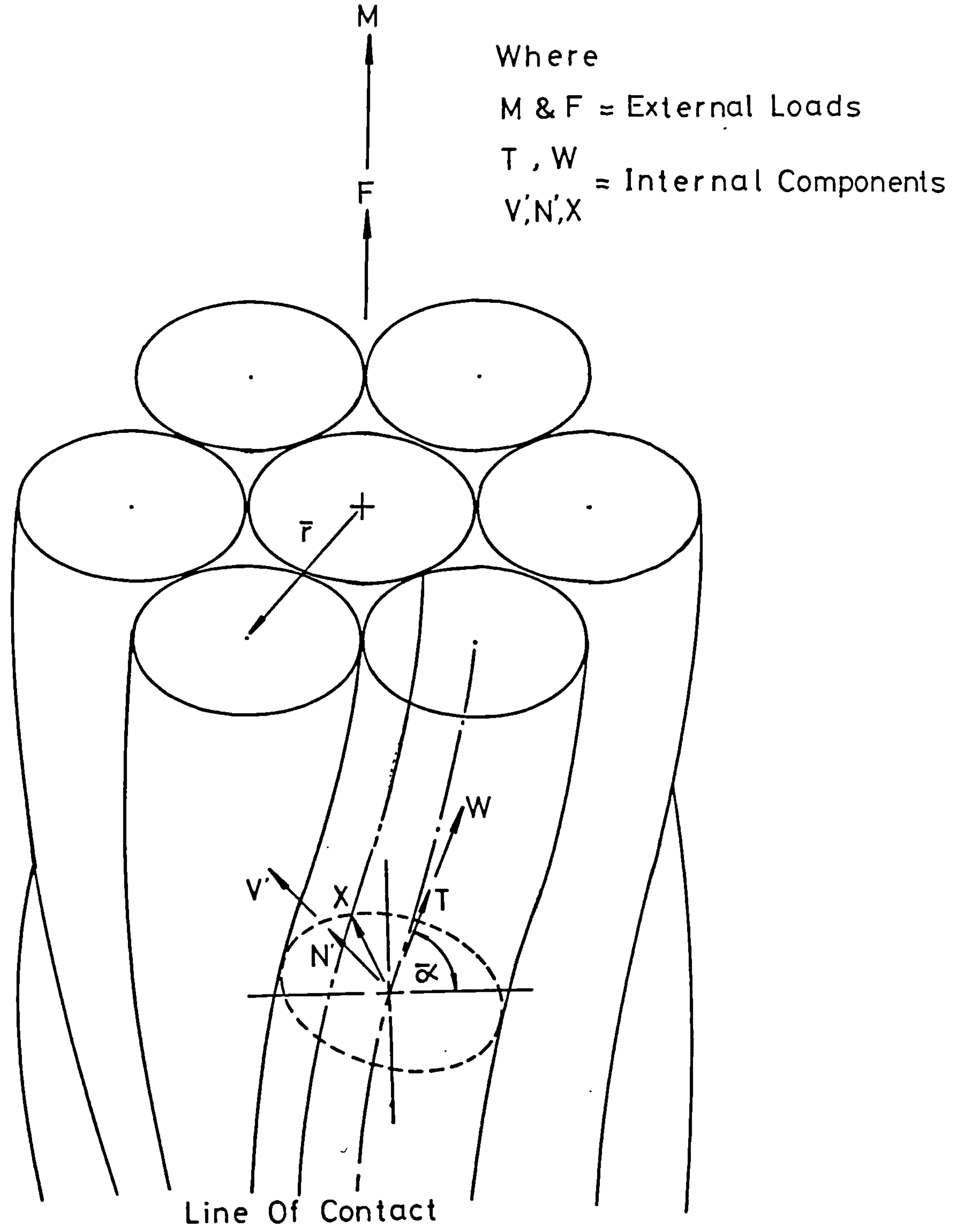

Figure 7·4-3
Typtical 6/1 Strand Model

7.4.2 Geometry of Deformation and Compatibility of Displacements

This section presents the approach to determine the geometry of deformation of core and helical wire in the single layer strand. It is organized into the following sub-sections.

a. Helix geometry required for the deformation analysis.
b. Wire sectional geometry.
c. Deformation geometry of core and helical wires.

7.4.2-1 Helix Geometry

Full details of cylindrical helix geometry have been presented in Chapter Four and Chapter Five. This sub-section gives important geometrical parameters which are used to relate the curvature and torsion with the bending and twisting moments along the helical wire. Expressions for these two parameters are:

a. Initial and Final Curvature of a Single Helix

$$k' = \frac{\cos^2 \alpha}{R} \quad ; \qquad \bar{k}' = \frac{\cos^2 \bar{\alpha}}{\bar{R}} \qquad (7.4\text{-}18)$$

b. Initial and Final Torsion

$$\tau = \frac{\sin \alpha \cos \alpha}{R} ; \qquad \bar{\tau} = \frac{\sin \bar{\alpha} \cos \bar{\alpha}}{\bar{R}} \qquad (7.4\text{-}19)$$

7.4.2-2 Sectional Geometry

Full details of sectional geometry have also been presented in Chapter Six. An admissible ratio between helical wire radius and helical radius as functions of number of helical wires per layer and helix angle is:

$$\frac{R}{r} = \{ 1 + \frac{\tan (\pi/2 + \pi/m)}{\sin^2 \alpha} \}^{1/2} \qquad (7.4\text{-}20)$$

For practical purpose, the helix angle should be between 60 and 90 degrees. Equation 7.4-20 was also given in Ref. 3.1.

7.4.2-3 Deformation Geometry Between Core and Helical Wire

The Development method can also be applied to determine the deformation of a helical wire in relation to the global displacement of the strand (with four strand termination conditions). A schematic representation of the axial deformation of strand and helical wires is shown in Figure 7.4-4. The geometrical imperfection, flattening effect, and second and higher order deformation terms are ignored in formulating the linearized model. Deformation equations, in terms of strand and helical wire axial strain are expressed as functions of changes in geometrical parameter and are given by:

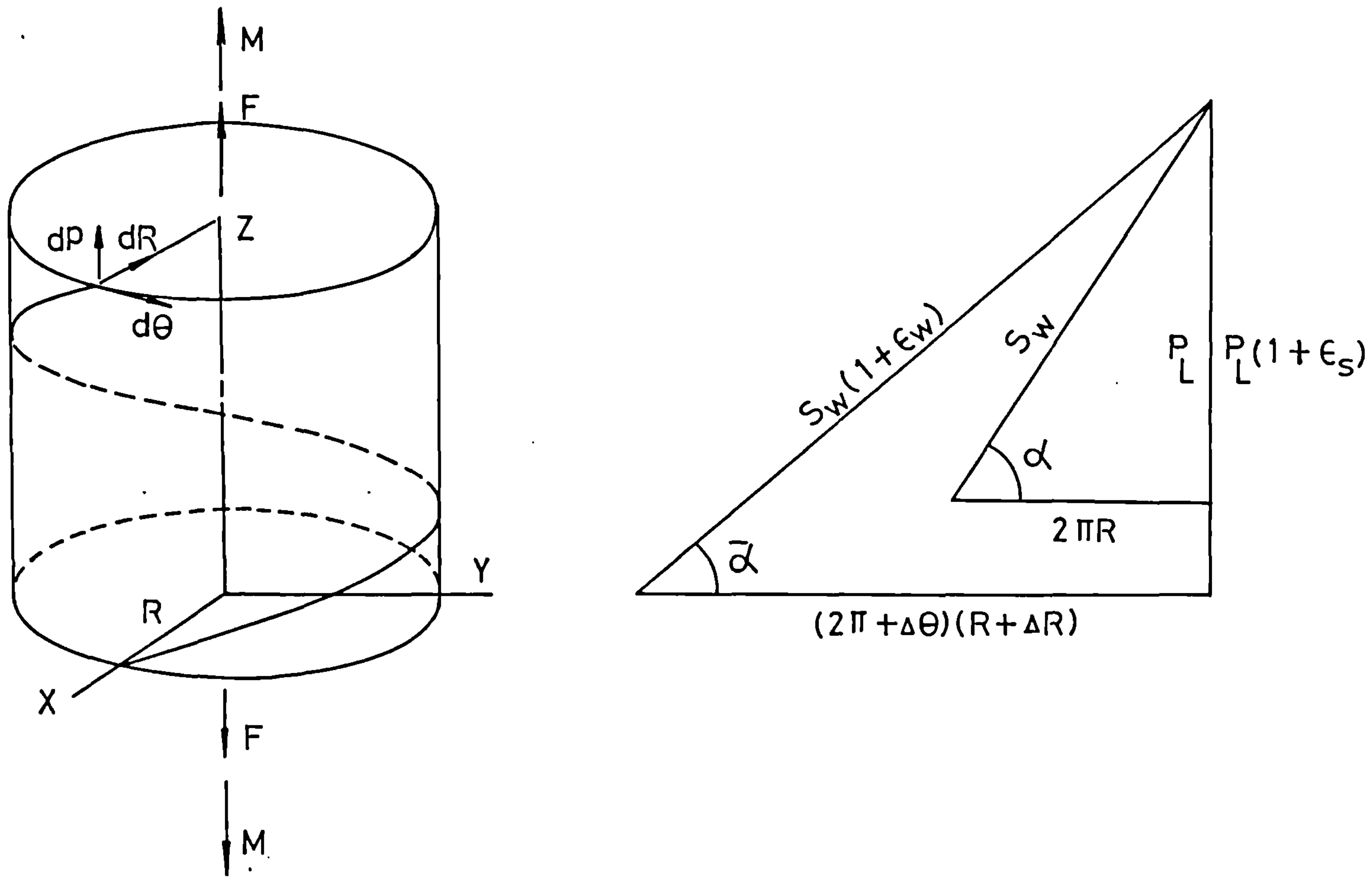

Figure 7.4-4

Cylindrical Helix And Its Development

$$\varepsilon_s = \varepsilon_w + \frac{\Delta\alpha}{\tan\alpha} \tag{7.4-21}$$

$$\varepsilon_s = \frac{\Delta R}{R} + \frac{\Delta\theta}{2\pi} + (\ \tan\alpha\ + \cot\alpha\ )\ \Delta\alpha \tag{7.4-22}$$

$$\varepsilon_w = \frac{\Delta R}{R} + \frac{\Delta\theta}{2\pi} + \Delta\alpha\ \ \tan\alpha \tag{7.4-23}$$

$$\varepsilon_w = \varepsilon_s\ \sin^2\alpha\ + \frac{\Delta R}{R}\cos^2\alpha\ + \frac{\Delta\theta}{2\pi}\cos^2\alpha \tag{7.4-24}$$

Where ΔR, $\Delta\theta$ and ε_s are global geometrical changes (in terms of cylindrical coordinates) of the single layer strand subjected to external axial load corresponding to the four termination conditions.

7.4.2-4 Deformations of Helical Wire

For a single layer strand subject to combined load, extension and rotation can be regarded as the known magnitudes in equations 7.2-21 and 7.4-24 whereas ε_w, ΔR and $\Delta\alpha$ are considered as the major unknowns in these equations. In order to solve equations 7.2-21 and 7.4-24, one additional known parameter is required. For convenience, ΔR is chosen to be approximated, by applying the classical approach (ie conservation of volume for incompressible material) and flattening effects. The change in helical radius can be found by:

$$\frac{\Delta R}{R} = \frac{\nu \, (a_c \, \varepsilon_s + a_h \, \varepsilon_w)}{R} + \delta R_f \qquad (7.4\text{-}25)$$

where δR_f is the flattening deformation due to radial force. It has been suggested by Utting and Jones[6.10] that the flattening term δR_f is very small and can be ignored in this analysis. Therefore, the change in helical radius is given by:

$$\frac{\Delta R}{R} = \frac{\nu \, (a_c \, \varepsilon_s + a_h \, \varepsilon_w)}{R} \qquad (7.4\text{-}26)$$

By substituting equation 7.4-26 into equation 7.4-24 the deformations of the helical wire can be written as:

$$\varepsilon_w = J_1 \, \varepsilon_s + J_2 \, \Delta\theta \qquad (7.4\text{-}27)$$

$$\Delta\alpha = J_3 \, \varepsilon_s + J_4 \, \Delta\theta \qquad (7.4\text{-}28)$$

The changes in curvature and torsion are given by

$$\Delta K' = J_5 \, \varepsilon_s + J_6 \, \Delta\theta \qquad (7.4\text{-}29)$$

$$\Delta\tau = J_7 \, \varepsilon_s + J_8 \, \Delta\theta \qquad (7.4\text{-}30)$$

where J_1, J_2, J_3, J_4, J_5, J_6, J_7 and J_8 are defined geometrical parameters. They are shown in Appendix.

7.4.3 Material Constants and Stress Strain Relationship

Rope steel is cold drawn (ie normally hypereutectoid steel) and the wire is considered to be a slender rod. In fact, the material properties along the wire are more important than the material properties across the transverse section in considering the structural properties of single layer strand. Rope steel, in this case, can be considered either as an isotropic material or an orthotropic material. The essential stress-strain relationships for the present model are given by Hooke's law and this is used to relate stress and strain along the centroidal axis of any wire resulted from tension. The stress-strain relationship is given by:

$$E = \frac{\sigma}{\varepsilon} \tag{7.4-31}$$

If the wire material is assumed isotropic, the shear modulus can be related to the Young's modulus. The shear modulus is used to relate the twisting stress with the twisting strain resulting from the change in torsion of the single helical wire.

$$G = \frac{E}{2\ (\ 1 + \nu\ )} \tag{7.4-32}$$

For an orthotropic material, the relationship described by equation 7.4-32 is no longer valid. Then individual material constants (E and G) are normally determined by experiment or recommended by wire manufacturer.

Remark:

In the current modelling, E and G are essentially employed to relate the change of curvature and torsion with the bending and twisting component of a single helical wire within a single layer strand subjected to external axial load.

7.4.4 Linearization

Costello and others suggested that geometrical non-linear characteristics do not appear to have significant influence to the linear load-extension behaviour; this mechanical behaviour is referred to as weakly non-linear.

The main purpose of model linearization is to derive element stiffnesses for individual wires, to allow assembly of stiffnesses for the single layer strand and to calculate the structural properties of a strand with respective termination conditions.

To proceed model linearization, the second and the higher order deformation terms, with respect to the axial deformation of a strand, are ignored. The following gives the linearized equations with respect to the axial deformations of the strand.

7.4.4-1 Linearized Internal Components

a. Bending Moment Acting on a Helical Wire

For a strand subjected to a tensile load, the bending moment on a single helical wire can be expressed as functions of change in curvature of the centroidal axis of the wire as:

$$V' = B_s' \ (\ \bar{K}' - K' \ ) = B_s' \ \Delta K' \qquad (7.4-33)$$

By substituting the linearized equation 7.4-29 into equation 7.4-33 the bending moment V' can be expressed as a function of the axial deformation of strand, as shown below:

$$V' = B_s' \ (\ J_5 \ \varepsilon_s - J_6 \ \Delta\theta \ ) \qquad (7.4-33)$$

where J_5 and J_6 are defined as element stiffness, given in Appendix.

b. Twisting Moment Acting on a Helical Wire

For a strand subjected to an axial load, the twisting moment on a single helical wire can be written as a function of change in torsion on the centroidal axis of that wire:

$$W = T_s \ (\ \bar{\tau} - \tau \ ) = T_s \ \Delta\tau \qquad (7.4-35)$$

By substituting the linearized equation 7.4-30 into equation 7.4-35. The twisting moment W can be expressed as a function of the axial deformation of strand:

$$W = T_s \ (\ J_7 \ \varepsilon_s - J_8 \ \Delta\theta \ ) \qquad (7.4-36)$$

where J_7 and J_8 are also defined as element stiffness, as given in Appendix.

c. Tensile Force Acting on a Helical Wire

The tensile component along the single helical wire can reasonably be approximated by:

$$T_h = \pi a_h^2 \; E \; \varepsilon_w \qquad (7.4\text{-}37)$$

again, by substituting the linearized equation 7.4-27 into equation 7.4-37, the tensile force equation can be written as functions of axial deformations of a strand:

$$T_h = \pi a_h^2 E \left(J_1 \varepsilon_s + J_2 \Delta\theta \right) \qquad (7.4\text{-}38)$$

where J_1 and J_2 are given in Appendix.

d. Shearing Force Acting on a Helical Wire

By substituting the linearized equations 7.4-34 and 7.4-35 into equation 7.4-11 the shear force along the helical wire can also be expressed as functions of axial deformation of a strand.

$$N' = J_{17} \varepsilon_s + J_{18} \Delta\theta \qquad (7.4\text{-}39)$$

e. Radial Force Acting on a Helical Wire

By substituting the linearized equations 7.4-38 and 7.4-39 into equation 7.4-12, the radial force on a helical wire can be written in term of axial deformation of strand:

$$X = J_{19} \varepsilon_s + J_{20} \Delta\theta \qquad (7.4\text{-}40)$$

again the element stiffness constants J_{17}, J_{18}, J_{19}, and J_{20} are given in Appendix.

7.4.4-2 Linearized Stresses Along Core and Single Helical Wire

The aim of the current sub-section is to relate the component stresses on each wire with the axial deformations of a strand. This procedure allows component stresses and strains on each wire within a strand to be expressed as functions of axial deformation (ie ε_s and $\Delta\theta$ of the strand).

For a strand subjected to axial load, the stresses and strains on each of the wires are given as follows:

a. Core Wire of a Strand

1. Strain and stress on the core wire resulting from tension alone are given by:

$$\varepsilon_c = \varepsilon_s \qquad (7.4\text{-}41)$$

$$\sigma_c = E\ \varepsilon_s \qquad (7.4\text{-}42)$$

2. Stress and strain along core wire resulting from twisting moment alone are given by

$$\tau_c = J_{10}\ a_{cy}\ \Delta\theta\ /\ J_c \qquad (7.4\text{-}43)$$

$$\gamma_c = \tau_c\ /\ G \qquad (7.4\text{-}44)$$

b. Helical Wires of a Strand

1. Stress and strain along the helical wire resulting from tension alone are given by:

$$\varepsilon_w = J_1 \varepsilon_s + J_2 \Delta\theta \tag{7.4-45}$$

$$\sigma_w = E \varepsilon_w \tag{7.4-46}$$

2. Stress and strain along the helical wire resulting from bending alone are given by:

$$\varepsilon_{wb} = \frac{a_{hy} J_5}{1 + k' a_{hy}} \varepsilon_s + \frac{a_{hy} J_6}{1 + k' a_{hy}} \Delta\theta \tag{7.4-47}$$

$$\sigma_{wb} = E \varepsilon_{wb} \tag{7.4-48}$$

3. Stress and strain along helical wire resulting from twisting alone are given by:

$$\gamma_w = (J_7 \varepsilon_s + J_8 \Delta\theta) \tag{7.4-49}$$

$$\tau_w = G \gamma_w \tag{7.4-50}$$

7.4.5 Structural Equilibrium and Properties of Single Layer Strand

In practice, rope users are interested finding out how a new rope will behave under tension with various termination conditions. The current section considers how the structural equilibrium and properties are related with the deformation of the single layer strand. The section is organized as follows:

a. Structural equilibrium of single layer strand.

b. Structural properties corresponding to termination conditions.

7.4.5-1 Linearized Structural Equilibrium of a Single Layer Strand

From the preceding linearized approach, general equations which represent the structural equilibrium of a single layer strand subjected to axial loads with four termination conditions can be obtained. This is done by substituting linearized internal component equations, presented in sub-section 7.4.4-1, into external equilibrium equations, as presented in sub-section 7.4.1-2 (ie equations 7.4-15 and 7.4-16). The linearized structural equilibrium equations expressed in a matrix form (ie equation 7.4-17), can also be expressed as functions of structural deformations (ie ε_s and $\Delta\theta$) of single layer strand.

7.4.5-2 Structural Response and Properties of Single Layer Strand

One of the main purposes of the stiffness matrix approach is to develop a comprehensive mathematical model which can be applied to evaluate the structural properties of a single layer strand subjected to combined load.

a. Strand With Free Ends

In this case, there is no torsional load applied to the terminations and tension is the only external load applied to the strand terminations. Therefore

$$M = 0 \tag{7.4-51}$$

From equation 7.4-17, the amount of unwinding rotation per lay length of the strand resulting from tensile load is given by

$$\Delta\theta = - K_3 \ \varepsilon_s \ / \ K_4 \tag{7.4-52}$$

The effective tensile modulus of the strand is defined as

$$E_{eff} = F/\varepsilon_s \tag{7.4-53}$$

and is, therefore, given by

$$E_{eff} = \frac{K_1 \ K_4 - K_2 \ K_3}{K_4} \tag{7.4-54}$$

b. Strand With Fixed Ends

In this case, the rotational displacement of terminations $\Delta\theta$ is constrained and tension is the only axial load allowed.

Therefore,

$$\Delta\theta = 0 \qquad (7.4.55)$$

assuming that the torque developed at the terminations is linearly proportional to the applied tension, the torque generated at the terminations as a result of restriction of rotations at the termination, is given by

$$M = \frac{K_3}{K_1} \cdot F \qquad (7.4.56)$$

The effective tensile modulus, as defined previously, is given by

$$E_{eff} = K_1 \qquad (7.4.57)$$

c. Strand Subjected to Twisting Alone

In this case, torsion is the only load applied to the terminations. Therefore,

$$F = 0 \qquad (7.5\text{-}58)$$

The shortening effect due to twisting of the strand induces a compressive strain to the core wire. This is given by

$$\varepsilon_s = -\frac{K_2}{K_1} \cdot \Delta\theta \qquad (7.4\text{-}59)$$

The effective torsional rigidity is defined as

$$G_{eff} = M / \Delta\theta \qquad (7.4\text{-}60)$$

and is, therefore, given by

$$G_{eff} = \frac{K_1 K_4 - K_2 K_3}{K_1} \qquad (7.4\text{-}61)$$

d. Strand Subject to Combined Axial Loads

In this case, both axial tensile and twisting loads are applied to the terminations of the strand. The equilibrium equations which applied to approximate this situation has been given by 7.4-17.

Again the effective tensile modulus and the effective torsional rigidity are defined as

$$E_{eff} = F \,/\, \varepsilon_s^{*} \qquad (7.4\text{-}62)$$

and

$$G_{eff} = M \,/\, \Delta\theta^{*} \qquad (7.4\text{-}63)$$

where

$$\varepsilon_s^{*} = \varepsilon_{s\ (fixed)} + \varepsilon_{s\ (twisting\ alone)} \qquad (7.4\text{-}64)$$

$$\Delta\theta^{*} = \Delta\theta_{(twisting\ alone)} + \Delta\theta_{(fixed)} \qquad (7.4.65)$$

where

$\varepsilon_{s\ (twisting\ alone)}$ is negative due to contraction.

$\Delta\theta_{\ (fixed)}$ is negative due to unwinding rotation.

e. Effective Poisson's Ratio of Single Layer Strand

At this point, it may be useful to evaluate the ratio of the change in strand diameter to the original diameter of the unloaded strand. This ratio, according to the literature [3.19] defined as an effective Poisson's ratio, is given by:

$$\nu_s = \frac{R - \bar{R}}{R} \qquad (7.4\text{-}66)$$

where

$$R = a_h + 2\ a_c \qquad (7.4\text{-}67)$$

$$R = \bar{a}_h + 2\ a_c \qquad (7.4.68)$$

To evaluate the effective Poisson's ratio in terms of the strand structural displacement (ie axial displacement), the essential parameters which are needed, are the final radii of core wire and helical wire corresponding to the deformation of strand subjected to axial loads. The expressions used to determine the final radii are:

$$\bar{a}_c = a_c\ (\ 1 - \nu\ \varepsilon_s\ ) \qquad (7.4\text{-}69)$$

$$\bar{a}_h = a_h\ (\ 1 - \nu\ \varepsilon_w\ ) \qquad (7.4\text{-}70)$$

By substituting equations 7.4-69 and 7.4-70 into equation 7.4-66 the effective Poisson's ratio of the straight single layer strand subjected to axial loads in terms of strand structural deformation is given by:

$$\nu_s = J_{21}\ \varepsilon_s + J_{22}\ \Delta\theta \tag{7.4-71}$$

where J_{21} and J_{22} are defined geometrical parameters given in Appendix.

7.5 OTHER CONSIDERATIONS

This section presents a discussion on another method for evaluating bending and twisting stress.

a. Discussion on The Bending of Large Diameter Helical Wire

The approximate theory, as presented in Love's treatise [3.21], various references [3.1 - 3.20] and equations 7.4-5 & 7.4-6 of this chapter, are applied to evaluate approximate bending and twisting components along a slender single helical wire. This is considered to be a reasonably closed form method, provided that the wire diameter is small and the helix angle is large, so that the wire diameter is very small compared with the radius of curvature. In fact, the stress distribution as the result of bending is almost linear. Reference [4.1] also suggests that the radius of curvature has to be large compared with the wire diameter when using this approximate method; for instance $\rho_k \geq 50\ d_h$ and helix angle around 85 degrees or above. On the other hand, when the diameter of a helical wire is of the same order of the radius of curvature, the distribution of bending stress across the wire section is non-linear as shown in Figure 7.5-1 a. A mathematical treatment of the migration of the neutral axis, for large diameter helical wires with a relatively small helix angle, is outline below:

If the radius of the helical wire is of the same order as the radius of curvature, the bending strain across the section of

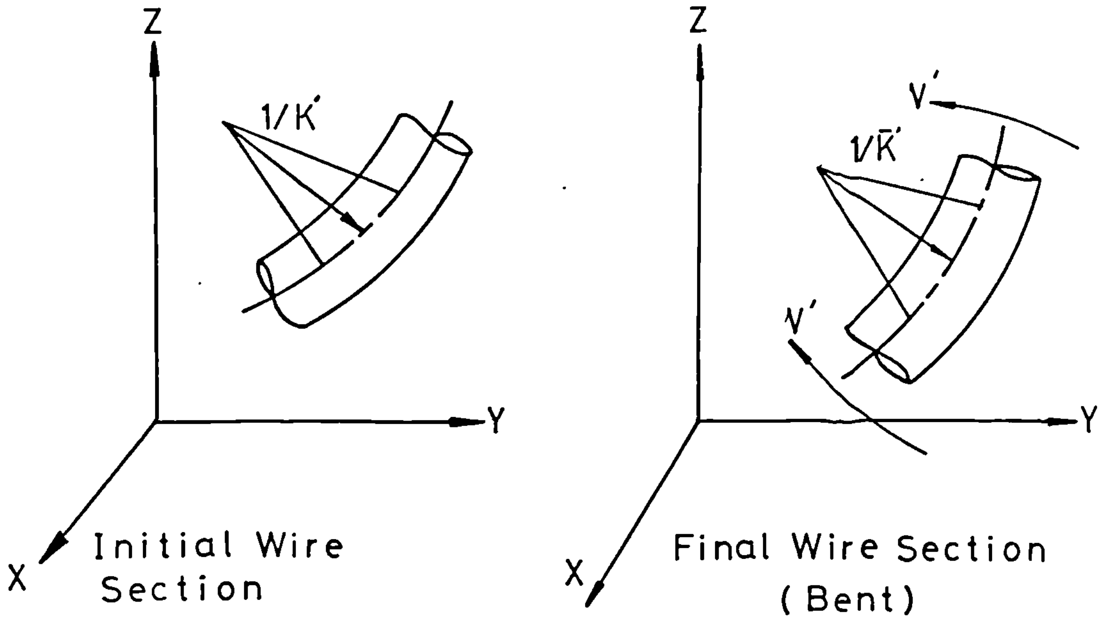

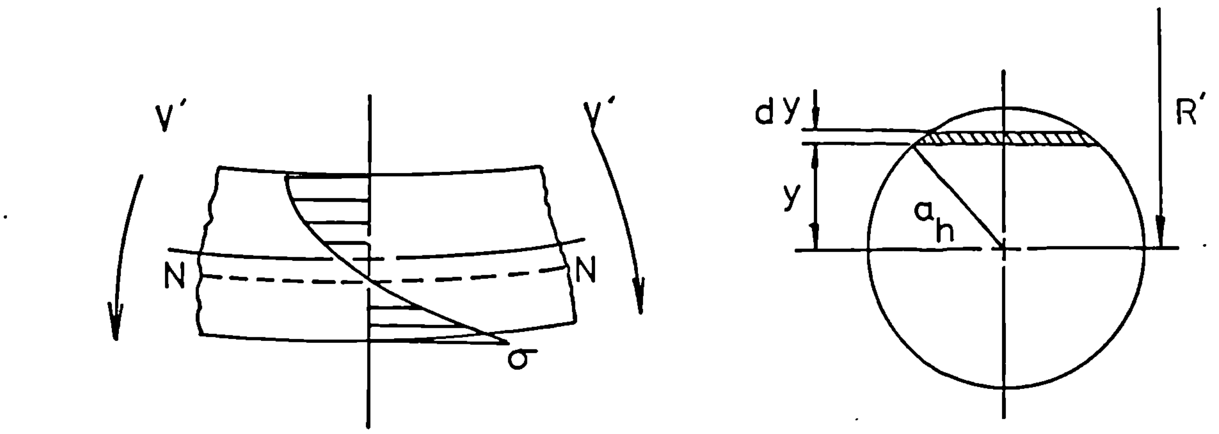

a. Stress Distribution Due To Migration Of Neutral Axis

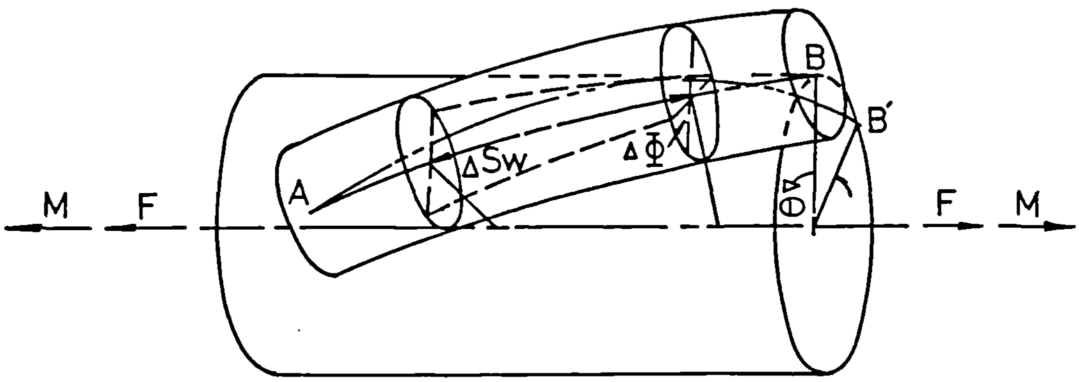

b. Twisting Model Of Helical Wire

Figure 7·5-1
Bending And Twisting On Helical Wire

the large diameter wire is given by:

$$\varepsilon_{wb} = \frac{a_{hy} \left(1/k' - 1/\bar{k}' \right)}{1/\bar{k}' \left(1/k' + a_{hy} \right)} \tag{7.5-1}$$

and the bending stress is given by

$$\sigma_b = E \, \varepsilon_{wb} \tag{7.5-2}$$

For equilibrium of internal and external bending moments, the general equation is given by

$$V' = \int_{A_h} \sigma_b \, a_{hy} dA_h \tag{7.5-3}$$

By substituting equations 7.5-1 and 7.5-2 into equation 7.5-3, the simplified bending moment is then given by

$$V' = \frac{N_h \, A_h \, E \left(1/k' - 1/\bar{k}' \right)}{1/\bar{k}'} \tag{7.5-4}$$

$$N_h = \frac{R'}{2} \left(\frac{1}{2} \left(a_h / R' \right)^2 + \frac{1}{8} \left(a_h / R' \right)^4 + \ldots \right) \tag{7.5-5}$$

For a circular section,

$$R' = 1 / K' \tag{7.5-6}$$

see Figure 7.5-1, At this stage, one can predict the stress distribution across a section of helical wire resulting from bending.

b. Twisting Moment on The Helical Wire (Alternative Method):

From the geometrical point of view, the torsion can be defined as

$$\tau = \lim_{\Delta \to 0} \frac{\Delta\phi}{\Delta S_w} \qquad (7.5\text{-}7)$$

Therefore, for a single layer strand subjected to axial load, the change in rotation of a helical wire, is given by

$$\Delta (\Delta\phi) = \Delta S_w (\tau \varepsilon_w + \Delta\tau) \qquad (7.5\text{-}8)$$

By using the flexural twisting theory, it can be shown that the twisting moment on the helical wire is given by

$$W = \frac{G J_h \Delta (\Delta\phi)}{\Delta S_w} \qquad (7.5\text{-}9)$$

At this point, one can also predict the approximate twisting stress across the section a helical wire resulting from twisting moment. See Figure 7.5-1 b for cross reference purpose.

c. Theoretical Analysis of Stress Due To Internal Components

Consider a helical wire subjected to internal components as illustrated in Figure 7.5-2. The following stress components on an element of material at the surface points A, B and C can be derived.

at A :

$$\sigma_1, \sigma_2 = \frac{1}{2}\sigma_{XA} \pm \frac{1}{2}\{ \sigma_{XA}^2 + 4 \tau_{XZ}^2 \}^{1/2} \quad (7.5\text{-}10)$$

at B:

$$\sigma_1 = -\sigma_2 = \tau_{XZ} \quad (7.5\text{-}11)$$

at C:

$$\sigma_1, \sigma_2 = \frac{1}{2}\sigma_{XC} \pm \frac{1}{2}\{ \sigma_{XC}^2 + 4 \tau_{XZ}^2 \}^{1/2} \quad (7.5\text{-}12)$$

where

$$\sigma_{XA} = \frac{4T}{\pi d^2} + \frac{32\ V'}{\pi d^3} \quad (7.5\text{-}13)$$

$$\tau_{XZ} = 16\ W / \pi d^3 \quad (7.5\text{-}14)$$

$$\sigma_{XC} = \frac{4T}{\pi d^2} + \frac{32\ V'}{\pi d^3} \quad (7.5\text{-}15)$$

The maximum shear stress is given by

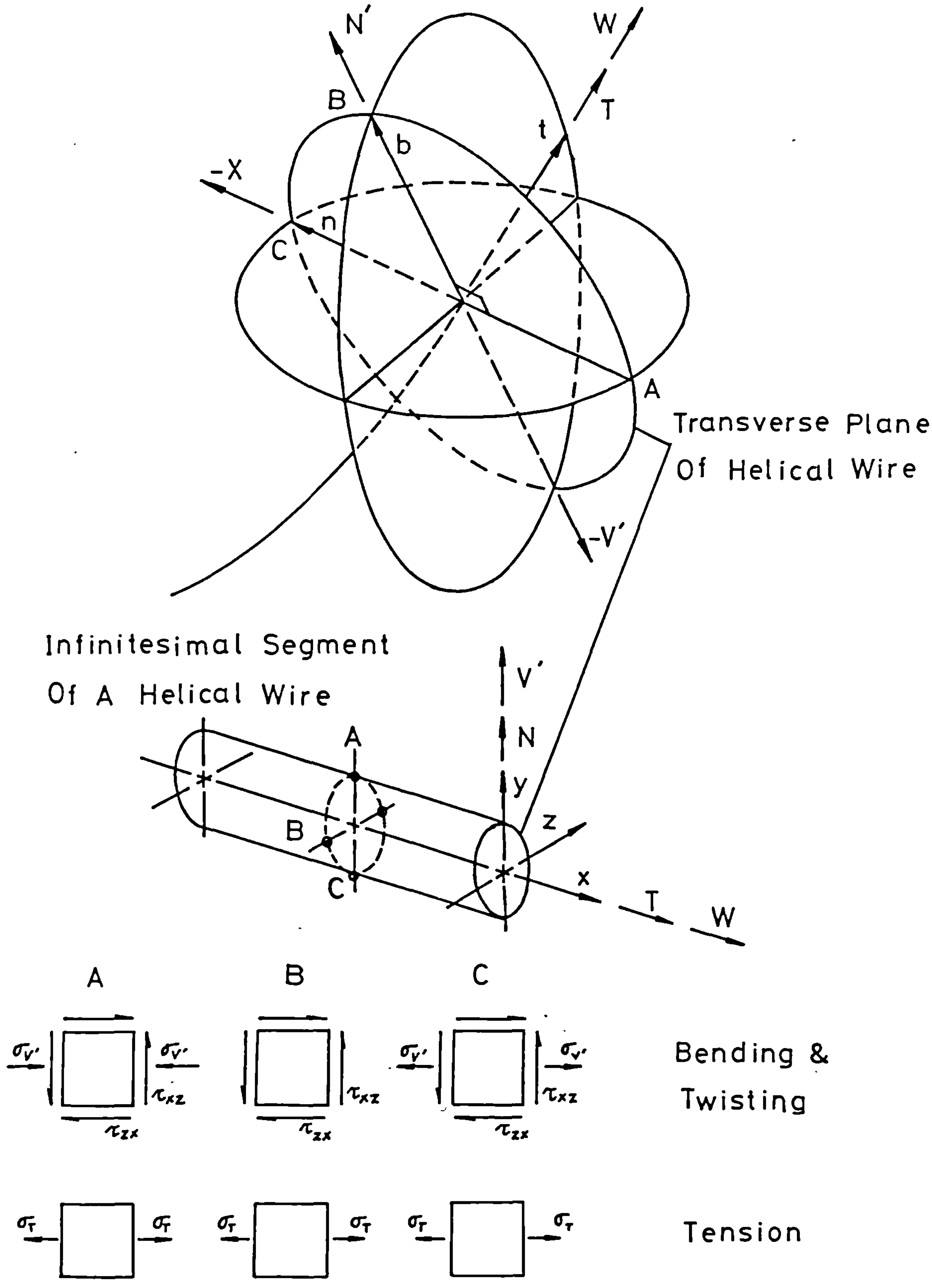

Figure 7·5-2
Stresses On An Element Of
The Helical Wire

$$\tau_{max} = (\sigma_1 - \sigma_2) / 2 \qquad (7.5\text{-}16)$$

d. Shear Stress Distribution Across The Helical Wire Section

The presence of shear force "N'" indicates that there must be shear stress on the transverse planes in the helical wire. It is not possible to use the conditions of geometry of deformation and the stress-strain relationships except in the development of an exact solution. However, from the assumptions about the validity of the bending stress distribution, it is possible to estimate the transverse and longitudinal shear stress distributions in the helical wire by using only the condition of equilibrium. Figure 7.5-3 shows the geometry of helical wire section from which the shear stress distribution is estimated. The general equation is given by:

$$\tau_{yx} = \frac{dM}{dS} \cdot \frac{1}{bI} \int_{A'} y \, dA \qquad (7.5\text{-}17)$$

since $dM/dS = N'$ (7.5-18)

Thus, equation 7.5-17 can be rewritten as

$$\tau_{XY} = \frac{N'}{I} \int_{A'} (y/b) \, dA \qquad (7.5\text{-}17)$$

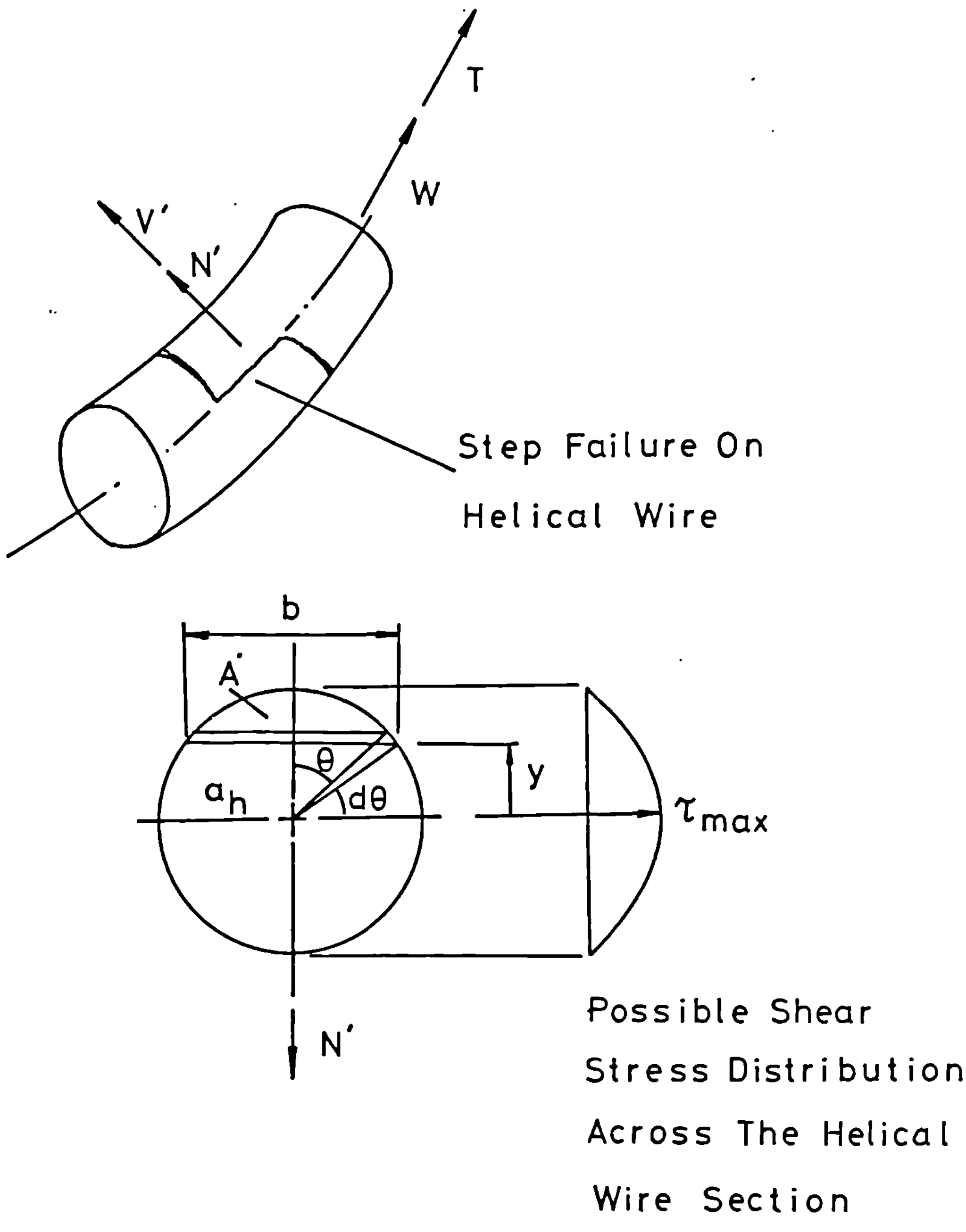

Figure 7.5-3

Shear Stress Distribution Across Helical Wire Transverse Section

$$= \frac{N' a_h^2}{4I} \left(\cos 2\theta - 1 \right) \qquad (7.5\text{-}18)$$

when M is the bending moment exerted on the helical wire.

7.6 Introduction to Non-linearized Model of Single Layer Strand

For a single layer strand subjected to an axial load, a linearized model with four known termination conditions has been developed in the preceding section. The current section will focus on the derivation of a non-linear geometrical model. The known structural deformations of strand which allow one to consider the higher order derivatives found the deformation of helical wire are bounded by the termination conditions. They are

a. Fixed ends ie, $\Delta\theta = 0$

b. Combined loads ie, both ε_s and $\Delta\theta$ are known

In order to highlight the nature of the solution, the organization of this section is slightly different from that of the previous section:

7.6-1 Geometry of Deformation

a. Deformation of Single Helical Wire

To proceed to the non-linear modelling for a single layer strand it is important to be able to relate the tensile strain along the helical wire with the known deformation of strand within limit of proportion. The relationships between strand and helical wire deformations have been illustrated in Figure 7.4-4, and the principal expressions required to solve the extension of a helical wire in terms of tensile strain, contractions and rotation are given by:

$$\varepsilon_s = \frac{\Delta P_L}{P_L} \tag{7.6-1}$$

$$\Delta\theta^* = \frac{\Delta\theta}{2\pi} \tag{7.6-2}$$

The radial contraction of helical radius is given by

$$\frac{\Delta R}{R} = - \frac{\nu \left(a_c \varepsilon_s + a_h \varepsilon_w \right)}{R} = \Delta R^* \tag{7.6-3}$$

From the triangle of the developed helix, as shown is Figure 7.4-4 one can obtain the following relationships

$$S_w^2 = (1 + \varepsilon_w)^2 \tag{7.6-4}$$

$$= P_L^2 (1 + \varepsilon_s)^2 + (2 \pi + \Delta\theta)^2 (R + \Delta R)^2$$

By substituting equations 7.6-1, 7.6-2 and 7.6-3 into equation equation 7.6-4, a quadratic equation can be found and is given by:

$$A\ \varepsilon_w^2 + B\ \varepsilon_w + C = 0 \tag{7.6-5}$$

where A, B and C are coefficients and have been given in Appendix.

From equation 7.6-5, one can evaluate the tensile strain on a helical wire within a strand. It can also be shown that the helical wire tensile strain is a quadratic function.

b. Deformed Helical Geometry

At this point, it is essential to evaluate the deformed geometry of a helical wire, so that the component forces and moments exerted along the helical wire can be related with the deformed geometry which is described by:

$$\sin \bar{\alpha} = \frac{\sin \alpha\ (\ 1 + \varepsilon_s)}{(\ 1 + \varepsilon_w\ )} \tag{7.6-6}$$

$$\cos \bar{\alpha} = \frac{2\pi\ (\ 1 + \Delta\theta^*\ )\ \bar{R}\ \sin \alpha}{P_L\ (\ 1 + \varepsilon_s\ )^2} \tag{7.6-7}$$

$$\bar{K}' = \frac{\cos 2\bar{\alpha}}{\bar{R}} \tag{7.6-8}$$

$$\bar{\tau} = \frac{\sin \bar{\alpha} \cos \bar{\alpha}}{\bar{R}} \qquad (7.6\text{-}9)$$

7.6-2 Internal Equilibrium

The internal component of forces and moments on a wire can be evaluated in respect to the deformed geometry of wires in the strand. The rod theory is applied to evaluate the internal components along the helical wire.

a. Tensile force and twisting moment on a core wire are given by.

$$T_c = (\pi \bar{a}_c^2 E) \varepsilon_s \qquad (7.6\text{-}10)$$

$$W_c = \frac{G \bar{J}_c \Delta\theta}{P_L} \qquad (7.6\text{-}11)$$

b. Tensile force, bending moment, twisting moment, shear force and radial force along the helical wire are given by

$$T_h = (\pi \bar{a}_h^2 E) \varepsilon_w \qquad (7.6\text{-}12)$$

$$V' = E \bar{I}_h \Delta K' \qquad (7.6\text{-}13)$$

$$W = G J_h \Delta\tau \qquad (7.6\text{-}14)$$

$$N' = W \bar{K}' - V' \bar{\tau} \qquad (7.6\text{-}15)$$

$$X = N' \bar{\tau} - T_h K' \qquad (7.6\text{-}16)$$

7.6-3 External Equilibrium of Strand

At the final stage, the internal components of forces and moments on each of the wires will be orientated and summed up to the direction of the axial load applied to the terminations of the strand. The equations of external equilibrium are given by:

$$F = m (T_h \sin \bar{\alpha} + N' \cos \bar{\alpha}) + T_c \qquad (7.6\text{-}17)$$

$$M = m (W \sin \bar{\alpha} + V' \cos \bar{\alpha} + T_h \bar{R} \cos \bar{\alpha} - N' \bar{R} \sin \bar{\alpha}) + W_c \qquad (7.6\text{-}18)$$

7.6-4 Other Considerations

a. Classical Linear Theory:

If wires are considered as being incompressible, it should be able to express the deformed cross sectional area as functions of initial sectional area of wire, helix angle and material properties. The deformed cross sectional area of wire is given by:

$$A = A_0 \{ 1 - (\nu / E) \alpha_h \}^{1/2} \qquad (7.6\text{-}19)$$

b. Logarithmic Strain Approach:

A Logarithmic strain approach appears to have been suggested for one dimensional problems. It would also be interesting to modify the tensile strain into logarithmic strain, the equations being given by:

$$\varepsilon'_s = \mathrm{Ln} (1 + \varepsilon_s) \qquad (7.6\text{-}20)$$

$$\varepsilon'_w = \mathrm{Ln} (1 + \varepsilon_w) \qquad (7.6\text{-}21)$$

c. Full Inter-wire Grasp Condition (ie infinite friction)

For a strand subjected to axial load with infinite friction, the tensile strain along the centroidal axis of a single helical wire can be expressed as:

$$\varepsilon_w = \frac{d\bar{S}_w - dS_w}{dS_w} \qquad (7.22)$$

where

$d\bar{S}_w$ is the final arc length of the centroidal axis of a single helical wire.

dS_w is the initial arc length of the centroidal axis of a single helical wire.

However, the full inter-wire grasp condition is outside the scope of this thesis. The details of derivations will not be discussed.

In view of the complexity of the problem, a micro-computer software has been written for the purpose of evaluating the results from both linear and non-linear mathematical models for the single layer strand. Sample results are given in the next section of this chapter.

7.7 DISCUSSION AND CONCLUSION

7.7-1 Computation for Single Layer Strands

A PC type of micro-computer package has been developed by the author for the purpose of evaluating stresses, strains, structural properties of the single layer strand, internal forces and moments on wires. A diagram representing the general structure of this computer package for the single layer strand is illustrated in block diagram 7.7-1. This package solves the mechanical problem of single layer strands, with or without a core wire and is valid within the static linear elastic regime.

7.7-2 Results and Discussion

a. Comparison of Results

For a strand subjected to an axial load, a number of rope investigators have described the difficulties arise from measuring the component strains on the surface of individual wires by using the strain gauging method. However, for measuring the global mechanical behaviours of a 6/1 strand, the extensometer approach has a better proven reliability. Experimental results from Martin and Packards'[6.4] for steel strand and those from Machida's[4.1] for epoxy strand under fixed end conditions have been compared with the present author's model for single layer strand. Good agreement is obtained.

MICRO-COMPUTER PACKAGE STRUCTURE FOR SINGLE LAYER STRAND

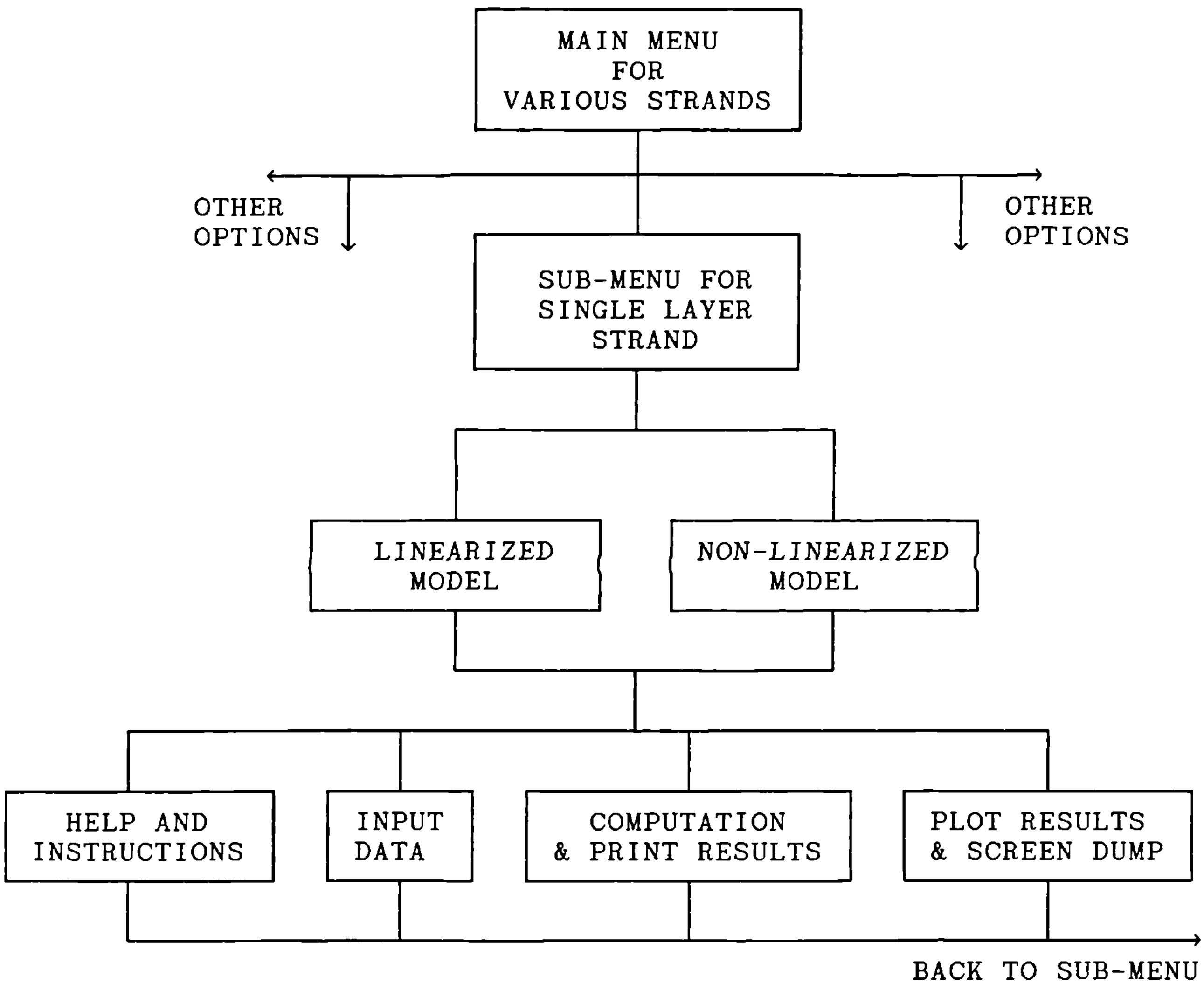

BLOCK DIAGRAM 7.7-1

STRUCTURE DIAGRAM OF SINGLE LAYER STRAND MODELLING

The comparisons are presented in Figure 7.7.1, 7.7.2, and 7.7.4. Results obtained from the author's free end model are also compared with those experimental results from Machida's

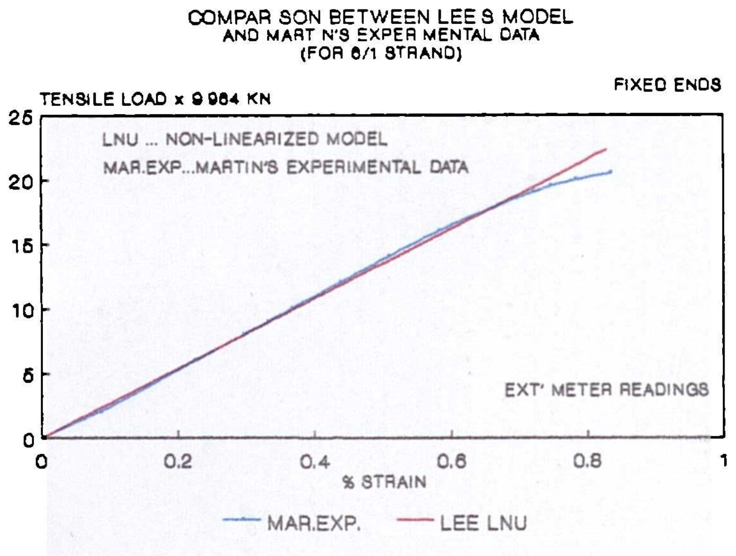

F GURE 7 7 1
TENSILE LOAD VS % STRA N

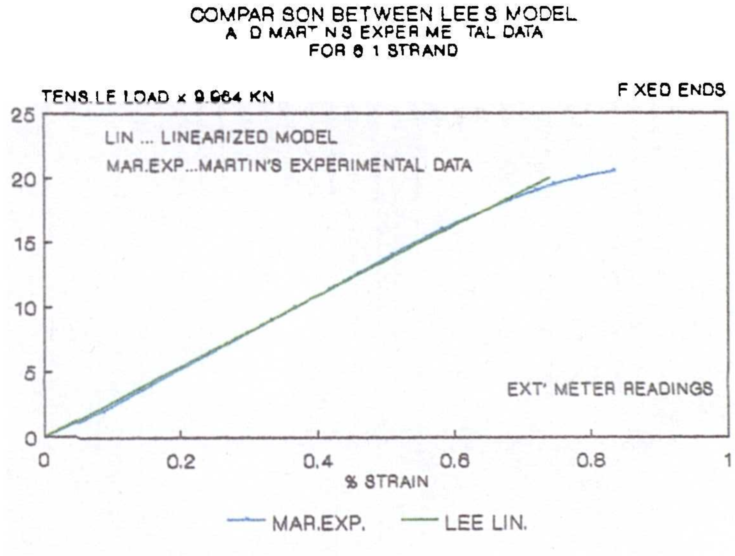

F GURE 7 7 2
TENSILE LOAD VS % STRAIN

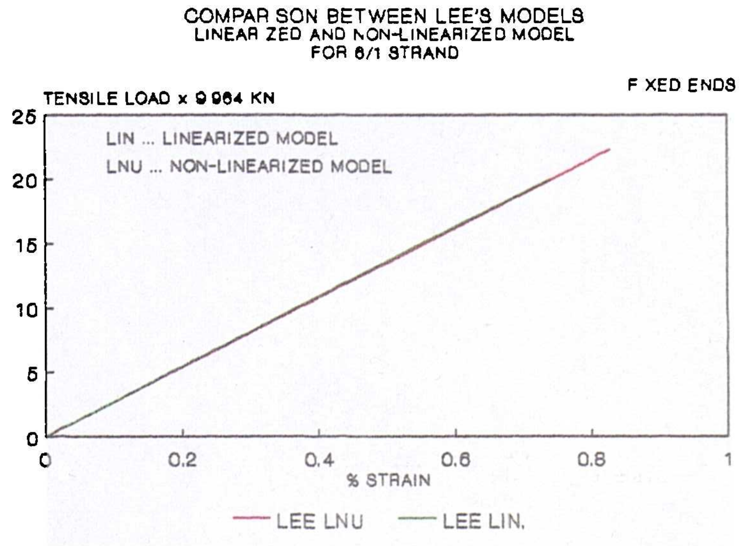

F GURE 7 7 3
TENS LE LOAD VS % STRA N

for epoxy strand under same termination condition, Figure 7.7.5. In addition to these, Figure 7.7.3 illustrates the author's own comparison between the linearized and non-linearized models for 6/1 strand. The two results appear to be very close to each other. This is because a very large helix angle (ie $\alpha > 80$ degrees) is chosen for the single helical wires. The linear tensile component is more dominant than the non-linear components contributed from the change in helix geometry.

The author's analytical model appears to be more accurate than Machida's model, Figure 7.7.4 and 7.7.5. This is because Machida's model ignored the shear component exerted on six single helical wires.

b. Discussion of Sample Results

Although the mathematical model and the computer package for the single layer strand were developed for solving general single layer strand problems, rotational rope carrying tensile load has to be equipped with fixed terminations for safety purpose. For this reason, sample results given in this section focus on 6/1 strand with fixed terminations. It is also noted that the helix angle is the dominant parameter with respect to change of helix geometry, the change of internal components along the single helical wire in the single layer strand subjected to external tensile load are, therefore, influenced by the helix angle. Figure 7.7.6 illustrates the influence of helix angle, as an example.

COMPARISON BEWTEEN MACHIDA AND LEE
FREE END

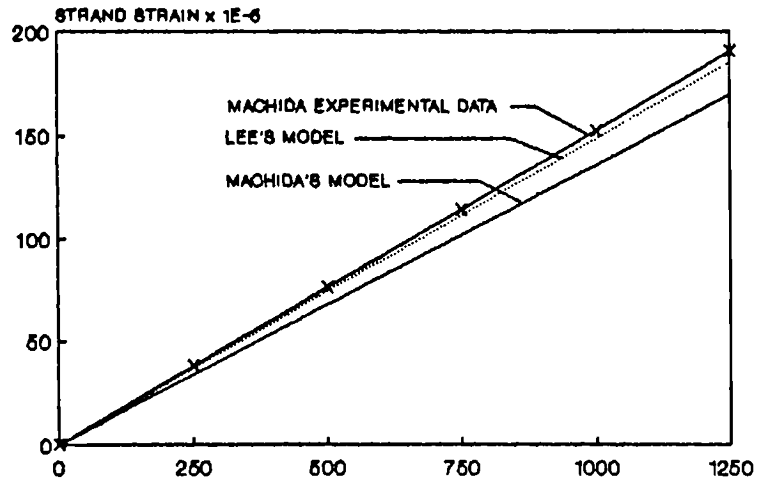

TENSILE LOAD - lbf
FIGURE 7.7.5
EXTENSION VS LOAD

COMPARISON BEWTEEN MACHIDA AND LEE
FIXED END

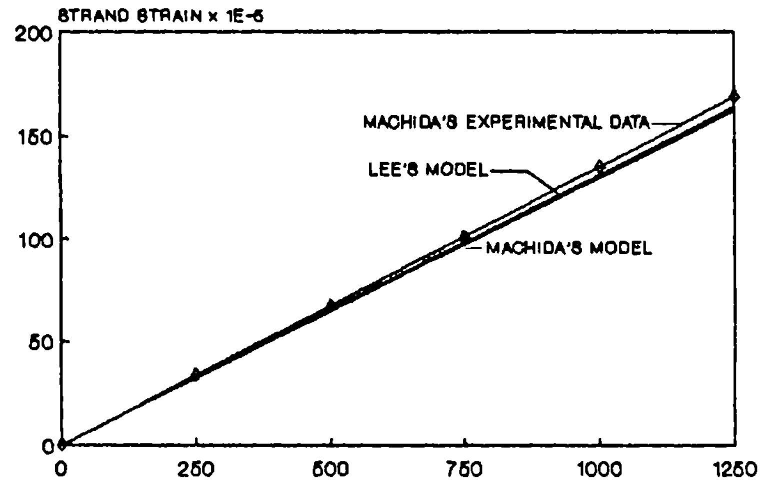

TENSILE LOAD - lbf
FIGURE 7.7.4
EXTENSION VS LOAD

Numerical analysis of a 6/1 strand with fixed ends within linear elastic regime is presented below:

1. Analysis Based on Steel Strand

The material properties used in the analysis are as specified in Martin and Parker's report[6.4] and the diameter of helical wire is retained. The diameter of the core wire is varied by considering the admissible "R/r" ratio to the helical wires (for details, see Chapter Six). The helix angle is varied from 60 degrees to 85 degrees. Results are presented in the following figures:

Figure 7.7.7 (a) shows how the tensile load shared by the core wire depends on the applied tensile load and helix angle. This figure shows that the share of tensile load carried by the core wire increases in inverse proportion to the helix angle.

Figure 7.7.7 (b) shows the resisting torque exerted at the terminations as functions of the tensile load and helix angle. This figure also shows that the resisting torque is inversely related to the helix angle chosen for the helical wire.

Figure 7.7.7 (c), (d), (e), (f) and (g) shows the variation of applied tensile load and helix angle with the internal component forces and moments on the helical wire. These figures show that all internal component forces and moments

An Example Which Illustrates The Influence Of Helix Angle.

Diagram a. Shows Components Exerted Along Helical Wire

Helix Angle < 90° Helix Angle = 90°

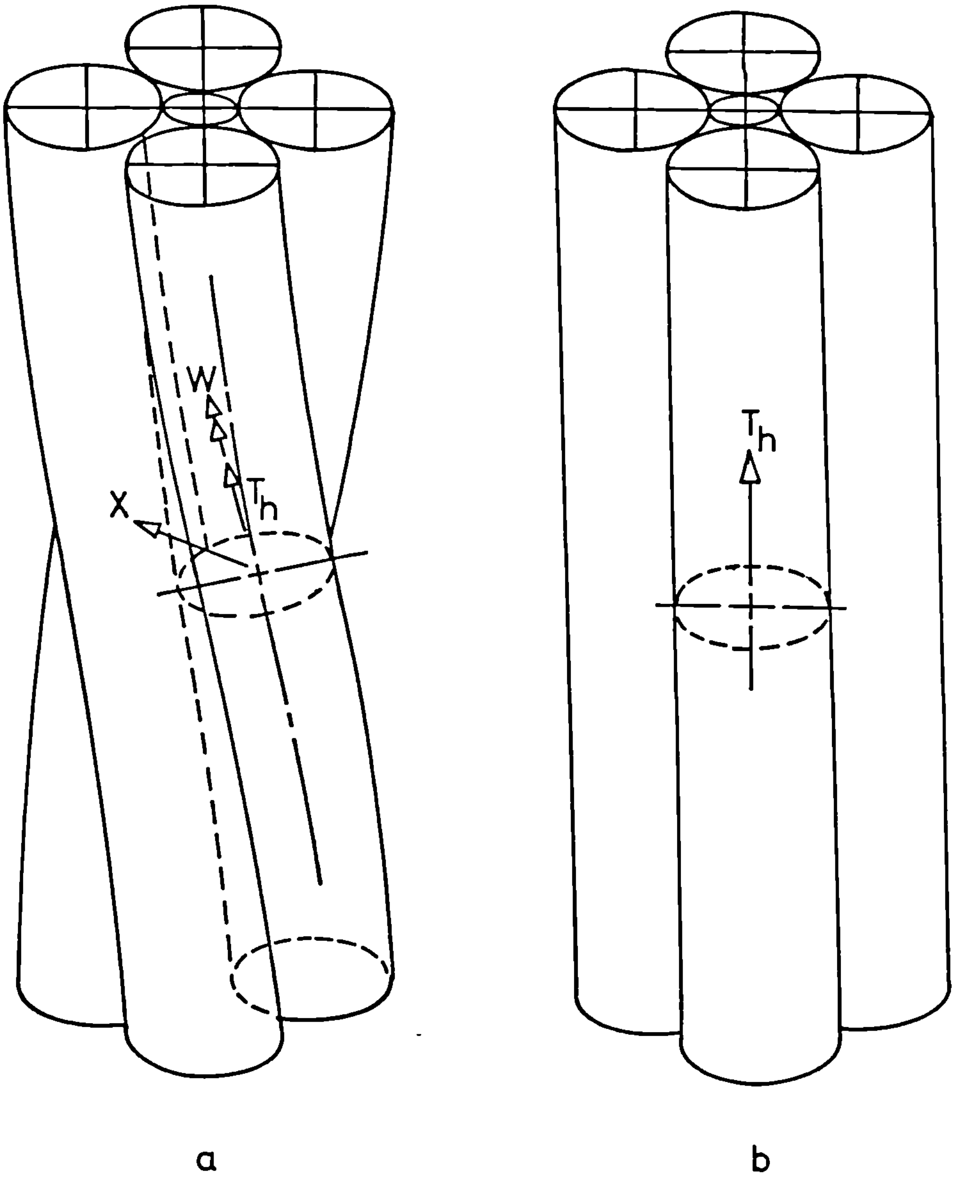

Figure 7·7·6

Parallel Wire Strand & Twisted Wire Strand Model

SINGLE LAYER STRAND

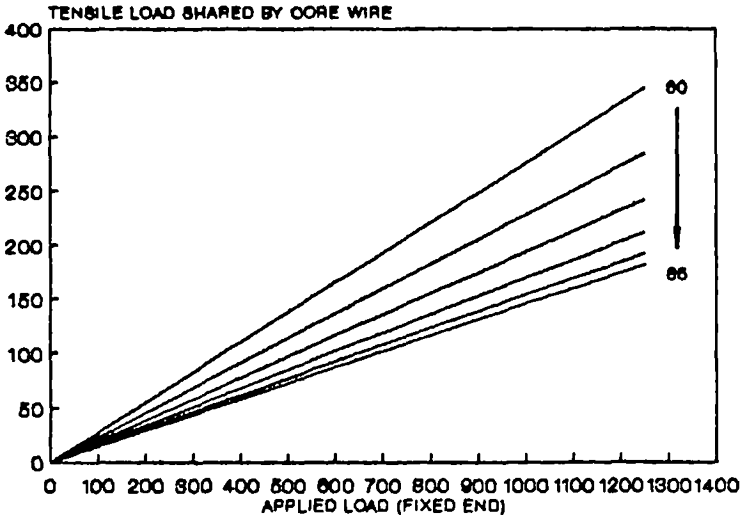

FIGURE 7.7.7 (a)
LOAD SHARED BY CORE WIRE

SINGLE LAYER STRAND

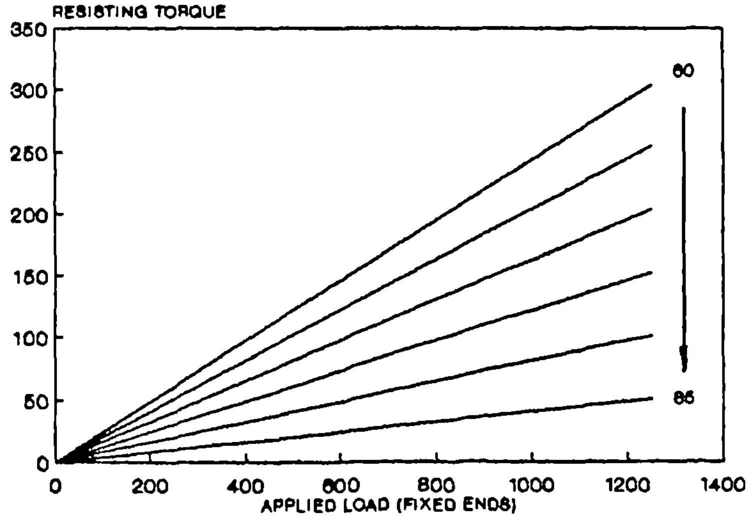

FIGURE 7.7.7 (b)
APPLIED LOAD VS RESISTING TORQ.

SINGLE LAYER STRAND

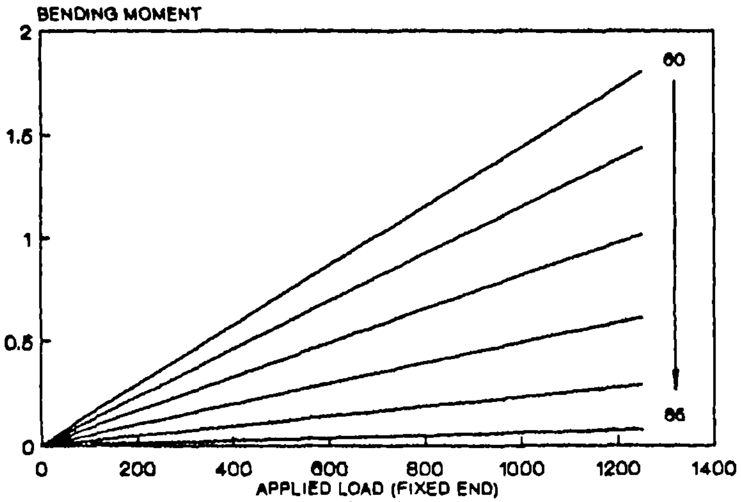

FIGURE 7.7.7 (c)
APPLIED LOAD VS BENDING MOMENT
(ON SINGLE HELICAL WIRE)

SINGLE LAYER STRAND

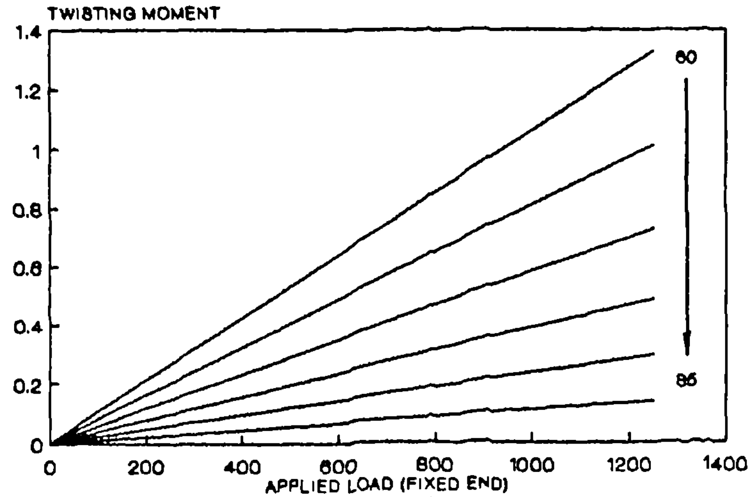

FIGURE 7.7.7 (d)
APPLIED LOAD VS TWISTING MOMENT
(ON SINGLE HELICAL WIRE)

SINGLE LAYER STRAND

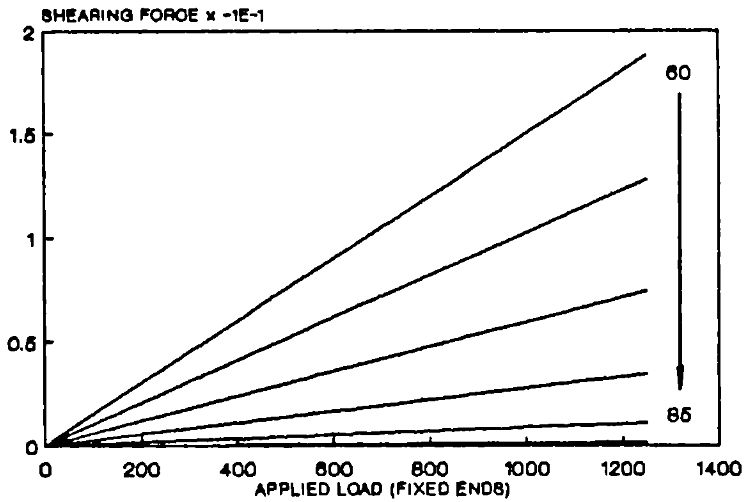

FIGURE 7.7.7 (e)
APPLIED LOAD VS SHEARING FORCE
(ON SINGLE HELICAL WIRE)

SINGLE LAYER STRAND

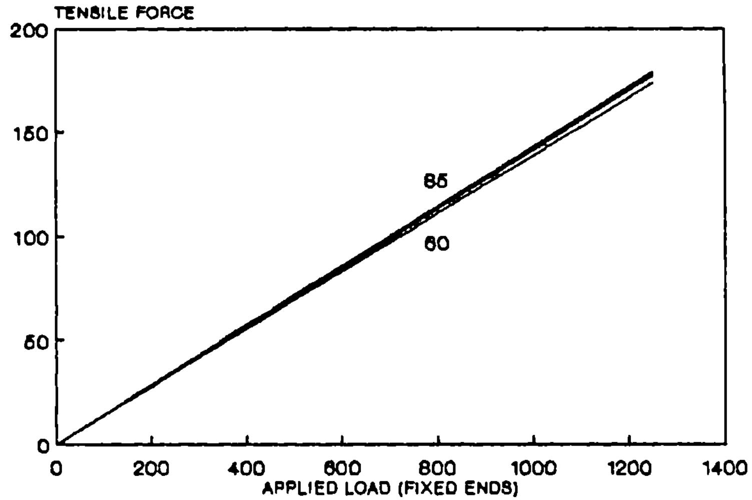

FIGURE 7.7.7 (f)
APPLIED LOAD VS TENSILE FORCE
(ON SINGLE HELICAL WIRE)

SINGLE LAYER STRAND

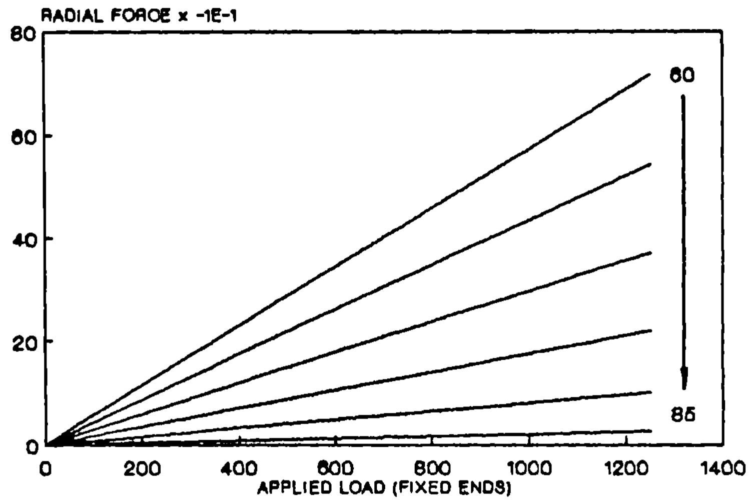

FIGURE 7.7.7 (g)
APPLIED LOAD VS RADIAL FORCE
(ON SINGLE HELICAL WIRE)

STRAND STRAIN VS HEL. WIRE STRAIN
(TENSILE STRAIN)

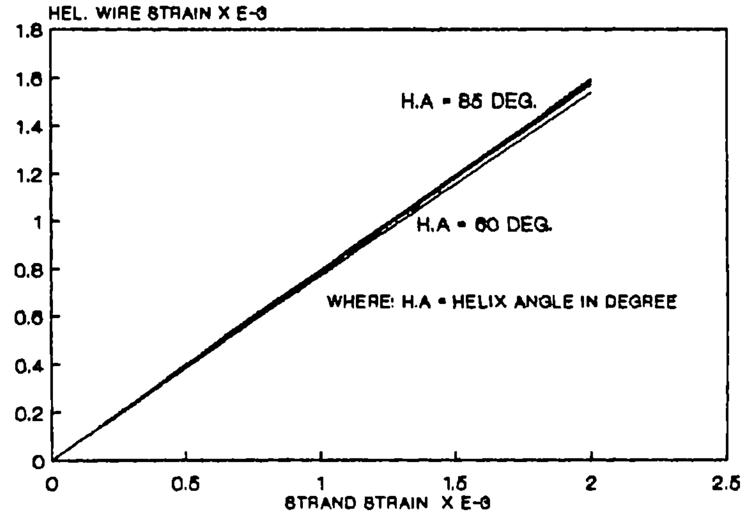

FIGURE 7.7.7 (h)

increase in inverse proportion to the helix angle, with the exception that the tensile component (see Figure 7.7.7 (f)) on single helical wire increases in proportion. By comparing these figures, one should note that the variation of tensile force exerted on the helical wire, as the result of variation of helix angle, is comparatively small compared to the variation of other components exerted on the same helical wire.

Figure 7.7.7 (h) shows the variation of strand strain and tensile strain as a function of helix angle. This figure shows the same properties as that in Figure 7.7.7 (f).

2. Analysis Based on Epoxy Strand

The material properties used in the following analysis are based on those specified in Machida's paper[4.1]. The admissible "R/r" ratio (see chapter six) is ignored so that the diameters of helical and core wire are kept unchanged as the helix angle is varied. In other words, the separation the core wire from the helical wires, as the result of reducing the helix angle, is ignored. In practical design, one should avoid this "separation". However, an attempt has been made to illustrate that the change in helical parameters appears to have non-linear characteristics with the variation of tensile load and helix angle.

Figure 7.7.8 (a) shows the change in helix angle vs the variation of helix angle and applied tensile load.

CHANGE IN WIRE HELIX ANGLE

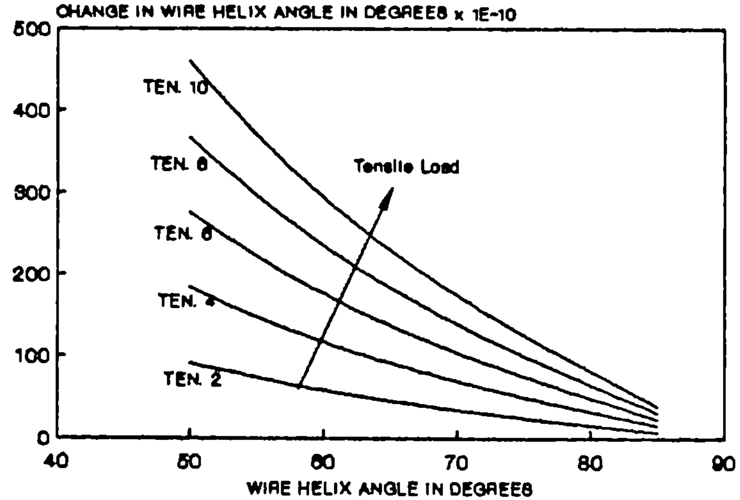

FIGURE 7.7.8 (a)
CHANGE IN WIRE HELIX ANGLE
VS ORIGINAL WIRE HELIX ANGLE

CHANGE IN CURVATURE

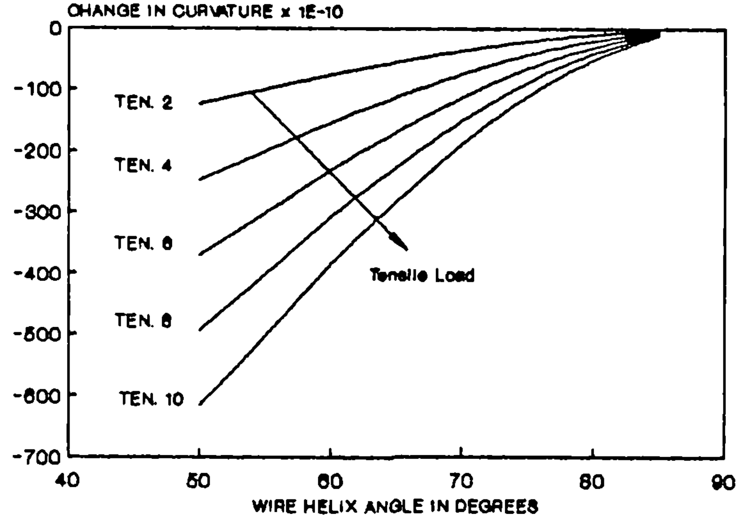

FIGURE 7.7.8 (b)
CHANGE IN CURVATURE VS HELIX ANGLE

CHANGE IN TORSION

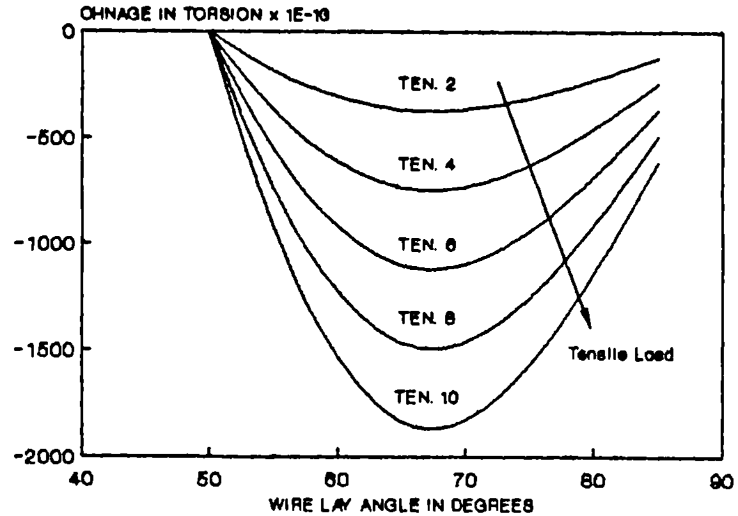

FIGURE 7.7.8 (c)
CHANGE IN TORSION VS LAY ANGLE

EFFECT POISON'S RATIO V LAY ANGLE

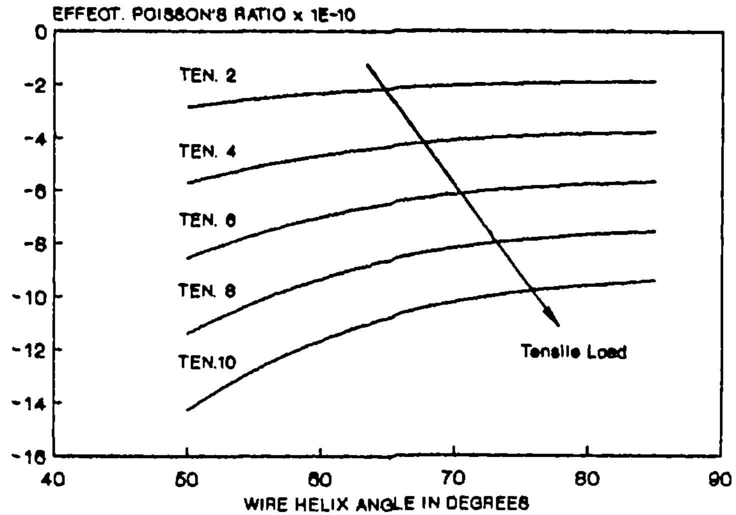

FIGURE 7.7.8 (d)
EFFECTIVE POISSON'S RATIO VS HELIX ANGLE

Figure 7.7.8 (b) shows the change in curvature vs the variation of helix angle and applied load to the strand.

Figure 7.7.8 (c) shows the change in torsion of the helical wire vs the variation of helix angle and applied load to the strand. The change in torsion is increased with respect to the helix angle and reaches a maximum at about 68 degrees

Figure 7.7.8 (d) shows the change in effective Poisson's ratio of the strand vs the variation of helix angle and applied load to the strand.

3. Sample Stress Components on Core and Helical Wire

Sample stress components are presented in this sub-section for a steel strand with 80 degrees helix angle . The material properties are the same as those specified in Martin and Parker's report. Results are presented in the following figures.

Figure 7.7.9 (a) shows the variation of bending and twisting stress exerted in the binormal and tangent directions of the helical wire vs the applied tensile load applied to the strand. The negative bending stress in the binormal direction indicates that the surface of the helical wire in that direction is under compression.

Figure 7.7.9 (b) shows the variation of tensile stress on the core and helical wire vs the tensile load applied to the

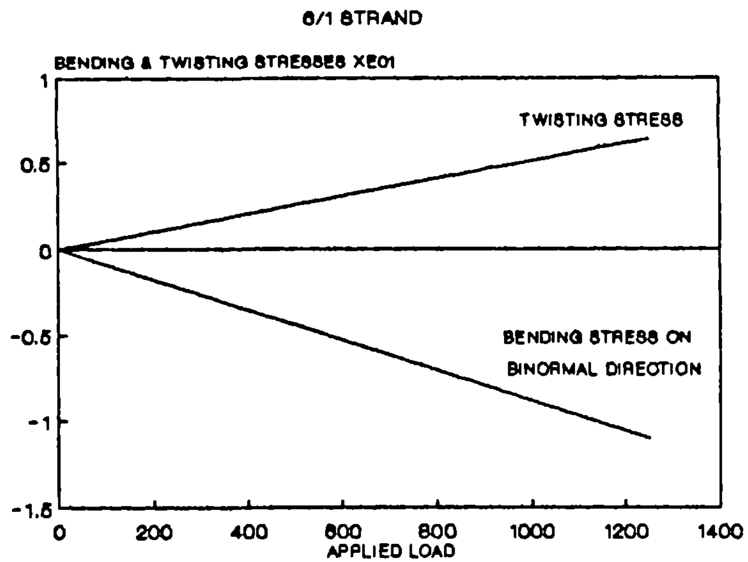

FIGURE 7.7.9 (a)
APP. LOAD VS BENDING & TWISTING STRESSES

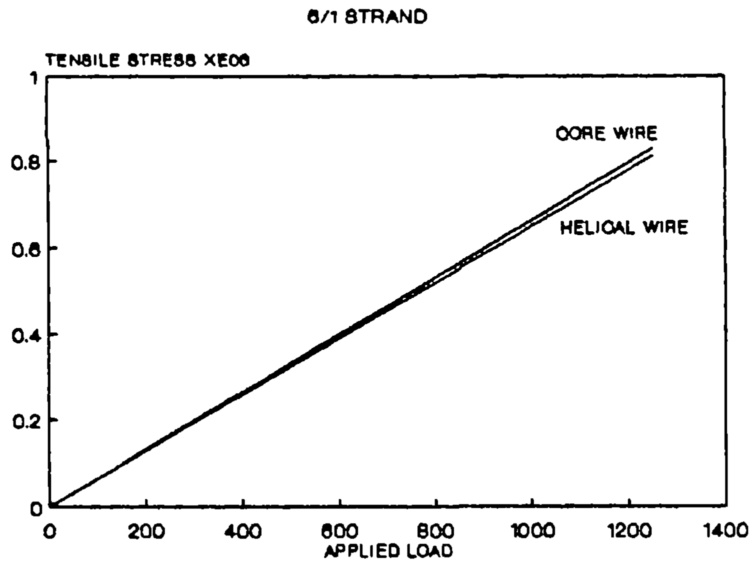

FIGURE 7.7.9 (b)
APPLIED LOAD VS TENSILE STRESS ON WIRES

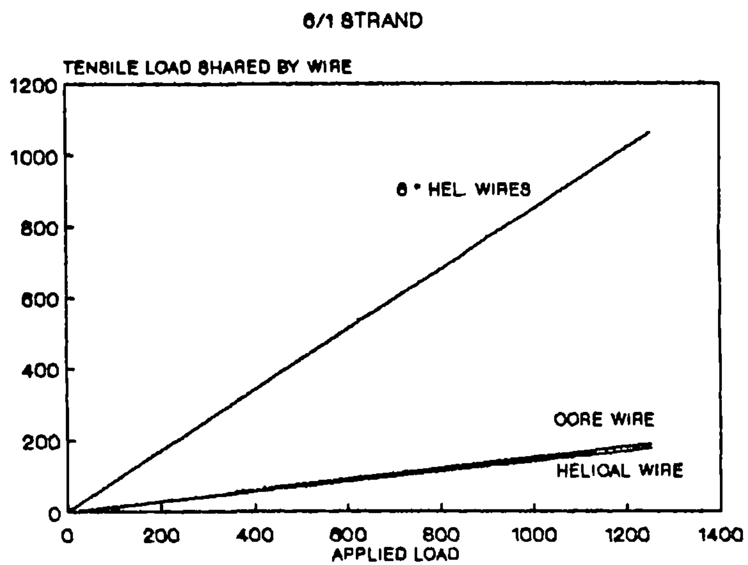

FIGURE 7.7.9 (c)
APPLIED LOAD VS LOAD SHARED BY WIRES

strand. By increasing the helix angle, one should be able to ensure that the tensile stress acting on the core wire is close to the order of those on the helical wires. In practice, one should design strands in which each wire carries same order of tensile load to avoid unbalancing tensile load carried by the core wire.

Figure 7.7.9 (c) shows the variation of tensile load carried on the core wire, helical wire and helical wires in a 6/1 strand.

7.7-3 Conclusions

These conclusions are based on the static analysis of a 6/1 strand subjected to axial load with four termination conditions,as described in the preceding section.

1. A single layer strand with fixed ends is stiffer than that with free ends. Therefore, the strand with fixed ends gives more control in maneuvering applications.

2. A single layer strand with large helix angle helical wires is stiffer than that with small helix angle.

3. For helix angle within the practical range (60 to

90 degrees) if the helix angle of the helical wires is being reduced all internal component forces and moments on the helical wires will increase correspondingly with the exception of the tensile component. Hence, the mechanical behaviour and fatigue performance of helical wire will be affected by the helix angle of the helical wire.

4. A decrease in helix angle does not have a significant influence on the tensile load shared by the helical wires.

5. The bending and twisting components are sensitive to the change in helix angle. Because of the geometrical properties of helical wire.

6. For a 6/1 strand, the tensile load shared by the core wire is of similar order of that carried by the helical wire.

7. For helical wires with large helix angle ($\alpha > 80$ degrees), most internal component forces and moments appeared to be less significant with the exception of the tensile component on the helical wire.

CHAPTER EIGHT

STRUCTURAL MODELLING OF

MULTI-LAYER STRANDS

NOMENCLATURE

a_c	Radius of core wire
a_f	Radius of filler wire
a_i	Radius of helical wire in ith layer, i = 2 and 3
E	Young Modulus
F	Tensile force exerted on the multi-layer strand
F_c	Tensile force exerted on the core wire of the strand
G	Modulus of rigidity
H_i	Defined parameters, i = 1, 2, 3, ...
I_i	Defined parameters, i =1, 2, 3, ...
I^*_j	Second moment of area of helical wire in jth layer
J_c	Polar moment of area of core wire
J_i	Defined parameters, i = 1, 2, 3, ...
J^*_j	Polar moment of area of helical wire in jth layer
K_i	Stiffness constants for multi-layer strand, i = 1, 2, 3 and 4
K'_f	Curvature of filler wire
K'_i	Curvature of helical wire in ith layer
M	Twisting moment applied to the strand terminations
M_c	Twisting moment exerted on the core wire
m_f	Number of filler wire
m_i	Number of helical wires in ith layer of the strand
N'_i	Shearing force on the helical wire in ith layer of a multi-layer strand
P_i	Cyclic length of a helical wire in ith layer of a

	multi-layer strand
r_f	Helical radius of filler wire
r_i	Helical radius of any helical wire in ith layer within a multi-layer strand
T_i	Tensile force exerted on any helical wire in ith layer
V_i	Bending moment exerted on any helical wire in ith layer
W_i	Twisting moment exerted on any helical wire in ith layer
X_i	Radius force exerted on any helical wire in ith layer
α_i	Helix angle of any helical wire in ith layer
α_f	Helix angle of filler wire
τ_f	Torsion of filler wire
τ_i	Torsion of any helical wire in ith layer
ε_s	Strand strain or tensile strain of core wire of a multi-layer strand
ε_i	Tensile strain on any helical wire in ith layer
ν	Poisson's ratio of wire
$\Delta\theta_s$	Angle of twist of a multi-layer strand per lay length
$\Delta\theta_i$	Angle of twist of any helical wire in ith layer
Δr_i	Change in helical radius of any helical wire in ith layer
$\Delta K_i'$	Change in curvature of any helical wire in ith layer

$\Delta\tau_i$	Change in torsion of any helical wire in ith layer
$\Delta\alpha_i$	Change in helix angle of any helical wire in ith layer
$\bar{\alpha}_i$	Final helix angle of any helical wire in ith layer
$\bar{K}'_i$	Final curvature of any helical wire in ith layer
$\bar{\tau}_i$	Final torsion of any helical wire in ith layer

SUBSCRIPTS

S	Strand
f	Filler wire
i	ith layer of strand
C	Core wire

8.1 INTRODUCTION TO LINEARIZED THEORY OF MULTI-LAYER STRAND

Multi-layered strands are constructed either in form of "cross lay" or in form of "equal lay". Generally speaking, "equal lay" strands are designed to prevent cross cutting and secondary bending of wires at the contact locations. As a result, "equal lay" strands are expected to have longer life than "cross lay" strands. However, "equal lay" strands are less flexible than "cross lay" strands. In addition, equal lay strands give rise to more rotation.

In practice, multi-layered strands are designed to carry static and dynamic load; flexibility, fatigue performance and other properties are considered to be secondary, depending upon the application and service conditions. In the present chapter, both "equal lay" and "cross lay" are considered, but in view of the geometric complexity of strand sections, only three typical multi-layer strands geometries studied, namely:

a. 9/9/1 equal lay strand
b. 12/6F+6/1 equal lay strand with filler wire
c. 12/6/1 cross lay strand

In this analysis, the deformation geometry of the single helical wire is linearized by ignoring the second and higher order deformation terms with respect to the structural displacements of the strand, (in other words, the second and higher order differential terms are ignored). Consequently, four termination conditions, as used in the linearized single layer strand model, can also be used in these models. Internal forces, moments, stresses, strains and the structural properties of the strands are considered in these linearized models under monotonic loading to be within the proportional limit of the strand. The factors which will influence the present analysis, are listed below.

a. Termination Conditions :

The structural properties of multi-layer strands are influenced by the termination conditionsn namely,

1. Fixed ends
2. Free ends
3. Moment alone
4. Combined loads (ie tension and twisting)

b. Wire Material:

The wire material which affects the constitutive relationships in this analysis, is cold drawn rope steel. It is assumed to be homogeneous, isotropic and linearly elastic.

8.2 STRUCTURE OF THE APPROACH TO THE MATHEMATICAL MODELLING OF MULTI-LAYER STRAND

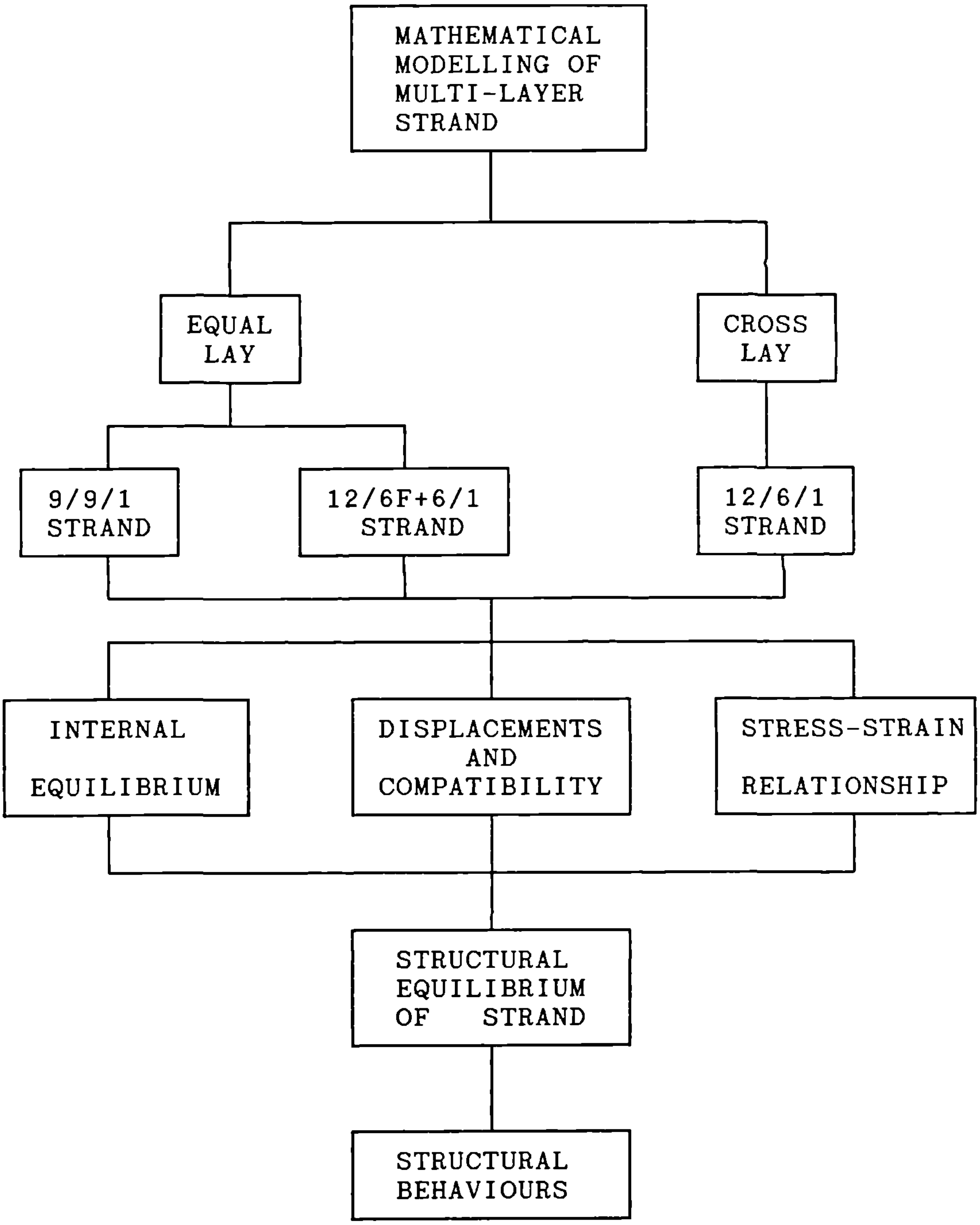

BLOCK DIAGRAM 8.2-1

STRUCTURAL MODELLING OF MULTI-LAYER STRAND

8.3 BASIC ANALYSIS AND ASSUMPTIONS

a. Basic Analysis

In this analysis, internal components of forces and moments on each wire are formulated based on the rod theory. Tensile strains on a core wire and helical wires in each layer are derived from the development of a deformed axis of a single helical wire as shown in Chapter 7 Figure 7.4-4. After established the equations of deformation. The linearied change in curvature and torsion can then be calculated by ignoring the second and the higher order derivative terms with respect to the structural displacements of the strand. The linearized stresses on the helical wire can be related with the linearized strains by means of the constitutive relationships. Finally, individual components of forces and moments on each of the wires can be resolved to and summed to the global direction of the strand. The principal procedures require to generate models for the multi-layer strands, are summarized below:

1. Establish equation(s) of internal equilibrium.
2. Relate internal and external equilibrium.
3. Establish relationship between deformation of helical wire and structural displacements of multi-layer strands.
4. Apply classical constitutive relationship to relate load-deformation and stress-strain along the wire.

b. Assumptions

The assumptions made in this chapter are similar to those made in Chapter Seven. Again, mechanical interactions are ignored, and only mechanical responses of wire and structural responses of strands are considered. The strands are considered to be loaded monotonically within the limit of proportionality.

8.4 LINEARIZED MULTI-LAYER STRANDS MODEL

In this section, the modelling of multi-layer strands is divided into three sub-sections, namely

a. External and internal equilibrium in strands
b. Deformation of single helical wires
c. Structural properties and applications

8.4-1 External and Internal Equilibrium

a. External Equilibrium

By ignoring the influence of mechanical interactions resulting from the small helix angle of single helical wires in each layer, the static equilibrium (ie external equilibrium) of the multi-layer strands is given by :

For 9/9/1 Multi-Layer Strands (Equal Lay)

$$F = \sum_{i=2}^{3} \{ m_i \, (T_i \sin \bar{\alpha}_i + N_i' \cos \bar{\alpha}_i) \} + F_c \quad (8.1)$$

$$M = \sum_{i=2}^{3} \{ m_i \, [\, (W_i - N_i' \bar{r}_i) \sin \bar{\alpha}_i + (V_i' + T_i \bar{r}_i) \cos \bar{\alpha}_i \,] \} + M_c \quad (8.2)$$

For 12/6F+6/1 Multi-Layer Strand With Filler Wires (Equal Lay Construction)

$$F = \sum_{i=2}^{4} \{ m_i \, (T_i \sin \bar{\alpha}_i + N_i' \cos \bar{\alpha}_i) \} + F_c \quad (8.3)$$

$$M = \sum_{i=2}^{4} \{ m_i \, [\, (W_i - N_i' \bar{r}_i) \sin \bar{\alpha}_i + (V_i' + T_i \bar{r}_i) \cos \bar{\alpha}_i \,] \} + M_c \quad (8.4)$$

For 12/6/1 Multi-Layer Strand (Cross Lay)

$$F = \sum_{i=2}^{3} \{ m_i \, (T_i \sin \bar{\alpha}_i + N_i' \cos \bar{\alpha}_i) \} + F_c \quad (8.5)$$

$$M = \sum_{i=2}^{3} \{ m_i \, [\pm (W_i - N_i' \bar{r}_i) \sin \bar{\alpha}_i \pm (V_i' + T_i \bar{r}_i) \cos \bar{\alpha}_i \,] \} + M_c \quad (8.6)$$

NB: The "±" sign in equation (8.6) relates to the direction of lay for the helical wire. The "+" sign corresponds to the conventional right hand lay, whereas, the "-" sign corresponds to the left hand lay.

Using the stiffness approach, external equilibrium can be expressed through a general stiffness matrix given by :

$$\begin{vmatrix} K_1 & K_2 \\ K_3 & K_4 \end{vmatrix} \begin{vmatrix} \varepsilon_R \\ \Delta\theta \end{vmatrix} = \begin{vmatrix} F \\ M \end{vmatrix} \qquad (8.7)$$

where the stiffness parameters for each of the strands are given in the Appendix.

b. Internal Equilibrium

The approximate rod theory given by Love is again applied to evaluate the internal components along the single helical wire in each layer. Equations which represent the internal equilibrium of single helical wire are similar to the internal equilibrium equations for single helical wire presented in Chapter Seven. For completeness, the internal equilibrium equations are listed below.

1. For Core Wire Of The Strand

$$F_c = \pi a_c^2 E \varepsilon_s \quad (8.8)$$

$$M_c = G J_c \Delta\theta_s / P_3 \quad (8.9)$$

2. For Helical Wire In Each Layer Of The Strand

$$T_i = \pi a_i^2 E \varepsilon_i \quad (8.10)$$

$$V_i' = \Delta K_i' E I_i^* \quad (8.11)$$

$$W_i = \Delta\tau_i G J_i^* \quad (8.12)$$

$$N_i' = W_i \bar{K}_i' - V_i' \bar{\tau}_i \quad (8.13)$$

$$X_i = N_i' \bar{\tau}_i - T_i \bar{K}_i \quad (8.14)$$

By substituting the corresponding linearized geometrical parameters obtained from the deformation geometry of the helix into above equations, the above internal equilibrium equations can be expressed as functions of the structural displacements (ie $\Delta\theta_s$ and ε_s) of the strand.

By substituting the linearized internal equilibrium equations, for each layer of the strands, into structural equilibrium equations 8.1, 8.2, 8.3, 8.4, 8.5 and 8.6. stiffness matrices for each of the strands, similar to equation 8.7, can be obtained.

8.4-2 Deformation Geometry

In this section, the "development technique" is again applied to evaluate the deformation of helical wire in each layer. However, the constructional and flattening displacements are ignored. Hence, the deformations of helical wires with respect to the structural displacements are given by:

a. Deformations Of Single Helical Wire In Each Layers

$$\varepsilon_s = \varepsilon_i + \frac{\Delta\alpha_i}{\tan \alpha_i} \tag{8.15}$$

$$\varepsilon_s = \frac{\Delta r_i}{r_i} + \frac{\Delta\theta_i}{\pi} + (\tan \alpha_i + \cot \alpha_i) \Delta\alpha_i \tag{8.16}$$

$$\varepsilon_i = \frac{\Delta r_i}{r_i} + \frac{\Delta\theta_i}{2\pi} + \Delta\alpha_i \tan \alpha_i \tag{8.17}$$

$$\varepsilon_i = \varepsilon_s \sin^2\alpha_i + \frac{\Delta r_i}{r_i} \cos^2 \alpha_i + \frac{\Delta\theta_i}{2\pi} \cos^2 \alpha_i \tag{8.18}$$

The above equations of deformation can be expressed in terms of structural displacements of the strand. The $\Delta\theta_i$ and Δr_i. are the unknowns. They can be evaluated by:

For Equal Lay Multi-Layer Strands

By ignoring the second and the higher order differential terms in the expression of R/r ratio, the change of helical radius for each layer of the helical wire is given by :

$$\frac{\Delta r_i}{r_i} = -\nu\,\varepsilon_i - \frac{\tan^2(\pi/2 - \pi/m_i)\,\Delta\alpha}{\tan\alpha_i\,\{\sin^2\alpha_i + \tan^2(\pi/2-\pi/m_i)\}}$$

(8.19)

For 12/6F+6/1 strand. the $\Delta r_f/r_f$ of filler wire is given by :

$$\frac{\Delta r_f}{r_f} = \frac{\nu\,(r_f - a_2)}{a_2^2} + \frac{\cos^2\pi/m_2\,\cot^2\pi/m_2\,\cos\alpha_2}{r_f\,\sin^2\alpha_2}$$

(8.20)

b. For Cross Lay Multi-layers Strand

For cross lay construction, one can either use the approximate equation 8.19 or use the classical strength of materials method to evaluate the following equations :

For first layer, $\Delta r/r$ is given by :

$$\frac{\Delta r_2}{r_2} = \frac{-\nu\,(a_1\,\varepsilon_s + a_2\,\varepsilon_2)}{r_2} \qquad (8.21)$$

For second layer, $\Delta r/r$ is given by :

$$\frac{\Delta r_3}{r_3} = \frac{-\nu \,(a_1 \varepsilon_s + 2\, a_2 \varepsilon_2 + a_3 \varepsilon_3)}{r_3} \tag{8.22}$$

Finally, the angle of twist "$\Delta\theta_i$" for i^{th} layer per lay length can be related to the angle of twist "$\Delta\theta_s$" of the strand per lay length by using the similar triangle method developed from the development of the cylindrical helix. This is given by :

$$\Delta\theta_i = \frac{\Delta\theta_s \; P_i}{P_s} \tag{8.23}$$

At this point, one should have sufficient known parameters to solve equations 8.15 to 8.18. Hence, the linearized geometrical changes of the single helical wire can be evaluated; for instance, the geometrical changes of a 9/9/1 strand are given by :

1. For first layer

$$\varepsilon_2 = I_1\, \varepsilon_s + I_2\, \Delta\theta_s \tag{8.24}$$

$$\Delta\alpha_2 = I_3\, \varepsilon_s + I_4\, \Delta\theta_s \tag{8.25}$$

$$\Delta K'_2 = I_5\, \varepsilon_s + I_6\, \Delta\theta_s \tag{8.26}$$

$$\Delta\tau_2 = I_7 \varepsilon_s + I_8 \Delta\theta_s \tag{8.27}$$

2. Similarly, for second layer

$$\varepsilon_3 = J_1 \varepsilon_s + J_2 \Delta\theta_s \tag{8.28}$$

$$\Delta\alpha_3 = J_3 \varepsilon_s + J_4 \Delta\theta_s \tag{8.29}$$

$$\Delta K'_3 = J_5 \varepsilon_s + J_6 \Delta\theta_s \tag{8.30}$$

$$\Delta\tau_3 = J_7 \varepsilon_s + J_8 \Delta\theta_s \tag{8.31}$$

The dimensionless geometrical parameters "I_i" and "J_i", in this chapter, are derived based on three displacements component; namely: extensional, rotational and radial displacement. They are given in the Appendix. In Costello's approach, only extensional and rotational displacements are considered.

Since the procedures for evaluating the linearized geometrical change of single helical wire for 12/6F+6/1 and 12/6/1 strands are similar to the procedure adopted for 9/9/1 strand, this work will not be duplicated in the current sub-section. At this point, one should have sufficient equations to evaluate the linearized internal components along the single helical wire in each layer of the multi-layer strand. By substituting these linearized changes of geometry into equations 8.10 to 8.14, the linearized internal components along each of the single helical wires in each layer can be evaluated in terms of the structural displacements of multi-layer strand.

8.5 DISCUSSION AND CONCLUSION

8.5-1 Computation For Multi-Layer Strands

In view of the complexity of the structural modelling for multi-layers strands, a PC micro-computer package has been developed by the author for the purpose of evaluating the stresses, strains forces and moments on helical wires as well as structural properties of the multi-layer strand (ie, 9/9/1, 12/6F+6/1 and 12/6/1 strands). A diagram representing the general structure of this computer package for the linearized multi-layer strand models is similar to that as shown in Chapter seven, Figure 7.7-1.

8.5-2 Results And Discussion

In this study (including construction of 9/9/1, 12/6F+6/1 and 12/6/1 multi-layer strand), material properties of steel wire are being used throughout the computation. The admissible "R/r" ratio for helical wires in each layer is also considered. Methods used to evaluate the stresses and strains on the helical wires of a multi-layer strand are similar to those in dealing with the single layer strand. No contact stresses, mechanical interactions and termination effects are considered. Therefore, for a multi-layer strand constructed with more than two layers, bigger discrepancies between the present model and experiment would expect.

In this sample study, results for structural equilibrium vs strand strain and the internal components exerted on the helical wires with fixed end condition under linear elastic regime are given. Discussion on the sample results of the multi-layer strand (ie, 9/9/1, 12/6F+6/1 and 12/6/1 strands) are obtained from the author's own computer program.

The wire dimensions used for the numerical analysis of the multi-layer strand are listed in the following tables:

TABLE 8.5-1

DIMENSION OF WIRES FOR 9/9/1 STRAND		
LAYER	DIAMETER OF WIRE	HELIX ANGLE
CORE	.424 IN	90 DEGREES
1ST LAYER	.216 IN	80 DEGREES
2ND LAYER	.424 IN	80 DEGREES

TABLE 8.5-2

DIMENSION OF WIRES FOR 12/6F + 6/1 STRAND		
LAYER	DIAMETER OF WIRE	HELIX ANGLE
CORE	.2711437 IN	90 DEGREES
1ST LAYER	.265 IN	80 DEGREES
FILLER	.10976 IN	80 DEGREES
2ND LAYER	.265 IN	80 DEGREES

Where : FILLER = Filler Wire

IN = Inch

TABLE 8.5-3

DIMENSION OF WIRES FOR 12/6/1 STRAND		
LAYER	DIAMETER OF WIRE	HELIX ANGLE
CORE	.2711437 IN	90 DEGREES
1ST LAYER	.265 IN	80 DEGREES
2ND LAYER	.265 IN	73.274 DEG.

a. Discussion of Sample Results on Strand

Figures 8.5-1 and 8.5-2 show the variation of applied tensile load vs the strand strain. In this example, a 12/6F+6/1 strand appears to be stiffer than a 9/9/1 and a 12/6/1 strand. This is simply because more wires are used to construct the 12/6F+6/1 strand.

b. Discussion of Internal Components on Helical Wire

For a 12/6/1 cross lay strand subjected to tensile load, shear force, bending moment, twisting moment and radial force acting on a helical wire in the outer layer appear to be larger than those acting on the helical wire in the inner layer. This is because the radius of curvature and torsion of the helical wire in the outer layer are smaller than that of the helical wire in the inner layer, Figure 8.5-3 and 8.5-7 (a), (b) and (d). However, the tensile force acting on the

9/9/1 MULTI-LAYERS STRAND
(EQUAL LAY)

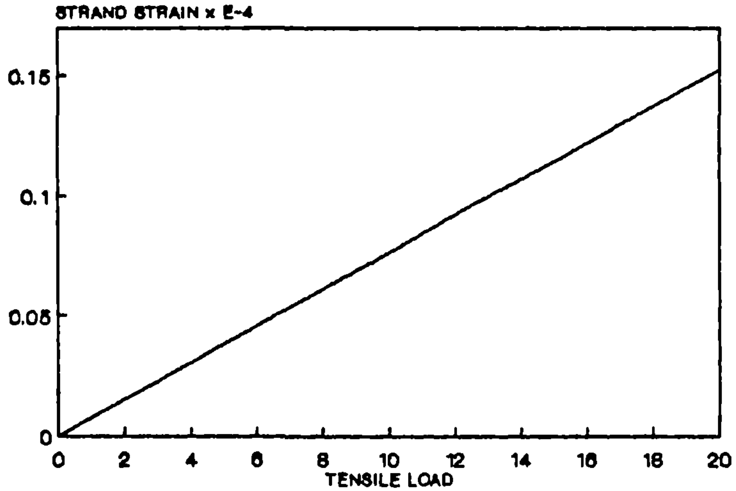

FIGURE 8.5-1
TENSILE LOAD VS STRAND STRAIN

12/6/1 AND 12/6F+6/1 STRAND
(CROSS AND EQUAL LAY STRAND)

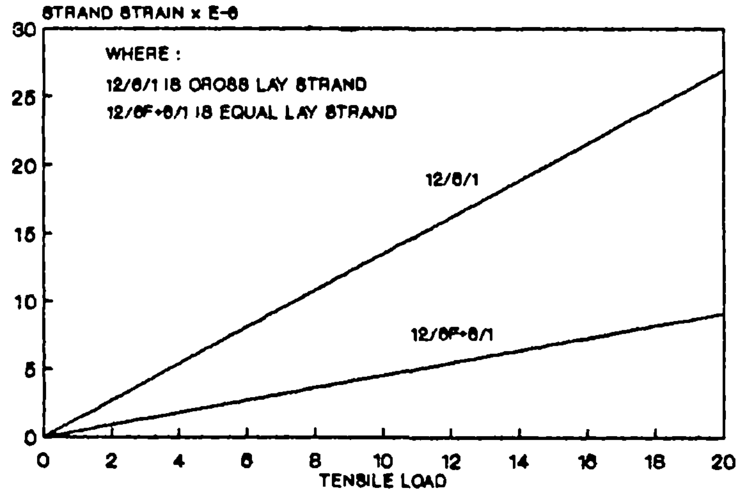

FIGURE 8.5-2
TENSILE LOAD VS STRAND STRAIN

12/6/1 STRAND
(SHEAR FORCE)

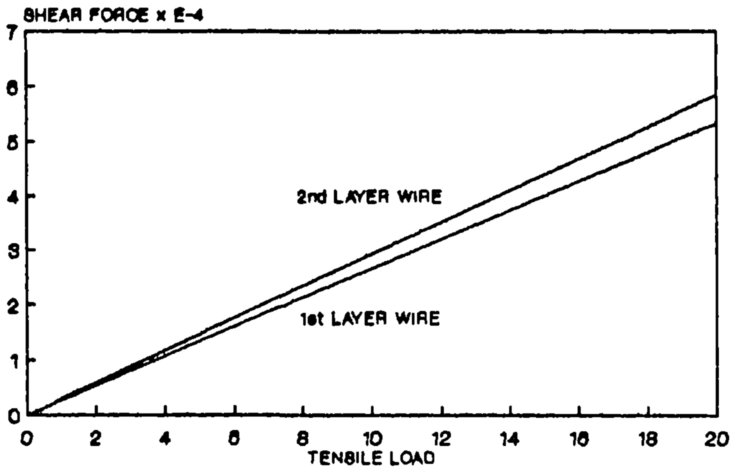

FIGURE 8.5-3
SHEAR FORCE EXERTED ON
HEL. WIRES IN EACH LAYER

12/6F+6/1 STRAND
(SHEAR FORCE)

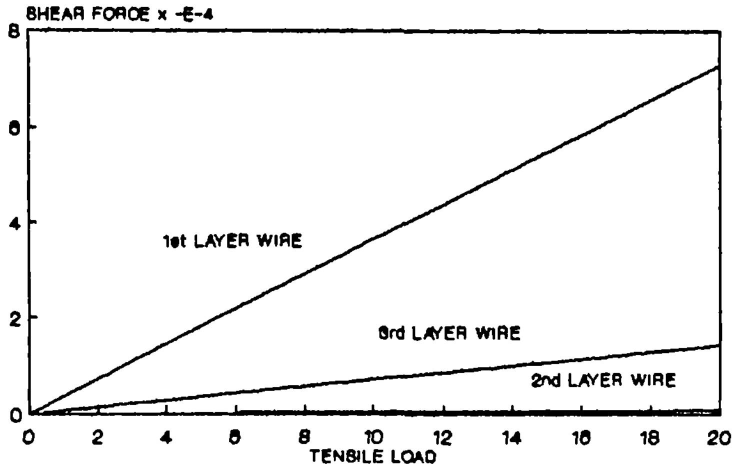

FIGURE 8.5-4
SHEAR FORCE EXERTED ON
HEL. WIRES IN EACH LAYER

helical wires of the inner layer appears to be greater than that acting on the helical wires of the outer layer. This is because the helix angle of a helical wire in the inner layer is larger than that of the helical wire in the outer layer.

For a 12/6F+6/1 equal lay strand, shear force, bending moment, twisting moment and radial force acting on the helical wire in the outer layer appear to be smaller than that of the helical wire in the inner layer. This is because the radius of curvature and torsion of the helical wire in the outer layer are larger than that of the helical wire in the inner layer, Figure 8.5-4 and 8.5-6 (a), (b) and (d). For the same reason, the tensile force acting on the helical wire in the outer layer appear to be larger than that of the helical wire in the inner layer, Figure 8.5-6 (c).

From a practical point of view, it is useful to study the component forces and moments acting on each layer of the helical wire. Any significant unbalance load shared by a layer of helical wires will weaken the fatigue performance of that particular layer of helical wires.

8.5-3 Conclusion

Since the construction of multi-layers strands are different, the size of wires, number of wires per layer and the helix angle chosen for the helical wire in each layer are restricted by geometrical factors of helices. Two multi-layer

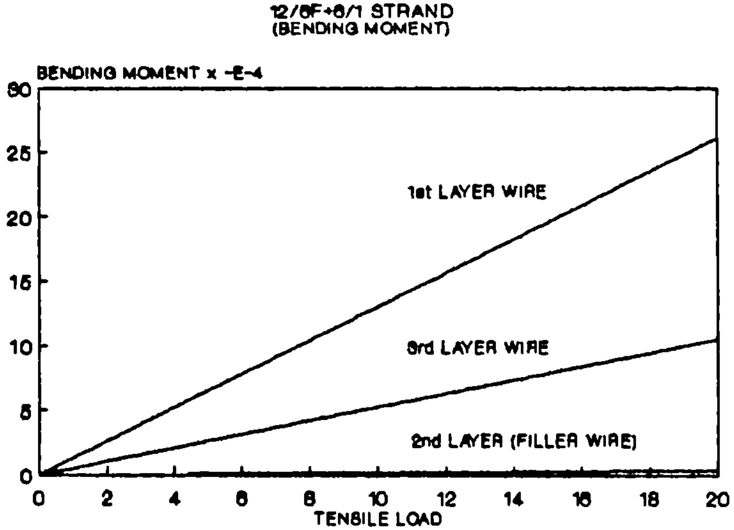

FIGURE 8.5-6 (a)
BENDING MOMENT EXERTED ON
HEL. WIRES IN EACH LAYER

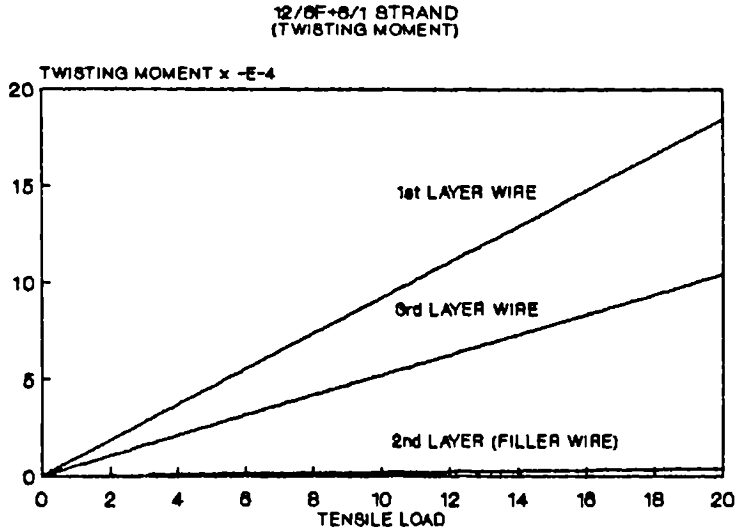

FIGURE 8.5-6 (b)
TWISTING MOMENT EXERTED ON
HEL. WIRES IN EACH LAYER

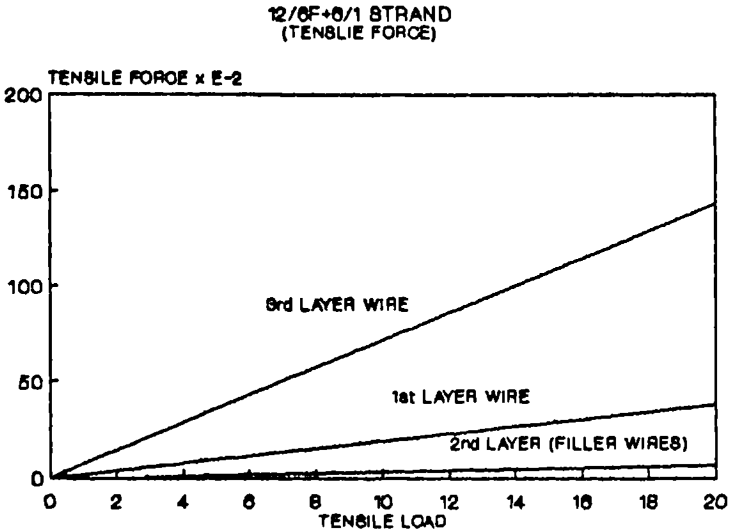

FIGURE 8.5-6 (c)
TENSILE FORCE EXERTED ON
HEL. WIRES IN EACH LAYER

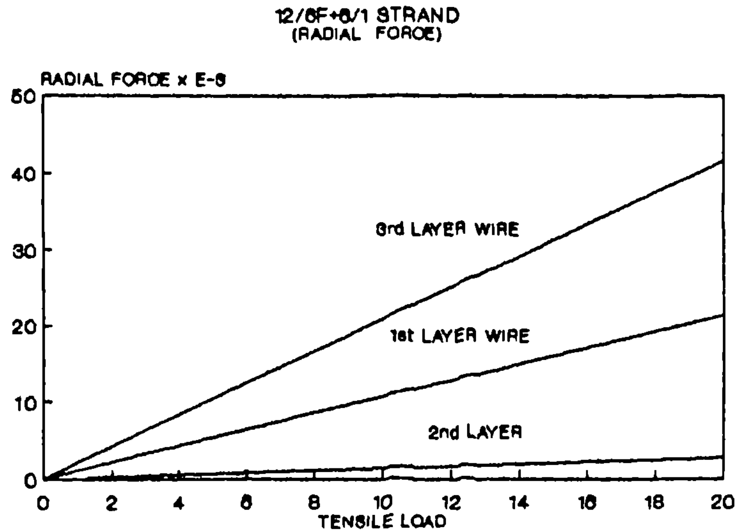

FIGURE 8.5-6 (d)
RADIAL FORCE EXERTED ON
HEL. WIRES IN EACH LAYER

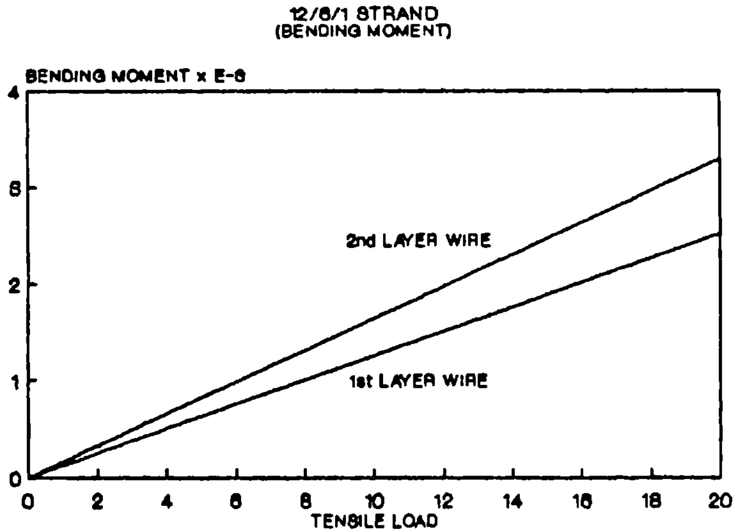

FIGURE 8.5-7 (a)
BENDING MOMENT EXERTED ON
HEL. WIRES IN EACH LAYER

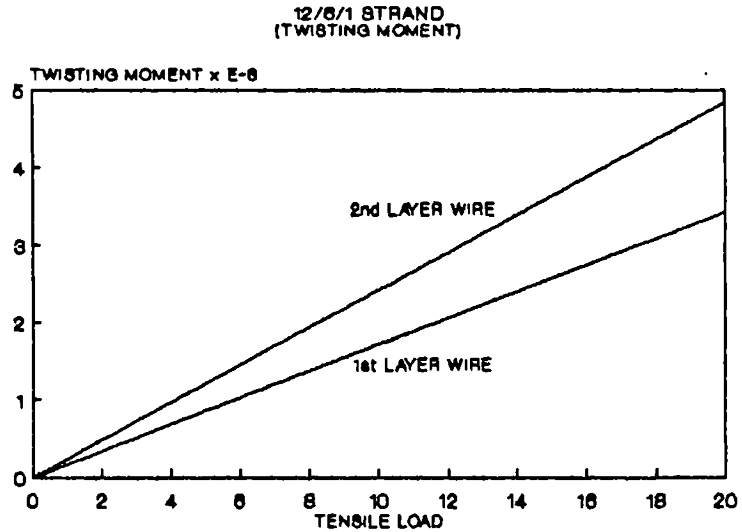

FIGURE 8.5-7 (b)
TWISTING MOMENT EXERTED ON
HEL. WIRES IN EACH LAYER

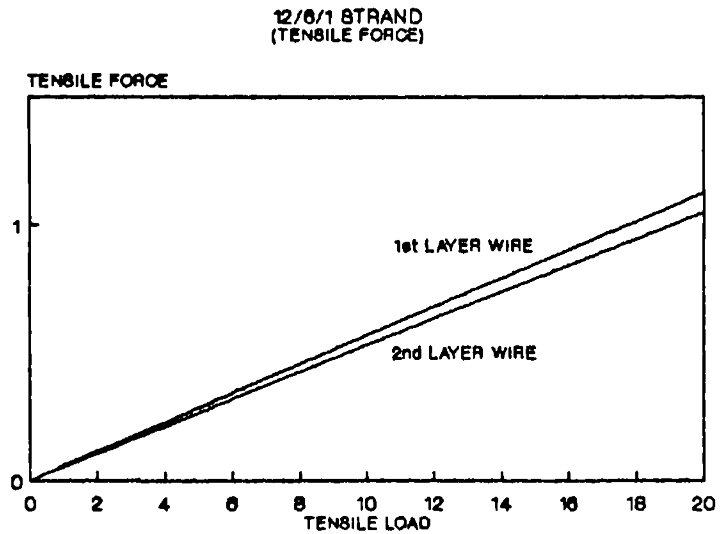

FIGURE 8.5-7 (c)
TENSILE FORCE EXERTED ON
HEL. WIRES IN EACH LAYER

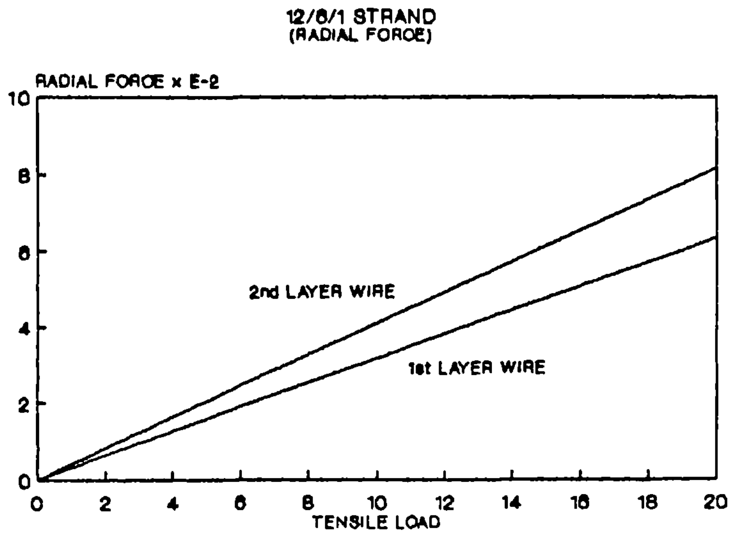

FIGURE 8.5-7 (d)
RADIAL FORCE EXERTED ON
HEL. WIRES IN EACH LAYER

strands with different constructions cannot have exactly the same strand diameter. In this analysis, the author has attempted to retain the same size of the helical wire by adjusting the helix angle and the diameter of core wire. Therefore, the conclusions are rather tentative:

1. The stiffness of the 12/6F+6/1 strand should be greater than that of the 12/6/1 and the 9/9/1 strand.

2. The load acting on the helical wire in each layer of the 12/6/1 strand is even greater than that acting on the helical wire in each layer of the 12/6F+6/1 strand.

3. The tensile force acting on the helical wire is less sensitive than the other internal component forces and moments to the change in helix angle.

Note: For helical wires with helix angle smaller than 60 degrees, the approximate admissible R/r ratio will diverge from exact R/r ratio. The component forces and moments acting on each layer of helical wires will increase significantly with the exception of torsion and tension. The influence of mechanical interaction will be more pronounced as the helix angle is reduced to below 50 degrees. These models will become less accurate. However, for multi-layer strands which are designed with helix angle less than 60 degrees, are considered as poor practice.

CHAPTER NINE

STRUCTURAL MODELLING OF IWRC

NOMENCLATURE

a	Defined parameter
a_c or a_{11}	Radius of king wire
a_{ch} or a_{12}	Radius of helical wire in main core strand (6/1)
a_{sc} or a_{21}	Radius of core wire in outer strand (6/1)
a_{sh} a_{22} a_{23} a_{24} a_{25} a_{26} a_{27}	Radius of helical wire (double helix) in outer strand (6/1)
AA_1 & AA_2	Defined parameters
A_s	Approximate bending stiffness of helical strand
BB_1 & BB_2	Defined parameters
b	Defined parameter
CC_1 & CC_2	Defined parameters
C	Defined parameter
DD_1 & DD_2	Defined parameters
d	Defined parameter
EE_1 & EE_2	Defined parameters
e	Defined parameter
E	Young modulus of wire material
FF_1 & FF_2	Defined parameters
f	Defined parameter
F_c	Tensile force acting on the main core strand
F_{Dh}	Summation of component forces on double helical wire to the global direction of the

	IWRC
F_R	External tensile force applied to IWRC terminations
F_{sc}	Summation of component forces on the core wire of the outer strands
G	Modulus of rigidity
G^*	Ratio of cyclic length of main core strand to the lay length of IWRC
GG_1 & GG_2	Defined parameter
g	Defined parameter
G_i	Element stiffness of helical wire in main core strand, i = 1, 2, 3, ...
HH_1 & HH_2	Defined parameters
h	Defined parameter
II_1 & II_2	Defined parameters
i	Defined parameter
I_i	Element stiffness of core wire in outer strand, i = 1, 2, 3, ...
J_i	Element stiffness of helical wire in outer strand, i = 1, 2, 3, ...
J_i^*	Element stiffness of helical wire in outer strand, i = 10, 11, 12 and 13
J_{ch} & I_{ch}	Polar moment and second moment of area of helical wire in main core strand
J_{sc} & I_{sc}	Polar moment and second moment of area of core wire in outer strand
J_{Dh} & I_{Dh}	Polar moment and second moment of area of

	helical wire in outer strand
K_i	Assemble stiffness for IWRC, i = 1, 2, 3 & 4
K'_{ch} $\bar{K}'_{ch}$ & $\Delta K'_{ch}$	Initial curvature, final curvature and change in curvature of helical wire in main core strand
K'_{sc} $\bar{K}'_{sc}$ & $\Delta K'_{sc}$	Initial curvature, final curvature and change in curvature of core wire in outer strand
K'_{Dh} $\bar{K}'_{Dh}$ & $\Delta K'_{Dh}$	Initial curvature, final curvature and change in curvature of helical wire in outer strand
K_i^c	Stiffness for core strand, i = 1, 2, 3, and 4
K_i^o	Stiffness for ordinary lay outer strand, i = 1, 2, 3 and 4
K_i^s	Stiffness for Lang's lay outer strand, i = 1, 2, 3 and 4
K_j^s	Stiffness for outer strand, j = 5, 6, 7, ..., 10
K_i^R	Stiffness for IWRC, i = 1, 2, 3 and 4
LL_i	Defined parameters, i = 1, 2, 3, ...
L_i^Δ	Defined parameters, i = 1 and 2
$L_i^\uparrow$	Defined parameters, i = 1, 2, 3 and 4
L_i^*	Defined parameters, i = 1, 2 and 3
L_i^+	Defined parameters, i = 1 and 2
M	Applied twisting moment to IWRC
M^*	Defined parameter
M_c	Twisting moment acting on the main core strand of an IWRC
m_c	Number of core wire of outer strand in an IWRC

M_{Dh}	Twisting moment acting on all the double helical wires
m_{Dh}	Number of double helical wire in an IWRC
M_k	Twisting moment acting on the king wire
M_R	Twisting moment acting on the IWRC
M_{sc}	Twisting moment acting on all helical core wire of outer strands in an IWRC
m_s	Number of helical strand in an IWRC
m_{22} m_{23} m_{24} m_{25} m_{26} m_{27}	Number of double helical wire at various locations
N'_{ch}	Shearing force acting on king wire
N'_{sc}	Shearing force acting on core wire of outer strand
N'_{sh}	Shearing force acting on helical wire of outer strand
N'_{Dh}	Shearing forces acting on double helical wire
P_{ch}	Lay length of core strand
P_L	Lay length of IWRC
r_{ch}	Helical radius of helical wire in main core strand
r_s	Helical radius of outer strand
r_w or r_{sh}	Helical radius of double helical wire
R_{Dh}	Radial distance from centre of IWRC to the centre of double helical wire
R_i	Defined constants, i = 1, 2, 3, ... 10
S_{ch}	Path length of helical wire of core strand
S_i	Defined constants, i = 1, 2, 3, ..., 18

S_{sc}	Path length of outer strand
S_{sh}	Path length of double helical wire
T_c	Tensile force acting on king wire
T_{ch}	Tensile force acting on helical wire in main core strand
T_{sc}	Tensile force acting on core wire in outer strand
T_{Dh}	Tensile force acting on double helical wire
T_k	Tensile force acting on king wire
T_s	Tensile force acting on helical strand
V_{ch}	Bending moment acting on helical wire in main core strand
V_{sc}	Bending moment acting on core wire of outer strand
V_{Dh}	Bending moment acting on double helical wire
W_c	Twisting moment acting on king wire
W_{ch}	Twisting moment acting on helical wire of main core strand
W_{sc}	Twisting moment acting on core wire of outer strand
W_{Dh}	Twisting moment acting on double helical wire
W_s	Twisting moment acting on helical strand
X_{ch}	Radial force acting on helical wire of main core strand
X_{sc}	Radial force acting on core wire of outer strand
X_{Dh}	Radial force acting on double helical wire

$\dot{\bar{X}}, \dot{\bar{Y}}, \dot{\bar{Z}}$	First derivative of the coordinate equations of a double helix
$\ddot{\bar{X}}, \ddot{\bar{Y}}, \ddot{\bar{Z}}$	Second derivative of the coordinate equations of a double helix
$\dddot{\bar{X}}, \dddot{\bar{Y}}, \dddot{\bar{Z}}$	Third derivative of the coordinate equations of a double helix
Δr_w or Δr_{sh}	Change in helical radius of wire due to external loads
Δr_s	Change in helical radius of strand due to external loads
$\Delta\theta_w$ or $\Delta\theta_{sh}$	Change in rotational coordinate of helical wire
$\Delta\theta_s$	Change in rotational coordinate of outer strand
$\Delta\theta_R$	Change in rotational displacement of IWRC per lay length
$\Delta\alpha_{ch}$	Change in helix angle of helical wire in main core strand
$\Delta\alpha_{Dh}$	Change in double helical angle
$\Delta\Omega$	Change in defined parameter resulted from external loads
$\Delta\beta$	Change in helix angle of outer strand
ε_R	Equivalent tensile strain on IWRC
ε_{ch}	Tensile strain of helical wire in main core strand
ε_{sc}	Tensile strain of core wire in outer strand
ε_{Dh} or ε_{sh}	Tensile strain of double helical wire

α_{ch}	Helix angle of helical wire in main core strand
β or α_{sc}	Helix angle of core wire of outer strand or helix angle of outer strand
α_{sh}	Helix angle (single helix angle) of helical wire of outer strand when it is in a straight line form
α_{Dh}	Double helix angle
ν	Poisson's ratio of wire material
τ_{ch} $\bar{\tau}_{ch}$ $\Delta\tau_{ch}$	Initial torsion, final torsion and change in torsion of helical wire in main core strand
τ_{sc} $\bar{\tau}_{sc}$ $\Delta\tau_{sc}$	Initial torsion, final torsion and change in torsion of core wire in outer strand
τ_{Dh} $\bar{\tau}_{Dh}$ $\Delta\tau_{Dh}$	Initial torsion, final torsion and change in torsion of helical wire in outer strand
τ_s $\bar{\tau}_s$ $\Delta\tau_s$	Initial torsion, final torsion and change in torsion of helical strand of IWRC
Ω	Defined parameter
Ω^*	Defined parameter
θ_i	Defined parameter, i = 1 and 2

SUBSCRIPTS:

R	Rope
S	Strand
W	Wire
C	Core
h	Helical wire

D	Double helical wire
Ch	Helical wire (single helix)
SC	Core wire of outer strand (single helix)
Sh	Helical wire of outer strand (single helix)
Dh	Double helical wire

9.1 INTRODUCTION TO LINEARIZED MODELLING OF IWRC

Independent wire rope core "IWRC" basically takes the form of 6x7 Lang's lay rope which is the simplest form of wire rope. It is constructed by laying six "6/1" strand around a "6/1" main core strand. The IWRC itself is also used as main core of a six stranded rope. It gives greater resistance to crushing without significantly reducing the flexibility of the rope. In addition to this, steel wire core provides higher strength which is essential for ropes operating in a high temperature environment.

Three main types of wire can be found in a straight IWRC, namely:

a. Straight king wire; 2.1 % in an IWRC.

b. Single helical wire; 24.5% in an IWRC.

c. Double helical wire; 73.4% in an IWRC.

The IWRC is generally constructed in form of right hand Lang's lay. However, in order to understand the mechanical response of double helical wire, the IWRC is assumed to be manufactured either in form of Lang's lay or in form of ordinary lay.

Costello and Velinsky[3.18-3.20] used the single helix approach for modelling the structural response of the Seale rope. However, double helical wires are considered in the present Chapter. Factors which will influence the present analysis, in the linear elastic regime, are listed below:

a. Termination Conditions:

1. Tensile load with fixed terminations.
2. Combined tension and torsion applied to the termination.

In addition to this, Velinsky's approach provides another two more termination conditions to be considered, namely:

3. Twisting moment alone.
4. Free ends

b. Termination Attachments:

Cone with epoxy type of terminations are assumed to be used for the rope terminations.

For model linearization, the 2nd and higher differential terms, in equations of deformation geometry, are ignored.

9.2 STRUCTURE OF THE APPROACH TO THE MATHEMATICAL MODELLING OF IWRC

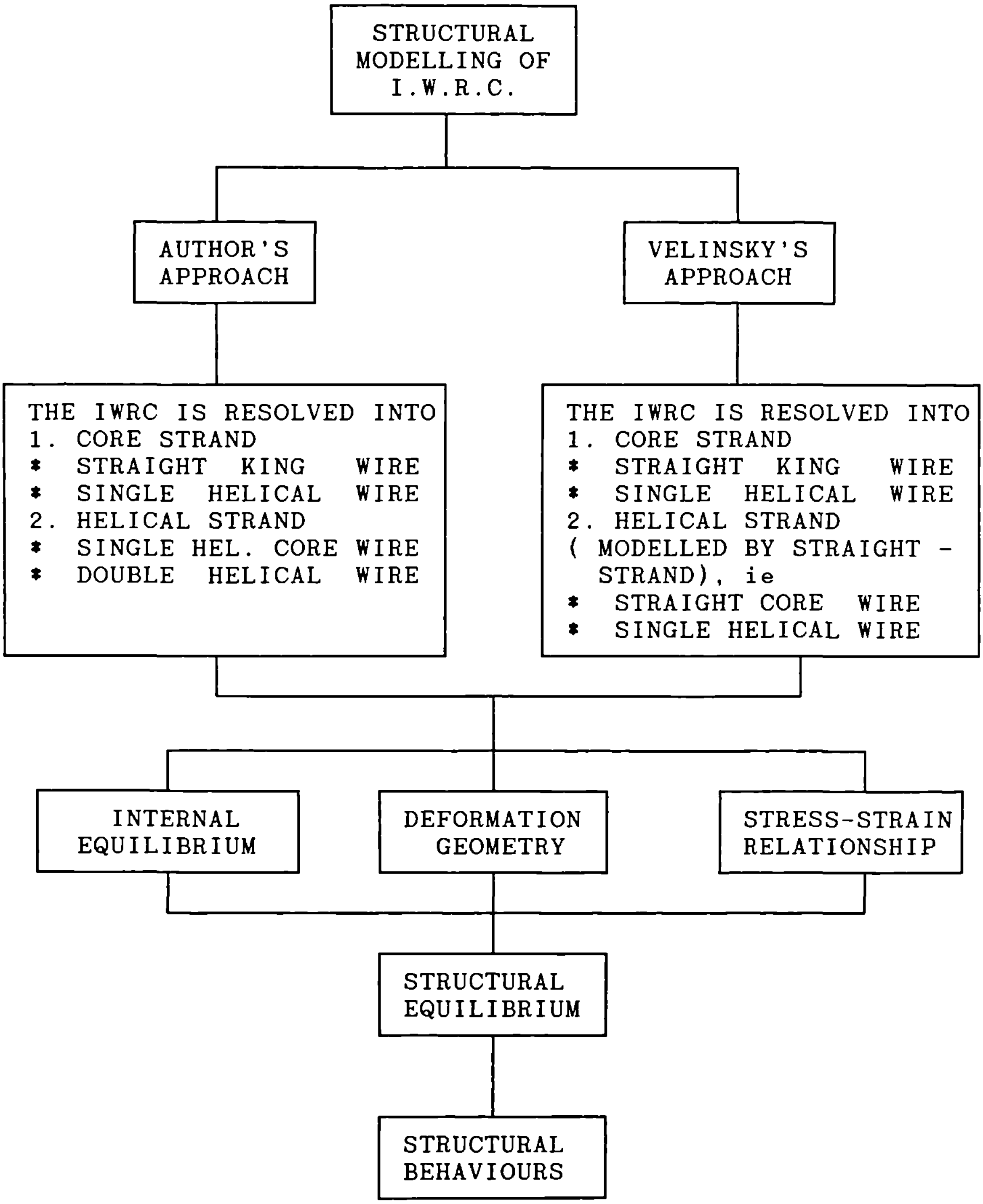

BLOCK DIAGRAM 9.1

STRUCTURAL MODELLING OF IWRC

9.3 BASIS OF APPROACH AND ASSUMPTIONS

An IWRC is considered as a statically indeterminate structure. Each of the internal component forces and moments acting on each of the wires will be resolved and summed in the loading direction. The basis of the current model approach is summarized as follows:

1. Establish equation(s) of internal equilibrium (based on naturally curved rod theory) for each individual wire in the IWRC.
2. Relate internal and external equilibrium using Costello's approach.
3. Establish relationships between the deformation of helical wire and structural displacements using the development technique and the author's method for double helix geometry.
4. Apply classical constitutive relationship to relate load-deformation or stress-strain along wires in the IWRC.

The assumptions made in this Chapter are similar to the assumptions made in Chapter 7. In addition to these, the influence of mechanical interactions is also ignored.

9.4 VELINSKY'S APPROACH TO THE ANALYSIS IWRC

Velinsky[3.18 & 3.19] suggested that the internal tension and twisting moment acting on outer strand of a Seale rope can be considered as the external tension and twisting moment applied to a straight strand of same size and construction. Based on this concept, the present author will modify Velinsky's model in order to form an analytical model to predict the structural behaviour of an IWRC. The procedure is presented in the following sub-sections.

9.4-1 Organization of This Section

This section is generally organized into two main sub-sections as shown in the block diagram below:

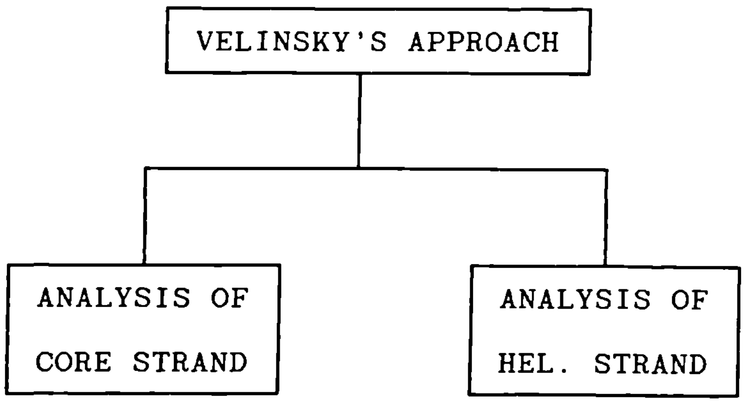

BLOCK DIAGRAM 9.2

VELINSKY'S APPROACH

9.4-2 External and Internal Equilibrium

External and internal equilibrium on an IWRC model are considered in this sub-section. These include:

1. external equilibrium on the IWRC and
2. internal equilibrium on main core strand and outer strand.

a. External Equilibrium on The IWRC

Velinsky's approach is to incorporate a outer strand (ie a single helical strand) with a main core strand of an IWRC is in much the same manner as a helical wire (ie a single helical wire) is incorporated with a core wire of a straight strand. In this approach, the total forces and moments exerted in each individual strands are oriented and summed to the global direction where external tensile force and twisting moment are applied. The external and internal equilibrium exerted on the IWRC model under combined loading condition (as presented in Chapter seven) are given by :

$$F_R = m_s \, (T_s \sin \bar{\beta} + N'_s \cos \bar{\beta} \,) + F_c \qquad (9.1)$$

$$M_R = m_s \, \{ \, (\, W_s - N'_s \, \bar{r}_s \,) \sin \bar{\beta} + (\, V'_s + T_s \, \bar{r}_s) \cos \bar{\beta} \, \} + M_c \qquad (9.2)$$

(The notation used in this Chapter is the present author's own, where T_s and W_s are the equivalent internal tension and twisting moment acting on a helical strand. The equivalent internal tension T_s and twisting moment W_s are obtained by considering the external and internal equilibrium on a straight strand of same size and construction.)

b. Internal Equilibrium of Main Core and Helical Strand

1. Internal Equilibrium of Main Core Strand

Procedures for the evaluation of total internal equilibrium will not be repeated as they are similar to those described earlier and one can refer to Chapter Seven for details. The equilibrium equations on the main core strand corresponding to the global displacement of the IWRC are given by :

$$\begin{vmatrix} K_1^c & K_2^c \\ K_3^c & K_4^c \end{vmatrix} \begin{vmatrix} \varepsilon_R \\ \Delta\theta_R \end{vmatrix} = \begin{vmatrix} T_c \\ M_c \end{vmatrix} \qquad (9.3)$$

whereas, the equilibrium equations corresponding to the external applied load are given by

$$T_c = m_{ch} \{ T_{ch} \sin \bar{\alpha}_{ch} + N'_{ch} \cos \bar{\alpha}_{ch} \} + F_{ch} \qquad (9.4)$$

$$W_c = m_{ch} \{ (W_{ch} - N'_{ch} \bar{r}_{ch}) \sin \bar{\alpha}_{ch} + (V'_{ch} + T_{ch} \bar{r}_{ch}) \cos \bar{\alpha}_{ch} \} + M_{ch} \qquad (9.5)$$

2. Internal Equilibrium of Helical Strand

In order to evaluate the equivalent internal component forces and moments acting on a single helical outer strand, rod theory from Love [3.21] together with Velinsky's approach for Seale rope will be applied to evaluate the equivalent tensile, shear and radial forces as well as the twisting moment. In addition to this, Timoshenko's theory for spring and Costello's approach for stranded spring will also be used to evaluate the equivalent bending moment acting on the same outer strand. Finally, the internal equilibrium on the outer strand can be regarded as functions of axial deformations of the IWRC model, and a system of equilibrium equations are given by :

$$T_s = K_1^h \varepsilon_R + K_2^h \Delta\theta_R \qquad (9.6)$$

$$W_s = K_3^h \varepsilon_R + K_4^h \Delta\theta_R \qquad (9.7)$$

$$V'_s = A_s \Delta K'_s \qquad (9.8)$$

$$N'_s = W_s \bar{K}'_s - V'_s \bar{\tau}_s \qquad (9.9)$$

$$X_s = N'_s \bar{\tau}_s - T_s \bar{K}_s \qquad (9.10)$$

Where the internal equilibrium force "T_s" and moment "W_s" acting on the outer strand, in accordance with Velinsky's approach, can be approximated by balancing the external and internal equilibrium on a straight strand of same size and construction. They are given by :

$$T_s = m_{sh} \{ T_{sh} \sin \bar{\alpha}_{sh} + N'_{sh} \cos \bar{\alpha}_{sh} \} + F_{sc} \tag{9.11}$$

i. For Lang's Lay:

$$W_s = m_{sh} \{ (W_{sh} - N'_{sh} \bar{r}_{sh}) \sin \bar{\alpha}_{sh} + (V'_{sh} + T_{sh} \bar{r}_{sh}) \cos \bar{\alpha}_{sh} \} + M_{sc} \tag{9.12}$$

ii For Ordinary Lay:

$$W_s = m_{sh} \{ -(W_{sh} - N'_{sh} \bar{r}_{sh}) \sin \bar{\alpha}_{sh} - (V'_{sh} + T_{sh} \bar{r}_{sh}) \cos \bar{\alpha}_{sh} \} + M_{sc} \tag{9.13}$$

By expressing the deformation of the centroidal axis of the outer strand in terms of the structural displacements of the IWRC equations 9.12 and 9.13 can be rewritten as functions of ε_R and $\Delta\theta_R$. These two equations can be expressed in the form of equations 9.6 and 9.7. Likewise, equations 9.8, 9.9 and 9.10 can also be expressed as functions of structural displacement* of the IWRC. They are given by :

$$V'_s = K_5^s \varepsilon_R + K_6^s \Delta\theta_R \tag{9.14}$$

$$N'_s = K_7^s \varepsilon_R + K_8^s \Delta\theta_R \tag{9.15}$$

$$X_s = K_9^s \varepsilon_R + K_{10}^s \Delta\theta_R \tag{9.16}$$

All expressions for geometrical and stiffness constants are collected in the Appendix.

Note: Structural displacement*

$\Delta\theta_R$ and ε_R are defined as structural (or axial) deformation of an IWRC.

9.4-3 Deformation of Single Helical Wire and Strand

Now the development technique is applied to relate the deformations of single helical wire and single helical outer strand as functions of the structural displacements of the IWRC. Since IWRC will be subjected to "constructional displacements" in the low load region (range normally from no load to 20 % of UBL). This phenomenon is pronounced in fibre core rope and is insignificant in single layer strand. However, both constructional and flattening displacements are ignored in this analysis. Finally, deformation of single helical wire and *single helical outer strand as functions of* the structural displacement of the IWRC are given below:

a. Single Helical Wire of Main Core Strand

By applying the "Development Technique" and taking the total partial derivative of the single helix geometry with respect to the structural displacements, the linearized deformation of a single helical wire can be expressed by the following equations:

$$\varepsilon_{ch} = G_1\, \varepsilon_R + G_2\, \Delta\theta_R \qquad (9.17)$$

$$\Delta\alpha_{ch} = G_3\, \varepsilon_R + G_4\, \Delta\theta_R \qquad (9.18)$$

$$\Delta K'_{ch} = G_5\, \varepsilon_R + G_6\, \Delta\theta_R \qquad (9.19)$$

$$\Delta\tau_{ch} = G_7\,\varepsilon_R + G_8\,\Delta\theta_R \qquad (9.20)$$

b. Outer Strand of The IWRC

The "Development Technique" can, similarly, be applied to relate the displacement of the centroidal axis of an outer strand as a function of the structural displacements of the IWRC. The corresponding equations are given by :

$$\varepsilon_{sc} = I_1\,\varepsilon_R + I_2\,\Delta\theta_R \qquad (9.21)$$

$$\Delta\beta_{sc} = I_3\,\varepsilon_R + I_4\,\Delta\theta_R \qquad (9.22)$$

$$\Delta K'_{sc} = I_5\,\varepsilon_R + I_6\,\Delta\theta_R \qquad (9.23)$$

$$\Delta\tau_{sc} = I_7\,\varepsilon_R + I_8\,\Delta\theta_R \qquad (9.24)$$

Velinsky[3.18] also showed that the twisting moment acting on the outer strand could be considered as the twisting moment acting on the straight strand of same size and construction. Hence, the change in torsion resulted from the same amount of the twisting moment applied to the straight strand is given by :

$$\Delta\tau_{sh} = J_7\,\varepsilon_R + J_8\,\Delta\theta_R \qquad (9.25)$$

where I, J and G are parametric variables dependent on the wire helix geometry. They are given in Appendix.

9.4-4 Stress-Strain Relationship

The material constant and stress-strain relationship applied in this analysis are exactly the same as those presented in Chapter 7.

9.4-5 Structural Equilibrium

By incorporating the outer strands with the main core strand, the structural equilibrium of the IWRC can then be obtained, by substituting equations 9.3, 9.6 - 9.9 into equations 9.1 and 9.2. A stiffness matrix which represents the external equilibrium of the IWRC, in terms of structural deformations, is given by :

$$\begin{vmatrix} K_1^R & K_2^R \\ K_3^R & K_4^R \end{vmatrix} \begin{vmatrix} \varepsilon_R \\ \Delta\theta_R \end{vmatrix} = \begin{vmatrix} F_R \\ M_R \end{vmatrix} \qquad (9.26)$$

at this stage, Velinsky's approach for solving the structural response of the IWRC has been completed and results will be discussed in section 9.6.

9.5 AUTHOR'S APPROACH TO THE ANALYSIS OF IWRC

An IWRC is constructed from 49 individual steel wires, including one straight King wire, twelve single helical wires and thirty six double helical wires. From the design point of view, therefore, it is useful, to know how double helical wires behave and how the load is shared by each type of wire. The helix geometry of the double helical wire is periodic; this implies that the internal components forces and moments also vary periodically on each cyclic length of the double helical wire. The present analysis has been stimulated by this concept.

9.5-1 The Organization of This Section

This section is organized into three portions as shown in the following block diagram.

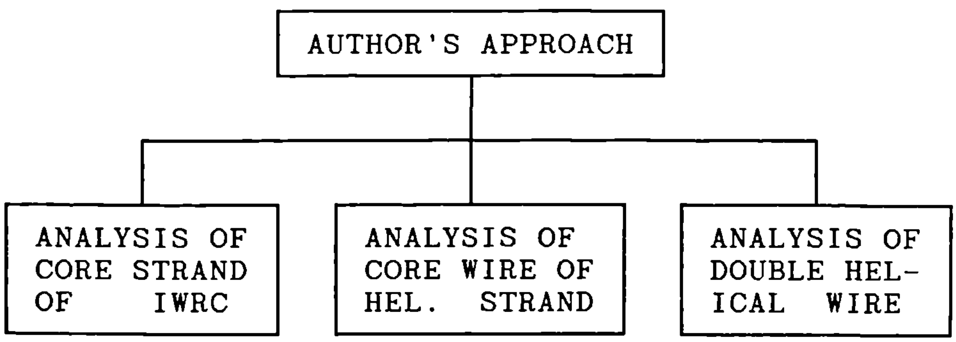

BLOCK DIAGRAM 9.3

AUTHOR'S APPROACH

9.5-2 External and Internal Equilibrium

External and internal equilibrium on the IWRC model are considered in this section. They include :

1. External equilibrium on the IWRC
2. Internal equilibrium on the main core strand.
3. Internal equilibrium on the core wire of the outer strand.
4. Internal equilibrium on the double helical wires.

a. External Equilibrium on The IWRC

The structural equilibrium on the IWRC model is obtained by orientating and summing all the component forces and moments acting on each individual wire to the global direction of the IWRC where the external load applied. The equilibrium equations are given by :

$$F_R = \sum F_w = T_c + F_{sc} + F_{dh} \quad (9.27)$$

$$M_R = \sum M_w = W_c + M_{sc} + M_{dh} \quad (9.28)$$

where the subscript of the equations are given by

R Rope

w wires in IWRC

c core strand

sc core wires of single helical strand

dh double helical wires

b. Internal Equilibrium on Core Strand

1. Internal tensile force and twisting moment acting on the King wire

$$T_K = F_{10} \, \varepsilon_R \tag{9.29}$$

$$M_K = F_{11} \, \Delta\theta_R \tag{9.30}$$

2. Internal component forces and moments acting on a helical wire

$$T_{ch} = G_{10} \, \varepsilon_R + G_{11} \, \Delta\theta_R \tag{9.31}$$

$$V'_{ch} = G_{12} \varepsilon_R + G_{13} \Delta\theta_R \tag{9.32}$$

$$W_{ch} = G_{14} \, \varepsilon_R + G_{15} \, \Delta\theta_R \tag{9.33}$$

$$X_{ch} = G_{16} \, \varepsilon_R + G_{17} \, \Delta\theta_R \tag{9.34}$$

Therefore, the external and internal equilibrium on the main core strand is given by :

$$T_c = m_c \{ T_{ch} \sin \bar{\alpha}_{ch} + N'_{ch} \cos \bar{\alpha}_{ch} \} + T_K \tag{9.35}$$

$$W_c = m_c \{ (W_{ch} - N'_{ch} \bar{r}_{ch}) \sin \bar{\alpha}_{ch} + (\bar{V}'_{ch} + T_{ch} \bar{r}_{ch}) \cos \bar{\alpha}_{ch} \} + M_K \tag{9.36}$$

d. Internal Equilibrium on a Core Wire Of Outer Strand

The approach which is applied to evaluate the internal component forces and moments acting on a single helical core wire within an outer strand is similar to those described in Chapter Seven. The linearized internal component forces and moments equations are given below :

1. Internal component forces and moments acting on a single helical core wire of outer strand are given by :

$$T_{sc} = I_{10}\, \varepsilon_R + I_{11}\, \Delta\theta_R \tag{9.37}$$

$$V'_{sc} = I_{12}\, \varepsilon_R + I_{13}\, \Delta\theta_R \tag{9.38}$$

$$W_{sc} = I_{14}\, \varepsilon_R + I_{15}\, \Delta\theta_R \tag{9.40}$$

$$N'_{sc} = I_{16}\, \varepsilon_R + I_{17}\, \Delta\theta_R \tag{9.41}$$

2. Total Equilibrium on a Single Helical Core Wire

$$F_{sc} = m_{sc} \{ T_{sc} \sin \bar{\beta} + N'_{sc} \cos \bar{\beta} \} \tag{9.42}$$

$$M_{sc} = m_{sc} \{ (W_{sc} - N'_{sc}\, \bar{r}_{sc}) \sin \bar{\beta} + (V'_{sc} + T_{sc}\, \bar{r}_{sc}) \cos \bar{\beta} \} \tag{9.43}$$

e. Internal Equilibrium on a Double Helical Wire

The centroidal axis of a double axis can be regarded as a three dimension space curve. By applying the rod theory, the general internal equilibrium equations applied to a single helical wire can also be applied to a double helical wire. However, the final form of the internal equilibrium equations for the double helical wire will heavily influenced by the geometry of the double helical wire. The general internal equilibrium equations for a double helical wire are given by:

1. Internal Component forces and moments acting on the double helical wire are given by :

$$T_{dh} = L_{10}\ \varepsilon_R + L_{11}\ \Delta\theta_R \qquad (9.44)$$

$$V'_{dh} = L_{12}\ \varepsilon_R + L_{13}\ \Delta\theta_R \qquad (9.45)$$

$$W_{dh} = L_{14}\ \varepsilon_R + L_{15}\ \Delta\theta_R \qquad (9.46)$$

$$N'_{dh} = L_{16}\ \varepsilon_R + L_{17}\ \Delta\theta_R \qquad (9.47)$$

2. Total Equilibrium Of Double Helical Wires

$$F_{dh} = m_{dh}\{\ T_{dh}\ \sin\bar{\alpha} + N'_{dh}\ \cos\bar{\alpha}\ \} \qquad (9.48)$$

For Lang's Lay :

$$M_{dh} = m_{dh}\{\ (\ W_{dh} - N'_{dh}\ \bar{r}_{dh}\ )\ \sin\bar{\alpha}_{dh} + (\ V'_{dh} + T_{dh}\ \bar{r}_{dh}\ )\ \cos\bar{\alpha}_{dh}\ \} \qquad (9.49)$$

For Ordinary Lay:

$$M_{dh} = m_{dh}\{-(\ W_{dh} - N'_{dh}\ \bar{r}_{dh}\ )\ \sin\bar{\alpha}_{dh} - (\ V'_{dh} + T_{dh}\ \bar{r}_{dh}\ )\ \cos\bar{\alpha}_{dh}\ \} \qquad (9.50)$$

A schematic diagram illustrating the significance of various parameters used in the above equations is shown in Figure 9.1.

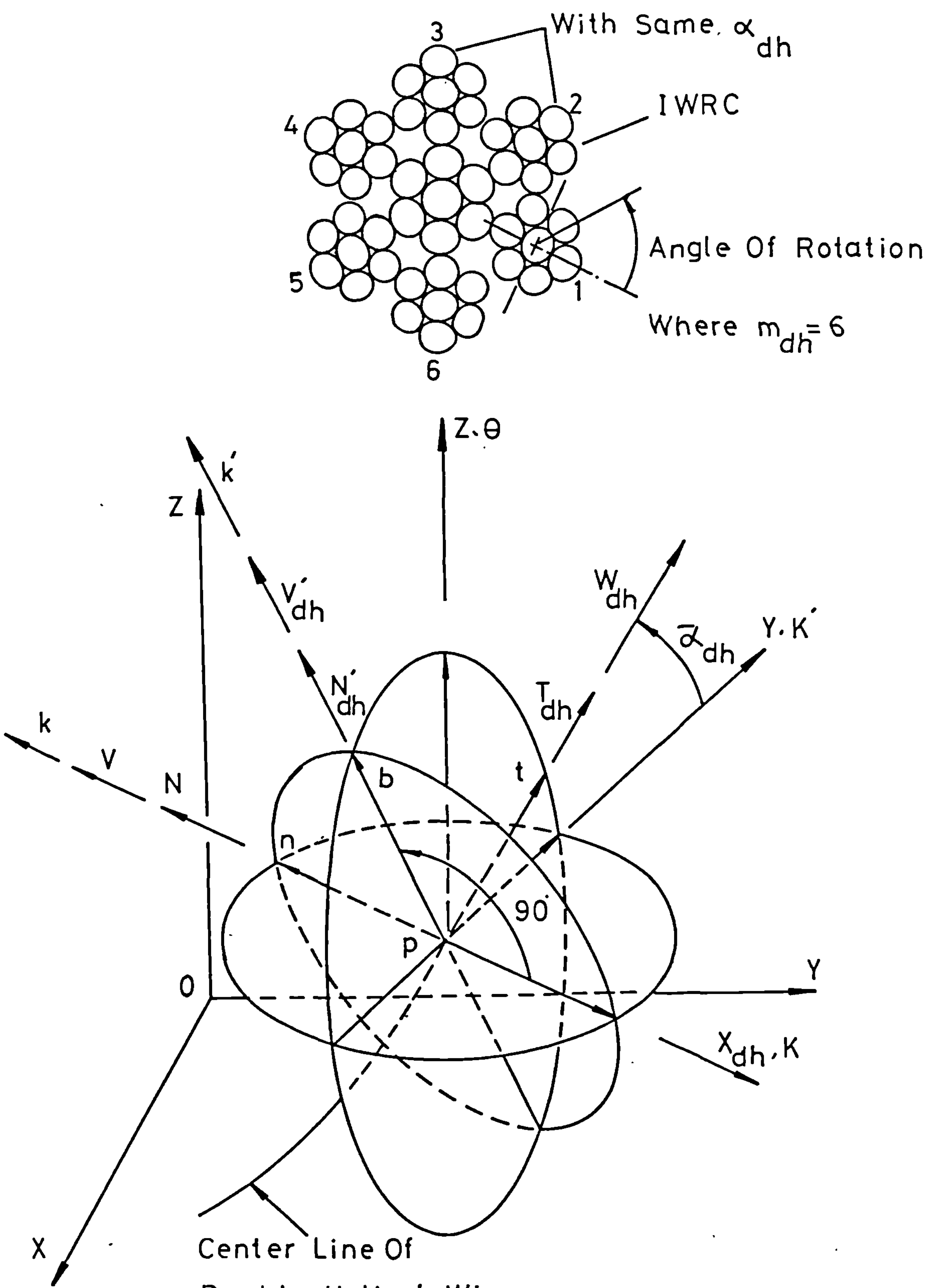

Figure 9.1

Line Model Representing Internal Components Exerted On Any Point 'p' Along The Double Helical Wire

9.5-3 Deformation of Helical Wires and Strand

In order to evaluate the deformation of helical wires and strands with respect to the structural displacements of the IWRC, both vector differential geometry and development technique are used. *Constructional and flattening* displacements are ignored.

Vector differential geometry is mainly used to evaluate the change in curvature and torsion along centroidal axis of a double helical wire. The development technique is used to evaluate the translational and rotational deformation of helical wires resulting from the application of external loads to the termination of the IWRC.

a. Deformation of a Single Helical Wire within the main Core Strand

By applying the "Development Technique", as illustrated in Figure 9.2 (a), the linearized deformation of single helical wire with respect to the structural displacements of the IWRC (in terms of tensile strains) is given by :

$$\varepsilon_R = \varepsilon_{ch} + \frac{\Delta\alpha_{ch}}{\tan \alpha_{ch}} \tag{9.51}$$

$$\varepsilon_R = \frac{\Delta r_{ch}}{r_{ch}} + \frac{\Delta\theta_{ch}}{2\pi} + (\tan \alpha_{ch} + \cot \alpha_{ch}) \, \Delta\alpha_{ch} \tag{9.52}$$

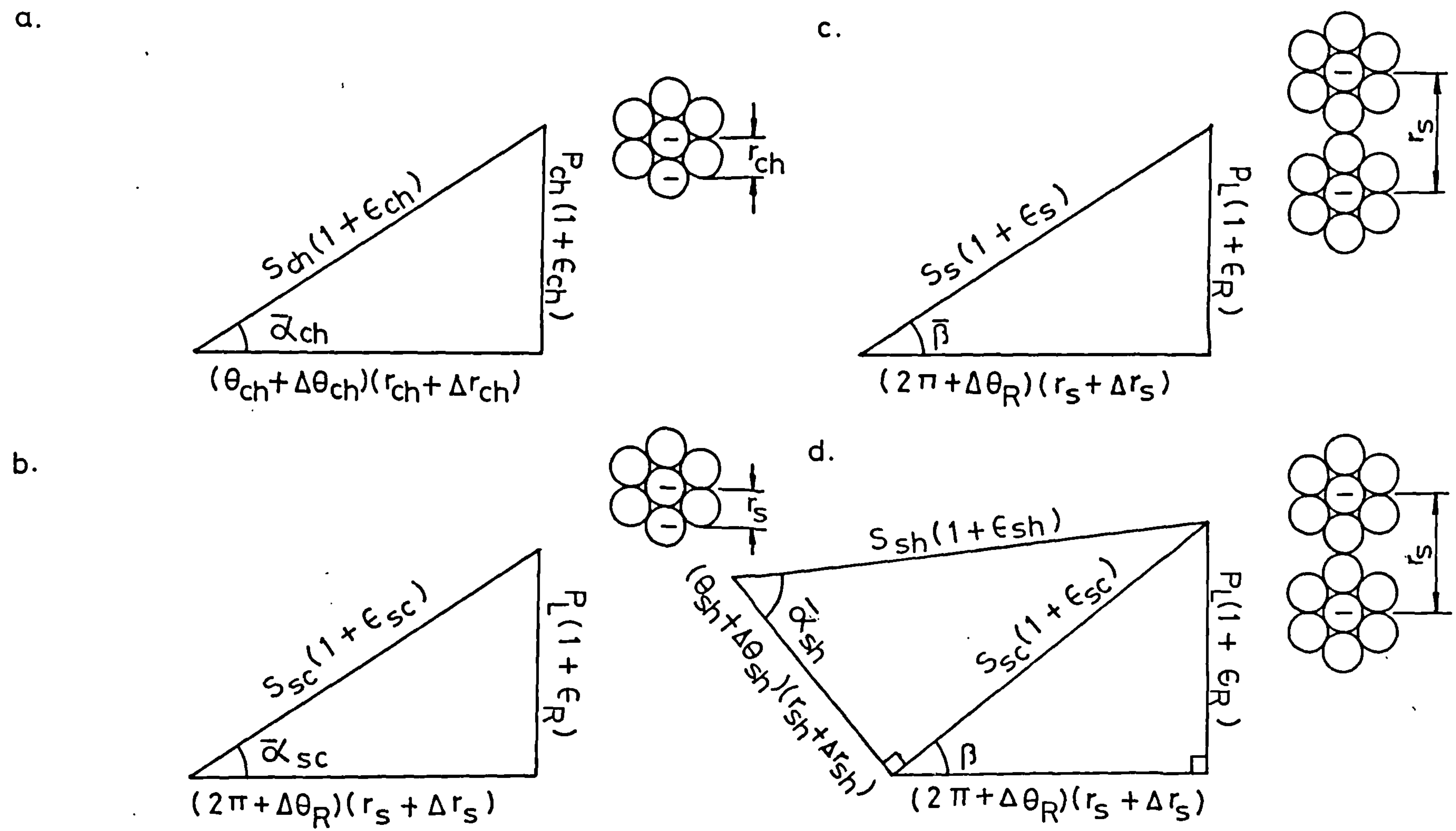

Figure 9.2

Development Of Helical Wires

$$\varepsilon_{ch} = \frac{\Delta r_{ch}}{r_{ch}} + \frac{\Delta\theta_{ch}}{2\pi} + \Delta\alpha_{ch} \tan \alpha_{ch} \tag{9.53}$$

$$\varepsilon_{ch} = \varepsilon_R \sin^2 \alpha_{ch} + \frac{\Delta r_{ch}}{r_{ch}} \cos^2 \alpha_{ch} + \frac{\Delta\theta_{ch}}{2\pi} \cos^2 \alpha_{ch} \tag{9.54}$$

Amongst these equations, the two unknowns are $\Delta r_{ch}/r_{ch}$ and $\Delta\theta_{ch}/2\pi$. However, $\Delta r_{ch}/r_{ch}$ can be determined by the classical linear elastic theory, and is given by :

$$\Delta r_{ch} = - \nu (a_c \varepsilon_R + a_{ch} \varepsilon_{ch}) \tag{9.55}$$

By applying the "development technique" to the deformed core strand, $\Delta\theta_{ch}$ can be obtained in terms of $\Delta\theta_R$:

$$\Delta\theta_{ch} = \frac{P_{ch}}{P_L} \Delta\theta_R \tag{9.65}$$

Substituting equations 9.55 and 9.56 into equation 9.54 and 9.51 respectively, the tensile strain and change in helix angle of the single helical wire in terms of structural displacements $\Delta\theta_R$ & ε_R of the IWRC are given by :

$$\varepsilon_{ch} = G_1 \varepsilon_R + G_2 \Delta\theta_R \tag{9.66}$$

$$\Delta\tau_{ch} = G_3 \varepsilon_R + G_4 \Delta\theta_R \tag{9.67}$$

By taking total partial derivatives of the equations of curvature and torsion with respect to the structural displacement of the IWRC, the change in curvature and torsion of a single helical wire can be expressed as linearized equations. They are given by :

$$\Delta K'_{ch} = G_5 \, \varepsilon_R + G_6 \, \Delta\theta_R \tag{9.68}$$

$$\Delta\tau_{ch} = G_7 \, \varepsilon_R + G_8 \, \Delta\theta_R \tag{9.69}$$

where the geometrical parameters G_i are given in Appendix, where i = 1, 2, 3, ...

b. Deformation of a Core Wire Within An Outer Strand

The core wire of the outer strand is a single helical wire. Thus, the deformation of the core wire is similar to the deformation of any single helical wire obtained by the "development technique". Therefore, the deformation of the single helical core wire is given by the following expressions :

$$\varepsilon_R = \varepsilon_{sc} + \frac{\Delta\beta}{\tan\beta} \tag{9.70}$$

$$\varepsilon_R = \frac{\Delta r_s}{r_s} + \frac{\Delta\theta_R}{2\pi} + (\tan\beta + \cot\beta)\,\Delta\beta \tag{9.71}$$

$$\varepsilon_{sc} = \frac{\Delta r_s}{r_s} + \frac{\Delta\theta_R}{2\pi} + \Delta\beta \tan\beta \tag{9.72}$$

$$\varepsilon_{sc} = \varepsilon_R \sin^2 \beta + \frac{\Delta r_s}{r_s} \cos^2 \beta + \frac{\Delta \theta_R}{2\pi} \cos^2 \beta \tag{9.73}$$

In these equations, the only unknown is $\Delta r_s/r_s$. However, by using the classical theory of elasticity and taking the Poisson's effect of wire material into consideration. The expression which relates the change of the strand helical radius is given by :

$$\frac{\Delta r_s}{r_s} = L_1^s \varepsilon_R + L_2^s \Delta\theta_R + L_3^s \varepsilon_{sh} + L_4^s \varepsilon_{sc} \tag{9.74}$$

This is obtained by equation 9.74 into equations 9.70 and 9.73 respectively. The linearized equations representing the deformation geometry of the single helical core wire are:

$$\varepsilon_{sc} = I_1 \varepsilon_R + I_2 \Delta\theta_R \tag{9.75}$$

$$\Delta\alpha_{sc} = I_7 \varepsilon_R + I_8 \Delta\theta_R \tag{9.76}$$

$$\Delta K'_{sc} = I_5 \varepsilon_R + I_6 \Delta\theta_R \tag{9.77}$$

$$\Delta\tau_{sc} = I_7 \varepsilon_R + I_8 \Delta\theta_R \tag{9.78}$$

where the geometrical parameters are given in Appendix.

c. Deformation of Double Helical Wire

For an IWRC subjected to axial deformation, the "Development Technique" is again the principal technique applied to evaluate the extension of the double helical wire. In addition to this, the vector differential geometry is also used to evaluate the double helix angle, curvature and torsion along the deformed double helical wire. The approach, which is used to evaluate the deformation of the double helical wire, is given below:

1. Extension of a Double Helical Wire

The extensional deformation of a double helical wire can be derived from its deformed centroidal axis as shown in Figure 9.2 (d). Expressions describing the extensional deformation of the double helical wire are given by :

$$\varepsilon_{sc} = \varepsilon_{sh} + \frac{\Delta\alpha_{sh}}{\tan \alpha_{sh}} \tag{9.79}$$

$$\varepsilon_{sc} = \frac{\Delta r_{sh}}{r_{sh}} + \frac{\Delta\theta^{*}_{sh}}{2\pi} + (\tan \alpha_{sh} + \cot \alpha_{sh}) \Delta\alpha_{sh} \tag{9.80}$$

$$\varepsilon_{sh} = \frac{\Delta r_{sh}}{r_{sh}} + \frac{\Delta\theta^{*}_{sh}}{2\pi} + \Delta\alpha_{sh} \tan \alpha_{sh} \tag{9.81}$$

$$\varepsilon_{sh} = \varepsilon_{sc} \sin^2 \alpha_{sh} + \frac{\Delta r_{sh}}{r_{sh}} \cos^2 \alpha_{sh} + \frac{\Delta\theta^{*}_{sh}}{2\pi} \cos^2 \alpha_{sh} \tag{9.82}$$

As usual, the unknowns are $\Delta r_{sh}/r_{sh}$ and $\Delta\theta^{*}_{sh}$ as found in the above equations. By applying the classical theory of elasticity the former parameter is given by:

$$\frac{\Delta r_{sh}}{r_{sh}} = L_1^o \varepsilon_R + L_2^o \Delta\theta_R + L_3^o \varepsilon_{sh} \qquad (9.81)$$

where L_i^o is given in Appendix.(i = 1, 2, 3)

The latter unknown $\Delta\theta^*_{sh}$ corresponds to the angle of twist per lay length of the "straightened" outer strand of the IWRC. It is necessary to relate the angle of twist per lay length of the IWRC to the induced angle of twist on each individual helical wires. By using the similar triangle developed from the double helical wire, an expression relating the angle of twist of the helical outer strand with the angle of twist of the IWRC is given by :

$$\Delta\theta^*_{sh} = P_{sh}\Delta\theta_{sh}/r_{sh} \qquad (9.82)$$

where

$$\theta_R = \Omega\,\theta_{sh} \qquad (9.83)$$

$$\Omega = r_{sh}\cos\beta\tan\alpha_{sh} / r_{sh} \qquad (9.84)$$

This relationship has been given in Chapter Four. By taking the total partial derivative of θ_R with respect to Ω and θ_{sh}, and then back substituting to equation 9.82 the second unknown in terms of the structural displacement of the IWRC is given by :

$$\frac{\Delta\theta^{*}_{sh}}{2\pi} = S_{15}\ \varepsilon_{R} + S_{15}\ \Delta\theta_{R} + S_{17}\ \varepsilon_{sc} + S_{18}\ \varepsilon_{sh} \qquad (9.85)$$

By substituting equation 9.85 back to equation 9.81, the linearized tensile strain along the double helical wire is given by :

$$\varepsilon_{sh} = J_1\ \varepsilon_{R} + J_2\ \Delta\theta_{R} \qquad (9.86)$$

where J_1 and J_2 are given in Appendix

2. Change of Double Helical Wire Geometry

The vector method, which is applied in this sub-section, is to determine the change of geometry of the double helical wire with respect to the extension of this wire.

i. Change in Double Helix Angle

The change in double helix angle corresponding to the change in structural displacements of the IWRC is given by :

$$\Delta\alpha_{dh} = \bar{\alpha}_{dh} - \alpha_{dh} \qquad (9.87)$$

where the final helix angle of the double helical wire resulted from the structural displacements is given by :

$$\alpha_{dh} = \tan^{-1}\left\{ \frac{|\ \dot{Z} + d\dot{Z}\ |}{[\ (\dot{X} + d\dot{X})^2 + (\dot{Y} + d\dot{Y})^2\ ]^{1/2}} \right\} \qquad (9.88)$$

ii. Change in Curvature and Torsion of a Double Helical Wire

The changes in curvature and torsion of the double helical wire are essential parameters for evaluating the flexural bending and twisting of the wire resulting from extension.

The change in curvature of the double helix is given by :

$$\Delta K'_{dh} = \bar{K}'_{dh} - K'_{dh} \qquad (9.89)$$

The change in torsion of the double helix is given by :

$$\Delta \tau_{dh} = \bar{\tau}_{dh} - \tau_{dh} \qquad (9.90)$$

where the final curvature and torsion of the double helix are given by :

$$\bar{k}'_{dh} = \frac{\{[(\dot{Y}\ddot{Z} + d\dot{Y}\ddot{Z})-(\dot{Z}\ddot{Y}+d\dot{Z}\ddot{Y})]^2+[(\dot{Z}\ddot{X}+d\dot{Z}\ddot{X})-(\dot{X}\ddot{Z}+d\dot{X}\ddot{Z})]^2+ \ldots\ldots [(\dot{X}\ddot{Y}+d\dot{X}\ddot{Y})-(\dot{Y}\ddot{X}+d\dot{Y}\ddot{X})]^2\}}{\{(\dot{X}+d\dot{X})^2 + (\dot{Y}+d\dot{Y})^2 + (\dot{Z}+d\dot{Z})^2\}^{3/2}} \qquad (9.91)$$

and

$$\bar{\tau}_{dh} = \frac{\begin{vmatrix} (\dot{X}+d\dot{X}) & (\dot{Y}+d\dot{Y}) & (\dot{Z}+d\dot{Z}) \\ (\ddot{X}+d\ddot{X}) & (\ddot{Y}+d\ddot{Y}) & (\ddot{Z}+d\ddot{Z}) \\ (\dddot{X}+d\dddot{X}) & (\dddot{Y}+d\dddot{Y}) & (\dddot{Z}+d\dddot{Z}) \end{vmatrix}}{[(\dot{Y}\ddot{Z} + d\dot{Y}\ddot{Z})-(\dot{Z}\ddot{Y}+d\dot{Z}\ddot{Y})]^2+[(\dot{Z}\ddot{X}+d\dot{Z}\ddot{X})-(\dot{X}\ddot{Z}+d\dot{X}\ddot{Z})]^2+}$$

$$\cdots\cdots\cdots \frac{}{[(\dot{X}\ddot{Y}+d\dot{X}\ddot{Y})-(\dot{Y}\ddot{X}+d\dot{Y}\ddot{X})]^2} \quad (9.92)$$

where $\cdot$ first derivative of coordinates

$\cdot\cdot$ second derivative of coordinates

$\cdots$ third derivative of coordinates

At this point, the analysis has sufficient known parameters to evaluate the mechanical responses of both Lang's lay and ordinary type of IWRC. In view of the complexity, Computer programmes have been produced for the numerical analysis of the mechanical response of the IWRC.

iii. Change in Length of a Double Helical Wire

As well as the development method applied to evaluate the change in length on the double helical wire under full inter-wire slip condition, ie frictionless condition. The change in axial length of the double helical wire under full inter-wire grasp condition (ie where full inter-wire slippage can occur between wires) can also be determined by the vector method. The change in axial length along the double helical wire is given by:

$$\delta S = d\bar{S}_{dh} - dS_{dh} \quad (9.94)$$

Where

$$dS_{dh} = (\ddot{X}^2 + \ddot{Y}^2 + \ddot{Z}^2)^{1/2}\, d\theta_{dh} \quad (9.95)$$

By substituting the change in coordinates resulting from the Poisson's effect and the change in wire rotation into equation 9.95, the final differential length $d\bar{S}_{dh}$ can be evaluated.

9.6 DISCUSSION AND CONCLUSION

Based on the author's and Velinsky's approaches, a micro-computer package has been developed for the purpose of evaluating the internal component forces & moments, stresses & strains acting on the wires and the structural responses & properties of the IWRC. A schematic diagram representing the structure of this computer package is illustrated in block diagram 9.6.1. This diagram is as shown below :

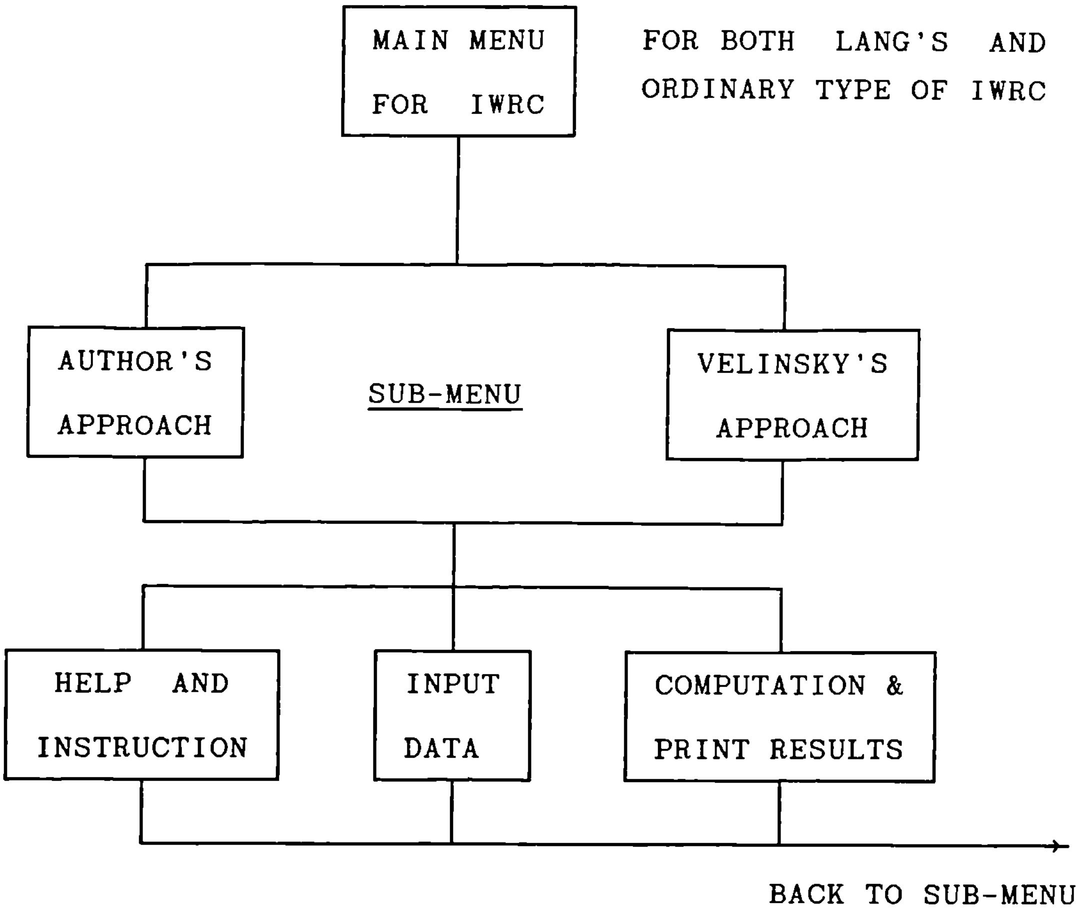

BLOCK DIAGRAM 9.6.1

STRUCTURE DIAGRAM OF THE APPROACH TO IWRC MODELLING

9.6-1 Brief Description of This Section

The sample results presented in the following sub-sections are obtained from the author's own computer package developed for the mathematical modelling of IWRC. The wires dimensions used for the sample analysis are extracted from Velinsky's thesis and are tabulated in section 9.6-2. The material properties of wires for the IWRC are based on those properties of steel wire. Finally, only the fixed end termination condition is considered. Various computer results for the IWRC are presented in section 9.6-2 and 9.6-3.

9.6-2 Results and Discussion (Velinsky's Approach)

The following tables give the dimensions of the IWRC within the 6x19 Seale rope (taken from Velinsky's Thesis) :

Table 9.1 lists the dimensions of wires in various strands (in straight form) used to construct the IWRC.

TABLE 9.1

CORE STRAND (6/1)			
WIRE	RADIUS OF WIRE	HELIX ANGLE	LIMITED HELIX ANGLE
CORE	0.03155 IN	90 DEG.	N.A.
HEL.	0.028925 IN	73.707 DEG.	70.619 DEG.
OUTER STRAND (6/1)			
CORE	0.027725 IN	90 DEG.	N.A.
HEL.	0.025815 IN	81.066 DEG.	72.4125 DEG.

Table 9.2 lists the dimensions of strands used to construct the IWRC.

TABLE 9.2

	RADIUS OF STRAND	HELIX ANGLE	LIMITED H.A.
CORE STRD.	0.0894 IN	90 DEG	N.A.
HEL. STRD.	0.079355 IN	70.83 DEG	67.3504 DEG

Abbreviations used in the figures of this section are given as follows:

C.STD.H.W Helical wire of core strand

HEL.C.W. Helical core wire of outer strand

D.H. WIRE Double helical wire of outer strand

H.W. Helical Wire

Discussion of The Results Obtained From Velinsky's Approach

Figure 9.6.1 shows the tensile strain acting on each of the wires within the IWRC subjected to external tensile load applied to the termination. Obviously, the king wire carries the highest tensile load and the double helical wire carries the smallest tensile load, as illustrated in Figure 9.6.2. This is because double helical wire is the longest wire whereas King wire is the shortest wire within the IWRC.

Figures 9.6.3 and 9.6.4 show the bending and twisting moment developed on the helical wire of the core strand and the outer strand of the IWRC. These two figures illustrate that the effective bending and twisting moments developed on the outer strand are higher than those developed on the single helical wire of the core strand. The author, in this example, intends to emphasize that there is "tertiary bending"* on the outer layer wires of the adjacent strands at the contact location resulted from the unwinding rotation of the outer strand.

Remark:*

For a rope subject to tension or twisting moment, the tertiary bending is regarded as one of the mechanical interactions. When the outer layer wires of a strand are resting in the valleys provided by outer layer wires of the

VELINSKY'S APPROACH
(IWRO)

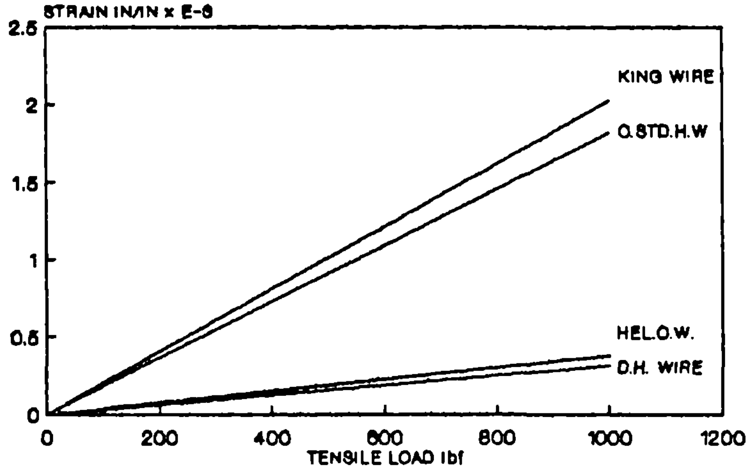

FIGURE 9.6.1
STRAINS VS TENSILE LOAD
(FIXED ENDS CONDITION)

VELINSKY'S APPROACH
(IWRO)

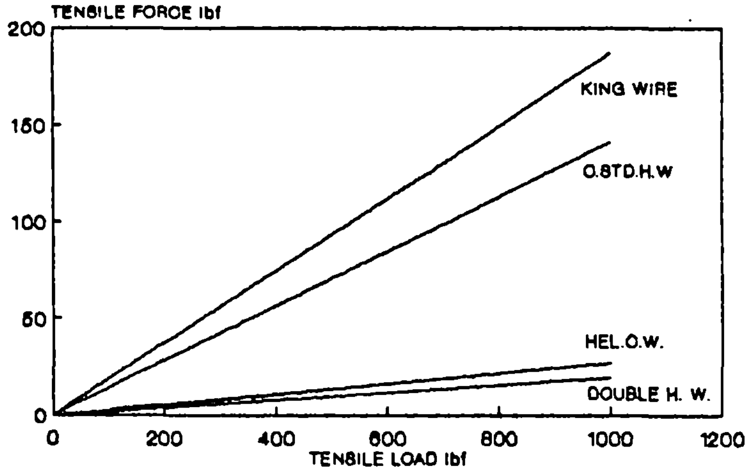

FIGURE 9.6.2
TENSILE COMPONENTS VS TENSILE LOAD
(FIXED ENDS CONDITION)

VELINSKY'S APPROACH
(IWRO)

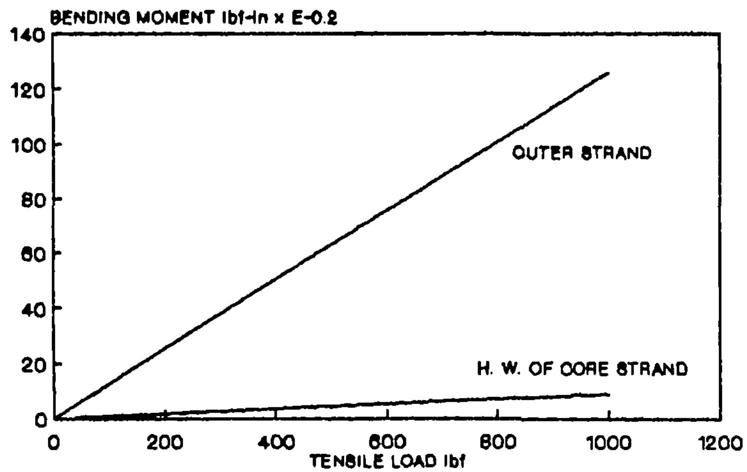

FIGURE 9.6.3
BENDING COMPONENTS VS TENSILE LOAD
(FIXED ENDS CONDITION)

VELINSKY'S APPROACH
(IWRO)

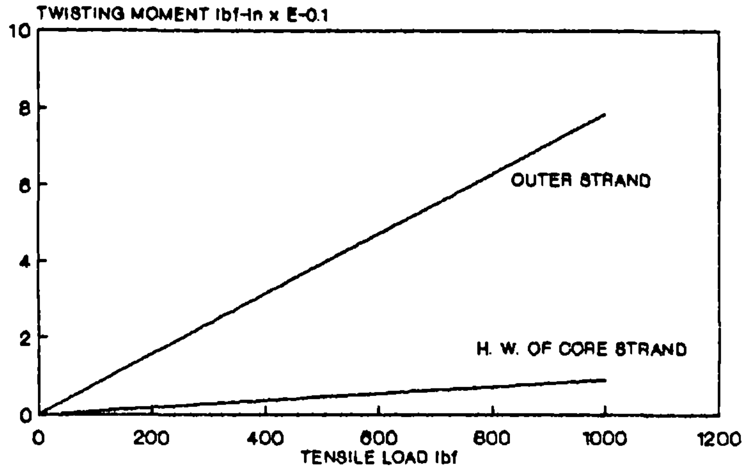

FIGURE 9.6.4
TWISTING COMPONENTS VS TENSILE LOAD
(FIXED ENDS CONDITION)

adjacent strands, then the third type of bending moment will develop on any outer layer wire of the strand resting in the valley at the contact locations provided by the outer wires of the adjacent strands resulted from the unwinding rotation of wires and strands.

The advantage of using Velinsky's approach is that one can evaluate the equivalent bending and twisting moment for each of the strands under the preceding defined termination conditions. The limitations of velinsky's approach are that it is:

a. applied only to frictionless condition,
b. used to evaluate equivalent component forces and moments acting on the single helical strand and
c. applied to evaluate the global mechanical behaviour of a rope; eg notional stiffness of a rope.

9.6-3 Results And Discussions (Author's Approach)

Results obtained from the author's computer package developed for the static analysis of IWRC are presented below:

Abbreviations used in the figures of this section are given as follows:

H.W.	Helical wire
STD & STRD	Strand
IWRC	Independent wire rope core

Figure 9.7.1 shows the tensile strain developed in each helical wire against the tensile strain of the IWRC. These results are similar to those obtained from Velinsky's model. It is because the results obtained are also based on a frictionless model.

Figure 9.7.2 illustrates the variation of bending and twisting component acting on the double helical wire. The "out-of-phase" characteristic between the bending and twisting component on the double helical wire arises basically from the "out-of-phase" characteristic between curvature and torsion of the double helical wire (see Chapter 5).

Figure 9.7.3 illustrates the variation of the shear force and

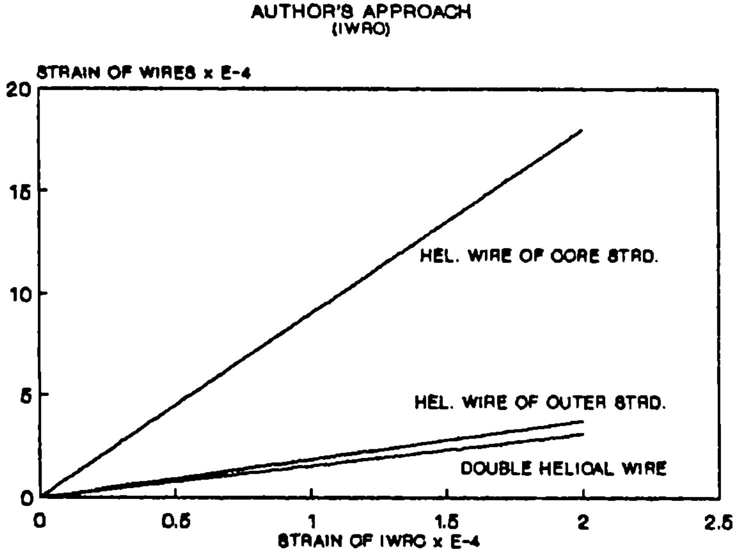

FIGURE 9.7.1
STRAIN OF IWRC VS WIRES STRAIN

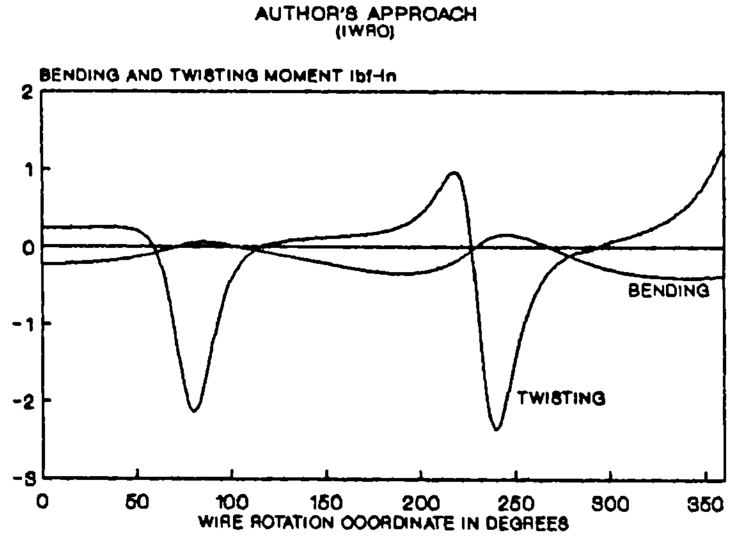

FIGURE 9.7.2
VARIATION OF BENDING & TWISTING
MOMENT ON DOUBLE HELICAL WIRE

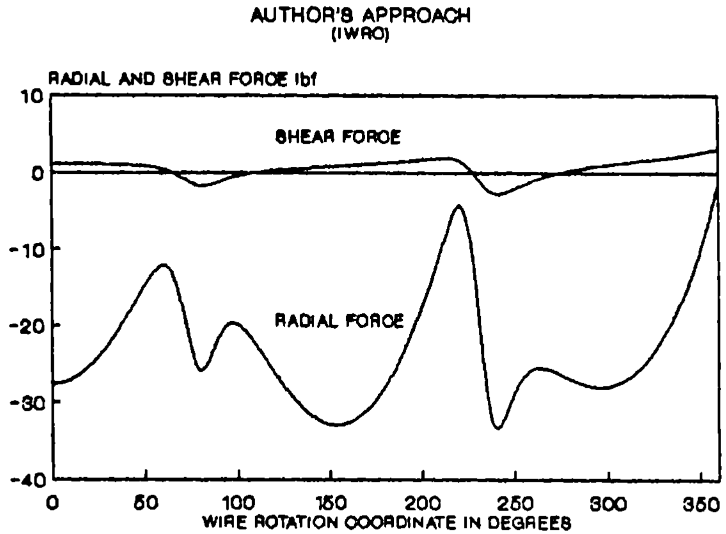

FIGURE 9.7.3
VARIATION OF RADIAL AND SHEAR FORCE
ON DOUBLE HELICAL WIRE

radial force along the double helical wire. The variation of radial force along the double helical wire arises from the variation of curvature, torsion and double helix angle. The variation of depth and width of "grooves" on the surface of the helical core wire of the outer strand reveals this physical significance (see Chapter three).

Figures 9.7.4-7 shows bending moment, twisting moment, shear force and radial force developed on the single helical wire of the main core strand and the core wire of the outer strand.

Figure 9.7.8-9 shows the variation of radius of curvature and torsion along a undeformed and deformed double helical wire.

9.7 CONCLUSION

a. Velinsky's approach is based on a stiffness matrix treatment. Hence, the structural properties of the IWRC under defined termination conditions (ie, fixed end, free end, twisting moment and combined loads) can be addressed. However, one can not apply this approach to evaluate the component forces and moments developed along the double helical wire and the helical core wire of the outer strand. On the other hand, the author's approach provides a closed form method to evaluate the component forces and moments along the double helical

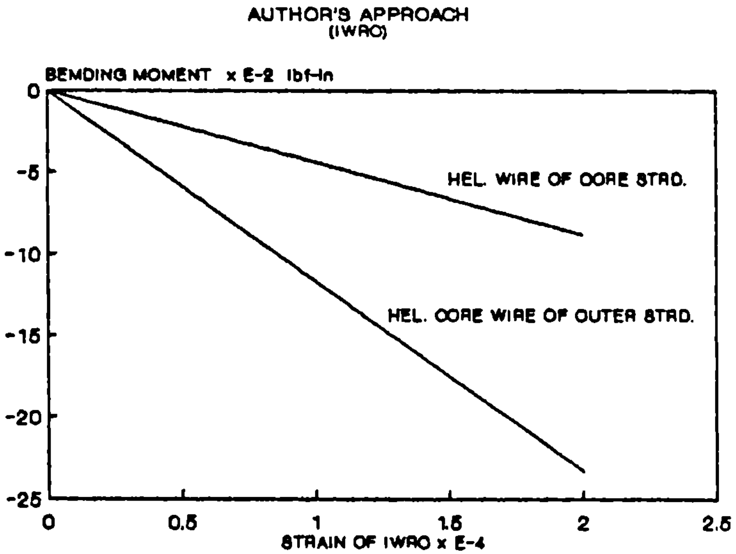

FIGURE 9.7.4
BENDING MOMENT VS IWRC STRAIN

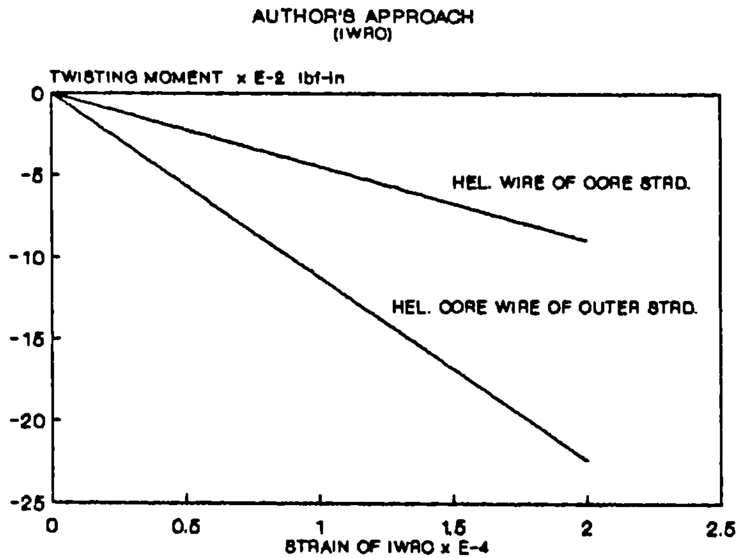

FIGURE 9.7.5
TWISTING MOMENT VS IWRC STRAIN

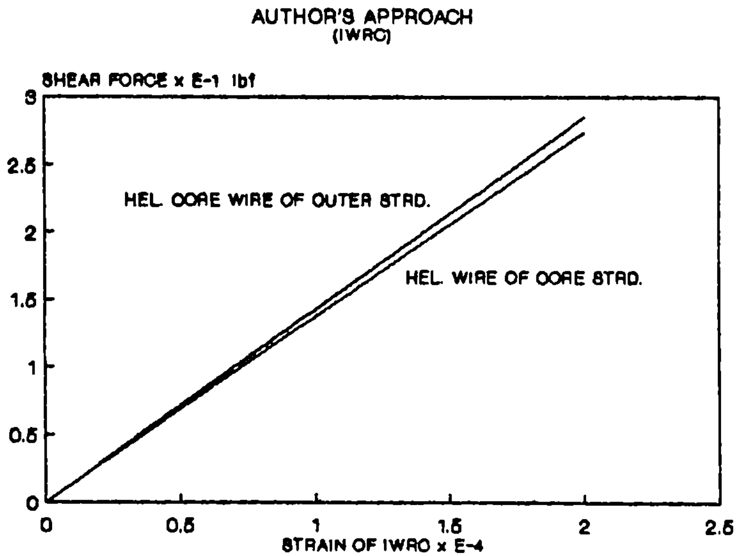

FIGURE 9.7.6
SHEAR FORCE VS IWRC STRAIN

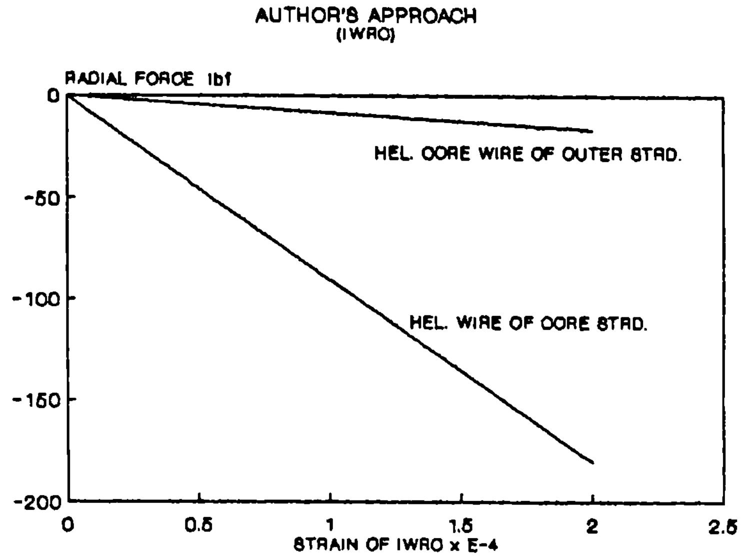

FIGURE 9.7.7
RADIAL FORCE VS IWRC STRAIN

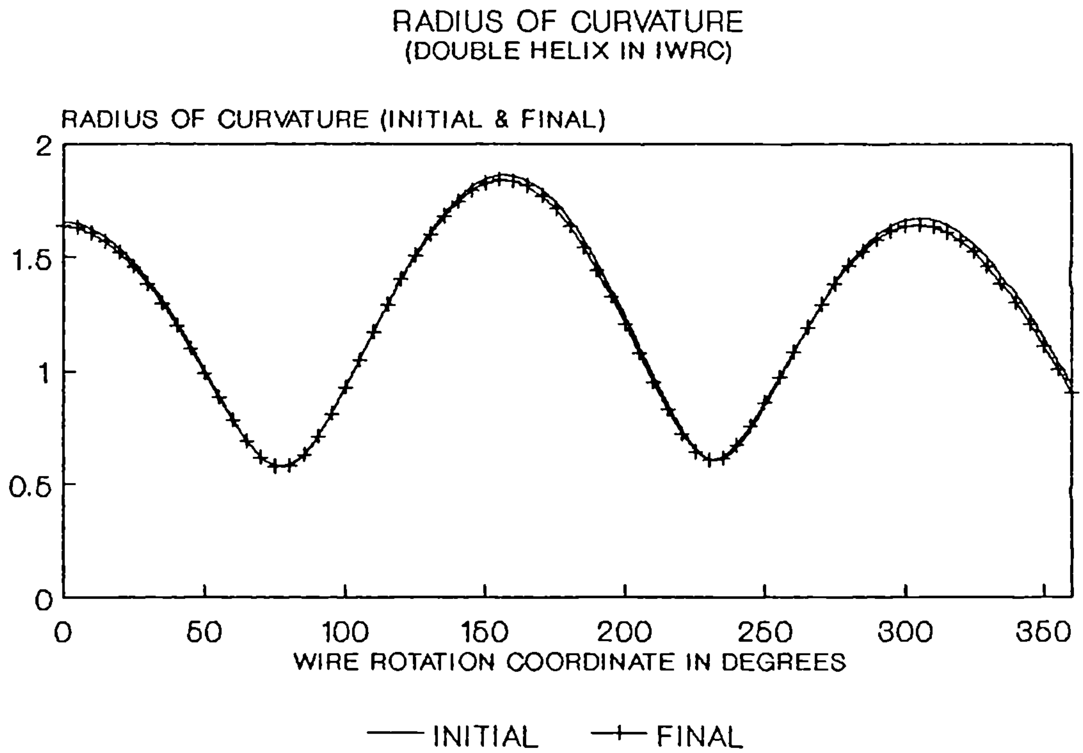

FIGURE 9.7.8
RADIUS OF CURVATURE ON UNDEFORMED
AND DEFORMED DOUBLE HELICAL WIRE

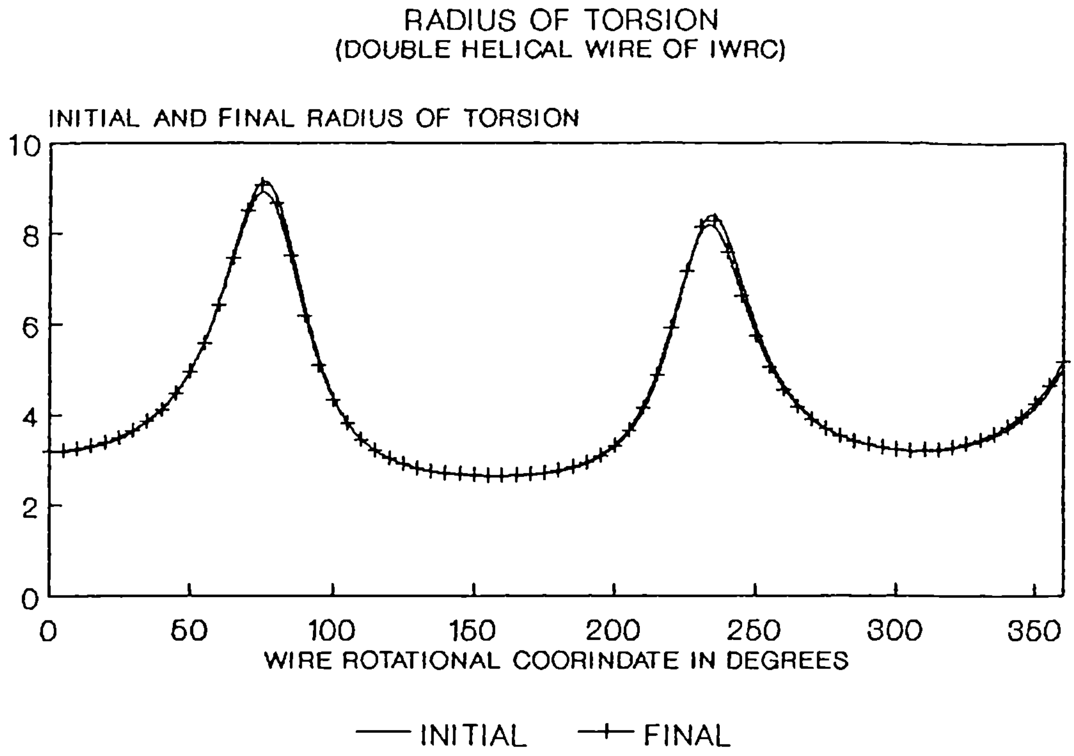

FIGURE 9.7.9
RADIUS OF TORSION ON UNDEFORMED
AND DEFORMED DOUBLE HELICAL WIRE

wire and the helical core wire of the outer strand of the IWRC. However, the author's method is limited to fixed end and combined load conditions.

b. The internal components of forces and moments developed on the single helical wire are constant along the length of the helical wire if the mechanical interactions are ignored.

c. The internal component forces and moments developed on the double helical wire vary along the length of that wire. This is fundamentally due to the variation of double helix geometry.

d. The "out-of-phase" characteristic between bending moment and twisting moment along the double helical wire corresponds to the "out-of-phase" characteristic between curvature and torsion of that wire.

e. The double helical wire develops the smallest tensile strain as compared with the king wire or single helical wires of the IWRC. This is because the double helical wire is longer than the king wire and the single helical wire within any longitudinal section of a rope structure.

9.8 SUGGESTION ON FUTURE RESEARCH WORKS

The author hopes that the present theoretical analysis and approach will be useful to both industry and academic world. It is also hoped that this thesis will motivate others to carry out further theoretical and experimental analysis of other rope problems. There are a number of suggestions about the theoretical analysis of wire rope worthy mentioning:

a. An analytical study of the influence of mechanical interactions, eg secondary and tertiary bending on the double helical wire.

b. To refine the analytical fretting and contact stresses analysis between wires at the contact locations.

c. Mathematical modelling of the strand and rope bent over sheave or wound around drum, eg for a large diameter wire rope subjected to tension-tension fatigue, the rope can be last for millions of block cycles. However, for a rope with similar construction subjected to bending-tension fatigue test, the rope can only last for many thousand block cycles.

d. The influence of kinking of strand and rope to the damage of wires within the region of kinked rope. For a rope subjected to kinking, the service life of the rope will be significantly reduced.

e. Mathematical modelling of the pattern of contact patches within any construction of round stranded ropes. Although it is a potential that the fretting may cause the propagation of fatigue cracks on the helical wires, see Chapter three. The locations of the contact patches on the helical wires and the geometrical configuration will *directly influence the fatigue performance of a* rope.

Wire ropes are complicated structures, characterized by a great variety of geometrical patterns. However, most designs are based on experiences and experimental grounds. Therefore, it will be very useful if more research work can be carried out on theoretical aspects.

APPENDIX

BIBLIOGRAPHY

REFERENCES ON WIRE ROPE HISTORY

1.1 Clark,P.R. (1930)
The Development Of The Wire Rope
Inst. Petroleum Tech. J1, Vol 16, 1930 PP464-471.

1.2 Forestier-Walker,E.R. (1952)
A History Of The Wrie Rope Industry In Grest Britain
British Wire rope Manufacturers, 1952

1.3 Hendrick,R.F. & Edwards, E.H. (1953)
Wire Rope Origin And Development,
Wire And Wire Products, Vol. 28, No. 8 August 1953, PP 777-833.

1.4 Vivian, C.H. (1961)
The Generalogy Of Wire Rope,
Compressed Air Mad.
V41, N11, Nov., 1961, PP5182-8

1.5 Pearsall, R. (1971)
Early Days Of Wire rope,
Wire Industry, August 1971, PP 558

1.6 Sayenga,D. (1980)
The Birth And Evolution Of The American Wire Rope Industry,
Proc. Of The First Annual Wire Rope Symposium, Denver, Colorado

Published By Engineering Extension service, Washington state University, Pullman, Washington, USA, March 1980, PP275-335.

1.7 Weber,W. (1974)
Development And Production Of Wire Rope (1)
Wire World International, Vol. 16,Nov/Dec., 1974 PP286-291

1.8 Weber,W. (1975)
Development And Production Of Wire Rope (2)
Wire World International, vol 17, Jan/Feb., 1975, PP20-24

1.9 Costello,G.A. (1978)
Analytical Investigation Of Wire Rope
Applied Mechanics Reviews, Vl .31, No.7, July 1978, PP897-899

1.10 Utting,W.S. (1984)
A Survey Of Literature On The Behaviour Of Wire Ropes,
Wire Industry, Sept, 1984, PP623-629

1.11 Bahke,E.H.E, (1985)
150 Years Of Wire Rope Research,
Wire, vol 35, Jul/Aug, 1985, PP 148-52

REFERENCES ON WIRE ROPE MODELLING (HRUSKA'S APPROACH)

2.1 Hall, H.M. (1951)
Stresses In Small Wire Ropes
Wire, March 1951, pp.228, & 258

2.2 Hruska, F.H. (1951)
GEOMETRIE IM DRAHTSEIL
DRAHT 4 1953 Nr.5

2.3 Hruska, F.H. (1951)
Calculation Of Stresses In Wire Ropes
Wire, September 1951 pp.766-801.

2.4 Hruska, F.H. (1952)
Radial Force In Wire Ropes
Wire, May 1952 vol 27 pp. 459-463

2.5 Hruska, F.H. (1953)
Tangential Forces In Wire Ropes
Wire Amd Wire Products, May, 1953 vol.28, pp. 455-460

2.6 Cress, H.A. (1955) MSc Thesis
A Theoretical Investigation Of Contact Stresses In A 6 x 7 Wire Rope The Ohio State University 1955

2.7 Starkey, W.L. & Cress, H.A. (1959)
An Analysis Of Critical Stresses And Mode Of Failure Of A Wire Rope. J, Of Engineering For Industry, Nov, 1959 pp.307-311

2.8 Leissa, A.W. (1959)
Contact Stresses In Wire Ropes
Wire And Wire Products, Vol. 34 March, 1959 pp. 307-314, pp 372-373

2.9 Bert, C.W. And Stein, R.A. (1962)
Stress Analysis Of Wire Rope In Tension And Torsion
(Determination Of Contact Forces) Part I & II
Wire and Wire Products, May,V37, pp.621-624 and June pp. 769-770,772 & 816

2.10 Gibson, P.T. Cress, H.A. Kaufman, W.J. Gallant, W.E (1970)
Torsional Properties Of Wire Rope
March 1, 1970 pp.1-11

2.11 Reemsnyder, H.S. (1972)
The Mechanical Behavior And Fatigue Resistance Of Steel Wire Strand And Rope
Internal Report, Bethleham Steel Corporation, June 1972

REFERENCES ON MATHEMATICAL MODELLING OF WIRE ROPE

(COSTELLO'S APPROACH)

3.1 Phillips, J.W. And Costello, G.A. (1973)
Contact Stresses in Twisted Wire Cables
Proc. ASME JL Eng. Mech.Div. 1973 Vol.99, pp.331-341

3.2 Costello, G.A. And Phillips, J.W. (1974)
A More Exact Theory For Twisted Cables
Proc. ASCE, J. ENG. Mech. DIV. 1974 Vol.100 pp.1096-9

3.3 Costello, G.A. And Phillips, J.W. (1976)
Effective Modulus Of Twisted Wire Cables
Journal Of The Engineering Mechanics Division, February, 1976
pp.171-181

3.4 Costello,G.A. (1977)
Large Deflections Of Helical Spring Due To Bending
J. Applied Mechanics Trans, Proc Paper 12964, June, 1977
pp.479-87

3.5 Costello, G.A. And Sinha, S.K. (1977)
Static Behavior Of Wire Rope
Journal Of The Engineering Mechanics Division December, 1977
pp.1011-1023

3.6 Costello, G.A. And Sinha S.K. (1977)
Torsional Stiffness of Twisted Wire Cables
J. Of Then Engineering Mechanics Division, Vol.103,No.EM4,
Aug, 1977 pp. 767-70

3.7 Phillips, J.W. And Costello, G.A. (1979)
General Axial Response Of Stranded Wire Helical Spring
Int,J.Linear Mechanics Vol14, pp.247-257.

3.8 Costello, G.A. And Miller, R.E. (1979)
Lay Effect Of Wire Rope
Engineering Mechanics Division Vol.105 No. EM4 August, 1979
pp.597-607

3.9 Costello, G.A. And Miller, R.E. (1980)
"Static Response of Reduced Rotation Rope
J, of The Engineering Mechanics Division Vol.106, No.EM4,
August 1980 pp. 623-631

3.10 Phillips,J.W., Miller,R.E. and Costello,G.A (1980)
Contact Stresses In A Straight Coss-Lay Wire Rope
Proc. 1st ann. Wire Rope Symp, Denver, March 1980 pp.177-199

3.11 Butson,G.J. (1981) PhD Thesis
Static And Dynamic Analysis Axially Loaded Wire ropes
University Of Illinois At Urbana-Champaign 1981

3.12 Velinsky,S.A. (1981) PhD Thesis
Analysis Of Wire Ropes With Complex Cross Section
University Of illinois At Urbana-Champaign 1981.

3.13 Costello, G.A. And Butson G.J. (1982)
Simplified Bending Theory For Wire Rope
ASCE J. ENG. MECH. DIV April, 1982 Vol.108, Nem2, pp.219-227

3.14 Phillips,J.W. and Fotch,P.D. (1983)
Preliminary Analysis Of Filler-Wire Hoisting Rope
Proc. 18th Midwestern Mechanics Conf., May 16-18 1983 PP397-340.

3.15 Costello,G.A. (1983)
Stresses In Multilayer Cables
J. Of Energy Resources Technology, Sept., 1983, Vol 105 PP337-340.

3.16 Velinsky,S.A., Anderson,G.L. and Costello G.A. (1984),
Wire Rope With Complex Corss Section,
J, Eng. Mech. Div. Mar,.1984, Vol.110 No.3, PP 380-91

3.17 Chi-Hui Chien And Costello, G.A. (1985)
Effective Length Of Fractured wire in Wire Rope
ASCE, Vol. 111, No. 7, July, 1985. pp.953-961

3.18 Velinsky, S.A. (1985)
Analysis of Fibe-Core Wire Rope
Transactions of the ASME, vol.107, Sep.,1985, pp.388-389.

3.19 Velinsky, S.A. (1985)
General Nonlinear Theory For Complex Wire Rope,
Int, J. Mech. Sci. Vol 27, No. 7/8 PP 497-507, 1985

3.20 Phillips, J.W. And Costello, G.A. (1985)
Analysis Of Wire Ropes With Internal Wire rope Cores
Transactions of the ASME, Vol.52, Sept,. 1985, pp. 510-516.

3.21 Love,A.E.H. (1944)
A treatise On The Mathematical Theory Of Elasticity
Dover Publication Inc., 1944

3.22 Kirchhoff,J.F. (1859)
Math (Crelle) ,BD 56, 1859

3.23 Timoskenko,S. (1956)
Strength Of Materials Part II 3rd Ed.
D. Van Nostrand Comapny, Inc. New York Mar., 1956 PP 295-298

3.24 LeClair R.A. & Costello G.A. (1988)
Axial Bending And Torsional Loading Of A Strand With friction
Journal Of Offshore Mechanics And Arctic Engineering Vol. 110
Feb. 1988 PP 38-42.

3.25 Velinsky S.A. & Schmidt J.D. (1988)
A Simplified Treatise On The Effect Of Wear In Cables
Journal Of Offshore Mechanics And Arctic Engineering vol. 110
Feb. 1988 PP-32-37

REFERENCES ON MATHEMATICAL MODELLING OF WIRE ROPE

(BY INDEPENDENT INVESTIGATOR)

4.1 Machida,S and Durelli,A.J. (1973) , (Supported By Experiments)
Response OF A Strand To Axial And Torsional Displacements,
Jnl Of Mech Eng Science,Vol15,No4,1973,PP241-251.

4.2 Nowak,G., (1974)
Computer Design Of Electronmechanical cables For Ocean application,
Proc of 10th Annual Conference, Marine Tech Society, Washington DC,1974, PP293-305.

4.3 Knapp,R.H. (1975)
Non-linear Analysis Of A Helically Armoured Cable With Non-Unform Mechanical Properties In Tension, IEEE Paper No 75CHO,(95-1,) OEC,Proc IEEE Conference On Engineering In the Ocean, Environmental And Marine Tech Sec,11th Annual Meeting,San Diego,Cal,1975,PP155-164

4.4 Huang,N.C. (1978)
Finite Extension Of An Elastic Strand With A Central Core,
ASME Jnl Of App. mechs, vol 45, No4, 1978, PP852-858

4.5 Knapp,R.H. (1979)
Derivation Of A New Stiffness Matrix For Helically Armoured Cables Considering Tension And Torsion, Intl J. For Numerical Methods In Engineering,vol14,1979, PP515-529

4.6 Knapp, R.H. (1988)
Helical Wire Stresses In Bent Cables
Journal Of Offshore Mechanics And Arctic Engineering
Feb., 1988 Vol. 110 PP 55-58.

REFERENCES ON ROPE GEOMETRY

5.1 Stein,R.A. And Bert,C.W. (1962)
Radius Of Curvature Of A Double Helix
J. Of Engineering For Industry, Transactions Of The ASME
Technical Briefs, August, 1962 PP394-95

5.2 Karamchetty,S.D.S.R. And Yuen,W.Y. (1979)
Contact Problems In Wire Ropes
J. Of Mechanical Design, Transactions Of The ASME Vol101 Oct,1979
PP 702-10

5.3 Karamchetty,S.D.S.R. (1978) & (1980)
Some Geometrical Characteristics Of Wires In Wire Ropes And Cables
Proc. of 9th SECTAM, developments In theoretical And Applied
Mechanics Vol 9, PP 519-541 May 1978 and Wire Journal 1980, V13,
N11, PP98-104

5.4 Kunoh,T and Leech,C.M. (1985)
Curvature Effects On Contact Position Of Wire Strands
Int.J. Mech Sci, Vol 27, No. 78, PP 465-70. 1985

5.5 Wiek,L. (1986)
Staalkables Geometrie en Levensduur Proefschrift,
Werktuigouwkundig Ingenieur Gebroen Te's Gravenhage, 7
October,1986 Te16.00 UUR

5.6 Spiegel, M.R. (1981)
Vector Analysis,
Schaum's Outline Series Asian Student Edition, May 1981, Chapter II

5.7 Robert, C.F. and Ziebur, A.D.
Calculus and Analytical Geometry,
2nd edition, Prentice-Hall Inc., Chapter IX

5.8 Angus, E.T.
Advanced Calculus
University of California, Los Angeles, Ginn & Company, Chapter XII

5.9 Lee, W.K. Casey, N.F. and Gray, T.G.F. (1987)
Helix Geometry In Wire Rope
Wire Industry, August, 1987, PP461-468

REFERENCES ON EXPERIMENTAL TEST OF ROPE IN BRITAIN

(WITH MATHEMATICAL MODEL)

6.1 Matheson, J.A.L. (1948)
The Mechanics Of Locked Coil Ropes
Engineering, June 18 and 25, 1948, PP578-581 and 601-604

6.2 Hansom, O.P. (1948)
Mechanics Of Locked coil Steel Wire Ropes, PhD Thesis
University Of Birmingham.

6.3 Slight, G.C. (1949)
The Torsional Properties Of Three & Seven Strand Wire Ropes
With The View To Their Use In Multiple Strand Helical Springs,
B.Sc Thesis, Woolwich Polytechnic Mechanical Engineering
Department.

6.4 Martin, B.C. and Packard, T.J. (1966)
Stresses IN Wire Strand, B.Sc Thesis
University Of Bristol June 1966

6.5 Jones, N. and Christodoulides, J.C. (1980)
Static Plastic Behaviour Of A Strand
Int J Mech Sci, Vol22, 1980, PP 185-195.

6.6 Raoof, M. (1983)
Interwire Contact Forces And The Statics, Hysteretic And
Fatigue

Properties Of Multi-Layer Structure Strands, PhD Thesis.
Imperial College Of Science And Technology, London.

6.7 Hobbs,R.E. and Raoof,M (1983), (With Experiments)
Interwire Slippage And Fatigue Prediction In Stranded Cables
For TLP Tethers, Behaviour Of Offshore structures,
Chryssostomiolis, C, And Connor, Hemisphere Publishing/Mcgraw
Hill, New York,1982, vol2 PP77-99.

6.8 Utting,W.S. (1984)
Experimental And Theoretical Studies On Stress In And
Deformation of Wire Ropes Under Axial Tensile Loads, PhD
Thesis
University Of Liverpool.

6.9 Cascy,N.F. (1984)
The Evaluation Of Wire Ropes By Acoustic Emission And Other
Techniques, PhD Thesis
University Of Cardiff.

6.10 W. S. Utting and N. Jones (1987)
The Response of Wire rope Strands To Axial Tensile Load
Part I and II Experimental Results And Theoretical Predictions
Int. J. Mech Sci 29, No. 9, PP 606-619 and PP 621-636, 1987

REFERENCES ON EXPERIMENTAL STUDY OF WIRE ROPE

7.1 Nesterov, P.O., Shabanov-Kushnarenko, Yu.P. and Kozyuberda, N.I. (1961)
A New Method Of determination Of Stresses In Wire Ropes
Translated From russian, Zavodskaya Laboratoriya, Vol.27, No.2, 1961, PP 191-194

7.2 Dong, R.G. and Steidel, R.P. (1965)
Contact Stress In Stranded Cable
Experimental Mechanics, May 1965, PP 142-147

7.3 Gibson, P.T., Cress, H.A., Kaufmann, W.J. and Gallant, W.E. (1969)
'Torsional Properties Of Wire Rope'
ASME Paper No. 69-DE-34, Proc. Design Eng. Div. conference, N.York, 1969.

7.4 Vandervelt, H.H., Laura, P.A. and Gaffney, P.G. (1969)
Mechanical Behaviour Of Stranded Wire Ropes
Dept Of Mech Engg. Themis prog. No. 893(1968-71) The Catholic Uni Of America, Washington, D.C. 20017

7.5 Durelli, A.J., Machida, S. and Parks, V.J. (1972)
Strains and Displacements On a Steel wire Strand, Naval Engineers Journal, Vol.13, 1973, PP 85-93

7.6 Durelli,A.J. and Machida,S (1973)
Response Of Epoxy Oversized Models Of Strands To Axial And Torsional Loads, Experimental Mechanics, Vol.13, 1973, PP 313-321

7.7 Wiek,L. (1975)
Measured Differences Between Steel Wire ropes In Normal Lay And In Lang Lay, Report,Techniske Hogeschool,Delft, 1975

7.8 Hankus,J. (1977)
The permanent and Percentage Elongation Of Winding ropes In factory Condition',
translated From Polish, Glowny Instytut Gornictwa Katowice 1977, Kommunikat No. 862, PP 3-14.

7.9 Hankus,J. (1978)
Elastic Modulus Of Mine Winding Ropes In conditions Of Static Loading',
In Polish With English Abstract, Glowny Instytut Gormictwo, Katowice 1978, Kommunikat No.695.

7.10 Hankus,J (1978)
Exmination OF Elastic Modulus Of Mine Winding Ropes In Conditions Of dynamic Loading'
In Polish With English Abstract. Katowice 1978, Glowny Instytut Gornictwa, Kom. No.700.

7.11 Wiek,L. (1979)

Strain Gauge Measurements At Multi-strand Non-spinning Ropes, Publ. No. 212, Technische Hogeschool, Delft, Transportkunde, 1979

7.12 Wiek,L. (1981)

Stress deviations In Steel wire Ropes', Proc. OIPEEC Round Table, Cracow, 1981.

REFERENCES ON ROPE TERMINATION AND ATTACHMENTS

8.1 Hilgers,W (1973)
Wire Rope Tail Cones And Alloys
Wire, Nov/Dec 1973, PP251-263

8.2 Christen,R (1973)
Tail cones: does doubling Back Of The Wire Increse Safety,
Wire, Vol.23, E4, 1973, PP 160-164

8.3 Myers,W.H. (1977)
Major Part Of Lifting Devices;Wire Rope End Attachments
Wire Journal, march 1977, PP 67-71

8.4 Gathman,D.W. (1979)
Resin Socketing For Wire Rope Attachments,
Wire Journal, Vol. 12, No. 6 1979, PP 82-85

8.5 Dodd,J.M. (1981)
Resin As a Socketing Medium,
Wire Industry, vol. 48, No. 569, 1981, PP 343-344

8.6 Matanzo,F.Jr. and Metcalf,J.T.Jr (1981)
Efficiency of Wire Rope terminations Used In the Mining Industry
Proc. OIPEEC Round Table, Luxemburg, 1977.

8.7 Chaplin,C.R. and Sharman,R.C. (1983)
Mechanisms Of Load transfer In Resin Socketed Terminations

Int. Wire and Mach. Assoc. Conference On Offshore Applications, Aberdeen, 1983.

8.8 Utting,W.S. (1988)
Wire Loading Near Rope terminations
Wire Industry, March 1988, PP 251-259

MISCELLANEOUS REFERENCES

9.1 National Coal Board. (1966)

Ropeman's handbook. 2nd Edition. 1966.

9.2 British Rope

Blue Strand Steel Rope. Publication No.1220

9.3 American Iron And Steel Institute. (1981)

Wire Rope Users Manual, 2nd Edition, 1981 Chapter 6

9.4 N.F. Casey (1988)

Control/Data Acquisition Systems For Monitoring Changes In Wire Rope Properties. NEL Internal Report DE/3/88

9.5 BS.2763 Round Steel Wire For Wire Ropes

9.6 The Manufacture And Properties Of Steel Wire

By Prof. Dr. Ing. Anton Pomp

The Wire Industry Ltd. 1954

9.7 Wire Rope In Offshore Application

C. Richard Chaplin And Andrew E.Potts

Dept. Of Engineering University Of Reading

Published By The Marine Technology Directorate Ltd.

London Feb., 1988 Fig. 33

9.8 N.F. Casey And W.K. LEE
The Fatigue Of Large Diameter Stranded Wire Rope
International J. Of Fatigue
March 1989, PP 77-84.

9.9 N.E.L. Internal Reports

9.10 SERC Marine Technology Directorate
Behaviours Of Wire Ropes In Offshore Applications
Progress Report On First Phase Of Research Program, January 1984

9.11 Mechanics Of Solids And Structures
By P.P. Benham & F.V. Warnock
Pitmans 1981, PP 98.

9.12 Seely, F.B. And Smith
Advanced Mechanics Of Materials

9.13 Abbott, W.,
Techanical Drawing, 4th Edition
Blackie & son Limited, 1978.

GLOSSARY

GLOSSARY OF WIRE ROPE TERMS

ABRASION Frictional surface wear on the wires of a rope.

AGGREGATE AREA See AREA, METALLIC.

AGGREGATE STRENGTH The estimate of strength derived by summing the individual breaking strengths of the elements of the strand or rope. This estimate does not give recognition to the reduction in strength resulting from the orientation of the wires in the rope, or other factors that may affect efficiency.

ALBERTS LAY See LAY, TYPES.

ALTERNATE LAY See LAY, TYPES.

AREA, METALLIC Sum of the cross-sectional areas of all the wires either in a wire rope or in a strand. Wire sectional shape is approximated by either a circle or an ellipse.

BENDING STRESS Stress that is imposed on the wires of strand or rope by bending.

BIRDCAGE A colloquial description of the appearance of a wire rope forced into compression. The outer strands form a cage shape and, at times, displace the core.

BREAKING STRENGTH The ultimate load at which a tensile failure occurs in the sample of wire rope being tested. The term breaking strength is synonymous with actual strength.

Minimum Acceptance Strength is the strength which is 2½% lower than the catalogue or norminal strength (normally provided by the rope manufacturer). This tolerance is used to offset variations that occur during sample preparation and actual physical test of a wire rope.

Nominal Strength is the published (catalogue) strength calculated by a standard procedure which is accepted by the wire rope industry. The wire rope manufacturer designs wire rope to this strength, and the user should consider this strength when making design calculations.

BRIDGE CABLE (Structural Strand or Rope) The all-metallic wire rope or strand used as the catenary and suspenders on a suspension bridge.

BRIDGE SOCKET A strand or wire rope end termination made of forged or cast steel that is designed with baskets - having adjustable bolts - for securing rope ends. There are two styles: 1) the closed type has a U-bolt with or without a bearing block in the U of the bolt, and 2) the open type has two eye-bolts and a pin.

BRIGHT ROPE Wire rope fabricated from wires that are not coated.

BRONZE ROPE Wire rope fabricated from bronze wires.

CABLEWAY System for transporting single loads along a suspended track cable.

CLASSIFICATION Group, or family designation of wire rope constructions with common strengths and weights.

CONSTRUCTION Geometrical design description of the wire rope. This includes the number of STRANDS in a rope, the number of WIRES per strand and the pattern of wire arrangement in each STRAND.

CONSTRUCTIONAL STRETCH The stretch that occurs when the rope is loaded. It is due to the helically laid wires and strands generating a constructing action that compresses the core of the rope and the core of the strand and generally brings all of the rope into close contact.

CORE The axial member of a wire rope about which the strands are laid.

CORROSION Chemical decomposition of the material of wires in a rope through the action of moisture, acids, alkalines or other destructive agents inside and outside the rope.

CORROSION-RESISTING STEEL Chrome-nickel steel alloys designed for increased resistance to corrosion of wires in the wire rope.

COVER WIRES Outer layer of wires of a strand.

CROSS LAY See LAY, TYPES.

CROWD ROPE A wire rope used to drive or force a power shovel bucket into the material that is to be handled.

CYLINDRICAL DRUM A hoisting drum of uniform diameter. See DRUM.

DESIGN FACTOR In a wire rope, it is the ratio of the norminal strength to the total working load.

DRAGlINE a) Wire rope used for pulling excavating or drag buckets, and b) name applied to a specific type of excavator.

ELASTIC LIMIT Stress limit above which permanent deformation will take place within a piece of material.

END ATTACHMENT The accessories which are attached to the end termination of ropes or strands for transmitting loads to the rope or strand body.

END CONDITIONS The mathematical term which is used to described how the external loads applied to the rope terminations. There are four common end conditions namely fixed ends, free ends, twisting alone and combined loads (ie, torsion and tension).

END TERMINATION The treatment at the end or ends of a length of wire rope. Usually made by forming an eye or attaching a fitting and designed to be the permanent end termination on the wire rope that connects it to the load.

FACTOR OF SAFETY In the wire rope industry, this term was originally used to express the ratio of nominal strength to the total working load. The term is no longer used since it implies a permanent existence for this ratio when, in practice, the rope strenght begins to reduce from the moment it is put into service. See DESIGN FACTOR.

FIBRE CENTER Cord or rope of vegetable or synthetic fiber used as the axial member of a strand (ie core of the strand).

FIBRE CORE Cord or rope of vegetable or synthetic fiber used as the axial member of a rope (ie fibre main core).

FILLER WIRE Small spacer wires within a strand which help position and support other wires. Also the name for the type of strand pattern utilizing filler wires.

FLAT ROPE Wire rope that is made of a series of parallel, alternating right-lay and left-lay ropes, sewn together with relatively soft wires.

FLEXIBLE WIRE ROPE An archaic and imprecise term to differentiate one rope construction from another, such as, 6 x 7 (least flexible) and 6 x 19 classification (somewhat more flexible).

GALVANIZED (of wire) coated with Zinc for protection against corrosion.

GALVANIZED ROPE Wire rope made up of galvanized wires.

GALVANIZED STRAND Strand made up of galvanized wires.

GALVANIZED WIRE Zinc-coated wire which is the most commonly used wire.

GEOMETRICAL PATTERN OF ROPE A geometrical term which is used to describe the pattern of wires in a transverse section of rope. The geometrical pattern of rope is governed by the helix geometry of rope and the sectional geometry of helical wire.

GRADE Wire rope or strand classification by strength and/or type of material, i.e., Improved Plow Steel, Type 302 Stainless, Phosphor Bronze, etc. It does not imply a strength of the basic wire used to meet the rope's nominal strength.

GRADES, ROPE Classification of wire rope by the wire's metallic composition and the rope's nominal strength.

GRADES, STRAND Classification of strand by the wire's metallic composition and the strand's nominal strength. In the order of increasing nominal strengths, the grades are Common, Siemens Martin, Hight-Strength and Extra-High Strength. A Utilities grade is also made to meet apecial rrequirements and its strength is usually greater than High Strength.

HAULAGE ROPE Wire Rope used for pulling movable devices such as cars that roll on a track.

HELIX GEOMETRY OF ROPE The three dimension geometry of wire found in a rounded stranded rope, such as single helix and double helix.

HELICAL RADIUS The distance from the centre of rope or strnad to the centre of any specific helical wire.

IMPROVED PLOW STEEL ROPE A specific grade of wire rope.

INDEPENDENT WIRE ROPE CORE (IWRC) A small flexible wire rope used as the axial member of a larger wire rope to increase the resistance to core crushing.

INNER WIRES All wires of a strand except the outer or cover wires.

INTERNALLY LUBRICATED Wire rope or strand having all of its wire components coated with lubricants.

KINK A deformation of a wire rope caused by a loop of rope tightened. It causes irreparable damage to and an indeterminate loss of strenght in the rope.

LAY a) The manner in which the wires in a strand or the strands in a rope are oriented, or b) the distance measured parallel to the axis of the rope (or strand) in which a strand (or wire) makes one complete helical convolution about the core (or centre). In this context, lay is also referred to as LAY LENGTH or PITCH.

LAY, TYPES

1) Right Lay: The direction of strand or wire helix corresponding to that of a right hand screw thread.

2) Left Lay: The direction of strand or wire helix corresponding to that of a left hand screw thread.

LAY LENGTH See LAY (b).

3) Cross Lay: rope or strand in which one or more operations are performed in opposite directions. A multiple operation product is described according to the direction of the outside layer.

4) Regular Lay (or Ordinary Lay): The type of rope in which the lay of the wires in the strand is in the opposite direction to the lay of the strand in the rope. The crowns of the wires appear to be parallel to the axis of the rope (N.B. appear to be parallel but are not necessarily so).

5) Lang's Lay: The type of rope in which the lay of the wires in the strand is in the same direction as the lay of the strand in the rope . The crowns of the wires appear to be at an angle to the axis of the rope.

(6) Albert's Lay: An old and rarely used term for Lang's lay.

7) Alternate Lay: Lay of a wire rope in which the strands are laid alternately ordinary and Lang lay.

8) Reverse Lay: Another tern for alternate lay.

LOCKED COIL STRAND Smooth-surfaced strand usually made up of shaped, outer wires arranged in concentric layers around a centre of round wires.

MECHANICAL INTERACTIONS The reaction forces, moments and other interactive effects (eg, friction and wear, secondary bending and twisting and other bending and twisting effects at the contact point) which are induced on the helical wires of adjacent strands at the contact points inside the rope due to the mechanical response. Mechanical interactions change as the geometry pattern of a rope changes.

MECHANICAL RESPONSES The internal conponent forces, moments and displacements which are induced along the helical wires (eg, single helix and double helix) due to the external loads applied to the end termination of the strand or rope.

METALLIC CORES See WIRE STRAND CORE and INDEPENDENT WIRE ROPE CORE.

NICKS The contact patches on the wire surface of the rope.

MODULUS OF ELASTICITY Mathematical quantity expressing the ratio, whithin the elastic limit, between stress on a wire rope and the corresponding elongation.

MOORING LINES Galvanized wire rope, usually 6 x 12, 6 x 24, or 6 x 3 x 19 spring lay, for holding ships to dock.

NON-PREFORMED Rope or strand that is not preformed. See PREFORMED STRANDS and PREFORMED ROPES.

NON-ROTATING WIRE ROPE Former term for 19 x 7 or 18 x 7 rope. See ROTATION RESISTANT ROPE or NON-SPINNING ROPE.

NON-SPINNING WIRE ROPE See ROTATION RESISTANT ROPE.

PREFORMED STRANDS Strand in which the wires are permanently formed during fabrication into the helical shape they will assume in the undeformed strand.

PREFORMED WIRE ROPE Wire rope in which the strands are permanently formed during fabrication into the helical shape they will assume in the undeformed wire rope.

PROPORTIONAL LIMIT As used in the rope industry, this term has virtually the same meaning as ELASTIC LIMIT. It is the (notional) value of the load beyond which an increase in load no longer produces a proportional increase in elongation and from which point recovery to the rope's original length is unlikely.

REVERSE BEND Reeving a wire rope over sheaves and drums so that it bends in opposing directions. See REEVE.

REVERSE LAY See LAY, TYPES.

RIGHT LAY See LAY, TYPES.

ROTATION-RESISTANT ROPE A wire rope specially constructed to reduce the tendency of the rope to rotate along its length or at the terminations.

SAFETY FACTOR See DESIGN FACTOR.

SAFE WORKING LOAD This term is potentially misleading. and its use should be avoided when referring to strand and rope. Essentially, it refers to that proportion of the nominal rope strength which can be applied either to move or sustain a load. It is misleading because it is only valid when the rope is new and equipment is in good condition. See RATED CAPACITY.

SEALE The name for a type of strand pattern that has two adjacent layers laid in one operation with any number of uniform sized wires in the outer layer, and with the same number of uniform but smaller sized wires in the inner layer.

SECONDARY BENDING AND TWISTING The interactive effects on the helical wires near the contact region due to the pattern of contact patches.

SECTIONAL GEOMETRY OF HELICAL WIRE The geometry of helical wire cross section, which provides imformation about the configuration of the wire in a rope.

SHEAVE A grooved pulley for wire rope.

SPRING LAY See LAY TYPES.

STAINLESS STEEL ROPE Wire rope made up of corrosion resistant steel wires.

STANDING ROPE (or GUY LINE) Strand or rope, usually galvanized, for stabilizing or maintaining a structure in fixed position.

STRAND A aggregate of round or shaped wires helically laid about a straight axis.

STRAND CORE See WIRE STRAND CORE.

STRETCH The elongation of a wire rope under load.

WARRINGTON The name for a type of strand pattern that is characteized by having one of its wire layers (usually the outer) made up of an arrangement of alternately large and small wires.

WIRE (ROUND) A single, continuous length of metal, with a circular cross-section that is a cold-drawn form rod.

WIRE (SHAPED) A single, continuous length of metal with a non-circular cross-section that is either a cold-drawn or a cold-rolled form rod.

WIRE ROPE A aggregate of wire strands helically laid about a straight axis.

WIRE STRAND CORE (WSC) A wire strand used as the axial member of a wire rope.

Brief Review On

Some Literatures

BRIEF REVIEW ON HRUSKA AND OTHERS

Hall,H.M.[2.1] (1951)

In this paper, the author attempted to prove that the tensile stress on the helical wires of an outer layer are appreciably higher than this on the helical wires of an inner layer within a strand. In his analysis, a strand was considered as a solid rod subjected to a tensile load. The tensile force exerted on the rod was then resolved in the direction of the helical wire. Based on this approach and his observations, he explained that, for a strand subjected to external load, the outer layer wires would break earlier than the inner layer wires. This theory was proved to be wrong by Hruska.

Hruska,F.H.[2.2-2.5] (1951 to 1953)

Hruska's first paper was essentially stimulated by Hall's work on small wire rope. For a strand subjected to a tensile load, the tensile strains of a core wire and of a helical wire can be evaluated from the triangular relationship established from the derived of a single helical wire. Expressions were then developed to determine the tensile stress ratio between the core wire and the helical wire. Finally, the internal tensile forces acting on each of the individual wires are summed in the direction of the external load. He also suggested that ropes could carry load even when the wires are broken at different locations. This is because of the existence of the inter-wire friction amongst the adjacent wires.

Hruska's second paper dealt specifically with radial forces in strands and ropes. A theory was developed in order to quantify these forces. He also explained that radial forces increase inwards for each layer of rope construction. Hence, this could produce very high contact stresses at the contact points for the wires in the inner layer of the strand.

Hruska's third paper considered tangential forces induced on the helical wires within a rope. For a rope subject to tensile load, he showed that unwinding torque will develop at the rope terminations. He then went further and explained that the unwinding moment of a Lang's lay rope is much greater than that of the ordinary lay rope (also called regular lay rope). If both terminations are firmly fastened, then the unwinding torque will be constrained.

Hruska's fourth paper dealt with sectional geometry of helical wire and reaction forces at the contact position. He showed that the cross sectional shape of the helical wire can be considered as an ellipse. Similar approach was also appeared in Costello and Phillips' paper[3.1].

Cress,H.A.[2.6] (1955)

A mathematical investigation of contact stresses in a 6 x 7 wire rope (ie IWRC) was explored by Cress in his MSc project. Hruska's approach and Hertzian contact stresses theory were applied to quantify the contact stresses at the helical wires of a 6/1 strand. The geometrical features of the helical wires at the contact location were idealized by two parallel cylinders and two cross cylinders with equal diameter.

Leissa,A.W.[2.8] (1959)

Leissa was probably stimulated by Cress's work on the contact stresses in a 6/1 strand subjected to tensile load. He showed that there are two types of possible contacts (contacts within same layer and contacts between adjacent layers) between neighbouring strands within a rope. Based on Hruska's model and Hertzian contact theory, he then considered the critical case of contact points between adjacent strands in the same layer. The results showed not only the severity of the contact stresses but also the complexity of the analysis.

Startkey,W.L. and Cress H.A.[2.7] (1959)

In response to Leissa's work, Startkey and Cress offered minor improvements to Lessa's analysis by introducing the failure theory. A similar type of contact stress analysis for a 6 x 7 wire rope under tensile load was also considered.

They suggested that the cross-over point contact between adjacent strands is more critical than the line contact between adjacent strands.

Bert,C.W. and Stein,R.A.[2.9] (1962)

Bert and Stein improved the geometry of curvature at the contact location which was initially approximated by the geometry of two cross-over straight cylinder as shown in Startkey and Cress's paper. However, Hruska's type of approach applied to evaluate the contact force, the tensile stress between a core wire and a helical wire was still being used.

Gibson,P.T., CRESS,H.A., Kaufman, W.J. & Gallant, W.E.[2.10] (1970)

The tension-torque characteristics of round stranded ropes were studied by Gibson and others. Hruska's approach was applied in their study. They concluded that the torque characteristics of round stranded ropes and fibre core ropes which were constructed either with round strands or with flattened strands, will behave linearly with respect to the applied tensile load.

Reemsnyder,H.S.[2.11] (1972)

A research report on the mechanical behaviour and fatigue resistance of steel wire, strand and rope was published by Bethlehem steel corporation. Hruska's type of approach to the analysis of tensile stress, tensile force, radial force and rope unwinding torque acting on the helical wire was used. In addition to this, the contact stress approach of Leissa and the bearing pressure ratio of Drucker-Tachau were also used.

BRIEF REVIEW ON COSTELLO AND OTHERS

G.A.Costello and J.W.Phillips[3.1, 3.2 & 3.3] (1973, 74 76)

Costello and Phillips took a more fundamental approach in modelling the responses of a helical wire within a strand. Each individual wire within a strand was treated as a thin rod [3.21] subjected to tension, bending, twisting, shear force and radial force. Fundamental expressions dealing with the evaluation of approximate helical radius, section of helical wire, contact forces, and contact angle between two adjacent wires, were developed. They then went further to predict the effective modulus of a twisted wire cable. In order to use a set of six indeterminate differential equations as established in the rod theory which they applied to model the helical wires two approximate expressions for bending and twisting (also from rod theory) were introduced in their analysis. These two expressions are:

$$G' = A(k_1' - k_0') \quad (1.2.1)$$

$$H = C(\tau_1 - \tau_0) \quad (1.2.2)$$

Hence, shear force, radial forces and effective modulus for twisted wire cables can be evaluated.

A similar study, for prediction of the radial force and wire sectional geometry for a 6/1 strand, had also been shown earlier by Hruska in a article called "Geometrie im Drahteil".

G.A.Costello[3.4] (1977)

In this paper, the six differential equations of equilibrium from rod theory were used for the prediction of the large deflection of helical spring due to bending. In order to evaluate the twisting moment, normal and binormal bending moment acting on the spring, Costello assumed that in the case where Poisson's ratio (ie ν) equals zero, the flexural bending stiffness equals the flexural twisting stiffness. Then bending and twisting component can be calculated by using the differential equations established in the rod theory. By substituting the twisting energy, normal and binormal bending energy, dissipated from the helical spring due to deformation, into the strain energy equation for the spring (see Timoshenko's[3.23] strain energy method), and by integrating the strain energy equation, the deflection of the spring in terms of curvature and rotation of the centroidal axis of the spring, resulting from bending, can be calculated.

G.A.Costello and S.K.Sinha[3.5-3.6] (1977)

Six differential equations from rod theory were further used to analyze the static behaviour of wire rope (ie 6 x 7 rope with fibre core) and torsional stiffness of twisted wire cables (ie 6/1 strand). In the first paper, it was assumed that the fibre core carried no external load. To proceed the analysis by rod theory, each helical strand was idealised by a helical rod. Results were presented as a normalized axial force as a function of axial strand strain. In the second paper, a cable was considered to be constructed without a core wire. The analytical procedure was similar to the first paper. Results were presented as a normalized axial moment as a function of rotational cable strain.

G.A.Costello and J.W.Phillips[3.7] (1978)

Again, six differential equations from rod theory were used to analyze the static response of a 3/1 stranded helical spring. In this paper, Timoshenko's spring theory was used to approximate the flexural bending stiffness of the stranded helical spring.

G.A.Costello and R.E.Miller[3.8] (1979)

Rod theory and approximate bending stiffness from spring theory were used to analyse the lay effect of wire rope. In this study, the tensile stiffness and flexural bending stiffness of ordinary lay rope and of Lang's lay rope were compared. Costello and Miller then concluded that, for a Lang's lay rope subjected to tension, it has effectively no stiffness due to unwinding moment. Therefore, Lang's lay rope should not be allowed to be used with terminations free from rotation. Ordinary lay rope, on the other hand, tends to stiffen as the load is increased, and therefore can be used with swivel termination.

G.A.Costello and R.E.Miller[3.9] (1980)

Equations from rod theory was still used. The static response of 'reduced rotation' rope (ie a 1 x 19 multi-layer strand with inner left lay wire and outer right lay wire) was studied. The results were presented in such the way that the initial helix angle of the outer layer wires was expressed as a function of the initial helix angle of the inner layer wires. Costello and Miller concluded that, for the outer layer wires with given helix angle, there are two possible helix angles for the inner layer wires. Then, for a cross-lay multi-layer strand subjected to tensile load, the rotation provoked from the inner layer wires can be counterbalanced by that of the outer layer wires (in this study, a "strand" was named as "rope").

J.W.Phillips, R. E. Miller and G.A.Costello[3.10] (1980)

The localized stresses resulting from contact forces at the contact points of wires between adjacent layers of wires of a 1 x 19 multi-layer strand (cross lay) were studied. Hertzian contact theory in conjunction with the analytical method introduced by a text book "Advanced Mechanics of Materials" by Boresi Sidebottom, were used. Results were presented in form of "contact forces/rope force as function of helix angle" for the inner layer wires.

G.J.Butson[3.11] (1981)

Mathematical models for the analysis of static and dynamic responses of a 6/1 strand were developed in a PhD study by Butson. In this study, 6 stranded rope was modelled by a 6/1 strand subjected to axial load and axial impulse respectively. In the static analysis, a vector method was used and frictional effects were taken into account. In the dynamic analysis, a impulse was assumed to be applied to one end of the rope and an equation of motion was formulated based on a traditional dynamic approach.

S.A.Velinsky[3.12] (1981)

The nonlinear geometrical equations for the analysis of change in geometry of a single helical wire, developed by Costello and others, were linearized by Velinsky in a PhD study. Based on the linearized approach, he then went further to study the static response of a 6 x 19 Seale type rope with IWRC. A breakthrough was claimed in analyzing similar types of static problems of the strands and wire ropes.

G.A.Costello and G.J.Butson[3.13] (1982)

The static response of a wire rope (ie 6/1 strand, in this paper called a "rope") subjected to external tension, torsion and bending was studied. Timoshenko's type of bending theory for calculating the flexual bending stiffness of a helical spring was modified. Equations from rod theory and single helix geometry were presented. Costello and Butson claimed that the approach can be extended to study ropes with more complex sections.

J.W.Phillips and P.D.Fotch[3.14] (1983)

A simplified bending theory for a 6/1 strand, developed by Costello and Butson, was used in this analysis. The authors illustrated results from the bending stress analysis for a 6 x 25F IWRC rope. However, relevant equations and modified theory were not given.

G.A.Costello[3.15] (1983)

Static strand theory and simplified bending theory for the analysis of static response of a single layer strand, developed by Costello and his fellow workers, were used to study the stress in the core wire of a three layered cable (ie a multi-layer strand with two layer of single helical wires and a core wire). The static responses of the strand was derived. From this study, Costello concluded that the highest axial tensile stress occurs on the central core wire of the strand.

S.A.Velinsky, G.L.Anderson and G.A.Costello[3.16] (1984)

The nonlinear geometrical parameters in the equations of equilibrium for the static analysis of helical rod were linearized. These equations, together with the analytical approach developed by Costello and others, were used to study the static response of a 6 x 19 Seale rope with IWRC. In this study, Velinsky and others concluded that:

a. The maximum tensile stress occurs in the King wire provided both terminations of the rope are fixed.
b. The effective modulus of a rope decreases when additional strands are added.
c. The theoretically determined modulus is higher than that obtained from experiments.
d. If the stress exceeds the elastic limit of the king wire, the king wire may become compressive when the external load is reduced to zero.

C.H.Chien and G.A.Costello[3.17] (1985)

A mathematical method used to predict the effective length of a fractured wire, in a 6 x 25 ordinary lay rope with IWRC after fatigue, was presented by Chien and Costello. Coulomb friction and rod theory were used throughout their analysis. From their study, they concluded that the effective length of the fractured wire is independent of the axial load.

S.A.Velinsky[3.18] (1985)

Rod theory and a modelling technique, for the analysis of stranded spring developed by Costello and his fellow workers, were used to model the mechanical response of the helical strand of a 6 x 19 Seale rope with fibre core. The mechanical properties of the fibre core were assumed to be linear. In order to evaluate the deformed strand helical radius, 'an effective' radius of fibre core was introduced. The nonlinear geometrical change of the helical strand was linearized as usual. Results were illustrated on a load-extension curve.

S.A.Velinsky[3.19] (1985)

A general nonlinear theory (ie geometrical nonlinear) for a 6 x 19 Seale rope with IWRC was presented. The stranded helical spring model and the straight strand model were applied in the analysis. The model was used to predict the static responses of the Seale rope. Results (ie the load-extension curves) were presented in dimensionless form. From this study, Velinsky concluded that the nonlinear theory for the 6 x 19 Seale rope with IWRC showed no significant advantage over the linearized theory.

J.W.Phillips and G.A.Costello[3.20] (1985)

A mathematical model for the static analysis of Seale rope, proposed by Velinsky, was generalised by Phillips and Costello. In this paper, no mechanical interactions were taken into consideration. They then summarized that the "effective modulus" of wire rope predicted by the model was slightly higher than this obtained from experiment. They explained that the discrepancy between the model and experiment was probably due to the model failing to take contact deformation, line loads and other possible interstitial movement into consideration.

R.A.LeClair & G.A.Costello[3.24] (1988)

As usual, six differential equations from rod theory and expressions from helix geometry of a single helical wire, were used to analyse the mechanical behaviour of strand resulted from axial bending and twisting moments applied to that strand. They claimed that this model, took friction into consideration, could be used to predict the stresses in a single layer strand subjected to axial, bending and torsional loading. However, no stresses equations in related with friction were given.

S.A.Velinsky and J.D.Schmidt[3.25] (1988)

A simplified treatise of static behaviour of worn cable (ie 6/1 strand) was presented. The wear, on the worn crown and at the contact locations between adjacent helical wires, was idealized by flat surfaces. By using this geometry, the helical radius of worn wire was then predicted. Based on the rod theory, they went on to analyze the mechanical responses of the worn cable.

PARAMETRIC EXPRESSIONS

OF

SINGLE LAYER STRAND

A1,1 Geometrical Constants Of single Layer Strand:

$$J_1 = \frac{a_c (\sin^2 \alpha - \nu \cos^2 \alpha) + a_h \sin^2 \alpha}{a_c + a_h (1 + \nu \cos^2 \alpha)} \qquad (A1,1)$$

$$J_2 = \frac{(a_c + a_h) \cos^2 \alpha}{2 \pi \{ a_c + a_h (1 + \nu \cos^2 \alpha) \}} \qquad (A1,2)$$

$$J_3 = \frac{(a_c + a_h) (1 + \nu) \cos \alpha \sin \alpha}{a_c + a_h (1 + \nu \cos^2 \alpha)} \qquad (A1,3)$$

$$J_4 = \frac{(a_c + a_h) \sin \alpha \cos \alpha}{2 \pi \{ a_c + a_h (1 + \nu \cos^2 \alpha) \}} \qquad (A1,4)$$

$$J_5 = \frac{\nu \cos^2 \alpha}{R^2} (a_c + a_h J_1) - \frac{2 \sin \alpha \cos \alpha}{R^2} J_3 \qquad (A1,5)$$

$$J6 = \frac{\nu \cos^2 \alpha \, a_h J_2}{R^2} - \frac{2 \sin \alpha \cos \alpha J_4}{R} \qquad (A1,6)$$

$$J_7 = \frac{\cos 2 \alpha 2}{R} J_3 + \frac{\nu \sin 2 \alpha}{2 R^2} (a_c + a_h J_1) \qquad (A1,7)$$

$$J_8 = \frac{\cos 2 \alpha}{R} J_4 + \frac{\nu \sin 2 \alpha}{2 R^2} a_h J_2 \qquad (A1,8)$$

$$J_9 = \pi a_h^2 E \qquad (A1,9)$$

$$J_{10} = G J_c \qquad (A1,10)$$

$$J_{11} = \pi a_h^2 E J_1 \qquad (A1,11)$$

$$J_{12} = \pi a_h^2 E J_2 \qquad (A1,12)$$

$$J_{13} = E I_h J_5 \qquad (A1,13)$$

$$J_{14} = E\ I_h\ J_6 \tag{A1,14}$$

$$J_{15} = G\ J_h\ J_7 \tag{A1,15}$$

$$J_{16} = G\ J_h\ J_8 \tag{A1,16}$$

$$J_{17} = G\ J_h\ J_7\ k' - E\ I_h\ J_5\ \tau \tag{A1,17}$$

$$J_{18} = G\ J_h\ J_8\ k' - E\ I_h\ J_6\ \tau \tag{A1,18}$$

$$J_{19} = (\ G\ J_h\ J_7\ k' - E\ I_h\ J_2\ \tau\ )\ \tau - \pi\ a_h\ E\ J_1\ k' \tag{A1,19}$$

$$J_{20} = (\ G\ J_h\ J_8\ k' - E\ I_h\ J_6\ \tau\ )\ \tau - \pi\ a_h\ E\ J_2\ k' \tag{A1,20}$$

$$J_{21} = \frac{-\ \nu\ (\ a_c + 2\ a_h\ J_1\ )}{a_c\ +\ 2\ a_h} \tag{A1,21}$$

$$J_{22} = \frac{-2\ \nu\ a_h\ J_2}{a_c + 2\ a_h} \tag{A1,22}$$

A1,2 The Effective Stiffness Constants:

$$K_1 = m\ \{\ \pi\ a_h^2\ E\ J_1\ \sin\alpha + (\ G\ J_h\ J_7\ k' - E\ I_h\ J_2\ \tau\ )\ \cos\alpha\ \} + \pi\ a_c^2\ E \tag{A1,21}$$

$$K_2 = m\ \{\ \pi\ a_h^2\ E\ J_2\ \sin\alpha + (\ G\ J_h\ J_8\ k' - E\ I_h\ J_6\ \tau\ )\ \cos\alpha\ \} \tag{A1,22}$$

$$K_3 = m\ \{\ G\ J_h\ J_7\ \sin\alpha + E\ I_h\ J_5\ \cos\alpha + \pi\ a_h\ E\ J_1\ R\ \cos\alpha - (\ G\ J_h\ J_7\ k' - E\ I_h\ J_5\ \tau\ )\ R\ \sin\alpha\ \} \tag{A1,23}$$

$$K_4 = m\ \{\ G\ J_h\ J_8\ \sin\alpha + E\ I_h\ J_6\ \sin\alpha + \pi\ a_h\ E\ J_2\ R\ \cos\alpha - (\ G\ J_h\ J_8\ k' - E\ I_h\ J_6\ \tau\ )\ R\ \sin\alpha\ \} + G\ J_c \tag{A1,24}$$

A.1.3 Global Mechanical Equilibrium Of Single Layer Strand

$$F = m (T_h \sin \bar{\alpha} + N' \cos \bar{\alpha}) + T_c \quad (A1,25)$$

$$M = m (W \sin \bar{\alpha} + V' \cos \bar{\alpha} + T_h R \cos \bar{\alpha} - N' R \sin \bar{\alpha}) + W_c \quad (A1,26)$$

Alternatively

$$\begin{vmatrix} K_1 & K_2 \\ K_3 & K_4 \end{vmatrix} \begin{vmatrix} \varepsilon_s \\ \Delta\theta \end{vmatrix} = \begin{vmatrix} F \\ M \end{vmatrix} \quad (A1,27)$$

A.1.4 Geometrical Responses Of Helical Wire

$$\varepsilon_w = J_1 \varepsilon_s + J_2 \Delta\theta \quad (A1,28)$$

$$\Delta\alpha = J_3 \varepsilon_s + J_4 \Delta\theta \quad (A1,29)$$

$$\Delta k' = J_5 \varepsilon_s + J_6 \Delta\theta \quad (A1,30)$$

$$\Delta\tau = J_7 \varepsilon_s + J_8 \Delta\theta \quad (A1,31)$$

A.1.5 Geometrical Responses Of Strand (Strand displacements)

$$\varepsilon_s = \frac{\text{Final strand length - Original strand length}}{\text{Original strand length}} \quad (A1,32)$$

$$\Delta\theta = \frac{\text{Rotational displacement}}{\text{lay length}} \quad (A1,33)$$

A.1.6 Internal Components In Wires:

Core Wire:

$$T_c = J_9 \varepsilon_s \quad (A1,34)$$

$$W_c = J_{10}\ \Delta\theta \qquad \text{(A1,35)}$$

Helical Wire:

$$T_h = J_{11}\ \varepsilon_s + J_{12}\ \Delta\theta \qquad \text{(A1,36)}$$

$$V' = J_{13}\ \varepsilon_s + J_{14}\ \Delta\theta \qquad \text{(A1,37)}$$

$$W = J_{15}\ \varepsilon_s + J^{16}\ \Delta\theta \qquad \text{(A1,38)}$$

$$N' = J_{17}\ \varepsilon_s + J_{18}\ \Delta\theta \qquad \text{(A1,39)}$$

$$X = J_{19}\ \varepsilon_s + J_{20}\ \Delta\theta \qquad \text{(A1,40)}$$

A.1.7 Strains In Helical Wire:

For helical wire

Due to tension alone

$$\varepsilon_w = J_1\ \varepsilon_s + J_2\ \Delta\theta \qquad \text{(A.1,41)}$$

Due to bending alone

$$\varepsilon_{wb} = \frac{a_{hY}\ J_5}{1 + k'a_{hY}}\ \varepsilon_s + \frac{a_{hY}\ J_6}{1 + k'a_{hY}}\ \Delta\theta \qquad \text{(A.1,42)}$$

Due to twisting alone

$$\gamma_w = (\ J_7\ \varepsilon_s + J_8\ \Delta\theta\ )\ a_{hY} \qquad \text{(A.1,43)}$$

A.1.8 Defined Parameters For Nonlinear Strain Strain Modelling

$$P_L = 2\pi\ R\ \tan\ \alpha \qquad \text{(A.1,44)}$$

$$\Delta\theta^* = \Delta\theta/2\pi \qquad \text{(A.1,45)}$$

$$a_h^* = -\ \nu\ a_h\ /\ R \qquad \text{(A.1,46)}$$

$$a_c^* = - \nu \, a_c \, / \, R \qquad (A.1,47)$$

$$P_L^{\Delta} = \sin^2 \alpha \, (1 + \varepsilon_s)^2 \qquad (A.1,48)$$

$$\Delta\theta^{\Delta} = \cos^2 \alpha \, (1 + \Delta\theta^*)^2 \qquad (A.1,49)$$

$$P_{L\theta} = 1 - P_L^{\Delta} - \Delta\theta^{\Delta} \qquad (A.1,50)$$

$$A = 1 - a_h^{*2} \, \Delta\theta^{\Delta} \qquad (A.1,51)$$

$$B = 2 \, (1 - \Delta\theta^{\Delta} \, a_c^* \, a_h^* \, \varepsilon_s - \Delta\theta^{\Delta} \, a_h^*) \qquad (A.1,52)$$

$$C = P_{L\theta} - 2 \, \Delta\theta^{\Delta} \, a_c^* \, \varepsilon_s - \Delta\theta^{\Delta} \, a_c^{*2} \, \varepsilon_s^2 \qquad (A.1,53)$$

PARAMETRIC EXPRESSIONS

OF

SIX STRANDED ROPE

A.2.1 Stiffness Constants Of King Wire.

$$F_{10} = \pi\ a^2_c\ E \quad (A.2.1)$$

$$F_{11} = G\ J_c\ /\ P_L \quad (A.2.2)$$

A.2.2 Geometrical Constant.

$$G^* = P_{ch}/P_L \quad (A.2.3)$$

$$G_1 = \frac{r_{ch}\ \sin^2 \alpha_{ch} - \nu\ a_c\ \cos_2 \alpha_{ch}}{r_{ch} + \nu\ a_{ch}\ \cos^2 \alpha_{ch}} \quad (A.2.4)$$

$$G_2 = \frac{r_{ch}\ \cos^2 \alpha_{ch}}{2\pi(r_{ch} + \nu\ a_{ch}\ \cos^2 \alpha_{ch})} .\ G^* \quad (A.2.5)$$

$$G_3 = (1 - G_1)\ \tan \alpha_{ch} \quad (A.2.6)$$

$$G_4 = -\ G_2\ \tan \alpha_{ch} \quad (A.2.7)$$

$$H_1 = \nu\ (\ a_c + a_{ch}\ G_1\ )\ /\ r^2_{ch} \quad (A.2.8)$$

$$H_2 = \nu\ a_{ch}\ /\ r^2_{ch} \quad (A.2.9)$$

$$G_5 = H_1\ \cos^2 \alpha_{ch} - \sin^2 \alpha_{ch}\ G_3\ /\ r_{ch} \quad (A.2.10)$$

$$G_6 = H_2\ \cos^2 \alpha_{ch} - \sin^2 \alpha_{ch}\ G_4\ /\ r_{ch} \quad (A.2.11)$$

$$G_7 = \frac{G_3\ \cos 2\ \alpha_{ch}}{r_{ch}} - \frac{H_1\ \sin^2 \alpha_{ch}}{2} \quad (A.2.12)$$

$$G_8 = \frac{G_4\ \cos 2\ \alpha_{ch}}{r_{ch}} - \frac{H_2\ \sin^2 \alpha_{ch}}{2} \quad (A.2.12)$$

$$P_L = 2\pi\ r_s\ \tan \beta \quad ; \quad P_{ch} = 2\pi\ r_{ch}\ \tan \alpha_{ch} \quad (A.2.13)$$

$$G_{10} = \pi\ a^2_{ch}\ E\ G_1 \quad (A.2.14)$$

$$G_{11} = \pi a^2_{ch} E G_2 \tag{A.2.15}$$

$$G_{12} = E I_{ch} G_5 \tag{A.2.16}$$

$$G_{13} = E I_{ch} G_6 \tag{A.2.17}$$

$$G_{14} = G J_{ch} G_7 \tag{A.2.18}$$

$$G_{15} = G J_{ch} G_8 \tag{A.2.19}$$

$$G_{16} = K'_{ch} G_{14} - \tau_{ch} G_{12} \tag{A.2.20}$$

$$G_{17} = K'_{ch} G_{15} - \tau_{ch} G_{13} \tag{A.2.21}$$

$$G_{18} = \tau_{ch} G_{16} - K'_{ch} G_{10} \tag{A.2.22}$$

$$G_{19} = \tau_{ch} G_{17} - K'_{ch} G_{11} \tag{A.2.23}$$

A.2.3 Parametric Constant For Helical Core Wire

$$S_1 = -\nu a_{sc} / r_{sh} \tag{A.2.24}$$

$$S_2 = -\nu a_{sh} / r_{sh} \tag{A.2.25}$$

$$S_3 = -\nu (a_c + 2 a_{ch} G_1)/ r_s \tag{A.2.26}$$

$$S_4 = -\nu (2 a_{ch} G_1) \tag{A.2.27}$$

$$S_5 = -\nu (2 a_{sh})/ r_s \tag{A.2.28}$$

$$S_6 = -\nu a_{sc} / r_s \tag{A.2.29}$$

$$S_7 = -S_3 \quad : \quad S_8 = -S_4 \tag{A.2.30}$$

$$S_9 = S_1 - S_6 \tag{A.2.31}$$

$$S_{10} = S_2 - S_5 \tag{A.2.32}$$

$$\Omega^* = \cos \beta \tan \alpha_{sh} \tag{A.2.33}$$

$$\Omega = r_{sh}\ \Omega^* / r_s \tag{A.2.34}$$

$$S_{11} = r_{sh}\ \Omega^*\ S_7 / r_s \tag{A.2.35}$$

$$S_{12} = r_{sh}\ \Omega^*\ S_8 / r_s \tag{A.2.36}$$

$$L^{\Delta}_1 = \frac{\cos\beta\ \tan\alpha_{sh}}{\cos^2\alpha_{sh}} + \sin\beta\ \tan\beta\ \tan\alpha_{sh} \tag{A.2.37}$$

$$L^{\Delta}_2 = \frac{-\cos\beta\ \tan\alpha_{sh}}{\cos^2\alpha_{sh}} \tag{A.2.38}$$

$$S_{13} = r_{sh}\ (\ L^{\Delta}_1 + \Omega^*\ S_9\ ) / r_s \tag{A.2.39}$$

$$S_{14} = r_{sh}\ (\ L^{\Delta}_2 + \Omega^*\ S_{10}\ ) \tag{A.2.40}$$

$$S_{15} = -\ S_{11} / \Omega \tag{A.2.41}$$

$$S_{16} = 1/2\pi - S_{12}/\Omega \tag{A.2.42}$$

$$S_{17} = -\ S_{13} / \Omega \tag{A.2.43}$$

$$S_{18} = -\ S_{14} / \Omega \tag{A.2.44}$$

$$A = (\ 1 - \cos^2\alpha_{sh}\ S_5 - \cos\alpha_{sh}\ S_{18}\ ) \tag{A.2.45}$$

$$B = (\ S_3\cos^2\alpha_{sh} + S_{15}\cos\alpha_{sh}\ ) \tag{A.2.46}$$

$$C = (\ \cos^2\alpha_{sh}\ S_4 + \cos\alpha_{sh}\ S_{16}\ ) \tag{A.2.47}$$

$$D = (\sin^2\alpha_{sh} + \cos^2\alpha_{sh}\ S_6 + \cos\alpha_{sh}\ S_{17}) \tag{A.2.48}$$

$$L^{*}_1 = -\ v\ (\ a_c + 2a_{ch}\ G_1\ ) / r_s \tag{A.2.49}$$

$$L^{*}_2 = -\ v\ (\ 2\ a_{ch}\ G_2\ ) / r_s \tag{A.2.50}$$

$$L^{*}_3 = -\ v\ (\ 2\ a_{sh}\ ) / r_s \tag{A.2.51}$$

$$L^{*}_{4} = - \nu \, a_{sc} \,/\, r_s \qquad (A.2.52)$$

$$I_1 = \frac{(A \sin^2 \beta + A \cos^2 \beta \, L^{*}_{1} + \cos^2 \beta \, L^{*}_{3} \, B)}{(A - \cos^2 \beta \, L^{*}_{3} \, D - A \cos^2 \beta \, L^{*}_{4})} \qquad (A.2.53)$$

$$I_2 = \frac{\left(A \cos^2 \beta \, L^{*}_{2} + \cos^2 \beta \, L^{*}_{3} \, C + A \dfrac{\cos^2 \beta}{2\pi}\right)}{(A - A \cos^2 \beta \, L^{*}_{3} \, D - \cos^2 \beta \, L^{*}_{4})} \qquad (A.2.54)$$

$$I_3 = (1 - I_1) \tan \beta \qquad (A.2.55)$$

$$I_4 = - I_2 \tan \beta \qquad (A.2.56)$$

$$LL_1^{*} = L^{*}_{1} + L^{*}_{2} \, J_1 + L^{*}_{3} \, I_2 \qquad (A.2.57)$$

$$LL_2^{*} = L^{*}_{2} + L^{*}_{3} \, J_2 + L^{*}_{4} \, I_2 \qquad (A.2.58)$$

$$I_5 = -(LL_1^{*} \cos^2 \beta + I_3 \sin 2\beta)/r_s \qquad (A.2.59)$$

$$I_6 = -(LL_2^{*} \cos^2 \beta + I_4 \sin 2\beta)/r_s \qquad (A.2.60)$$

$$I_7 = (I_3 \cos 2\beta - LL_1^{*} \sin \beta \cos \beta)/r_s \qquad (A.2.61)$$

$$I_8 = (I_4 \cos 2\beta - LL_2^{*} \sin \beta \cos \beta)/r_s \qquad (A.2.62)$$

$$I_{10} = \pi \, a^2_{sc} \, E \, I_1 \qquad (A.2.63)$$

$$I_{11} = \pi \, a^2_{sc} \, E \, I_2 \qquad (A.2.64)$$

$$I_{12} = E \, I_{sc} \, I_5 \qquad (A.2.65)$$

$$I_{13} = E \, I_{sc} \, I_6 \qquad (A.2.66)$$

$$I_{14} = G \, J_{sc} \, I_7 \qquad (A.2.67)$$

$$I_{15} = G \, J_{sc} \, I_8 \qquad (A.2.68)$$

$$I_{16} = I_{14} \, K'_{sc} - I_{12} \, \tau_{sc} \qquad (A.2.69)$$

$$I_{17} = I_{15} K'_{sc} - I_{13} \tau_{sc} \quad (A.2.70)$$

$$I_{18} = I_{16} \tau_{sc} - I_{10} K'_{sc} \quad (A.2.71)$$

$$I_{19} = I_{17} \tau_{sc} - I_{11} K'_{sc} \quad (A.2.72)$$

A.2.4 Parametric Constant For Double Hleical Wire:

$$L^{*}_{3} = - \sin\beta \tan\beta \tan\alpha_{sh} \quad (A.2.73)$$

$$L_1^* = \frac{\sin^2\beta + L^{*}_{1} \cos^2\beta}{1 - L^{*}_{4} \cos^2\beta} \quad (A.2.74)$$

$$L_2^* = \frac{\sin^2\beta + L^{*}_{2} \cos^2\beta}{1 - L^{*}_{4} \cos^2\beta} \quad (A.2.75)$$

$$L_3^* = \frac{L^{*}_{3} \cos^2\beta}{1 - L^{*}_{4} \cos^2\beta} \quad (A.2.76)$$

$$J_1 = \frac{(B + D L_1^*)}{(A - D L_3^*)} \quad (A.2.77)$$

$$J_2 = \frac{(C + D L_2^*)}{(A - D L_3^*)} \quad (A.2.78)$$

$$J_3 = (I_1 - J_1) \tan\alpha_{sh} \quad (A.2.79)$$

$$J_4 = (I_2 - J_2) \tan\alpha_{sh} \quad (A.2.80)$$

A.2.5 Parametric Constants In Velinsky's Approach To Analyze IWRC

$$\theta_1 = - 2\pi (S_{11} + S_{13} I_1 + S_{14} J_1)/ \Omega^2 \quad (A.2.81)$$

$$\theta_2 = - 2\pi (S_{12} + S_{13} I_2 + S_{14} J_2)/ \Omega^2 + 1/\Omega \quad (A.2.82)$$

$$L^{+}_{1} = - \nu (a_{sc} I_1 + a_{sh} J_1) \quad (A.2.83)$$

$$L^{+}_{2} = -\nu\ (a_{sc}\ I_2 + a_{sh}\ J_2) \qquad (A.2.84)$$

$$J_5 = \frac{-L^{+}_{1}\cos^2\alpha_{sh}}{r_{sh}} - \frac{J_3\sin 2\alpha_{sh}}{r_{sh}} \qquad (A.2.85)$$

$$J_6 = \frac{-L^{+}_{2}\cos^2\alpha_{sh}}{r_{sh}} - \frac{J_4\sin 2\alpha_{sh}}{r_{sh}} \qquad (A.2.86)$$

$$J_7 = (J_3\cos 2\alpha_{sh} - L^{+}_{1}\sin\alpha_{sh}\cos\alpha_{sh})/r_{sh} \qquad (A.2.87)$$

$$J_8 = (J_4\cos 2\alpha_{sh} - L^{+}_{2}\sin\alpha_{sh}\cos\alpha_{sh})/r_{sh} \qquad (A.2.88)$$

$$J^{*}_{10} = \pi\ a^2_{sc}\ E\ I_1 \qquad (A.2.89)$$

$$J^{*}_{11} = \pi\ a^2_{sc}\ E\ I_2 \qquad (A.2.90)$$

$$J^{*}_{12} = G\ J_{sc}\ \theta_1 \qquad (A.2.91)$$

$$J^{*}_{13} = G\ J_{sc}\ \theta_2 \qquad (A.2.92)$$

$$J_{10} = \pi\ a^2_{sc}\ E\ J_1 \qquad (A.2.93)$$

$$J_{11} = \pi\ a^2_{sc}\ E\ J_2 \qquad (A.2.94)$$

$$J_{12} = E\ I_{sh}\ J_5 \qquad (A.2.95)$$

$$J_{13} = E\ I_{sh}\ J_6 \qquad (A.2.96)$$

$$J_{14} = G\ J_{sh}\ J_7 \qquad (A.2.97)$$

$$J_{15} = G\ J_{sh}\ J_8 \qquad (A.2.98)$$

$$J_{16} = J_{14}\ K'_{sh} - J_{12}\ \tau_{sh} \qquad (A.2.99)$$

$$J_{17} = J_{15}\ K'_{sh} - J_{13}\ \tau_{sh} \qquad (A.2.100)$$

$$J_{18} = J_{16}\ \tau_{sh} - J_{10}\ K'_{sh} \qquad (A.2.101)$$

$$J_{19} = J_{17}\,\tau_{sh} - J_{11}\,K'_{sh} \qquad (A.2.102)$$

$$A_s = m_{sh}\,\frac{\pi\,E\,a^4_{sh}}{2} \cdot \frac{\sin\alpha_{sh}}{2 + \nu\cos\alpha_{sh}} + \frac{\pi\,E\,a^4_{sc}}{4} \qquad (A.2.103)$$

Stiffness Constants For Core Strand:

$$K^c_1 = m_c\,(\,G_{10}\sin\alpha_{ch} + G_{16}\cos\alpha_{ch}\,) + F_{10} \qquad (A.2.104)$$

$$K^c_2 = m_c\,(\,G_{11}\sin\alpha_{ch} + G_{17}\cos\alpha_{ch}\,) \qquad (A.2.105)$$

$$K^c_3 = m_c\,\{(\,G_{14} - G_{16}\,r_{ch}\,)\sin\alpha_{ch} + (\,G_{12} + G_{10}\,r_{ch}\,)\cos\alpha_{ch}\,\} \qquad (A.2.106)$$

$$K^c_4 = m_c\,\{(\,G_{15} - G_{17}\,r_{ch}\,)\sin\alpha_{ch} + (\,G_{13} + G_{11}\,r_{ch}\,)\cos\alpha_{ch}\,\} + F_{11} \qquad (A.2.107)$$

Stiffness Constant For Helical Strand (Lang's Lay)

$$K^s_1 = J^*_{10} + m_{sh}\,(\,J_{10}\sin\alpha_{sh} + J_{16}\cos\alpha_{sh}\,) \qquad (A.2.108)$$

$$K^s_2 = J^*_{11} + m_{sh}\,(\,J_{11}\sin\alpha_{sh} + J_{17}\cos\alpha_{sh}\,) \qquad (A.2.109)$$

$$K^s_3 = J^*_{12} + m_{sh}\,\{(\,J_{14} - J_{16}\,r_{sh}\,)\sin\alpha_{sh} + (\,J_{12} + J_{10}\,r_{sh}\,)\cos\alpha_{sh}\,\} \qquad (A.2.110)$$

$$K^s_4 = J^*_{13} + m_{sh}\,\{(\,J_{15} - J_{17}\,r_{sh}\,)\sin\alpha_{sh} + (\,J_{13} + J_{11}\,r_{sh}\,)\cos\alpha_{sh}\,\} \qquad (A.2.111)$$

Common Stiffness Constants For Helical Strand (Both Lang and Ordinary Lay)

$$K^s_5 = A_s\,I_5 \qquad (A.2.112)$$

$$K^s_6 = A_s\,I_6 \qquad (A.2.113)$$

$$K^{s}_{7} = K^{s}_{3} K'_{s} - K^{s}_{5} \tau_{s} \quad (A.2.114)$$

$$K^{s}_{8} = K^{s}_{4} K'_{s} - K^{s}_{6} \tau_{s} \quad (A.2.115)$$

$$K^{s}_{9} = K^{s}_{7} \tau_{s} - K^{s}_{1} K'_{s} \quad (A.2.116)$$

$$K^{s}_{10} = K^{s}_{8} K'_{s} - K^{s}_{2} \tau_{s} \quad (A.2.117)$$

Stiffness Constant For Helical Strand (Ordinary Lay)

$$K^{o}_{1} = J^{*}_{10} + m_{sh} (J_{10} \sin \alpha_{sh} + J_{16} \cos \alpha_{sh}) \quad (A.2.112)$$

$$K^{o}_{2} = J^{*}_{11} + m_{sh} (J_{11} \sin \alpha_{sh} + J_{17} \cos \alpha_{sh}) \quad (A.2.113)$$

$$K^{o}_{3} = J^{*}_{12} - m_{sh} \{(J_{14} - J_{16} r_{sh}) \sin \alpha_{sh} + (J_{12} + J_{10} r_{sh}) \cos \alpha_{sh} \} \quad (A.2.114)$$

$$K^{o}_{4} = J^{*}_{13} - m_{sh} \{(J_{15} - J_{17} r_{sh}) \sin \alpha_{sh} + (J_{13} + J_{11} r_{sh}) \cos \alpha_{sh} \} \quad (A.2.115)$$

Stiffness Constants For IWRC:

$$K^{R}_{1} = K^{c}_{1} + m_{s} (K^{s}_{1} \sin \beta + K^{s}_{7} \cos \beta) \quad (A.2.116)$$

$$K^{R}_{2} = K^{c}_{2} + m_{s} (K^{s}_{2} \sin \beta + K^{s}_{8} \cos \beta) \quad (A.2.117)$$

$$K^{R}_{3} = K^{c}_{3} + m_{s} \{(K^{s}_{3} - K^{s}_{7} r_{s}) \sin \beta + (K^{s}_{5} + K^{s}_{1} r_{s}) \cos \beta \} \quad (A.2.118)$$

$$K^{R}_{4} = K^{c}_{4} + m_{s} \{(K^{s}_{4} - K^{s}_{8} r_{s}) \sin \beta + (K^{s}_{7} + K^{s}_{2} r_{s}) \cos \beta \} \quad (A.2.119)$$

Note: $L^{\dagger} = L^{*}$

PARAMETRIC EXPRESSIONS

OF

MULTI–LAYER STRAND

A.3.1 Geometrical Parameters For 9/9/1 Equal Lay Strand.

First Layer:

$$I_R = \frac{\cos^2 \alpha_2 \tan^2 (\pi/2 - \pi/m_2)}{\mathrm{Sin}^2 \alpha_2 + \tan^2 (\pi/2 - \pi/m_2)} \qquad \text{(A.3.1.1)}$$

$$I_1 = \frac{1}{(1 + v \cos^2 \alpha_2 - I_R)} \{ \sin^2 \alpha_2 - I_R \} \qquad \text{(A.3.1.2)}$$

$$I_2 = \frac{1}{(1 + v \cos^2 \alpha_2 - I_R)} \{ \frac{\cos^2 \alpha_2}{2\pi} \} \qquad \text{(A.3.1.3)}$$

$$I_3 = (1 - I_1) \tan \alpha_2 \qquad \text{(A.3.1.4)}$$

$$I_4 = - I_2 \tan \alpha_2 \qquad \text{(A.3.1.5)}$$

$$I_A = - v I_1 - I_R I_3 \qquad \text{(A.3.1.6)}$$

$$I_B = - v I_2 - I_R I_4 \qquad \text{(A.3.1.7)}$$

$$I_5 = - \frac{\sin 2\alpha_2}{r_2} I_3 - \frac{\cos^2 \alpha_2}{r_2} I_A \qquad \text{(A.3.1.8)}$$

$$I_6 = - \frac{\sin 2\alpha_2}{r_2} I_4 - \frac{\cos^2 \alpha_2}{r_2} I_B \qquad \text{(A.3.1.9)}$$

$$I_7 = \frac{\cos 2\alpha_2}{r_2} I_3 - \frac{\sin 2\alpha_2}{2 r_2} I_A \qquad \text{(A.3.1.10)}$$

$$I_8 = \frac{\cos 2\alpha_2}{r_2} I_4 - \frac{\sin 2\alpha_2}{2 r_2} I_B \qquad \text{(A.3.1.11)}$$

$$I_{11} = \pi a^2{}_2 E I_1 \qquad \text{(A.3.1.12)}$$

$$I_{12} = \pi\, a^2{}_2\, E\, I_2 \qquad (A.3.1.13)$$

$$I_{13} = E\, I^*{}_2\, I_5 \qquad (A.3.1.14)$$

$$I_{14} = E\, I^*{}_2\, I_6 \qquad (A.3.1.15)$$

$$I_{15} = G\, J^*{}_2\, I_7 \qquad (A.3.1.16)$$

$$I_{16} = G\, J^*{}_2\, I_8 \qquad (A.3.1.17)$$

$$I_{17} = I_{15}\, K'_2 - I_{16}\, \tau_2 \qquad (A.3.1.18)$$

$$I_{18} = I_{16}\, K'_2 - I_{17}\, \tau_2 \qquad (A.3.1.19)$$

Second Layer:

$$J_R = \frac{\cos^2 \alpha_3 \tan^2 (\pi/2 - \pi/m_3)}{\text{Sin}^2 \alpha_3 + \tan^2 (\pi/2 - \pi/m_3)} \qquad (A.3.1.20)$$

$$J_1 = \frac{1}{(1 + \nu \cos^2 \alpha_3 - J_R)} \{ \sin^2 \alpha_3 - J_R \} \qquad (A.3.1.21)$$

$$J_2 = \frac{1}{(1 + \nu \cos^2 \alpha_3 - J_R)} \{ \frac{\cos^2 \alpha_3}{2\pi} \} \qquad (A.3.1.23)$$

$$J_3 = (1 - J_1) \tan \alpha_3 \qquad (A.3.1.24)$$

$$J_4 = - J_2 \tan \alpha_3 \qquad (A.3.1.25)$$

$$J_A = - \nu\, J_1 - J_R\, J_3 \qquad (A.3.1.26)$$

$$J_B = - \nu\, J_2 - J_R\, J_4 \qquad (A.3.1.27)$$

$$J_5 = - \frac{\sin 2\alpha_3}{r_3} J_3 - \frac{\cos^2 \alpha_3}{r_3} J_A \qquad (A.3.1.28)$$

$$J_6 = -\frac{\sin 2\alpha_3}{r_3} J_4 - \frac{\cos^2 \alpha_3}{r_3} J_B \qquad (A.3.1.29)$$

$$J_7 = \frac{\cos 2\alpha_3}{r_3} J_3 - \frac{\sin 2\alpha_3}{2\, r_3} J_A \qquad (A.3.1.30)$$

$$J_8 = \frac{\cos 2\alpha_3}{r_3} J_4 - \frac{\sin 2\alpha_3}{2\, r_3} J_B \qquad (A.3.1.31)$$

$$J_9 = \pi\, a^2{}_1\, E \qquad (A.3.1.32)$$

$$J_{10} = G\, J^*{}_1 / P_1 \qquad (A.3.1.33)$$

$$J_{11} = \pi\, a^2{}_3\, E\, J_1 \qquad (A.3.1.34)$$

$$J_{12} = \pi\, a^2{}_3\, E\, J_2 \qquad (A.3.1.35)$$

$$J_{13} = E\, I^*{}_3\, J_5 \qquad (A.3.1.36)$$

$$J_{14} = E\, I^*{}_3\, J_6 \qquad (A.3.1.37)$$

$$J_{15} = G\, J^*{}_3\, J_7 \qquad (A.3.1.38)$$

$$J_{16} = G\, J^*{}_3\, J_8 \qquad (A.3.1.39)$$

$$J_{17} = J_{15}\, K'_3 - J_{16}\, \tau_3 \qquad (A.3.1.40)$$

$$J_{18} = J_{16}\, K'_3 - J_{17}\, \tau_3 \qquad (A.3.1.41)$$

The Stiffness Constants For 9/9/1:

$$K_1 = m_2\, (I_{11} \sin \alpha_2 + I_{17} \cos \alpha_2) + m_3\, (J_{11} \sin \alpha_3 + J_{17} \cos \alpha_3) + J_9 \qquad (A.3.1.42)$$

$$K_2 = m_2 \, (I^{\Delta}_{12} \sin \alpha_2 + I^{\Delta}_{18} \cos \alpha_2) + m_3 \, (J_{12} \sin \alpha_3 + J_{18} \cos \alpha_3) \qquad \text{(A.3.1.43)}$$

$$K_3 = m_2 \, (I_{15} \sin \alpha_2 + I_{13} \cos \alpha_2 + r_2 \, I_{11} \cos \alpha_2 - r_2 \, I_{17} \sin \alpha_2) + m_3 \, (J_{15} \sin \alpha_3 + J_{13} \cos \alpha_3 + r_3 \, J_{11} \cos \alpha_3 - r_3 \, J_{17} \sin \alpha_3) \qquad \text{(A.3.1.44)}$$

$$K_4 = m_2 \, (I^{\Delta}_{16} \sin \alpha_2 + I^{\Delta}_{14} \cos \alpha_2 + r_2 \, I^{\Delta}_{12} \cos \alpha_2 - r_2 \, I^{\Delta}_{18} \sin \alpha_2) + m_3 \, (J_{16} \sin \alpha_3 + J_{14} \cos \alpha_3 + r_3 \, J_{12} \cos \alpha_3 - r_3 \, J_{18} \sin \alpha_3) + J_{10} \qquad \text{(A.3.1.45)}$$

A.3.2 Geometrical Constant For 12/6/1 Cross Lay Strand:

For First Layer:

$$I_1 = \frac{r_2 \sin^2 \alpha_2 - \nu \, a_1 \cos^2 \alpha_2}{r_2 + \nu \, a_2 \cos^2 \alpha_2} \qquad \text{(A.3.2.1)}$$

$$I_2 = \frac{r_2 \cos^2 \alpha_2}{2 \, \pi \, (r_2 + \nu \, a_2 \cos^2 \alpha_2)} \qquad \text{(A.3.2.2)}$$

$$I_3 = (1 - I_1 \,) \tan \alpha_2 \qquad \text{(A.3.2.4)}$$

$$I_4 = - I_2 \tan \alpha_2 \qquad \text{(A.3.2.5)}$$

$$H_4 = \frac{\nu}{r^2_2} (a_1 + a_2 \, I_1 \,) \qquad \text{(A.3.2.6)}$$

$$H_5 = \nu \, a_2 \, I_2 \, / \, r^2_2 \qquad \text{(A.3.2.7)}$$

$$I_5 = H_4 \cos^2 \alpha_2 - 2 \, I_3 \sin 2\alpha_2 \, / \, r_2 \qquad \text{(A.3.2.8)}$$

$$I_6 = H_5 \cos^2 \alpha_2 - 2 I_4 \sin 2\alpha_2 / r_2 \qquad (A.3.2.9)$$

$$I_7 = (H_4 \sin 2 \alpha_2)/2 + (I_3 \cos 2 \alpha_2)/r_2 \qquad (A.3.2.10)$$

$$I_8 = (H_5 \sin 2 \alpha_2)/2 + (I_4 \cos 2 \alpha_2)/r_2 \qquad (A.3.2.11)$$

The expressions I_{11}, I_{12}, I_{13}, ... I_{18} used for 12/6/1 strand are exactly the same as those used for 9/9/1 strand.

Second Layer:

$$J_1 = \frac{r_3 \sin^2 \alpha_3 - (a_1 + 2 a_2 I_1) v \cos^2 \alpha_3}{r_3 + a_3 v \cos^2 \alpha_3} \qquad (A.3.2.12)$$

$$J_2 = \frac{r_3 \cos^2 \alpha_3 - 4 \pi a_2 I^{\Delta}_2 v \cos^2 \alpha_3}{2 \pi (r_3 + a_3 v \cos^2 \alpha_3)} \qquad (A.3.2.13)$$

$$J_3 = (1 - J_1) \tan \alpha_3 \qquad (A.3.2.14)$$

$$J_4 = - J_2 \tan \alpha_3 \qquad (A.3.2.15)$$

$$H_1 = v (a_1 + 2 a_2 I_1) / r_3 \qquad (A.3.2.16)$$

$$H_2 = 2 v a_2 I^{\Delta}_3 / r_3 \qquad (A.3.2.17)$$

$$H_3 = a_3 v / r_3 \qquad (A.3.2.18)$$

$$J_5 = (H_1 + H_3 J_1)\cos^2 \alpha_3/r^2_3 - 2 J_3 \sin 2\alpha_3/r_3 \qquad (A.3.2.8)$$

$$J_6 = (H_2 + H_3 J_2)\cos^2 \alpha_3/r^2_3 - 2 J_4 \sin 2\alpha_3/r_3 \qquad (A.3.2.9)$$

$$J_7 = (H_1 + H_3 J_1)\sin 2\alpha_3/2 r^2_3 + J_3 \cos 2\alpha_3/r_3 \quad (A.3.210)$$

$$J_8 = (H2 + H_3 J_2)\sin 2\alpha_3/2 r^2_3 + J_4 \cos 2\alpha_3/r_3 \quad (A.3.210)$$

The expressions J_{11}, J_{12}, J_{13}, ... J_{18} and the stiffness constant K_1, K_2, K_3 & K_4 used for 12/6/1 strand are exactly the same as those used for 9/9/1 strand.

A.3.3 Geometrical Constant For 12/6F + 6/1 Equal Lay Filler Wire Strand:

$$J_A = - \nu \quad (A.3.3.1)$$

$$J_B = - \frac{\cos^2 \alpha_2 \tan^2 (\pi/2 - \pi/m_2)}{\text{Sin}^2 \alpha_2 + \tan^2 (\pi/2 - \pi/m_2)} \quad (A.3.3.2)$$

$$J_C = - \nu (r_f - a_2) / a^2_2 \quad (A.3.3.3)$$

$$J_D = - \frac{\cos^2 \alpha_2 \tan^2 (\pi/2 - \pi/m_2) \cos^2 \pi/m_2}{r_f \sin^3 \alpha_2} \quad (A.3.3.4)$$

$$J_E = J_A \quad (A.3.3.5)$$

$$J_F = \frac{- \cot \alpha_3 \tan^2 (\pi/2 - \pi/m_3)}{\text{Sin}^2 \alpha_3 + \tan^2 (\pi/2 - \pi/m_3)} \quad (A.3.3.6)$$

$$J_G = J_C H_1 + J_D H_3 \quad (A.3.3.7)$$

$$J_H = J_C H_2 + J_D H_4 \quad (A.3.3.8)$$

For First Layer Of Helical Wire:

$$H_h = 1 - J_A \cos^2 \alpha_2 + J_B \sin \alpha_2 \cos \alpha_2 \qquad (A.3.3.9)$$

$$H_1 = (\sin^2 \alpha_2 + J_B \sin \alpha_2 \cos \alpha_2) \;/\; H_h \qquad (A.3.3.10)$$

$$H_2 = \cos^2 \alpha_2 \;/\; (2 \pi H_h) \qquad (A.3.3.11)$$

$$H_3 = (1 - H_1) \tan \alpha_2 \qquad (A.3.3.12)$$

$$H_4 = - H_2 \tan \alpha_2 \qquad (A.3.3.13)$$

$$H_5 = (1 - H_1) J_B \tan \alpha_2 + J_A H_1 \qquad (A.3.3.14)$$

$$H_6 = (J_A - J_B \tan \alpha_2) H_2 \qquad (A.3.3.15)$$

$$H_7 = - (H_3 \sin 2\alpha_2 + H_5 \sin^2 \alpha_2) \;/\; r_2 \qquad (A.3.3.16)$$

$$H_8 = - (H_4 \sin 2\alpha_2 + H_7 \cos^2 \alpha_2) \;/\; r_2 \qquad (A.3.3.17)$$

$$H_9 = (H_3 \cos 2\alpha_2 - H_5 \sin \alpha_2 \cos \alpha_2) \;/\; r_2 \qquad (A.3.3.18)$$

$$H_{10} = (H_4 \cos 2\alpha_2 - H_6 \sin \alpha_2 \cos \alpha_2) \;/\; r_2 \qquad (A.3.3.19)$$

For Helical Filler Wire:

$$I_1 = \sin^2 \alpha_2 + J_G \cos^2 \alpha_3 \qquad (A.3.3.20)$$

$$I_2 = \{ J_H + 1/(2 \pi) \} \cos^2 \alpha_3 \qquad (A.3.3.21)$$

$$I_3 = (1 - H_1) \tan \alpha_3 \qquad (A.3.3.22)$$

$$I_4 = - I_2 \tan \alpha_3 \qquad (A.3.3.23)$$

$$I_5 = J_G \qquad (A.3.3.24)$$

$$I_6 = J_H \qquad (A.3.3.25)$$

$$I_7 = - (I_3 \sin 2\alpha_3 + I_5 \sin^2 \alpha_3) / r_f \quad (A.3.3.26)$$

$$I_8 = - (I_4 \sin 2\alpha_3 + I_7 \cos^2 \alpha_3) / r_f \quad (A.3.3.27)$$

$$I_9 = (I_3 \cos 2\alpha_3 - I_5 \sin \alpha_3 \cos \alpha_3) / r_f \quad (A.3.3.28)$$

$$I_{10} = (I_4 \cos 2\alpha_3 - I_6 \sin \alpha_3 \cos \alpha_3) / r_f \quad (A.3.3.29)$$

For Second Layer Of Helical Wire:

$$J_J = 1 - J_E \cos^2 \alpha_3 + J_F \sin \alpha_3 \cos \alpha_3 \quad (A.3.3.30)$$

$$J_1 = (\sin^2 \alpha_3 + J_F \sin \alpha_3 \cos \alpha_3) / J_J \quad (A.3.3.31)$$

$$J_2 = \cos^2 \alpha_3 / (2 \pi J_J) \quad (A.3.3.32)$$

$$J_3 = (1 - J_1) \tan \alpha_3 \quad (A.3.3.33)$$

$$J_4 = - J_2 \tan \alpha_3 \quad (A.3.3.34)$$

$$J_5 = J_F \tan \alpha_3 + (J_E - J_F \tan \alpha_3) J_1 \quad (A.3.3.35)$$

$$J_6 = (J_E - J_F \tan \alpha_3) J_2 \quad (A.3.3.36)$$

$$J_7 = - (J_3 \sin 2\alpha_3 + J_5 \sin^2 \alpha_3) / r_3 \quad (A.3.3.37)$$

$$J_8 = - (J_4 \sin 2\alpha_3 + J_7 \cos^2 \alpha_3) / r_3 \quad (A.3.3.38)$$

$$J_9 = (J_3 \cos 2\alpha_3 - J_5 \sin \alpha_3 \cos \alpha_3) / r_3 \quad (A.3.3.39)$$

$$J_{10} = (J_4 \cos 2\alpha_3 - J_6 \sin \alpha_3 \cos \alpha_3) / r_3 \quad (A.3.3.40)$$